UNIVERSIDADE FEDERAL DE SANTA CATARINA
CENTRO TECNOLÓGICO
PROGRAMA DE PÓS-GRADUAÇÃO EM ENGENHARIA MECÂNICA

Humberto Reder Cazangi

DISCOVERY OF POTENTIAL INNOVATIVE GAPS IN AUTOMOTIVE PLANETARY GEAR MECHANISMS DATABASE

Florianópolis
2024

Humberto Reder Cazangi

DISCOVERY OF POTENTIAL INNOVATIVE GAPS IN AUTOMOTIVE PLANETARY GEAR MECHANISMS DATABASE

Tese submetida ao Programa de Pós-Graduação em Engenharia Mecânica da Universidade Federal de Santa Catarina como requisito parcial para a obtenção do título de Doutor em Engenharia Mecânica, na área de Projeto de Sistemas Mecânicos.

Orientador: Prof. Daniel Martins, Dr. Eng.
Coorientador: Prof. Estevan Hideki Murai, Dr. Eng.

Florianópolis
2024

Ficha catalográfica gerada por meio de sistema automatizado gerenciado pela BU/UFSC.
Dados inseridos pelo próprio autor.

Cazangi, Humberto Reder
DISCOVERY OF POTENTIAL INNOVATIVE GAPS IN AUTOMOTIVE PLANETARY GEAR MECHANISMS DATABASE / Humberto Reder Cazangi ; orientador, Daniel Martins, coorientador, Estevan Hideki Murai, 2024.
518 p.

Tese (doutorado) - Universidade Federal de Santa Catarina, Centro Tecnológico, Programa de Pós-Graduação em Engenharia Mecânica, Florianópolis, 2024.

Inclui referências.

1. Engenharia Mecânica. 2. planetary gear train. 3. automatic transmission. 4. mechanism design. 5. innovation sets. I. Martins, Daniel. II. Murai, Estevan Hideki. III. Universidade Federal de Santa Catarina. Programa de Pós Graduação em Engenharia Mecânica. IV. Título.

Humberto Reder Cazangi

DISCOVERY OF POTENTIAL INNOVATIVE GAPS IN AUTOMOTIVE PLANETARY GEAR MECHANISMS DATABASE

O presente trabalho em nível de Doutorado foi avaliado e aprovado, em 06 de dezembro de 2023, por banca examinadora composta pelos seguintes membros:

Profa. Ludmila Corrêa de Alkmin e Silva, Dra.
Universidade Estadual de Campinas

Prof. Luis Paulo Laus, Dr.
Universidade Tecnológica Federal do Paraná

Prof. Alexandre Leopoldo Gonçalves, Dr.
Universidade Federal de Santa Catarina

Prof. Andrea Piga Carboni, Dr.
Universidade Federal de Santa Catarina

Certificamos que esta é a **versão original e final** do trabalho de conclusão que foi julgado adequado para obtenção do título de Doutor em Engenharia Mecânica, na área de Projeto de Sistemas Mecânicos.

ICP-Edu
Documento assinado digitalmente
Henrique Simas
Data: 04/06/2024 06:37:36-0300
CPF: ***.194.639-**
Verifique as assinaturas em https://v.ufsc.br

Coordenação do Programa de
Pós-Graduação

ICP-Edu
Documento assinado digitalmente
Daniel Martins
Data: 04/06/2024 08:14:28-0300
CPF: ***.746.219-**
Verifique as assinaturas em https://v.ufsc.br

Prof. Daniel Martins, Dr. Eng.
Orientador

ICP-Edu
Documento assinado digitalmente
Estevan Hideki Murai
Data: 04/06/2024 08:07:09-0300
CPF: ***.016.409-**
Verifique as assinaturas em https://v.ufsc.br

Prof. Estevan Hideki Murai, Dr. Eng.
Coorientador

Florianópolis, 2024.

This thesis is dedicated to all those who never gave up.

Esta tese é dedicada à todos aqueles que nunca desistiram.

ACKNOWLEDGEMENTS

I am grateful to my parents and family.
I thank my therapists and facilitators.
I thank my supervisors.
I thank my colleagues at IFSC and UFSC.
I thank life.

Agradeço aos meus pais e à minha família.
Agradeço aos meus terapeutas e facilitadores.
Agradeço aos meus orientadores.
Agradeço aos meus colegas do IFSC e da UFSC.
Agradeço à vida.

"My soul, a nomad spark.
I must always be ready,
To swiftly take flight,
For new lands to find.
It is always rebirth."
(Unknown)

"Minha alma é nômade.
Eu preciso estar sempre pronto,
A levantar acampamento,
Para novas terras conhecer.
E isto é sempre um renascer."
(Desconhecido)

RESUMO

Esta tese apresenta um processo inovador para identificar requisitos potencialmente inovadores no projeto de trens de engrenagens planetárias (PGTs) utilizados em transmissões automáticas (ATs). Uma abordagem multidisciplinar, integrando ciência de mecanismos e máquinas, teoria dos grafos e técnicas avançadas de ciência de dados, é empregada para abordar esta desafiadora tarefa de projeto. Para viabilizar a análise, novos conceitos de juntas redundantes e virtuais sao introduzidos, permitindo uma representação aprimorada de mecanismos de engrenagens planetárias (PGMs) em modelos de grafos. Também propõe uma equação geral de mobilidade revisada para PGMs, permitindo a análise integral dos mecanismos sem necessidade de simplificação. Além disso, novas métricas de complexidade estrutural e capacidade funcional são desenvolvidas, suportando avaliações comparativas abrangentes de PGMs. O processo apresentado envolve a construção de um banco de dados abrangente de PGMs, seguido por análise estratégica de atributos e descoberta de lacunas inovadoras. Este processo foi aplicado em um estudo de caso de 155 transmissões automotivas (6-10 velocidades), analisando 143 atributos distintos e resultando na identificação de treze conjuntos de atributos inovadores com múltiplos potenciais construtivos. Com base em um desses conjuntos, dois PGMs potencialmente inovadores foram sintetizados. Esta pesquisa também resultou em um valioso banco de dados enriquecido e uma extensa revisão da literatura sobre PGTs automotivos. Embora o tamanho do banco de dados seja atualmente limitado pela natureza meticulosa da extração de dados, uma aplicabilidade mais ampla é prevista através da futura automação do processo de coleta de dados e da integração de modelos de aprendizado de representação de grafos (GRL).

Palavras-chave: trens de engrenagens planetárias; transmissão automática; projeto de mecanismos; inovação; teoria dos grafos; ciência de dados.

RESUMO EXPANDIDO

Introdução

As transmissões automotivas desempenham um papel essencial na otimização do desempenho de veículos, abordando desafios de transferência de potência, conversão de torque, eficiência de combustível e adaptabilidade. Enquanto o mercado ainda é dominado por veículos com motor de combustão interna (ICE), emergem oportunidades para avanços em desempenho e redução de emissões, paralelamente ao crescimento dos veículos elétricos (EVs). Diversos tipos de transmissão, incluindo manual (MT), mecânica automatizada (AMT), automática (AT), de dupla embreagem (DCT) e continuamente variável (CVT), oferecem características operacionais e de eficiência distintas. Historicamente, as transmissões automáticas evoluíram consideravelmente desde o século XIX, focando em eficiência de combustível e redução de emissões. Os AT modernos incorporam complexos trens de engrenagens planetárias (PGTs), variando de 4 a 10 velocidades. O projeto de novos PGTs para AT requer essencialmente um estudo aprofundado da estrutura cinemática do mecanismo, o que se apresenta como uma tarefa desafiadora. Embora seja um tema amplamente estudado, exige uma combinação única de criatividade e habilidades técnicas. Os métodos tradicionais de projeto frequentemente se baseiam em adaptação ou busca exaustiva, havendo limitações de escopo em ambos os casos. Portanto, o principal desafio é identificar com maior precisão e detalhamento os requisitos de projeto de maior potencial inovador, minimizando o investimento dedicado a soluções inviáveis. Nesse contexto, a análise de mecanismos obtidos em fontes como patentes, pesquisa acadêmica e dados industriais, aliada com técnicas avançadas de ciência de dados, emerge como uma estratégia valiosa para impulsionar a inovação.

Objetivos

Esta pesquisa tem o intuito de criar e explorar bases de dados extensas e diversificadas para revelar oportunidades inovadoras nos projetos de mecanismos de engrenagens planetárias (PGMs) automotivos. O principal objetivo é desenvolver um processo para auxiliar projetistas na identificação de tais oportunidades. Durante o estudo de diferentes mecanismos de transmissão automotiva, identificou-se que as representações por grafo existentes e a equação geral de mobilidade se limitam à análise da cadeia cinemática, inviabilizando uma abordagem abrangente. Portanto, um objetivo adicional desta tese é apresentar um arcabouço para análise comparativa de mecanismos PGT completos englobando: conceitos de juntas redundantes e virtuais na representação por grafos, equação geral de mobilidade atualizada, e métricas para avaliação da complexidade estrutural e capacidade funcional. Essas métricas permitem avaliações comparativas minuciosas dos projetos de PGM. Os objetivos específicos incluem a investigação de processos de análise e síntese de PGMs, a construção de um banco de dados abrangente, o estabelecimento de abordagens sistemáticas para identificar atributos relevantes, descobrir lacunas inovadoras para os requisitos de projeto e implementar o processo em um estudo de caso com transmissões automáticas.

Metodologia

Foi proposto um processo que integra conceitos multidisciplinares — incluindo análise de requisitos de projeto, ciência de mecanismos e máquinas, bancos de dados de

patentes e teoria dos grafos — com métodos avançados de *data science*, como a descoberta de conhecimento em bases de dados (KDD) e técnicas de mineração de dados. Está estruturado em quatro fases, cada uma com quatro etapas distintas, visando ampliar o domínio de análise dos mecanismos para identificar atributos não-triviais que usualmente não são considerados nos projetos. A primeira fase é a *Pesquisa de Mecanismos*, onde um estudo abrangente reúne dados e informações relevantes de mecanismos em bases de patentes, acadêmicas e industriais. A segunda fase é o *Enriquecimento de Dados*, em que é criado um dicionário diversificado de atributos para caracterização dos mecanismos e formação da base de dados completa. A terceira fase é a *Análise de Atributos*, quando os mecanismos e atributos da base de dados são revisados quanto à sua integridade, avaliados estatistica e estrategicamente, e os atributos mais relevantes para o projeto dos mecanismos são selecionados. A quarta fase é a *Descoberta de Lacunas*, compreendendo a varredura nos atributos mais relevantes para a descoberta de lacunas nos dados, que na sequência são priorizadas, combinadas em *clusters* e, as mais promissoras, são selecionadas como potenciais conjuntos de inovações que servem como requisitos para o projeto de novos mecanismos. Apesar deste estudo ser focado em transmissões automotivas, o processo foi proposto para atender a projetos de mecanismos em geral.

Resultados e Discussão

O processo proposto foi aplicado como estudo de caso a transmissões automotivas automáticas de 6 a 10 marchas baseadas em mecanismos de engrenagens planetárias (PGMs), sendo construído um banco de dados com 160 mecanismos caracterizados por 186 atributos. Após revisão e limpeza dos dados, resultaram 155 mecanismos e 143 atributos distintos, que foram analisados em contextos de grupo único e, também, agrupados por condição comercial, número de conjuntos planetários (PGSs) e número de marchas à frente. A análise estratégica dos principais corpos fixo (F), entrada (IN) e saída (OUT) permitiu caracterizá-los quanto a sua constituição e acoplamentos. A análise estratégica sobre complexidade revelou que a métrica de complexidade estrutural proposta é mais precisa que outras métricas, diferenciando 143 mecanismos únicos, sendo altamente correlacionada com seu termo relativo à complexidade das juntas. Ainda, a métrica de complexidade estrutural foi utilizada em conjunto com a métrica de capacidade para apresentar um mapa de fronteira tecnológica dos mecanismos da base de dados. A seleção de atributos utilizou técnicas como *Random Forest*, *Recursive Feature Elimination (RFE)*, regularização L1 usando método Lasso e métodos estatísticos univariados para determinar os atributos mais relevantes conforme os contextos de análise previamente estabelecidos. Por fim, utilizando uma função própria para a descoberta de lacunas, foram selecionados 13 conjuntos de inovação envolvendo atributos topológicos e funcionais com múltiplos conjuntos de PGSs que podem ser aplicados como requisitos de projeto para novos mecanismos de transmissão planetária automotiva. Uma síntese baseada nas lacunas de inovação foi apresentada propiciando a descoberta de dois novos mecanismos em potencial. A pesquisa apresentou avanços significativos na análise e síntese de mecanismos de engrenagens planetárias (PGTs) automotivos, destacando-se:

1. Novos conceitos de juntas redundantes e virtuais permitem uma representação mais abrangente da estrutura dos mecanismos em modelos de grafos, considerando o PGM integralmente, facilitando a análise e o projeto de mecanismos complexos.

2. Nova equação geral da mobilidade revisada para PGMs possibilita o cálculo preciso da mobilidade de mecanismos de transmissões planetárias completos, considerando as juntas redundantes e virtuais.
3. Novos conceitos de complexidade estrutural e capacidade funcional fornecem uma avaliação mais completa, precisa e abrangente do mecanismos de PGT, auxiliando na tomada de decisões durante o projeto.
4. Novo processo de análise e descoberta de lacunas inovadoras em base de dados de mecanismos permite a identificação de lacunas inovadoras em bases de dados de mecanismos, abrindo caminho para o desenvolvimento de novos conceitos e soluções tecnológicas.
5. Aplicação do processo proposto em um estudo de caso comprovou sua viabilidade e efetividade na identificação de sete conjuntos de inovação relevantes para o projeto de novos mecanismos de PGT.
6. Processo de síntese baseado em conjuntos inovadores resultou no desenvolvimento de duas novas transmissões automotivas com potencial inovador.
7. Base de dados enriquecida com 143 atributos distintos representa um recurso valioso para pesquisas futuras na área de projeto de transmissões automotivas.

Considerações Finais

As contribuições científicas envolvem a revisão do grafo e da equação de mobilidade para PGMs, a introdução de métricas de complexidade e capacidade funcional, o desenvolvimento e a aplicação de um procedimento para identificar conjuntos de inovação, e a síntese de dois PGMs potencialmente novos, enriquecendo o processo de desenvolvimento de novos mecanismos. O estudo possui limitações, como o número restrito de instâncias na base de dados devido ao processo manual meticuloso que toma tempo na conversão de patentes em modelos na base de dados, influenciando a generalização dos resultados. A necessidade de competência técnica para a análise dos atributos também pode ser uma barreira para a adoção do processo. Trabalhos futuros deverão focar na automação da coleta de dados, expansão da caracterização dos PGMs, aprimoramento das métricas de complexidade e generalização do processo para outros mecanismos complexos. Utilizar modelos de aprendizagem por representação com grafos (GRL) para descoberta de conhecimento e mineração de dados é um caminho promissor. Em resumo, a pesquisa apresenta uma abordagem estruturada para identificar e analisar configurações inovadoras em PGMs, contribuindo significativamente para o avanço da pesquisa e projeto neste campo. Esforços futuros podem aprimorar ainda mais o processo, transformando-o em metodologia para ampliar sua aplicabilidade prática.

Palavras-chave: trens de engrenagens planetárias; transmissão automática; projeto de mecanismos; inovação; teoria dos grafos; ciência de dados.

ABSTRACT

This thesis presents a novel process for identifying potential innovative requirements in the design of automotive planetary gear trains (PGTs) used within automatic transmissions (AT). A multidisciplinary approach, integrating mechanism and machine science, graph theory, and advanced data science techniques, is employed to address this challenging design task. To enable the analysis, this research introduces new concepts of redundant and virtual joints, allowing an improved representation of planetary gear mechanisms (PGMs) within graph models. It is proposed a revised general mobility equation for PGMs, allowing the full analysis of the mechanisms without the need for simplifications. Furthermore, new metrics of structural complexity and functional capability are developed, supporting comprehensive comparative evaluations of PGM designs. The proposed process involves constructing a comprehensive database of PGMs, followed by strategic feature analysis and discovery of potentially innovative gaps. This process was applied in a case study of 155 automotive transmissions (6-10 speeds), analyzing 143 distinct attributes and resulted in the identification of thirteen innovative feature sets with multiple candidates PGSs. Based on one of these sets, two potentially innovative PGMs were synthesized. This research also resulted in a valuable enriched database and an extensive literature review on automotive PGTs. While the database size is currently constrained by the meticulous nature of data extraction, broader applicability is envisioned through future automation of the data collection process and the integration of graph representation learning (GRL) models.

Keywords: planetary gear train; automatic transmission; mechanism design; innovation sets; graph theory, data science.

LIST OF FIGURES

Figure 1 – 6-speed manual transmission (MT) for passenger cars Mercedes-Benz SG6-300. 34
Figure 2 – 7-speed automated manual transmission (AMT) for passenger cars Getrag 247. 34
Figure 3 – 9-speed automatic transmission (AT) for passenger cars Mercedes-Benz 9G-Tronic. 35
Figure 4 – 7-speed dual clutch transmission (DCT) for passenger cars Volkswagen DQ200-7F. 36
Figure 5 – Continuously variable transmission (CVT) for passenger cars Audi Multitronic. 36
Figure 6 – Hybrid transmission for passenger cars BMW/Chrysler/Daimler/GM. 37
Figure 7 – Shiftable planetary gear transmission in 1834. 38
Figure 8 – Configuration of a 3-speed AT based on Simpson PGT. 45
Figure 9 – Drivetrain arrangements for a front-wheel driven vehicle. 48
Figure 10 – Overview of machine's constitution. 54
Figure 11 – Overview of a typical kinematic structure found in AT. 55
Figure 12 – Planetary Gear Sets (PGS) 55
Figure 13 – Typical configuration of a planetary gear train in automotive transmissions. 57
Figure 14 – Schematic representation of a simple planetary gear train. 57
Figure 15 – Functional diagram of a GM 6-speed automatic transmission 58
Figure 16 – Kinematic structural representation of a simple planetary gear train. 58
Figure 17 – Simple PGS kinematic chain representations. 60
Figure 18 – Double PGS kinematic chain representations. 60
Figure 19 – Subgraph of vertices F, IN, and OUT to generate a PGM. 61
Figure 20 – Representations of a PGM with one SPGS. 62
Figure 21 – Graph representation of the GM 6-speed automatic transmission. . . 62
Figure 22 – Representations of a Simpson PGT. 69
Figure 23 – Mechanism and Machine design. 70
Figure 24 – Declarative design model for a two-stage PGT. 72
Figure 25 – Topology representation of a 4-speed PGT 72
Figure 26 – Overview of a library based topology synthesis process for EVs. . . 73
Figure 27 – Flowchart of a creative design methodology for structural synthesis. 74
Figure 28 – Patent survey and technological boundary. 77
Figure 29 – Case 1: Simple PGT with 2 brakes 82
Figure 30 – Case 2: Simple PGT with 2 brakes and 1 clutch 83
Figure 31 – Case 3: Simple PGT with 2 brakes, 2 clutches and output link 85

Figure 32 – Case 4: GM 6-speed model 6T40 86
Figure 33 – Overview of the structural complexity metric. 93
Figure 34 – Process for Discovering Potential Innovative Gaps. 101
Figure 35 – Overview of the KDD process. 102
Figure 36 – Front page of an international patent application. 105
Figure 37 – LAR Patent Survey Methodology 106
Figure 38 – Example of an EDA process. 116
Figure 39 – Categories of Feature Selection output. 119
Figure 40 – User's perspective categorization for FS methods. 120
Figure 41 – Unified framework view of FS methods. 121
Figure 42 – Automotive PGM patents published per year. 129
Figure 43 – Automotive PGM published patents segmented by gear ratios (since 1965). 130
Figure 44 – Automotive PGM published patents by applicants. 131
Figure 45 – Toyota 8-speed automatic transmission for transverse application. . 132
Figure 46 – Bibliographic data excerpt from the patent US10563738B2. 133
Figure 47 – Toyota 8-speed AT functional diagram. 133
Figure 48 – Functional and technical data of *US10563738B2__FIG_1*. 135
Figure 49 – PGM and DBG graphs of *US10563738B2__FIG_1*. 136
Figure 50 – Distribution of data types in the database. 146
Figure 51 – Distribution of data types in the database after the cleansing step. . 149
Figure 52 – Distribution of the correlation pairs by strength in database. 151
Figure 53 – Correlation heatmap of PGM Complexity metrics. 156
Figure 54 – Technological Boundary Map for PGMs. 160
Figure 55 – Diagram of the reference PGSs sequence *1S+1D+1R [S,R,D]*. . . . 179
Figure 56 – Schematic diagram of the PGT *1S+1D+1R__277*. 183
Figure 57 – Lever diagram of the PGT *1S+1D+1R__277*. 184
Figure 58 – Lever diagram of the PGT *1S+1D+1R__277* with potential shift couplings. 186
Figure 59 – Diagram of Longitudinal PGM *1S+1D+1R__277*. 190
Figure 60 – Graph of the longitudinal PGM *1S+1D+1R__277*. 190
Figure 61 – Diagram of the transverse PGM *1S+1D+1R__277*. 191
Figure 62 – Graph of the transverse PGM *1S+1D+1R__277*. 191
Figure 63 – PGM *1S+1D+1R__277* in the Technological Boundary Map. 192
Figure 64 – PGM Dataset Template Map. 219
Figure 65 – Sector 1: Dataset Identification (manual) 220
Figure 66 – Sector 2: Topological and functional data input (manual) 220
Figure 67 – Sector 3: Links creation (automatic) 220
Figure 68 – Sector 4: Joints creation (automatic) 221

Figure 69 – Sector 5: PGM Graph analysis (automatic) 221
Figure 70 – Sector 6: Gear specifications (automatic) 222
Figure 71 – Sector 7: PGM Graph link assortment (automatic) 222
Figure 72 – Sector 8: PGT Kinematic chain - DBG graph creation (automatic) . . 223
Figure 73 – Sector 9: Validators checklist (automatic) 224
Figure 74 – Sector 10: Dataset summary (automatic) - 1 of 2 225
Figure 75 – Sector 10: Dataset summary (automatic) - 2 of 2 226
Figure 76 – Sector 11: PGM and DBG General validation (automatic) 227
Figure 77 – Sector 12: Topological and Functional classification (automatic) . . . 227
Figure 78 – Sector 13: Unique dataset identifier and version control (automatic) . 227
Figure 79 – Sector 14: Dataset references (manual) 227
Figure 80 – Sector 15: PGM Figures (manual) 228
Figure 81 – AISIN_TOYOTA__AT_6_speed_L representations. 229
Figure 82 – AISIN_TOYOTA__AT_8_speed_L representations. 230
Figure 83 – AISIN_TOYOTA__AT_10_speed_L representations. 231
Figure 84 – AISIN_TOYOTA__AT_6_speed_FT representations. 232
Figure 85 – AISIN_TOYOTA__AT_8_speed_FT representations. 233
Figure 86 – CN100480537C__FIG1 representations. 234
Figure 87 – CN100480537C__FIG3 representations. 235
Figure 88 – CN101036001A__FIG1 representations. 236
Figure 89 – CN113503344A__FIG1 representations. 237
Figure 90 – CN113503347A__FIG1 representations. 238
Figure 91 – CN114810958A__FIG1 representations. 239
Figure 92 – JP3519037B2__7GTronic representations. 240
Figure 93 – CN105229337B__9GTronic representations. 241
Figure 94 – EP2655929B1__FIG1 representations. 242
Figure 95 – EP2655929B1__FIG5 representations. 243
Figure 96 – FORD__AT_8_speed_FT_8F24 representations. 244
Figure 97 – FORD__AT_8_speed_FT_8F35 representations. 245
Figure 98 – FORD__AT_8_speed_FT_8F57 representations. 246
Figure 99 – US8545362B1__AT_10_speed_L_10R80 representations. 247
Figure 100–GM__AT_8_speed_L representations. 248
Figure 101–GM__AT_10_speed_L representations. 249
Figure 102–GM__AT_6_speed_FT representations. 250
Figure 103–GM__AT_9_speed_FT representations. 251
Figure 104–CN108691965A__AT_10_speed_FT representations. 252
Figure 105–CN105179615A__MECH1 representations. 253
Figure 106–CN105090394A__MECH2 representations. 254
Figure 107–CN109764095A__MECH3 representations. 255

Figure 108–CN109798334A__MECH4 representations. 256
Figure 109–JP3519037B2__FIG1 representations. 257
Figure 110–JP3519037B2__FIG3 representations. 258
Figure 111–JP3519037B2__FIG5 representations. 259
Figure 112–JP3519037B2__FIG7 representations. 260
Figure 113–JP3710180B2__FIG2 representations. 261
Figure 114–JP3710180B2__FIG5 representations. 262
Figure 115–JP3710180B2__FIG8 representations. 263
Figure 116–JP3710180B2__FIG23 representations. 264
Figure 117–JP3710180B2__FIG44 representations. 265
Figure 118–KR101154689B1__FIG1 representations. 266
Figure 119–KR102417360B1__FIG1 representations. 267
Figure 120–KR20090096701A__FIG1 representations. 268
Figure 121–KR20090096701A__FIG1A representations. 269
Figure 122–PIGAMARTINS__FIG2 representations. 270
Figure 123–PIGAMARTINS__FIG3 representations. 271
Figure 124–US10161483B2__FIG2 representations. 272
Figure 125–US10161483B2__FIG3 representations. 273
Figure 126–US10323726B2__FIG1 representations. 274
Figure 127–US10323726B2__FIG4 representations. 275
Figure 128–US10563738B2__FIG1 representations. 276
Figure 129–US10612627B2__FIG1 representations. 277
Figure 130–US10612627B2__FIG2 representations. 278
Figure 131–US10612627B2__FIG3 representations. 279
Figure 132–US10612627B2__FIG4 representations. 280
Figure 133–US10612627B2__FIG5 representations. 281
Figure 134–US10612627B2__FIG6 representations. 282
Figure 135–US10612627B2__FIG7 representations. 283
Figure 136–US10612627B2__FIG8 representations. 284
Figure 137–US10612627B2__FIG9 representations. 285
Figure 138–US10612627B2__FIG10 representations. 286
Figure 139–US11199246B2__FIG1 representations. 287
Figure 140–US11231105B2__FIG2 representations. 288
Figure 141–US11248699B2__FIG_1 representations. 289
Figure 142–US11248699B2__FIG_3 representations. 290
Figure 143–US5599251A__FIG1 representations. 291
Figure 144–US6422969B1__FIG1 representations. 292
Figure 145–US6422969B1__FIG3 representations. 293
Figure 146–US6422969B1__FIG5 representations. 294

Figure 147–US6422969B1__FIG7 representations. 295
Figure 148–US6422969B1__FIG9 representations. 296
Figure 149–US6514170B1__FIG1 representations. 297
Figure 150–US6514170B1__FIG2 representations. 298
Figure 151–US6514170B1__FIG3 representations. 299
Figure 152–US6514170B1__FIG4 representations. 300
Figure 153–US6514170B1__FIG5 representations. 301
Figure 154–US6514170B1__FIG6 representations. 302
Figure 155–US6514170B1__FIG7 representations. 303
Figure 156–US6514170B1__FIG8 representations. 304
Figure 157–US6514170B1__FIG9 representations. 305
Figure 158–US6514170B1__FIG10 representations. 306
Figure 159–US6514170B1__FIG11 representations. 307
Figure 160–US6514170B1__FIG12 representations. 308
Figure 161–US6530858B1__FIG1 representations. 309
Figure 162–US6530858B1__FIG3 representations. 310
Figure 163–US6530858B1__FIG5 representations. 311
Figure 164–US6530858B1__FIG7 representations. 312
Figure 165–US6530858B1__FIG9 representations. 313
Figure 166–US6530858B1__FIG11 representations. 314
Figure 167–US6530858B1__FIG13 representations. 315
Figure 168–US6530858B1__FIG15 representations. 316
Figure 169–US6530858B1__FIG17 representations. 317
Figure 170–US6530858B1__FIG19 representations. 318
Figure 171–US6530858B1__FIG21 representations. 319
Figure 172–US6530858B1__FIG23 representations. 320
Figure 173–US6530858B1__FIG25 representations. 321
Figure 174–US6595892B2__FIG1 representations. 322
Figure 175–US6595892B2__FIG3 representations. 323
Figure 176–US6595892B2__FIG5 representations. 324
Figure 177–US6595892B2__FIG7 representations. 325
Figure 178–US6595892B2__FIG9 representations. 326
Figure 179–US6595892B2__FIG11 representations. 327
Figure 180–US6595892B2__FIG13 representations. 328
Figure 181–US6595892B2__FIG15 representations. 329
Figure 182–US6595892B2__FIG17 representations. 330
Figure 183–US6595892B2__FIG19 representations. 331
Figure 184–US6595892B2__FIG21 representations. 332
Figure 185–US6595892B2__FIG23 representations. 333

Figure 186–US6595892B2__FIG25 representations. 334
Figure 187–US6595892B2__FIG27 representations. 335
Figure 188–US6623398B2__FIG1 representations. 336
Figure 189–US6623398B2__FIG3 representations. 337
Figure 190–US6623398B2__FIG5 representations. 338
Figure 191–US6623398B2__FIG7 representations. 339
Figure 192–US6623398B2__FIG9 representations. 340
Figure 193–US6623398B2__FIG11 representations. 341
Figure 194–US6623398B2__FIG13 representations. 342
Figure 195–US6623398B2__FIG15 representations. 343
Figure 196–US6623398B2__FIG17 representations. 344
Figure 197–US6623398B2__FIG19 representations. 345
Figure 198–US6705967B2__FIG1 representations. 346
Figure 199–US6705967B2__FIG3 representations. 347
Figure 200–US6705967B2__FIG5 representations. 348
Figure 201–US6705967B2__FIG7 representations. 349
Figure 202–US6705967B2__FIG9 representations. 350
Figure 203–US6705967B2__FIG11 representations. 351
Figure 204–US6705967B2__FIG13 representations. 352
Figure 205–US6705967B2__FIG15 representations. 353
Figure 206–US6705967B2__FIG17 representations. 354
Figure 207–US6705967B2__FIG19 representations. 355
Figure 208–US6705967B2__FIG21 representations. 356
Figure 209–US6705967B2__FIG23 representations. 357
Figure 210–US6705967B2__FIG25 representations. 358
Figure 211–US6705967B2__FIG27 representations. 359
Figure 212–US6705967B2__FIG29 representations. 360
Figure 213–US6705967B2__FIG31 representations. 361
Figure 214–US6705967B2__FIG33 representations. 362
Figure 215–US7621841B2__FIG1 representations. 363
Figure 216–US7621841B2__FIG4 representations. 364
Figure 217–US7621841B2__FIG5 representations. 365
Figure 218–US7628726B2__FIG1 representations. 366
Figure 219–US7967716B2__FIG2 representations. 367
Figure 220–US7985160B2__FIG1 representations. 368
Figure 221–US8012059B2__FIG1 representations. 369
Figure 222–US8029405B2__FIG1 representations. 370
Figure 223–US8029405B2__FIG4 representations. 371
Figure 224–US8029405B2__FIG5 representations. 372

Figure 225–US8123650B2__FIG1 representations. 373
Figure 226–US8202192B2__FIG1 representations. 374
Figure 227–US8506443B2__FIG1 representations. 375
Figure 228–US8597153B2__FIG1 representations. 376
Figure 229–US8597153B2__FIG4 representations. 377
Figure 230–US8657718B2__FIG1 representations. 378
Figure 231–US8663055B2__FIG1 representations. 379
Figure 232–US8678973B2__FIG1 representations. 380
Figure 233–US8992374B2__FIG1 representations. 381
Figure 234–US8992374B2__FIG5 representations. 382
Figure 235–US9587716B1__FIG1 representations. 383
Figure 236–US9726262B1__FIG1 representations. 384
Figure 237–US9841085B2__FIG1 representations. 385
Figure 238–DE10140424A1__6HP representations. 386
Figure 239–ZF__8HP representations. 387
Figure 240–US8398522B2__9HP representations. 388
Figure 241–Violin plot explanation 390
Figure 242–Violin plots of numerical features - *FWD GEARS* (1 of 8) 391
Figure 243–Violin plots of numerical features - *FWD GEARS* (2 of 8) 392
Figure 244–Violin plots of numerical features - *FWD GEARS* (3 of 8) 393
Figure 245–Violin plots of numerical features - *FWD GEARS* (4 of 8) 394
Figure 246–Violin plots of numerical features - *FWD GEARS* (5 of 8) 395
Figure 247–Violin plots of numerical features - *FWD GEARS* (6 of 8) 396
Figure 248–Violin plots of numerical features - *FWD GEARS* (7 of 8) 397
Figure 249–Violin plots of numerical features - *FWD GEARS* (8 of 8) 398
Figure 250–Charts of boolean features - *FWD GEARS* 399
Figure 251–Charts of categorical feature - Unique Sources ID - *FWD GEARS* . 400
Figure 252–Charts of categorical feature - PGSs Sequences - *FWD GEARS* . . 401
Figure 253–Charts of categorical feature - DBG Classification - *FWD GEARS* . 401
Figure 254–Charts of categorical feature - DBG Link Assortments - *FWD GEARS* 402
Figure 255–Charts of categorical feature - PGM Classification - *FWD GEARS* . 403
Figure 256–Charts of categorical feature - PGM Link Assortments - *FWD GEARS* 404
Figure 257–Violin plots of numerical features - *PGSs Total* (1 of 8) 406
Figure 258–Violin plots of numerical features - *PGSs Total* (2 of 8) 407
Figure 259–Violin plots of numerical features - *PGSs Total* (3 of 8) 408
Figure 260–Violin plots of numerical features - *PGSs Total* (4 of 8) 409
Figure 261–Violin plots of numerical features - *PGSs Total* (5 of 8) 410
Figure 262–Violin plots of numerical features - *PGSs Total* (6 of 8) 411
Figure 263–Violin plots of numerical features - *PGSs Total* (7 of 8) 412

Figure 264–Violin plots of numerical features - *PGSs Total* (8 of 8) 413
Figure 265–Charts of boolean features - *PGSs Total* 414
Figure 266–Charts of categorical feature - Unique Sources ID - *PGSs Total* . . 415
Figure 267–Charts of categorical feature - PGSs Sequences - *PGSs Total* . . . 416
Figure 268–Charts of categorical feature - DBG Classification - *PGSs Total* . . . 416
Figure 269–Charts of categorical feature - DBG Link Assortments - *PGSs Total* 417
Figure 270–Charts of categorical feature - PGM Classification - *PGSs Total* . . 418
Figure 271–Charts of categorical feature - PGM Link Assortments - *PGSs Total* 419
Figure 272–Violin plots of numerical features - *Commercial?* (1 of 8) 421
Figure 273–Violin plots of numerical features - *Commercial?* (2 of 8) 422
Figure 274–Violin plots of numerical features - *Commercial?* (3 of 8) 423
Figure 275–Violin plots of numerical features - *Commercial?* (4 of 8) 424
Figure 276–Violin plots of numerical features - *Commercial?* (5 of 8) 425
Figure 277–Violin plots of numerical features - *Commercial?* (6 of 8) 426
Figure 278–Violin plots of numerical features - *Commercial?* (7 of 8) 427
Figure 279–Violin plots of numerical features - *Commercial?* (8 of 8) 428
Figure 280–Charts of boolean features - *Commercial?* 429
Figure 281–Charts of categorical feature - Unique Sources ID - *Commercial?* . 430
Figure 282–Charts of categorical feature - PGSs Sequences - *Commercial?* . . 431
Figure 283–Charts of categorical feature - DBG Classification - *Commercial?* . 431
Figure 284–Charts of categorical feature - DBG Link Assortments - *Commercial?* 432
Figure 285–Charts of categorical feature - PGM Classification - *Commercial?* . 433
Figure 286–Charts of categorical feature - PGM Link Assortments - *Commercial?* 434
Figure 287–Normality Tests Results (1 of 24) 436
Figure 288–Normality Tests Results (2 of 24) 437
Figure 289–Normality Tests Results (3 of 24) 438
Figure 290–Normality Tests Results (4 of 24) 439
Figure 291–Normality Tests Results (5 of 24) 440
Figure 292–Normality Tests Results (6 of 24) 441
Figure 293–Normality Tests Results (7 of 24) 442
Figure 294–Normality Tests Results (8 of 24) 443
Figure 295–Normality Tests Results (9 of 24) 444
Figure 296–Normality Tests Results (10 of 24) 445
Figure 297–Normality Tests Results (11 of 24) 446
Figure 298–Normality Tests Results (12 of 24) 447
Figure 299–Normality Tests Results (13 of 24) 448
Figure 300–Normality Tests Results (14 of 24) 449
Figure 301–Normality Tests Results (15 of 24) 450
Figure 302–Normality Tests Results (16 of 24) 451

Figure 303–Normality Tests Results (17 of 24) 452
Figure 304–Normality Tests Results (18 of 24) 453
Figure 305–Normality Tests Results (19 of 24) 454
Figure 306–Normality Tests Results (20 of 24) 455
Figure 307–Normality Tests Results (21 of 24) 456
Figure 308–Normality Tests Results (22 of 24) 457
Figure 309–Normality Tests Results (23 of 24) 458
Figure 310–Normality Tests Results (24 of 24) 459
Figure 311–Correlation Heatmap Slice Map 460
Figure 312–Correlation Heatmap (1 of 21) 461
Figure 313–Correlation Heatmap (2 of 21) 462
Figure 314–Correlation Heatmap (3 of 21) 463
Figure 315–Correlation Heatmap (4 of 21) 464
Figure 316–Correlation Heatmap (5 of 21) 465
Figure 317–Correlation Heatmap (6 of 21) 466
Figure 318–Correlation Heatmap (7 of 21) 467
Figure 319–Correlation Heatmap (8 of 21) 468
Figure 320–Correlation Heatmap (9 of 21) 469
Figure 321–Correlation Heatmap (10 of 21) 470
Figure 322–Correlation Heatmap (11 of 21) 471
Figure 323–Correlation Heatmap (12 of 21) 472
Figure 324–Correlation Heatmap (13 of 21) 473
Figure 325–Correlation Heatmap (14 of 21) 474
Figure 326–Correlation Heatmap (15 of 21) 475
Figure 327–Correlation Heatmap (16 of 21) 476
Figure 328–Correlation Heatmap (17 of 21) 476
Figure 329–Correlation Heatmap (18 of 21) 477
Figure 330–Correlation Heatmap (19 of 21) 477
Figure 331–Correlation Heatmap (20 of 21) 478
Figure 332–Correlation Heatmap (21 of 21) 478
Figure 333–Perfectly Correlated Features (1 of 1) 479
Figure 334–Highly Correlated Features (1 of 19) 480
Figure 335–Highly Correlated Features (2 of 19) 481
Figure 336–Highly Correlated Features (3 of 19) 481
Figure 337–Highly Correlated Features (4 of 19) 482
Figure 338–Highly Correlated Features (5 of 19) 483
Figure 339–Highly Correlated Features (6 of 19) 484
Figure 340–Highly Correlated Features (7 of 19) 485
Figure 341–Highly Correlated Features (8 of 19) 485

Figure 342–Highly Correlated Features (9 of 19) 486
Figure 343–Highly Correlated Features (10 of 19) 487
Figure 344–Highly Correlated Features (11 of 19) 487
Figure 345–Highly Correlated Features (12 of 19) 488
Figure 346–Highly Correlated Features (13 of 19) 488
Figure 347–Highly Correlated Features (14 of 19) 489
Figure 348–Highly Correlated Features (15 of 19) 489
Figure 349–Highly Correlated Features (16 of 19) 489
Figure 350–Highly Correlated Features (17 of 19) 490
Figure 351–Highly Correlated Features (18 of 19) 490
Figure 352–Highly Correlated Features (19 of 19) 491
Figure 353–Frame (F) compound links analysis 493
Figure 354–Frame (F) adjacency analysis by *FWD GEARS* 494
Figure 355–Frame (F) adjacency analysis by *Commercial* 495
Figure 356–Frame (F) adjacency analysis by *PGSs Total* 496
Figure 357–Frame (F) centrality analysis 497
Figure 358–Input (IN) compound links analysis 498
Figure 359–Input (IN) adjacency analysis by *FWD GEARS* 499
Figure 360–Input (IN) adjacency analysis by *Commercial* 500
Figure 361–Input (IN) adjacency analysis by *PGSs Total* 501
Figure 362–Input (IN) centrality analysis 502
Figure 363–Output (OUT) compound links analysis 503
Figure 364–Output (OUT) adjacency analysis by *FWD GEARS* 504
Figure 365–Output (OUT) adjacency analysis by *Commercial* 505
Figure 366–Output (OUT) adjacency analysis by *PGSs Total* 506
Figure 367–Output (OUT) centrality analysis 507
Figure 368–15 most relevant features for commercial status 'TRUE'. 509
Figure 369–15 most relevant features for total count of 3 elementary PGSs. . . . 510
Figure 370–15 most relevant features for total count of 4 elementary PGSs. . . . 511
Figure 371–15 most relevant features for total count of 5 elementary PGSs. . . . 512
Figure 372–15 most relevant features for 6 forward speeds. 513
Figure 373–15 most relevant features for 7 forward speeds. 514
Figure 374–15 most relevant features for 8 forward speeds. 515
Figure 375–15 most relevant features for 9 forward speeds. 516
Figure 376–15 most relevant features for 10 forward speeds. 517

LIST OF TABLES

Table 1 – Mainstream transmissions comparison. 37
Table 2 – Gear ratio conditions. 48
Table 3 – Gear ratios truth table of a 6-speed transmission. 50
Table 4 – Kinematic pairs and their characteristics. 52
Table 5 – Simple Planetary Gear Set (SPGS) 56
Table 6 – Double Planetary Gear Set (DPGS) 56
Table 7 – Correspondences between mechanisms and graphs. 62
Table 8 – Degrees of freedom and constraints of revolute and gear joints in each motion space. 65
Table 9 – Link assortments of the GM 6-speed AT graph (Fig. 21). 66
Table 10 – Compound link transition cost conditions. 94
Table 11 – Relative individual complexity attributed to elementary links of PGMs. 94
Table 12 – Relative pairwise complexities attributed to couplings of PGMs. 96
Table 13 – Common univariate analysis according to feature type. 117
Table 14 – Common bivariate analysis according to feature type. 117
Table 15 – Summary of PGMs' collected data. 131
Table 16 – *US10563738B2__FIG_1* input identification data. 134
Table 17 – *US10563738B2__FIG_1* input topological data. 134
Table 18 – *US10563738B2__FIG_1* input functional data. 135
Table 19 – *US10563738B2__FIG_1* input technical data. 136
Table 20 – *US10563738B2__FIG_1* data dictionary of features. 139
Table 21 – Missing values in features. 147
Table 22 – Database overview. 149
Table 23 – Correlation classes for absolute values. 150
Table 24 – Fundamental PGS types in sequence arrangements. 154
Table 25 – PGSs sequences in the database. 155
Table 26 – Statistical overview of complexity metrics. 155
Table 27 – Four PGMs complexity comparison. 158
Table 28 – Comparison of the least and most complex PGMs in database. 161
Table 29 – Top 15 most relevant features for each target variable. 162
Table 30 – Identified gaps in PGSs sequence arrangements for global context. . 165
Table 31 – Gaps in requisite properties for *commercial status "TRUE"* context. . . 166
Table 32 – Gaps in requisite properties for *total count of 3 elementary PGSs* context.166
Table 33 – Gaps in requisite properties for *total count of 4 elementary PGSs* context.166
Table 34 – Gaps in requisite properties for *total count of 5 elementary PGSs* context.167
Table 35 – Gaps in requisite properties for *6 forward speeds* context. 167
Table 36 – Gaps in requisite properties for *7 forward speeds* context. 168

Table 37 – Gaps in requisite properties for *8 forward speeds* context. 168
Table 38 – Gaps in requisite properties for *9 forward speeds* context. 168
Table 39 – Gaps in requisite properties for *10 forward speeds* context. 169
Table 40 – Prioritization scheme for feature gaps by innovation potential. 170
Table 41 – Innovation potential rank of gaps in property requisite features. 172
Table 42 – Gaps clustered by contexts. 174
Table 43 – Innovation Sets within local contexts. 176
Table 44 – Characterization of 10 forward speed local context. 179
Table 45 – Top 10 new potential PGTs. 180
Table 46 – Summary of preliminary gear modes for PGM *1S+1D+1R__277*. . . . 186
Table 47 – Gear teeth suggested for PGM *1S+1D+1R__277*. 187
Table 48 – PGM *1S+1D+1R__277* Lever diagrams and gear modes. 187
Table 49 – Preliminary gear specifications for the *PGM 1S+1D+1R__277* 189
Table 50 – *PGM* 1S+1D+1R__277 topological data. 189
Table 51 – Analysis of Objective Attainment 193
Table 52 – AISIN_TOYOTA__AT_6_speed_L dataset information. 229
Table 53 – AISIN_TOYOTA__AT_8_speed_L dataset information. 230
Table 54 – AISIN_TOYOTA__AT_10_speed_L dataset information. 231
Table 55 – AISIN_TOYOTA__AT_6_speed_FT dataset information. 232
Table 56 – AISIN_TOYOTA__AT_8_speed_FT dataset information. 233
Table 57 – CN100480537C__FIG1 dataset information. 234
Table 58 – CN100480537C__FIG3 dataset information. 235
Table 59 – CN101036001A__FIG1 dataset information. 236
Table 60 – CN113503344A__FIG1 dataset information. 237
Table 61 – CN113503347A__FIG1 dataset information. 238
Table 62 – CN114810958A__FIG1 dataset information. 239
Table 63 – JP3519037B2__7GTronic dataset information. 240
Table 64 – CN105229337B__9GTronic dataset information. 241
Table 65 – EP2655929B1__FIG1 dataset information. 242
Table 66 – EP2655929B1__FIG5 dataset information. 243
Table 67 – FORD__AT_8_speed_FT_8F24 dataset information. 244
Table 68 – FORD__AT_8_speed_FT_8F35 dataset information. 245
Table 69 – FORD__AT_8_speed_FT_8F57 dataset information. 246
Table 70 – US8545362B1__AT_10_speed_L_10R80 dataset information. 247
Table 71 – GM__AT_8_speed_L dataset information. 248
Table 72 – GM__AT_10_speed_L dataset information. 249
Table 73 – GM__AT_6_speed_FT dataset information. 250
Table 74 – GM__AT_9_speed_FT dataset information. 251
Table 75 – CN108691965A__AT_10_speed_FT dataset information. 252

Table 76 – CN105179615A__MECH1 dataset information. 253
Table 77 – CN105090394A__MECH2 dataset information. 254
Table 78 – CN109764095A__MECH3 dataset information. 255
Table 79 – CN109798334A__MECH4 dataset information. 256
Table 80 – JP3519037B2__FIG1 dataset information. 257
Table 81 – JP3519037B2__FIG3 dataset information. 258
Table 82 – JP3519037B2__FIG5 dataset information. 259
Table 83 – JP3519037B2__FIG7 dataset information. 260
Table 84 – JP3710180B2__FIG2 dataset information. 261
Table 85 – JP3710180B2__FIG5 dataset information. 262
Table 86 – JP3710180B2__FIG8 dataset information. 263
Table 87 – JP3710180B2__FIG23 dataset information. 264
Table 88 – JP3710180B2__FIG44 dataset information. 265
Table 89 – KR101154689B1__FIG1 dataset information. 266
Table 90 – KR102417360B1__FIG1 dataset information. 267
Table 91 – KR20090096701A__FIG1 dataset information. 268
Table 92 – KR20090096701A__FIG1A dataset information. 269
Table 93 – PIGAMARTINS__FIG2 dataset information. 270
Table 94 – PIGAMARTINS__FIG3 dataset information. 271
Table 95 – US10161483B2__FIG2 dataset information. 272
Table 96 – US10161483B2__FIG3 dataset information. 273
Table 97 – US10323726B2__FIG1 dataset information. 274
Table 98 – US10323726B2__FIG4 dataset information. 275
Table 99 – US10563738B2__FIG1 dataset information. 276
Table 100–US10612627B2__FIG1 dataset information. 277
Table 101–US10612627B2__FIG2 dataset information. 278
Table 102–US10612627B2__FIG3 dataset information. 279
Table 103–US10612627B2__FIG4 dataset information. 280
Table 104–US10612627B2__FIG5 dataset information. 281
Table 105–US10612627B2__FIG6 dataset information. 282
Table 106–US10612627B2__FIG7 dataset information. 283
Table 107–US10612627B2__FIG8 dataset information. 284
Table 108–US10612627B2__FIG9 dataset information. 285
Table 109–US10612627B2__FIG10 dataset information. 286
Table 110–US11199246B2__FIG1 dataset information. 287
Table 111–US11231105B2__FIG2 dataset information. 288
Table 112–US11248699B2__FIG_1 dataset information. 289
Table 113–US11248699B2__FIG_3 dataset information. 290
Table 114–US5599251A__FIG1 dataset information. 291

Table 115–US6422969B1__FIG1 dataset information. 292
Table 116–US6422969B1__FIG3 dataset information. 293
Table 117–US6422969B1__FIG5 dataset information. 294
Table 118–US6422969B1__FIG7 dataset information. 295
Table 119–US6422969B1__FIG9 dataset information. 296
Table 120–US6514170B1__FIG1 dataset information. 297
Table 121–US6514170B1__FIG2 dataset information. 298
Table 122–US6514170B1__FIG3 dataset information. 299
Table 123–US6514170B1__FIG4 dataset information. 300
Table 124–US6514170B1__FIG5 dataset information. 301
Table 125–US6514170B1__FIG6 dataset information. 302
Table 126–US6514170B1__FIG7 dataset information. 303
Table 127–US6514170B1__FIG8 dataset information. 304
Table 128–US6514170B1__FIG9 dataset information. 305
Table 129–US6514170B1__FIG10 dataset information. 306
Table 130–US6514170B1__FIG11 dataset information. 307
Table 131–US6514170B1__FIG12 dataset information. 308
Table 132–US6530858B1__FIG1 dataset information. 309
Table 133–US6530858B1__FIG3 dataset information. 310
Table 134–US6530858B1__FIG5 dataset information. 311
Table 135–US6530858B1__FIG7 dataset information. 312
Table 136–US6530858B1__FIG9 dataset information. 313
Table 137–US6530858B1__FIG11 dataset information. 314
Table 138–US6530858B1__FIG13 dataset information. 315
Table 139–US6530858B1__FIG15 dataset information. 316
Table 140–US6530858B1__FIG17 dataset information. 317
Table 141–US6530858B1__FIG19 dataset information. 318
Table 142–US6530858B1__FIG21 dataset information. 319
Table 143–US6530858B1__FIG23 dataset information. 320
Table 144–US6530858B1__FIG25 dataset information. 321
Table 145–US6595892B2__FIG1 dataset information. 322
Table 146–US6595892B2__FIG3 dataset information. 323
Table 147–US6595892B2__FIG5 dataset information. 324
Table 148–US6595892B2__FIG7 dataset information. 325
Table 149–US6595892B2__FIG9 dataset information. 326
Table 150–US6595892B2__FIG11 dataset information. 327
Table 151–US6595892B2__FIG13 dataset information. 328
Table 152–US6595892B2__FIG15 dataset information. 329
Table 153–US6595892B2__FIG17 dataset information. 330

Table 154–US6595892B2__FIG19 dataset information. 331
Table 155–US6595892B2__FIG21 dataset information. 332
Table 156–US6595892B2__FIG23 dataset information. 333
Table 157–US6595892B2__FIG25 dataset information. 334
Table 158–US6595892B2__FIG27 dataset information. 335
Table 159–US6623398B2__FIG1 dataset information. 336
Table 160–US6623398B2__FIG3 dataset information. 337
Table 161–US6623398B2__FIG5 dataset information. 338
Table 162–US6623398B2__FIG7 dataset information. 339
Table 163–US6623398B2__FIG9 dataset information. 340
Table 164–US6623398B2__FIG11 dataset information. 341
Table 165–US6623398B2__FIG13 dataset information. 342
Table 166–US6623398B2__FIG15 dataset information. 343
Table 167–US6623398B2__FIG17 dataset information. 344
Table 168–US6623398B2__FIG19 dataset information. 345
Table 169–US6705967B2__FIG1 dataset information. 346
Table 170–US6705967B2__FIG3 dataset information. 347
Table 171–US6705967B2__FIG5 dataset information. 348
Table 172–US6705967B2__FIG7 dataset information. 349
Table 173–US6705967B2__FIG9 dataset information. 350
Table 174–US6705967B2__FIG11 dataset information. 351
Table 175–US6705967B2__FIG13 dataset information. 352
Table 176–US6705967B2__FIG15 dataset information. 353
Table 177–US6705967B2__FIG17 dataset information. 354
Table 178–US6705967B2__FIG19 dataset information. 355
Table 179–US6705967B2__FIG21 dataset information. 356
Table 180–US6705967B2__FIG23 dataset information. 357
Table 181–US6705967B2__FIG25 dataset information. 358
Table 182–US6705967B2__FIG27 dataset information. 359
Table 183–US6705967B2__FIG29 dataset information. 360
Table 184–US6705967B2__FIG31 dataset information. 361
Table 185–US6705967B2__FIG33 dataset information. 362
Table 186–US7621841B2__FIG1 dataset information. 363
Table 187–US7621841B2__FIG4 dataset information. 364
Table 188–US7621841B2__FIG5 dataset information. 365
Table 189–US7628726B2__FIG1 dataset information. 366
Table 190–US7967716B2__FIG2 dataset information. 367
Table 191–US7985160B2__FIG1 dataset information. 368
Table 192–US8012059B2__FIG1 dataset information. 369

Table 193–US8029405B2__FIG1 dataset information. 370
Table 194–US8029405B2__FIG4 dataset information. 371
Table 195–US8029405B2__FIG5 dataset information. 372
Table 196–US8123650B2__FIG1 dataset information. 373
Table 197–US8202192B2__FIG1 dataset information. 374
Table 198–US8506443B2__FIG1 dataset information. 375
Table 199–US8597153B2__FIG1 dataset information. 376
Table 200–US8597153B2__FIG4 dataset information. 377
Table 201–US8657718B2__FIG1 dataset information. 378
Table 202–US8663055B2__FIG1 dataset information. 379
Table 203–US8678973B2__FIG1 dataset information. 380
Table 204–US8992374B2__FIG1 dataset information. 381
Table 205–US8992374B2__FIG5 dataset information. 382
Table 206–US9587716B1__FIG1 dataset information. 383
Table 207–US9726262B1__FIG1 dataset information. 384
Table 208–US9841085B2__FIG1 dataset information. 385
Table 209–DE10140424A1__6HP dataset information. 386
Table 210–ZF__8HP dataset information. 387
Table 211–US8398522B2__9HP dataset information. 388

LIST OF ABBREVIATIONS AND ACRONYMS

A	arm (planet carrier)
AMT	automated mechanical transmission
AT	automatic transmission
B	brake
C	clutch
CL	compound link
CVT	continuously variable transmission
DBG	double bicolor graph
DCT	dual clutch transmission
DOF	degrees-of-freedom
DPGS	double planetary gear set
EDA	exploratory data analysis
EGT	epicyclic gear train
EM	electric motors
EV	electric-powered vehicle
F	frame or fixed link (housing)
FS	feature selection
ICE	internal combustion engine
IN	input shaft or link
KC	kinematic chain
MT	manual transmission
OUT	output shaft or link
OWC	one-way clutch
P	planet gear
PGM	planetary gear mechanism
PGS	planetary gear set
PGT	planetary gear train
PR	outer planet
PS	inner planet
R	ring gear
RF	random forest
RFE	recursive feature elimination
S	sun gear
SC	shift coupling
SPGS	simple planetary gear set
SVM	support vector machine
TCM	transmission control module

CONTENTS

1	**INTRODUCTION**	**33**
1.1	THESIS OBJECTIVES	41
1.2	METHODOLOGY APPROACH	41
1.3	CONTRIBUTION AND EXPECTED OUTCOMES	42
1.4	THESIS OUTLINE	43
2	**REVIEW OF AUTOMOTIVE PLANETARY GEAR TRAINS**	**45**
2.1	AT OVERVIEW	45
2.1.1	**AT Functional Requirements**	**46**
2.1.1.1	*Gear ratios*	*47*
2.2	MECHANISM AND MACHINE SCIENCE REVIEW FOR PGTS	51
2.2.1	**Concepts and Definitions**	**51**
2.3	PLANETARY GEAR MECHANISM (PGM)	53
2.3.1	**Graph representations**	**59**
2.3.2	**Structural Analysis**	**63**
2.3.2.1	*Mobility Equation*	*63*
2.3.2.2	*Link Assortments*	*65*
2.3.2.3	*Structural Characteristics of PGTs*	*66*
2.3.2.4	*Isomorphism in PGTs*	*68*
2.4	PGT DESIGN	69
2.4.1	**PGM Structural Synthesis**	**71**
2.4.1.1	*PGM Atlas-based Methodologies*	*71*
2.4.1.2	*PGM Abstraction-based Methodologies*	*72*
2.4.2	**Design specifications**	**76**
2.5	CHAPTER HIGHLIGHTS	79
3	**PGM MODELING REVISED AND NEW METRICS**	**80**
3.1	REVISION OF THE PGM GRAPH MODEL	80
3.1.1	**PGM Case Studies**	**81**
3.1.1.1	*Case 1: Simple PGT with 2 brakes*	*81*
3.1.1.2	*Case 2: Simple PGT with 2 brakes and 1 clutch*	*82*
3.1.1.3	*Case 3: Simple PGT with 2 brakes, 2 clutches and output link*	*84*
3.1.1.4	*Case 4: GM 6-speed automatic transmission*	*85*
3.1.2	**Definition of Redundant Joints j_Q and Virtual Joints j_V in PGMs**	**87**
3.1.3	**A Revised Mobility Equation for PGMs**	**88**
3.1.4	**Mobility Review of the Case Studies**	**89**
3.1.4.1	*Case 1: $j_Q = j_V = 0$*	*89*
3.1.4.2	*Case 2: $j_Q = 1$*	*89*
3.1.4.3	*Case 3: $j_Q = 2$*	*89*

3.1.4.4 *Case 4: $j_Q = 2$ and $j_V = 1$* . . . *89*
3.1.5 **Mobility Discussions and Contributions for PGMs** . . . **90**
3.2 PGM: COMPLEXITY AND CAPABILITY . . . 91
3.2.1 **PGM Structural Complexity Metric** . . . **92**
3.2.1.1 *PGM Link Complexity (Cx_1)* . . . *93*
3.2.1.2 *PGM Coupling Complexity (Cx_2)* . . . *95*
3.2.1.3 *PGM Topological Complexity (Cx_3)* . . . *97*
3.2.2 **PGM Capability Metric** . . . **97**
3.2.2.1 *PGM Performance metric (Ca_1)* . . . *98*
3.2.2.2 *PGM Actuation Efficiency metric (Ca_2)* . . . *98*
3.3 CHAPTER HIGHLIGHTS . . . 98
4 PROCESS FOR DISCOVERING INNOVATIVE GAPS IN MECHANISMS DATABASE . . . **100**
4.1 REVIEW OF KNOWLEDGE DISCOVERY IN DATABASES (KDD) . . . 101
4.2 PHASE 1: MECHANISM SURVEY . . . 103
4.2.1 **Study Goals** . . . **104**
4.2.2 **Data Collection** . . . **104**
4.2.2.1 *Patent Search* . . . *104*
4.2.2.2 *Academic and Industry Search* . . . *106*
4.2.3 **Datasets Creation** . . . **107**
4.2.4 **Raw Datasets** . . . **108**
4.3 PHASE 2: DATA ENRICHMENT . . . 108
4.3.1 **Features Diversification** . . . **109**
4.3.1.1 *Local features* . . . *109*
4.3.1.2 *Global features* . . . *111*
4.3.2 **Dictionary of Features** . . . **112**
4.3.3 **Data Evaluation** . . . **113**
4.3.4 **Database** . . . **114**
4.4 PHASE 3: FEATURE ANALYSIS . . . 114
4.4.1 **Data Cleansing** . . . **115**
4.4.2 **Data Insights** . . . **116**
4.4.3 **Strategic Analysis** . . . **117**
4.4.4 **Feature Selection** . . . **118**
4.5 PHASE 4: GAP DISCOVERY . . . 122
4.5.1 **Gap Search** . . . **123**
4.5.2 **Gap Analysis** . . . **124**
4.5.3 **Gap Clustering** . . . **124**
4.5.4 **Innovation Sets** . . . **125**
5 PROCESS APPLICATION IN AUTOMOTIVE PGMS DATABASE . . . **126**

5.1 APPLICATION: AUTOMOTIVE PGMS FOR PASSENGER CARS . . 126
5.2 PHASE 1: MECHANISM SURVEY - PGMS 126
5.2.1 Step 1. Study Goals 126
5.2.2 Step 2. Data Collection 127
5.2.3 Step 3. Dataset Creation 131
5.2.4 Step 4. Raw Datasets 137
5.3 PHASE 2: DATA ENRICHMENT - PGMS 137
5.3.1 Step 1. Features Diversification 137
5.3.2 Step 2 and 3. Dictionary of Features and Data Evaluation 138
5.3.3 Step 4. Database 146
5.4 PHASE 3: FEATURE ANALYSIS - PGMS 146
5.4.1 Step 1. Data Cleansing 146
5.4.2 Step 2. Data Insights 149
5.4.3 Step 3. Strategic Analysis 151
5.4.3.1 Links Analysis 152
5.4.3.2 PGSs Sequence Arrangement Analysis 153
5.4.3.3 Complexity Analysis 154
5.4.3.4 Technological Boundary Map for PGMs 159
5.4.4 Step 4. Feature Selection 160
5.5 PHASE 4: GAP DISCOVERY - PGMS 164
5.5.1 Step 1. Gap Search 164
5.5.2 Step 2. Gap Analysis 169
5.5.3 Step 3. Gap Clustering 173
5.5.4 Step 4. Innovation Sets 175
6 PGMS DESIGN USING INNOVATION SETS 178
6.1 SYNTHESIS PROCESS 178
7 CONCLUSIONS AND FUTURE WORK 193
7.1 ANALYSIS OF OBJECTIVE ATTAINMENT 193
7.2 SCIENTIFIC CONTRIBUTIONS 194
7.3 CHALLENGES AND LIMITATIONS 195
7.4 FUTURE WORK 196
References 198
APPENDIX A – PLANETARY GEAR MECHANISMS DATABASE . 219
A.1 PGM DATASET TEMPLATE 219
A.2 PGM COMPLETE DATABASE 228
APPENDIX B – VISUAL RESULTS FROM THE PROCESS APPLICATION 389
B.1 RESULTS OF UNIVARIATE DATA ANALYSIS 389
B.1.1 Features Distribution Segmented by *FWD GEARS* 390

B.1.2 Features Distribution Segmented by *PGSs Total* **406**
B.1.3 Features Distribution Segmented by *Commercial?* **421**
B.1.4 Univariate Normality Results **435**
B.2 RESULTS OF BIVARIATE DATA ANALYSIS 460
B.2.1 Perfectly Correlated Features **479**
B.2.2 Highly Correlated Features **479**
B.3 RESULTS OF LINK ANALYSIS 492
B.3.1 Frame (F) Link Results **493**
B.3.2 Input (IN) Link Results **498**
B.3.3 Output (OUT) Link Results **503**
B.4 RESULTS OF FEATURE SELECTION 508

1 INTRODUCTION

Automotive transmissions are essential in optimizing vehicle performance by addressing requirements imposed by the limitations of both internal combustion engines (ICEs) and electric motors (EMs). These needs include power transfer from the engine to the wheels, torque conversion during startup, power distribution at different speeds, fuel efficiency optimization, and adaptability to different power sources.

Despite the growing presence of electric-powered vehicles (EVs) in the automotive market, ICE vehicles will remain dominant in the foreseeable future (ZHANG; MI, 2018). This is primarily due to existing challenges in the development of key electric vehicle technologies, such as battery energy density, durability, and charging time, as well as the lack of necessary infrastructure for widespread electric vehicle adoption.

In 2022, according to ANFAVEA (2023), the estimated fleet of automobiles (passenger vehicles) in Brazil was approximately 38 million, being only 129,000 electric vehicles, representing 0.3% of the total. Despite the high expectations of transitioning towards electrification, 35% of global market share in 2030 according to IEA (2023), the combustion engine vehicle market remains significantly larger, providing opportunities to address challenges related to the limitations of ICE in terms of performance and emissions.

Currently, there are five mainstream transmission types for ICE passenger vehicles: manual transmission (MT), automated mechanical transmission (AMT), automatic transmission (AT), dual clutch transmission (DCT), and continuously variable transmission (CVT). A brief summary of each type is described below based on Naunheimer et al. (2011), Fischer et al. (2015), Zhang and Mi (2018) and Chen (2021).

Manual transmission (MT) is a mechanical transmission that enables manual gear shifting, providing variable speed ratios. It offers high transmission efficiency, torque transfer, and a simple structure. MT is commonly utilized in smaller vehicles and some sport cars, typically available in 5 or 6-speed variants. Recent MT advancements include compact designs with improved synchronizers and advanced lubricants. Although MTs are popular in Europe and emerging markets, ATs are gaining traction due to their improved fuel economy and reduced costs. As environmental standards rise, automated powertrains may become mandatory in some markets due to their efficiency and reduced emissions (FOLKSON; SAPSFORD, 2022). Figure 1 provides an example of a 6-speed manual transmission utilized by Mercedes-Benz in their C-Class passenger vehicles during the 2000s.

Automated mechanical transmission (AMT) utilizes electronic control, hydraulic, or electric actuation systems to automate clutch engagement, gear selection, and shifting. AMT offers high transmission efficiency, ease of manufacturing, and cost-effectiveness. It is predominantly employed in mini and small cars but has limited

Figure 1 – 6-speed manual transmission (MT) for passenger cars Mercedes-Benz SG6-300.

(a) Two-stage 6-speed MT

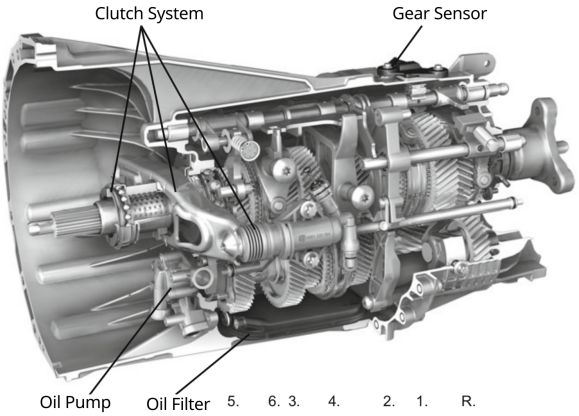

(b) MT diagram

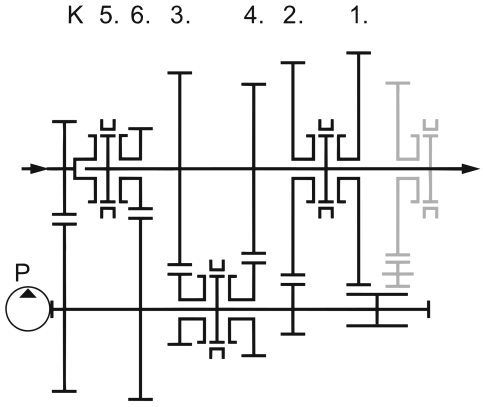

Source: Naunheimer et al. (2019).

potential for larger models due to power failure during shifts. AMT includes electrically controlled hydraulic AMT (with an electrohydraulic actuator) and electrically driven AMT, with the latter featuring a simpler structure, improved reliability, and lower cost, representing the mainstream trend in AMT development. Figure 2 shows an example of a 7-speed automated manual transmission utilized by BMW in M5 and M6 models of passenger vehicles since 2005.

Figure 2 – 7-speed automated manual transmission (AMT) for passenger cars Getrag 247.

(a) Two-stage 7-speed AMT

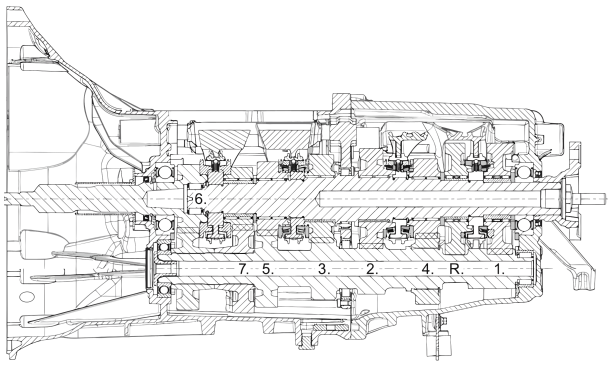

(b) AMT diagram

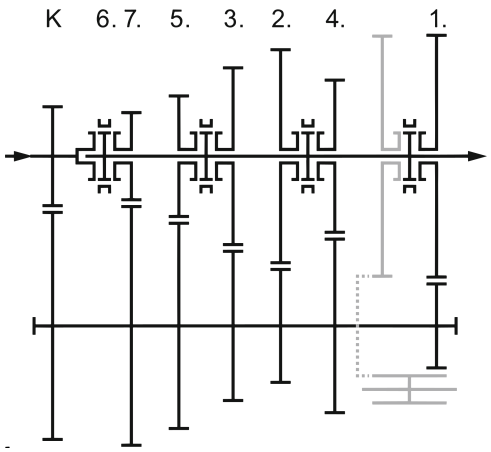

Source: Naunheimer et al. (2019).

Automatic transmission (AT) allows for the automatic shifting of gears without requiring driver input. The hydraulic automatic transmission is the most common type and operates using a combination of a planetary gear train (PGT), hydraulic controls, and a torque converter. Until the turn of the century, 4-speed ATs were popular in small cars despite reduced comfort and economy. Currently, six-speed ATs are stan-

dard equipment across the industry, and luxury brands use 7-speed and 8-speed ATs for improved performance and efficiency (ZHANG; MI, 2018). Advanced options like 9-speed and 10-speed AT have been successfully developed by automotive companies like Daimler (DÖRR et al., 2014), ZF (GAERTNER; EBENHOCH, 2013), Aisin (SUZUKI et al., 2017), and GM (MARTIN; HENDRICKSON, 2018), among others. Figure 3 showcases an example of a 9-speed automatic transmission utilized by Mercedes-Benz in several passenger car models such as the C, E, S, GL, and AMG Classes. Additionally, Nissan and Infiniti's top level vehicles have also been granted permission to use this transmission (HENRY, 2015).

Figure 3 – 9-speed automatic transmission (AT) for passenger cars Mercedes-Benz 9G-Tronic.

(a) Planetary 9-speed AT

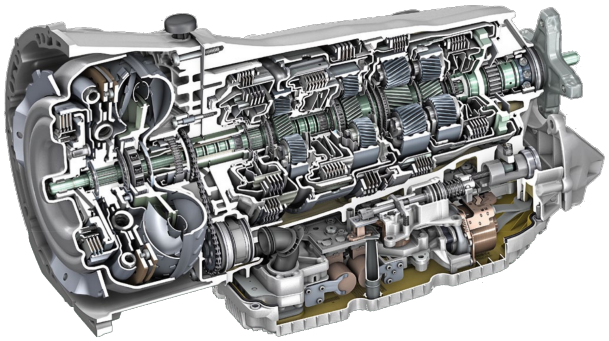

(b) AT diagram

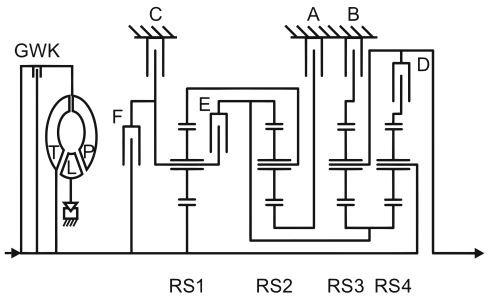

Source: (a) Dörr et al. (2014), and (b) Naunheimer et al. (2019).

Dual clutch transmission (DCT) arranges transmission gears on two input shafts connected with two clutches, combining the advantages of AT and AMT. It delivers high transmission efficiency, simplicity, and cost-effectiveness. DCT is classified into dry DCT (DDCT) and wet DCT (WDCT). Electric DDCT, featuring a simple and reliable structure, is expected to become the mainstream choice for small to medium torque transmissions, while WDCT, with a high carrying capacity, is suitable for application in intermediate and higher-class vehicles (CHEN, 2021). Figure 4 shows an example of a 7-speed dual clutch transmission introduced in 2008 by Volkswagen and utilized in all models from the Polo to the Arteon (VOLKSWAGEN, 2023). Manufacturers such as BMW believe that the 8-speed planetary AT can perform as well as a DCT in performance vehicles with the right software and calibration (MARSHALL, 2022).

Continuously variable transmission (CVT) optimizes engine and powertrain performance for smooth operation, enhanced safety, and improved emissions. Launch devices include torque converters and clutches, with a planetary gear set providing a reverse gear. Park lock is common. Two common types of CVTs are metal pushing V-belt and chain CVT. Metal pushing V-belt CVT offers unparalleled comfort but requires cost and maintenance improvements, while chain CVT has higher transmission efficiency and a compact structure but may produce some noise. Figure 5 provides an example

Figure 4 – 7-speed dual clutch transmission (DCT) for passenger cars Volkswagen DQ200-7F.

(a) 3.5 stage 7-speed DCT

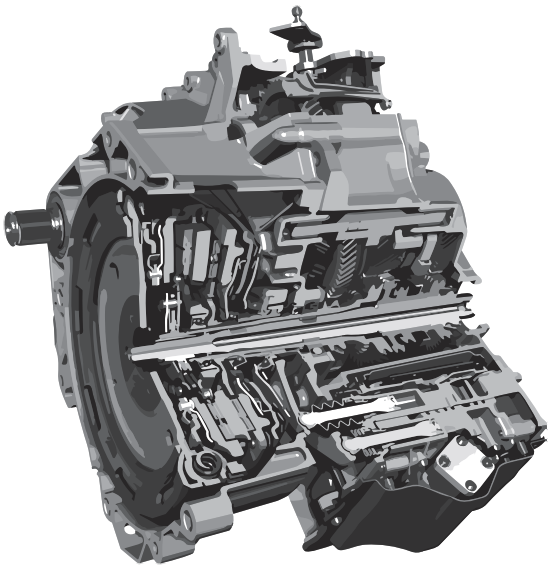

(b) DCT diagram

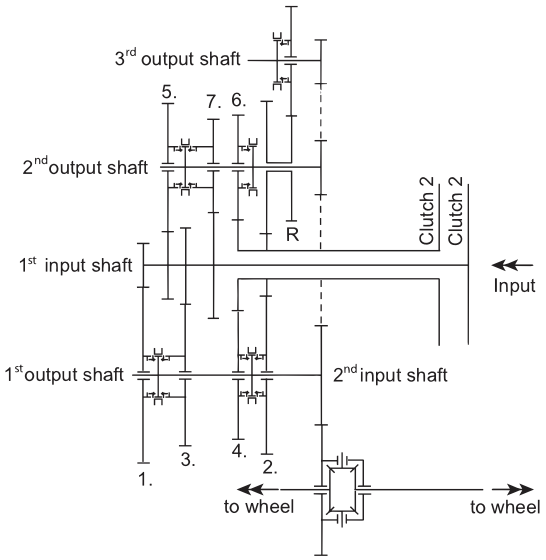

Source: Fischer et al. (2015).

of Audi Multitronic CVT utilized in passenger cars such as A4, A5, A6 and A7 models up to 2014 (DEGASPERI, 2014).

Figure 5 – Continuously variable transmission (CVT) for passenger cars Audi Multitronic.

(a) Audi Multitronic CVT

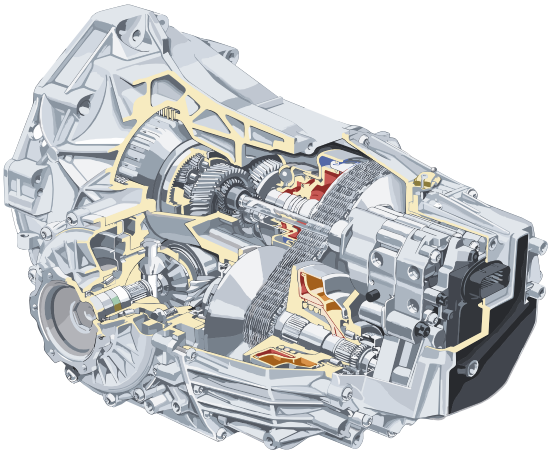

(b) CVT diagram

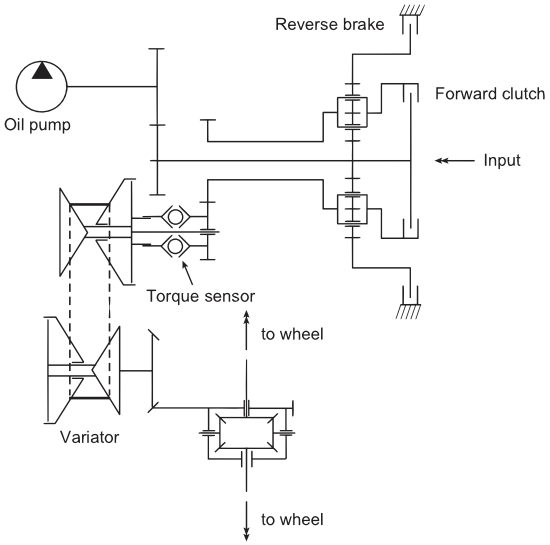

Source: Fischer et al. (2015).

A comparative analysis of the five main transmission types can be seen in Tab. 1.

Additionally, there is a projected substantial increase in the utilization of hybrid

Table 1 – Mainstream transmissions comparison.

TYPE	**MT**	**AMT**	**AT**	**DCT**	**CVT**
Operation	manual	automatic	automatic	automatic	automatic
Torque	▲	▲	▲	▲	▼
Efficiency	▲	▲	▼	▲	▼
Comfort	▼	●	▲	▲	★
Shifting	▼	▼	▲	▲	★
Reliability	▲	▼	▲	●	●
Economy	▲	▲	▼	●	●
Emissions	●	●	●	▲	▲
Durability	★	●	●	●	▼
Cost	★	●	▼	▼	▼
Scope	▲Power ▲Cost	▲Power ▲Cost	▲Power ▼Cost	▲Power ▼Cost	▼Power ▼Cost

Legend: Best (★), Good (▲), Average (●), Bad (▼)

Source: Author based on Chen (2021).

transmissions (HT), driven by the expanding market share of hybrid electric vehicles (HEV) and battery electric vehicles (BEV). This shift towards hybrid transmissions aligns with evolving consumer demands and industry trends in the automotive sector. Figure 6 shows an example of a two-mode dedicated hybrid transmission (DHT) developed in cooperation by BMW, Chrysler, Daimler, and General Motors in 2009. The ML 450 HYBRID from Mercedes used this technology, which integrated two EMs into the housing as permanently excited synchronous machines (NAUNHEIMER et al., 2019).

Figure 6 – Hybrid transmission for passenger cars BMW/Chrysler/Daimler/GM.

(a) Two-mode DHT

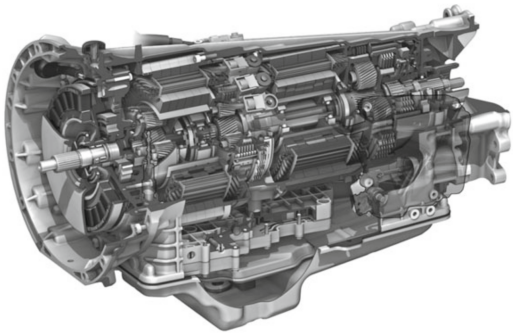

(b) DHT diagram

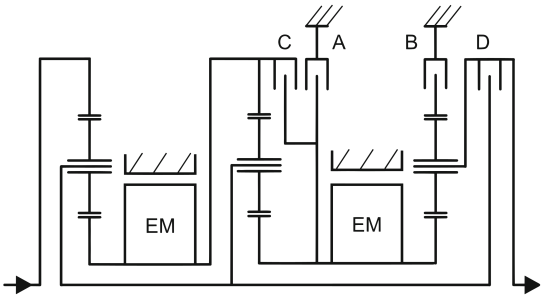

Source: Naunheimer et al. (2019).

This research focuses on the topology of PGT's automatic transmissions, a complex yet critical component of modern automotive transmissions. The ATs have gained significant importance in the automotive industry since the 19th century, as highlighted in Naunheimer et al. (2019). In 1834, Bodmer designed a partially power-shiftable

planetary gear (Fig. 7), followed by H. Rieseler in 1925, who designed an automatic transmission with a torque converter and rear-mounted planetary transmission. The essential components of Rieseler's transmission, such as the torque converter, planetary gear, and shifting mechanisms, became the foundation for conventional automatic transmission systems as found these days. The General Motors Hydramatic, introduced in 1939, marked the first mass-produced automatic transmission, rapidly gaining popularity in the USA after World War II. In Europe, automatic transmissions had a lower market share until German manufacturers like Borgward, Daimler-Benz, and ZF developed their own designs in the 1950s and 1960s. Over time, automatic transmissions underwent continuous development for fuel efficiency, with electronic-hydraulic control units becoming the standard in the mid-1990s.

Figure 7 – Shiftable planetary gear transmission in 1834.

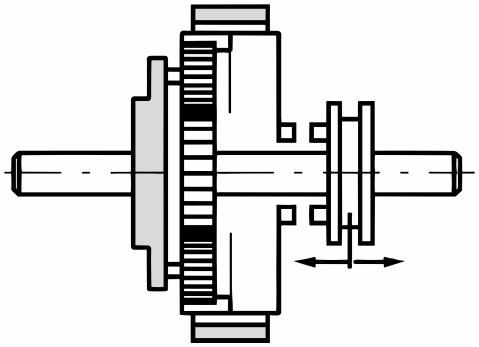

Source: Naunheimer et al. (2019).

Advancements include slip-controlled torque converter lock-up clutches, transmissions with up to 10 speeds for improved gear ratio adaptation, and the reintroduction of claw shift elements in 2013 to reduce drag losses. At the moment, according to Chen (2021), ATs are found in 4 up to 10 speeds. Smaller or older cars usually carry 4-speed ATs, which has poor comfort and economy. 5-speed ATs are slightly better but has an abrupt shift and limited late development space. 6-speed ATs are the mainstream for modern small, compact, and middle-sized vehicles. High-end models have 7 or 8-speed ATs, while larger vehicles have 9 or 10-speeds ATs. Increasing the number of ratios allows for optimum engine conditions, but frequent shifting has disadvantages, including higher energy consumption in the hydraulic shift system and a poor driver experience referred to as 'shift busyness' (FOLKSON; SAPSFORD, 2022).

The PGT technological advancements in automotive transmissions boasted several advantages, including a wide range of motion states, a compact design, high power density, improved efficiency, and seamless shifting. PGTs typically consist of a hydrodynamic torque converter in combination with planetary gear sets (PGS), enabling the power transmission through gear clutches and gear rolling to achieve a high number

of gear ratios. The electronic control system is essential in operating the brakes and clutches through electrohydraulic valves, ensuring smooth and efficient shifting.

Xu et al. (2018) offers an insightful review of the progress in automotive transmission technology. This includes the development of new transmission schemes assisted by computer-aided programs, optimization of transmission parameters, and a shift towards electrification in the industry. The challenges highlighted encompass optimizing speed numbers, determining the appropriate number of degrees-of-freedom (DOF), and enhancing mechanical and hydraulic systems, among others.

In the innovation field concerning automotive ATs, the topological structure of PGTs stands out as the central area of interest. The design complexities of these mechanisms dictate key transmission specifications, including the number of gears and their sequential arrangement during shifting. Yet, the design process for new PGTs is intricate, requiring a blend of creativity and technical skills to address specific engineering challenges within set constraints.

Historically, reliance on designers' intuition and experience in early design phases can occasionally result in suboptimal outcomes, potentially limiting innovation (TSAI, 2001). The conceptual phase, where mechanisms are designed, is particularly challenging due to its requirement for creativity and knowledge (YAN, 1992). According to Ding et al. (2013), traditional methods for mechanism design are time-consuming and have limitations in conceiving all possible kinematic structures. As a result, deriving the optimal solution for the design task becomes challenging, if not impossible.

In the literature, two main approaches for mechanism design have been identified (FREUDENSTEIN; MAKI, 1979). The atlases-based methodologies involve designing from a library of elementary mechanisms grouped according to their function. While these methodologies are relatively easier to analyze and design, they have limitations in terms of the number of possible solutions due to structural constraints and restrictions (KOTA; CHIOU, 1992; SUBRAMANIAN; WANG, 1995; OU et al., 2010; TSAI et al., 2010; HE; HUANG, 2016; HU et al., 2017). On the other hand, the abstraction-based methodologies involve designing based on structural characteristics derived from abstract representations of mechanisms, such as equations, matrices, and graphs (HARTENBERG; DENAVIT, 1964; FREUDENSTEIN; MAKI, 1979; CHATTERJEE; TSAI, 1994; YAN, 1998; MURAI, 2019; DING, 2015). This approach offer more numerous and detailed solutions with greater potential for innovation compared to atlases-based approaches, but they can be more time-consuming and challenging to visualize in early stages (YAN, 1998).

An undeniable challenge in mechanism design is the precise identification of key requirements and parameters driving the creation of new mechanisms, while minimizing the time spent on non-viable solutions. This becomes particularly crucial in abstraction-based methodologies, where the high level of abstraction makes it challenging for

designers to identify parameters significantly affecting design and performance of the mechanisms.

Researchers and designers frequently turn to diverse information sources to improve mechanism design processes, with patents being a particularly valuable repository of technological insights (WIPO, 2015; ARISTODEMOU; TIETZE, 2018). Comprehensive patent analyses can reveal existing solutions and highlight potential design innovations (HOELTGEBAUM et al., 2016a; MARTINS et al., 2018; OLIVEIRA E COSTA et al., 2018). Ding and Cai (2019) further emphasized the essence of patent analyses by conducting an in-depth examination of PGTs in 673 ATs. Their research accentuated the necessity to comprehend the structural attributes of PGTs to augment AT performance and instigate innovation. Notably, the study addressed the pseudo-isomorphism challenge, paving the way for the development of novel PGT configurations, and unearthed important challenges for future works, encompassing the efficient synthesis of PGT configurations and the optimization of AT design processes. However, the study's primary focus remained on basic mechanism characteristics, such as the number of links, degrees of freedom, and link assortments.

Several methods involve patent in engineering design, including TRIZ, design-by-analogy, concept-knowledge (C-K) theory, and genetic algorithms (ALTSHULLER et al., 1999; JEONG; KIM, 2014; FELK et al., 2011; KOZA et al., 2004). Hoeltgebaum et al. (2016b) introduced a patent survey methodology specifically tailored for automotive mechanisms, such as gear trains and suspensions. This methodology delineates a structured six-step process, encompassing preliminary searches, meticulous analysis, and the classification of key mechanisms. This approach is significantly dependent on the designer's subjective analysis and might overlook essential design characteristics. The resulting narrowing of technological mapping may unintentionally exclude critical information necessary for innovative solutions.

Despite the extensive research on the subject of automotive planetary gear trains, it is evident that there are still significant gaps and challenges that can be improved.

While the potential of patent research in revealing valuable insights is recognized, current methodologies appear to possess limitations. Specifically, the designer's limited capacity to deal with a large and diverse number of mechanism characteristics reduces the possibility of delving deeper into the inherent potential of these surveys (CHEN, 2021). Such restrictions prevent accessing less trivial patterns of mechanism characteristics that may have the potential for innovation. Moreover, the current landscape lacks a holistic and comprehensive process to support the designer, emphasizing the opportunity to improve methodologies.

Discovering innovative requirements for designing new automotive planetary transmissions includes the need for a systematic approach to innovation, determining relevant parameters and characteristics for evaluation, and identifying gaps with

potential for innovation in the topology of the mechanisms.

1.1 THESIS OBJECTIVES

This thesis aims to **develop a systematic process for identifying potential innovative gaps within the design requirements of automotive planetary gear train mechanisms in a comprehensive and diverse database**. The central research question guiding this work is: *How can an extensive and diverse database support the discovery of potential innovative gaps in automotive planetary gear train designs?*

During the study of different automotive transmission mechanisms, it was determined that existing graph-based representations and the general mobility equation are limited solely on kinematic chain analysis, making the comprehensive study unfeasible. Therefore, an additional objective of this thesis is to **present a framework for the comparative analysis of complete PGT mechanisms**. This framework encompasses the *concepts of redundant and virtual joints* within the graph representation, a *revised form of the general mobility equation*, and *metrics for assessing structural complexity and functional capabilities*.

To accomplish the primary objective, the research is decomposed into specific objectives, each serving as a systematic step towards the overall goal:

1. To investigate analysis and synthesis processes in automotive planetary gear trains to identify diverse evaluation features.
2. To construct a structured database centered on automotive ATs based on planetary gear trains, analyzing inherent mechanism features.
3. To establish a systematic approach to identify relevant features in synthesizing automotive planetary gear trains.
4. To develop an analysis method for discovering innovative gaps in the design requirements of automotive planetary gear trains.
5. To implement the process in a case study to analyze results and extract insights for innovation in automotive AT design.

1.2 METHODOLOGY APPROACH

The process proposed in this research integrates multidisciplinary concepts — including analysis of design requirements, mechanism and machine science, patent analysis and graph theory — with advanced *data science* methods, such as data mining and feature selection. The process is systematically structured into four sequential phases, each comprising four distinct steps. Its framework was intentionally designed to broaden the scope of mechanism analysis, capturing non-trivial features often not considered in conventional designs. The first phase is *Mechanism Survey*, where a

comprehensive study brings together relevant data and information from mechanisms in patent, academic and industrial sources. The second phase is *Data Enrichment*, in which a diverse dictionary of features is created to characterize the mechanisms and complete the database construction. The third phase is *Feature Analysis*, when the mechanisms and features of the database are revised for their integrity, evaluated statistically and strategically, and the most relevant features for the design of the mechanisms are selected. The fourth phase is *Gap Discovery*, comprising scanning the most relevant features for discovering gaps in data, which are then prioritized, combined into *clusters* and, the most promising, are selected as potential innovation sets that can be used as requirements for the design of new mechanisms.

Although this study is focused on automotive transmissions, the process was proposed to cover mechanism designs in general.

1.3 CONTRIBUTION AND EXPECTED OUTCOMES

This thesis contributes to the fields of analysis and synthesis of automatic automotive transmissions, specifically focusing on defining potential innovative design requirements for the topology of planetary gear train mechanisms. It is introduced new equations for the characterization of PGTs and a systematic process for database investigation and requirement discovery that has the potential for innovation in the synthesis of new automotive transmissions, with potential extensions to other types of mechanisms.

By conducting extensive and diverse analysis of features involved in the analysis and synthesis process, it is expected to identify characteristics that are often overlooked in traditional design processes. To the best of the author's knowledge, the process introduced in this thesis is the first to incorporate data mining techniques for discovery of potential innovative design requirements in automatic automotive transmissions based on planetary gear trains.

The main contributions of this thesis are summarized below, organized by their level of relevance:

1. **Novel Concepts of Redundant and Virtual Joints:** The introduction of innovative concepts for redundant and virtual joints has enabled the enhanced representation of PGT mechanisms in graph form. This advancement facilitates improved modeling and analysis of the complete structure of these mechanisms.
2. **Revised General Mobility Equation:** A refined general mobility equation for calculating the mobility of PGT mechanisms has been proposed. This equation expands the analytical capabilities to encompass complete mechanisms without the need for simplifications.

3. **Novel Structural Complexity and Functional Capability Metrics:** The development of novel concepts for structural complexity and functional capability has paved the way for more comprehensive comparative evaluations of PGT performance. These concepts provide valuable support to designers during the synthesis process.
4. **New Process for Analyzing and Discovering Innovative Gaps in Mechanism Databases:** A systematic process for identifying innovative gaps in mechanism databases has been created. This process opens up avenues for the development of new concepts and technological solutions.
5. **Application of the Proposed Process in a Case Study:** The proposed process for analyzing and discovering innovative gaps was applied in a case study involving 155 automotive transmissions with 6 to 10 speeds. This application resulted in the identification of thirteen innovative sets of attributes with potential for developing new mechanisms.
6. **Synthesis Process Based on Innovative Sets:** Building upon one of the discovered innovative sets of attributes, two potentially innovative automotive transmissions were developed through the synthesis of new planetary gear train mechanisms.
7. **Enriched Database with 186 Attributes:** This thesis has led to the development of a database comprising 155 automotive planetary transmissions enriched with 180 analyzed attributes for each transmission. This comprehensive dataset provides a valuable resource for future research.
8. **Extensive Literature Review:** The thesis presents an extensive review of the literature on automatic automotive transmissions based on planetary gear trains. This review provides a solid foundation for the new concepts, methods, and results presented in the research.

1.4 THESIS OUTLINE

In alignment with the stated objectives, the thesis structure has been organized into chapters as detailed below.

In Chapter 1, an overview of the automotive transmissions landscape is given. The debate surrounding the design of new mechanisms is initiated, with problems and challenges being identified. The main research question of the thesis is introduced, followed by the objectives that have been established to explore, assess, and suggest potential solutions. The anticipated contributions of this work are then delineated.

In Chapter 2, a detailed examination of automatic transmissions that employ planetary gear trains is presented. This encompasses their definitions, types, appli-

cations, structural characteristics, methods of analysis, synthesis, and the challenges linked with PGTs.

In Chapter 3, an in-depth revision of the mobility equation, particularly as it pertains to planetary gear trains with redundant and virtual constraints, is undertaken. Metrics for evaluating the structural complexity and performance capability of the PGTs are also introduced.

In Chapter 4, a novel process for the analysis and synthesis of mechanisms, including planetary gear trains, is introduced. This process is divided into four distinct phases: a survey of mechanisms, data enrichment, feature analysis, and gap discovery. Each phase is presented in detail, aiding in the identification of requirements for potential innovations in mechanism design.

In Chapter 5, a preliminary implementation of the proposed process is applied to the analysis of planetary automatic transmissions ranging from 6 to 10 speeds. Subsequently, the obtained innovations sets and pertinent discussions are presented.

In Chapter 6, a synthesis process based on gaps and innovation sets is presented to design potentially new PGMs.

In Chapter 7, a summary of the achieved objectives and the scientific contributions made is provided. References to pertinent publications, the challenges and restrictions of the thesis, and suggestions for future research directions are also offered.

2 REVIEW OF AUTOMOTIVE PLANETARY GEAR TRAINS

Automatic transmissions consist of mechanisms with complex topologies and necessitate an extensive study to fully mastery their design. This chapter offers a comprehensive analysis of planetary gear train mechanisms, specifically concentrating on the analysis and synthesis of their kinematic structures within the scope of automotive transmission design.

Initially, a comprehensive overview of automatic transmissions is provided, delineating their primary functional requisites. Subsequently, definitions pertinent to mechanism and machine science are reviewed, followed by a detailed analysis of the planetary gear train structure. In conclusion, the principal methodologies applied to these mechanisms are presented, emphasizing the significance of design specifications and requirements specially tailored for planetary gear trains.

2.1 AT OVERVIEW

Automatic transmissions based on planetary gear trains are widely employed in passenger cars. These transmissions consist of a torque converter, an oil pump, a planetary gear train, a set of shift couplings (clutches and brakes), and a shifting controller. This kind of transmission is also known as conventional automatic transmissions (AT). Figure 8 illustrates a typical configuration of automotive AT based on PGTs.

Figure 8 – Configuration of a 3-speed AT based on Simpson PGT.

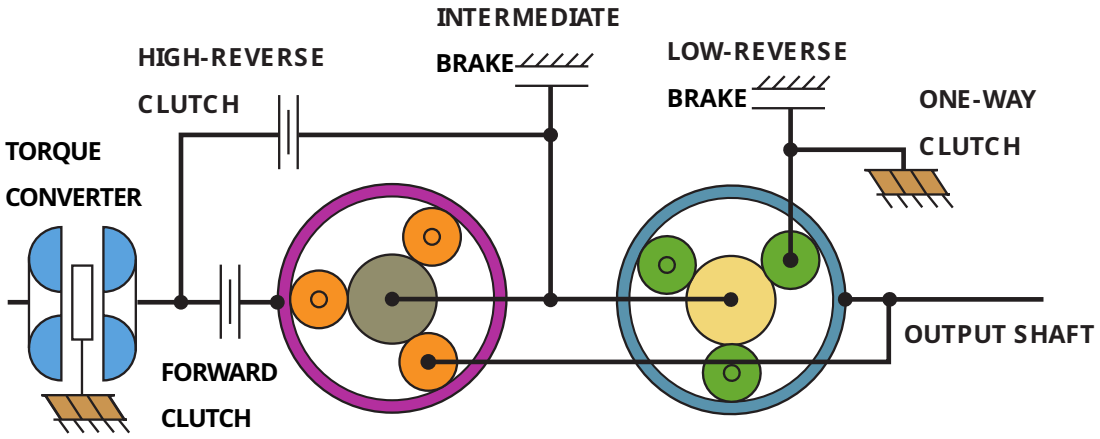

Source: Adapted from Halderman and Birch (2017).

The torque converter works as a fluid coupling between the engine and transmission, enabling torque multiplication during acceleration, smooth vehicle stops without engine stalling, and seamless gear changes while transmitting torque from the engine to the wheels.

Oil pumps are responsible by ensuring a consistent flow and pressure of fluid in the hydraulic circuit of the AT. This is essential for lubricating and cooling moving parts,

supplying fluid to the valve body, and maintaining fluid circulation within the torque converter. The oil pump is directly connected to the engine speed through the torque converter and relies on the operation of the ICE to properly pressurize the fluid.

Shift couplings (SC), also referred to as shifting elements, are used in the design of AT to provide frictional power transfer among internal transmission elements. This enables torque supply between different ratios without interrupting the power flow to the output shaft. Shift quality, particularly shift impact and shift time, holds significant importance in transmission development and calibration (FISCHER et al., 2015). When one element is stationary (housing), it is referred to as a brake (B) or reaction coupling. On the other hand, when both elements are movable, it is referred to as a clutch (C) or coupling clutch. Additionally, one-way clutches (OWCs) allow rotation in one direction while blocking it in the opposite direction, contributing to smoother gear changes during shifting (ZHANG; MI, 2018).

Most modern automatic transmissions incorporate a Transmission Control Module (TCM) to manage their operation. The TCM communicates with the vehicle's Electronic Control Unit (ECU) to ensure proper shift timing and quality. The actuation of each shift coupling is achieved through hydraulically controlled electrovalves (solenoids) contained within a valve body submerged in transmission fluid. The TCM utilizes various sensors such as rotation, pressure, temperature, and position to adapt transmission operation to optimal conditions, a process known as transmission adaptive learning or adaptive control.

While there are various technologies associated with the systems mentioned above in automatic transmissions, their detailed discussion is beyond the scope of this thesis, which focuses on PGTs. For more in-depth understanding of these topics, it is recommended to refer to specific literature (CHEN, 2021; NAUNHEIMER et al., 2019; HALDERMAN; BIRCH, 2017; BOSCH, 2014).

2.1.1 AT Functional Requirements

According to Naunheimer et al. (2011), the main functions of a vehicle transmission are to:

- Enable the vehicle to move-off from rest.
- Adpat power flow by:
  - converting output torque and speed,
  - enabling reverse motion.
- Enable permanent power transmission with minimal loss.
- Control power matching.

The inherent characteristics of PGTs make them an essential component in achieving multiple gear ratios and enabling smooth shifting operations in automatic

transmissions.

To ensure optimal performance and fuel economy, these transmissions must meet specific functional requirements that are summarized as follows (TSAI, 2001):

1. Provide multiple speed ratios, including reverse, by engaging different links within the transmission mechanism.
2. Have a wide overall speed ratio range to accommodate both high-load and low-load operations.
3. Ensure small step ratios between speeds, following an adequate progression for smooth and gradual transitions.
4. Enable single clutch-to-clutch shifts for seamless and uninterrupted gear changes.

In addition to the main functional requirements, there are ancillary requirements that impact the competitiveness of the transmission system (NAUNHEIMER et al., 2011). These include operational reliability, gearbox costs, ease of repair, ease of operation, power matching, efficiency, installation dimensions and weight, customization, and emissions (noise, oil, etc.).

The arrangement of the driving wheels and the engine in the vehicle also exerts an important influence on the transmission design. There are three main configurations according to driving wheels: front-wheel drive (FWD), rear-wheel drive (RWD), and all-wheel drive (AWD). Additionally, the drivetrain can be arranged in two ways based on the relative direction of its main rotating shaft to the wheel axle: transverse (parallel) and longitudinal (perpendicular).

A specific type of transmission commonly used in FWD vehicles and some RWD configurations is the transaxle. It combines the functions of the transmission and a differential into a single integrated unit, simplifying the drivetrain layout and reducing weight. The Fig. 9 illustrates transaxle transmissions in transverse (Fig. 9a) and longitudinal (Fig. 9b) mountings for a front-wheel drivetrain.

The importance of these supplementary requirements can be assessed through a requirements profile, which aids in identifying design and economic goal conflicts and seeking suitable compromises based on assigned weightings.

2.1.1.1 Gear ratios

The gear ratio i_G is the relationship between the input shaft (IN) and the output shaft (OUT) of a transmission as follows:

$$i_G = \frac{n_{IN}}{n_{OUT}} = \frac{T_{OUT}}{T_{IN}} = \frac{Z_{OUT}}{Z_{IN}} \quad , \tag{1}$$

where n denotes speed, T represents torque, and Z indicates the number of teeth on the respective shafts.

Figure 9 – Drivetrain arrangements for a front-wheel driven vehicle.

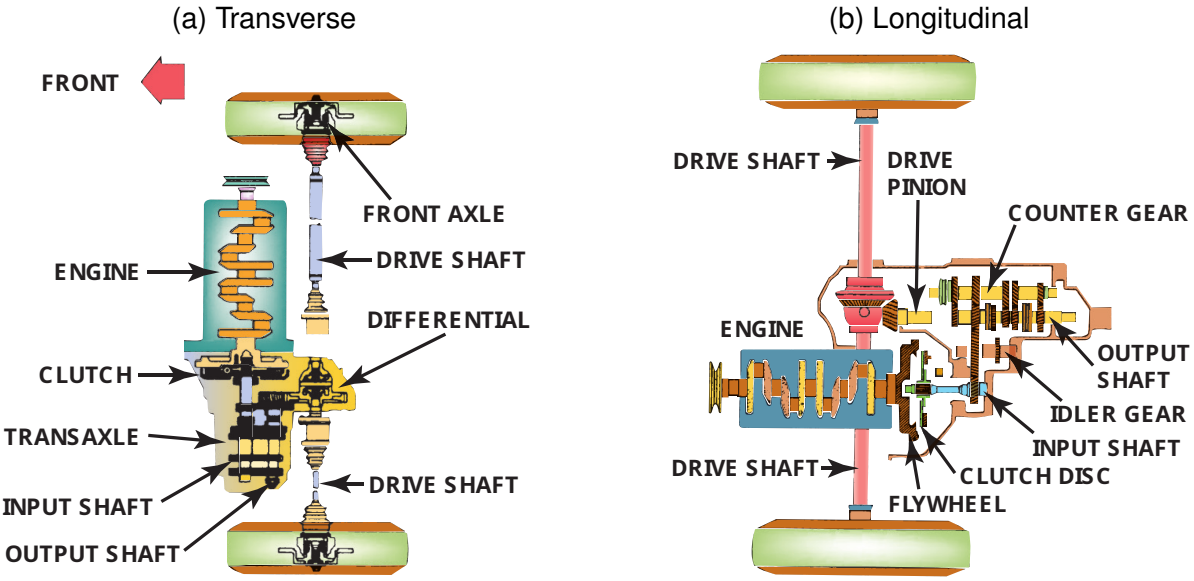

Source: Adapted from Halderman and Birch (2017).

In planetary gear trains, gear ratios are achieved by engaging and disengaging shift couplings to create power flow between the input and output shafts. According to the engaged couplings, these power flow provide the following conditions (Tab. 2):

Table 2 – Gear ratio conditions.

Gear ratio	Condition
$i_G < 0$	Reverse
$i_G = 0$	Neutral
$i_G > 1$	Underdrive (speed reduction)
$i_G = 1$	Direct-drive (1:1)
$0 < i_G < 1$	Overdrive (speed multiplication)

Source: Author.

Specific reduction and multiplication transmission ratios are achieved by varying the number of teeth on the gears. To avoid continuous noise repetition, engineers usually avoid using whole number transmission ratios (e.g., 3:1 or 4:1) in gear pairs and instead apply a margin of approximately 10% (e.g., 3.29:1 or 4.34:1) (HALDERMAN; BIRCH, 2017). In higher gears, overdrive gear ratios ($0 < i_G < 1$) are selected to achieve higher vehicle speeds while keeping the engine speed low, promoting fuel efficiency. The detailed gear ratios for automatic transmissions are discussed in the following sections.

The total powertrain ratio i_A is the relative speed between engine output shaft

and the wheel shaft, and is given by Eq. (2)

$$i_A = i_S \cdot i_G \cdot i_E \quad . \tag{2}$$

Where i_S is the torque converter ratio, i_G is the gear ratio, i_E is the final drive ratio.

As hydrodynamic torque converters convert both rotational speed and torque, their ratio is $i_S \geq 1$.

The final drive ratios i_E can vary depending on factors such as vehicle type, performance requirements, and terrain conditions. Common ranges for different axle drives in passenger cars include approximately 3.0-5.5 for spur gear axle drive, 2.5-5.0 for bevel gear axle drive, and 5.0 for worm gear axle drive.

The maximum ratio required $i_{A,max}$ is defined by the greatest traction requirement given in the worst considered condition to move-off. The smallest powertrain ratio $i_{A,min}$ is given by operating in the fuel-efficient ranges of the engine performance map. The required maximum speed condition gives the maximum road speed ratio $i_{A(v_{max,th})}$ (NAUNHEIMER et al., 2019).

The overall gear ratio $i_{G,tot}$ of the transmission relates the largest and the smallest gear ratio (Eq. (3)):

$$i_{G,tot} = \frac{i_{G,max}}{i_{G,min}} = \frac{i_1}{i_z} \quad , \tag{3}$$

with the gears from $n = 1$ to z.

The highest gear ratio for passenger cars is, in general, fixed within the range $0.7 \leq i_z \leq 1.0$.

The $i_{G,tot}$ is influenced by several factors, including the specific power of the vehicle (in kW/t), the engine's spread, and the intended use of the vehicle. In the case of AT for passenger cars, the overall gear ratio $i_{G,tot}$ spreads into 4.5 to 10 (NAUNHEIMER et al., 2019).

The number of gears is selected based on the gear ratio steps strategy. The ratio between two sequential gears (Eq. (4)) is considered the *ratio step* φ:

$$\varphi = \frac{i_{n-1}}{i_n} \quad . \tag{4}$$

The goal is to achieve an optimal balance between power utilization, shifting frequency, and overall transmission size and weight. Increasing the number of gear ratios offer better power utilization by closely following the torque curve, but they also increase the frequency of gear shifting, the weight, the size, and add complexity to the transmission. On the other hand, fewer gear ratios lead to larger step ratios, requiring the engine to operate in less efficient ranges, resulting in significant engine RPM changes between shifts and potentially decreasing performance and fuel efficiency. Factors such as specific vehicle power, road profile, traffic conditions, and driver behavior play a role in determining the ideal gear ratios.

The progressive gear ratio step method, commonly used for passenger cars, employs the Eq. (5) by relating the base ratio change φ_1 and the progression factor φ_2 to determine the intermediate ratios:

$$i_n = i_z \cdot \varphi_1^{(z-n)} \cdot \varphi_2^{0.5(z-n)(z-n-1)} \quad . \tag{5}$$

Initial values of $1.1 \leq \varphi_1 \leq 1.7$ and $1.0 \leq \varphi_2 \leq 1.2$ are typically chosen, but further adjustment and fine-tuning are necessary to optimize the gear ratios for specific vehicles (SINGH et al., 2012; BERA, 2019).

The gear ratios of a transmission and their corresponding characteristics are typically displayed in a truth table, outlining the engagement sequence for the shift couplings. In Table 3, which is based on Figures 1 and 2 of Raghavan and Usoro (2000), the truth table for a 6-speed automatic transmission illustrates each gear ratio along with the engaged shift couplings (denoted by ⊗) and their respective ratio steps. This particular AT comprises five shift couplings, including three brakes ($B1$, $B2$, and $B3$) and two clutches ($C1$ and $C2$). These couplings are engaged in pairs, with one clutch disengaging while the other engages, resulting in the changing of only one shift coupling from one gear to the next. The engaging sequence in this transmission follows a clutch-to-clutch pattern. This arrangement enables the transmission to operate with one reverse gear (R), three underdrive gears (1, 2, and 3), one direct gear (4), and two overdrive gears (5 and 6). The overall gear ratio is $i_{G,tot} = 6.15$.

Table 3 – Gear ratios truth table of a 6-speed transmission.

		shift couplings					
Gear	Gear Ratio	B_1	B_2	B_3	C_1	C_2	Ratio Step φ
R	-3.46	⊗		⊗			
1	3.94			⊗		⊗	-0.87
2	2.05		⊗			⊗	1.91
3	1.33	⊗				⊗	1.54
4	1.00				⊗	⊗	1.33
5	0.78	⊗		⊗			1.27
6	0.64		⊗		⊗		1.22

Source: Adapted from Raghavan and Usoro (2000).

The subsequent sections will delve into the technical definitions, analysis, and synthesis processes of planetary gear trains. Special attention will be given to the parameters governing the kinematic structure of these mechanisms, laying a solid foundation for the subsequent chapters, which will present methodologies and tools for discovering innovative gaps.

2.2 MECHANISM AND MACHINE SCIENCE REVIEW FOR PGTS

Mechanism and Machine Science, a field that explores the relationship between geometry, motion of machine parts, and the forces involved, is essential in the analysis and synthesis of mechanisms (MATA et al., 2016). Analysis involves evaluating existing mechanisms' ability to perform required tasks, while synthesis focuses on designing mechanisms capable of meeting those tasks. This may involve modifying existing solutions or inventing entirely new mechanisms based on new requirements and constraints. To establish a clear understanding of mechanisms and their characteristics, this thesis follows the terminology of IFToMM (STANDARDIZATION OF TERMINOLOGY, 2014; STARZHINSKY et al., 2017; ARTELT et al., 2019) and definitions from relevant publications (REULEAUX, 1876; HUNT, 1990; DAVIES, 1995b; TSAI, 2001; IONESCU, 2003; MATA et al., 2016) are briefly introduced below.

2.2.1 Concepts and Definitions

Mechanisms are represented in a motion space, where the dimension is referred as the *order of the system (λ)* or the degree of freedom of the space. It indicates the number of possible independent motions that a free body can exhibit within that space. For instance, in a 3-D space, the order of the system is $\lambda = 6$, representing three rotations and three translations. On the other hand, in a 2-D space (plane), the order of the system is $\lambda = 3$, consisting of one rotation and two translations.

A **link** or an element is defined as an individual rigid body subjected to negligible deformation. The relative motion between two links can be constrained by a specific form of connection, termed as a *coupling*. In situations where the links are in contact and exhibit passive relative motion, the coupling is classified as a *kinematic pair*. On the other hand, a coupling allowing active power transmission between the links is categorized as an *active coupling*.

The classification of a link is based on the number of kinematic pairs it belongs to. For example, a link can be binary (belonging to two kinematic pairs), ternary (belonging to three kinematic pairs), quaternary (belonging to four kinematic pairs), and so on. Additionally, when a set of links is connected together with no relative motion, it is considered as one single link.

A **joint** is the physical representation of a kinematic pair. It restricts the relative motion between its constituent links based on the geometric characteristics of the contact. Kinematic pairs are classified as *lower pair* when the contact between links occurs on a surface, or *higher pair* when the contact occurs at a line or a point. For two links in a motion space denoted by λ, inserting a joint i between them will impose c_i *degrees of constraint* and will result in f_i *degrees of freedom* as shown in Eq. (6):

$$\lambda = c_i + f_i \quad . \tag{6}$$

The most common kinematic pairs are summarized in Table 4, presenting their classification and degrees of constraint and freedom according to the motion space.

Table 4 – Kinematic pairs and their characteristics.

Class	Pair	Drawing	Symbol	Degrees	Line (1-D) $\lambda = 2$	Plane (2-D) $\lambda = 3$	Space (3-D) $\lambda = 6$
Lower	Revolute		J_R	c_R	1	2	5
				f_R	1	1	1
	Prismatic	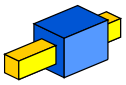	J_P	c_P	1	2	5
				f_P	1	1	1
	Cylindrical	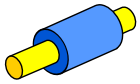	J_C	c_C	0	-	4
				f_C	2	-	2
	Helical		J_H	c_H	1	-	5
				f_H	1	-	1
	Spherical	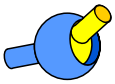	J_S	c_S	-	-	3
				f_S	-	-	3
	Planar		J_E	c_E	-	0	3
				f_E	-	3	3
Higher	Helical Gear	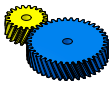	J_G	c_G	1	1	1
				f_G	1	2	5
	Spur Gear	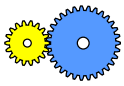	J_G	c_G	1	1	2
				f_G	1	2	4
	Spherical Cam		J_{C_P}	c_{C_P}	1	1	1
				f_{C_P}	1	2	5
	Roller Cam	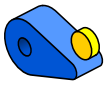	J_{C_P}	c_{C_P}	1	1	2
				f_{C_P}	1	2	4

Source: Author.

A set of links interconnected by joints forms a **kinematic chain (KC)**. Any subset of a kinematic chain is named a *subchain* and, if it forms a closed circuit, it is named *loop*.

The set of links that belong to a kinematic chain is named a *partition*. Each possible arrangement of the links of a partition to generate a kinematic chain is named a *variation*.

A kinematic chain is designated *fractionated* when there is a link or joint whose removal results in two separated chains (disconnected chain).

A **mechanism** can be defined as a kinematic chain that allows a controlled output motion to be generated from an input motion, where one of the links is considered fixed to the ground or reference frame. Alternatively, it can be said it is a constrained system

of bodies designed to convert motions of, and forces on, one or several bodies into motions of, and forces on, the remaining bodies.

The grounded link is named the **frame link** or fixed link, denoted as 'F', and the process of fixing different links of the same kinematic chain to obtain different mechanisms is named *kinematic inversion*. Thus, from a single partition, it is possible to create several variations, each of which allows a number of kinematic inversions equal to the number of links.

The **input link(s)**, denoted as 'IN', form joint(s) with the frame through which motion and action are transmitted to the mechanism, being referred to as *input joints*. On the other hand, the **output link(s)**, denoted as 'OUT', form joint(s) with the frame where the required motion and action intended for the mechanism are performed, being referred to as *output joints*. A kinematic chain that has all input joints defined is referred to as a *constrained kinematic chain*, as all the links perform a constrained motion when the input moves in a prescribed manner.

In general, an external source provides motion and force to the input joint(s) such as an electric motor, a hydraulic piston, a combustion engine, human action, etc., which is named an *actuator*. When one or more mechanisms are connected with actuators (and optionally sensors, controllers, etc.) in order to carry out work, it becomes a *machine*.

Thus, a **machine** can be defined as a set of interrelated movable units - *mechanisms* - with supporting structures for transmit/modify motions and forces for a suitable task (Fig. 10).

In this thesis, the conventional automatic transmissions (AT) are considered the machine, a mechanical system designed to perform specific tasks such as allowing the vehicle to move-off and providing multiple ratios by controlling the power flow between the engine and wheels. The mechanism responsible for achieving different gear ratios in AT is based on the planetary gear train, also known as epicyclic gear train (EGT), which consists of gears with mobile axes.

2.3 PLANETARY GEAR MECHANISM (PGM)

A **planetary gear mechanism (PGM)** is constituted by a kinematic chain, denoted as a planetary gear train (PGT), integrated to a frame link (housing), input and output links, and shift couplings to constrain its motion and establish a power flow. This arrangement results in a multi-degree-of-freedom mechanism capable of generating gear ratios.

PGTs belong to a special class of geared kinematic chains where the joints consist exclusively of revolute and gear pairs, enabling unlimited rotation (TSAI, 2001). A PGT is essentially composed of one or more elementary interconnected kinematic chains (HSIEH; TSAI, 1996b), referred in this research as to planetary gear sets (PGS).

Figure 10 – Overview of machine's constitution.

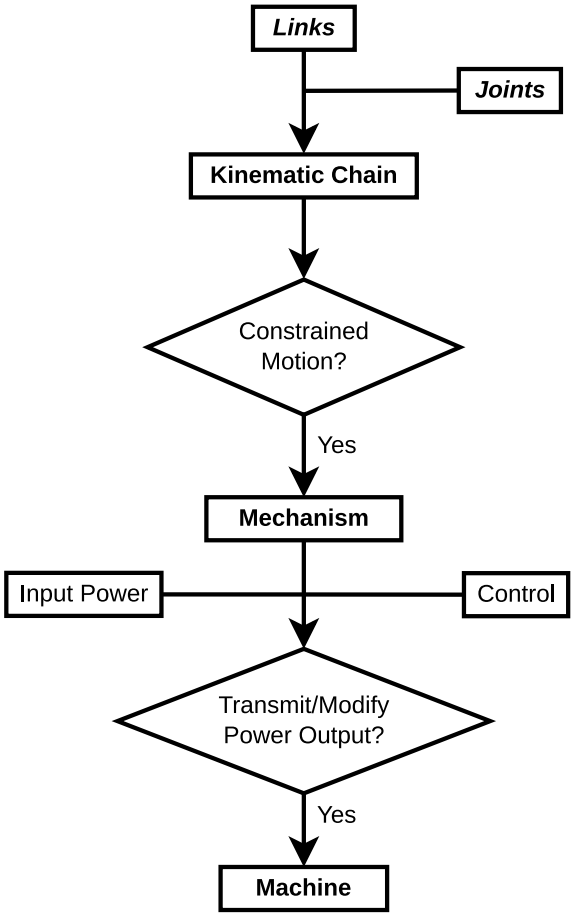

Source: Adapted from Yan (1998).

Within these sets, some links might be rigidly interconnected, referred to as *compound links (CL)* in this research.

Furthermore, the *shift couplings* contained in a PGM are active couplings that can be actuated to temporarily allow the transmission of torque between PGM links.

In Figure 11, an overview of a typical kinematic structure found in automatic transmissions is presented. The diagram highlights the constituent elements of its kinematic chain, providing a clear overview of its structural configuration.

As previously shown in Figure 8 and detailed in the diagram of Figure 11, an automatic transmission is characterized by multiple PGSs interconnected through compound links and shift couplings providing a multiplicity of gear ratios between input and output links when shift control actuate a combination of clutches and brakes.

There are two elementary topologies of PGSs based on the planet sets: simple and double.

A simple PGS (SPGS) consists of four basic links: a sun gear (S) and a ring gear (R) that rotate about a central stationary axis (first level), and a planet gear (P) that rotates about a second-level axis supported by a planet carrier (arm - A), maintaining a

Figure 11 – Overview of a typical kinematic structure found in AT.

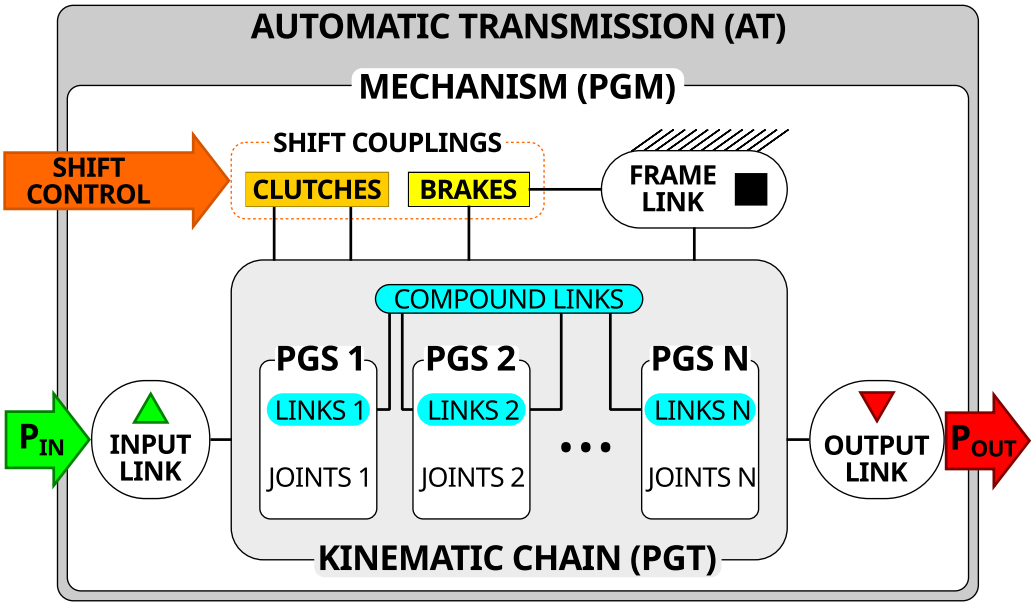

Source: Author.

constant center distance between the gear meshes. Since the SPGS has only one level connecting the sun and the ring, it results in opposite rotating directions between them. Figure 12a illustrates a SPGS, while Tab. 5a lists its links and Tab. 5b lists its joints.

Figure 12 – Planetary Gear Sets (PGS)

(a) Simple PGS (SPGS)

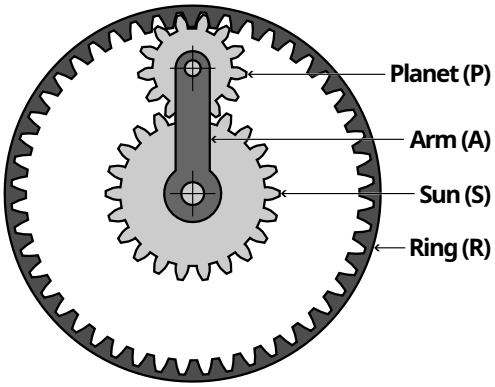

(b) Double PGS (DPGS)

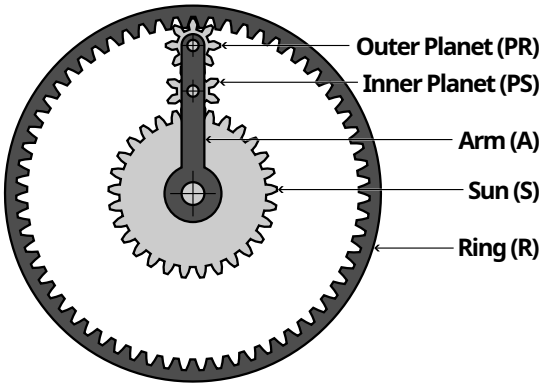

Source: Author.

A double PGS (DPGS) has two meshing planet gears connecting the sun and the ring, the inner planet (PS) and the outter planet (PR), resulting in the same direction of rotation between them. Figure 12b illustrates a DPGS, while Tab. 6a lists its links and Tab. 6b lists its joints.

The axes of rotation in PGTs are denoted by revolute joints, which are labeled with letters to distinguish their relative positions with respect to the central axis. Notably, the column 'Level' in both Table 5b and Table 6b presents revolute joints listed in alphabetical ascending order based on the level location of their axes. The letter 'a' is

Table 5 – Simple Planetary Gear Set (SPGS)

(a) SPGS links

Links	Symbol
Sun	S
Ring	R
Planet	P
Arm (carrier)	A

(b) SPGS joints

Joints	Type	Level
P-S	external gear	g
P-A	revolute	b
P-R	internal gear	g
A-S	revolute	a

Source: Author.

Table 6 – Double Planetary Gear Set (DPGS)

(a) DPGS links

Links	Symbol
Sun	S
Ring	R
Inner Planet (sun)	PS
Outer Planet (ring)	PR
Arm (carrier)	A

(b) DPGS joints

Joints	Type	Level
PS-PR	external gear	g
PS-S	external gear	g
PS-A	revolute	b
PR-R	internal gear	g
PR-A	revolute	b
A-S	revolute	a

Source: Author.

assigned to joints located along the central axis, while letters 'b' or higher are designated for planet axis joints found in upper levels. Gear joints are always referred to as letter 'g' without any distinction regarding their location.

In Fig. 13, a simple PGT is illustrated and showcases the arrangement of sun gear as the input link, the planet carrier (arm) as the output link, the ring gear is a reaction link, and three equally distributed planets. By alternating the combination of input, output and reaction links, this configuration allows for various gear ratios and torque distribution capabilities, making it suitable for achieving a wide range of vehicle speed and load requirements in a compact mechanism.

The kinematic structure of PGTs can be represented in various formats to aid in the analysis and synthesis of the mechanisms. In general, the following assumptions are made for all representation methods (TSAI, 2001):

1. Due to symmetry on central axis, the PGT is represented by its upper half.
2. The multiplicity of planets is represented as a single planet for simplicity. In general, two or more planets are employed to balance the planetary structure and to increase load capacity.
3. Multiple revolute joints are represented as an equivalent set of coaxial binary revolute joints.
4. Links that are permanently connected (rigid) are represented as a single link

Figure 13 – Typical configuration of a planetary gear train in automotive transmissions.

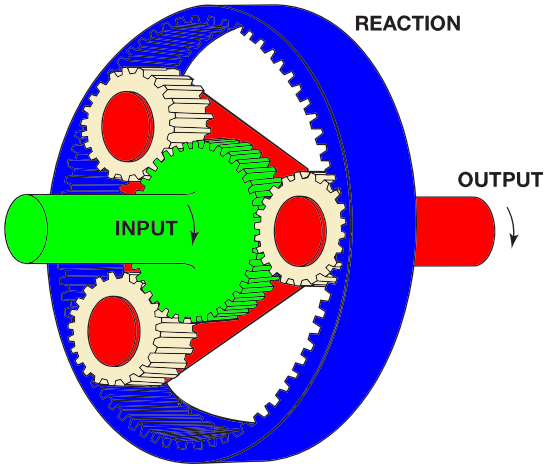

Source: Adapted from Halderman and Birch (2017).

(compound links).

The *functional schematic representation* is a simplified cross-sectional drawing that presents only functional links as gears, shafts, and their respective couplings identified by labels. This representation aims to maintain the evident mechanism's geometry and topology, ensuring comprehensibility. Figure 14 has an example of a *schematic representation* of a simple PGT with three equally distributed planets. Figure 15 con-

Figure 14 – Schematic representation of a simple planetary gear train.

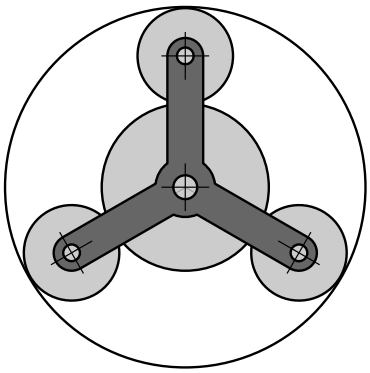

Source: Author.

tains the *functional diagram*, also known as kinematic skeleton, representing the upper half PGM of a GM 6-speed automatic transmission composed of three SPGSs and five shift couplings comprising 3 brakes (B1, B2, B3), and 2 clutches (C1, C2). The housing (F), input (IN), and output (OUT) links, as well as the one-wheel-clutch (OWC), parallel to brake B2, are also visible. In the functional diagram, for each PGS, the multiplicity of equally distributed planets is usually represented by only one single planet (SPGS) or one double planet set (DPGS).

The *structural representation* is an abstraction of the kinematic chain relating

Figure 15 – Functional diagram of a GM 6-speed automatic transmission

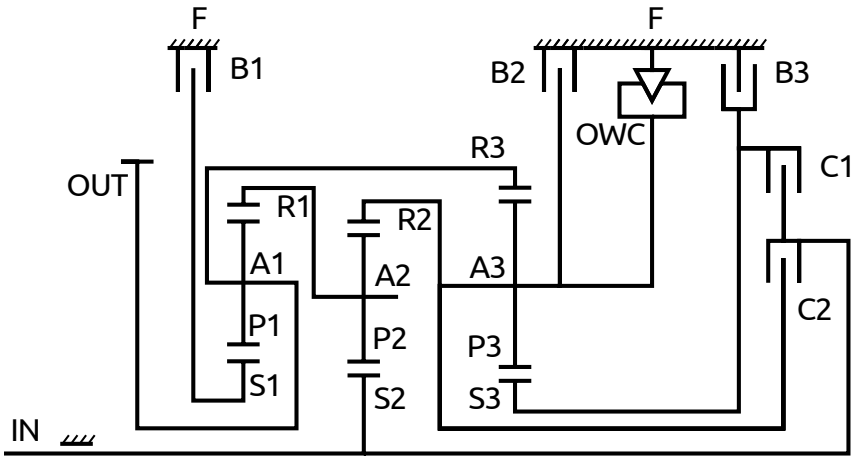

Source: Author based on Singh and Olenzek (2010).

links to polygons, with vertices representing kinematic pairs. In this case, dimensions are not considered. Figure 16 is the structural representation of the SPGS (Fig. 12a) where arm (A) and ring (R) are binary links represented by lines and sun (S) and planet (P) are ternary links represented by a cross-hatched triangle. The plain vertices '○' represent revolute pairs, whereas the solid vertices '●' denote gear pairs.

Figure 16 – Kinematic structural representation of a simple planetary gear train.

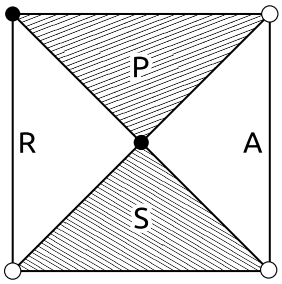

Source: Author based on Tsai (2001).

The topology of mechanism refers to the number and types of links and kinematic pairs, as well as the connection relationship between them (DING et al., 2022). A mechanism and its kinematic chain can be represented using a more abstract model known as *topological graph representation*. This approach belongs to the research field of graph theory and has been widely utilized in the analysis and synthesis of gear trains since Buchsbaum and Freudenstein (1970). Graph representations play a significant role in aiding the analysis and synthesis of PGTs and is presented in more detail in the following Section 2.3.1, as this model of representation is the primary focus of this thesis.

Furthermore, there are alternatively other representations used to study PGTs such as linkages (JOHNSON; TOWFIGH, 1967), nomographs (ESMAIL, 2013), network theory (POLDER, 1969), ports (MOLIAN, 1970), lever analogy (BENFORD; LEIS-

ING, 1981), building blocks (KOTA; CHIOU, 1992), model-based (KARHULA; NICOLAI, 2018), and zebra (S.; GHOSE, 2022), among others.

2.3.1 Graph representations

Graph theory has been utilized in the analysis of kinematic chains and mechanisms since the 1960s, when it was first introduced by Crossley (1965). This approach has greatly improved the design process by providing a more elegant and rational method, while also allowing for computer implementation, as stated by (DOBRJANSKYJ; FREUDENSTEIN, 1967). The *graph representations* have many advantages (TSAI, 2001), including the direct application of network properties to mechanisms, allowing for the analysis of kinematics, statics, and dynamics with the aid of computers. It also enables the systematic enumeration, classification, and atlas generation of mechanisms, and the generation of functional schematic and structural representations. Therefore, this research is based, but not restricted, on the graph representation of PGTs.

Buchsbaum and Freudenstein (1970) were the first to present a graph representation for the structure of geared kinematic chains including PGTs. Since then, this field was extensively discussed by researchers as summarized in these reviews (MRUTHYUNJAYA, 2003; PENNESTRI; BELFIORE, 2015; XUE et al., 2016b; JUBER et al., 2022).

In the work of Davies (1995b), a generalized model for representing mechanisms is presented through the use of a coupling graph. This model represents the relationship between links without distinguishing their mechanical nature. Two graphs can be derived based on the purpose of analysis. The motion graph represents the possible freedoms between links, and the action graph represents the constraints imposed between links. These graphs are applied by Davies (1995a) to model and analyze a two-stage turbine PGM using screw theory. A comprehensive review on Davies methods for PGT kinematic and static analysis is presented in Cazangi and Martins (2007) and Cazangi (2008).

The **conventional topological graph** of PGTs, equivalent to the motion graph, represents links as solid vertices and joints as undirected edges. Vertices are labeled or enumerated according to links. Revolute pairs are represented by solid edges labeled in alphabetic ascending order according to the level location of their axes, and gear pairs are distinguished by dashed edges. In Figure 17, the SPGS kinematic chain (Fig. 12a) is represented by its functional diagram (Fig. 17a) and its associated topological graph (Fig. 17b) evidencing two joint levels, the central axis with label 'a', and the planet (P) axis with label 'b'.

In Figure 18, the DPGS kinematic chain (Fig. 12b) is represented by its functional diagram (Fig. 18a) and its associated topological graph (Fig. 18b) evidencing three joint

Figure 17 – Simple PGS kinematic chain representations.

(a) Functional diagram

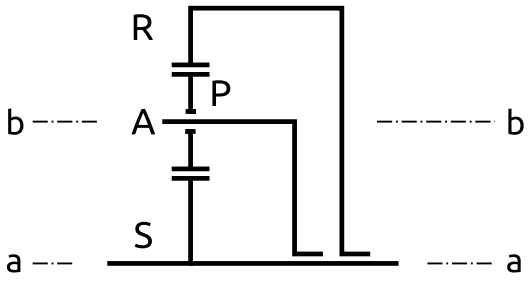

(b) Topological graph

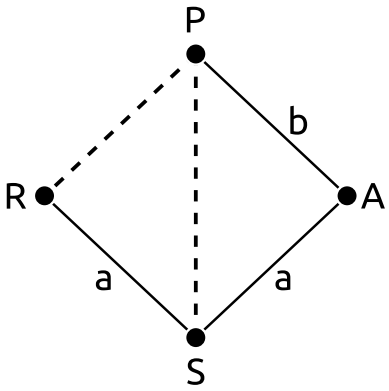

Source: Author.

levels, the central axis with label 'a', the inner planet (PS) axis with label 'b', and the outer planet (PR) axis with label 'c'.

Figure 18 – Double PGS kinematic chain representations.

(a) Functional diagram

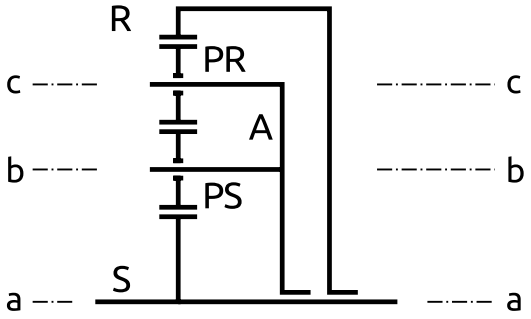

(b) Topological graph

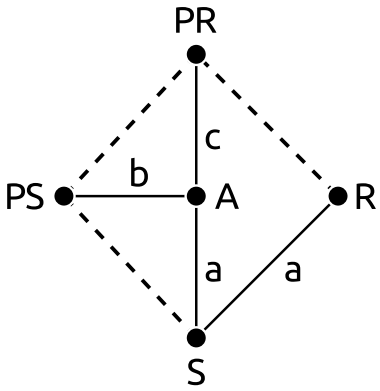

Source: Author.

A link is referred to as the *transfer vertex* when it maintains a constant center distance between the axes of two geared links, positioning them at different levels. In the case of the simple PGS (Fig. 17), and the double PGS (Fig. 18), the arm (A) link serves as the transfer vertex. In the simple PGS, the arm (A) link rotates around the central axis (level 'a') and supports the planet axis in level 'b'. Similarly, in the double PGS, the arm (A) link rotates around the central axis (level 'a') and supports the inner planet (PS) axis in level 'b' and the outer planet (PR) in level 'c'.

In a PGT, the interconnection of n links through j joints is represented by a connected topological graph containing at least two circuits. Each *circuit (or loop)* is a path through existing edges starting and ending at the same vertex, without repeating any vertex. On the other hand, a *tree* is a connected graph that has no circuits. The tree

is considered a *spanning tree* if it is a subgraph of the topological graph that includes all vertices and only a subset of its edges. Specifically, the edges belonging to the spanning tree are named *branches*, and the remaining edges are named *chords*. The subgraph obtained by removing all geared edges from the topological graph of an PGT must be a tree. Any geared edge added onto the tree forms a unique circuit named the *fundamental circuit (f-circuit)*, i.e., each f-circuit is comprised by one gear pair (chord) and several revolute pairs (branches).

In order to generate a PGM, the housing or frame (F), input (IN), and output (OUT) links, as well as the joints related to shift couplings, must be incorporated into the PGT. Due to these links, a subgraph of three vertices and two revolute edges in level 'a' should be aggregated to the graph representation (Fig. 19). In this thesis, to

Figure 19 – Subgraph of vertices F, IN, and OUT to generate a PGM.

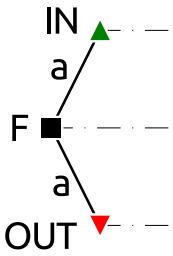

Source: Author.

enhance the readability of mechanism graphs, a slight distinction in vertex symbols is introduced for three specific links: frame (■), input (▲), and output (▼). These links can either be associated with existing kinematic chain links or included as new ones. Likewise, the addition of shift couplings (brakes and clutches) requires proper actuation and should be located in level 'a', being connected to existing level 'a' revolute joints or added as new ones between existing links.

In Figure 20, the PGM containing one SPGS is represented by its functional diagram (Fig. 20a) and its associated topological graph (Fig. 20b). The frame (F) and output (OUT) links are added as new vertices in the graph, and the input link (IN) was associated to the existing sun (S). The two clutches (C1, C2) and two brakes (B1, B2) were added as four new edges in the graph.

In Figure 21, is presented the graph representation of the GM 6-speed automatic transmission (Fig. 15) to exemplify a more complex PGM.

In Table 7, a summary of basic correspondences between mechanisms and graphs is presented.

In the literature, various other graph representations for mechanisms are discussed, such as rotational and displacement graphs (FREUDENSTEIN, 1971), closed rotation and displacement graphs (RAVISANKAR; MRUTHYUNJAYA, 1985), coincident-joint graph (OLSON et al., 1991), coincident-joint graph with solid polygons to de-

Figure 20 – Representations of a PGM with one SPGS.

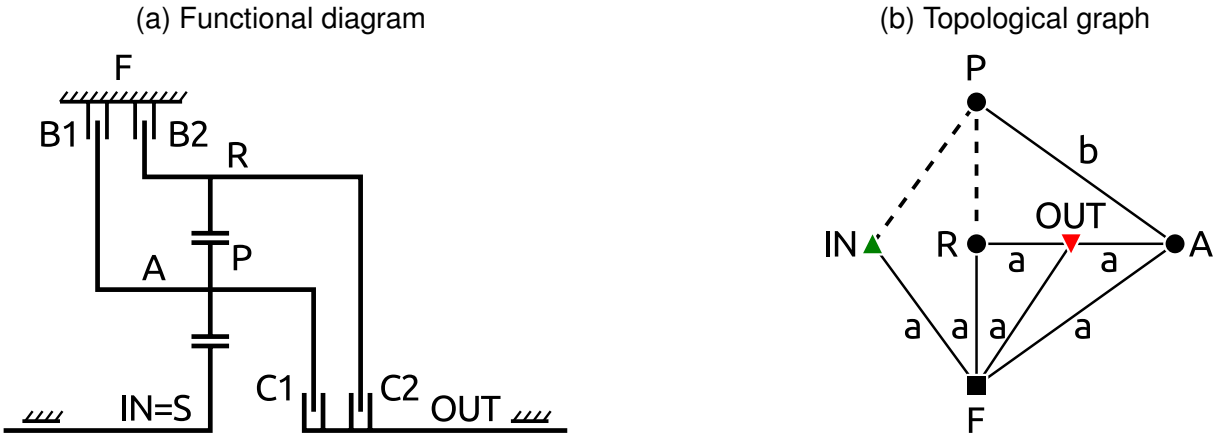

Source: Author.

Figure 21 – Graph representation of the GM 6-speed automatic transmission.

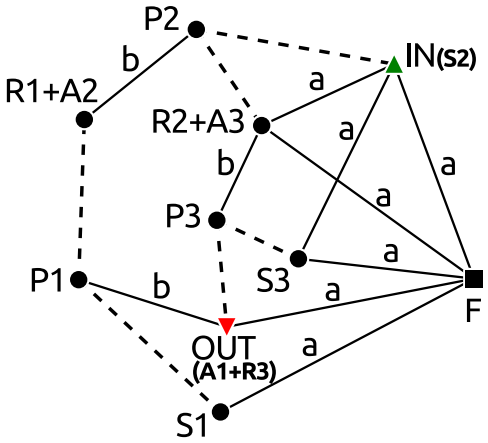

Source: Author.

Table 7 – Correspondences between mechanisms and graphs.

Mechanisms	*Symbol*	Graphs	*Symbol*
No. of links	n	No. of vertices	v
No. of links with i joints	n_i	No. of vertices with i edges	v_i
No. of joints	j	No. of edges	e
No. of joints on link i	d_i	Degree of vertex i	k_i
No. of independent kinematic equations	v	No. of fundamental loops	L
No. of kinematic equations with i joints	v_i	No. of loops with i edges	L_i
Total No. of kinematic equations	$\tilde{v}$	Total No. of loops	$\tilde{L}$

Source: Adapted from Tsai (2001).

note multiple joints (HSU; LAM, 1992), canonical graphs (CHATTERJEE; TSAI, 1994), graphs based on functional constraints (CASTILLO, 2002), and double bicolored graphs (DBG) (YANG et al., 2018). For a comprehensive review of graph representations for PGTs, refer to (XUE et al., 2016b).

The *matrix representation* of PGTs is an extension of the close relationship between graphs and matrices, which has greatly facilitated the computational analysis of mechanisms. The main matrix is the adjacency matrix (A), which correlates adjacent links by representing them with 1 and the others with 0, as follows:

$$A = [a_{xy}]_{n\times n} = \begin{cases} 1 & \text{if link } x \text{ is connected to link } y, \\ 0 & \text{otherwise (including } x = y), \end{cases}$$

where x is a link in row, y is a link in column and n is the total of links in the mechanism.

The incidence matrix (B) correlates links in each row with their respective incident joints in each column, as follows:

$$B = [b_{xy}]_{n\times j} = \begin{cases} 1 & \text{if link } x \text{ contains incident joint } y, \\ 0 & \text{otherwise,} \end{cases}$$

where x is a link in the row, y is a joint in column, n is the total of links and j is the total of joints in the mechanism.

Both matrices serve as the unequivocal representations of the graph; all other matrices are derivatives of these two. Operations such as contractions, expansions, and property analysis in graphs can be directly applied to matrix representations for computational analysis of mechanisms.

2.3.2 Structural Analysis

The structural analysis of planetary gear trains involves studying the interconnections and mobility of their components, with a specific focus on fundamental relationships, including degrees of freedom, number and type of links, joints, and loops, among other relevant properties. Graphs are utilized to represent the kinematic structure of PGTs, facilitating the translation of useful characteristics and properties from graphs to features of kinematic chains and mechanisms. According to Tsai et al. (1988), the structural analysis of the PGM reveals both the specific PGT utilized in the transmission and the arrangement of the shifting couplings. The following sections provide indispensable analyses to comprehend the overall functional characteristics of PGTs and PGMs.

2.3.2.1 Mobility Equation

The mobility M is the primary characteristic that determines the number of inputs (independent variables) required to drive the mechanism. Also named the net degree of freedom, it is defined as the sum of all degrees of freedom F of each link that composes a mechanism, moving freely in space, minus the motion constraints C imposed by the joints between them and the definition of a fixed body (Eq. (7)).

$$M = F - C \tag{7}$$

For two links in a motion space denoted by λ, inserting a joint i between them will impose c_i degrees of constraint and will result in f_i degrees of freedom as shown in Eq. (8):

$$\lambda = c_i + f_i \tag{8}$$

Considering a mechanism where one link is fixed and all the remaining $n-1$ links are free to move in space λ, its degree of freedom F is given by $\lambda(n-1)$. Now, inserting j joints among the links impose $C = \sum_{i=1}^{j} c_i$ constraints and the mobility (Eq. (7)) of the mechanism results in (Eq. (9)):

$$M = \lambda(n-1) - \sum_{i=1}^{j} c_i \tag{9}$$

Expressing the mobility equation in terms of degrees of freedom (Eq. (8)) results in the Grübler-Kutzbach criterion (GRÜBLER, 1917; KUTZBACH, 1929) shown in Equation (10):

$$M = \lambda(n-j-1) + \sum_{i=1}^{j} f_i \tag{10}$$

where λ is the motion space, n is the number of links, j is the number of joints (kinematic pairs) and f_i is the degree of freedom of the i-th joint. The Grübler criterion, as stated by Tsai (2001), holds true when the constraints imposed by the joints in a mechanism are independent and do not introduce redundant degrees of freedom. A redundant degree of freedom refers to a motion that does not affect the transfer of motion from the input to the output link of the mechanism.

The general form of the mobility equation is discussed for almost two centuries, and there are still challenges as shown in these reviews (GOGU, 2005; PENNESTRI et al., 2005; DVORNIKOV; ZHUKOV, 2022).

In PGTs, the only kinematic pairs considered are revolute and gear types. So, the total number of joints j is given by (Eq. (11)):

$$j = j_R + j_G \tag{11}$$

where j_R is the number of revolute joints and j_G is the number of gear joints in the mechanism.

Revolute joints j_R allow only one relative motion of rotation between links, independently of the motion space, resulting $f_{R,\lambda} = 1$ degree of freedom (REULEAUX, 1876).

Gear joints j_G constrain only the relative rotation between links about their own axes as a function of the transmission ratio, independently of the motion space, resulting $c_{R,\lambda} = 1$ degree of constraint (KHULIEF, 2013).

The degrees of freedom and constraints for revolute and gear joints are summarized in the Tab. 8, according to the motion space.

Table 8 – Degrees of freedom and constraints of revolute and gear joints in each motion space.

	j_R		j_G	
λ	$f_{R,\lambda}$	$c_{R,\lambda}$	$f_{G,\lambda}$	$c_{G,\lambda}$
2	1	1	1	1
3	1	2	2	1
6	1	5	5	1

Source: Author.

The mobility equation (Eq. (7)) applied to PGTs can be expressed as follows (Eq. (12)):

$$M = \lambda(n-1) - j_R \cdot c_{R,\lambda} - j_G \cdot c_{G,\lambda} \tag{12}$$

The Grübler-Kutzbach criterion (Eq. (10)) for PGTs can be written as (Eq. (13)):

$$M = \lambda(n-j-1) + j_R \cdot f_{R,\lambda} + j_G \cdot f_{G,\lambda} \tag{13}$$

The mobility of PGMs represents the motion at the input joint plus the number of shift couplings that need to be actuated to achieve a transmission ratio at the output joint. The total number of possible modes of generating a gear ratio is given by the following combination (Eq. (14)):

$$\text{Total Modes} = \binom{SC}{M-1} = \frac{SC!}{(M-1)!(SC-M+1)!} \quad . \tag{14}$$

Where SC denotes the total number of shift couplings, and M represents the mobility of the PGT.

2.3.2.2 Link Assortments

Given a PGT with $\tilde{L}$ loops, n links, and j joints, the *Euler's equation* relates them as (Eq. (15)):

$$\tilde{L} = j - n + 2 \quad . \tag{15}$$

Considering the PGTs are always a closed-loop kinematic chains, the minimum number of joints comprising a corresponding link must be 2. On the upper side, the maximal degree p allowed for a link in a partition is limited by the number of loops ($\tilde{L}$) in the kinematic chain. By relating the link maximal degree and the Equation (15), it is possible to obtain (Eq. (16)):

$$p \leq \tilde{L} = L + 1 = j - n + 2 \quad , \tag{16}$$

where L is the number of fundamental loops in the graph.

The link assortments is the process of distribution of links by their degree of adjacency, generating partitions. Considering n_k the number of links with k joints, the total number of links (n) of a PGT graph can be described as (Eq. (17)):

$$n_2 + n_3 + n_4 + \ldots + n_p = n \quad . \tag{17}$$

Each joint is a coupling between two links and each link n_i contains i joints, describing another relation (Eq. (18)):

$$2n_2 + 3n_3 + 4n_4 + pn_p = 2j \quad . \tag{18}$$

Combining both Equations (17) and (18), it is possible to identify the lower bound number of binary links n_2 as (Eq. (19)):

$$n_2 \geq 3n - 2j \quad . \tag{19}$$

Given the number of links n and joints j, all possible partitions can be determined by solving the system of equations involving Equations (17) to (19).

As explained in Section 2.2.1, it is possible to have multiple PGMs for a single partition. As an example, the GM 6-speed AT (Fig. 15) PGM partition is detailed in Table 9.

Table 9 – Link assortments of the GM 6-speed AT graph (Fig. 21).

Degree of vertex	k	Graph	Links	Link Assortment
binary	2		S1, R1+A2	$n_2 = 2$
ternary	3		OUT, P1, P2, P3, S3	$n_3 = 5$
quaternary	4		IN, R2+A3	$n_4 = 2$
quinary	5		F	$n_5 = 1$

Source: Author.

The concept of link assortments is commonly used to group PGTs into families based on the similarity of their degrees. Furthermore, the maximal degree is utilized in the synthesis equations of mechanisms to establish an upper bound for generating link assortments.

2.3.2.3 Structural Characteristics of PGTs

The topology of a mechanism is defined by its structural characteristics, relating its kinematic chain to the required functionalities. Buchsbaum and Freudenstein (1970) described a set of structural characteristics about the geared kinematic chains of PGTs based on topology graph. Subsequently, in their follow-up study (FREUDENSTEIN, 1971), it was synthesized in a set of rules as follows:

S1. The mechanism must satisfy the general degree-of-freedom (DOF) equation represented by the Grübler-Kutzbach criterion Eq. (13).
S2. For a PGT with n links and mobility M-DOF, the corresponding graph must have n vertices, $j_R = n-1$ revolute edges, and $j_G = n-1-M$ geared edges.
S3. The subgraph obtained by removing the geared edges must be a tree.
S4. Each geared edge added to the tree forms a unique fundamental circuit.
S5. The number of f-circuits (L) is equal to the number of geared edges (j_G).
S6. Each vertex n_i must have at least one incident edge that represents a revolute pair.
S7. The subgraphs' mobility (M') must be at least one, to avoid structures.
S8. In each f-circuit, there is one transfer vertex, such that all revolute edges on one side of the vertex are at the same level, and all revolute edges on the other side of the vertex are at a different level.

Moreover, Tsai (2001) suggests additional structural characteristics concerning PGTs:

S9. The torque converter, clutch controller, final reduction, and differential can be temporarily ignored for the purpose of structure synthesis.
S10. Turning-pair edges of the same level and their end vertices form a tree.
S11. The graph of a PGT should not contain any circuit that is made up of only geared edges to avoid complexity.
S12. A PGT is a fractionated two-DOF mechanism. Specifically, it is made up of a one-DOF PGT supported by the housing of a transmission mechanism on a central axis.
S13. Only coaxial links of a PGT are used as the input link (IN), output link (OUT), and shift couplings.
S14. For a one-DOF PGT with m_r desired gear ratios, the number of coaxial links n_c (with revolute joints in level 'a') should satisfy the inequality:

$$(n_c - 1)(n_c - 2) + 1 \geq m_r \quad .$$

S15. There shall be no redundant links (the removal of the link does not affect the mobility of the mechanism) or partially locked subchains.

The inequality in Item S14, as proposed by Tsai et al. (1988) as a necessary condition for single-DOF mechanisms, is based on two assumptions: the potential to alternate input power among coaxial links, and the permanent designation of one of the coaxial links as the output. Furthermore, this condition can be extrapolated to serve as a requisite for mechanisms with multiple degrees of freedom, as illustrated in Equation (20):

$$n_c \geq \frac{1}{2} \cdot \left(1 + \sqrt{4m_r - 3}\right) + M \quad . \tag{20}$$

Then, given the desired m_r gear ratios (including reverse), it is possible to determine the minimum number of coaxial links n_c for any mobility M.

These structural characteristics form the fundamental basis for analyzing the feasibility of PGTs through the use of graph representation.

2.3.2.4 Isomorphism in PGTs

Isomorphism refers to the property of mechanisms and graphs sharing the same topological structure (MCKAY; PIPERNO, 2014). In the context of innovation, isomorphism represents identical mechanisms or kinematic chains, which is undesirable. Detecting graph isomorphism is a critical step in the analysis and synthesis process, and various solutions have been proposed, such as methods based on string codes (YANG; LI, 2022), perimeter loops(YANG; DING, 2018), matrix operations (MUSTAFA et al., 2019a; XU et al., 2020; SUN et al., 2021), characteristic polynomials (MUSTAFA et al., 2019b), among others.

According to Tsai (2001), an ideal algorithm for detecting structural isomorphism should provide a unique, efficient, and decodable representation of kinematic chains, facilitating automated identification and storage for practical design applications. Despite the existence of several reliable solutions, researchers are continually exploring computationally agile approaches to expedite the analysis process.

Pseudoisomorphism, another challenge in the comparative analysis of PGTs (HSU; LAM, 1992), refers to the situation where PGTs are structurally and mathematically non-isomorphic graphs but are functionally isomorphic. This phenomenon often arises when multiple links are coaxial, meaning they rotate among themselves sharing the same axis, resulting in circuits with edges solely in level 'a' in the graph, indicating a circular dependency. These multiple joints give rise to numerous constructive combinations of mechanisms that are structurally different but functionally identical. Chatterjee and Tsai (1994) proposed a canonical graph to deal with pseudoismomorphic topologies.

Yang et al. (2018) and Yang and Ding (2019) introduced a double bicolor graph (DBG) representation aiming to reduce the number of potential pseudoisomorphisms resulting from coaxial revolute joints. In their graph model, fictitious multiple joints (hollow vertices '○') are introduced as references at each axis location with a multiplicity of links (solid vertices '●') rotating among themselves. The original revolute joints are removed and substituted by edges between the hollow vertices and the related links. This process aids in identify and reduce the number of isomorphisms and pseudoisomorphisms during synthesis process. The graph attend to the fundamental structural characteristics rules similarly to the conventional topological graph, with the following differences: gear edges cannot connect to hollow vertices; revolute edges incident to hollow vertices must be at the same level; the degree 'k' of the hollow vertex is equivalent to 'k-1'

revolute pairs; graphs with different numbers of hollow vertices are non-isomorphic; and graphs containing hollow vertices of different degrees are non-isomorphic; the mobility of DGB graph is equal the mobility of PGT plus the number of hollow vertices. In this graph model, only the PGT kinematic chain is considered.

An illustration of the application of the DBG graph model to the well-known Simpson PGT is presented in Figure 22. The functional diagram (Fig. 22a) is followed by its corresponding conventional topological graph (Fig. 22b), and the double bicolored graph (DBG) representation (Fig. 22c). In this case, the DBG graph comprises the hollow vertex '7' as a multiple joint (*MJ*) with degree $d = 3$ representing the coaxial links (1, 3, 4, 6) rotating in the central axis (level 'a').

Figure 22 – Representations of a Simpson PGT.

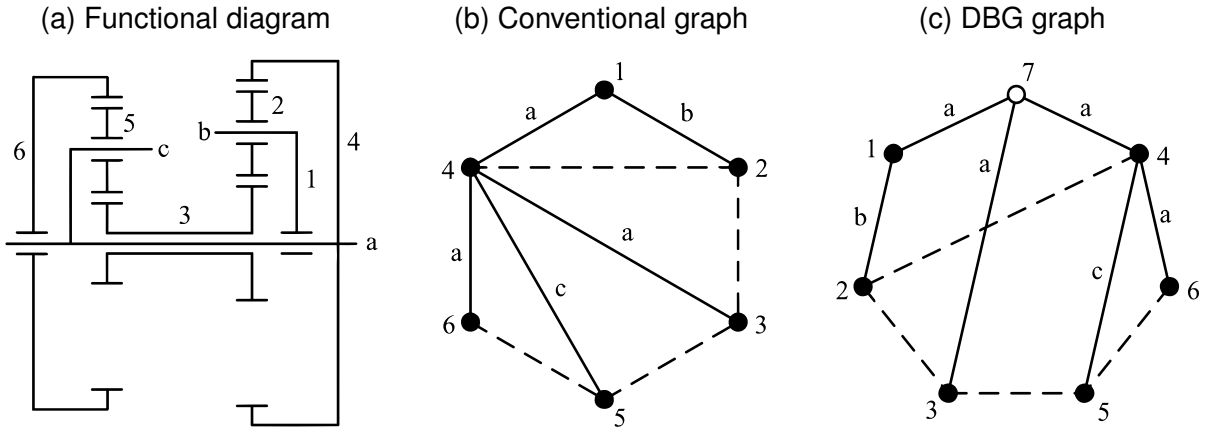

Source: Adapted from Yang et al. (2018).

In this thesis, the DBG graph is used to model the PGTs in parallel with the conventional topological graph model, which is employed to represent PGMs.

2.4 PGT DESIGN

Machine design is a logical process that demands high creative and technical skills to solve a particular problem surrounded by engineering constraints. It can be divided in 4 major design phases: Informational, Conceptual, Detailing and Product (YAN, 1998; TSAI, 2001; NORTON, 2006; PAHL et al., 2007; BACK et al., 2008). The *Informational* phase comprises to identify customer's needs and translate them into engineering specifications for the machine to be designed. The *Conceptual* is the creativity phase, where a pool of design alternatives are generated, evaluated and the most promising concept is selected. The *Detailing* phase comprises engineering studies as design analysis, optimization, and simulation to detail function, shape, material and production methods. The *Product* is the last phase, comprising construction of prototypes, testing and validation of the detailed design for documentation and manufacturing of the final product.

Decisions made in the two initial design phases, Informational and Conceptual, significantly influence the manufacturing cost of the final product and rely on the designer's intuition, ingenuity, and experience. For Yan (1998), the Conceptual phase is the most difficult and least understood step in the design process due to its requirements for creativity and knowledge. It is also in the Conceptual phase that mechanisms are designed.

Mechanism design is described by Yan (1998) as the generation or selection of a particular type of mechanism, the determination of the required numbers and types of elements and joints, and the derivations of geometric dimensions of elements between joints to achieve the desired requirements of the constrained motion (Fig. 23).

Figure 23 – Mechanism and Machine design.

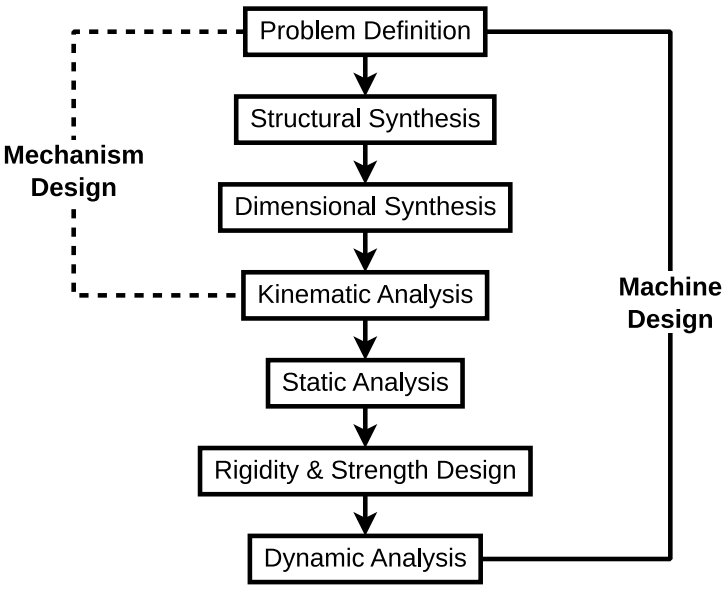

Source: Yan (1998).

A typical mechanism design process involves (HARTENBERG; DENAVIT, 1964; YAN, 1998; TSAI, 2001; MATA et al., 2016):

- KINEMATIC SYNTHESIS: design of a new mechanism that satisfies required motion characteristics from the input to output links to perform a task. It is subdivided in two main phases:
  - **Structural Synthesis:** enumeration of all feasible kinematic structures or linkage topologies for a given number of degrees of freedom, number of links, and type of joints. It is comprised by two steps:
    - *Number Synthesis:* determination of the number of links, joints and their interconnection needed to achieve a given mobility of the desired mechanism.
    - *Type Synthesis:* determination of specific type of kinematic pairs to meet the functional requirements of the mechanism. Other considera-

tions such as materials, manufacturing processes, and cost also can influence in the type synthesis.

  - **Dimensional Synthesis:** determination of appropriate dimensions of links as lengths, angles, and proportions for the mechanism to perform the desired motion.

- KINEMATIC ANALYSIS: study of relative motions associated with the links of a mechanism such as displacement, velocity, acceleration, etc., given an input motion and joint constraints.

The scope of this thesis is to investigate the structural characteristics of PGMs aiming to identify potential innovative gaps in design requirements for assisting designers in the structural synthesis of new mechanisms.

2.4.1 PGM Structural Synthesis

As stated in Chapter 1, it is possible to distinguish PGM design methodologies in two main approaches (FREUDENSTEIN; MAKI, 1979): *atlases of mechanisms* grouped according to function and *abstract representation* of the structure of mechanisms.

2.4.1.1 PGM Atlas-based Methodologies

The *atlases-based methodologies* represent an approach to mechanism design that involves utilizing a library of elementary mechanisms, known as building blocks, which are categorized based on their function (KOTA; CHIOU, 1992; SUBRAMANIAN; WANG, 1995; YAN; OU, 2005; HAN; LEE, 2006; OU et al., 2010; HU et al., 2017). These building blocks serve as design concepts with rules rather than specific structural forms. To create new mechanisms, at least two building blocks are combined, and their parameters are adjusted to meet the desired task.

Karhula and Nicolai (2018) presents a computational design synthesis using a block-based approach for PGMs. Design requirements are selected from a patent survey, and a declarative design model (Fig. 24) with constraints is used to generate multiple mechanism candidates. Three new 4-speed PGMs were discovered. In (KARHULA et al., 2019), the block-based method was extended considering symmetry breaking to exhaustively synthesize 2-, 3-, and 4-speed PGT designs (Fig. 25), resulting in new topologies. However, the method is computationally demanding.

In a recent study conducted by Köller and Schmitz (2022), an automated method for the synthesis of transmission topologies and the pre-design of gears for electric vehicles was introduced. Their method utilizes a library of topologies and employs a multi-criteria evaluation to optimize and rank the solutions (Fig. 26). The methodology was applied using a BMW i3 passenger car and a 40-ton truck as reference data to validate the model and reach new topologies.

Figure 24 – Declarative design model for a two-stage PGT.

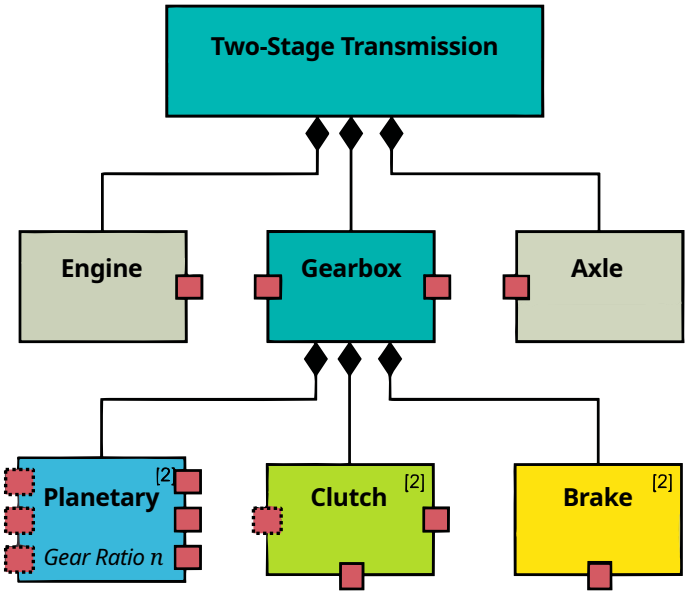

Source: Karhula and Nicolai (2018).

Figure 25 – Topology representation of a 4-speed PGT

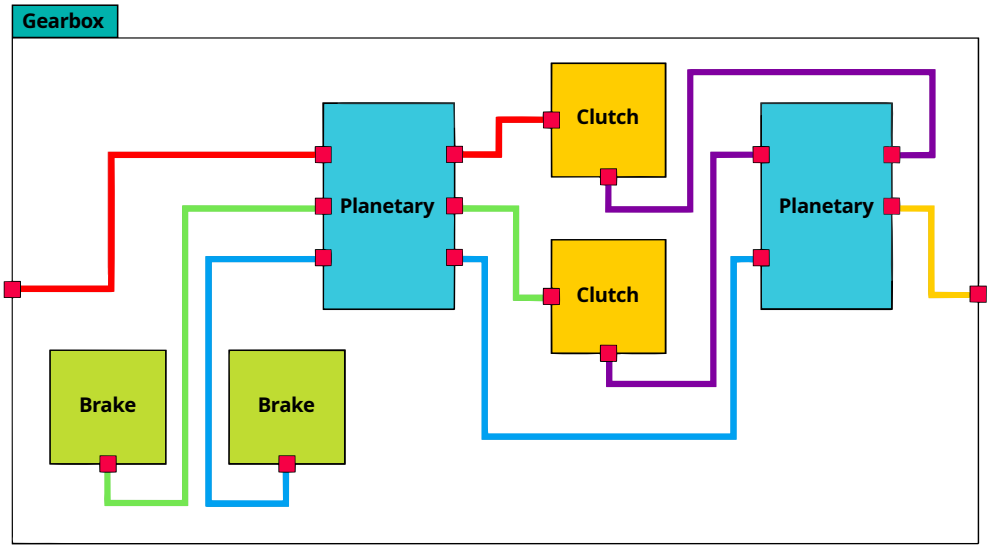

Source: Karhula et al. (2019).

2.4.1.2 PGM Abstraction-based Methodologies

The *abstraction-based methodologies* use representations such as equations, matrices, and graphs to design mechanisms. These considered creative design methodologies, also known as *enumeration-based methodologies*, systematically enumerate all possible kinematic structures of the same mobility, type of motion (planar, spatial, etc.), and complexity using graph theory, combinatorial analysis, and computer algorithms. Each kinematic structure is evaluated based on a subset of design specifications to select the most suitable mechanisms for further analyses, optimization, and detailing.

Figure 26 – Overview of a library based topology synthesis process for EVs.

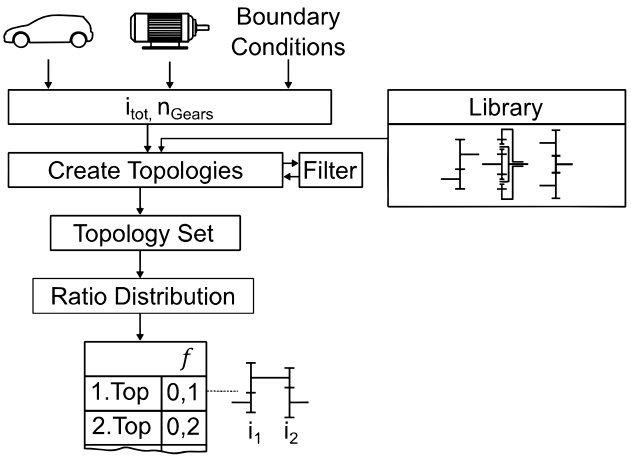

Source: Köller and Schmitz (2022).

Dobrjanskyj and Freudenstein (1967) proposed a systematic approach for enumeration of mechanisms using graph theory by separating the kinematic structure from functional considerations. Their approach was a significant development in the structural synthesis phase of the mechanism design process, and comprehensive reviews can be found in (YAN, 1992; TSAI, 2001; MRUTHYUNJAYA, 2003; SIMONI et al., 2011; YAN; CHIU, 2015; MURAI, 2019; DING et al., 2022).

In the structural synthesis of PGTs, graphs have significantly enhanced the capacity for abstraction in the design process, and their use has been extensively investigated. To achieve a feasible topology, any graph representing a PGT must comply with the structural characteristics detailed in Section 2.3.2.3. Buchsbaum and Freudenstein (1970) by separating the kinematic structure from functional considerations. Subsequently, Freudenstein (1971) presented the concepts of rotation and displacement graphs. The rotation graph is associated with the rotational displacement equations of a PGT based on the transfer vertex (arm link) and is derived from the topological graph by omitting revolute edges and transfer vertices. Then, each gear pair is labeled with the respective transfer vertex identifier. In contrast, the displacement graph pertains to the linear displacement equations of a PGT, depending on the center distance between gear pair axes. The displacement graph is generated from the rotation graph, with vertices labeled based on the edge pair levels connecting them to transfer vertices in the f-circuits where they reside. According to the review of Shanmukhasundaram et al. (2021), the structural synthesis of PGTs centers on enumerating all non-isomorphic displacement graphs given a specific number of links and degrees of freedom. The synthesis is categorized into three primary stages. Firstly, candidate PGT kinematic chains are based on graphs derived from existing PGTs. Then, isomorphism detection is performed to discard graphs with duplicate kinematic structures. Finally, non-isomorphic graphs are assessed to remove those corresponding to degenerate or rigid PGT chains (ALI et al.,

2022), which are subchains exhibiting zero DOF. Two main methodologies have been identified: generating all rotation graphs first and then producing displacement graphs for each non-isomorphic rotation graph, or directly enumerating all displacement graphs from a set of parent graphs. In both methodologies, an isomorphism test is imperative.

Various synthesis techniques for PGTs, such as the parent graph (BUCHSBAUM; FREUDENSTEIN, 1970; DING, 2015; SHANMUKHASUNDARAM et al., 2019), genetic graph (TSAI, 1987), and acyclic graph (HSU; HSU, 2000), have been adopted. Irrespective of the method chosen, the inventive design process typically relies on the intersection between a generalized atlas of topology candidates and design specifications to generate feasible mechanisms.

An example of a creative design methodology for structural synthesis is illustrated in Figure 27.

Figure 27 – Flowchart of a creative design methodology for structural synthesis.

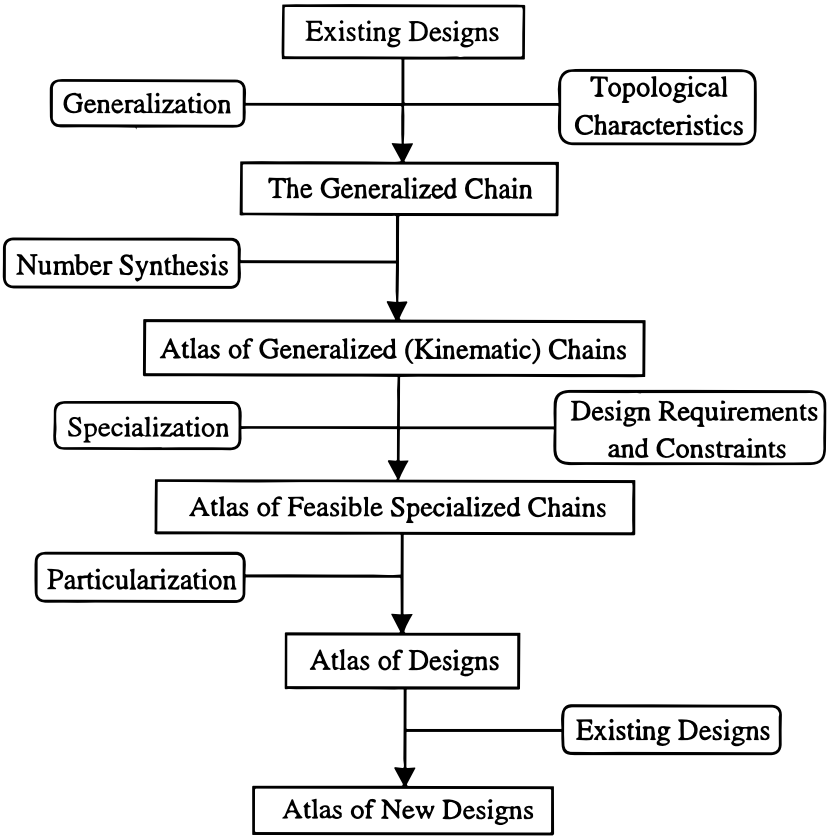

Source: Yan (1998).

In order to transform a PGT into a PGM, it is required to integrate the frame (F), input (IN), and output (OUT) links, as well as to identify the shift couplings essential for actuation. This procedure, referred to as *configuration synthesis*, involves making decisions about the positioning of each link, determining the number and location of shift couplings, and specifying their types. Generally, the most viable PGT kinematic structure (topology) from the enumeration are selected for further investigation. An ex-

haustive search method is subsequently utilized to generate all possible configurations of the mechanisms. Later on, three main criteria are used to evaluate these mechanisms: a kinematic analysis, which determines the number of unique gear ratios; an assemblability analysis, ensuring the absence of topological interferences; and a feasibility analysis, ensuring alignment with design specifications. For the configuration synthesis, a range of methods have been employed, such as coded sketches (HWANG; HUANG, 2011), the lever method (ROSS; ROUTE, 1991; HO; HWANG, 2020; KE et al., 2021), matrix-based strategies (DONG et al., 2023), and even relying on the expertise of designers (HWANG; HUANG, 2005; DING et al., 2020).

When it comes to mechanism design, each structural synthesis methodology has its own set of advantages and disadvantages. However, they all share core steps in the design process. Here are the key steps that are consistent across these methodologies:

1. **Define design specifications** by encompassing functional and structural requirements, design constraints, and relevant characteristics based on both customer needs and existing design analyses. The fundamental set of structural characteristics, including mobility, spatial order, and the number of links or independent loops, serve as the basis for enumeration. These values are usually derived from an existing design chosen as a reference benchmark. Any supplementary features, requirements, or constraints are then regarded as selection criteria for further feasibility evaluations.
2. **Formulate link assortments** by allocating the kinematic pairs among the links. Structural characteristics and design constraints are used to exclude non-viable partitions.
3. **Enumerate the kinematic chains** by generating all variations for each viable link assortment. Unviable kinematic chains are excluded, specifically those that are *degenerated* by being fractionated or having null mobility subchains ($M' = 0$), and those that are *isomorphisms* by having identical kinematic structures.
4. **Generate mechanisms** designs by:
   (a) Determine the *fixed link* for each feasible kinematic chain, thus generating all kinematic inversions.
   (b) Specify the *input* and *output links*, based on functional requirements translated to the mechanism's structural characteristics;
   (c) Specify the *shift couplings*, detailing their quantity, type, and placement.
5. **Eliminate potential isomorphisms and pseudoisomorphisms**.
6. Compare the generated mechanisms against existing designs to **discover innovation**.

From the preceding discussion, the significance of design specifications and structural characteristics throughout each step of the structural synthesis of mechanisms becomes evident. It is noteworthy that this procedure exhibits a combinatorial nature, leading to an exponential growth in the generation of solution candidates. Design specifications are pivotal in filtering out and discarding non-viable candidates. The primary challenge lies in determining requirements towards innovation that can effectively reduce unnecessary enumerations, minimize computational effort, and improve solution quality.

2.4.2 Design specifications

Design specifications, the detailed written descriptions of the mechanism, are obtained from a variety of sources such as customers needs, commercial products, academic publications, patent databases, among others.

A survey of existing designs in commercial products and an exhaustive search of patents is the primary step conducted by Yan (1998) to determine design specifications and deduce the minimal set of structural characteristics essential for enumeration. A transformation of functional requirements from customer needs into structural characteristics is proposed by Tsai (2001). In the mechanism design methodology presented by Murai (2019), based on previous studies (MURAI et al., 2013; MURAI et al., 2015), a state-of-the-art survey was initiated based on searches in commercial, academic, and patent domains for developing stitching devices. They introduced four structural characteristics and one structural requirement to help designers in the selection of enumerated kinematic chains. At the Laboratory of Applied Robotics Prof. Raul Guenther - LAR (LAR, 2018), where the author of this thesis is affiliated, a methodology for patent surveys on automotive mechanisms was presented by Hoeltgebaum et al. (2016b). Despite being tailored for mechanisms enumeration, the approach predominantly relies on subjective assessments and expertise, possible overlooking a diverse analysis of features. Consequently, the depth and effectiveness of the analysis may be limited by the narrow scope of features considered by the design team.

Focusing on determining PGT design specifications, Karhula and Nicolai (2018) conducted an assessment of 1022 patented automatic transmissions. Block models were employed, as described earlier, to delineate a technological boundary based on the complexity and capability of the mechanisms, as illustrated in Figure 28. Through their analysis, an innovation opportunity was identified in the domain of four-speed transmissions characterized by a complexity level of 8 (sum of gear contacts and shift couplings). Consequently, an exhaustive synthesis was applied, resulting in the proposal of three novel designs. The modeling of PGTs through the use of topological graphs was criticized by the authors, asserting that such representation does not include clutches and brakes. This perspective holds merit since topological graphs, as

commonly presented in the literature, predominantly represent and synthesize only the kinematic chains of the mechanisms, which inherently exclude the shift couplings. *However, in this thesis, topological graphs are applied to represent the entire mechanism, including the shifting couplings.* These couplings are regarded as revolute joints between link pairs. Subsequent analyses, as presented in Chapter 3, determine whether these are genuinely integrated actuators at the revolute joints or only actuators.

Figure 28 – Patent survey and technological boundary.

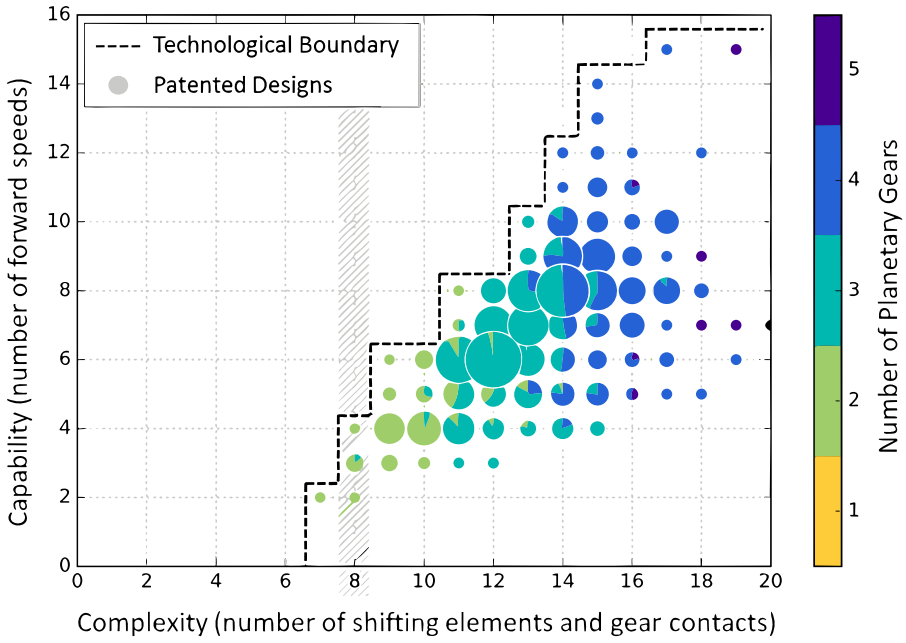

Source: Karhula and Nicolai (2018).

In a distinct study examining 673 patents to delve into the design specifications of PGTs used in existing AT designs, Ding and Cai (2019) employed double bicolored graphs for model representation. This approach identified 274 distinct topologies, which were further classified into 67 basic graphs (without differentiation of joint types). These graphs were sorted into 13 groups based on the mobility of the DBG and the adjacency degree of the hollow vertex. Upon analysis, certain characteristics of PGTs were observed: a range of 6 to 14 links, 4 to 9 coaxial links (level 'a'), a mobility ranging from 1 to 4, 2 to 6 gear rows, a singular input link per AT, and recommendable fewer than 4 engaging shift couplings for 2 or 3-DOF PGTs. Despite the extensive preliminary work cited, the authors proposed a methodology for deriving new PGT configurations based on basic graphs, with the intent to enhance the likelihood of innovation. This work results in 9 new DBG topologies with potential to numerous mechanisms. However, the invested research effort in patent analysis was utilized only to support decisions taken along the proposed synthesis process rather than to directly inform design specifications, optimizing the domain for an innovation-focused development.

From an industrial perspective, General Motors has developed hundreds of novel

architectures for multi-speed AT over recent decades, leading to designs that have been widely produced (RAGHAVAN, 2011). These achievements were result of an algebraic procedure rooted in the methodology of Hsieh and Tsai (1996a), which incorporates graph-based enumeration and transmission powerflow to complement traditional design approaches. This procedure was employed to synthesize AT and electrically variable transmissions (EVTs) with three PGSs and six or seven shift couplings, resulting in 8-speed transmissions (RAGHAVAN et al., 2007). Extensions to the lever analogy method (BENFORD; LEISING, 1981) for PGSs, including negative lever ratios, are presented by Raghavan (2010). Discussions on the utilization of long pinion (compound planets) for alternative AT architectures are provided in Raghavan (2013, 2018). Furthermore, the algebraic procedure was applied to produce AT and EVTs with four PGSs and five or six shift couplings, achieving eight or more forward speed ratios and a reverse ratio; this led to the introduction of the GM 8L90 model (RAGHAVAN, 2015; HART, 2014). Based on the General Motors researches, a range of selection criteria for AT topology can be summarized as:

- *Structural Requirements:*
  - Reduction in component count
  - Minimization of active shift couplings
  - Maximization of speed ratios
  - Emphasis on simple PGS
  - Maximization of input clutches
  - Reduction in spin losses (open actuators)
  - Accessibility of shift couplings to hydraulic circuitry
  - Requirement for a planar graph for feasibility
  - Ensuring uniqueness by checking isomorphisms
- *Functional Requirements:*
  - Achieving a wider ratio spread
  - Prioritizing single transition clutching
  - Inclusion of direct drive
  - Adherence to progressive ratio steps
- *Technical Requirements:*
  - Evaluation of both quantitative and qualitative measures of perceived quality in areas such as safety, dependability, reliability, cost, efficiency, performance, comfort, payload, excitement, noise reduction, compactness, and delivery timing for each candidate powerflow to determine the optimal selection for a range of vehicle applications.

Throughout this thesis, efforts are directed towards improving the challenges previously mentioned by proposing a process for a state-of-the-art survey and analysis of mechanisms, driven to the discovery of potential innovative design requirements. Emphasis is placed on the analysis of patent databases, though the scope is not limited exclusively to them.

2.5 CHAPTER HIGHLIGHTS

In Chapter 2, a detailed review of automotive automatic transmissions for passenger cars employing planetary gear trains is presented. Emphasis is placed on elucidating the kinematic structure of such mechanisms using graph representation and on understanding their associated characteristics. This review enables the comprehensive analysis of a wide collection of mechanisms and the examination of their design specifications. The ultimate objective is to assist transmission design engineers in identifying potential innovative requirements for the synthesis process within the domain of automotive AT design.

3 PGM MODELING REVISED AND NEW METRICS

Planetary gear mechanisms (PGMs), based on the structural characteristics of geared kinematics chains enumerated in Section 2.3.2.3, are expected to adhere to the Grübler-Kutzbach general mobility equation (Eq. (13)). This requirement has been followed in various studies on mechanism synthesis, including works by (RAVISANKAR; MRUTHYUNJAYA, 1985; TSAI, 2001; CAZANGI; MARTINS, 2007; KHULIEF, 2013; SHANMUKHASUNDARAM et al., 2021; DING et al., 2022).

However, it is essential to acknowledge that applying the general mobility equation to the topological graph of PGMs may present limitations due to the topological complexities that arise when active couplings, such as shift couplings, are incorporated into the PGT to generate the PGM. A revision in the graph model representation is proposed to attend to the research demands, giving rise to redundant and virtual constraints in the PGMs' graph representation. Case studies are presented to demonstrate these constraints, which are further considered for the revision of the general mobility equation accordingly.

Additionally, this chapter delves into the complex structural characteristics of PGMs. A discussion is instigated, and novel metrics are proposed to critically assess their performance according to topological characteristics. The complexity and capability metrics for mechanisms, including PGMs, are explored and presented to characterize technological performance indexes for innovation.

3.1 REVISION OF THE PGM GRAPH MODEL

In this research, attention is particularly given to an in-depth study of the topology of AT to compare their mechanisms and identify potential characteristics relevant to innovative design requirements.

As mentioned in Section 2.3.2, the PGM is usually a fractioned mechanism encompassing two degrees of freedom, being a one-DOF PGT supported by the housing of a transmission mechanism on a central axis. The ATs are actuated through an input joint and shift couplings to obtain the possible gear ratios. These active couplings impose additional constraints to those set by the kinematic pairs of the PGT, enabling torque transmission between the links to establish the power flow. Typically, for each configuration of active shift couplings that yields a power flow, the AT is recognized as a distinct PGM. In this regard, the edges of the topological graphs exhibited in Section 2.3.1 only represent the kinematic pairs of the mechanism, such as gear and revolute joints, without considering active couplings.

Shift couplings can be placed between any two links that revolve around the PGT's central axis, at level 'a'. There are two potential scenarios for allocating shift couplings:

1. Between links directly connected by a revolute joint, as a parallel coupling.
2. Between links not directly connected by a revolute joint, thereby working as a novel direct coupling.

In scenario one, the shift coupling is represented in the topological graph through the parallel revolute joint edge. However, in scenario two, the shift coupling is not included in the topological graph as there is no kinematic pair between the links.

One of the objectives of this research is the comprehensive analysis and comparison of the kinematic structure (topology) of each AT, representing them as unique PGM embodiments comprising all their couplings. To this end, all the shift couplings existing in the PGM will be assumed to have revolute joints in parallel and represented as edges in the topological graph.

However, by considering this hypothesis, a revision of the general mobility equation is necessary in order to avoid possible overconstraint conditions caused by redundancy among the kinematic pairs in PGMs. This revision is discussed through the presentation of case studies in the following section.

3.1.1 PGM Case Studies

In this section, four PGMs are depicted as case studies and their mobility is analyzed using the Grübler-Kutzbach criterion (Eq. (13)), ordered by increasing complexity. The results are discussed on a case-by-case basis to provide clarity on the mobility calculation for each topology.

3.1.1.1 Case 1: Simple PGT with 2 brakes

This PGM case refers to the simple PGT illustrated in Figure 29a, comprising:

- PGT:
  - one SPGS
  - no compound links
- PGM:
  - housing (F, ■)
  - input link (▲) in the Sun (S)
  - output link (▼) in the Ring (R) or the Arm (A)
  - two shift couplings:
    - ∗ two brakes (B1 and B2)

The PGM has a total of $n = 5$ links, $j = 6$ joints ($j_R = 4$ revolute and $j_G = 2$ gear joints), and 2 fundamental circuits as shown in the graph of Figure 29b. Considering

$\lambda = 3$, the mobility of this PGM is calculated as follows (Eq. (21)):

$$M = 3(5-6-1) + 4 \cdot 1 + 2 \cdot 2 = 2 \text{ DOFs} \tag{21}$$

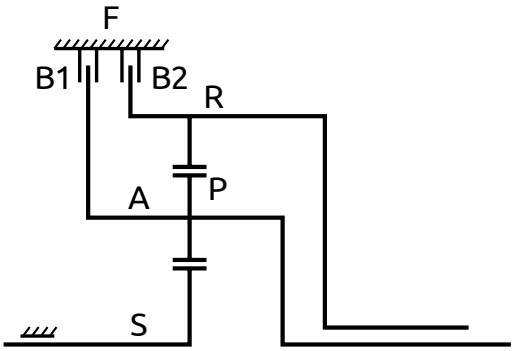

(a) Schematic representation

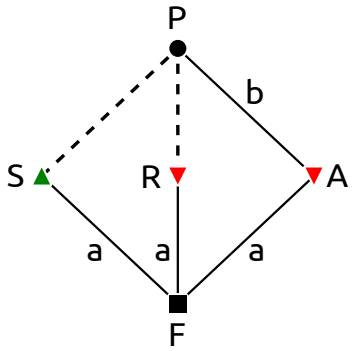

(b) Topological graph

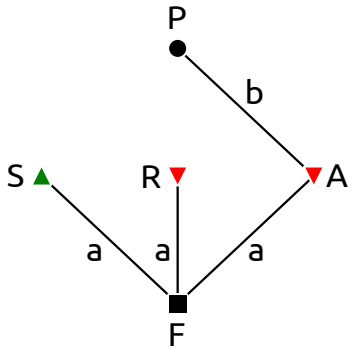

(c) Graph without $j_G = 2$

Figure 29 – Case 1: Simple PGT with 2 brakes

The obtained result of two DOFs is correct, comprising 1 DOF for the input rotation in the Sun, and the remaining 1 DOF associated with the actuation of one brake to create power flow to the selected output link. This is consistent with the structural characteristic of a fundamental circuit existing for each gear pair. The removal of the $j_g = 2$ gear pairs from the graph in Figure 29b results in a tree, as shown in Figure 29c.

3.1.1.2 Case 2: Simple PGT with 2 brakes and 1 clutch

This PGM, illustrated in Figure 30a, is a variation of the previous case (Section 3.1.1.1) by the addition of a clutch between links A and R for the direct gear ratio. It comprises:

- PGT:
  - one SPGS
  - no compound links
- PGM:
  - housing (F, ■)

- input link (▲) in the Sun (S)
- output link (▼) in the Ring (R) or the Arm (A)
- three shift couplings:
  - two brakes (B1 and B2)
  - one clutch (C1)

The PGM has a total of $n = 5$ links, $j = 7$ joints ($j_R = 5$ revolute and $j_G = 2$ gear joints), and 3 fundamental circuits as shown in the graph of Figure 30b. Considering $\lambda = 3$, the mobility of the PGM is calculated as follows (Eq. (22)):

$$M = 3(5 - 7 - 1) + 5 \cdot 1 + 2 \cdot 2 = 0 \text{ DOF.} \tag{22}$$

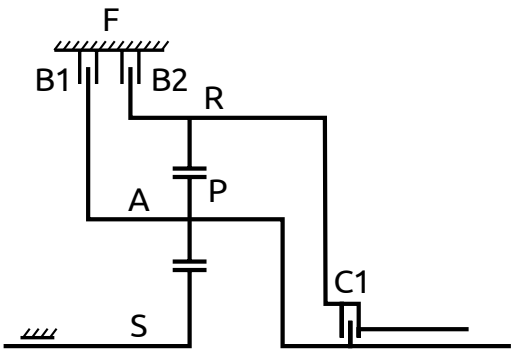

(a) Schematic representation

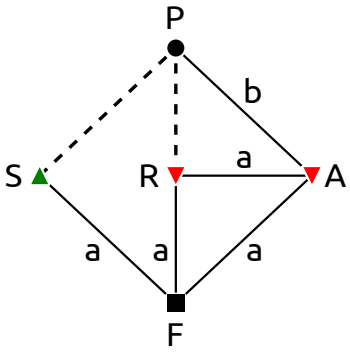

(b) Topological graph

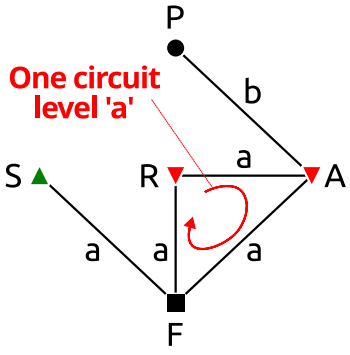

(c) Graph without $j_G = 2$

Figure 30 – Case 2: Simple PGT with 2 brakes and 1 clutch

The obtained result of zero degrees of freedom (DOF) is incorrect, as the expected mobility should be 2 DOF, comprising 1 DOF for the input rotation in the Sun, and the remaining 1 DOF associated with the actuation of 1 shift coupling to create power flow between input link and the selected output link. The inclusion of the clutch (C1) between links A and R, which already have the necessary structural constraints, resulted in redundant constraints, leading to an additional DOF in the mechanism. This situation violates the structural characteristic of existing a fundamental circuit for each pair of gears and can be identified by removing all gear pairs from the graph (Fig. 30b), resulting in a still connected graph as seen in Figure 30c when it should be a tree. The

remaining circuit is formed only by revolute joints at level 'a' as follows: B1:F-A, C1:A-R, B2:R-F.

3.1.1.3 Case 3: Simple PGT with 2 brakes, 2 clutches and output link

In this case, illustrated in Figure 31a, the previous PGM of Section 3.1.1.1 received the addition of an output link (OUT) and two clutches (C1 and C2). It comprises:

- PGT:
  - one SPGS
  - no compound links
- PGM:
  - housing (F, ■)
  - input link (▲) in the Sun (S)
  - output link (OUT, ▼)
  - four shift couplings:
    - two brakes (B1 and B2)
    - two clutches (C1 and C2)

The PGM has a total of $n = 6$ links, $j = 9$ joints ($j_R = 7$ revolute and $j_G = 2$ gear joints), and 4 fundamental circuits as shown in the graph of Figure 31b. Considering $\lambda = 3$, the mobility of the PGM is calculated as follows (Eq. (23)):

$$M = 3(6-9-1) + 7 \cdot 1 + 2 \cdot 2 = -1 \text{ DOF}. \tag{23}$$

The obtained result of one negative DOF is incorrect, as the expected mobility should be 3 DOF, comprising 1 DOF for the input rotation in the Sun, and the remaining 2 DOFs are associated with the actuation of 2 shifting elements to create power flow between input and output links. The inclusion of the output link (OUT) with clutches C1 and C2 to select the output rotation resulted in two circuits formed only by revolute joints at level 'a': B1:F-A, C1:A-OUT, a:OUT-F and B2:F-R, C2:R-OUT, a:OUT-F. As explained in the previous Section 3.1.1.2, this situation violates the structural characteristic of existing a fundamental circuit for each gear pair and can be identified by removing all gear pairs from the graph (Fig. 31b), resulting in a still connected graph as seen in Figure 31c.

Incorporating a shift coupling between coaxial links leads to the formation of a redundant circuit, violating the structural characteristics of the mechanism. However, this type of circuit can be inherent in the topology of PGMs and should be considered in the mobility equation by including their respective redundant joints.

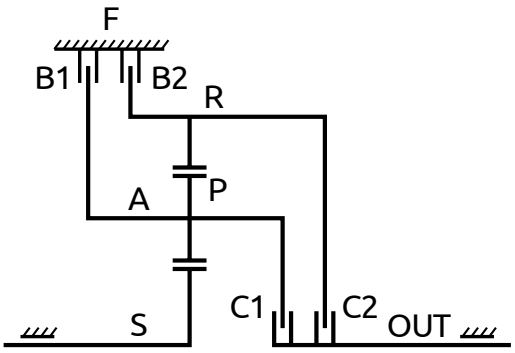

(a) Functional Schematic

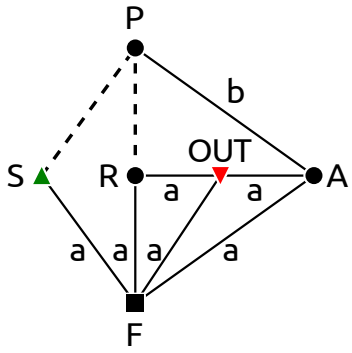

(b) Topological graph

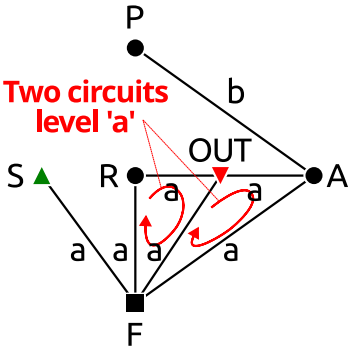

(c) Graph without $j_G = 2$

Figure 31 – Case 3: Simple PGT with 2 brakes, 2 clutches and output link

3.1.1.4 Case 4: GM 6-speed automatic transmission

The GM 6T40 (SINGH; OLENZEK, 2010), illustrated in Figure 32a, is a transversal commercial 6-speed automatic transmission model studied in this case. It comprises:

- PGT:
  - three SPGS
  - three compound links:
    - A1;R3
    - R1;A2
    - R2;A3
- PGM:
  - housing (F, ■)
  - input link (IN, ▲) in the Sun (S2)
  - output link (OUT, ▼) in compound link (A1;R3)
  - five shift couplings:
    - three brakes (B1, B2, and B3)

∗ two clutches (C1 and C2)

The PGM has a total of $n = 10$ links, $j = 16$ joints ($j_R = 10$ revolute and $j_G = 6$ gear joints), and 7 fundamental circuits as shown in the graph of Figure 32b. Considering $\lambda = 3$, the mobility of this PGM is calculated as follows (Eq. (24)):

$$M = 3(10 - 16 - 1) + 10 \cdot 1 + 6 \cdot 2 = 1 \text{ DOF.} \tag{24}$$

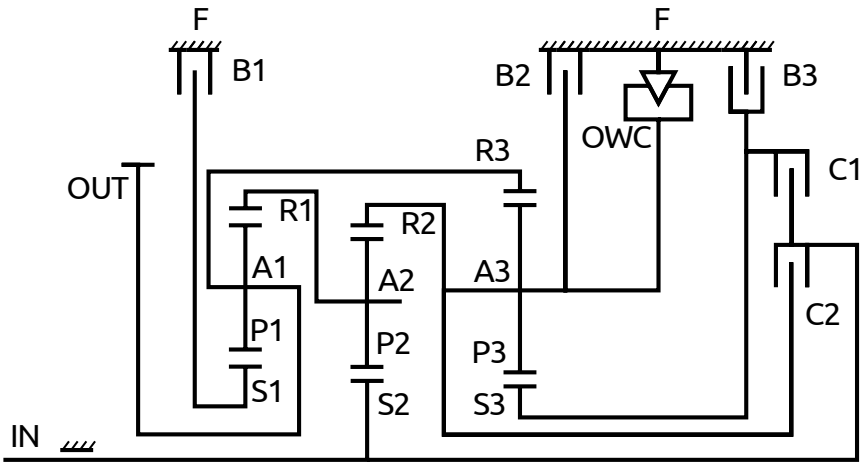

(a) Functional Schematic

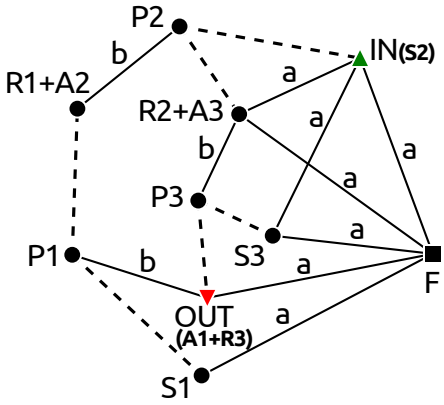

(b) Topological graph

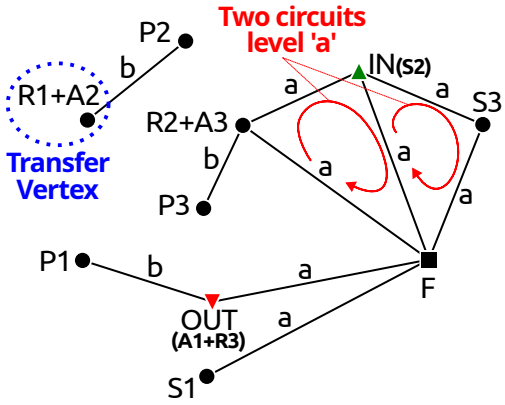

(c) Graph without $j_G = 6$ gear joints

Figure 32 – Case 4: GM 6-speed model 6T40

The obtained result of 1 DOF is incorrect, as the expected mobility should be 3 DOF, comprising 1 DOF for the input rotation, and the remaining 2 DOFs for the actuation of 2 shift couplings to create power flow between the input and output links. Further analysis of the structural characteristics of the 6T40 mechanism reveals that three fundamental circuits violate structural characteristics. By removing all gear pairs from the graph (Fig. 32b), it results in a disconnected graph with two components as shown in Figure 32c.

The bigger component has two remaining circuits formed only by revolute joints at level ‘a’ as follows: B2:F-R2, C1:R2-IN, a:IN-F, and B3:F-S3, C1:S3-IN, a:IN-F. These are redundant circuits and must be included in the mobility calculation.

The smaller component comprises the planet (P2) connected to its corresponding arm formed by the link (R1;A2) through a revolute joint at level ‘b’. According to PGT structural characteristics (BUCHSBAUM; FREUDENSTEIN, 1970), this subgraph should have the link (R1;A2) connected to a link at level ‘a’ through a revolute joint to function as a transfer vertex (Fig. 32c). However, the real mechanism is manufactured and operates without this joint in its topology. This phenomenon is attributed to the presence of multiple planets that are equidistantly distributed around the sun and the ring, not being assigned in the graph model. This arrangement of planets results in a combination of constraints that statically balance the arm (R1;A2) and ensure its rotation around the central axis, eliminating the need for a physical revolute joint at level ‘a’. This virtual constraint should be considered in the mobility calculation.

3.1.2 Definition of Redundant Joints j_Q and Virtual Joints j_V in PGMs

As demonstrated in the case studies (Section 3.1.1), topological complexities as redundant and virtual constraints should be accounted for in the mobility equation of PGMs.

Definition 3.1.1 (Redundant Joints (j_Q))**.** In PGM analysis, redundant joints refer to revolute joints introduced in parallel to shift couplings between coaxial links that lack a pre-existing revolute joint. These joints represent hypothetical excess of constraints within the kinematic structure, often leading to overconstrained circuits composed solely of revolute joints at level ’a’. While feasible due to potential coaxial link arrangements, redundant joints complicate the analysis of a mechanism’s motion (kinematics) and its degrees of freedom (mobility).

Redundant joints typically appear in the graph model when a shift coupling is added between coaxial links already constrained by revolute joints with other links. This connection necessitates the representation of the shift coupling but also implies the presence of an additional revolute joint. Although this configuration is physically possible (e.g., a shaft with multiple bearings), it impacts PGM mobility calculations. To ensure consistency, one revolute joint must be excluded from each redundant circuit during mobility analysis. This excluded joint is termed a "redundant joint j_{Q_i}".

Each redundant joint corresponds to an active revolute joint at level ’a’, representing $c_{R,\lambda}$ redundant constraints to the mechanism. Since redundant joints are initially included in the revolute joint count j_R in the graph representation, they must be subtracted to accurately assess the mechanism’s mobility. Therefore, the accurate total joint count (j) is given by (Eq. (25)):

$$j = j_R - j_Q + j_G \quad , \tag{25}$$

where j_Q is the sum of all j_{Q_i} redundant joints in the graph.

Definition 3.1.2 (Virtual Joints (j_V))**.** In PGM analysis, virtual joints represent passive revolute joints at level 'a' that implicitly arise from specific arrangements of planets, sun gear, and ring gear.

Their presence is implied by the symmetrical distribution of planets, which creates a balanced set of constraints that enforce rotation of the arm around the central axis. This configuration eliminates the need for a physical revolute joint at level 'a'. While not explicitly modeled in the graph, each virtual joint (j_{V_i}) represents $c_{R,\lambda}$ constraints on the mechanism, necessitating their inclusion in mobility calculations.

Therefore, to accurately assess PGT mobility, the total joint count (j) within the mobility equation must be modified as follows (Eq. (26)):

$$j = j_R + j_V + j_G \quad , \tag{26}$$

where j_V is the sum of all j_{V_i} virtual joints in the PGM.

Considering both effects (Equations (25) and (26)), the total number of joints j must be revised as follows (Eq. (27)):

$$j = j_R - j_Q + j_V + j_G \tag{27}$$

where j_Q is the sum of each redundant joint j_{Q_i} and j_V is the sum of each virtual joint j_{V_i}.

3.1.3 A Revised Mobility Equation for PGMs

A revised mobility equation for PGMs, accounting for the effects of redundant and virtual constraints, can be obtained by substituting the total number of joints (Eq. (27)) in the general mobility equation (Eq. (9)). This results in the following expression (Eq. (28)):

$$M = \lambda(n-1) - \underbrace{(j_R + j_V - j_Q) \cdot c_{R,\lambda}}_{\text{revolute joints}} - \underbrace{j_G \cdot c_{G,\lambda}}_{\text{gear joints}} \quad . \tag{28}$$

Table 4 indicates that the degree of constraint for revolute joints is $c_{R,\lambda} = \lambda - 1$. For gear joints, the degree of constraint is $c_{G,\lambda} = 1$ with the exception to spur gear pairs in cases where $\lambda > 3$. By substituting these constraints in Equation (28), the revised mobility equation for PGMs for motion spaces up to $\lambda \leq 3$ is presented in a simple and concise form (Eq. (29)):

$$M = \lambda(n-1) - (j_R + j_V - j_Q) \cdot (\lambda - 1) - j_G \quad . \tag{29}$$

The Equation (29) is a general equation able to analyze the mobility of PGMs as only a function of the motion space and the number of joints of each type in the mechanism. When there are no redundant or virtual joints, i.e., $j_Q = j_V = 0$, the mobility equation becomes the original Grüebler-Kutzbach criterion (Eq. (10)).

3.1.4 Mobility Review of the Case Studies

Next, the revised mobility equation (Eq. (29)) is applied to each case study (Section 3.1.1) to demonstrate its validity.

3.1.4.1 Case 1: $j_Q = j_V = 0$

In Case 1 (Section 3.1.1.1), there are no redundant or virtual joints, and the mobility equation (Eq. (29)) reverts to the original Equation (10).

3.1.4.2 Case 2: $j_Q = 1$

In Case 2 (Section 3.1.1.2), the addition of clutch (C1) between arm (A) and ring (R) resulted in one redundant circuit (B1:F-A, C1:A-R, B2:R-F), which is represented by $j_Q = 1$ redundant joint. There are no virtual joints ($j_V = 0$) in this case. Substituting these joints into Equation (29) result in (Eq. (30)):

$$M = 3(5-1) - (5+0-1) \cdot (3-1) - 2 = 2 \text{ DOF.} \tag{30}$$

The obtained result aligns with the expected mobility of 2 DOF for this PGM, as discussed in the previous Section 3.1.1.2.

3.1.4.3 Case 3: $j_Q = 2$

In Case 3 (Section 3.1.1.3), the inclusion of the output link (OUT) with clutches C1 and C2 resulted in two redundant circuits (B1:F-A, C1:A-OUT, a:OUT-F and B2:F-R, C2:R-OUT, a:OUT-F), which are represented by $j_Q = 2$ redundant joints. There are no virtual joints ($j_V = 0$) in this case. Substituting these joints into Equation (29) result in (Eq. (31)):

$$M = 3(6-1) - (7+0-2) \cdot (3-1) - 2 = 3 \text{ DOF.} \tag{31}$$

The obtained result aligns with the expected mobility of 3 DOF for this PGM, as discussed in the previous Section 3.1.1.3.

3.1.4.4 Case 4: $j_Q = 2$ and $j_V = 1$

In Case 4 (Section 3.1.1.4), the PGM contains three circuits that violates the structural characteristics stated for PGTs. The first two are redundant circuits formed only by revolute joints at level ‘a’ (B2:F-R2, C1:R2-IN, a:IN-F, and B3:F-S3, C1:S3-IN, a:IN-F) which are represented by $j_Q = 2$ redundant joints. The third circuit (g:R2-P2, b:P2-R1, g:R1-P1, b:P1-OUT, g:OUT-P3, b:P3-R2) does not form a transfer vertex in the arm integrating the link (R1;A2). However, the presence of multiple equidistantly distributed planets (P2) around the sun (S2) and the ring (R2) statically balances the link (R1;A2), eliminating the need for a physical revolute joint at level ‘a’. Although not

explicitly represented in the graph model, the virtual constraint must be accounted for by considering $j_V = 1$ virtual joint. Substituting these joints into Equation (29) yields (Eq. (32)):

$$M = 3(10-1)-(10+1-2)\cdot(3-1)-6 = 3 \text{ DOF}. \tag{32}$$

The obtained result aligns with the expected mobility of 3 DOF for this PGM, as discussed in the previous Section 3.1.1.4.

Another evaluation of the revised mobility equation (Eq. (29)) is to consider different motion spaces as $\lambda = 2$ and 6. Applying the revised mobility equation in the motion space $\lambda = 2$ to this Case 4 results in (Eq. (33)):

$$M = 2(10-1)-(10+1-2)\cdot(2-1)-6 = 3 \text{ DOF}. \tag{33}$$

And going to the spatial motion space $\lambda = 6$ to this Case 4 results in (Eq. (34)):

$$M = 6(10-1)-(10+1-2)\cdot(6-1)-6 = 3 \text{ DOF}. \tag{34}$$

Both obtained results align with the expected mobility of 3 DOF for this PGM, showing the applicability of the revised mobility equation (Eq. (29)) in different motion spaces.

3.1.5 Mobility Discussions and Contributions for PGMs

The analysis of mobility in PGMs has led to important discussions and contributions. One significant aspect is the consideration of redundant and virtual joints within the mobility equation.

Redundant joints offer the potential to expand the number of gear ratios in PGMs by introducing additional shift couplings. However, it is essential to exclude the redundant constraints from the mobility calculation.

On the other hand, virtual joints arise due to combined constraints resulting from the equidistant distribution of multiple planets, ensuring rotational degrees of freedom relative to the central axis of certain links, such as the arm and the ring. These constraints cannot be directly identified in the graph representation of PGMs, as they depend on the complete graph (not simplified) and the geometric position of components not assigned in topological graph representation. Thus, it is necessary to include these combined constraints in the mobility equation.

The identification of redundant and virtual joints in PGMs can be achieved by removing all gear joints from the graph and applying search algorithms (SKIENA, 2008), such as Depth-First Search (DFS) or Breadth-First Search (BFS), to detect remaining circuits (indicating redundant joints) and disconnections (indicating virtual joints).

3.2 PGM: COMPLEXITY AND CAPABILITY

In the preceding sections, the complex topology of PGMs has been highlighted, illustrating the myriad of combination possibilities available to meet functional requirements.

As this metrics section begins, it is crucial to emphasize a few points. While there is an abundance of methods for the enumeration and synthesis of kinematic chains, these methods produce a considerable volume of chains. However, bridging the gap between theoretical outcomes and their practical applications poses challenges. Predominantly in industrial practice, solutions are frequently driven by economic factors and the pursuit of manufacturing efficiency, with a common objective of simplifying assembly processes. This inclination towards simplicity often leads to a reduction in overall complexity. Such simplified solutions demand thorough evaluation, emphasizing the need for a well-defined complexity criterion. Rare works like Karhula and Nicolai (2018) and Köller and Schmitz (2022) do utilize certain complexity metrics; however, these metrics do not adequately capture the topological complexity inherent to the PGMs.

Within this section, the objective is to present and refine a more suitable complexity criterion. Once articulated, this metric will be subsequently employed for the analysis or optimization of planetary gear trains.

Suh (2005) refers to complexity, in this context, as the uncertainty in satisfying functional requirements within the design range. The author highlights the importance of measuring topological complexity in engineered systems to improve design and operation efficiency and move away from trial-and-error approaches. According to Hennig et al. (2022), understanding the complexity of systems is considered a primary driver of adverse project outcomes, including cost, schedule, and scope overruns. They conducted a rigorous benchmarking study on complexity measures for engineering systems and found numerous studies but little consensus on "how" complexity should be measured and what constitutes a good measure. However, the literature consistently expects that complexity growth is correlated with increases in size, the number of interconnections, and the randomness of the system architecture. As stated by Sinha and Suh (2018), structural complexity arises when a system has many components, and the interaction between them is difficult to describe or understand. Elmaraghy et al. (2012) reviewed in deep the complexity metrics for design process, products, manufacturing, and business. For them, the increase in complexity should be justified only if it improves system capabilities and performance, but should otherwise be minimized. Regardless of the objective, it is important to characterize and measure complexity at all levels.

It becomes evident that measurement of the topological complexity of PGMs can assist in the decision-making process for design, enabling the determination of more suitable design requirements, including parameters and values. Mechanisms with

higher functional capacity and lower topological complexity are considered more topologically efficient, potentially impacting costs, production, operation, and maintenance. Moreover, in cases of isomorphisms and pseudoisomorphisms, complexity serves as a decisive metric in differentiating between them.

Although the term *complexity* is widely used in discussions about PGM topology, but there is limited literature on measuring the complexity itself of these mechanisms. Freudenstein and Maki (1979) attribute the complexity to the number of independent circuits or closed loops in the mechanism. Tsai (2001) suggests parameters that may increase mechanism topology complexity, such as the number of loops, vertices, length of peripheral loops, use of clutches for connecting PGSs, and presence of floating carriers, but does not utilize them for this purpose. Similarly, Karhula and Nicolai (2018) and Karhula et al. (2019) emphasize that the complexity of automatic transmissions can be assessed by the sum of shift couplings and gear pairs, wherein the design process aims to optimize capability while minimizing complexity. In a recent work, Köller and Schmitz (2022) restricted the complexity of PGMs to the cumulative count of major components, including gears, synchronizers, clutches, and brakes.

The aforementioned parameters are important for analyzing PGM complexity; however, they are limited to individual entities or subchains of the mechanism. Solely, they fall short in capturing the overall complexity of the mechanisms. A more in-depth metric for complexity can improve the comparative assessment of mechanisms and support the selection of optimal parameters during the design phase. In the subsequent sections, improved metrics to quantify complexity and capability inherent to PGMs will be presented.

3.2.1 PGM Structural Complexity Metric

The PGM structural complexity metric applied in this thesis is an adaptation of the work of Sinha and Weck (2013), which presents an interesting approach to measuring structural complexity for engineered complex systems. This approach provides a comprehensive characterization by capturing complexities of individual components (local effect), pairwise interfaces (local effect), and the system's architecture (global effect). An overview of the structural complexity metric is shown in Figure 33.

In this thesis, the structural complexity metric (Fig. 33) is adapted to fit the domain of PGMs. In order to avoid misinterpretation on symbols of variables, the structural complexity metric will be designated by Cx, and thus also extended to its components as shown below (Eq. (35)).

$$Cx(n, j, A) = \underbrace{Cx_1}_{\text{links}} + \underbrace{Cx_2}_{\text{joints}} \cdot \underbrace{Cx_3}_{\text{topology}} \quad , \tag{35}$$

where n is the number of links, j is the number of joints and A is the adjacency matrix.

Figure 33 – Overview of the structural complexity metric.

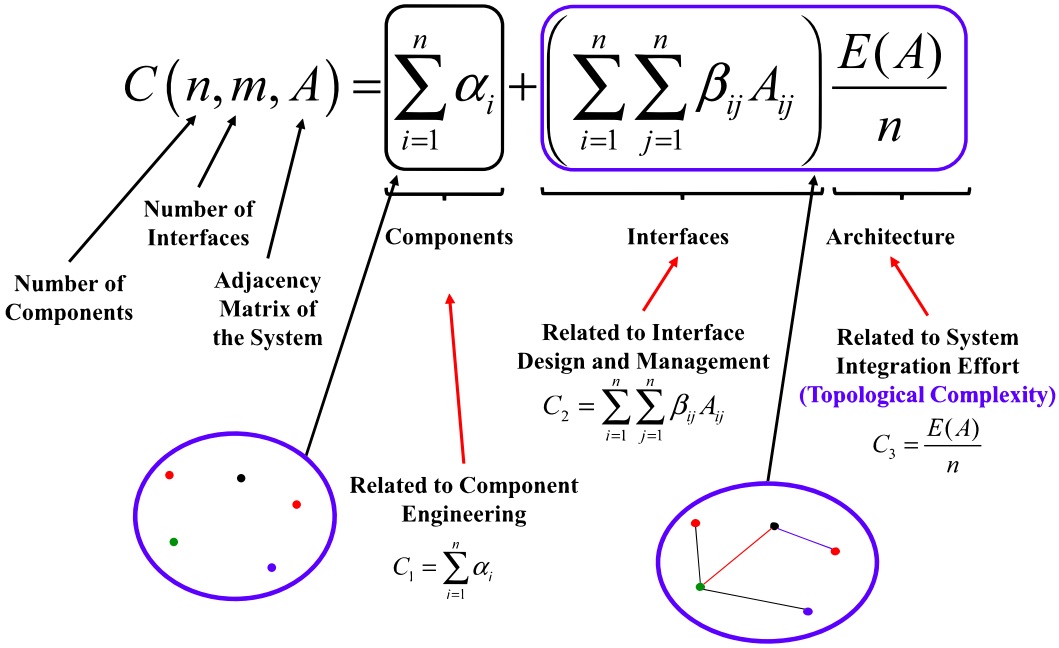

Source: Adapted from Sinha and Suh (2018).

3.2.1.1 *PGM Link Complexity (Cx_1)*

Link complexity (Cx_1) represents the combined complexity of all links in a mechanism and is calculated by summing (Eq. (36)) their individual complexities (α_i):

$$Cx_1 = \sum_{i=1}^{N} \alpha_i \tag{36}$$

Individual complexities (α_i) focus on the technical design difficulty of each component, without considering complexity stemming from interfaces (SINHA, 2014). Factors such as performance, size, reliability, knowledge requirements, and reusability should inform this assessment. Estimation methods may include expert opinion (when reliable data are unavailable), technological maturity (Technology Readiness Level - TRL), or data analytics.

An improved mathematical formulation is presented in this thesis to represent individual complexity (α_i) of a PGM link i, described as (Eq. (37)):

$$\alpha_i = k(i) + \left(CL_{factor}(links_i) \cdot \sum_{l=1}^{l_i} \alpha_{link,l} \right) \quad , \tag{37}$$

where:

- $k(i)$ is the degree of adjacency (e.g., binary, ternary).
- $links_i$ is the sequence of elementary links composing link i.
- $CL_{factor}(links_i)$ is a weighting factor for compound links (CL), accounting for radial transition costs between elementary links.

- $\alpha_{link,I}$ is the relative individual complexity of each elementary link within link i, as presented in Table 11.

For compound links, the CL_{factor} weights the complexity based on radial level transitions between elementary links. It is calculated as the product of individual transition costs (Eq. (38)). Transitions among sun gear (S), arm (A), and ring gear (R) incur complexity penalties as outlined in Table 10. Higher values indicate more complex radial transitions within the compound link. For single links, the CL_{factor} is 1.

$$CL_{factor} = \prod_{i=1}^{n-1} C(link_i, link_{i+1}) \quad , \tag{38}$$

where $C(link_i, link_{i+1})$ is the transition cost between two consecutive elementary links.

Table 10: Compound link transition cost conditions.

Condition	**Transition**	$C(link_i, link_{i+1})^*$
C1	Same link level (ex. S1;S2, A1;A2, R1;R2.)	1.03
C2	Between arm (A) level to other levels (ex. A1;S2, A1;R2)	1.05
C3	Between sun (S) and ring (R) levels (ex. S1;R2, R1;S2)	1.07

* Cost of each individual transition.

Source: Author.

Relative complexity values are assigned based on the author's expertise, comparing all elementary links within a PGS and treating the input shaft (singly) as the simplest component. Factors considered include geometry, design uniqueness, manufacturing processes, modularity, tolerances, and material requirements. Individual complexity (α_i) of a compound link is the sum of the complexities of its constituent elementary links multiplied by their transition factors.

Table 11 – Relative individual complexity attributed to elementary links of PGMs.

Link	Symbol	α_{link}
Input shaft	IN	1.0
Output shaft	OUT	1.0
Sun	S	1.5
Planet	P, PS, PR	1.6
Arm	A	1.8
Ring	R	1.9
Frame	F	5.0
Others		1.0

Source: Author.

As an illustrative example, consider a quinary ($k(i) = 5$) compound link consisting of the following elementary links sequence: A1 $\rightarrow$ R2 $\rightarrow$ S3 $\rightarrow$ S4. The compound link factor (CL_{factor}) is calculated as follows:

- A1 $\rightarrow$ R2: *(C2) Transition between arm level and other level* $\rightarrow C(A1, R2) = 1.05$
- R2 $\rightarrow$ S3: *(C3) Transition between sun and ring levels* $\rightarrow C(R2, S3) = 1.07$
- S3 $\rightarrow$ S4: *(C1) Same link level* $\rightarrow C(S3, S4) = 1.03$

Therefore:

$$\begin{aligned} CL_{factor} &= C(A1, R2) \cdot C(R2, S3) \cdot C(S3, S4) \\ &= 1.05 \cdot 1.07 \cdot 1.03 \\ &\approx 1.157 \end{aligned}$$

The relative individual complexity $\alpha_{link,I}$ is calculated as follows:

- A1: *Arm* $\rightarrow \alpha_{link}(A1) = 1.8$
- R2: *Ring* $\rightarrow \alpha_{link}(R2) = 1.9$
- S3: *Sun* $\rightarrow \alpha_{link}(S3) = 1.5$
- S4: *Sun* $\rightarrow \alpha_{link}(S4) = 1.5$

Therefore:

$$\begin{aligned} \sum_{I=1}^{4} \alpha_{link,I} &= \alpha_{link}(A1) + \alpha_{link}(R2) + \alpha_{link}(S3) + \alpha_{link}(S4) \\ &= 1.8 + 1.9 + 1.5 + 1.5 \\ &= 6.7 \end{aligned}$$

And finally, the individual complexity (α_i) of this compound link result as:

$$\alpha_i = 5 + (1.157 \cdot 6.7) \approx 12.753 \quad .$$

It is important to note that this assessment is qualitative and serves as a starting point for individual complexity analysis.

3.2.1.2 PGM Coupling Complexity (Cx_2)

The coupling complexity (Cx_2) in the mechanism represents the complexities arising from their couplings, encompassing joints (kinematic pairs) and actuators (active couplings). It is calculated by summing the pairwise complexities ($\beta_{i,j}$) of each coupling (Eq. (39)):

$$Cx_2 = \sum_{i=1}^{n} \sum_{j=1}^{n} \beta_{i,j} \cdot A_{i,j} \quad , \tag{39}$$

where $A_{i,j}$ is the adjacency matrix related to the PGM graph.

As suggested by Sinha (2014), the pairwise complexity ($\beta_{i,j}$) of each coupling interface (i and j) can be estimated based on a function that considers the complexities of the interfacing components (α_i, α_j) and the characteristic properties of the interface

type. In this thesis, for simplicity, the pairwise complexity of each coupling in a PGM is given by (Eq. (40)):

$$\beta_{i,j} = \beta_{kp} \cdot \max(\alpha_i, \alpha_j) \quad . \tag{40}$$

Where $\max(\alpha_i, \alpha_j)$ captures the higher link complexity in the pair and β_{kp} is the relative pairwise complexity attributed to couplings based on the pair characteristics such as type, level, and function, according to the author's expertise as detailed in Table 12.

Table 12 – Relative pairwise complexities attributed to couplings of PGMs.

Coupling Type	Level	β_{kp}
Virtual	*a*	0.0
Revolute (planets)	*b* or higher	1.0
Revolute (coaxial)	*a*	1.2
Input	*a*	1.3
Output	*a*	1.3
External Gear	*g*	1.4
Internal Gear	*g*	1.5
Brake	*a*	1.8
Clutch	*a*	2.0

Source: Author.

The planets revolute joints (level 'b' or higher) were considered the simplest joint in PGMs and has been designated a reference complexity value of 1.0. The coaxial revolute joints (level 'a'), which require critical alignment, lubrication channels, and the inclusion of additional components such as bearings, have been rated at 1.2 in complexity. Owing to their sealing prerequisites, input/output shaft joints have been assigned a relative complexity of 1.3. In addition to geometric complexity, gear meshes require precise tolerances to maintain center distances. Sun-planet external gearing has been attributed a complexity of 1.4, while planet-ring internal gearing has been assigned a value of 1.5. Shift couplings, typically multifaceted in design and demanding precision in hydraulic operation, are regarded as having the highest complexity among joints. Brakes, which are anchored to the housing, were given a complexity rating of 1.8. Furthermore, clutches between two movable links have been determined to have a complexity of 2.0, primarily attributed to the increased challenges associated with accessing the hydraulic fluid essential for their operation.

It is imperative to acknowledge that these values serve as an initial reference, and real-world complexities might be detailed depending on specific design requirements and operational scenarios. A more rigorous complexity index for lower kinematic pairs, grounded in the concept of *loss-of-regularity*, is introduced by Khan et al. (2007). However, no literature addresses the complexity of higher kinematic pairs, especially gear pairs in PGM transmissions.

3.2.1.3 PGM Topological Complexity (Cx_3)

The topological complexity metric (Cx_3) originates from interaction between elements and depends on the nature of such connectivity structure, being determined as (Eq. (41)):

$$Cx_3 = \frac{1}{n} \cdot E(A) \quad , \tag{41}$$

where

$$E(A) = \sum_{i=1}^{n} \sigma_i \quad . \tag{42}$$

$E(A)$ is the graph energy resulted as the sum of the singular values (σ_i) obtained by the singular value decomposition of the adjacency matrix A.

As depicted by Sinha (2014), the Cx_3 is associated with the topology pattern of the graphs as follows:

$Cx_3 < 1$: *hypoenergetic* $\Rightarrow$ Centralized Architecture

$1 \leq Cx_3 < 2$: *transitional* $\Rightarrow$ Hierarchical/Layered Architecture

$Cx_3 \geq 2$: *hyperenergetic* $\Rightarrow$ Distributed Architecture

The structural complexity metric can provide a comprehensive assessment of mechanisms, considering both individual and collective complexities. It is important to note that the specific formulation and calculation methods for these features must be adapted depending on the mechanisms and specific requirements of each study.

3.2.2 PGM Capability Metric

Capability metrics are designed to quantify the ability of mechanisms to perform their designated tasks and to evaluate their performance. Such metrics are commonly associated with the functional requirements of mechanisms and are sometimes referred to as performance metrics. Parameters related to the kinematics, statics, and dynamics of mechanisms in both local and global configurations are evaluated by these metrics (RUSSO, 2022).

In this thesis, a mechanism functional capability metric (Ca) is introduced. This metric intends to capture a functional trade-off between benefit and cost: a quantifiable output related to the primary function of the mechanism and its actuation efficiency. It is defined as follows (Eq. (43)):

$$Ca = Ca_1 + Ca_2 \quad , \tag{43}$$

where Ca_1 is the term associated with a quantifiable output performance metric, and Ca_2 is the term associated with actuation efficiency.

3.2.2.1 PGM Performance metric (Ca_1)

The choice of a performance metric (Ca_1) is influenced by the type of mechanism and the specific function under consideration. It might be the global conditioning index for robots, the maximum displacement for a linkage, or other relevant metrics.

For PGMs, the output performance metric is determined by their number of forward gears, as given by (Eq. (44)):

$$Ca_1 = \text{Gears}_{FWD} \tag{44}$$

3.2.2.2 PGM Actuation Efficiency metric (Ca_2)

The actuation efficiency metric (Ca_2) is defined as the reciprocal of the mechanism's mobility:

$$Ca_2 = \frac{1}{M} \quad , \tag{45}$$

where M denotes the mobility.

Thus, when mechanisms are compared, a higher output response combined with a reduced required actuation for its achievement indicates a superior mechanism functional capability metric Ca.

Such a capability metric offers a quantitative assessment of mechanisms' abilities and facilitates a thorough analysis of their functionality.

3.3 CHAPTER HIGHLIGHTS

In Chapter 3, a thorough review of the PGM graph model was conducted. An assumption was made wherein all shift couplings possess a parallel revolute joint to be depicted accurately in the topological graph. This assumption can yield overconstraints, resulting in redundant circuits of revolute joints at level 'a'. Additionally, virtual constraints were recognized, emerging from the assembly of equidistantly distributed planets around the sun and ring. A revised mobility equation, referenced as (Eq. (29)), has been introduced in this thesis. This revised equation enhances the Grübler-Kutzbach criterion (Eq. (10)), providing a comprehensive analysis of the mobility of complex PGMs by incorporating considerations for redundant and virtual constraints. The equation's accuracy was validated through four case studies, demonstrating its effectiveness in predicting the correct mobility of PGMs in any motion space. This contribution enhances the understanding of PGM kinematic structures as a whole and supports advancements in PGM design and innovation.

Moreover, novel metrics designed for evaluating the performance of mechanisms, premised on their topological characteristics, were introduced in this chapter. These metrics, conceived to analyze complexity and capability of various mechanisms, are

discussed with particular emphasis on their application to PGMs. An in-depth application and discussion on the structural complexity and capability metrics for PGMs is presented in Chapter 5, wherein the technological performance indexes for innovation are characterized.

4 PROCESS FOR DISCOVERING INNOVATIVE GAPS IN MECHANISMS DATABASE

This chapter provides an overview of the process proposed for this thesis research. As mentioned in Chapter 1, the design process of automotive planetary transmissions can benefit from a systematic approach for innovation to assist engineers in identifying relevant structural parameters and characteristics to design new mechanisms. To address these challenges, the research question posed is: *"Is it possible to discover potential innovative gaps in the requirements for designing automotive planetary gear trains by analyzing an extensive and diverse database?"* The primary objective of this thesis is **to introduce a new process for identifying potential innovative gaps in the requirements for designing new automotive planetary gear mechanisms through comprehensive database analysis**.

The proposed process is divided into four key phases:

1. **MECHANISM SURVEY:** Conduct a comprehensive study and review of existing Planetary Gear Mechanisms (PGMs) by gathering relevant data and information from patent, academic, and industry sources. This phase involves generating extensive datasets.
2. **DATA ENRICHMENT:** Create a diverse dictionary of features related to automotive Automatic Transmissions (AT) based on planetary gear trains. Evaluate the datasets and generate a structured comprehensive database.
3. **FEATURE ANALYSIS:** Use data science strategies to analyze the characteristics of features involved in the design of automotive planetary gear trains. Select the most relevant features as a result of this analysis.
4. **GAP DISCOVERY:** Assess the boundaries of the selected features and discover gaps in data. Combine the relevant feature gaps and select the most promising ones as potential innovation sets for input in the design of new automotive transmissions.

In Figure 34, a diagram illustrating the proposed workflow of the process for discovering potential innovative gaps in automotive planetary gear trains database is presented, containing each phase and their associated methods.

As depicted in Figure 34, the process is versatile and is not exclusively limited to PGMs, it can be applied to projects involving various types of mechanisms. This chapter introduces the process tailored for the discovery of potential innovative gaps in generic mechanisms. The subsequent Chapter 5 delves into its application specifically to the case study of PGTs.

To provide a thorough understanding of the process, a brief review on the knowledge discovery in databases is presented in Section 4.1. Subsequently, each phase is described in detail in the following Sections 4.2 to 4.5, highlighting the significance

Figure 34 – Process for Discovering Potential Innovative Gaps.

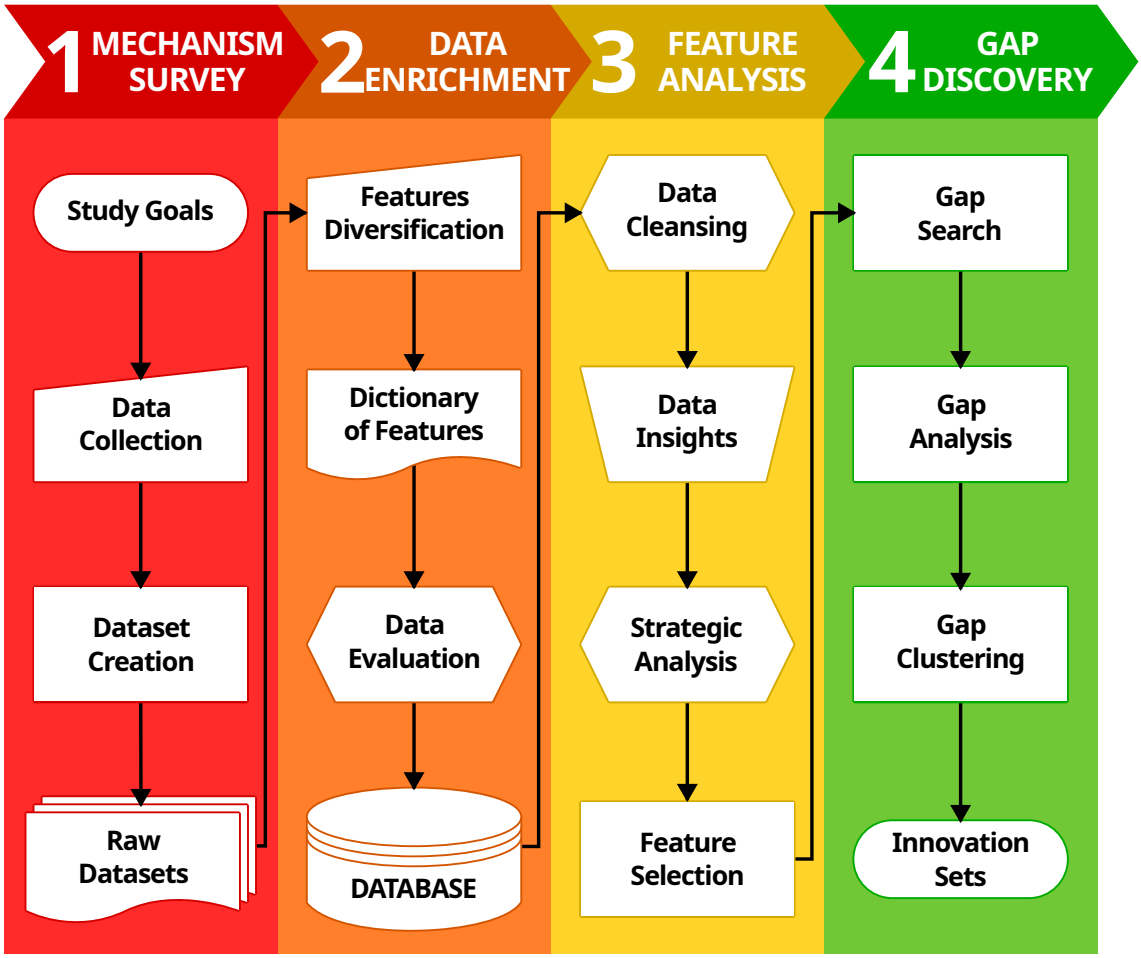

Source: Author.

of the methods employed, their relevance in the research context, and any limitations associated with their implementation.

4.1 REVIEW OF KNOWLEDGE DISCOVERY IN DATABASES (KDD)

According to Witten et al. (2017), *information* is the set of patterns or expectations existing in recorded facts in its raw form, known as *data*. There is a huge amount of information locked up in databases-information that is potentially important but has not yet been discovered or articulated.

The *Knowledge Discovery in Databases (KDD)* is defined by Fayyad (1996) as:

> ... the nontrivial *process* of identifying *valid*, *novel*, potentially *useful*, and ultimately *understandable patterns* in *data*.

Data is typically obtained through observations or measurements, which can be unprocessed or processed. It is described by *features* (also known as attributes, properties, characteristics, parameters, or variables) associated with *values* represented as text, numbers, or multimedia. The data associated with a unique body of work is

referred to as an *instance*, and these instances are stored in a structured collection named a *dataset*. Multiple datasets form a *database*, which is an organized collection of data that can be electronically accessed, manipulated, and updated.

The *dimensionality of the data* is determined by the number of features it contains, while *patterns* represent abstract representations of subsets of the data. Instances within a dataset can be categorized into *classes* based on specific aspects.

Formally, a dataset can be simply represented as $\mathbf{X} = \{\mathbf{x_1}, \ldots, \mathbf{x_d}\} \in \mathbb{R}$. The class label is represented as $\mathbf{Y} = \{\mathbf{y_1}, \ldots, \mathbf{y_N}\}$. A typical dataset is organized as a matrix of N rows (instances) by d columns (features) and an extra column with the class labels (Eq. (46)):

$$\mathbf{X}_{N\times d} = \overbrace{\begin{bmatrix} x_{11} & x_{12} & \cdots & x_{1d} \\ x_{21} & x_{22} & \cdots & x_{2d} \\ \vdots & \vdots & \ddots & \vdots \\ x_{N1} & x_{N2} & \cdots & x_{Nd} \end{bmatrix}}^{features} \Bigg\} \; instances \quad , \quad \mathbf{Y}_{N\times 1} = \overbrace{\begin{bmatrix} y_1 \\ y_2 \\ \vdots \\ y_N \end{bmatrix}}^{class} \tag{46}$$

The primary objective of the KDD process is to extract knowledge by exploring databases through a series of iterative steps, including data preparation, selection, preprocessing, transformation, data mining, and evaluation. The KDD process is illustrated in Figure 35. It is important to note that the term Data Mining (DM) is often used inter-

Figure 35 – Overview of the KDD process.

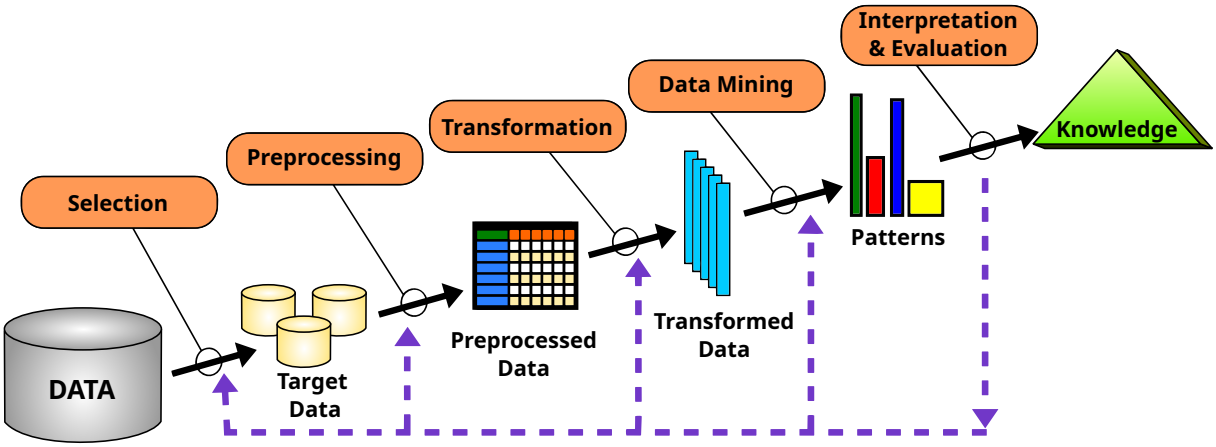

Source: Adapted from Fayyad (1996).

changeably with KDD, but it specifically refers to the step within the KDD process where specific algorithms are applied to extract patterns from the data (HAN et al., 2012). Data mining focuses on the computational techniques used to uncover meaningful patterns, relationships, and trends in the data. From understanding the problem to its completion with useful knowledge, the KDD process can be briefly described in the following steps:

1. PROBLEM DEFINITION: Define the application domain, incorporate relevant prior knowledge, and identify the KDD's goal to establish the context and objectives of the data analysis.
2. SELECTION: Gather and select the necessary data from multiple sources to create a dataset that accurately represents the problem domain.
3. PREPROCESSING: Remove noise and outliers, handle missing data fields, account for time-sequence information and known changes, and apply appropriate normalization techniques to enhance data quality and consistency.
4. TRANSFORMATION: Extract relevant attributes, perform dimensionality reduction, and transform the data to ensure its suitability for data mining algorithms and techniques.
5. DATA MINING: Search for patterns of interest and usefulness within the dataset using selected algorithms and models suitable for the KDD's goal.
6. INTERPRETATION & EVALUATION: Validate and explain the results of the data mining process for reliability and significance, and utilize visualization techniques to present the findings in a comprehensible manner.
7. KNOWLEDGE: Present the mined knowledge to users and integrated into existing systems or applications to enhance their functionality.

KDD is an interdisciplinary field that encompasses various disciplines such as statistics, machine learning, artificial intelligence, reasoning with uncertainty, databases, knowledge acquisition, pattern recognition, information retrieval, visualization, intelligent agents, digital libraries, and management information systems (FAYYAD, 1996).

As mentioned earlier in this chapter, the focus of this thesis is to determine relevant features (characteristics) for identifying gaps (values not covered in patterns) in a mechanism database. The ultimate goal is to generate potentially innovative sets of requirements for designing new mechanisms. In the following sections, each phase of the proposed process (as shown in Figure 34) is described.

4.2 PHASE 1: MECHANISM SURVEY

The *Mechanism Survey* phase is characterized by the establishment of study objectives and the collection of essential information required for the generation of datasets related to the mechanisms under study. This phase encompasses the subsequent steps:

1. STUDY GOALS: Review of the research scope, specifying the mechanism type, and articulating the objectives.
2. DATA COLLECTION: Retrieving initial data related to the essential design requirements of existing mechanisms from reliable sources such as patent databases,

academic articles, and reports from manufacturers.

3. DATASET CREATION: Creation of a dataset template for inputting and validating the collected data of each mechanism to ensure accuracy.
4. RAW DATASETS: Set of datasets containing all valid mechanisms collected data intended for further analysis.

The output of phase 1 is the formulation of raw datasets that encompass existing mechanisms, thereby facilitating subsequent analytical and synthesis processes.

4.2.1 Study Goals

The initial step in phase 1 involves translating customer requirements into clear, technical, and objective directives. This step aids in the identification of the mechanism type and the delineation of the study's objectives, guiding the overall process. Key information and their attributes include:

1. *Mechanism Type Identification*
2. *Goal and Objective Specification:* Definition of the overall goal and specific objectives to be accomplished through data analysis.
3. *Data Source Specification:* Identification of sources from which data will be retrieved.
4. *Scope Definition:* Determining the boundaries pertinent to the analysis.
5. *Constraint Consideration:* Identification of potential constraints or limitations that might influence the data analysis process.
6. *Evaluation Criteria Establishment:* Delineating the criteria for assessing the efficacy of the data analysis efforts.

4.2.2 Data Collection

The second step of phase 1 is focused on collecting essential data related to existing mechanisms. This involves sourcing data from trustworthy repositories such as patent databases, academic publications, and manufacturers' documentation.

4.2.2.1 Patent Search

According to WIPO (2015), patent information is a valuable source of technological information presented in a standardized format. It is considered the world's largest repository of technological information (ARISTODEMOU; TIETZE, 2018).

A patent typically consists of various fields of information, including bibliographic data, claims, detailed description, drawings, background, abstract, and summary (WIPO, 2011). Figure 36 illustrates an example of the front page of an international patent application.

Figure 36 – Front page of an international patent application.

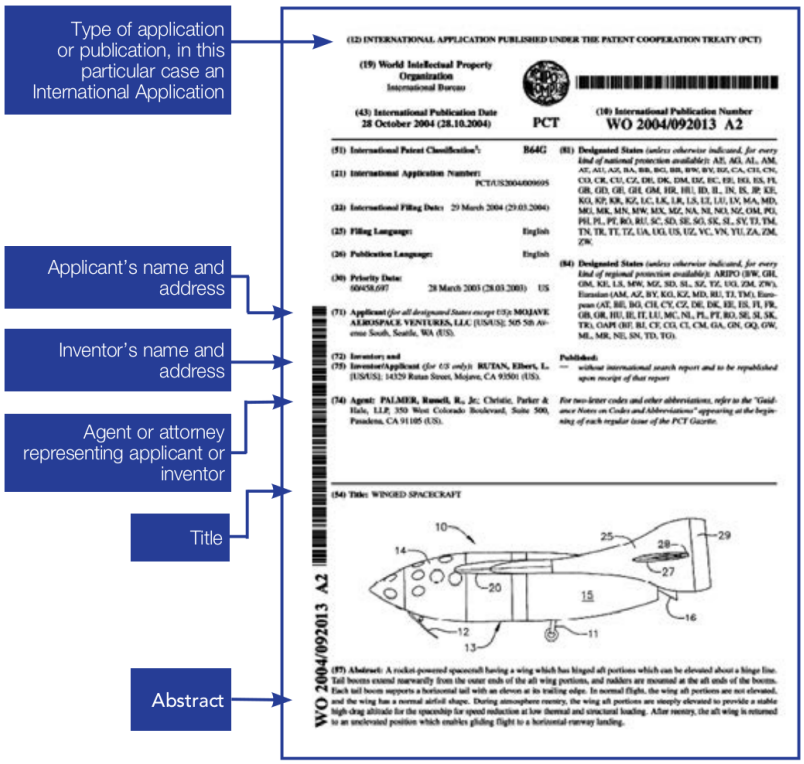

Source: Adapted from WIPO (2015).

In the context of enumeration-based mechanism design, patent analysis is used to review existing designs, identify relevant information on structural and functional characteristics of mechanisms, and inspire designers to create new concepts while avoiding protected solutions. Freudenstein and Maki (1979) suggested cross-indexing mechanical patents with a simple structural formula to facilitate prior art searches.

LAR Patent Search Methodology Proposed by the author's research group (HOELTGEBAUM et al., 2016b), this process focuses on patent search for automotive mechanisms. The primary objective is to identify the structural characteristics, such as mobility, number of independent loops, and order of the space , of the inventions and use them as initial structural requirements for the design of new mechanisms. The process consists of six steps: preliminary search and analysis, detailed search and analysis, mechanism analysis, and technology mapping (Fig. 37). The preliminary and detailed search steps are iterative in nature.

The LAR methodology is the recommended patent search method for this step.

Patent Data Sources When conducting a patent search, it is essential to utilize reliable and comprehensive sources of patent data. There are several recognized world-wide open databases that can be utilized for this purpose. Some of the recommended sources include:

Figure 37 – LAR Patent Survey Methodology

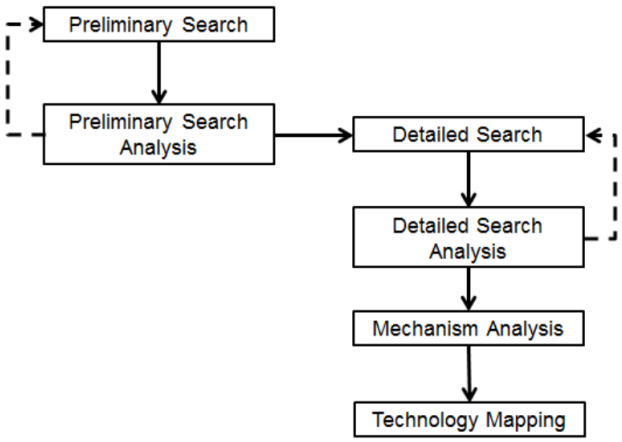

Source: Hoeltgebaum et al. (2016b).

1. *ESPACENET:* A free online patent database provided by the European Patent Office (EPO) offering access to patent documents from around the world, including the EPO, WIPO, USPTO, and many other national patent offices.
2. *USPTO:* A comprehensive database of patents provided by the United States Patent and Trademark Office (USPTO). It is a valuable resource for accessing patent information from the United States.
3. *WIPO:* The World Intellectual Property Organization (WIPO) offers a global database named PATENTSCOPE, which provides access to both international and national patent applications from various countries and regions.
4. *INPI:* The National Institute of Industrial Property (INPI) is an important source for accessing patent information specific to Brazil.
5. *Google Patents:* An extensive online database that provides access to a wide range of patent documents from various jurisdictions around the world such as USPTO, EPO, WIPO, and many others.

4.2.2.2 Academic and Industry Search

Not all the required information is available in patents, such as the functional characteristics and physical properties of the related commercial product, e.g., weight, torque capacity, and others. Therefore, information beyond patent search can be accessed through academic and industry search.

Academic Search This step involves finding books, studies, and research papers that focus on the properties and characteristics of mechanisms. Academic databases such as IEEE Xplore, ScienceDirect, and Google Scholar can be valuable sources for accessing scientific literature. By reviewing academic publications, it is possible to

gather insights into the performance, efficiency, durability, and other important attributes of mechanisms.

Industry Search This step involves exploring suppliers' technical reports and product documentation. These sources provide detailed information about the commercial aspects of mechanisms, including specifications, performance data, operational parameters, and design considerations. Manufacturers' websites, product catalogs, and technical manuals can be used to extract essential information for mechanism analysis and comparison.

By incorporating both academic and industry search approaches to the patent search results, it is possible a comprehensive understanding of mechanisms, considering both their technical and commercial aspects. This enriched information enables a more thorough evaluation of existing mechanisms and facilitates the identification of opportunities for innovation and improvement.

4.2.3 Datasets Creation

The data collected from each mechanism in the previous step must be transformed into a suitable graph representation (Section 2.3.1), validated, and stored as datasets for subsequent analysis.

Typically, the structural characteristics are extracted from mechanism representations in figures of data sources, requiring visual analysis by the designer.

Functional characteristics vary depending on the type and purpose of the mechanism. They are often presented in tables or sentences that need to be read and interpreted before being input into the dataset.

Technical characteristics, such as dimensions, cost, weight, and others are typically retrieved from industrial and academic sources.

In order to achieve standardized, reliable, and replicable data collection with facilitated data input and automated data validation, the adoption of a dataset template is highly recommended. This template should encompass the identification of each mechanism, along with its structural, functional, and technical attributes. Moreover, to ensure data accuracy and reliability, the automated validation of the mechanism's structural characteristics within the dataset template is essential.

A proposed dataset template for mechanisms comprises the following fields:

A. **Dataset Template**: A structured format designed for the data insertion of each mechanism, equipped with automated validation functionalities for enhanced reliability (e.g., spreadsheet templates).

B. **Input data**: Required data to create each dataset.

   (a) Identification: Data pertinent to the recognition of individual mechanisms.

i. *Source*: Data origin, such as patents, academic articles, manufacturer brochures, among others.

ii. *Date*: Release date associated with the mechanism, predominantly available in the source.

iii. *Model*: Mechanism identifier or descriptor as presented in the source.

iv. *Others*: Any supplementary information deemed vital to the mechanism's categorization.

(b) Structural Characterization: Data related to the topology and inherent structural attributes based on the mechanism representation.

i. *Topology*: List of the mechanism's links and joints.

ii. *Actuators*: List of the mechanism's actuators.

iii. *Structural Validation*: Automated methods for evaluating and validating structural characteristics such as mobility, among others.

(c) Functional Characterization: Data addressing functional requirements of the mechanisms, including performance metrics, power outputs, controls, among others.

(d) Technical Characterization: Data related to product specifications like dimensions, cost, application, among others.

By employing this dataset creation method, data relevant to each mechanism is systematically organized, thus facilitating subsequent steps towards the identification of potential innovative gaps in the mechanism database.

4.2.4 Raw Datasets

The output of Phase 1 is a collection of raw datasets, consisting of essential and reliable data generated from the analyzed mechanisms. For effective management of this collected data, the implementation of a dataset control system is recommended. This system should encompass a comprehensive dashboard, and be supplemented with version control functionalities. Such provisions are essential to ensure the data integrity and organization throughout the research process.

4.3 PHASE 2: DATA ENRICHMENT

In the second phase, termed *Data Enrichment*, datasets are augmented with additional features to maximize the available information regarding the mechanisms. This phase encompasses the following core steps:

1. FEATURES DIVERSIFICATION: Identify additional features from diverse related domains for inclusion.

2. DICTIONARY OF FEATURES: Create a dictionary to characterize and recognize all features to be assessed within the datasets.
3. DATA EVALUATION: Assess all instances in the datasets with respect to the newly introduced features.
4. DATABASE: Store the enriched data in an organized collection, ensuring efficient retrieval and subsequent analysis.

The output of phase 2 is a comprehensive database containing enriched data aiming to enhance the understanding of the studied mechanisms. This enriched foundation opens the way for potential discovery of patterns and relationships in the following phases of the process.

4.3.1 Features Diversification

The diversification of features is essential in augmenting the utility and insights obtained from the collected data. This process includes the incorporation of additional features, which elucidate the structural, functional, and technical characteristics of the mechanisms. More precisely, it involves the identification and enhancement of measures sourced from diverse related domains for inclusion into the feature set.

Graph theory represents an essential domain in the study of mechanisms. Due to their multidisciplinary nature, numerous properties and measurements are possible for graph characterization (F. COSTA et al., 2007). Within the scope of this research, a detailed emphasis is given to the topological properties for the representation of mechanisms.

Metrics of topological nature, depending solely on the information within the adjacency matrix (Section 2.3.1), can be associated with various attributes such as distance, connectivity, clustering, centrality, and spectral measures, to name a few (HERNÁNDEZ; MIEGHEM, 2011). These metrics, either on a global scale, representing the mechanism as an entirety (graph topology), or on a local scale, illustrating the features of individual links (vertices) or joints (edges), can be found in the literature (OEHLERS; FABIAN, 2021).

In the subsequent sections, two primary approaches are proposed: local and global features.

4.3.1.1 Local features

Local features are measures related to individual components of the mechanism, namely links and joints. When the interrelations of key individual components, such as frame, input and output links, and actuators, are evaluated, characteristic patterns of interest may be potentially revealed. Presented below are suggested a small set of *local features* along with their respective definitions:

- *Vertex Degree:* The count of adjacent edges (i.e., neighboring vertices) connected to a vertex.
- *Vertex Eccentricity:* The maximum shortest distance between the vertex and any other vertex in the graph, it is a metric that can help in identifying links in mechanisms distanced farthest from other links, thus potentially playing a role in long-distance motion transmission.
- *Vertex Centrality:* The importance of the vertex in a graph is measured according to various centrality metrics (RODRIGUES, 2019).
  - *Degree Centrality:* The simplest of measures, identical to the vertex degree. It operates on the premise that vertices of importance possess numerous connections. Within the mechanism's graph representation, it correlates to the number of joints linked to a link and has a direct association with link assortments (Section 2.3.2.2).
  - *Closeness Centrality:* The average distance of the vertex to all other vertices, this metric assumes that vertices of importance are close to other vertices. Within the mechanism graph, it might be indicative of links required to transmit power transmission over shorter spans, such as input links.
  - *Betweenness Centrality:* The extent to which the vertex lies on the shortest paths between pairs of other vertices in a graph. This can reveal the importance of links serving as bridges between disparate sections of the mechanism.
  - *Eigenvector Centrality:* Derived from the principal eigenvalue correlated to the vertex in the adjacency matrix's eigenvector, it assumes a vertex's importance based on the importance of its surrounding neighborhood. Links with elevated eigenvector centrality within the mechanism graph might be key components in the mechanism's efficiency.
  - *Katz Centrality:* An eigenvector centrality variant, it measures a vertex's relative influence within a graph, factoring in both immediate and secondary degree neighbors. Within the mechanism graph, it might reflect the aggregated influence of links directly and indirectly tethered to a given link. For instance, a link with high Katz centrality might substantially affect the mobility of neighboring links, thus being important to the control of the mechanism.

The aforementioned list is not exhaustive. Depending on the distinct mechanism under consideration, the exploration and assessment of supplementary metrics and properties can provide invaluable insights.

4.3.1.2 Global features

Global features refer to measures related to the entire topology of the mechanism. A selection of *global features* is proposed below, along with their respective definitions (STEEN, 2010):

- *Planarity:* A graph is termed planar when it can be embedded in a plane without any edge intersections. Such a characteristic might be relevant for mechanisms requiring spatial arrangements avoiding intersecting links, like planar robotic arms or linkages used in manufacturing systems.
- *Average Degree:* This is the mean adjacency degree of vertices in a graph. For instance, the average degree may provide insights on the complexity of mechanisms.
- *Density:* Defined as the relative ratio of the number of existing edges to the total potential edges among all vertices, this metric describes the graph's degree of interconnectedness. For mechanisms, density may aid in determining the degree of component interconnectivity and interdependency.
- *Diameter:* Representing the greatest shortest distance between any two graph vertices, this quantifies the largest eccentricity value of a vertex in the graph. In the context of mechanisms, the diameter may offer insights into the efficiency of power transmission.
- *Radius:* This quantifies the least eccentricity value of a vertex, representing the center of the graph. Within mechanisms, a smaller radius might indicate quicker responses, whereas a larger one could hint at increased redundancy.
- *Average Clustering:* This metric involves the extent to which graph vertices tend to cluster together. For mechanisms, average clustering can spotlight clusters or groups of links with strong interconnections.
- *Average Shortest Path Length:* This is the average of the minimum count of edges that need to be navigated to go from one vertex to another in the graph. It can be applied to analyze the efficiency of power transmission within the mechanism.
- *Network Complexity Coefficient:* Calculated as the ratio of the variance in the degree distribution to the graph's average degree, this metric becomes more pronounced with an increase in the variability of vertex degrees (BARABÁSI; PÓSFAI, 2016). Such a coefficient can be used to quantify complexity within mechanisms.

To further enhance the data, other features can be assessed to capture nontrivial information about mechanisms (NEWMAN, 2010). The main objective here is to improve the description of mechanisms through the datasets by incorporating valuable new

insights into the characteristics of the mechanisms under study.

4.3.2 Dictionary of Features

The creation of a dictionary of features is suggested in order to standardize and organize the datasets effectively. The aim is to identify and provide comprehensive descriptions for the features that will be evaluated in the mechanisms under study. Following, a structure for the dictionary is proposed:

- *Feature Name*: Name of the feature as a variable in the database.
- *Description*: A brief explanation detailing the significance or purpose of the feature.
- *Rule or Equation*: Mathematical or logical relations explaining how to obtain the feature.
- *Feature Type*: Representation of the feature type, e.g., *textual, categoric, numeric, or time series.*
- *Data Type*: Specification of data storage format, e.g., *string, int, float, bool, or datetime.*
- *Boundaries*: Limits in which the feature's value can lie, detailing the *lower and upper bounds*.
- *Example*: A practical instance or use-case scenario showcasing the feature's application.
- *Machine Scope*: Feature level in a machine hierarchy breakdown (Fig. 10), whether it's a *machine, mechanism, kinematic chain, joint, link*.
- *Requisite Scope*: Inherent essence of the feature requirement, whether it's a *structural, functional, or technical*.
- *Requisite Type*: Classification of design requirements into *property* for inherent attributes, *metric* for measurable assessments, and *information* for additional context.
- *Knowledge Domain*: Research field or domain the feature belongs to, e.g., *information retrieval, mechanism design, graph theory, or data mining*.
- *Acquisition*: Method of obtention of feature's data, whether it's *measured, calculated, inferred* (based on other features), or *implied* (based on intuition).

For ease of reference and effective documentation, it's recommended to implement this dictionary in a spreadsheet format in the project.

4.3.3 Data Evaluation

The *Data Evaluation* step aims to calculate the value of all features listed in the dictionary for each mechanism instance. Their values must be evaluated according to the defined rules or equations and following the data type and the specified units. To accomplish this, the collected data from each mechanism in the datasets must be read, converted into the chosen representation model (e.g., graphs), and appropriate libraries can be used to evaluate the features.

Python (FOUNDATION, 2023) is the most popular programming language for data science (CARBONNELLE, 2023) and offers several specialized libraries, including:

- *Pandas:* Data structures for statistical computing (MCKINNEY, 2010)
- *NumPy:* Array programming for accessing, manipulating and operating on data in vectors, matrices and higher-dimensional arrays (HARRIS et al., 2020).
- *SciPy:* Numerical routines for solving a wide range of scientific problems, including optimization, integration, interpolation, and differential equations. It provides specialized data structures and is built on top of NumPy (VIRTANEN et al., 2020).
- *NetworkX:* Package that enables the exploration, analysis, and calculation of network properties in various scientific fields through a variety of data structures and graph algorithms (HAGBERG et al., 2008).
- *Matplotlib:* 2D graphics package used for application development, interactive scripting,and publication-quality image generation across user interfaces and operating systems (HUNTER, 2007).
- *Seaborn:* Dataset-oriented API for creating statistical graphics, automating the mapping of data values to visual attributes, performing statistical transformations, and enhancing plots with informative labels and legends (WASKOM, 2021).
- *SciKit-Learn:* State-of-the-art machine learning algorithms accessible to non-specialists through a general-purpose high-level language, is suitable for medium-scale supervised and unsupervised problems (PEDREGOSA et al., 2012).
- *Statsmodels:* Extensive tools for statistical modeling and hypothesis testing, including linear and non-linear models, statistical tests, and data exploration, making it integral for econometrics, statistical analysis, and data science (SEABOLD; PERKTOLD, 2010).
- *SageMath:* Open-source mathematics software system that integrates several libraries and packages into a unified interface, providing a comprehensive environment for advanced algebra, calculus, and various other domains of mathematics (DEVELOPERS, 2023).

- *Orange:* Open-source data visualization and analysis tool for both novice and expert users, offering a range of components for machine learning and data mining through a visual programming interface (DEMŠAR et al., 2013).

Once all instances have their enriched features been evaluated, storing the data in a database becomes essential for further analysis.

4.3.4 Database

The mechanism *Database*, the output of Phase 2, refers to the structured organization and storage of the collected and enriched data. There is a wide range of formats for databases, from simple flat table to specialized systems to record data (HAN et al., 2012). Independently of their complexity, the database must ensure data integrity, facilitate efficient retrieval, and serves as the foundational layer upon which analytical algorithms operate to extract meaningful patterns and insights.

Considering the diverse landscape of database structures, for many academic projects, a simpler database structure such as a flat table (Eq. (46)) might suffice. Flat tables are straightforward, easy to understand, and often more than adequate for datasets that do not require complex relationships or queries. Their simplicity ensures faster data retrieval times, minimalistic design, and often easier data management. Additionally, flat tables can be directly imported into a multitude of statistical software, facilitating quick and seamless analysis.

4.4 PHASE 3: FEATURE ANALYSIS

The phase 3, *Feature Analysis*, focuses on identifying the optimal subsets of most relevant features for further gap discovery. Four steps comprise this phase:

1. DATA CLEANSING: Correction of the database by handling possible issues to ensure data consistency for further analysis.
2. DATA INSIGHTS: Exploration of the database by applying statistics to summarize the main characteristics and getting insights into data.
3. STRATEGY ANALYSIS: Formulation of data mining strategy procedures for attending to the study goals (Section 4.2.1).
4. FEATURE SELECTION: Identification of the minimal features to represent the most relevant design requirements throughout the strategies.

The output of phase 3, based on the chosen strategies, yields subsets of essential features that best represent the design requirements for each study goal.

4.4.1 Data Cleansing

The first step in the feature analysis is Data Cleansing, which aims to verify and correct possible issues with inconsistent data. Among the most important factors for the quality of data, Han et al. (2012) highlights: accuracy, completeness, consistency, timeliness, believability and interpretability. Organizing and cleaning the data ensure its quality and reliability, helping to eliminate any inconsistencies or errors in the dataset.

The main work involves cleaning routines to check data type, handle missing values and outliers, and removing duplicates in instances (rows) and features (columns).

Validating the data types of features is very important in the data evaluation process. For instance, if a feature is expected to contain numerical values, it is imperative to ensure that all values are indeed numeric. In cases where a feature has a different data type than expected, appropriate methods for data type conversion should be applied to guarantee consistency within the dataset.

Handling missing values is another critical aspect of data evaluation, and several techniques can be employed (HAIR et al., 2019). If the amount of missing data is relatively small compared to the overall dataset, one approach is to remove the instances containing missing values. Similarly, if a significant portion of a feature's values are missing, removing that feature might be necessary. Alternatively, missing values can be imputed using statistical measures, such as mean, median, or mode, when the number of missing values is relatively small or removing them would result in a significant loss of information.

Duplicated features or instances can also present challenges during data evaluation. To address duplicated features, it is important to check for identical column names and compare the values within each column. In case of identical values, the duplicated columns must be removed from database.

Duplicated instances occur when multiple records in the dataset have the same values across all features. In case of mechanisms represented by graphs, it is crucial to detect these duplicates as they can represent isomorphisms (Section 2.3.2.4). The appropriate course of action is removing or consolidating duplicate instances into a single representative instance. There are several methods for checking for isomorphism such as VF algorithm (JÜTTNER; MADARASI, 2018), graph edit distance (ABU-AISHEH et al., 2015), graph kernel hashing (SHERVASHIDZE et al., 2011), perimeter loop (DING; HUANG, 2009), among others.

This step requires significant time and necessitates meticulous manual review by the engineer.

4.4.2 Data Insights

The second step in feature analysis is an exploratory data analysis (EDA) aiming to improve understanding on existing data by performing statistical analysis (KOMOROWSKI et al., 2016). Visual methods are often used to support three main approaches: descriptive (univariate), correlative (bivariate) and contextual analysis. The latter involves events that are time or agent based, not being related to the scope of this study. A general EDA process steps are exemplified in Figure 38.

Figure 38 – Example of an EDA process.

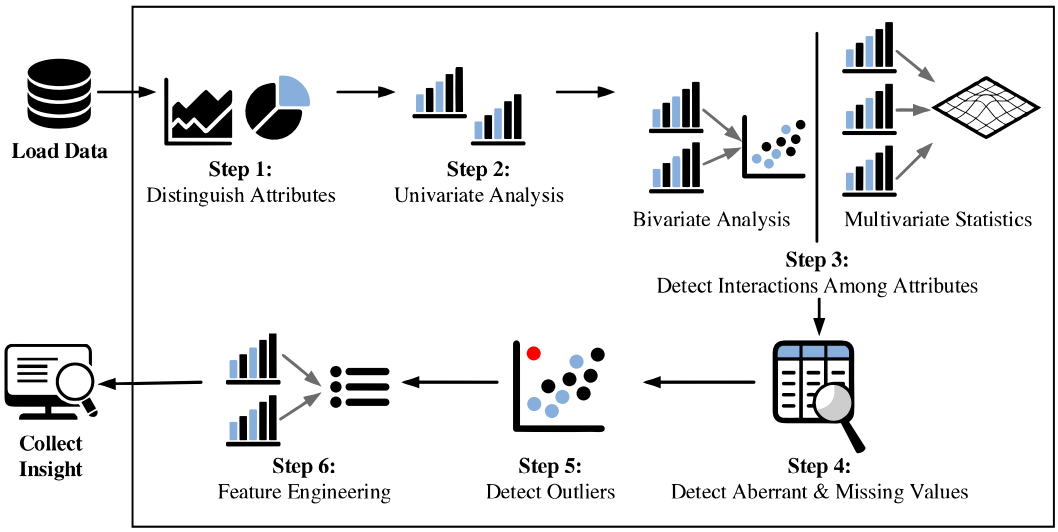

Source: Ghosh et al. (2018).

The descriptive analysis, often referred to as univariate analysis, focuses on summarizing the main features of a single variable in a dataset. This approach seeks to provide insights into the central tendency, spread, and shape of the data distribution. While measures like mean, median, and mode convey the data's central position, the variance, standard deviation, and range delineate its spread. Additionally, the shape of the distribution is characterized by attributes like skewness and kurtosis. Testing normality is vital for determining appropriate statistical methods and for selecting measures of central tendency and dispersion in continuous data (MISHRA et al., 2019). For small sample sizes ($n < 50$), the Shapiro–Wilk test is recommended due to its superior power in detecting non-normality. However, for sample sizes of at least 50, various methods and visualizations like the Kolmogorov–Smirnov test, histogram, box plot, P–P Plot, Q–Q Plot, and others can be employed to assess data normality. In Table 13, some of the most useful univariate analysis is presented for the attribute type, including visualization charts.

The correlative analysis is concerned with understanding the relationships or associations between two or more variables in a dataset. This approach employs measures like Pearson's correlation coefficient r to quantify linear relationships between

Table 13 – Common univariate analysis according to feature type.

Attribute type	Statistic/Calculation	Details	Visualization
Categorical	Cardinality	Number of unique values for the categorical attribute	Bar plot
	Unique counts	Number of occurrences for each unique value of the categorical attribute	Stacked bar
Numerical	Quantile statistics	Q1, Q2, Q3, min, max, range, interquartile range	Boxplot, Violin plot
	Descriptive statistics	Mean, mode, standard deviation, median, absolute deviation, kurtosis, skewness	Histogram, Line
	Distribution	Based on the appropriate number of bins	Histogram

Source: Adapted from Shixin (2020).

paired variables. Visual aids, such as scatter plots, play a pivotal role in visually assessing the nature and strength of these relationships. When examining multiple variables, heatmaps of correlation matrices can provide a holistic view of inter-variable relationships (BRUCE et al., 2020). Additionally, significance testing methods, like the *t*-test for correlation coefficients, help determine the statistical significance of observed correlations. For non-linear or monotonic relationships, alternative correlation measures such as Spearman's rank ρ or Kendall's τ coefficient might be employed (LEWICKI; HILL, 2006). In Table 14, some of the most useful univariate analysis is presented for the attribute type, including visualization charts.

Table 14 – Common bivariate analysis according to feature type.

X	Analysis	Y	
		Categorical	Numerical
Categorical	Qualitative	Contingency table with unique counts of X per unique value of Y	Descriptive statistics or histogram of Y per unique value of X
	Quantitative	Chi-square test Information gain	Student T-test ANOVA Logistic regression *Discretize Y*
Numerical	Quantitative	Student T-test ANOVA Logistic regression *Discretize X*	Correlation Linear Regression *Discretize X and Y*

Source: Adapted from Shixin (2020).

This is a foundational step in the data analysis process, offering critical insights into the nature and structure of data, guiding further analyses, and assisting in hypothesis generation and testing.

4.4.3 Strategic Analysis

Once the database has been prepared, explored, and characterized, the third step in the feature analysis phase is focused to the formulation of precise data mining

strategies that align with the objectives of the study. Three main components structure each strategy: a clearly defined objective, a systematic procedure, and a robust evaluation protocol.

The *objective* should articulate the central question or challenge of the data analysis, providing a clear achievement.

The *systematic procedure* constitutes a detailed, step-by-step pipeline, which demonstrates the sequence of tasks and methods to be used. This procedure ensures clarity and offers reproducibility.

The *evaluation protocol* is determined using relevant metrics, such as scores or significance levels. These metrics should be statistically significant and hold practical value (HAIR et al., 2019). The use of visual tools is suggested to augment the understanding of the results.

Employing this systematic method ensures that the strategy analysis is both comprehensive and reproducible, and it is firmly rooted in data science principles.

To guide the search for gaps with potential for innovation in mechanism design requirements, it is first essential to map existing mechanisms comparatively. This map assists in evaluating areas with innovation potential and subsequently determining the most critical project requirements. The technology boundary chart (Fig. 28), as referenced in Karhula and Nicolai (2018), serves as a beneficial tool in this context. Therefore, at this stage, the creation of a technological map comparing the capabilities and complexities of the database mechanisms is recommended. Other attributes might be considered to segment the data using symbols, colors, and the size representation of each mechanism on the technological map.

Analysis of the map allows for the identification of the technological frontier that distinguishes the area of existing mechanisms in the database from the disruptive innovation region. Generally, potential for disruptive innovation increases when moving left (reducing complexity) and upwards (increasing capability). Furthermore, it is possible to identify subregions within the technological frontier where mechanisms are absent, indicating local innovation potential.

Database analysis strategies should be crafted with the aim of assisting in identifying the most relevant design requirements in the technological map regions with the highest innovation potential.

4.4.4 Feature Selection

In the fourth step, key features in mechanism design should be identified through the application of strategies. Algorithms for Feature Selection (FS) aid in determining a subset of the most pertinent and informative features from the original dataset (LIU; MOTODA, 1998b), thereby reducing dimensionality and enhancing interpretability (GUYON; ELISSEEFF, 2003). The goal is to identify a concise set of features that best represent

the most important design requirements, aiding in the identification of innovation gaps.

The relevance of a feature is determined by the characteristics of the data, not by its value (VENKATESH; ANURADHA, 2019). A feature is termed *relevant* if its removal leads to a deterioration in the performance measure of the remaining features (LIU; MOTODA, 1998a). A *strongly relevant* feature becomes indispensable for an optimal subset, and its absence would change the original conditional class distribution. Conversely, a *weakly relevant* feature may not always be vital, but under certain circumstances, it becomes essential for an optimal subset. Notably, a weakly relevant feature is deemed redundant if correlated entirely with another feature (YU; LIU, 2004). An *irrelevant* feature has no necessity.

Methods of feature selection can be categorized in two manners. The first categorization relates to the output (Fig. 39): either a ranked list of all features by relevance, termed Feature Ranking (FR), or a subset of relevant features, termed Subset Search.

Figure 39 – Categories of Feature Selection output.

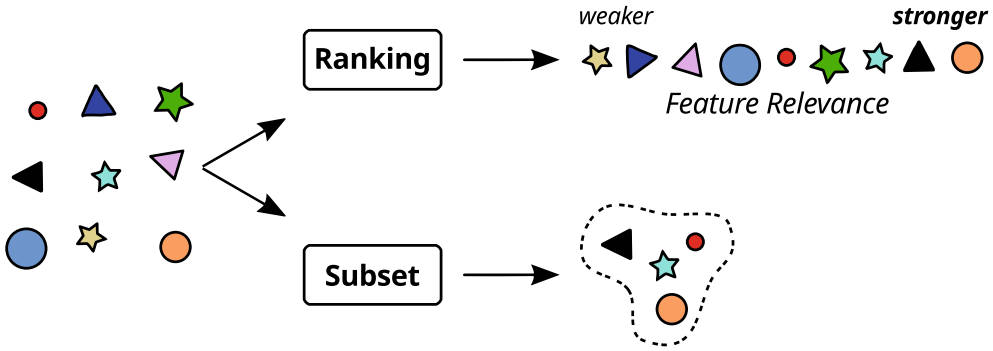

Source: Adapted from Bolón-Canedo and Alonso-Betanzos (2018).

The second categorization is based on the inductive learning method used to infer a model, encompassing three primary methods (BOLÓN-CANEDO; ALONSO-BETANZOS, 2018; SAHU et al., 2018):

- *Filter:* Evaluates features using statistical metrics such as correlation and mutual information, independent of a learning model (unsupervised).
- *Wrapper:* Evaluates feature subsets by training them on a supervised learning model and then measuring its performance. Examples include recursive feature elimination (RFE) and genetic algorithms. Though more accurate than filter methods, they are computationally demanding.
- *Embedded:* Combines an independent measure within the training of the supervised learning model. Techniques like Lasso or Ridge regressions and Random Forest are employed. It often outperforms other methods, being less resource-intensive than wrapper methods but remains model-specific.

Given the multitude of algorithms available for feature selection, a categorization was proposed by Liu and Yu (2005) from a user's perspective, as depicted in Figure 40.

Figure 40 – User's perspective categorization for FS methods.

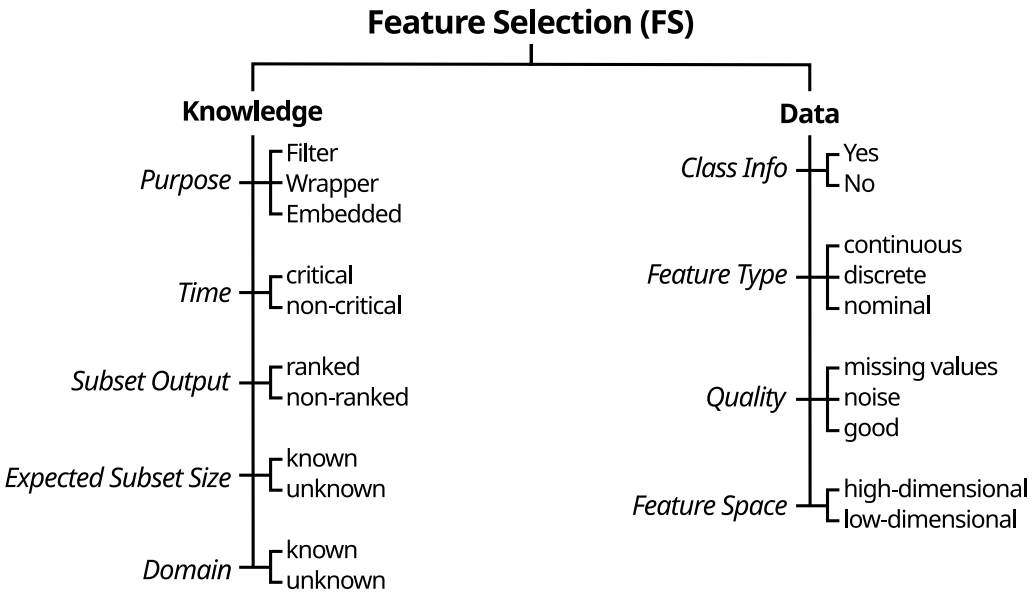

Source: Adapted from Liu and Yu (2005).

Feature selection methods are useful in enhancing knowledge discovery, particularly in high-dimensional data contexts, where there are as many or more features as instances. However, the challenge lies in selecting the optimal FS method. Khalid et al. (2014) conducted a comparative analysis of nine distinct feature selection algorithms. Their findings indicated that most methods address the elimination of redundant or irrelevant features in isolation, with only a few considering noisy data. In their work, Chandrashekar and Sahin (2014) introduced FS techniques predominantly associated with supervised learning models. They further integrated Sequential Feature Selection (SFS) methods with classification models such as the Support Vector Machine (SVM) and Radial Basis Function Network (RBF).

Chen et al. (2020) executed an evaluation on three high-dimensional datasets using three feature selection (FS) methods: Random Forest (RF), Recursive Feature Elimination (RFE), and Boruta. They compared the accuracy and performance of four classification models: RF, SVM, K-Nearest Neighbors (KNN), and Linear Discriminant Analysis (LDA). RF was found to be the superior model due to its simplicity, ability to handle both categorical and numerical features, and lack of distribution assumptions.

Evolutionary computation for FS has garnered attention, with methods like genetic algorithms (GA), genetic programming (GP), and particle swarm optimization (PSO) being at the forefront (XUE et al., 2016a). Cai et al. (2018) not only discussed evaluation measures for feature selection but also surveyed methods across supervised, unsupervised, and semisupervised domains. They presented these methods within a unified framework (Fig. 41). Ensemble methods, which involve the integration of multiple

models, have shown promise in augmenting predictive performance (BOLÓN-CANEDO; ALONSO-BETANZOS, 2018). Techniques like boosting and bagging of inductive learning models have been employed to enhance accuracy and stability over singular FS methods. Given the myriad of potential ensemble structures, numerous studies have aimed to compare and recommend optimal combinations (KIZILOZ, 2021; SPOONER et al., 2023). Some research efforts have also focused on creating frameworks to refine the FS process. For instance, Georges et al. (2020) introduced the *FS-Select* framework to pinpoint optimal feature selection methods, while Overschie et al. (2022) developed a benchmarking platform named *fseval* for comprehensive comparisons and validations of Feature Ranking and Feature Selection algorithms.

Figure 41 – Unified framework view of FS methods.

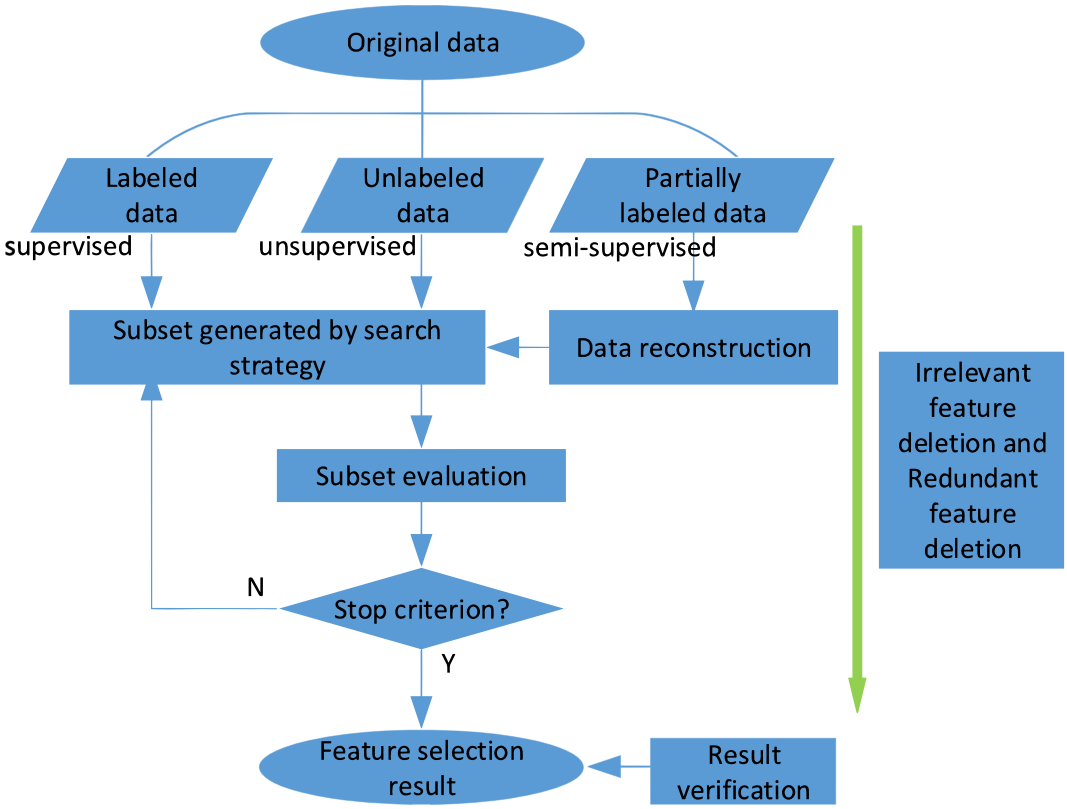

Source: Adapted from Cai et al. (2018).

A review of the literature was conducted, and the robustness of ensemble-based methods in feature selection is evident. Given the nature of mechanism design data, strategies capturing both linear and non-linear relationships among features, while also addressing potential feature interactions, are essential. Despite the numerous possibilities, a basic ensemble setup for Feature Selection is suggested as follows:

- **Models**
  - *Random Forest (RF)*: Recognized for its ability to provide feature importance metrics, this method adeptly captures non-linear relationships.

  - *Gradient Boosted Trees*: Supplementing RF, these models offer distinct importance scores due to their sequential learning mechanism, which focuses on previously mispredicted instances.
  - *Recursive Feature Elimination (RFE) with Logistic Regression or Linear SVM*: Inherently, linear models discern linearly separable patterns. Particularly, RFE ranks features based on their coefficients in the linear model.
  - *Lasso Regression*: Due to its regularization attributes, this method selects a subset of features by reducing certain coefficients to zero.

- **Ensemble Aggregation**
  - Features can be ranked by majority voting, summing their importance scores from both tree-based and linear models. Higher aggregate scores indicate features consistently considered as important across methods.

- **Evaluation**
  - Model performance with selected features can be validated using a test set or cross-validation to ensure feature generalizability.

In summary, for the domain of mechanism design, an ensemble-based approach for feature selection can aid in determining the most relevant features related to design requirements. The proposed ensemble setup provides a harmonious blend of methods, ensuring an exhaustive exploration of the feature space. Iterative refinement is essential as research progresses, ensuring alignment with the characteristics of the studied mechanism.

The output of this phase 3 yields optimal features' subset that aligns with the research goals for further analysis to discover potential innovative gaps within their values.

4.5 PHASE 4: GAP DISCOVERY

The final phase, called *Gap Discovery*, aims to uncover innovative requirements for new mechanism designs by identifying gaps in existing features. Comprising four steps, this phase elucidates the process of systematically discovering and leveraging these gaps:

1. GAP SEARCH: Examine features to identify gaps, i.e., non-existent values or intervals in database.
2. GAP ANALYSIS: Evaluate and rank gaps in features based on their potential for innovation.
3. GAP CLUSTERING: Aggregate gaps to form meaningful clusters.
4. INNOVATION SETS: Select promising gap clusters to derive innovation sets for new design requirements.

4.5.1 Gap Search

The *Gap Search*, as the initial step in Gap Discovery, examine mechanism features to identify gaps, defined as values or intervals missing on database. This step adopts a comprehensive procedure to analyze features in desired contexts, ensuring an exhaustive exploration of the data landscape.

A custom Python function, outlined in Algorithm 1, was developed to systematically scan each feature in the dataset, classifying them by data type and uncovering gaps. This inclusive process encompasses both global and local contexts, facilitating an in-depth data examination.

Algorithm 1 Gap Search for Features

```
procedure GapSearch(database)
    results ← {}
    for each feature in database do
        Detect data_type of feature
        if data_type is numeric then
            database_rounded, precision ← round_array(feature.dropna().unique())
            Update data_type if necessary
            Identify lower_bound and upper_bound of database_rounded
            if data_type is integer then
                eps ← 1
            else if data_type is float then
                eps ← 10^(−precision)
            end if
            Calculate difference between each adjacent element of database_rounded
            if any value in difference > eps then
                Identify gaps using the indices where difference > eps
                Store these gaps
            end if
            Update results with the details for the numeric feature
        else
            List unique items in the non-numeric feature
            Update results with the details for the non-numeric feature
        end if
    end for
    return results
end procedure
procedure round_array(arr)
    Get unique values of arr and sort them
    Identify the number of unique values in arr
    if all values in arr are integers then
        return sorted integer values of arr, 0
    end if
    Find smallest decimal value to round arr while maintaining unique values
    Round arr using this decimal value
    return rounded_arr and precision
end procedure
```

For each considered feature, the function distinguish its data type and, for numeric features, refines values to the smallest representable increment. This precision approach is essential for accurately detecting gaps. The function also check the lower and upper data bounds and computes differences between adjacent elements for numerical features, thereby identifying missing intervals.

The algorithm's output is a structured summary of each feature, detailing its type, unique elements, and observed gaps. Additionally, it provides a quantification of

features with gaps, offering a comprehensive overview of areas lacking data.

4.5.2 Gap Analysis

Following, *Gap Analysis* step focus on prioritizing gaps based on essential ranking criteria including:

- Global context presence, indicating gaps that are unrepresented intervals in database existing designs.
- Association with features of elevated design importance, particularly those with a property requisite type and high relevance in local contexts.
- Correlation with features that simplify complexity or augment capabilities.
- Recurrence across analyses, emphasizing prevalent gaps.

A custom Python function was developed to process and rank gaps, integrating data from diverse contexts such as global mechanism and local links and joints. This procedure creates a dataset connecting each gap to its respective feature, incorporating attributes like repetition count, global context occurrence, scope, and correlations with complexity and capability enhancement.

The result is an ordered list of gaps, ranked by their importance. This list is useful in identifying innovation opportunities for new mechanism designs. Special emphasis is placed on gaps related to features with 'property' requisite type, acknowledging their essential design role.

This systematic approach ensures the identification of most relevant gaps, guiding subsequent steps towards reaching these intervals. It promotes informed design of new mechanisms by focusing on intervals with greatest potential for innovation and improvement.

4.5.3 Gap Clustering

Gap Clustering step involves categorizing identified gaps into clusters based on their context and importance. This step consolidates insights from Gap Analysis into actionable clusters, informing innovative design strategies.

This phase transforms abstract Gap Analysis findings (Section 4.5.2) into structured groupings. Clustering gaps by shared contexts such as global mechanisms, local market status, or specific design parameters, establishes a comprehensive understanding of unexplored innovation areas in mechanism design.

The process employs combinatorial methods for exhaustive gap combinations, targeting groupings that indicate significant mechanical advancements. The outcome is a set of distinct clusters, each embodying a unique combination of identified gaps. These clusters assist engineers and designers in the decision-making process by em-

phasizing areas of mechanism design that hold the greatest potential for groundbreaking innovation.

4.5.4 Innovation Sets

The last step, *Innovation Sets*, consists on selecting the most relevant feature gap subsets within each cluster. This method aims to optimize innovation potential by selecting viable independent sets, based on an in-depth analysis of feature interdependencies.

Innovation sets are derived by ranking these independent sets according to a predefined analytical strategy. These top-ranked sets, referred to as innovation sets, are potential sources for generating innovative design requirements for new mechanisms.

The output of this phase comprises design requirements derived from the innovation sets. By aligning with existing mechanisms in the database, these requirements offer valuable insights for potential innovations, contributing significantly to the advancement of new mechanism designs.

5 PROCESS APPLICATION IN AUTOMOTIVE PGMS DATABASE

This chapter explores the application of the process, as proposed in Chapter 4, for identifying innovative gaps within the database of automotive Planetary Gear Mechanisms. The study focuses on the analysis of automotive planetary gear trains with six to ten speeds, examining their features to determine requirements for innovation. Each phase of the process is exemplified through selected samples, and the resulting findings are presented and discussed in detail.

A total of seven innovation sets have been identified, each representing a promising avenue for the development of new and innovative Planetary Gear Mechanisms. These sets address the identified gaps and capitalize on the potential inherent in each context. The chapter culminates in a thorough discussion of these innovation sets, providing insights into future directions for PGM development in the automotive industry.

5.1 APPLICATION: AUTOMOTIVE PGMS FOR PASSENGER CARS

In this section, the proposed process (Fig. 34) is applied to discover potential innovative gaps in automotive PGMs of passenger cars in the range of 6 to 10 gears. The interest lies in answering the following questions:

1. *Is it possible to identify potential innovation opportunities for the design requirements of an extensive and diverse database of PGMs for passenger cars automatic transmissions in a range of 6 to 10 gears?*
2. *What are the main "property" features that distinguish commercial mechanisms from those patented but not yet built?*
3. *What "property" features distinguish PGMs based on their total number of PGSs?*
4. *What "property" features distinguish PGMs based on their number of forward gears?*
5. *What are the most promising innovation sets for the design requirements of new PGMs?*

The step-by-step application of the four phases of the proposed process is presented in the following sections.

5.2 PHASE 1: MECHANISM SURVEY - PGMS

5.2.1 Step 1. Study Goals

In alignment with the objectives outlined in the thesis (Section 1.1), and highlighted in the previous section, the study goals can be summarized as follows:

1. **Mechanism Type:** The focus is on planetary gear mechanisms in automotive automatic transmissions.
2. **Main Goal:** The main objective is to identify potential innovation opportunities in the topology design requirements of PGMs for automatic transmissions in passenger cars.
3. **Specific Objectives:**
   (a) Identify the most relevant features of planetary gear mechanisms with six to ten gears.
   (b) Identify the most relevant features of commercial automatic transmissions.
   (c) Identify the most promising innovation sets for different automatic transmission design contexts.
4. **Data:** The analysis must include sources such as patented data, academic articles, and manufacturer reports.
5. **Scope:** The study focuses on transmissions with six to ten gears, specifically for passenger cars.
6. **Constraints:** PGMs and their associated kinematic chains will be represented as graph models described in Section 3.1.
7. **Evaluation Criteria:** The evaluation will be based on gaps identified in a database of over one hundred mechanisms.

5.2.2 Step 2. Data Collection

The data was primarily collected from patent databases, particularly ESPACENET, along with books, academic articles, and manufacturers' technical manuals related to automatic transmissions.

To gather relevant information on automotive automatic transmissions with 6 to 10 forward speeds, a patent search was conducted using diverse criteria. The search was performed on ESPACENET, a recognized worldwide open database, as it provided more consistent and comprehensive results when compared to other databases such as PATENTSCOPE, USPTO, and Google Patents. The search query used was as follows:

```
(((nftxt = "automatic" OR nftxt any "multi speed")
AND (nftxt = "transmission" OR nftxt = "gearbox")
AND pd <= "2023-03-20")
AND ((ipc =/low "F16H3/66" OR ipc =/low "F16H3/44"
OR ipc =/low "F16H3/62") AND cpc =/low "F16H2200"))
NOT ((ti any "electric*" OR ti = "hybrid"
OR ti=("method" prox/distance<5 "operation"))
```

```
OR (cpc = "F16H3/724" OR cpc = "F16H3/727"
OR cl = "F16H2057/02034" OR cl =/low "H02K7/00"
OR cl =/low "B60K6/20" OR cl =/low "B62"
OR cl =/low "F16K" OR cl =/low "G06F"
OR cl =/low "B60W" OR cl =/low "F15B"))
```

The search query includes specific criteria, such as the terms "automatic" or "multi-speed" in combination with "transmission" or "gearbox," limited to patents published before March 20, 2023. Additionally, International Patent Classification (IPC) and Cooperative Patent Classification (CPC) symbols related to automatic transmissions were used, and certain exclusions were applied to filter out irrelevant patents, as listed below:

- Specific IPC codes were used to *refine the search*:
  - IPC symbols included "F16H3/66" (Controlled change-speed gears), "F16H3/44" (Epicyclic or planetary gearings), and "F16H3/62" (Multiple forward speeds).
  - CPC symbol "F16H2200" (Automatic control in gearings) was utilized to further refine the search.
- To exclude irrelevant patents, specific *exclusion criteria* were applied:
  - These criteria involved excluding patents related to electric or hybrid technologies.
  - CPC symbols ("F16H3/724" - Electric or hybrid drive, "F16H3/727" - Continuously-variable gearings).
  - IPC symbols ("F16H2057/02034" - Electric propulsion with power supplied within the vehicle, "H02K7/00" - Arrangements for handling mechanical energy structurally associated with the machine, "B60K6/20" - Arrangement or mounting of plural diverse prime-movers, "B62" - Land vehicles, "F16K" - Valves, "G06F" - Electric digital data processing, "B60W" - Conjoint control of vehicle sub-units, "F15B" - Systems acting by means of fluids).

Further filtering was performed to narrow down the search results based on the number of forward speeds:

- *Number of Forward Speeds (CPC code):*
  - 6 forward speeds: F16H2200/0052
  - 7 forward speeds: F16H2200/0056
  - 8 forward speeds: F16H2200/006
  - 9 forward speeds: F16H2200/0065
  - 10 forward speeds: F16H2200/0069

The patent search returned 3125 published patents relating to 6 to 10 forward speeds automotive automatic transmissions, published between 1925 and 2022. The

resulting data was stored in a Google Sheets spreadsheet in Google Drive. In particular, the annual number of patents in the results showed an average of 200 applications between 2002 and 2017. However, there was a peak of 295 patents in 2007, of which 219 were from GM, which was the highest number of applications during this period. There was then a decline after 2017, possibly due to the increased popularity of hybrid and electric vehicles, which may have shifted the focus of innovation towards transmissions for these types of vehicles. A chart of annual patents for automatic transmissions for cars is shown in Figure 42.

Figure 42 – Automotive PGM patents published per year.

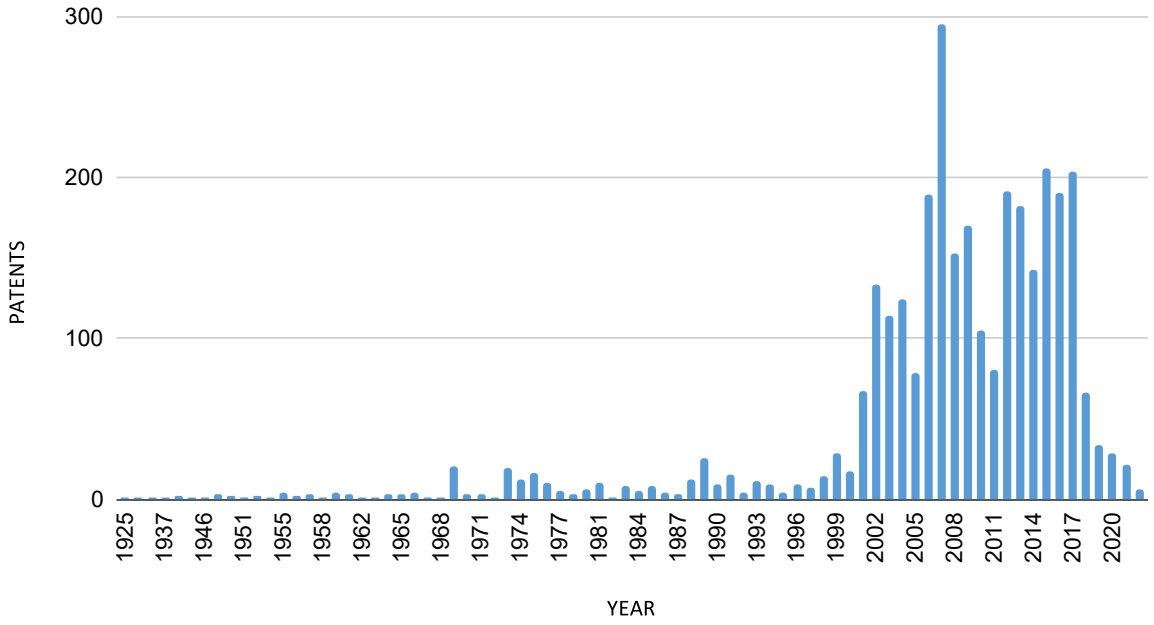

Source: Author.

Identifying all mechanisms protected by a single patent is a laborious task, as patents typically claim a family of mechanisms. Nevertheless, it is possible to estimate the minimum number of PGMs protected by each patent by examining their CPC code related to the number of forward gears. Based on this analysis, it was found that 734 patents claimed 6-speed transmissions, 445 patents covered 7-speed transmissions, 1,009 patents referred to 8-speed transmissions, 710 patents included 9-speed transmissions, and 693 patents were associated with 10-speed transmissions. This data suggests a minimum of 3,591 possible mechanisms. However, it is essential to note that patents may not always indicate all classification codes covered by them, making this analysis an estimate of the minimum number of mechanisms with a specific number of forward gears.

Figure 43 provides a visualization of the yearly patent applications for automotive automatic transmissions, categorized by the number of gears. While there was a slight

increase in patents for 6 and 7-speed transmissions in the early 1970s, the trend gained significant momentum in the early 2000s, with a notable focus on 8-speed transmissions, representing approximately 75% of patented transmissions during the peak in 2007. Subsequently, from 2012 onwards, inventors shifted their focus to increasing the number of gears, leading to more patents for 9 and 10-speed transmissions.

Figure 43 – Automotive PGM published patents segmented by gear ratios (since 1965).

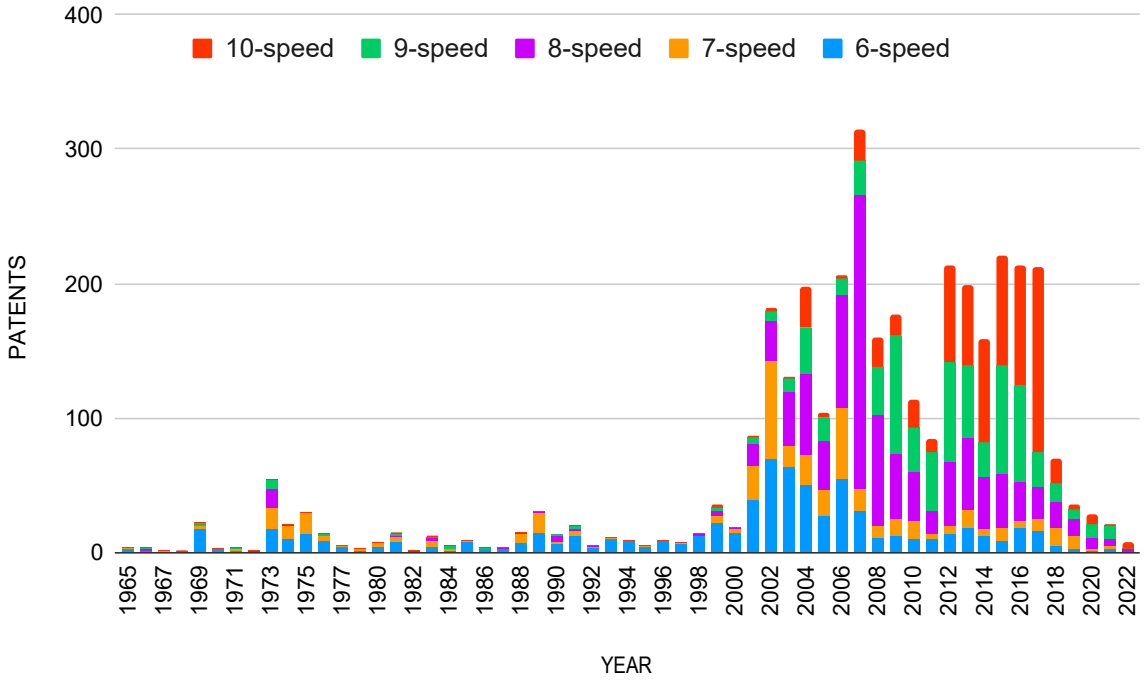

Source: Author.

Furthermore, the analysis of patent applicants (Fig. 44) revealed that GM (USA) and HYUNDAI (South Korea) are the companies with the highest number of patents for automotive automatic transmissions, each accounting for just over 20% of the total patents. This is followed by ZF (Germany) with almost 15% of total patents and AISIN (Japan) with about 5%. FORD (USA), TOYOTA (Japan), and HONDA (Japan) held 3.4%, 2.9%, and 2.4% of the patents respectively. Notably, several universities also patented automatic transmissions for cars, accounting for 1.7% of the total, with China's BEIHANG, ZHAOQING, and CHINA GEOSCIENCES WUHAN universities standing out. Other applicants, with a share of 1.5% or less of published patents, accounted for about 15% of the total.

Based on the results of the patent search, data from 1995 onwards were selected for further analysis, as these years contain the most representative data in terms of patent distribution. Random samples of patents were then selected for each group of forward speeds to ensure a balanced dataset. To complement the dataset, additional samples were selected from other sources such as academic articles and

Figure 44 – Automotive PGM published patents by applicants.

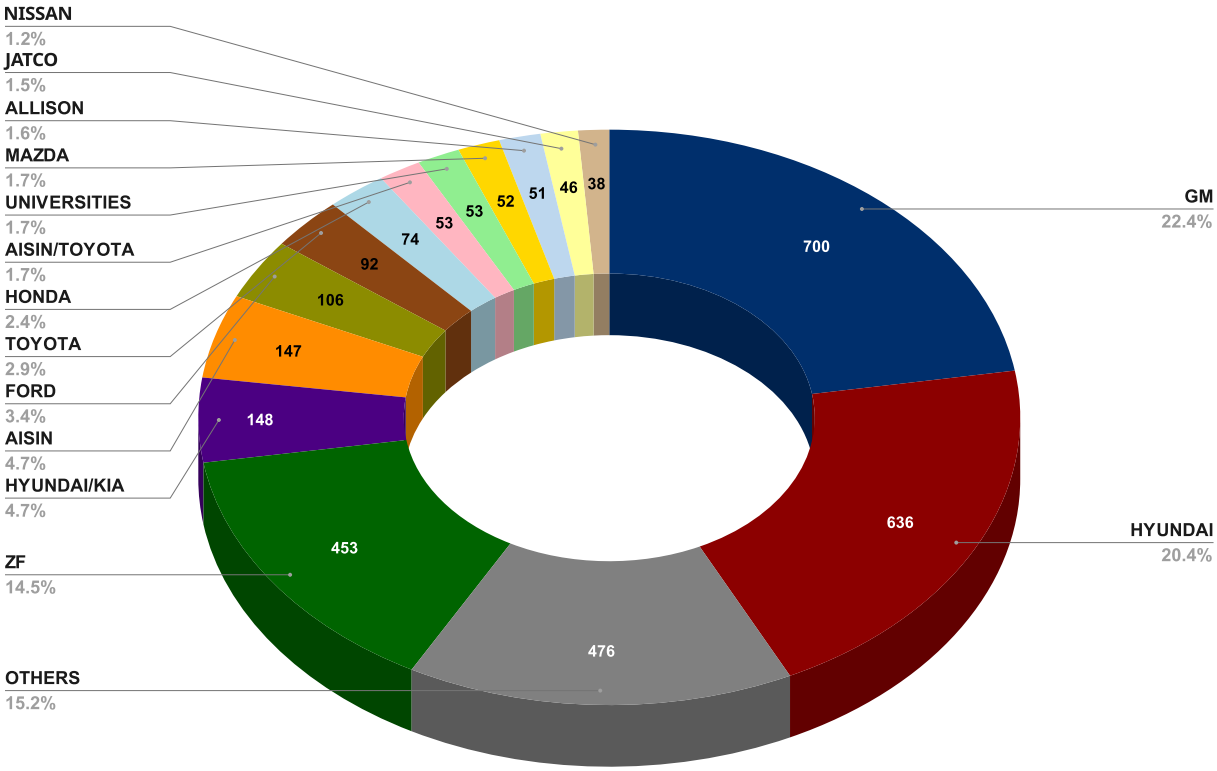

Source: Author.

industry brochures, including commercial transmissions. In total, 51 patents and 15 other sources from 17 different owners were selected for analysis. A meticulous manual analysis of each source was performed to identify and collect data on 160 existing PGMs. A summary of the data collected is presented in Table 15.

Table 15 – Summary of PGMs' collected data.

	Sources Collected			
FWD GEARS	**Patents**	**Other Sources**	**Owners**	***PGMs***
6	12	3	7	77
7	10	0	6	16
8	15	7	10	24
9	11	3	8	16
10	13	2	8	27
Unique	**51**	**15**	**17**	**160**

Source: Author.

5.2.3 Step 3. Dataset Creation

For this step, a standard automated dataset template has been developed to convert the collected PGMs data from the previous step (Section 5.2.2) into suitable graph representations (Section 2.3.1) for posterior analysis. For reasons of space, the template worksheet is presented in Appendix A.1. It requires manual input of minimal

data to characterize mechanisms in terms of identification, topology, functionality, and technical details. The dataset template was automated to generate the PGM topological graph, and the kinematic chain graph (DBG), evaluate and validate structural and functional characteristics, ensuring data consistency and reliability.

The PGM dataset files were created as spreadsheets in Google Sheets and stored in a dedicated folder in Google Drive. Each spreadsheet represents a source of collected data, which may contain one or more related PGMs. In cases where a source contains multiple mechanisms, they are represented by one spreadsheet with multiple worksheets. Conversely, if a source contains only one mechanism, it is represented by a spreadsheet with a single worksheet. The process of creating each PGM dataset begins with copying the standard template as a new dataset file and manually inputting the mechanism's identification, topology, functional, and technical data.

The application of this method is illustrated by a sample from the collected data, an 8-speed automatic transmission developed by Toyota, shown in Figure 45.

Figure 45 – Toyota 8-speed automatic transmission for transverse application.

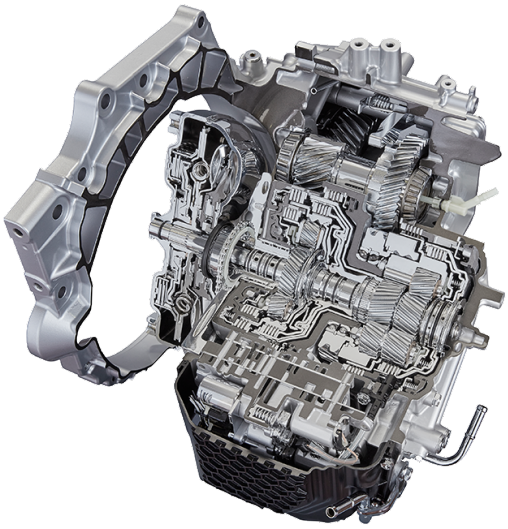

Source: Adapted from Toyota (2016).

The dataset is identified based on the data source, such as the patent number or owner name for academic and industry, and the mechanism model, such as the figure number in the source or commercial name. Spreadsheet files are named according to the source, and worksheets are named according to the model of the PGM they represent. The Toyota's 8-speed AT (Fig. 45) patent publication number is US10563738B2 (IKEMURA et al., 2016), and an excerpt of its bibliographic data is provided in Figure 46. The PGM is based on 'FIG. 1' of the referred patent and its functional diagram is shown in Fig. 47. From this point, the Toyota's 8-speed PGM is identified by its unique identification as *US10563738B2__FIG_1*. Its input identification data is presented in Table 16.

Figure 46 – Bibliographic data excerpt from the patent US10563738B2.

US010563738B2

(12) **United States Patent**
Ikemura et al.

(10) **Patent No.: US 10,563,738 B2**
(45) **Date of Patent: Feb. 18, 2020**

(54) **VEHICULAR AUTOMATIC TRANSMISSION**

(71) Applicant: **TOYOTA JIDOSHA KABUSHIKI KAISHA**, Toyota-shi, Aichi-ken (JP)

(72) Inventors: **Masashi Ikemura**, Toyota (JP); **Hirofumi Ota**, Toyota (JP); **Yasuyuki Hagino**, Toyota (JP); **Mitsuhiro Toyoda**, Miyoshi (JP); **Yosuke Michikoshi**, Toyota (JP)

(73) Assignee: **TOYOTA JIDOSHA KABUSHIKI KAISHA**, Toyota (JP)

(56) **References Cited**

U.S. PATENT DOCUMENTS

5,052,535 A * 10/1991 Vandervoort F16D 11/10 192/69.91
8,360,927 B2 1/2013 Murata et al.
(Continued)

FOREIGN PATENT DOCUMENTS

JP H06-59653 U 8/1994
JP 2003-139157 A 5/2003
(Continued)

Source: Adapted from Ikemura et al. (2016).

Figure 47 – Toyota 8-speed AT functional diagram.

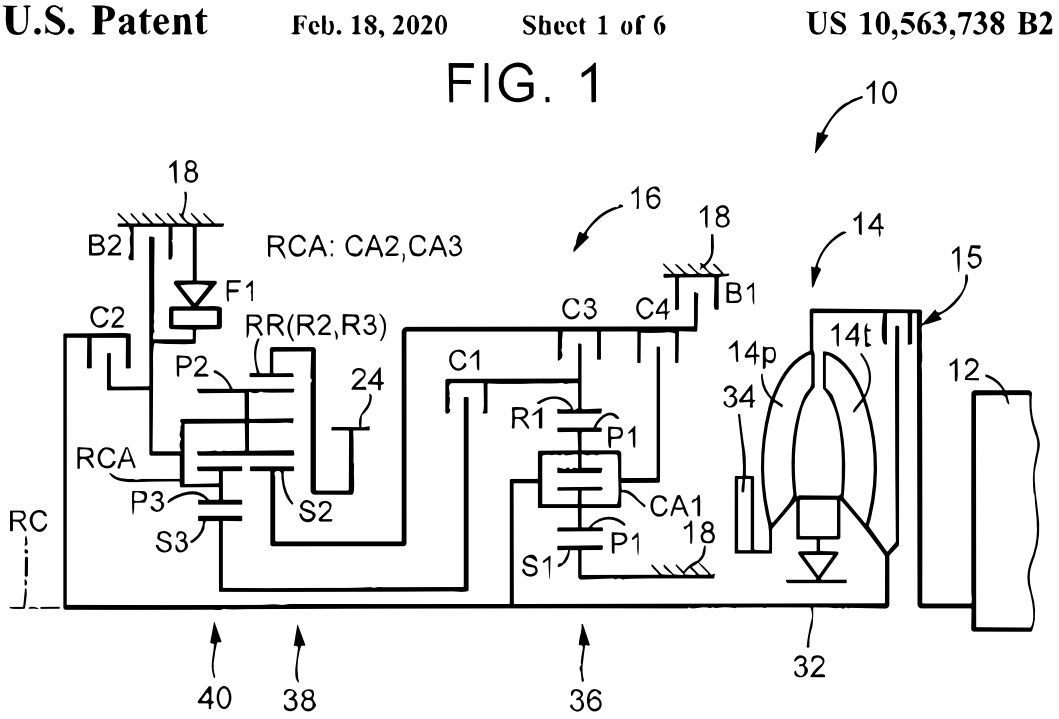

Source: Adapted from Ikemura et al. (2016).

The main topological characteristics are identified by analyzing the mechanism's functional diagram (Fig. 47). This process starts with determining the number of elementary PGSs and their classification as simple (S) or double (D). An adopted standard procedure was to label the elementary PGSs, numbering them from the closest to the input joint as PGS1 and sequentially numbering the adjacent PGSs up to the opposite side of the transmission. All the elementary links of each PGS are labeled according

Table 16 – *US10563738B2__FIG_1* input identification data.

PGM DATA	
Source	patent
Owner	Toyota
Patent Number	US10563738B2
Earliest Priority Date	2015-11-26 [JP]
Model	FIG. 1
PGM DATASET [a]	
Spreadsheet Name (SOURCE_ID)	US10563738B2
PGM Worksheet Name (UNIQUE_ID)	US10563738B2__FIG1

[a] automatically generated by the dataset template.
Source: Author.

to their respective symbols (see Tables 5a and 6a) along with the additional number of the PGS they belong to.

Next, it is reported the inclusion of any additional links in the mechanism beyond the elementary links of the PGSs, including frame, input, and output links. Furthermore, any elementary link that belongs to the declared PGSs but is not present in the PGM is excluded and indicated with a '-' sign. The compound links (CLs) are then input by listing the elementary links they consist of.

To complete the topological characterization of the PGM, the shifting couplings (SCs) are recorded by indicating each pair of links forming the joints and their classification as clutch (C) or brake (B), followed by sequential numbering. The necessary and sufficient topological input to generate the graph of *US10563738B2__FIG_1* is shown in Table 17. The semicolon character ';' is used to separate entities in the input data, facilitating parsing of the information for automated graph generation. It's worth noting that link labels in Table 17 differ from the existing nomenclature in the diagram of Figure 47, as it follows the standard procedure described above.

Table 17 – *US10563738B2__FIG_1* input topological data.

PGS		**LINKS**		**JOINTS**
ID	**Simple (S), Double (D)**	**Include, Exclude (-)**	**Compound (CL)**	**Shift Couplings (SC)**
1	D	F	F;S1	R1;S3;C1
2	S	IN	IN;A1	IN;A2;C2
3	D	OUT	P2;P3R	R1;S2;C3
			OUT;R2;R3	A1;S2;C4
			A2;A3	F;S2;B1
				F;A2;B2

Source: Author.

The required information for the functional characteristics of the PGM involves gear ratios specifications. It's mandatory to input at least the number of forward and reverse (R) gears. If available in the source, the gear ratio values and their respective set of active shifting couplings can also be input in the dataset. Figure 48a provides the engagement operation sequence, present as 'FIG. 2' in the *US10563738B2__FIG_1*'s

patent, containing the number of gear ratios and the active shifting couplings, but misses additional information. To complete the functional characteristics, the gear ratios values (Fig. 48b) were retrieved from an academic source (AOKI et al., 2013), and input in the dataset as presented in Table 18.

Figure 48 – Functional and technical data of *US10563738B2__FIG_1*.

(a) *US10563738B2__FIG_1* shift table.

FIG. 2

	ENGAGEMENT OPERATION TABLE					
	C1	C2	C3	C4	B1	B2
1st	○					○
2nd	○				○	
3rd	○		○			
4th	○			○		
5th	○	○				
6th		○		○		
7th		○	○			
8th		○			○	
Rev			○			○

(b) *US10563738B2__FIG_1* technical info.

Torque converter	**Φ260 with Lock up clutch**
Control	**Electro-Hydraulic**
Gear ratio (Gear step)	**1st 5.200 > (1.75)** **2nd 2.971 > (1.52)** **3rd 1.950 > (1.33)** **4th 1.469 > (1.20)** **5th 1.223 > (1.22)** **6th 1.000 > (1.22)** **7th 0.817 > (1.19)** **8th 0.685** **Rev. 4.254** **Spread 7.58**
Final Gear Ratio	**3.329**
Shift elements	**4 Clutches** **2 Brakes** **1 One-Way Clutch**
Max. Torque Capacity	**Engine Torque : 350Nm**
Mass (Wet)	**96 kg**

Source: (a) Ikemura et al. (2016), (b) Aoki et al. (2013).

Table 18 – *US10563738B2__FIG_1* input functional data.

GEARS		Gear Ratios		Engaged SCs		
R1	;	-4.254	;	C3	;	B2
1	;	5.2	;	C1	;	B2
2	;	2.971	;	C1	;	B1
3	;	1.95	;	C1	;	C3
4	;	1.469	;	C1	;	C4
5	;	1.223	;	C1	;	C2
6	;	1	;	C2	;	C4
7	;	0.817	;	C2	;	C3
8	;	0.685	;	C2	;	B1

Source: Author.

The last data to input in the dataset creation includes the technical characteristics of the PGM regarding the commercial status, and arrangement (longitudinal, transversal, or both). Additionally, if available, the weight (kg) and the maximum torque (N.m) can be

informed. The input technical data for the *US10563738B2__FIG_1*, presented in Table 19, were also retrieved from Aoki et al. (2013).

Table 19 – *US10563738B2__FIG_1* input technical data.

TECHNICAL INFO	
Commercial	TRUE
Arrangement	Transverse
Weight (kg)	96
Torque (N.m)	350

Source: Author.

After inputting the required data, the dataset template automatically generates the list of vertices and edges of the topological graph of PGM and the double bicolored graph (DBG) of the kinematic chain. The list of vertices in the mechanism is generated based on elementary links of PGSs (Tables 5a and 6a) and subsequently contracted based on the compound links declarations. In the list is provided a sequential enumeration of all links, beginning with the frame (F) as number 1, the input (IN) as number 2, the output (OUT) as number 3, and so on for the other links.

Next, the list of edges is created based on the elementary joints of PGSs (Tables 5b and 6b) including the comprising pair of links, the characterization of the joint by type and level, and the joint label (for actuators). Each edge is sequentially enumerated, starting with the input joint as number 1, followed by the output joint as number 2, the kinematic chain joints, and finally, the shifting couplings based on the provided sequence. Both graphs are visually presented in Figure 49.

Figure 49 – PGM and DBG graphs of *US10563738B2__FIG_1*.

(a) *US10563738B2__FIG_1* PGM graph. (b) *US10563738B2__FIG_1* DBG graph.

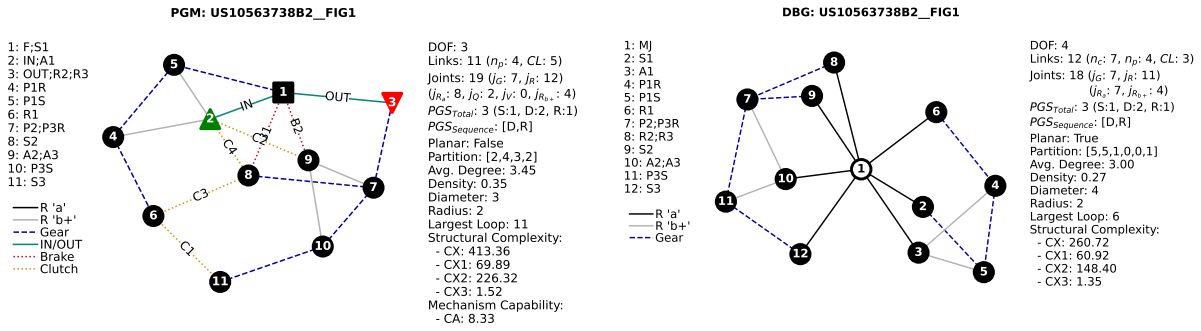

Source: Author.

The structural characteristics (Section 2.3.2.3) are automatically validated by the dataset template, which analyzes the number of loops, revolute and gear joints, and calculates the mobility. Redundant and virtual constraints are checked from the edges list of the graph, ensuring accurate mobility calculation using the revised equation (Eq. (29)).

Furthermore, the dataset template automatically checks if all planetary gear sets are simple and determines the numbers of shifting couplings, brakes, and clutches. Additionally, the number of clutches containing the input link in the joint pair and its input clutch rate are evaluated. The spin losses are determined from the shifting couplings by counting the number of open actuators. Functionality evaluation involves analyzing the gear modes by calculating the total number of possible gear modes, the number of gear modes used as gear ratio, and the utilization rate of gear modes.

The gear specifications are automatically validated, with the number of gears being the only mandatory input functional data. If informed, the gear ratio values are considered to calculate the overall ratio spread, gear steps, and step deviation by comparing the PGM gear steps to an ideally progressive gear ratio progression (as discussed in Section 2.1.1.1) based on the first gear and the average step between gears. The count of underdrive gears, overdrive gears, and direct gears are also assessed. If the sequence of active shift couplings is provided, the calculated mobility through the revised equation is compared to the declared mobility, and the transition between gears is checked for single clutch-to-clutch shift transitions.

Ending validations, the dataset template checks all the verifications results for the minimum set of data compatible to be inserted into the dataset database.

The output of each PGM dataset template is a summarized list of feature values, which are later inserted into a centralized dataset control with all other PGMs analyzed. The results of this step are exemplified for the *US10563738B2__FIG_1* PGM in the following Section 5.3.2.

5.2.4 Step 4. Raw Datasets

The datasets were created as spreadsheets in Google Sheets and stored in a Google Drive folder. Each spreadsheet is a source of the collected data which contains one or more related PGMs. Each worksheet in spreadsheet is a PGM dataset template representing a single mechanism.

A link to the Google Drive folder containing all datasets is available at PGM Datasets folder.

5.3 PHASE 2: DATA ENRICHMENT - PGMS

In this section, the raw datasets of PGMs are enriched by the evaluation and inclusion of a diverse set of new features as shown below.

5.3.1 Step 1. Features Diversification

The features selected to diversify and attempt to uncover nontrivial information about PGMs are presented and integrated on Table 20.

5.3.2 Step 2 and 3. Dictionary of Features and Data Evaluation

In these steps, the complete data dictionary of features (Section 4.3.2) is created by including the new features identified and selected in the Section 5.3.1. A summary of the data associated with the PGMs' graphs was retrieved from a control spreadsheet on Google Drive. This data was then imported into the Google Colab (BISONG, 2019) environment, where SageMath (DEVELOPERS, 2023), used as the local computation backend associated to other libraries Section 4.3.3, calculated the enriched data. An example of the results for the *US10563738B2__FIG_1* PGM is provided in Table 20.

Table 20: *US10563738B2__FIG_1* data dictionary of features.

FEATURE	Description	Feature Type	Data Type	VALUE	Machine Scope	Requisite Scope	Requisite Type	Acquisition
SOURCE †	Data source	categoric	string	patent	AT	technical	information *	measured
OWNER †	Data owner	categoric	string	TOYOTA	AT	technical	information *	measured
PATENT †	Patent number	categoric	string	US10563738B2	AT	technical	information *	measured
DATE †	Release year	datetime	date	2015	AT	technical	information *	measured
MODEL †	Transmission model ID	textual	string	FIG1	AT	technical	information *	measured
SOURCE_ID †	Data source ID	categoric	string	US10563738B2	AT	technical	information *	inferred
UNIQUE_ID †	Transmission unique ID	textual	string	US10563738B2__FIG1	AT	technical	information *	inferred
CHECKLIST COMPLETE? †	Validations passed?	binary	bool	`TRUE`	AT	technical	information *	inferred
Commercial? †	Marketed transmission?	binary	bool	`FALSE`	AT	technical	information	measured
Weight (kg) †	Transmission weight [kg]	numeric	float	96	AT	technical	property	measured
Máx. Torque (N·m) †	Torque capacity [N.m]	numeric	float	350	AT	technical	property	measured
GEAR SPECS Check †	All gear specs informed?	binary	bool	`TRUE`	PGM	functional	information *	inferred
Gears †	Reverse/forward gears informed?	binary	bool	`TRUE`	PGM	functional	information *	inferred
Gear Ratios †	Gear ratios informed?	binary	bool	`TRUE`	PGM	functional	information *	inferred
Gear Shiftings †	Shiftings informed?	binary	bool	`TRUE`	PGM	functional	information *	inferred
RWD GEARS †	Reverse gear count	numeric	int	1	PGM	functional	property	measured
RWD Máx. Ratio †	Max reverse ratio	numeric	float	-4.254	PGM	functional	property	measured
FWD GEARS †	Forward gear count	numeric	int	8	PGM	functional	property	measured
FWD Underdrive Gears †	Underdrive count ($i > 1$)	numeric	int	5	PGM	functional	property	inferred
FWD Direct Drive Ratio †	Direct drive count ($i = 1$)	numeric	int	1	PGM	functional	property	inferred
FWD Overdrive Gears †	Overdrive count ($i < 1$)	numeric	int	2	PGM	functional	property	inferred
FWD Overall Ratio †	Gear ratio spread	numeric	float	7.59124	PGM	functional	property	calculated
FWD Base ratio change (φ_1) †	Base ratio change (φ_1)	numeric	float	1.09596	PGM	functional	property	calculated
FWD Avg Progression Factor (φ_2) †	Average progression factor (φ_2)	numeric	float	1.06821	PGM	functional	property	calculated
FWD φ_2 STDEV †	Standard deviation of φ_2	numeric	float	0.07499	PGM	functional	metric	calculated
FWD φ_2 VAR COEF †	Coefficient of variation of φ_2	numeric	float	0.0702	PGM	functional	metric	calculated
FWD Reference diff †	Ideal vs PGM gear steps difference	numeric	float	0.67976	PGM	functional	metric	calculated
Direct drive? †	Has direct drive ($i = 1$)?	binary	bool	`TRUE`	PGM	functional	metric	inferred
Total Modes †	Total modes for gears	numeric	int	15	PGM	functional	metric	calculated
Used Modes †	Used modes for gears	numeric	int	9	PGM	functional	property	measured
Modes ratio †	Mode utilization ratio	numeric	float	0.6	PGM	functional	metric	calculated

Continued on next page

Table 20: *US10563738B2__FIG_1* data dictionary of features. (Continued)

FEATURE	Description	Feature Type	Data Type	VALUE	Machine Scope	Requisite Scope	Requisite Type	Acquisition
Open Actuators †	Inactive shift couplings in gears	numeric	int	4	PGM	functional	property	inferred
Spin Losses †	Ratio of inactive shift couplings	numeric	float	0.66667	PGM	functional	metric	calculated
Single transition? †	Single shift coupling transitions?	binary	bool	TRUE	PGM	functional	property	inferred
PGM__Ca ‡	PGM capability	numeric	float	8.33333	PGM	functional	metric	calculated
PGM__Ca$_1$ ‡	PGM performance	numeric	int	8	PGM	functional	metric	calculated
PGM__Ca$_2$ ‡	PGM actuation efficiency	numeric	float	0.33333	PGM	functional	metric	calculated
Longitudinal †	Longitudinal arrangement?	binary	bool	FALSE	PGM	structural	property	measured
Transversal †	Transversal arrangement?	binary	bool	TRUE	PGM	structural	property	measured
PGSs Total †	PGS count	numeric	int	3	PGT	structural	property	calculated
PGSs Sequence †	PGSs arrangement (S: Simple, D: Double, R: Ravigneaux)	textual	string	[D, R]	PGT	structural	property	inferred
Simple PGSs †	Simple PGS count	numeric	int	1	PGT	structural	property	measured
Double PGSs †	Double PGS count	numeric	int	2	PGT	structural	property	measured
Ravigneaux PGSs †	Ravigneaux PGS count	numeric	int	1	PGT	structural	property	measured
All simple PGSs? †	All PGSs simple?	binary	bool	FALSE	PGT	structural	metric	inferred
Shifting Couplings (SC) †	PGM shift couplings	numeric	int	6	PGM	structural	property	measured
Brakes (B) †	Brake count	numeric	int	2	PGM	structural	property	measured
Clutches (C) †	Clutch count	numeric	int	4	PGM	structural	property	measured
Input Clutches †	IN link clutches	numeric	int	1	PGM	structural	property	inferred
Clutches as Input †	Ratio of input clutches	numeric	float	0.25	PGM	structural	metric	calculated
All clutches are input? †	All clutches are input?	binary	bool	FALSE	PGM	structural	metric	inferred
Active SCs per gear †	Active shift couplings in gears	numeric	int	2	PGM	structural	property	measured
PGM_Edges †	PGM edges list	textual	string	[a]	PGM	structural	information *	calculated
PGM_Nodes †	PGM vertices list	textual	string	[b]	PGM	structural	information *	calculated
PGM CLASS †	PGM topology classification	categoric	string	[c]	PGM	structural	metric *	inferred
PGM DOFs †	PGM mobility	numeric	int	3	PGM	structural	property	calculated
PGM Loops (L_{PGM}) †	PGM fundamental circuits	numeric	int	9	PGM	structural	property	calculated
PGM LINKS (n) †	PGM links count	numeric	int	11	PGM	structural	property	calculated
PGM JOINTS (j) †	PGM joints count	numeric	int	19	PGM	structural	property	calculated
PGM Gear pairs (j_G) †	PGM gear joints count	numeric	int	7	PGM	structural	property	calculated
PGM Revolute pairs (j_R) †	PGM revolute joints count	numeric	int	12	PGM	structural	property	calculated

Continued on next page

Table 20: *US10563738B2__FIG_1* data dictionary of features. (Continued)

FEATURE	Description	Feature Type	Data Type	VALUE	Machine Scope	Requisite Scope	Requisite Type	Acquisition
PGM Revolute pairs 'a' (j_{R_a}) †	PGM revolute joints in level 'a'	numeric	int	8	PGM	structural	property	calculated
PGM Revolute pairs 'b' (j_{R_b}) †	PGM revolute joints > level 'a'	numeric	int	4	PGM	structural	property	calculated
PGM Redundant circuits (j_Q) †	PGM redundant joints count	numeric	int	2	PGM	structural	property	calculated
PGM Virtual joints (j_V) †	PGM virtual joints count	numeric	int	0	PGM	structural	property	calculated
PGM Compound links (CL_{PGM}) †	PGM compound links	numeric	int	5	PGM	structural	property	calculated
PGM Maximal degree (p_{PGM}) †	PGM max. possible vertex degree	numeric	int	8	PGM	structural	metric	calculated
PGM Link Assortment (LA_{PGM}) †	PGM partition	textual	string	2;4;3;2;0;0;0;0;0;0;0	PGM	structural	property	inferred
PGM LA n_2 †	PGM binary links	numeric	int	2	PGM	structural	property	calculated
PGM LA n_3 †	PGM ternary links	numeric	int	4	PGM	structural	property	calculated
PGM LA n_4 †	PGM quaternary links	numeric	int	3	PGM	structural	property	calculated
PGM LA n_5 †	PGM quinary links	numeric	int	2	PGM	structural	property	calculated
PGM LA n_6 †	PGM senary links	numeric	int	0	PGM	structural	property	calculated
PGM LA n_7 †	PGM septenary links	numeric	int	0	PGM	structural	property	calculated
PGM LA n_8 †	PGM octary links	numeric	int	0	PGM	structural	property	calculated
PGM LA n_9 †	PGM nonary links	numeric	int	0	PGM	structural	property	calculated
PGM LA n_10 †	PGM denary links	numeric	int	0	PGM	structural	property	calculated
PGM LA n_11 †	PGM undenary links	numeric	int	0	PGM	structural	property	calculated
PGM LA n_12 †	PGM duodenary links	numeric	int	0	PGM	structural	property	calculated
PGM Complexity Karhula †	Karhula and Nicolai (2018) complexity	numeric	int	13	PGM	structural	metric	calculated
PGM__Is_planar ‡	Planar PGM graph?	binary	bool	FALSE	PGM	structural	metric	calculated
PGM__Avg_Degree ‡	Average PGM vertex degree	numeric	float	3.45455	PGM	structural	metric	calculated
PGM__Variance_Degree ‡	PGM vertex degree coeff. var.	numeric	float	0.97521	PGM	structural	metric	calculated
PGM__STD_Degree ‡	PGM vertex degree std. dev.	numeric	float	0.98753	PGM	structural	metric	calculated
PGM__Density ‡	PGM graph density	numeric	float	0.34545	PGM	structural	metric	calculated
PGM__Diameter ‡	PGM graph diameter	numeric	int	3	PGM	structural	metric	calculated
PGM__Radius ‡	PGM graph radius	numeric	int	2	PGM	structural	metric	calculated
PGM__Largest_Loop ‡	Largest PGM independent circuit	numeric	int	11	PGM	structural	metric	calculated
PGM__Avg_Clustering ‡	Average PGM graph clustering	numeric	float	0.24545	PGM	structural	metric	calculated
PGM__Avg_Shortest_Path ‡	Average shortest path in PGM	numeric	float	1.85455	PGM	structural	metric	calculated
PGM__Complexity_Coeff ‡	Complexity coeff. of PGM graph	numeric	float	3.73684	PGM	structural	metric	calculated

Continued on next page

Table 20: *US10563738B2__FIG_1* data dictionary of features. (Continued)

FEATURE	Description	Feature Type	Data Type	VALUE	Machine Scope	Requisite Scope	Requisite Type	Acquisition
PGM__CL_size_F ‡	Elementary links in compound F	numeric	int	2	link	structural	metric	calculated
PGM__CL_size_IN ‡	Elementary links in compound IN	numeric	int	2	link	structural	metric	calculated
PGM__CL_size_OUT ‡	Elementary links in compound OUT	numeric	int	3	link	structural	metric	calculated
PGM__CL_count_single__F ‡	Single F link	numeric	int	0	link	structural	metric	calculated
PGM__CL_count_S__F ‡	Sun links in compound F	numeric	int	1	link	structural	metric	calculated
PGM__CL_count_A__F ‡	Arm links in compound F	numeric	int	0	link	structural	metric	calculated
PGM__CL_count_R__F ‡	Ring links in compound F	numeric	int	0	link	structural	metric	calculated
PGM__CL_count_single__IN ‡	Single IN link	numeric	int	0	link	structural	metric	calculated
PGM__CL_count_S__IN ‡	Sun links in compound IN	numeric	int	0	link	structural	metric	calculated
PGM__CL_count_A__IN ‡	Arm links in compound IN	numeric	int	1	link	structural	metric	calculated
PGM__CL_count_R__IN ‡	Ring links in compound IN	numeric	int	0	link	structural	metric	calculated
PGM__CL_count_single__OUT ‡	Single OUT link	numeric	int	0	link	structural	metric	calculated
PGM__CL_count_S__OUT ‡	Sun links in compound OUT	numeric	int	0	link	structural	metric	calculated
PGM__CL_count_A__OUT ‡	Arm links in compound OUT	numeric	int	0	link	structural	metric	calculated
PGM__CL_count_R__OUT ‡	Ring links in compound OUT	numeric	int	2	link	structural	metric	calculated
PGM__degree_F ‡	Adjacency degree of F link	numeric	int	5	link	structural	metric	calculated
PGM__degree_IN ‡	Adjacency degree of IN link	numeric	int	5	link	structural	metric	calculated
PGM__degree_OUT ‡	Adjacency degree of OUT link	numeric	int	2	link	structural	metric	calculated
PGM__neighbors_F ‡	Adjacent links of F	textual	string	[d]	link	structural	property	inferred
PGM__neighbors_IN ‡	Adjacent links of IN	textual	string	F;S1,P1R,P1S,A2;A3,S2	link	structural	property	inferred
PGM__neighbors_OUT ‡	Adjacent links of OUT	textual	string	F;S1,P2;P3R	link	structural	property	inferred
PGM__joints_F ‡	Adjacent joints of F	textual	string	I-a,O-a,Ge-g,B-a,B-a	link	structural	property	inferred
PGM__joints_IN ‡	Adjacent joints of IN	textual	string	I-a,R-b,R-c,C-a,C-a	link	structural	property	inferred
PGM__joints_OUT ‡	Adjacent joints of OUT	textual	string	O-a,Gi-g	link	structural	property	inferred
PGM__eccentricity_F ‡	F eccentricity	numeric	int	3	link	structural	metric	calculated
PGM__eccentricity_IN ‡	IN eccentricity	numeric	int	3	link	structural	metric	calculated
PGM__eccentricity_OUT ‡	OUT eccentricity	numeric	int	3	link	structural	metric	calculated
PGM__degree_centrality_F ‡	F degree centrality	numeric	float	0.5	link	structural	metric	calculated
PGM__between_centrality_F ‡	F betweenness centrality	numeric	float	0.15852	link	structural	metric	calculated
PGM__close_centrality_F ‡	F closenness centrality	numeric	float	0.625	link	structural	metric	calculated

Continued on next page

Table 20: *US10563738B2__FIG_1* data dictionary of features. (Continued)

FEATURE	Description	Feature Type	Data Type	VALUE	Machine Scope	Requisite Scope	Requisite Type	Acquisition
PGM__katz_centrality_F ‡	F Katz centrality	numeric	float	0.34756	link	structural	metric	calculated
PGM__degree_centrality_IN ‡	IN degree centrality	numeric	float	0.5	link	structural	metric	calculated
PGM__between_centrality_IN ‡	IN betweenness centrality	numeric	float	0.14	link	structural	metric	calculated
PGM__close_centrality_IN ‡	IN closenness centrality	numeric	float	0.625	link	structural	metric	calculated
PGM__katz_centrality_IN ‡	IN Katz centrality	numeric	float	0.34994	link	structural	metric	calculated
PGM__degree_centrality_OUT ‡	OUT degree centrality	numeric	float	0.2	link	structural	metric	calculated
PGM__between_centrality_OUT ‡	OUT betweenness centrality	numeric	float	0.01185	link	structural	metric	calculated
PGM__close_centrality_OUT ‡	OUT closenness centrality	numeric	float	0.47619	link	structural	metric	calculated
PGM__katz_centrality_OUT ‡	OUT Katz centrality	numeric	float	0.25903	link	structural	metric	calculated
PGM__Cx ‡	PGM structural complexity	numeric	float	413.35851	PGM	structural	metric	calculated
PGM__Cx_1 ‡	PGM component complexity	numeric	float	69.88908	PGM	structural	metric	calculated
PGM__Cx_2 ‡	PGM interface complexity	numeric	float	226.3168	PGM	structural	metric	calculated
PGM__Cx_3 ‡	PGM topological complexity	numeric	float	1.51765	PGM	structural	metric	calculated
DBG_Edges †	DBG edges list	textual	string	[e]	PGT	structural	information *	calculated
DBG_Nodes †	DBG vertices list	textual	string	[f]	PGT	structural	information *	calculated
DBG CLASS †	DBG topology classification	categorical	string	[g]	PGT	structural	metric *	inferred
DBG DOFs †	DBG mobility	numeric	int	4	PGT	structural	property	calculated
DBG Loops (L_{DBG}) †	DBG fundamental circuits	numeric	int	7	PGT	structural	property	calculated
DBG LINKS (v) †	DBG all links count	numeric	int	12	PGT	structural	property	calculated
DBG Number links (N_l) †	DBG links count w/o hollow vertices	numeric	int	11	PGT	structural	property	calculated
DBG Coaxial links (N_c) †	DBG coaxial links in 'a'	numeric	int	7	PGT	structural	property	calculated
DBG Planet links (N_p) †	DBG planet links count	numeric	int	4	PGT	structural	property	calculated
DBG Hollow Vertices (N_m) †	DBG hollow vertices count	numeric	int	1	PGT	structural	property	calculated
DBG JOINTS (e) †	DBG all joints count	numeric	int	18	PGT	structural	property	calculated
DBG Gear pairs (N_G) †	DBG gear joints count	numeric	int	7	PGT	structural	property	calculated
DBG Revolute pairs (N_R) †	DBG revolute joints count	numeric	int	10	PGT	structural	property	calculated
DBG Revolute pairs 'a' (N_{Ra}) †	DBG revolute joints in level 'a'	numeric	int	6	PGT	structural	property	calculated
DBG Revolute pairs 'b' (N_{Rb}) †	DBG revolute joints in level 'b'	numeric	int	4	PGT	structural	property	calculated
DBG Solid lines (N_s) †	DBG solid lines count	numeric	int	11	PGT	structural	property	calculated
DBG Dashed lines (N_d) †	DBG dashed lines count	numeric	int	7	PGT	structural	property	calculated

Continued on next page

Table 20: *US10563738B2__FIG_1* data dictionary of features. (Continued)

FEATURE	Description	Feature Type	Data Type	VALUE	Machine Scope	Requisite Scope	Requisite Type	Acquisition
DBG Compound links (CL_{DBG}) †	DBG compound links count	numeric	int	3	PGT	structural	property	calculated
DBG Maximal degree (p_{DBG}) †	DBG max. possible vertex degree	numeric	int	8	PGT	structural	metric	calculated
DBG Link Assortment (LA_{DBG}) †	DBG partition	textual	string	5;5;1;0;0;1;0;0;0;0;0;0	PGT	structural	property	inferred
DBG LA n_2 †	DBG binary links	numeric	int	5	PGT	structural	property	calculated
DBG LA n_3 †	DBG ternary links	numeric	int	5	PGT	structural	property	calculated
DBG LA n_4 †	DBG quaternary links	numeric	int	1	PGT	structural	property	calculated
DBG LA n_5 †	DBG quinary links	numeric	int	0	PGT	structural	property	calculated
DBG LA n_6 †	DBG senary links	numeric	int	0	PGT	structural	property	calculated
DBG LA n_7 †	DBG septenary links	numeric	int	1	PGT	structural	property	calculated
DBG LA n_8 †	DBG octary links	numeric	int	0	PGT	structural	property	calculated
DBG LA n_9 †	DBG nonary links	numeric	int	0	PGT	structural	property	calculated
DBG LA n_10 †	DBG denary links	numeric	int	0	PGT	structural	property	calculated
DBG LA n_11 †	DBG undenary links	numeric	int	0	PGT	structural	property	calculated
DBG LA n_12 †	DBG duodenary links	numeric	int	0	PGT	structural	property	calculated
DBG__Is_planar ‡	Planar DBG graph?	binary	bool	TRUE	PGT	structural	metric	calculated
DBG__Avg_Degree ‡	Average DBG vertex degree	numeric	float	3	PGT	structural	metric	calculated
DBG__Variance_Degree ‡	DBG vertex degree coeff. var.	numeric	float	1.83333	PGT	structural	metric	calculated
DBG__STD_Degree ‡	DBG vertex degree std. dev.	numeric	float	1.35401	PGT	structural	metric	calculated
DBG__Density ‡	DBG graph density	numeric	float	0.27273	PGT	structural	metric	calculated
DBG__Diameter ‡	DBG graph diameter	numeric	int	4	PGT	structural	metric	calculated
DBG__Radius ‡	DBG graph radius	numeric	int	2	PGT	structural	metric	calculated
DBG__Largest_Loop ‡	Largest DBG independent circuit	numeric	int	6	PGT	structural	metric	calculated
DBG__Avg_Clustering ‡	Average DBG graph clustering	numeric	float	0.15278	PGT	structural	metric	calculated
DBG__Avg_Shortest_Path ‡	Average shortest path in DBG	numeric	float	2.06061	PGT	structural	metric	calculated
DBG__Complexity_Coeff ‡	Complexity coefficient of DBG	numeric	float	3.61111	PGT	structural	metric	calculated
DBG__eccentricity_MJ ‡	MJ eccentricity	numeric	int	2	link	structural	metric	calculated
DBG__degree_centrality_MJ ‡	MJ degree centrality	numeric	float	0.63636	link	structural	metric	calculated
DBG__between_centrality_MJ ‡	MJ betweenness centrality	numeric	float	0.65455	link	structural	metric	calculated
DBG__close_centrality_MJ ‡	MJ closeness centrality	numeric	float	0.73333	link	structural	metric	calculated
DBG__katz_centrality_MJ ‡	MJ Katz centrality	numeric	float	0.38682	link	structural	metric	calculated
DBG__Cx ‡	DBG structural complexity	numeric	float	260.72415	PGT	structural	metric	calculated

Continued on next page

Table 20: *US10563738B2__FIG_1* data dictionary of features. (Continued)

FEATURE	Description	Feature Type	Data Type	VALUE	Machine Scope	Requisite Scope	Requisite Type	Acquisition
DBG__Cx$_1$ [‡]	DBG component complexity	numeric	float	60.918	PGT	structural	metric	calculated
DBG__Cx$_2$ [‡]	DBG interface complexity	numeric	float	148.3968	PGT	structural	metric	calculated
DBG__Cx$_3$ [‡]	DBG topological complexity	numeric	float	1.34643	PGT	structural	metric	calculated
DBG__C_code [‡]	Yang and Ding (2018) canonical code	textual	string	[h]	PGT	structural	metric	calculated

[†] Output of dataset template (Section 5.2.3).

[‡] Output of data enrichment (Section 5.3.2).

[*] Feature is metadata.

[a] PGM__US10563738B2__FIG1 = ["1 2 'Type': 'I', 'Level': 'a', 'Label': 'IN'", "1 3 'Type': 'O', 'Level': 'a', 'Label': 'OUT'", "4 5 'Type': 'Ge', 'Level': 'g', 'Label': ''", "4 6 'Type': 'Gi', 'Level': 'g', 'Label': ''", "4 2 'Type': 'R', 'Level': 'b', 'Label': ''", "5 1 'Type': 'Ge', 'Level': 'g', 'Label': ''", "5 2 'Type': 'R', 'Level': 'c', 'Label': ''", "7 3 'Type': 'Gi', 'Level': 'g', 'Label': ''", "7 9 'Type': 'R', 'Level': 'd', 'Label': ''", "7 8 'Type': 'Ge', 'Level': 'g', 'Label': ''", "7 10 'Type': 'Ge', 'Level': 'g', 'Label': ''", "7 3 'Type': 'Gi', 'Level': 'g', 'Label': ''", "7 9 'Type': 'R', 'Level': 'e', 'Label': ''", "10 11 'Type': 'Ge', 'Level': 'g', 'Label': ''", "10 9 'Type': 'R', 'Level': 'f', 'Label': ''", "6 11 'Type': 'C', 'Level': 'a', 'Label': 'C1'", "2 9 'Type': 'C', 'Level': 'a', 'Label': 'C2'", "6 8 'Type': 'C', 'Level': 'a', 'Label': 'C3'", "2 8 'Type': 'C', 'Level': 'a', 'Label': 'C4'", "1 8 'Type': 'B', 'Level': 'a', 'Label': 'B1'", "1 9 'Type': 'B', 'Level': 'a', 'Label': 'B2'"]

[b] PGM__US10563738B2__FIG1_Nodes = 1: 'F;S1', 2: 'IN;A1', 4: 'P1R', 5: 'P1S', 6: 'R1', 7: 'P2;P3R', 3: 'OUT;R2;R3', 8: 'S2', 9: 'A2;A3', 10: 'P3S', 11: 'S3'

[c] M03_L09_n11_j19_LA24320000000

[d] IN;A1,OUT;R2;R3,P1S,S2,A2;A3

[e] DBG__US10563738B2__FIG1 = ["1 2 'Type': 'R', 'Level': 'a', 'Label': ''", "1 3 'Type': 'R', 'Level': 'a', 'Label': ''", "1 6 'Type': 'R', 'Level': 'a', 'Label': ''", "1 8 'Type': 'R', 'Level': 'a', 'Label': ''", "1 9 'Type': 'R', 'Level': 'a', 'Label': ''", "1 10 'Type': 'R', 'Level': 'a', 'Label': ''", "1 12 'Type': 'R', 'Level': 'a', 'Label': ''", "4 5 'Type': 'Ge', 'Level': 'g', 'Label': ''", "4 6 'Type': 'Gi', 'Level': 'g', 'Label': ''", "4 3 'Type': 'R', 'Level': 'b', 'Label': ''", "5 2 'Type': 'Ge', 'Level': 'g', 'Label': ''", "5 3 'Type': 'R', 'Level': 'c', 'Label': ''", "7 8 'Type': 'Gi', 'Level': 'g', 'Label': ''", "7 10 'Type': 'R', 'Level': 'd', 'Label': ''", "7 9 'Type': 'Ge', 'Level': 'g', 'Label': ''", "7 11 'Type': 'Ge', 'Level': 'g', 'Label': ''", "7 8 'Type': 'Gi', 'Level': 'g', 'Label': ''", "7 10 'Type': 'R', 'Level': 'e', 'Label': ''", "11 12 'Type': 'Ge', 'Level': 'g', 'Label': ''", "11 10 'Type': 'R', 'Level': 'f', 'Label': ''"]

[f] DBG__US10563738B2__FIG1_Nodes = 1: 'MJ', 2: 'S1', 3: 'A1', 4: 'P1R', 5: 'P1S', 6: 'R1', 7: 'P2;P3R', 8: 'R2;R3', 9: 'S2', 10: 'A2;A3', 11: 'P3S', 12: 'S3'

[g] FD04_L07_Nm1_Nl11_Nr10_Ng07_LA551001000000

[h] 710101111100-02000000000-0120200000-010000000-02000000-0000000-000000-00020-0011-002-02-0

Source: Author.

5.3.3 Step 4. Database

A comprehensive database has been developed to house the full set of features corresponding to each PGM. This database encompasses 160 PGM instances, each characterized by 186 features. Given the large amount of data, aiming to organize a more streamlined understanding of the thesis, each mechanism within the database is detailed in Appendix A. This includes identification, topological, and functional data, along with the mechanism's functional diagram, and the PGM and DBG graphs. The distribution of data types in the database is depicted in the following Figure 50.

Figure 50 – Distribution of data types in the database.

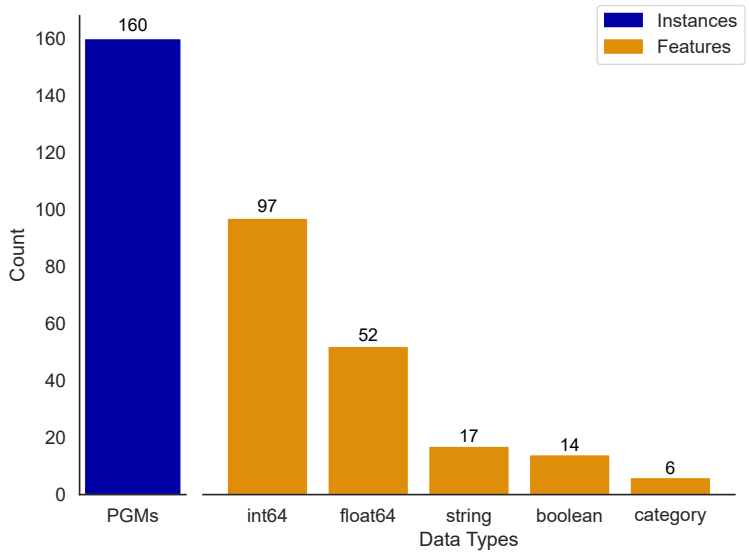

Source: Author.

The complete database can be found in the PGM Complete Database Spreadsheet.

5.4 PHASE 3: FEATURE ANALYSIS - PGMS

The Feature Analysis phase was carried out in the environment mentioned in Section 5.3.2. Subsequently, the processes of Data Preparation, Data Insights, Strategy Analysis, and Feature Selection were elaborated. These processes provided a comprehensive evaluation of the PGMs database leading to the identification of an optimal subset of features for the forthcoming gap discovery.

5.4.1 Step 1. Data Cleansing

During the Data cleansing step, the database, as referenced in Section 5.3.3, was first verified for correct data types based on the feature dictionary detailed in Section 5.3.2. Following this verification, thirteen features exhibiting constant values

were eliminated due to their lack of significance for the analysis. These features included *PGM LA* n_7, *PGM LA* n_8, *PGM LA* n_9, *PGM LA* n_{10}, *PGM LA* n_{11}, *PGM LA* n_{12},*PGM__CL_count_simple__OUT*, *DBG Hollow Vertices (Nm)*, *DBG LA* n_{11}, *DBG LA* n_{12}, *Gears*, *DBG__Radius*, and *DBG__eccentricity_MJ*.

The investigation for missing values within the features was conducted, and the results can be found in Table 21. Features such as *Weight (kg)* and *Máx. Torque(N·m)* were excluded due to the absence of over 90% of their values. Missing values in other features, including *DATE*, *FWD Underdrive Gears*, *FWD Direct Drive Ratio*, and *FWD Overdrive Gears*, were replaced with the median value of their respective *FWD GEARS* group. This strategy was adopted to potentially extract valuable information in subsequent feature analyses.

Table 21 – Missing values in features.

Feature	Missing count	Missing %
Weight (kg)	151	94.38
Máx. Torque (N·m)	150	93.75
RWD Máx. Ratio	24	15.00
FWD Underdrive Gears	24	15.00
FWD Direct Drive Ratio	24	15.00
FWD Overdrive Gears	24	15.00
FWD Overall Ratio	24	15.00
FWD Base ratio change (φ_1)	24	15.00
FWD Avg Progression Factor (φ_2)	24	15.00
FWD φ_2 *STDEV*	24	15.00
FWD φ_2 *VAR COEF*	24	15.00
FWD Reference diff	24	15.00
Direct drive?	24	15.00
PATENT	15	9.38
DATE	9	5.62

Source: Author.

There were 24 PGMs (15% of total) with unspecified gear ratios, resulting in the absence of associated gear specifications. Estimation of these values was deemed unreliable; hence, the related eight features, including *RWD Máx. Ratio*, *FWD Overall Ratio*, *FWD Base ratio change* (φ_1), *FWD Avg Progression Factor* (φ_2), *FWD* φ_2 *STDEV*, *FWD* φ_2 *VAR COEF*, *FWD Reference diff*, and *Direct drive?*, were removed. Additionally, twelve obsolete metadata features, including *SOURCE*, *OWNER*, *PATENT*, *MODEL*, *CHECKLIST COMPLETE?*, *PGM_Edges*, *PGM_Nodes*, *DBG_Edges*, *DBG_Nodes*, *GEAR SPECS Check*, *Gear Ratios*, and *Gear Shiftings*, were also removed from the database.

A comprehensive comparison of all features was carried out to detect duplicates, i.e., identical column values. Five groups of duplicated features were identified, as listed:

1. ***PGM Gear pairs*** *(j_G), DBG Loops (L_{DBG}), DBG Gear pairs (N_G), DBG Dashed lines (N_d)*
2. ***FWD GEARS****, PGM__Ca_1*
3. ***PGM Maximal degree*** *(p_{PGM}), DBG maximal degree (p_{DBG})*
4. ***DBG Number links*** *(N_l), DBG Solid lines (N_s)*
5. ***PGM Revolute pairs*** *(j_{Rb}), DBG Planet links (N_p), DBG Revolute pairs 'b' (N_{Rb})*

Among the groups mentioned above, the five boldfaced features were retained, while the eight others were removed from the database.

A total of 43 features were removed from the database in the cleansing step, remaining 143 useful features.

Subsequent efforts were made to identify any duplicates in the database's instances (rows). Although no completely identical rows were discovered, a meticulous review for isomorphisms, especially regarding PGMs, was deemed essential. Four algorithms, namely VF2++, Weisfeiler Lehman (WL) Hash Test, Perimeter Loop, and Graph Edit Distance (GED), as mentioned in Section 4.4.1, were employed for this purpose. Five sets, comprising a total of ten mechanisms, were identified as potential isomorphisms. A manual comparison of the PGM and DBG graph model representations confirmed their isomorphism. The sets of isomorphic PGMs, represented by their *UNIQUE_ID*, included:

1. **US6595892B2__FIG3**, US6595892B2__FIG9
2. **US6623398B2__FIG7**, US6623398B2__FIG9
3. **US6705967B2__FIG7**, US6705967B2__FIG9
4. **US6705967B2__FIG27**, US6705967B2__FIG31
5. **GM__AT_10_speed_L**, US8545362B1__AT_10_speed_L_10R80

It was noted that these isomorphic PGMs are often variants disclosed in patents, representing fundamentally the same mechanism. An instance of this observation was the collaboration between General Motors and Ford in developing a 10-speed AT, as cited in (SCHIRMER, 2013; GOLESKI; BALDWIN, 2013). The five instances listed in boldface were retained in database, while the five others were removed.

After the database receive essential cleansing processes, it was made ready for further exploration. The cleansed database now comprises 155 PGM instances and 143 features, as depicted in Figure 51.

The database containing all PGM data after cleansing (Section 5.4.1) is available in PGM Prepared Database Spreadsheet.

Figure 51 – Distribution of data types in the database after the cleansing step.

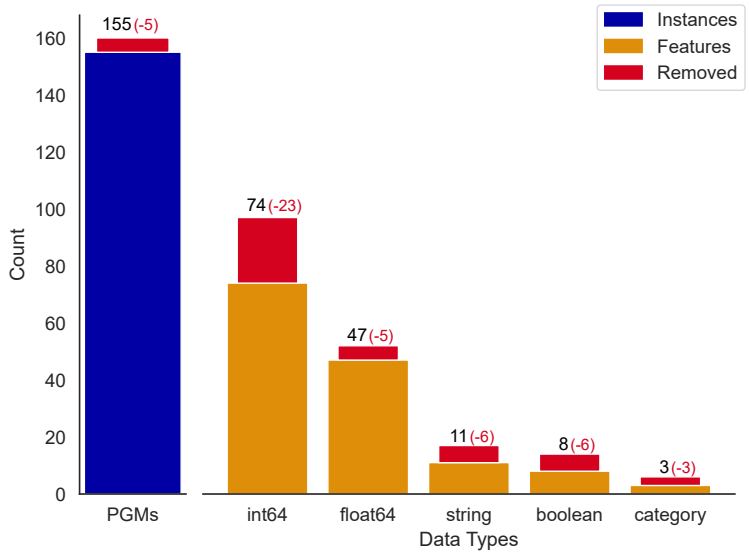

Source: Author.

5.4.2 Step 2. Data Insights

An overview of the database is provided in Table 22. The 155 mechanisms (PGMs) are categorized based on the number of forward gears into five distinct groups. A total of 81 unique kinematic chains have been identified, differentiated by their respective DBG representation. A predominant portion of the PGMs has been designed for a longitudinal arrangement, with a single instance designed for dual usage. Out of the total, 20 PGMs have been identified as commercial products in the market. Structurally, the PGMs in database are composed of three, four, or five planetary gear sets (PGSs).

Table 22 – Database overview.

Forward Gears	PGMs	Unique DBGs	Arrangement			Commercial		No. of PGSs		
			Longitudinal	Transversal	Both	TRUE	FALSE	3	4	5
6	73	34	71	2	0	4	69	73	0	0
7	16	13	16	0	0	1	15	10	6	0
8	24	15	12	11	1	9	15	11	12	1
9	16	15	5	11	0	3	13	1	15	0
10	26	16	21	5	0	3	23	1	13	12
Total	*155*	*81*	*126*	*30*	*1*	*20*	*135*	*96*	*46*	*13*

Source: Author.

Given the large amount of space required for charts, aiming to organize a more streamlined understanding of the thesis, the visual analysis of features is provided in Appendix B. Charts are segmented by the number of forward gears (Appendix B.1.1), the total number of PGSs (Appendix B.1.2), and the commercial status (Appendix B.1.3). Following, the key insights of data analysis are detailed.

Univariate Analysis

A detailed visualization of the distribution for each feature, based on its data type, is presented in Appendix B.1.

The dataset's feature distributions underwent statistical testing to check their normality (Appendix B.1.4). Besides visual inspections, the Shapiro-Wilk, D'Agostino's K^2, and Anderson-Darling tests were applied, and only features that met all three test hypotheses were considered normally distributed. However, it was found that most features in the dataset did not follow Gaussian distributions. Notable exceptions included the betweenness centrality of the input link (denoted as *PGM__between_centrality_IN*) and the topological complexity of the mechanisms (designated as *PGM__*Cx_3). Both displayed Gaussian-like tendencies. Given these findings, nonparametric methods were primarily selected for subsequent statistical analyses to ensure an accurate representation and understanding of the data underlying patterns and distributions.

Bivariate Analysis

A detailed visualization of the correlation matrix is provided in Appendix B.2, and the spreadsheet containing all correlations (Section 5.4.2) is available in PGM Database Correlation Matrix Spreadsheet.

The correlation assessment between numerical features was conducted using Pearson's method when both features adhered to a normal distribution. Conversely, Spearman's method was utilized when at least one of the features deviated from a normal distribution. For the evaluation of categorical features, which encompass boolean data types, Cramér's V with bias correction was employed. In instances where the statistical significance (p-value) exceeded 0.05, the null hypothesis asserting no correlation between the feature pairs was accepted.

In this analysis, correlations were classified based on their absolute values, ensuring the classifications were valid for both positive and negative correlations. The correlation classes are specified in Table 23.

Table 23 – Correlation classes for absolute values.

Class	**Value Range**	
	Low	High
Perfect	1	1
Very Strong	0.9	<1
Strong	0.7	<0.9
Moderate	0.5	<0.7
Weak	>0	<0.5
None	0	0

Source: Author.

In the database investigation, a total of 10,153 unique correlation pairs were analyzed. Among these, 13 pairs exhibited perfect correlations, and 170 showcased very high correlations, jointly accounting for 1.8% of the database. On the contrary, 4,464 pairs displayed weak correlations, and 3,275 pairs revealed no correlation, together making up 76.2% of the entire dataset. A thorough representation of the correlation strengths is provided in Figure 52.

Figure 52 – Distribution of the correlation pairs by strength in database.

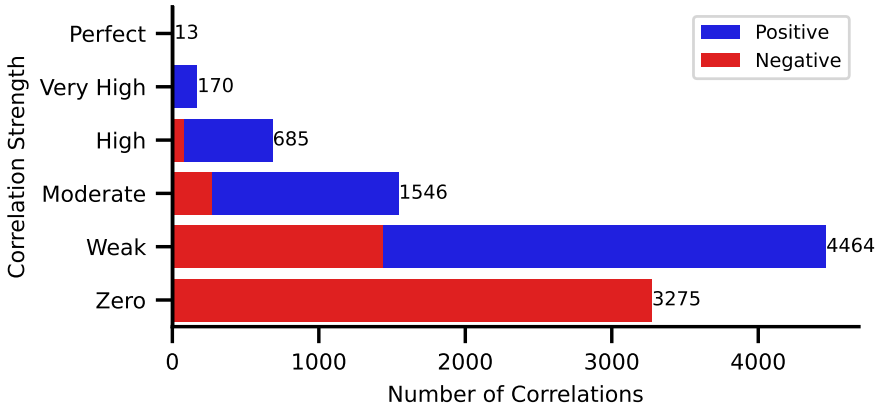

Source: Author.

Based on the analysis of the perfect correlations, nine groups comprising 20 unique features were identified, as enumerated below:

- *PGM Gear pairs (j_G)*, *PGM Maximal degree (p_{PGM})*
- *DBG Number links (N_l)*, *DBG VERTICES (v)*, *DBG Revolute pairs (N_R)*
- *DBG Link Assortment (LA)*, *DBG CLASS*
- *DBG__STD_Degree*, *DBG__Variance_Degree*
- *DBG__degree_centrality_MJ*, *DBG__close_centrality_MJ*
- *DBG Coaxial links (N_c)*, *DBG Revolute pairs 'a' (N_{Ra})*
- *PGM DOFs*, *PGM__Ca_2*, *Active SCs per gear*
- *PGM__CL_size_F*, *PGM__CL_count_single__F*

Within these groups, three features presented perfect negative correlations in their respective groups: *PGM__Ca_2*, *PGM__CL_size_F*, and *PGM__CL_count_single__F*.

5.4.3 Step 3. Strategic Analysis

This step presents strategic analyses for both local and global features within PGMs. For the local features, a link analysis focuses on the characterization of frame (F), input (IN), and output (OUT) with respect to compound links and their adjacency. For the global features, three strategic analyses are conducted: sequence arrangement

of PGSs within each PGM, structural complexity of PGMs, and technological boundary map for PGMs.

These analyses provide insights into the local and global characteristics of PGMs in database, enabling a comprehensive understanding of its structure and functionality.

5.4.3.1 Links Analysis

The frame (F), input (IN), and output (OUT) links were analyzed to determine their compound compositions, adjacency connections, and centrality measures. The results were segmented by three primary characteristics: the number of forward gears, the total count of PGSs, and the commercial status. Due to space limitations, graphical representations of these results for each link are provided in Appendix B.3, and serve as a source of consultation for specific designs for each segment. The overall results are discussed below.

Frame (F) link

In the frame (F) link composition analysis, it is predominantly a single (not compound) link, accounting for 52.9% of the 155 instances. The remaining are compounds with only one elementary link of which 32.3% is a sun (S), 8.4% is an arm (A), and 6.5% is a ring (R).

The adjacency analysis conducted on the Frame (F), it was found that the link frequently exhibited an adjacency degree of 5 (33.5%), an eccentricity of 3 (62.6%), and was associated with 2 brakes (34.8%). On average, the adjacent elementary links composition is 27.9% S, 33.0% A, 30.5% R, and 8.6% P, being the combination of 'S:2,A:3,R:1,P:0' as the most prevalent, representing 6.5% of the instances. On average, the adjacent joints composition is 45.1% j_{R_a}, 2.6% j_{R_b}, 9.0% j_G, and 43.3% B, being the combination of 'j_{R_a}:2, j_{R_b}:0, j_G:0, B:3' as the most prevalent, representing 20.6% of the instances.

Input (IN) link

In the composition analysis of the Input (IN) link, compounds predominantly contain one elementary link, representing 80.0% of the instances. Within this category, 31.0% are identified as an arm (A), 29.7% as a sun (S), and 19.4% as a ring (R). Other compositions include 14.3% with two elementary links, 5.2% with a single link, and solely 0.6% with three elementary links.

The adjacency analysis conducted on the Input (IN), it was found that the link frequently exhibited an adjacency degree of 3 (49.0%), an eccentricity of 3 (71.6%), and was associated with 1 clutches (73.5%). On average, the adjacent elementary links composition is 25.2% S, 27.1% A, 16.8% R, and 30.9% P, being the combination of

'S:1,A:2,R:0,P:1' as the most prevalent, representing 8.4% of the instances. On average, the adjacent joints composition is 27.8% j_{R_a}, 13.4% j_{R_b}, 19.5% j_G, and 39.2% C, being the combination of 'j_{R_a}:1, j_{R_b}:0, j_G:1, C:1' as the most prevalent, representing 27.7% of the instances.

Output (OUT) link

In the composition analysis of the Output (OUT) link, compounds predominantly contain one elementary link, representing 61.9% of the instances. Within this category, 34.8% are identified as a ring (R), 21.9% as an arm (A), and 5.2% as a sun (S). Other compositions include 35.5% with two elementary links, solely 2.6% with three elementary links, and no single link.

The adjacency analysis conducted on the Output (OUT), it was found that the link frequently exhibited an adjacency degree of 2 (46.5%), an eccentricity of 3 (80.6%), and was associated with Longitudinal arrangements (80.6%). On average, the adjacent elementary links composition is 16.9% S, 13.0% A, 12.8% R, and 57.3% P, being the combination of 'S:0,A:0,R:0,P:1' as the most prevalent, representing 25.2% of the instances. On average, the adjacent joints composition is 37.4% j_{R_a}, 22.0% j_{R_b}, 25.4% j_G, and 15.2% C, being the combination of 'j_{R_a}:1, j_{R_b}:0, j_G:1, C:0' as the most prevalent, representing 35.5% of the instances.

5.4.3.2 PGSs Sequence Arrangement Analysis

This strategic analysis examines the sequence in which PGSs are arranged and interconnected within the overall PGM structure. Three fundamental PGS types, defined in Table 24, are considered to compose a PGM: Simple PGS (S), Double PGS (D), and Ravigneaux PGS (R) which is a composition of Simple and Double elementary PGSs.

The arrangement of PGSs in sequence was determined based on the PGM diagrams in Appendix A.2. The PGS connected to the input (IN) link was identified as PGS number 1, with subsequent PGSs enumerated towards the opposite side of the transmission. The arrangement orders, essential for this structural analysis, are represented as PGSs sequences enclosed in brackets, with the input PGS positioned leftmost, followed by the remaining PGSs.

Table 25 presents 15 unique PGSs sequence arrangements identified in the database, segmented by commercial status ('TRUE'), total count of elementary PGSs (3 to 5), and number of forward speeds (6 to 10). The sequence with three Simple PGSs is the most prevalent, found in 63 PGMs, of which 53 represent mechanisms with six forward speeds, 7 with seven, and 3 with eight (only one being commercial). The

Table 24 – Fundamental PGS types in sequence arrangements.

Features	Simple (S)	Double (D)	Ravigneaux (R)
Diagram	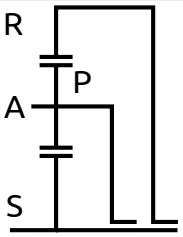	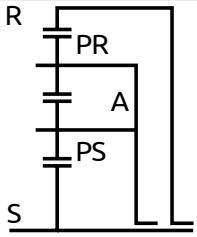	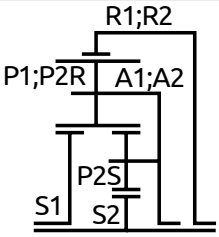
PGS Count	1	1	2
Links (n)	4	5	6
Planet links (n_p)	1	2	2
Coaxial links (n_c)	3	3	4
Compound Links (CL)	0	0	3
Joints (j)	5	7	9
Gear joints (jG)	2	3	4
Revolute joints (j_R)	4	5	6
Revolute joints 'a' (j_{Ra})	2	2	3
Revolute joints 'b' (j_{Rb})	1	2	2
Mobility (DOF)	1	1	1

Source: Author.

sequence with four simple PGSs is the second most common (33 PGMs), with mechanisms generating between seven and ten forward speeds (being ten commercial).

This analysis also highlights the diversity of PGMs showing variations in the sequence arrangements for the same PGS type compositions. For instance, in the case of sequences with two simple and one double PGSs, there are eight [S,S,D], three [S,D,S], and five [D,S,S] sequences.

In the subsequent Section 5.5, PGSs sequences are analyzed to identify potential innovation gaps.

5.4.3.3 Complexity Analysis

This study compares the structural complexity metric '*PGM__Cx*' presented in Section 3.2.1 with other metrics potentially related to the complexity of PGMs. The goal is to identify the metric that best distinguishes and represents the complexity of different mechanisms. For this purpose, the individual terms of '*PGM__Cx*', namely component '*PGM__Cx*$_1$', interface '*PGM__Cx*$_2$', and topological '*PGM__Cx*$_3$', were considered. Additionally, metrics as the number of independent loops '*PGM Loops (L_{PGM})*', the aggregate of shift couplings and gear pairs termed '*PGM Complexity Karhula*', and the network complexity coefficient '*PGM__Complexity_Coeff*' (Section 4.3.1.2) were evaluated. A statistical overview of these complexity features is provided in Table 26.

The analysis of Table 26 reveals that '*PGM__Cx*' exhibits the highest number of unique values (143) and spans a broad range (270.592 to 553.213). This suggests

Table 25: PGSs sequences in the database.

PGSs Sequence*	Commercial?	PGSs Total			FWD GEARS				
	TRUE	*3*	*4*	*5*	*6*	*7*	*8*	*9*	*10*
[S,R]	3	4			4				
[D,R]	3	7					7		
[S,S,S]	1	63			53	7	3		
[S,S,D]		8			7			1	
[S,D,S]		3			2		1		
[S,D,D]		2			1	1			
[D,S,S]		5			4	1			
[D,S,D]		4			2	1			1
[S,S,R]			3				1	2	
[S,D,R]			2				2		
[S,R,S]			1					1	
[D,S,R]			3						3
[R,S,S]	2		4			3			1
[S,S,S,S]	10		33			3	9	12	9
[S,S,S,S,S]	1			13			1		12
Total	***20***	***96***	***46***	***13***	***73***	***16***	***24***	***16***	***26***

* PGS: S - simple, D - double, R - Ravigneaux

Source: Author.

Table 26 – Statistical overview of complexity metrics.

Feature	unique	mode	freq.	mean	std.	min.	max.
PGM Loops (L_{PGM})	6	7	66	7.729	1.089	6	11
PGM Complexity Karhula	6	11	56	12.697	1.649	11	16
PGM__Complexity_Coeff	46	3.000	16	3.372	0.257	2.938	4.000
PGM__Cx	143	413.359	6	377.873	61.104	270.592	553.213
PGM__Cx_1	123	69.889	7	69.017	8.730	59.979	88.671
PGM__Cx_2	143	226.317	6	208.383	33.866	147.389	297.103
PGM__Cx_3	124	1.518	6	1.480	0.051	1.356	1.629

Source: Author.

its potential for providing fine-grained distinctions between mechanisms, even among isomorphic ones. Furthermore, its constituent terms offer insights into various facets of structural complexity.

The link complexity term '*PGM__Cx_1*' possesses 123 unique values, with a mode of 69.889 observed in 49 PGMs. This observation implies that groups of mechanisms may share similar link characteristics, possibly due to common patent origins. The coupling complexity '*PGM__Cx_2*' distinguishes 143 unique values, the same granularity of the structural complexity, while the topological complexity '*PGM__Cx_3*' demonstrates lower sensitivity (124 unique values) in differentiating PGM complexity.

Among other complexity-related metrics, the network complexity coefficient '*PGM__Complexity_Coeff*' stands out with 46 unique values. Both '*PGM Loops (L_{PGM})*' and '*PGM Complexity Karhula*' identify only 6 distinct mechanism groups, demonstrat-

ing their limited ability to capture the nuances of PGM complexity. These shortcomings likely stem from their limitation to consider the interaction between compound links, joint characteristics, and overall kinematic structure.

Several other metrics within the database exhibit a high number of unique values. However, these metrics focus on local link-specific features (F, IN, OUT). Examples include centrality metrics like '*PGM__katz_centrality_IN*' (135 unique values), '*PGM__katz_centrality_OUT*' (134 unique values), and others as detailed in Appendix B.3.

Furthermore, a correlation analysis was conducted to examine relationships between complexity metrics. Figure 53 presents the results as a heatmap.

Figure 53 – Correlation heatmap of PGM Complexity metrics.

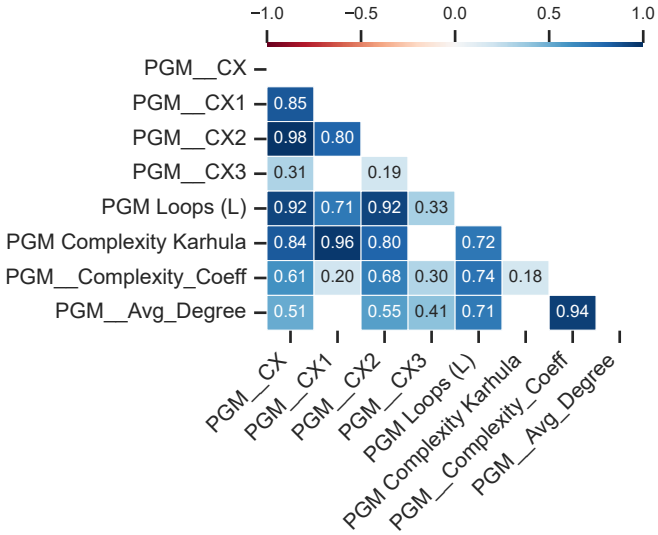

Source: Author.

The structural complexity metric '*PGM__Cx*' exhibits strong positive correlations with multiple features and no observed negative correlations. Specific findings include:

- Structural Complexity '*PGM__Cx*':
  - A very strong positive correlation with its interface component '$PGM__Cx_2$', suggesting a potential linear relationship.
  - A very strong positive correlation with the number of independent loops '$PGM\ Loops\ (L_{PGM})$', reinforcing its relationship with the interface component '$PGM__Cx_2$'.
- Link Complexity '$PGM__Cx_1$':
  - A very strong positive correlation with '*PGM Complexity Karhula*', indicating that the latter metric may be primarily influenced by link complexity.
- Topological Complexity '$PGM__Cx_3$':
  - Demonstrates weak to non-significant correlations with other metrics, em-

phasizing its unique ability to capture distinct aspects of complexity of the topology.

- Network Complexity Coefficient '*PGM__Complexity_Coeff*':
  - Exhibits strong positive correlation with '*PGM__Avg_Degree*', meaning it is mostly an average metric of the graph.

Table 27 presents four similar planetary gear mechanisms arranged in order of increasing structural complexity. Information in the table highlights their distinct characteristics and use complexity metrics (indicated in gray) to quantify these differences. Despite sharing several features, subtle variations in their configurations result in increasing complexity. All four PGMs exhibit the following commonalities: longitudinal arrangement, six forward (FWD) and one reverse (RWD) speeds, three planetary gear sets (PGSs), five shifting couplings (SCs), one input clutch, and seven revolute pairs at level 'a'. Furthermore, they have compound links for frame (F), input (IN), and output (OUT), each composed with a single elementary link.

The comparative analysis of the four PGMs reveals the following insights:

- PGM *US6530858B1__FIG25* exhibits the highest complexity due to:
  - a combination of one double PGS and two simple PGSs (versus three simple PGSs in others)
  - one brake and four clutches (versus only clutches in others)
  - 12 links (highest in the comparison)
  - 18 joints (two more than others)
  - 7 gear pairs (one more than others)
  - 4 revolute pairs in level 'b' (one more than others)
  - a link partition with 2 binary, 8 ternary, and 2 quaternary links
  - a non-planar graph
- PGMs *US6514170B1__FIG4* and *US6595892B2__FIG1* are similar in most aspects. However, *US6595892B2__FIG1* is considered more complex due to:
  - an additional joint in the input (IN) link, indicating increased coupling complexity
  - this complexity exists despite having a planar graph
- PGM *US6530858B1__FIG23* exhibits the lowest complexity, primarily due to:
  - a higher proportion of binary links and fewer ternary links in its partition compared to the others.

An analysis of complexity metrics indicates that the number of loops (L) and the Karhula complexity metric provide limited insight into the complexity differences among these PGMs. While the network complexity coefficient successfully identifies the least

Table 27: Four PGMs complexity comparison.

	US6530858B1__FIG23 (Fig. 172)	**US6514170B1__FIG4 (Fig. 152)**	**US6595892B2__FIG1 (Fig. 174)**	**US6530858B1__FIG25 (Fig. 173)**
Diagram	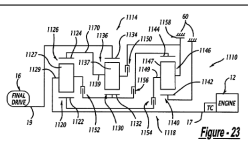	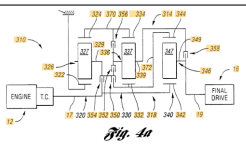	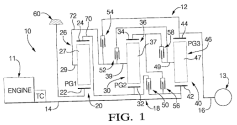	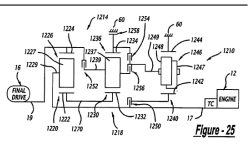
PGM Graph	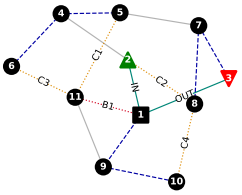	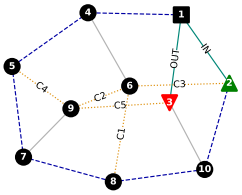	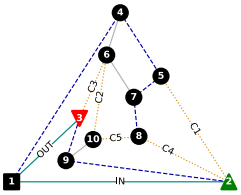	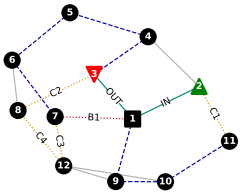
PGSs Sequence	[S,S,S] ★	[S,S,S] ★	[S,S,S] ★	[S,S,D] ▲
Simple PGSs	3 ▲	3 ▲	3 ▲	2 ★
Double PGSs	0 ★	0 ★	0 ★	1 ▲
Brakes (B)	1 ▲	0 ★	0 ★	1 ▲
Clutches (C)	4 ★	5 ▲	5 ▲	4 ★
DOFs	4 ▲	3 ★	3 ★	4 ▲
Loops (L)	6 ★	7 ▲	7 ▲	7 ▲
LINKS (n)	11 ●	10 ★	10 ★	12 ▲
JOINTS (j)	16 ★	16 ★	16 ★	18 ▲
Gear pairs (j_G)	6 ★	6 ★	6 ★	7 ▲
Revolute pairs (j_R)	10 ★	10 ★	10 ★	11 ▲
Revolute pairs (j_{Ra})	7 ●	7 ●	7 ●	7 ●
Revolute pairs (j_{Rb})	3 ★	3 ★	3 ★	4 ▲
Redundant pairs (j_Q)	0 ★	1 ▲	1 ▲	1 ▲
Virtual joints (j_V)	0 ★	0 ★	0 ★	1 ▲
Compound links (CL)	4 ★	5 ▲	5 ▲	4 ★
Partition	3;6;2;0;0;0 ★	0;8;2;0;0;0 ●	0;8;2;0;0;0 ●	2;8;2;0;0;0 ▲
Neighbors F	4 ▲	3 ★	3 ★	4 ▲
Neighbors IN	3 ★	3 ★	4 ▲	3 ★
Neighbors OUT	2 ★	3 ▲	3 ▲	3 ▲
Is planar?	FALSE ▲	FALSE ▲	TRUE ★	FALSE ▲
Complexity Karhula	11 ★	11 ★	11 ★	12 ▲
Complexity Coeff.	3.06 ★	3.25 ▲	3.25 ▲	3.11 ●
PGM__Cx	306.948 ★	307.338 ▼	311.697 ●	333.110 ▲
PGM__Cx_1	60.383 ★	60.422 ▼	60.479 ▼	65.640 ▲
PGM__Cx_2	166.176 ★	167.341 ▼	172.054 ●	178.794 ▲
PGM__Cx_3	1.484 ●	1.476 ▼	1.460 ★	1.496 ▲

Relative complexity based on correlations with the structural complexity metric '*PGM__Cx*' (Appendix B.1):
Best (lowest) (★), Low (▼), Average (●), High (▲)

Source: Author.

complex mechanism, it rates both *US6514170B1__FIG4* and *US6595892B2__FIG1* as highly complex. This coefficient demonstrates strong correlations with link assortments (0.947) and average degree of adjacency (0.937). However, these network features offer limited characterization of specific link and joint types within PGMs.

A detailed examination of the structural complexity metric '*PGM__Cx*' and its components reveals the following:

- Link Complexity '$PGM__Cx_1$':
  - This metric offers limited differentiation among the first three PGMs. Despite an additional link in *US6530858B1__FIG23*, its lower average degree of adjacency contributes to its perceived similarity. Notably, the highest link complexity is exhibited by *US6530858B1__FIG25* due to its 12 links.
- Coupling Complexity '$PGM__Cx_2$':
  - This metric effectively distinguishes joints complexity among the PGMs, accurately capturing local link-specific features (F, IN, OUT), even when PGMs share similar joint counts.
- Topological Complexity '$PGM__Cx_3$':
  - This metric indicates that all PGM topologies are hierarchical (as defined in Section 3.2.1.3). Their partitions support this finding, with each PGM possessing two quaternary links, several ternary links, and few binary links. *US6595892B2__FIG1*, being the unique planar graph, is identified as having the least complex topology. *US6530858B1__FIG23* exhibits a more complex topology than *US6514170B1__FIG4* due to having more links for an equivalent number of joints. As expected, *US6530858B1__FIG25* has the most complex topology, aligning with findings from Table 27.
- Overall Structural Complexity '*PGM__Cx*':
  - Despite limitations in its '$PGM__Cx_1$' component, this metric provides the most accurate and comprehensive assessment of PGM complexity when compared to the previously discussed metrics.

5.4.3.4 Technological Boundary Map for PGMs

This section introduces an updated technological boundary map for PGMs, inspired by the model presented in Figure 28. The updated map utilizes PGM Structural Complexity ('*PGM__Cx*') on the x-axis and PGM Capability ('*PGM__Ca*') on the y-axis. This new representation offers a more precise view of each mechanism, as illustrated in Figure 54.

Analysis of the chart reveals that PGMs positioned further to the left on the x-axis exhibit lower complexity. The integer values of capability on the y-axis correspond

Figure 54 – Technological Boundary Map for PGMs.

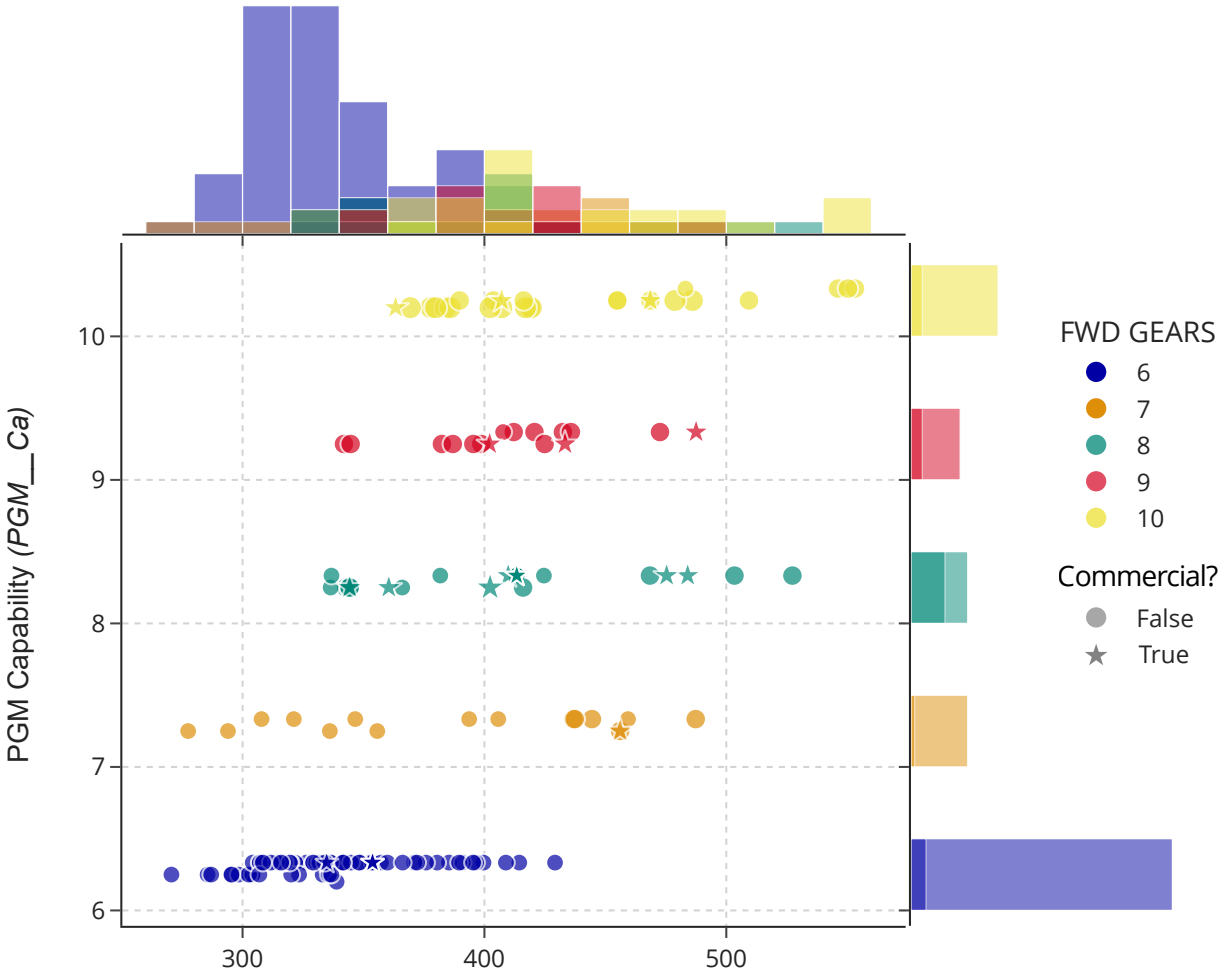

Source: Author.

to the number of forward speeds, with higher positions indicating greater capability. Additionally, within the interval between two integer capability values, a higher position of a PGM suggests less mobility needed to achieve that specific number of forward speeds. As well as, the mechanisms are segmented by the number of speeds (represented by different colors) and by their commercial status (symbolized by '○' for `FALSE` and '⋆' for `TRUE`).

Table 28 presents the two PGMs that represent the extremes of the technological map (Fig. 54) in terms of the structural complexity. These PGMs represent the simplest and the most structurally complex mechanisms identified in the analysis.

5.4.4 Step 4. Feature Selection

This study implemented a multi-faceted approach to evaluate and select the most relevant features for PGM design. The analysis focused on three main characteristics:

Table 28: Comparison of the least and most complex PGMs in database.

	US6530858B1__FIG5 (Fig. 163)	US8029405B2__FIG4 (Fig. 223)
Complexity	**LEAST** ★	**MOST** ▲
Diagram	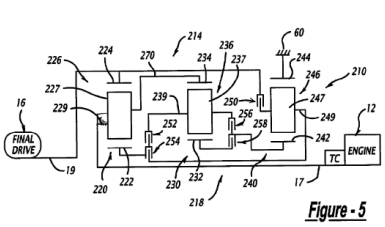	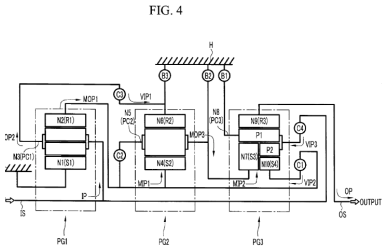
PGM Graph	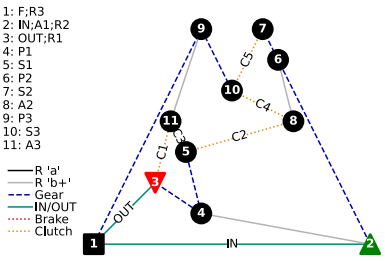	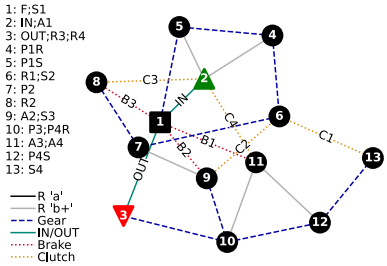
RWD Speeds	1	3
FWD Speeds	6	10
PGSs Total	3★	4▲
PGSs Sequence	[S,S,S]★	[D,S,R]▲
Simple PGSs	3▲	2★
Double PGSs	0★	2▲
Ravigneaux PGSs	0★	1▲
Brakes (B)	0★	3▲
Clutches (C)	5▲	4★
DOFs	4▲	3★
Loops (L)	6★	11▲
LINKS (n)	11★	13▲
JOINTS (j)	16★	23▲
Gear pairs (j_G)	6★	9▲
Revolute pairs (j_R)	10★	14▲
Revolute pairs (j_{Ra})	7★	9▲
Revolute pairs (j_{Rb})	3★	5▲
Redundant pairs (j_Q)	0★	2▲
Virtual joints (j_V)	0★	0★
Compound links (CL)	3★	7▲
Partition	1;A;0;0;0;0★	2;5;4;1;1;0▲
Is planar?	TRUE★	FALSE▲
Neighbors F	3★	6▲
Neighbors IN	3★	5▲
Neighbors OUT	3▲	2★
Complexity Karhula	11★	16▲
Complexity Coeff.	2.938★	3.870▲
PGM__Cx	270.592★	553.213▲
PGM__Cx_1	60.292★	85.092▲
PGM__Cx_2	149.974★	296.840▲
PGM__Cx_3	1.402★	1.577▲

Relative complexity based on correlations with the structural complexity metric '*PGM__Cx*' (Appendix B.1):
Best (lowest) (★), Low (▼), Average (●), High (▲)

Source: Author.

the commercial status of the PGMs, the count of PGSs, and the number of forward gears.

A comprehensive Python function was developed for this purpose, encompassing data preparation, splitting and preprocessing, evaluation of feature importance, and aggregation of feature rankings from various methods.

Initially, the data was processed to address missing values in both numerical and categorical features. Subsequently, it was divided into predictor variables and a target variable. The following features were selected as target variables:

- For the commercial status '*Commercial?*':
  - the PGMs with a status of "TRUE".
- For the planetary gear sets:
  - total count of PGSs.
- For forward speeds '*FWD GEARS*':
  - each forward gear in the range from 6 to 10 speeds.

A *Column Transformer* was utilized to standardize numerical features and *One-Hot Encoding* was applied to categorical features.

The evaluation of feature importance was conducted through a series of methods. A *Random Forest Classifier* was trained to determine feature importance. Additionally, *Recursive Feature Elimination (RFE)* with a *Logistic Regression* estimator was used to identify the top features. Univariate statistical methods, such as *F-scores* for numerical features and *Chi-squared scores* for categorical features, provided further insights. *L1 Regularization* using *LassoCV* also contributed to the feature selection process by highlighting the most significant features.

A two-step approach was employed to identify the most relevant features for each target variable. In the first step, feature rankings were aggregated using *weighted rank aggregation* and *mean rank computation*. This was followed by *score normalization* to ensure all features were on a comparable scale and contribute equally to the final ranking. The *weighted rank* was chosen as the primary metric for this analysis, and the top 15 most relevant features for each target variable are presented in Table 29, listed by order of importance.

Table 29: Top 15 most relevant features for each target variable.

Features	Commercial?	PGSs Total			Forward Speeds				
	TRUE	3	4	5	6	7	8	9	10
PGM__*Ca*		9	3		1		13	1	1
Used Modes		12	2		2			2	2
PGM__Cx_1		4	15		6			15	8
PGM__CL_count_A__IN	2					8	4	7	
DBG__*Cx*		6		4	3				10

Continued on next page

Table 29: Top 15 most relevant features for each target variable. (Continued)

Features	Commercial?	PGSs Total			Forward Speeds				
	TRUE	3	4	5	6	7	8	9	10
PGM__Cx_2			8			9	9	6	
Simple PGSs		5	4	15				13	
DBG__Cx_1		2		2	8				
DBG__Cx_2		7		5	4				
PGM__between_centrality_IN	1						8	9	
PGM LINKS (n)		14		3					3
PGM Complexity Karhula		11			5				5
Clutches as Input	7		11					8	
Total Modes					13		14		9
DBG__Avg_Degree		3	1						
DBG Compound links (CL)	5	1							
PGM__Avg_Clustering	3						3		
PGM__Cx_3						6	1		
DBG__Cx_3	6						2		
PGM__CL_count_R__OUT						2	6		
PGM__between_centrality_F			6					3	
FWD Direct Drive Ratio	12					4			
DBG__Complexity_Coeff		15		1					
PGM JOINTS (j)					12				4
PGM Revolute pairs (j_{Ra})					9				7
PGM Revolute pairs (j_R)					11				6
PGM__Density			10	8					
PGM Gear pairs (j_G)		10		10					
PGM__Cx			7		15				
FWD GEARS		13	9						
PGM__CL_size_OUT			12					10	
PGM Virtual joints (j_V)	11			13					
PGM__katz_centrality_F						13			12
Modes ratio					14	11			
DBG JOINTS (e)				12					14
PGM LA n_6			14			12			
Single transition?	13					14			
RWD GEARS						1			
DBG LA n_3						3			
DBG__between_centrality_MJ	4								
PGM__CL_count_S__IN								4	
PGM__CL_count_A__OUT								5	
PGM__CL_count_S__OUT						5			
DBG__Avg_Clustering							5		
DBG LA n_8			5						
PGM__Avg_Shortest_Path				6					
DBG LA n_4						7			
PGM__close_centrality_OUT							7		
Shifting Couplings (SC)					7				
PGM LA n_2				7					
Brakes (B)	8								
PGM Maximal degree (p_{PGM})		8							
Ravigneaux PGSs	9								
DBG Revolute pairs 'a' (N_{Ra})				9					
Clutches (C)	10								
PGSs Total					10				
PGM__eccentricity_IN						10			

Continued on next page

Table 29: Top 15 most relevant features for each target variable. (Continued)

Features	Commercial?	PGSs Total			Forward Speeds				
	TRUE	3	4	5	6	7	8	9	10
PGM__degree_F							10		
Longitudinal								11	
PGM__between_centrality_OUT							11		
DBG Coaxial links (N_c)				11					
PGM__Largest_Loop									11
PGM__eccentricity_OUT							12		
Input Clutches								12	
DBG__katz_centrality_MJ			13						
PGM__CL_count_R__IN									13
PGM__eccentricity_F	14								
PGM__close_centrality_F								14	
DBG Revolute pairs (N_R)				14					
PGM LA n_5							15		
PGM__katz_centrality_IN	15								
PGM__katz_centrality_OUT									15
PGM__Diameter						15			

Any values exceeding position 15 in the rank are omitted.

Source: Author.

These results may provide a valuable reference for prioritizing essential features in the design process.

Visual representations of the top features identified through all six methods for each target are delineated in Appendix B.4, providing a clear and comprehensive detailing of the results.

5.5 PHASE 4: GAP DISCOVERY - PGMS

5.5.1 Step 1. Gap Search

The gap discovery step investigated features in both global and local contexts to identify ranges of missing values based on the database segmentation.

Analyzing the **global context**, which encompasses features from the entire PGM database, 46 features were identified as containing gaps, suggesting potential opportunities for innovation. Notably, PGS sequence arrangements is the only feature related to property type of the structural scope that exhibited gaps.

The analysis of PGSs sequence arrangements in Section 5.4.3.2 revealed potential innovation gaps due to their role as a global structural property of PGMs. All possible combinations of fundamental PGS types were generated covering the range of gear pairs (j_G) (6 to 10) and total number of elementary PGSs (3 to 5) present in the database (details on these fundamental PGS types are provided in Table 24). Disregarding the exclusion of PGS links during PGT construction, a total of 44 sequence arrangements were identified, distributed across 16 possible combinations of fundamental PGS types. By analyzing these arrangements for gaps, 24 sequence arrangements

were identified as missing entries (gaps) in the database, distributed across 8 combinations of fundamental PGS types. Details on these gaps in sequence arrangements for global context are presented in Table 30.

Table 30: Identified gaps in PGSs sequence arrangements for global context.

PGM Gear pairs (j_G)	PGSs Total	PGSs Combination*	PGSs Sequences Gaps*
8	4	0S + 0D + 2R	[R,R]
9	3	0S + 3D + 0R	[D,D,D]
9	4	1S + 1D + 1R	[S,R,D], [D,R,S]
9	4	3S + 1D + 0R	[S,S,S,D], [S,S,D,S], [S,D,S,S], [D,S,S,S]
10	4	0S + 2D + 1R	[D,D,R], [D,R,D], [R,D,D]
10	4	2S + 2D + 0R	[S,S,D,D], [S,D,S,D], [S,D,D,S], [D,S,S,D], [D,S,D,S], [D,D,S,S]
10	5	1S + 0D + 2R	[S,R,R], [R,S,R], [R,R,S]
10	5	3S + 0D + 1R	[S,S,S,R], [S,S,R,S], [S,R,S,S], [R,S,S,S]

* PGSs: S - simple, D - double, R - Ravigneaux

Source: Author.

Of the remaining 45 features with gaps identified in the global context, 40 are structural metrics, and the remaining 5 are functional metrics. These gaps in features representing metrics requirements can be valuable for decision-making in subsequent stages once kinematic chain structures have been generated.

Analyzing the **local context**, the search for gaps focused on three principal characteristics: the commercial status of the PGMs, the total count of PGSs, and the number of forward speeds.

The analysis of PGMs segmented by ***commercial status "TRUE"*** identified 52 features containing gaps, suggesting potential opportunities for innovation. The most significant gaps were observed in six requisite properties, which are detailed in Table 31. The remaining gaps were identified in 41 structural metrics and 5 functional metrics.

The analysis of PGMs segmented by ***total count of 3, 4, and 5 elementary PGSs*** is summarized below.

An examination of PGMs with a *total count of 3 elementary PGSs* revealed 48 features containing gaps, suggesting potential for innovation. The most significant gaps were observed in two requisite properties, detailed in Table 32. The remaining gaps were identified in 41 structural metrics and 5 functional metrics.

Similarly, for PGMs with a *total count of 4 elementary PGSs*, 48 features containing gaps were identified, indicating potential innovation opportunities. The most significant gaps resided in two requisite properties, presented in Table 33. The remaining gaps were found in 41 structural metrics and 5 functional metrics.

Finally, the analysis of PGMs with a *total count of 5 elementary PGSs* identified 50 features containing gaps, suggesting potential for innovation. In this segment, the most significant gaps were observed in six requisite properties, detailed in Table 34. The remaining gaps were identified in 39 structural metrics and 5 functional metrics.

Table 31: Gaps in requisite properties for *commercial status "TRUE"* context.

Requisite	**Machine**	**Feature**	**Gaps**	
Scope	*Scope*	*Description*	*Count*	*Values*
structural	PGM	PGSs sequences*	19	[R,R], [S,S,D], [S,D,S], [S,D,D], [S,D,R], [S,R,S], [S,R,D], [D,S,S], [D,S,D], [D,S,R], [D,D,S], [D,D,D], [D,R,S], [R,S,D], [R,D,S], [S,S,S,D], [S,S,D,S], [S,D,S,S], [D,S,S,S]
structural	PGT	No. edges in the DBG graph ('*DBG JOINTS (e)*')	1	21
structural	PGT	No. compound links in the DBG graph ('*DBG Compound links (CL)*')	1	5
structural	PGM	No. joints in the PGM ('*PGM JOINTS (j)*')	1	17
structural	PGM	No. ternary links in the PGM graph ('*PGM LA* n_3')	1	7
functional	PGM	No. used modes ('*Used Modes*')	1	8

* PGSs: S - simple, D - double, R - Ravigneaux

Source: Author.

Table 32: Gaps in requisite properties for *total count of 3 elementary PGSs* context.

Requisite	**Machine**	**Feature**	**Gaps**	
Scope	*Scope*	*Description*	*Count*	*Values*
structural	PGM	PGSs sequences*	1	[D,D,D]
functional	PGM	No. used modes ('*Used Modes*')	1	11

* PGSs: S - simple, D - double, R - Ravigneaux

Source: Author.

Table 33: Gaps in requisite properties for *total count of 4 elementary PGSs* context.

Requisite	**Machine**	**Feature**	**Gaps**	
Scope	*Scope*	*Description*	*Count*	*Values*
structural	PGM	PGSs sequences*	16	[R,R], [S,R,D], [D,D,R], [D,R,S], [D,R,D], [R,D,D], [S,S,S,D], [S,S,D,S], [S,S,D,D], [S,D,S,S], [S,D,S,D], [S,D,D,S], [D,S,S,S], [D,S,S,D], [D,S,D,S], [D,D,S,S]
structural	PGT	No. edges in the DBG graph ('*DBG JOINTS (e)*')	1	18

* PGSs: S - simple, D - double, R - Ravigneaux

Source: Author.

Table 34: Gaps in requisite properties for *total count of 5 elementary PGSs* context.

Requisite	**Machine**	**Feature**	**Gaps**	
Scope	*Scope*	*Description*	*Count*	*Values*
structural	PGM	PGSs sequences*	7	[S,R,R], [R,S,R], [R,R,S], [S,S,S,R], [S,S,R,S], [S,R,S,S], [R,S,S,S]
structural	PGT	No. ternary links in DBG graph ('*DBG LA* n_3')	1	9
structural	PGM	No. joints in the PGM ('*PGM JOINTS (j)*')	1	22
structural	PGM	No. ternary links in PGM graph ('*PGM LA* n_3')	1	9
functional	PGM	No. forward gears ('*FWD GEARS*')	1	9
functional	PGM	No. used gear modes ('*Used Modes*')	1	10

* PGSs: S - simple, D - double, R - Ravigneaux

Source: Author.

The analysis of PGMs segmented by ***6, 7, 8, 9, and 10 forward speeds*** is summarized below.

An examination of PGMs with *6 forward speeds* revealed 47 features containing gaps, suggesting potential for innovation. The most significant gaps were observed in two requisite properties, detailed in Table 35. The remaining gaps were identified in 40 structural metrics and 5 functional metrics.

Table 35: Gaps in requisite properties for *6 forward speeds* context.

Requisite	**Machine**	**Feature**	**Gaps**	
Scope	*Scope*	*Description*	*Count*	*Values*
structural	PGM	PGSs sequences*	7	[D,R], [R,D], [R,R], [S,S,R], [S,R,S], [R,S,S], [S,S,S,S]
structural	PGM	No. joints in the PGM ('*PGM JOINTS (j)*')	1	19

* PGSs: S - simple, D - double, R - Ravigneaux

Source: Author.

For *7 forward speeds*, 49 features containing gaps were identified, indicating potential innovation opportunities. The most significant gaps were observed in four requisite properties, presented in Table 36. The remaining gaps resided in 40 structural metrics and 5 functional metrics.

The analysis of PGMs with *8 forward speeds* revealed 50 features containing gaps, suggesting potential for innovation. The most significant gaps were observed in five requisite properties provided in Table 37. The remaining gaps were identified in 40 structural metrics and 5 functional metrics.

An examination of PGMs with *9 forward speeds* identified 48 features containing gaps, with the most significant gaps residing in two requisite properties detailed in Table 38). The remaining gaps were found in 41 structural metrics and 5 functional metrics.

Table 36: Gaps in requisite properties for *7 forward speeds* context.

Requisite	**Machine**	**Feature**	**Gaps**	
Scope	*Scope*	*Description*	*Count*	*Values*
structural	PGM	PGSs sequences*	7	[S,R], [D,R], [R,S], [R,D], [R,R], [S,D,S], [S,R,S]
structural	PGM	No. brakes ('*Brakes (B)*')	1	1
structural	PGM	No. joints in the PGM ('*PGM JOINTS (j)*')	2	18, 19
structural	PGM	No. ternary links in PGM graph ('*PGM LA* n_3')	1	5

* PGSs: S - simple, D - double, R - Ravigneaux

Source: Author.

Table 37: Gaps in requisite properties for *8 forward speeds* context.

Requisite	**Machine**	**Feature**	**Gaps**	
Scope	*Scope*	*Description*	*Count*	*Values*
structural	PGM	PGSs sequences*	18	[S,R], [R,S], [R,R], [S,S,D], [S,D,D], [S,R,S], [S,R,D], [D,S,S], [D,S,D], [D,S,R], [D,D,S], [D,D,D], [D,R,S], [R,S,D], [S,S,S,D], [S,S,D,S], [S,D,S,S], [D,S,S,S]
structural	PGT	No. edges in the DBG graph ('*DBG JOINTS (e)*')	1	21
structural	PGM	No. brakes ('*Brakes (B)*')	1	1
structural	PGM	No. joints in the PGM ('*PGM JOINTS (j)*')	1	21
structural	PGM	No. binary links in PGM graph ('*PGM LA* n_2')	1	4

* PGSs: S - simple, D - double, R - Ravigneaux

Source: Author.

Table 38: Gaps in requisite properties for *9 forward speeds* context.

Requisite	**Machine**	**Feature**	**Gaps**	
Scope	*Scope*	*Description*	*Count*	*Values*
structural	PGM	PGSs sequences*	7	[D,R], [R,D], [R,R], [S,D,S], [S,D,D], [D,S,D], [D,D,S]
structural	PGM	No. redundant circuits in the PGM ('*PGM Redundant circuits* (j_Q)')	1	2

* PGSs: S - simple, D - double, R - Ravigneaux

Source: Author.

Finally, for PGMs with *10 forward speeds*, 50 features containing gaps were identified. The most significant gaps were observed in four requisite properties, presented in Table 39. The remaining gaps resided in 41 structural metrics and 5 functional metrics.

Table 39: Gaps in requisite properties for *10 forward speeds* context.

Requisite	**Machine**	**Feature**	**Gaps**	
Scope	*Scope*	*Description*	*Count*	*Values*
structural	PGM	PGSs sequences*	29	[R,R], [S,D,D], [S,D,R], [S,R,S], [S,R,D], [S,R,R], [D,D,S], [D,D,D], [D,D,R], [D,R,S], [D,R,D], [R,S,R], [R,D,S], [R,D,D], [R,R,S], [S,S,S,D], [S,S,S,R], [S,S,D,S], [S,S,D,D], [S,S,R,S], [S,D,S,S], [S,D,S,D], [S,D,D,S], [S,R,S,S], [D,S,S,S], [D,S,S,D], [D,S,D,S], [D,D,S,S], [R,S,S,S]
structural	PGT	No. edges in the DBG graph (’*DBG JOINTS (e)*’)	1	21
structural	PGT	No. ternary links in DBG graph (’*DBG LA* n_3’)	1	9
structural	PGM	No. ternary links in PGM graph (’*PGM LA* n_3’)	1	9

* PGSs: S - simple, D - double, R - Ravigneaux

Source: Author.

5.5.2 Step 2. Gap Analysis

This section focuses on analyzing and prioritizing gaps in features based on their innovation potential for PGM topology. A prioritization scheme is established, detailed in Table 40, which ranks criteria in descending order of importance.

The *Topology and Performance ranks* criteria consider the correlation values between features and the position of gap values according to optimization goals. The feature correlations are evaluated to three strategic metrics relevant to structural complexity and capability of the mechanisms:

- *’DBG__Cx’*: Kinematic chain structural complexity. Goal: ↓ *minimize*.
- *’PGM__Cx’*: Mechanism structural complexity. Goal: ↓ *minimize*.
- *’PGM__Ca’*: Mechanism capability. Goal: ↑ *maximize*.

Considering only numeric features, the *Gap Correlation Index* for each metric is calculated using the general formula (Eq. (47)):

$$\text{Gap Correlation Index} = \text{Normalized Gap Value} \cdot (|\text{Correlation Value}|)^{\text{Weighting Factor}}, \quad (47)$$

where:

- *Normalized Gap Value* represents the position of a gap within the valid range of its corresponding feature in the local context. This value is calculated to account for both individual and range-based gaps. It is determined as follows:

Table 40: Prioritization scheme for feature gaps by innovation potential.

Rank	Criteria	Ordered Values
1	**Database Context** *Feature gaps in global contexts are prioritized over those in local contexts. The risk of representing infeasible solutions must be evaluated by the designer.*	global local
2	**Requisite Scope and Type** *Gaps in features of the structural scope (particularly those related to property requirements) receive the highest priority as they represent potential innovation in PGM structural synthesis. Features of the functional and technical scopes (particularly those related to property and metric requirements) are more relevant to dimensional synthesis.*	structural property structural metric functional property functional metric technical property technical metric
3	**Machine Scope** *Gaps in features associated with the kinematic chain (PGT), represented by DBG graph features, are considered more innovative. This prioritizes gaps in features related to the core topology of the mechanisms, as PGMs are built upon kinematic chains.*	PGT PGM AT link joint
4	**Topology** *Gaps with a strong correlation to reducing PGM structural complexity are considered to have more innovation potential.*	
5	**Performance** *Gaps with a strong correlation to enhancing PGM capability are considered to have more innovation potential.*	
6	**Feature Relevance** *Gaps are ordered by the most relevant features for each context.*	Table 29
7	**Frequency** *Gaps that appear most frequently across multiple local context analyses are considered more significant.*	

Source: Author.

  - For features where higher values are desirable (e.g., *'PGM__Ca'*):

$$\text{Normalized Gap Value}_{\uparrow\text{maximize}} = \frac{\textit{Max}\ \text{Gap Value} - \text{Feature Lower Bound}}{\text{Feature Upper Bound} - \text{Feature Lower Bound}}$$

  - For features where lower values are desirable (e.g., *'DBG__Cx'*, *'PGM__Cx'*):

$$\text{Normalized Gap Value}_{\downarrow\text{minimize}} = \frac{\text{Feature Upper Bound} - \textit{Min}\ \text{Gap Value}}{\text{Feature Upper Bound} - \text{Feature Lower Bound}}$$

- *Correlation Value* represents the correlation coefficient between the feature with a gap and the corresponding strategic feature, as determined in Section 5.4.2. Weak correlations (< |0.5|) are disregarded.
- *Weighting Factor* emphasizes the importance of correlation value in this ranking. An empirical value of 1.5 was used in this case.

Therefore, features with stronger correlations (positive or negative depending on the optimization direction) to the strategic features receive higher correlation ranks.

The *Feature Relevance rank* is based on the features relative importance within their local context. The *Relevance Index* is the inverse of the ranking resulted from the feature selection process (Tab. 29) and is calculated as follows (Eq. (48)):

$$\text{Relevance Index} = \frac{1}{\text{Feature Rank}_{\text{Local Context}}} \quad . \tag{48}$$

Otherwise, the relevance index for features not present in the local context is 0. Thus, a higher relevance index indicates a significantly greater potential for innovation within that context.

Following the established prioritization scheme (Tab. 40), the gaps in property requisite features were ranked based on stronger correlations to strategic metrics in the desired optimization direction, higher relevance, and higher frequency across contexts. The resulting rank, detailed in Table 41, identifies gaps in features with the highest potential for innovation in PGMs.

Table 41: Innovation potential rank of gaps in property requisite features.

Requisite *Scope*	**Machine** *Scope*	**Feature**	**Gap** *Value*	**Context** *Local*	**Topology** *Rank*[1]	**Performance** *Rank*[2]	**Relevance** *Rank*[3]	**Frequency** *Count*
structural	*PGT*	DBG JOINTS (e)	21	FWD GEARS=10	0.591	0.147	0.042	3
structural	*PGT*	DBG JOINTS (e)	18	PGSs Total=4	0.391	0.000	0.021	1
structural	*PGT*	DBG Compound links (CL)	5	Commercial?=TRUE	0.124	0.000	0.333	1
structural	*PGT*	DBG JOINTS (e)	21	FWD GEARS=8	0.140	0.000	0.019	3
structural	*PGT*	DBG JOINTS (e)	21	Commercial?=TRUE	0.116	0.000	0.012	3
structural	*PGT*	DBG LA n_3	9	PGSs Total=5	0.103	0.000	0.013	2
structural	*PGT*	DBG LA n_3	9	FWD GEARS=10	0.000	0.000	0.033	2
structural	*PGM*	PGM JOINTS (j)	20	PGSs Total=5	0.629	0.110	0.026	1
structural	*PGM*	PGM LA n_3	9	FWD GEARS=10	0.071	0.614	0.018	2
structural	*PGM*	PGM Revolute pairs (j_R)	11	PGSs Total=5	0.559	0.146	0.010	1
structural	*PGM*	PGM JOINTS (j)	22	PGSs Total=5	0.210	0.329	0.026	1
structural	*PGM*	PGM JOINTS (j)	17	Commercial?=TRUE	0.423	0.112	0.015	1
structural	*PGM*	PGM Redundant circuits (j_Q)	2	FWD GEARS=9	0.245	0.275	0.012	1
structural	*PGM*	Brakes (B)	1	FWD GEARS=7	0.405	0.000	0.015	2
structural	*PGM*	PGM Virtual joints (j_V)	2	Commercial?=TRUE	0.000	0.000	0.500	2
structural	*PGM*	PGM JOINTS (j)	(18, 19)	FWD GEARS=7	0.341	0.000	0.010	1
structural	*PGM*	PGM Virtual joints (j_V)	2	FWD GEARS=8	0.000	0.296	0.014	2
structural	*PGM*	PGM Revolute pairs (j_{Ra})	7	PGSs Total=5	0.000	0.249	0.019	1
structural	*PGM*	PGM JOINTS (j)	19	FWD GEARS=6	0.143	0.000	0.083	1
structural	*PGM*	PGM JOINTS (j)	21	FWD GEARS=8	0.114	0.000	0.023	1
structural	*PGM*	Brakes (B)	1	FWD GEARS=8	0.000	0.000	0.017	2
structural	*PGM*	PGM LA n_3	9	PGSs Total=5	0.000	0.000	0.010	2
structural	*PGM*	PGM LA n_3	5	FWD GEARS=7	0.000	0.000	0.021	1
functional	*PGM*	Used Modes	11	PGSs Total=3	0.000	0.502	0.083	1
functional	*PGM*	Used Modes	8	Commercial?=TRUE	0.275	0.227	0.037	1
functional	*PGM*	FWD GEARS	9	PGSs Total=5	0.000	0.249	0.026	1
functional	*PGM*	Used Modes	10	PGSs Total=5	0.000	0.249	0.011	1

[1] Based on Gap Correlation Index (Eq. (47)) computed for structural complexity (Cx) of the related machine scope.
[2] Based on Gap Correlation Index (Eq. (47)) computed for PGM capability (Ca).
[3] Based on Relevance Index (Eq. (48)).

Source: Author.

The analysis revealed 27 potentially innovative gaps within 12 distinct property features across 9 local contexts. For structural requirements related to kinematic chains (PGTs), the gap with the highest potential for innovation is 21 joints in the DBG graph for transmissions with 10 forward speeds. For entire mechanisms (PGMs), the gap with the most significant potential for innovation is 20 joints in the PGM graph for transmissions with 5 elementary PGSs. When analyzing the gaps associated with functional properties, PGMs with 9 forward speeds and 5 elementary PGSs exhibit the most noteworthy potential for innovation. Further analysis in the following sections details the remaining potentially innovative gaps.

5.5.3 Step 3. Gap Clustering

Gaps in PGSs sequence arrangements were clustered with structural and functional property features gaps within specific local contexts (Tab. 41). Nine potential clusters for innovation were identified across various contexts, as detailed in Table 42, utilizing the feature gap prioritization scheme (Tab. 40). These clusters are presented in descending order of priority. Forward gear configurations ranging from six to ten speeds, particularly ten-speed configurations, demonstrate significant potential for innovation. Additionally, all planetary gear set (PGS) configurations offer development opportunities, with five-PGS transmissions exhibiting notable potential for innovation in mechanisms with nine gears.

Table 42: Gaps clustered by contexts.

Cluster	Context	Requisite	Machine	Feature	Gap
	Local	*Scope*	*Scope*		*Values*
1	**FWD GEARS=10**	*structural*	*PGT*	DBG JOINTS (e)	21
				DBG LA n_3	9
				PGSs Sequence	[R,R], [S,R,S], [S,D,D], [S,R,D], [D,D,S], [D,D,D], [D,R,S], [S,S,S,D], [S,S,D,S], [S,D,S,S], [D,S,S,S], [S,D,R], [S,R,R], [D,D,R], [D,R,D], [R,S,R], [R,D,S], [R,D,D], [R,R,S], [S,S,S,R], [S,S,D,D], [S,S,R,S], [S,D,S,D], [S,D,D,S], [S,R,S,S], [D,S,S,D], [D,S,D,S], [D,D,S,S], [R,S,S,S]
			PGM	PGM LA n_3	9
2	**PGSs Total=5**	*structural*	*PGT*	DBG LA n_3	9
				PGSs Sequence	[S,R,R], [R,S,R], [R,R,S], [S,S,S,R], [S,S,R,S], [S,R,S,S], [R,S,S,S]
			PGM	PGM JOINTS (j)	20, 22
				PGM LA n_3	9
				PGM Revolute pairs (j_R)	11
				PGM Revolute pairs ($j_R a$)	7
		functional	*PGM*	FWD GEARS	9
		functional	*PGM*	Used Modes	10
3	**PGSs Total=3**	*structural*	*PGT*	PGSs Sequence	[D,D,D]
		functional	*PGM*	Used Modes	11
4	**Commercial?=**`TRUE`	*structural*	*PGT*	DBG Compound links (CL)	5
				DBG JOINTS (e)	21
				PGSs Sequence	[R,R], [S,R,S], [S,D,D], [S,R,D], [D,D,S], [D,D,D], [D,R,S], [S,S,S,D], [S,S,D,S], [S,D,S,S], [D,S,S,S], [S,D,S], [D,S,D], [S,S,D], [S,D,R], [D,S,S], [D,S,R], [R,S,D], [R,D,S]
			PGM	PGM JOINTS (j)	17
				PGM Virtual joints (j_V)	2
		functional	*PGM*	Used Modes	8
5	**FWD GEARS=9**	*structural*	*PGT*	PGSs Sequence	[R,R], [S,D,D], [D,D,S], [D,R], [R,D], [S,D,S], [D,S,D]
			PGM	PGM Redundant circuits (j_Q)	2
6	**FWD GEARS=7**	*structural*	*PGT*	PGSs Sequence	[R,R], [S,R,S], [D,R], [R,D], [S,D,S], [S,R], [R,S]
			PGM	Brakes (B)	1
				PGM JOINTS (j)	18, 19
				PGM LA n_3	5
7	**PGSs Total=4**	*structural*	*PGT*	DBG JOINTS (e)	18
				PGSs Sequence	[R,R], [S,R,D], [D,R,S], [S,S,S,D], [S,S,D,S], [S,D,S,S], [D,S,S,S], [D,D,R], [D,R,D], [R,D,D], [S,S,D,D], [S,D,S,D], [S,D,D,S], [D,S,S,D], [D,S,D,S], [D,D,S,S]
8	**FWD GEARS=8**	*structural*	*PGT*	DBG JOINTS (e)	21
				PGSs Sequence	[R,R], [S,R,S], [S,D,D], [S,R,D], [D,D,S], [D,D,D], [D,R,S], [S,S,S,D], [S,S,D,S], [S,D,S,S], [D,S,S,S], [D,S,D], [S,R], [R,S], [S,S,D], [D,S,S], [D,S,R], [R,S,D]
			PGM	Brakes (B)	1
				PGM JOINTS (j)	21
				PGM Virtual joints (j_V)	2
9	**FWD GEARS=6**	*structural*	*PGT*	PGSs Sequence	[R,R], [S,R,S], [D,R], [R,D], [S,S,R], [R,S,S], [S,S,S,S]
			PGM	PGM JOINTS (j)	19

Source: Author.

5.5.4 Step 4. Innovation Sets

Innovation sets for each local context were generated by combining PGT features gaps based on the clusters identified in Table 42. The feasibility of each PGSs sequence arrangement was evaluated for every feature combination to ensure the practicality and potential utility of the proposed innovation sets. The corresponding local context PGM features and gaps were integrated to complete each innovation set. This process resulted in at least 13 innovation sets of feasible combinations organized and prioritized based on their innovation potential, as presented in Table 43.

Table 43: Innovation Sets within local contexts.

SET	Context Local	Features & Gaps	PGSs Sequences
1	*FWD GEARS=10*	DBG LA n_3=9, DBG JOINTS (e)=21, PGM LA n_3=9	[S,S,R,S], [R,D,S], [S,S,D,D], [S,D,D,S], [S,R,D], [S,D,S,D], [D,S,D,S], [D,D,S,S], [R,S,S,S], [D,R,S], [S,S,S,R], [S,R,S,S], [R,D,D], [D,S,S,D], [D,S,S,S], [D,R,D], [S,S,D,S], [D,D,D], [R,R,S], [S,D,S,S], [D,D,R], [R,S,R], [S,S,S,D], [S,R,R], [S,D,R]
2	*FWD GEARS=10*	DBG LA n_3=9, PGM LA n_3=9	[S,S,R,S], [R,D,S], [S,S,D,D], [S,D,D,S], [S,R,D], [S,D,S,D], [D,S,D,S], [D,D,S], [D,D,S,S], [R,R], [R,S,S,S], [D,R,S], [S,S,S,R], [S,R,S,S], [R,D,D], [S,R,S], [S,D,D], [D,S,S,D], [D,S,S,S], [D,R,D], [S,S,D,S], [D,D,D], [R,R,S], [S,D,S,S], [D,D,R], [R,S,R], [S,S,S,D], [S,R,R], [S,D,R]
3	*FWD GEARS=10*	DBG JOINTS (e)=21, PGM LA n_3=9	[S,S,R,S], [R,D,S], [S,S,D,D], [S,D,D,S], [S,R,D], [S,D,S,D], [D,S,D,S], [D,D,S,S], [R,S,S,S], [D,R,S], [S,S,S,R], [S,R,S,S], [R,D,D], [D,S,S,D], [D,S,S,S], [D,R,D], [S,S,D,S], [D,D,D], [R,R,S], [S,D,S,S], [D,D,R], [R,S,R], [S,S,S,D], [S,R,R], [S,D,R]
4	*PGSs Total=5*	DBG LA n_3=9, PGM JOINTS (j)=20, 22, PGM Revolute pairs (j_R)=11, PGM Revolute pairs ($j_R a$)=7, PGM LA n_3=9, FWD GEARS=9, Used Modes=10	[S,S,R,S], [S,R,S,S], [R,S,S,S], [R,R,S], [S,S,S,R], [R,S,R], [S,R,R]
5	*PGSs Total=3*	Used Modes=11	[D,D,D]
6	*Commercial?=TRUE*	DBG Compound links (CL)=5, DBG JOINTS (e)=21, PGM JOINTS (j)=17, PGM Virtual joints (j_V)=2, Used Modes=8	[R,S,D], [D,S,S,S], [S,S,D,S], [R,D,S], [D,D,D], [D,R,S], [S,R,D], [S,D,S,S], [D,S,R], [S,S,S,D], [S,D,R]
7	*Commercial?=TRUE*	DBG Compound links (CL)=5, PGM JOINTS (j)=17, PGM Virtual joints (j_V)=2, Used Modes=8	[D,S,S,S], [R,S,D], [S,S,D,S], [R,D,S], [S,R,S], [S,D,D], [D,D,D], [D,R,S], [S,D,S], [D,S,S], [S,R,D], [S,D,S,S], [S,S,D], [D,S,R], [S,S,S,D], [D,D,S], [D,S,D], [S,D,R]
8	*Commercial?=TRUE*	DBG JOINTS (e)=21, PGM JOINTS (j)=17, PGM Virtual joints (j_V)=2, Used Modes=8	[D,S,S,S], [R,S,D], [S,S,D,S], [R,D,S], [D,D,D], [D,R,S], [S,R,D], [S,D,S,S], [D,S,R], [S,S,S,D], [S,D,R]
9	*FWD GEARS=9*	PGM Redundant circuits (j_Q)=2	[R,R], [S,D,D], [D,D,S], [D,R], [R,D], [S,D,S], [D,S,D]
10	*FWD GEARS=7*	Brakes (B)=1, PGM JOINTS (j)=18, 19, PGM LA n_3=5	[R,R], [S,R,S], [D,R], [R,D], [S,D,S], [S,R], [R,S]
11	*PGSs Total=4*	DBG JOINTS (e)=18	[D,S,S,S], [D,R,D], [S,S,D,S], [R,R], [R,D,D], [S,S,D,D], [D,R,S], [D,D,S,S], [S,D,D,S], [S,R,D], [S,D,S,S], [D,D,R], [S,D,S,D], [S,S,S,D], [D,S,S,D], [D,S,D,S]
12	*FWD GEARS=8*	DBG JOINTS (e)=21, PGM Virtual joints (j_V)=2, PGM JOINTS (j)=21, Brakes (B)=1	[D,S,S,S], [R,S,D], [S,S,D,S], [D,D,D], [D,R,S], [S,R,D], [S,D,S,S], [D,S,R], [S,S,S,D]
13	*FWD GEARS=6*	PGM JOINTS (j)=19	[R,R], [S,R,S], [D,R], [R,D], [S,S,R], [R,S,S], [S,S,S,S]

Source: Author.

These sets may be further combined based on additional criteria, as determined by the designer's expertise and the study's objectives. The innovation sets represent promising requisites for the development of novel PGMs, effectively addressing identified gaps focused on the potential of each context.

Using these innovation sets as design requirements for new PGMs substantially reduces the design space. This reduction, facilitated by the identified attribute gaps, can guide the generation of alternative mechanism solutions. Consequently, this approach streamlines the design process, optimizing time and resources while promoting innovative solutions without the need for an exhaustive search.

6 PGMS DESIGN USING INNOVATION SETS

This chapter demonstrates how innovation sets identified in Chapter 5 are used to design potentially novel Planetary Gear Mechanisms (PGMs). The following section will detail the PGM synthesis process by presenting a discussion of initial concept generation and then progressing to an examination of the proposed diagrams for the two potentially new PGM configurations.

6.1 SYNTHESIS PROCESS

The first innovation set in Table 43 was chosen to exemplify the synthesis process of potential novel PGMs. This specific innovation set was identified for the local context of 10 forward speeds and presents four features with clearly defined gaps, as follows:

- DBG LA n_3 = 9
- DBG JOINTS (e) = 21
- PGM LA n_3 = 9
- PGSs Sequences = [S,S,S,D], [S,S,D,S], [S,D,S,S], [S,S,D,D], [S,D,D,S], [S,D,S,D], [S,S,S,R], [S,S,R,S],[S,R,S,S], [D,S,S,S], [D,S,D,S], [D,D,S,S], [D,S,S,D], [R,S,S,S], [S,D,R], [S,R,D], [S,R,R], [D,D,D], [D,D,R], [D,R,D], [D,R,S], [R,D,S], [R,D,D], [R,R,S], [R,S,R].

This implies that PGMs with 10 forward speeds and exhibiting any of these specific feature values are absent from the existing database. Given the context, the desired number of gears will be m_r = 11, consisting of ten forward speeds and one reverse speed.

To characterize the context of ten-speed transmissions, key features, their respective values, and correlations with PGT complexity and PGM capability were identified through analysis of the 26 mechanisms in the database. These are highlighted below in Table 44.

The PGSs sequence *1S+1D+1R [S,R,D]*, shown in Figure 55, was selected as a reference for the synthesis of potentially novel PGMs. This selection was motivated by two key factors. First, the chosen sequence possesses a more compact and less complex structure compared to the other alternative sequences. Second, the sum of the joints in the kinematic chain is e = 21, which aligns with the target number of joints desired for the innovation set.

To form the kinematic chain, all possible compound links between the coaxial links of the PGSs were generated, totaling 7881 PGTs represented by DBG graphs. However, an analysis of degeneration (rigid sub-chains) led to the removal of almost half of the PGTs, resulting in 4086 non-degenerated kinematic chains. Isomorphism evaluation further eliminated a significant number of candidate solutions, ultimately

Table 44: Characterization of 10 forward speed local context.

Feature	Unique Values	Correlations	
		Complexity *(DBG__Cx)*	**Capability** *(PGM__Ca)*
PGM Gear pairs (j_G)	[8, 9, 10] (Fig. 243)	*0.939*	*0.446*
DBG JOINTS (e)	[19, 20, 22, 23, 24, 25] (Fig. 247)	*0.922*	*0.581*
DBG LINKS (v)	[12, 13, 14, 15, 16] (Fig. 247)	*0.898*	*0.627*
PGSs Total	[3, 4, 5] (Fig. 242)	*0.868*	*0.781*
PGM LINKS (n)	[12, 13, 14, 15, 16] (Fig. 243)	*0.840*	*0.841*
Simple PGSs	[1, 2, 3, 4, 5] (Fig. 242)	*0.733*	*0.851*
PGM JOINTS (j)	[20, 21, 22, 23] (Fig. 243)	*0.705*	*0.002*
DBG DOFs	[3, 4, 5] (Fig. 247)	*0.662*	*0.801*
PGM Redundant circuits (j_Q)	[0, 1, 2, 3] (Fig. 243)	*0.619*	*0.791*
PGM Virtual joints (j_V)	[0, 1, 2] (Fig. 244)	*0.589*	*0.872*
PGM__Is_planar	69.2% of PGMs are `FALSE` (Fig. 250)	*0.568*	*0.371*
Shifting Couplings (SC)	[6, 7, 8] (Fig. 243)	*0.506*	*0.701*
PGM DOFs	[3, 4, 5] (Fig. 243)	*0.488*	*1.000*
PGM LA (n_3)	[4, 5, 6, 7, 8, 10] (Fig. 244)	*0.405*	*0.815*
PGM Compound links (CL_{PGM})	[4, 5, 6, 7] (Fig. 244)	*0.386*	*0.191*
PGM Loops (L_{PGM})	[7, 8, 9, 10, 11] (Fig. 243)	*0.222*	*0.865*
DBG LA (n_3)	[4, 5, 6, 7, 8, 10] (Fig. 248)	*0.214*	*0.140*
Double PGSs	[0, 1, 2] (Fig. 242)	*0.176*	*0.686*
PGM Revolute pairs (j_R)	[12, 13, 14] (Fig. 243)	*0.120*	*0.513*
Ravigneaux PGSs	[0, 1] (Fig. 242)	*0.057*	*0.564*
PGM__*CX*	min=363.27, max=553.21, avg=438.29 (Fig. 247)	*0.048*	*0.786*
Commercial?	11.5% of PGMs are `TRUE` (Fig. 250)	*0.000*	*0.000*

Source: Author.

Figure 55 – Diagram of the reference PGSs sequence *1S+1D+1R [S,R,D]*.

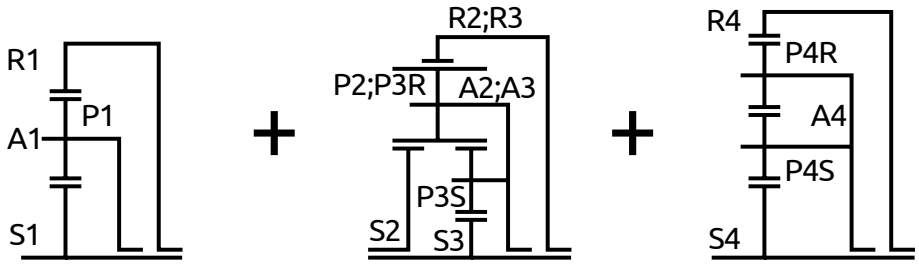

Source: Author.

yielding 710 non-isomorphic kinematic chains.

Each PGT was assessed according to its DBG graph to generate features consistent with the existing database. Potential new PGTs were arranged in ascending order by structural complexity (*Cx*), and the top 10 are shown in Table 45 along with their respective DBG graphs and primary attributes.

Table 45: Top 10 new potential PGTs.

Rank	DBG Graph of PGT
1	**DBG: 1S+1D+1R__277** 1: MJ 2: P1 3: R1 4: P3S 5: P4R 6: P4S 7: R4 8: A4 9: P2;P3R 10: A2;A3 11: A1;R2;R3 12: S1;S2 13: S3;S4 R_a R_{b+} Gear IN/OUT Brake Clutch 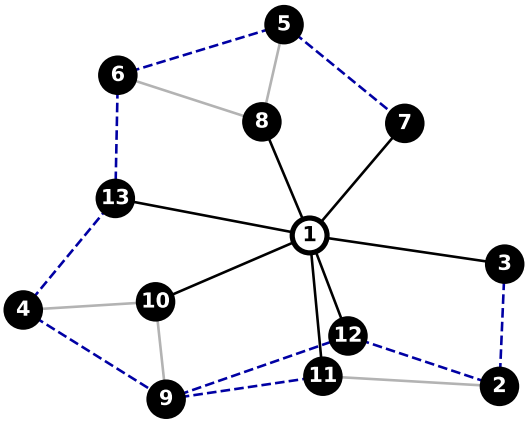 DOF: 3 Links: 13 (n_c: 7, n_p: 5, CL: 5) Joints: 21 (j_G: 9, j_R: 12) (j_{R_a}: 7, $j_{R_{b+}}$: 5) PGS_{Total}: 4 (S: 2, D: 2, R: 1) $PGS_{Sequence}$: [S,R,D] Planar: True Partition: [2,9,1,0,0,1] Avg. Degree: 3.23 Density: 0.27 Diameter: 4 Radius: 2 Largest Loop: 12 Structural Complexity: - CX: 325.67 - CX1: 74.24 - CX2: 180.96 - CX3: 1.39
2	**DBG: 1S+1D+1R__247** 1: MJ 2: P1 3: S1 4: P3S 5: P4R 6: P4S 7: R4 8: A4 9: P2;P3R 10: A2;A3 11: R1;R2;R3 12: A1;S2 13: S3;S4 R_a R_{b+} Gear IN/OUT Brake Clutch 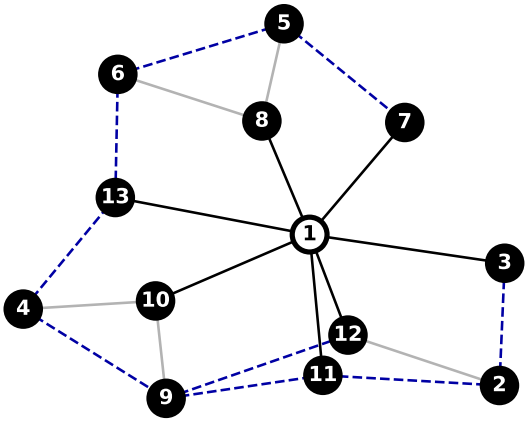 DOF: 3 Links: 13 (n_c: 7, n_p: 5, CL: 5) Joints: 21 (j_G: 9, j_R: 12) (j_{R_a}: 7, $j_{R_{b+}}$: 5) PGS_{Total}: 4 (S: 2, D: 2, R: 1) $PGS_{Sequence}$: [S,R,D] Planar: True Partition: [2,9,1,0,0,1] Avg. Degree: 3.23 Density: 0.27 Diameter: 4 Radius: 2 Largest Loop: 12 Structural Complexity: - CX: 328.37 - CX1: 74.21 - CX2: 182.93 - CX3: 1.39
3	**DBG: 1S+1D+1R__257** 1: MJ 2: P1 3: A1 4: P3S 5: P4R 6: P4S 7: R4 8: A4 9: P2;P3R 10: A2;A3 11: R1;R2;R3 12: S1;S2 13: S3;S4 R_a R_{b+} Gear IN/OUT Brake Clutch 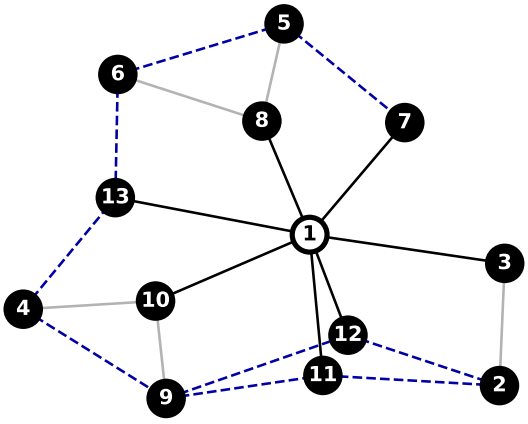 DOF: 3 Links: 13 (n_c: 7, n_p: 5, CL: 5) Joints: 21 (j_G: 9, j_R: 12) (j_{R_a}: 7, $j_{R_{b+}}$: 5) PGS_{Total}: 4 (S: 2, D: 2, R: 1) $PGS_{Sequence}$: [S,R,D] Planar: True Partition: [2,9,1,0,0,1] Avg. Degree: 3.23 Density: 0.27 Diameter: 4 Radius: 2 Largest Loop: 12 Structural Complexity: - CX: 328.60 - CX1: 74.13 - CX2: 183.15 - CX3: 1.39

Continued on next page

Table 45: Top 10 new potential PGTs. (Continued)

Rank	DBG Graph of PGT
4	**DBG: 1S+1D+1R__273** 1: MJ 2: P1 3: P3S 4: S3 5: P4R 6: P4S 7: R4 8: A4 9: P2;P3R 10: A2;A3 11: A1;R2;R3 12: S1;S2 13: R1;S4 R_a R_{b+} Gear IN/OUT Brake Clutch 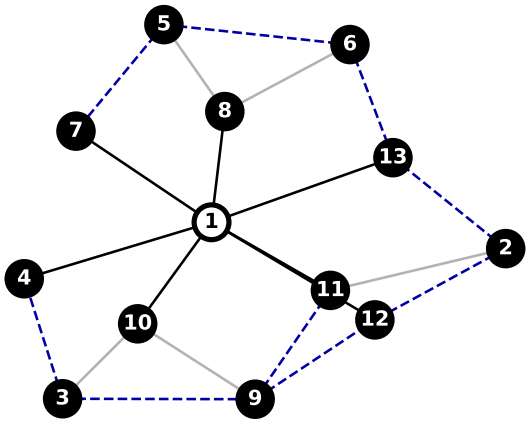 DOF: 3 Links: 13 (n_c: 7, n_p: 5, CL: 5) Joints: 21 (j_G: 9, j_R: 12) (j_{R_a}: 7, $j_{R_{b+}}$: 5) PGS_{Total}: 4 (S: 2, D: 2, R: 1) $PGS_{Sequence}$: [S,R,D] Planar: True Partition: [2,9,1,0,0,1] Avg. Degree: 3.23 Density: 0.27 Diameter: 4 Radius: 2 Largest Loop: 12 Structural Complexity: - CX: 328.91 - CX1: 74.39 - CX2: 182.70 - CX3: 1.39
5	**DBG: 1S+1D+1R__253** 1: MJ 2: P1 3: P3S 4: S3 5: P4R 6: P4S 7: R4 8: A4 9: P2;P3R 10: A2;A3 11: R1;R2;R3 12: S1;S2 13: A1;S4 R_a R_{b+} Gear IN/OUT Brake Clutch 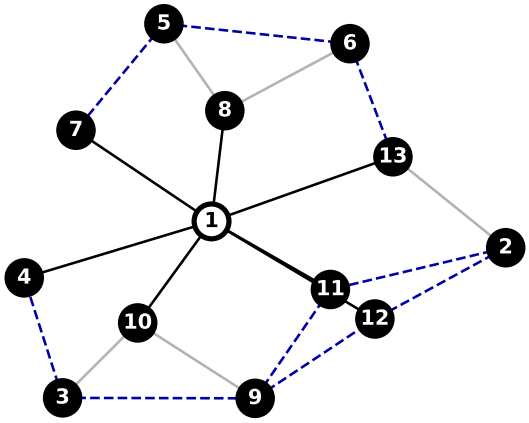 DOF: 3 Links: 13 (n_c: 7, n_p: 5, CL: 5) Joints: 21 (j_G: 9, j_R: 12) (j_{R_a}: 7, $j_{R_{b+}}$: 5) PGS_{Total}: 4 (S: 2, D: 2, R: 1) $PGS_{Sequence}$: [S,R,D] Planar: True Partition: [2,9,1,0,0,1] Avg. Degree: 3.23 Density: 0.27 Diameter: 4 Radius: 2 Largest Loop: 12 Structural Complexity: - CX: 329.78 - CX1: 74.21 - CX2: 183.45 - CX3: 1.39
6	**DBG: 1S+1D+1R__675** 1: MJ 2: P1 3: R1 4: A1 5: P3S 6: S3 7: P4R 8: P4S 9: P2;P3R 10: A2;A3 11: S1;S4 12: S2;A4 13: R2;R3;R4 R_a R_{b+} Gear IN/OUT Brake Clutch 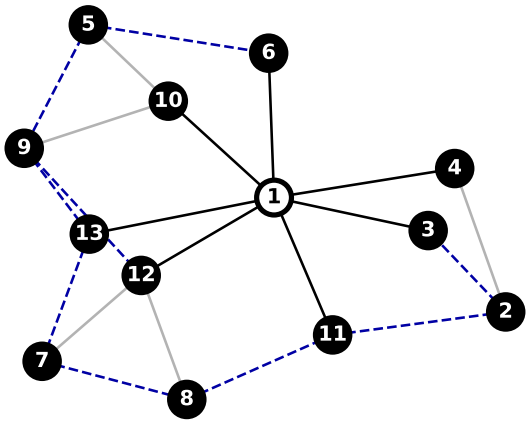 DOF: 3 Links: 13 (n_c: 7, n_p: 5, CL: 5) Joints: 21 (j_G: 9, j_R: 12) (j_{R_a}: 7, $j_{R_{b+}}$: 5) PGS_{Total}: 4 (S: 2, D: 2, R: 1) $PGS_{Sequence}$: [S,R,D] Planar: True Partition: [3,7,2,0,0,1] Avg. Degree: 3.23 Density: 0.27 Diameter: 4 Radius: 2 Largest Loop: 12 Structural Complexity: - CX: 330.09 - CX1: 74.21 - CX2: 186.63 - CX3: 1.37

Continued on next page

Table 45: Top 10 new potential PGTs. (Continued)

Rank	DBG Graph of PGT
7	**DBG: 1S+1D+1R__316** 1: MJ 2: P1 3: R1 4: S1 5: P3S 6: P4R 7: P4S 8: A4 9: P2;P3R 10: A2;A3 11: A1;R2;R3 12: S2;S4 13: S3;R4 R_a R_{b+} Gear IN/OUT Brake Clutch 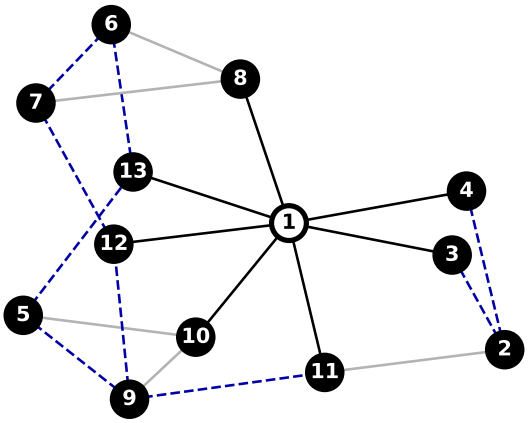 DOF: 3 Links: 13 (n_c: 7, n_p: 5, CL: 5) Joints: 21 (j_G: 9, j_R: 12) (j_{R_a}: 7, $j_{R_{b+}}$: 5) PGS_{Total}: 4 (S: 2, D: 2, R: 1) $PGS_{Sequence}$: [S,R,D] Planar: True Partition: [2,9,1,0,0,1] Avg. Degree: 3.23 Density: 0.27 Diameter: 4 Radius: 2 Largest Loop: 12 Structural Complexity: - CX: 330.10 - CX1: 74.39 - CX2: 182.70 - CX3: 1.40
8	**DBG: 1S+1D+1R__298** 1: MJ 2: P1 3: R1 4: P3S 5: S3 6: P4R 7: P4S 8: A4 9: P2;P3R 10: A2;A3 11: A1;R2;R3 12: S1;S4 13: S2;R4 R_a R_{b+} Gear IN/OUT Brake Clutch 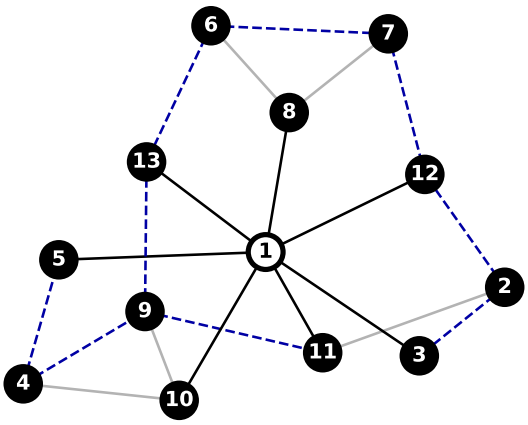 DOF: 3 Links: 13 (n_c: 7, n_p: 5, CL: 5) Joints: 21 (j_G: 9, j_R: 12) (j_{R_a}: 7, $j_{R_{b+}}$: 5) PGS_{Total}: 4 (S: 2, D: 2, R: 1) $PGS_{Sequence}$: [S,R,D] Planar: True Partition: [2,9,1,0,0,1] Avg. Degree: 3.23 Density: 0.27 Diameter: 4 Radius: 2 Largest Loop: 12 Structural Complexity: - CX: 330.39 - CX1: 74.39 - CX2: 181.93 - CX3: 1.41
9	**DBG: 1S+1D+1R__636** 1: MJ 2: P1 3: R1 4: S1 5: P3S 6: S3 7: P4R 8: P4S 9: P2;P3R 10: A2;A3 11: A1;S4 12: S2;A4 13: R2;R3;R4 R_a R_{b+} Gear IN/OUT Brake Clutch 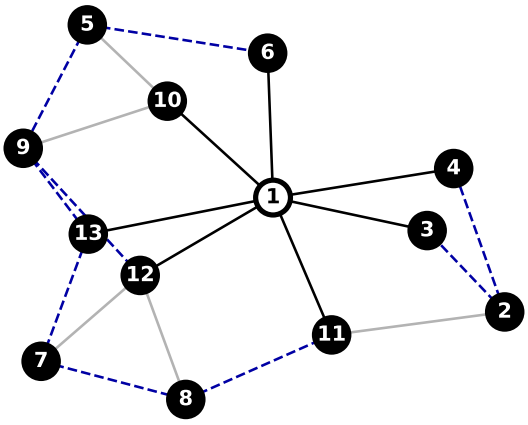 DOF: 3 Links: 13 (n_c: 7, n_p: 5, CL: 5) Joints: 21 (j_G: 9, j_R: 12) (j_{R_a}: 7, $j_{R_{b+}}$: 5) PGS_{Total}: 4 (S: 2, D: 2, R: 1) $PGS_{Sequence}$: [S,R,D] Planar: True Partition: [3,7,2,0,0,1] Avg. Degree: 3.23 Density: 0.27 Diameter: 4 Radius: 2 Largest Loop: 12 Structural Complexity: - CX: 330.58 - CX1: 74.28 - CX2: 186.93 - CX3: 1.37

Continued on next page

Table 45: Top 10 new potential PGTs. (Continued)

Rank	DBG Graph of PGT
10	**DBG: 1S+1D+1R__434** 1: MJ 2: P1 3: R1 4: A1 5: P3S 6: P4R 7: P4S 8: A4 9: P2;P3R 10: A2;A3 11: S1;R2;R3 12: S2;S4 13: S3;R4 R_a R_{b+} Gear IN/OUT Brake Clutch 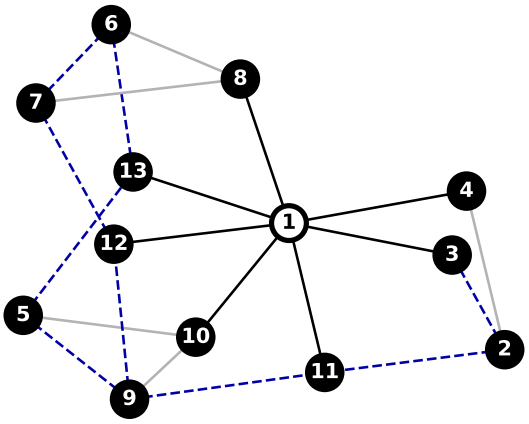 DOF: 3 Links: 13 (n_c: 7, n_p: 5, CL: 5) Joints: 21 (j_G: 9, j_R: 12) (j_{R_a}: 7, $j_{R_{b+}}$: 5) PGS_{Total}: 4 (S: 2, D: 2, R: 1) $PGS_{Sequence}$: [S,R,D] Planar: True Partition: [2,9,1,0,0,1] Avg. Degree: 3.23 Density: 0.27 Diameter: 4 Radius: 2 Largest Loop: 12 Structural Complexity: - CX: 331.44 - CX1: 74.47 - CX2: 183.60 - CX3: 1.40

Source: Author.

An initial investigation into the Table 45 identified the PGT *1S+1D+1R__277* as a promising candidate for the development of a new PGMs. This selection was motivated by two key factors. First, PGT *1S+1D+1R__277* exhibits the lowest structural complexity metric among all entries within the table, with a DBG complexity value (DBG__C_X) of 325.67. Second, this PGT possesses nine ternary links in its kinematic chain. The schematic diagram of the PGT *1S+1D+1R__277* is presented in Figure 56 for further visualization.

Figure 56 – Schematic diagram of the PGT *1S+1D+1R__277*.

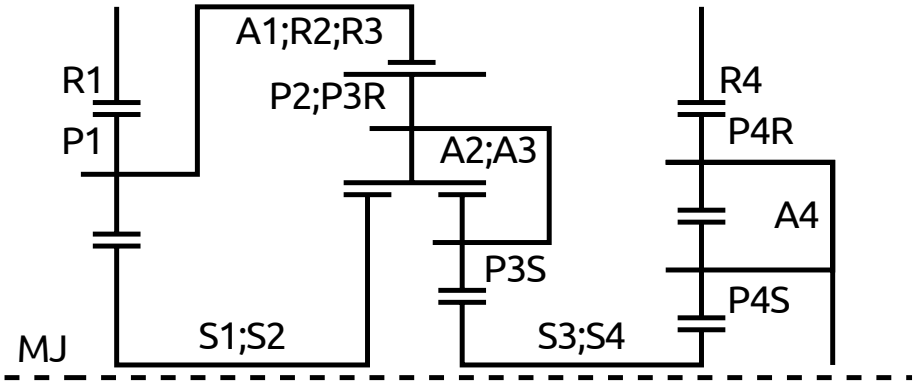

Source: Author.

The next step involved determining the Frame (F), Input (IN), and Output (OUT) links. Database strategic link analysis (Section 5.4.3.1) for the context of PGMs with four total PGSs revealed a prevalence of single links used as Frames (Fig. 353). Input (IN) links were most frequently identified as compound links joined to a single elementary link, typically the sun gear (S) Fig. 358). Similarly, Output (OUT) links were consistently

observed to be compound links formed by one or two elementary links, with the arm link (A) being the most common (Fig. 363).

Based on these findings, the following links were selected for the construction of the PGM:

- Frame (F): Single link.
- Input (IN): Compound link associated with the sun gear of PGS 1 (IN;S1).
- Output (OUT): Compound link associated with the arm of PGS 4 (OUT;A4).

The PGT *1S+1D+1R__277* is composed of n = 13 links and j = 21 joints (j_G = 9 gear pairs, j_{Ra} = 7 revolute pairs in level 'a', and j_{Rb+} = 5 revolute pairs in level 'b+'). Applying Equation (29), this initial configuration results in a mechanism with 3 degrees of freedom (DOF).

A preliminary kinematic analysis of the PGM's gear modes (Eq. (14)) was performed. The lever analogy method (BENFORD; LEISING, 1981; DING et al., 2020; YANG et al., 2022) was employed to identify the necessary shift couplings (SC) as brakes (B) and clutches (C). Each elementary PGS within the PGT *1S+1D+1R__277* is represented by a lever. These levers are interconnected through the compound links (Fig. 57), facilitating the evaluation of all possible gear modes.

Figure 57 – Lever diagram of the PGT *1S+1D+1R__277*.

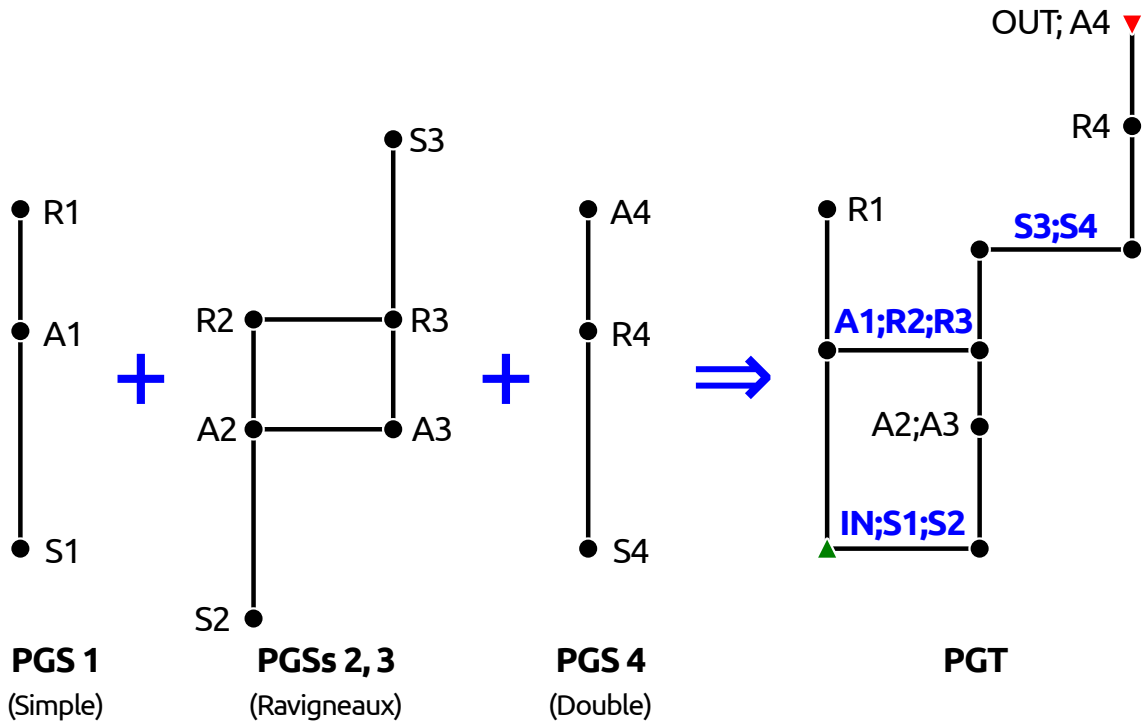

Source: Author.

The Simple PGS (1) connects directly to the Ravigneaux PGS (2 and 3) through two compound links: (IN;S1;S2) and (A1;R2;R3). This configuration restricts the internal mobility of the Simple PGS. Conversely, the Double PGS (4) has only one direct

connection to the Ravigneaux PGS, the compound link (S2;S3). Consequently, shift couplings should prioritize connections to PGS 4 to reduce its internal mobility to one.

Considering the PGM's 3-DOF configuration, each pair of shift couplings represents a potential gear mode. Five of the seven coaxial links have the potential to serve as brakes when connected to the housing (F). Four of these are selected, excluding the input (IN;S1;S2) and output (OUT;A4) links, which cannot be constrained, and the arm (A2;A3) to avoid blocking potential clutches.

Initial analysis identified 21 pairs of coaxial links as potential clutches. However, 10 of these pairs would result in atresia, a condition where all links within a PGS rotate as a single unit (DING et al., 2020), and are therefore discarded. Further analysis of the remaining 11 pairs within the schematic diagram (Fig. 56) reveals that 8 pairs are either infeasible or can be eliminated. The pair (IN;S1;S2, R4) is considered inaccessible. Four pairs containing link 'R1' are discarded to prevent blocking of potential brakes and clutches and to prioritize connections with PGS 4. Two pairs would lock the mechanism: (R1;S3;S4) and (IN;S1;S2, S3;S4). The pair (IN;S1;S2, OUT;A4) represents a direct input-output connection. This leaves 3 clutches and 4 brakes for potentially further evaluation, as shown in Figure 58 and listed below:

- Clutches
  - C_1: (A1;R2;R3, R4)
  - C_2: (A2;A3, R4)
  - C_3: (A2;A3, OUT;A4)
- Brakes
  - B_1: (F, R1)
  - B_2: (F, A1;R2;R3)
  - B_3: (F, R4)
  - $B_4{}^*$: (F, S3;S4)
    - $*$ *Note: the access of the link (S3;S4) to the housing (F) only occurs when the output is transversal, i. e., the link (OUT;A4) is a gear connecting another gear in an external parallel axis.*

Of the six possible brake pair combinations, three contain links from the same PGS, resulting in a locked mechanism. Additionally, the pair (B_1,B_4) would not transmit rotation to the fourth PGS. These combinations are discarded, leaving only two viable brake pairs: (B_1,B_3), and (B_2,B_3).

The total number of potential gear modes is determined by the feasible brake pairs, the combination of a brake and a clutch, and three direct modes achievable by engaging any pair of clutches (Eq. (49)):

$$\text{Potential Gear Modes} = 2 + 4 \times 3 + 3 = 17. \tag{49}$$

Figure 58 – Lever diagram of the PGT *1S+1D+1R__277* with potential shift couplings.

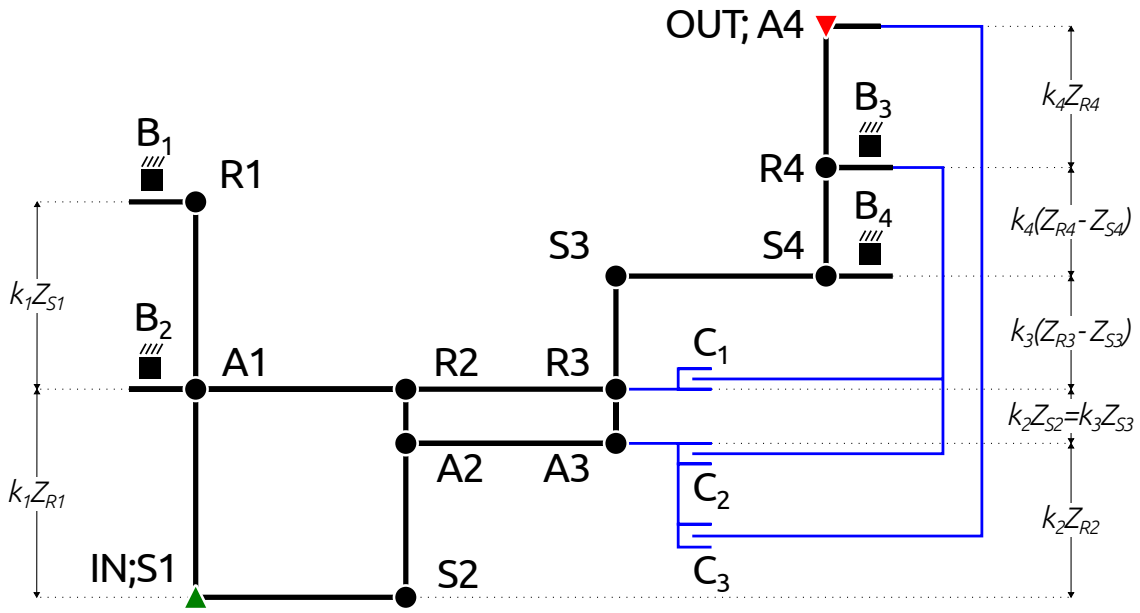

Source: Author.

A preliminary kinematic analysis using the lever method geometrically identified all possible gear modes as shown in Table 46.

Table 46: Summary of preliminary gear modes for PGM *1S+1D+1R__277*.

Shift Couplings	B_1	B_2	B_3	B_4	C_1	C_2	C_3
B_1		X	R	X	U	O	U
B_2			U†	X	U†	O	U
B_3				X	U†	O	U
B_4					U	O	U
C_1						D	D
C_2							D
C_3							

Gear ratios: R - reverse ($i_G < 0$), U - underdrive ($i_G > 1$) , D - direct ($i_G = 1$), O - overdrive ($0 < i_G < 1$), X - locked ($i_G = 0$)
† Clutch C_1 connects the links related to the brakes B_1 and B_2, resulting in the same gear ratio for three modes.

Source: Author.

To numerically validate the kinematic analysis and obtain preliminary transmission ratios, gear teeth numbers assigned to the PGSs are presented in Table 47.

Using the dimensional data in Table 47, lever diagrams were generated for 13 gear modes and are represented in Table 48. The remaining four gear modes are omitted from the table: three are direct drive modes resulting from clutch combinations, and the mode (B_2,B_3) yields the same transmission ratio as the modes (C_1,B_2) and (C_1,B_3), which are already represented. Due to the two compound links between the

Table 47: Gear teeth suggested for PGM *1S+1D+1R__277*.

	PGSs			
	Simple	Ravigneaux		Double
Gears	**1**	**2**	**3**	**4**
Ring (Z_R)	60	71*	71*	46
Sun (Z_S)	54	25	23	26

* This Ravigneaux PGS has only one ring (R) gear.

Source: Author.

Simple PGS and the Ravigneaux PGS, scaling constants k_i ($i = 1, 2, 3, 4$) between levers 1, 2, and 3 remain the same for all modes. The scaling constant k_4 for lever 4 (Double PGS) varies depending on the gear mode and is presented in each respective lever diagram.

Table 48: PGM *1S+1D+1R__277* Lever diagrams and gear modes.

Lever Diagram	Gear Modes ($\frac{\omega_{OUT}}{\omega_{IN}}$)
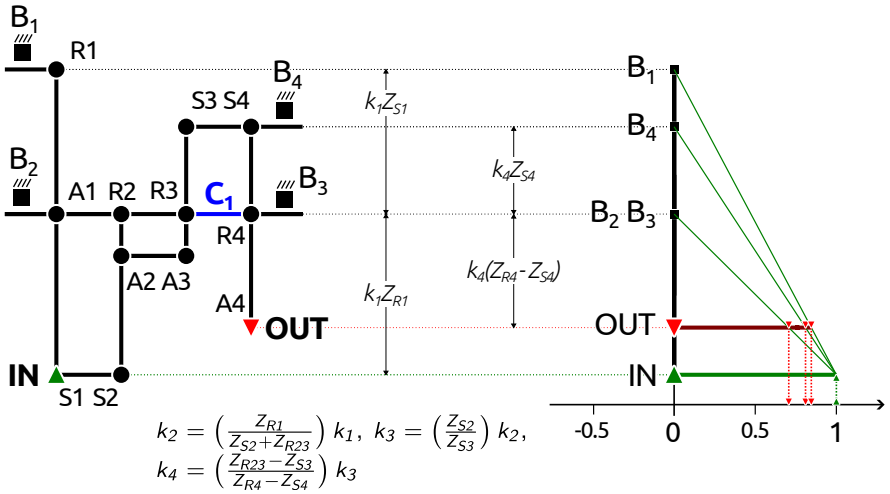	C_1, B_1: 0.8455 C_1, B_2: 0.7065 C_1, B_3: 0.7065 C_1, B_4: 0.8099
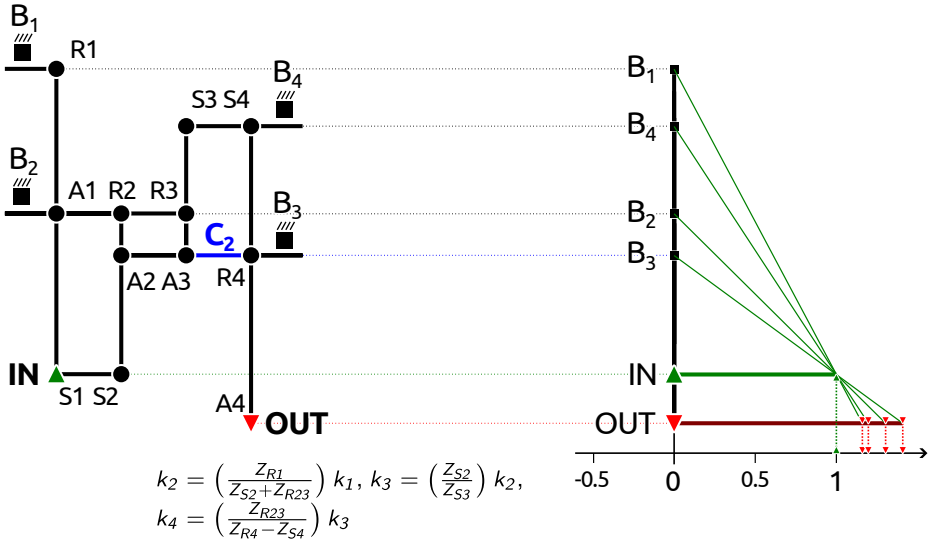	C_2, B_1: 1.1608 C_2, B_2: 1.3055 C_2, B_3: 1.4130 C_2, B_4: 1.1979

Continued on next page

Table 48: PGM *1S+1D+1R__277* Lever diagrams and gear modes. (Continued)

Lever Diagram	Gear Modes ($\frac{\omega_{OUT}}{\omega_{IN}}$)
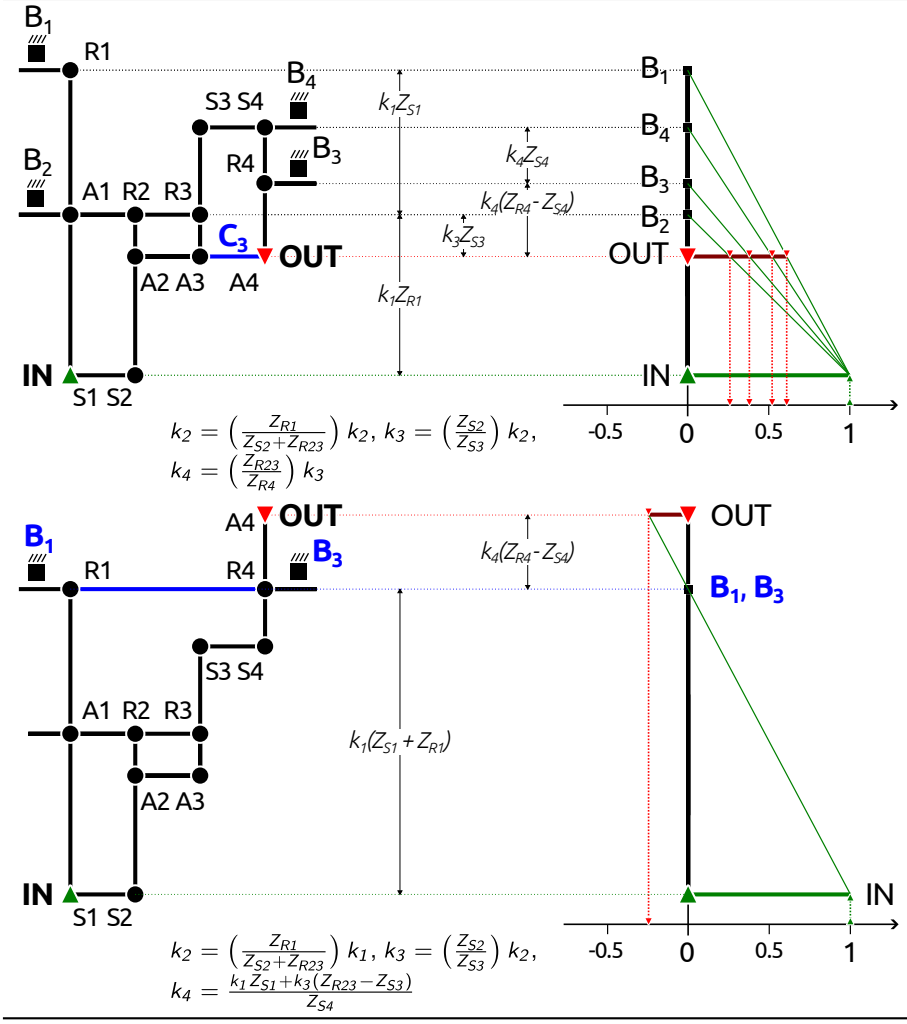	C_3,B_1: 0.6107 C_3,B_2: 0.2604 C_3,B_3: 0.3806 C_3,B_4: 0.5208
	B_1,B_3: –0.2439

Source: Author.

Lever diagrams are used to illustrate the speed ratios between transmission input and output links. For automotive transmissions, gear ratios are conventionally expressed as the ratio of input shaft speed to output shaft speed (see Section 2.1.1.1). Analysis of individual gear modes within the lever diagrams facilitates identification of shift coupling sequences requiring single transitions and their corresponding gear ratios, as demonstrated in Table 49. The transmission *PGM 1S+1D+1R__277* results in one reverse gear and twelve distinct forward gears. An overall gear ratio of $i_{G,tot}$ = 5.426 is achieved, and gear steps reasonably adhere to the progressive gear ratio method (Eq. (5)). Among the forward speeds, the first gear provides a suitable reduction with a ratio of i_1 = 3.840. Additionally, six progressively reduced gears, three direct drive options, and four overdrive ratios exist. The final overdrive ratio of i_12 = 0.708 falls within the typical range for passenger cars. A drawback of this design involves the transition from fourth to fifth gear (with a ratio of i_5 = 1.4154), which requires the simultaneous disengagement and engagement of two shift couplings, disrupting the otherwise simple

transition clutch-to-clutch sequence.

Table 49: Preliminary gear specifications for the *PGM 1S+1D+1R__277*

Gear	Ratio ($\frac{\omega_{IN}}{\omega_{OUT}}$)	Active Shift Couplings							Step φ	Transitions
		B_1	B_2	B_3	B_4	C_1	C_2	C_3		
R1	-4.0994	⊗		⊗						0
1	3.8400		⊗					⊗		2
2	2.6277			⊗				⊗	1.461	1
3	1.9200				⊗			⊗	1.369	1
4	1.6373	⊗						⊗	1.173	1
5a†	1.4154		⊗			⊗			1.157	2
5b†	1.4154			⊗		⊗			1.000	2
5c†	1.4154		⊗	⊗					1.000	2
6	1.2348				⊗	⊗			1.146	1
7	1.1827	⊗				⊗			1.044	1
8a‡	1.0000					⊗	⊗		1.183	1
8b‡	1.0000					⊗		⊗	1.000	1
8c‡	1.0000						⊗	⊗	1.000	1
9	0.8615	⊗					⊗		1.161	1
10	0.8348				⊗		⊗		1.032	1
11	0.7660		⊗				⊗		1.090	1
12	0.7077			⊗			⊗		1.082	1

† Underdrive gear ratio repeated in three different modes.
‡ Direct gear ratio repeated in three different modes.

Source: Author.

The topological characterization summary of the PGM *1S+1D+1R__277*, including the shift couplings (SC) is presented in Table 50.

Table 50 – *PGM* 1S+1D+1R__277 topological data.

PGS		LINKS		JOINTS
ID	**Simple (S), Double (D)**	**Include, Exclude (-)**	**Compound (CL)**	**Shift Couplings (SC)**
1	S	F	IN;S1;S2	F;R1;B1
2	S	IN	A1;R2;R3	F;A1;B2
3	D	OUT	P2;P3R	F;R4;B3
4	D		A2;A3	F;S4;B4
			S3;S4	R3;R4;C1
			OUT;A4	A3;R4;C2
				A3;A4;C3

Source: Author.

The PGM *1S+1D+1R__277* was generated in two mounting configurations: longitudinal and transverse. The longitudinal version, depicted in Figure 59, features 6 shift couplings (3 brakes and 3 clutches). As the brake B_4 is eliminated in this configuration, it has the potential to produce up to 9 forward speeds - all except gears 3, 6 and 10

of Table 49 - and 1 reverse speed. As a 3-DOF (degrees of freedom) transmission, it requires only 2 active shift couplings for each gear mode.

Figure 59 – Diagram of Longitudinal PGM *1S+1D+1R__277*.

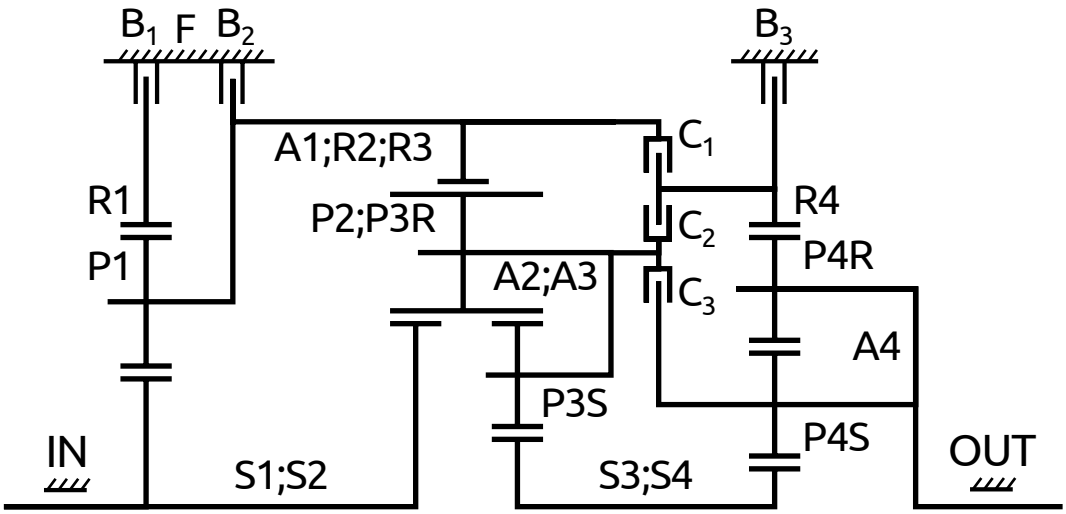

Source: Author.

The complete graph representation of the PGM *1S+1D+1R__277* longitudinal is illustrated in Figure 60. A detailed evaluation of the mechanism was also introduced, showing it is not planar and have high structural complexity is PGM__*Cx*=458.18, despite its good capability of PGM__*Ca*=9.33.

Figure 60 – Graph of the longitudinal PGM *1S+1D+1R__277*.

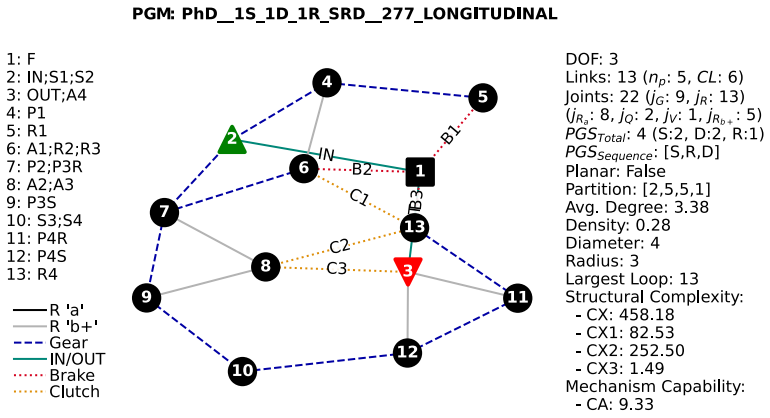

Source: Author.

The transverse-mount version of the PGM *1S+1D+1R__277*, illustrated in Figure 61, differs from the longitudinal version by the addition of brake B_4 within the sun compound link (S3;S4). This modification results in a total of 7 shift couplings (4 brakes and 3 clutches), potentially generating up to 12 forward speeds (7 underdrive, 4 overdrive, and 1 direct) and 1 reverse speeds. Like its counterpart, it is a 3-DOF transmission requiring the engagement of 2 shift couplings per gear mode.

Figure 61 – Diagram of the transverse PGM *1S+1D+1R__277*.

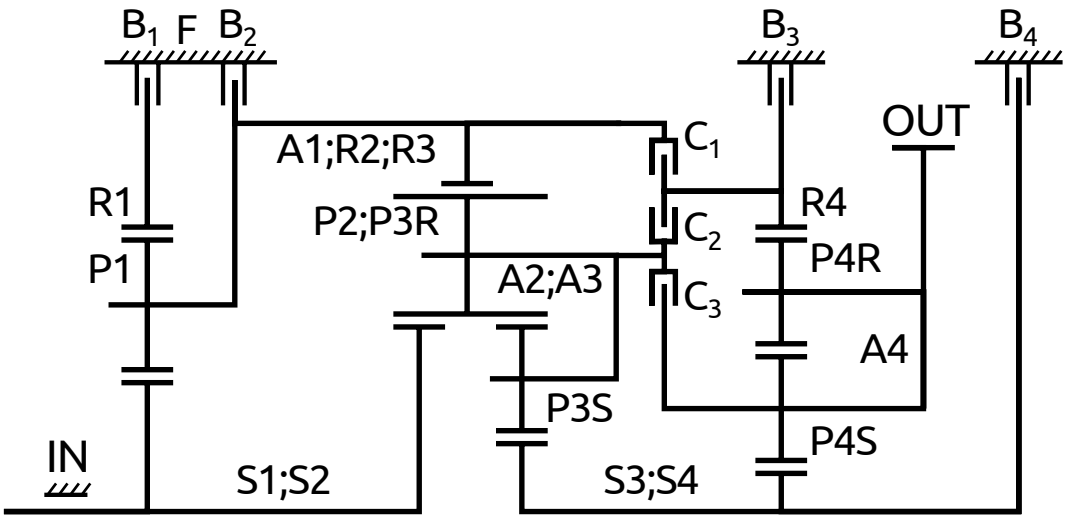

Source: Author.

The complete graph representation of the PGM *1S+1D+1R__277* transverse is illustrated in Figure 62. A detailed evaluation of the mechanism was also introduced, showing it is not planar and have high structural complexity is PGM__*Cx*=518.64, despite its good capability of PGM__*Ca*=12.33.

Figure 62 – Graph of the transverse PGM *1S+1D+1R__277*.

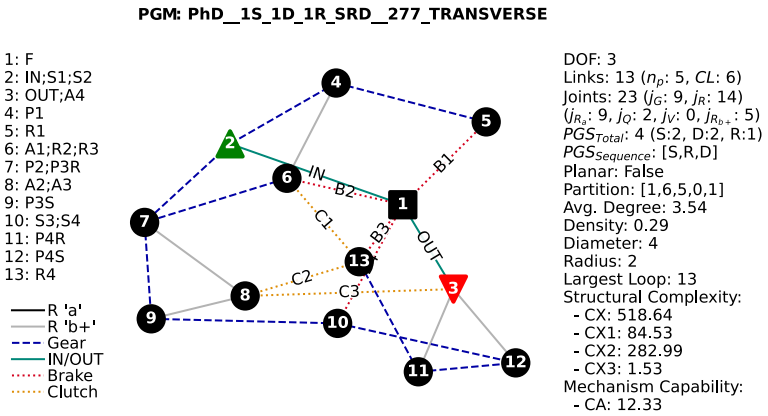

Source: Author.

Figure 63 displays the possible configurations of the PGM *1S+1D+1R__277* within the updated technological boundary map. This visualization offers insights into the PGM's potential design space and complexity variations.

Further dimensional synthesis is required to fully evaluate the feasibility of the preliminary gear ratios of Table 49. The absence of these mechanisms in this thesis database suggests potential novelty. To confirm their innovative status and patentability, a comprehensive patent search is necessary.

Figure 63 – PGM *1S+1D+1R__277* in the Technological Boundary Map.

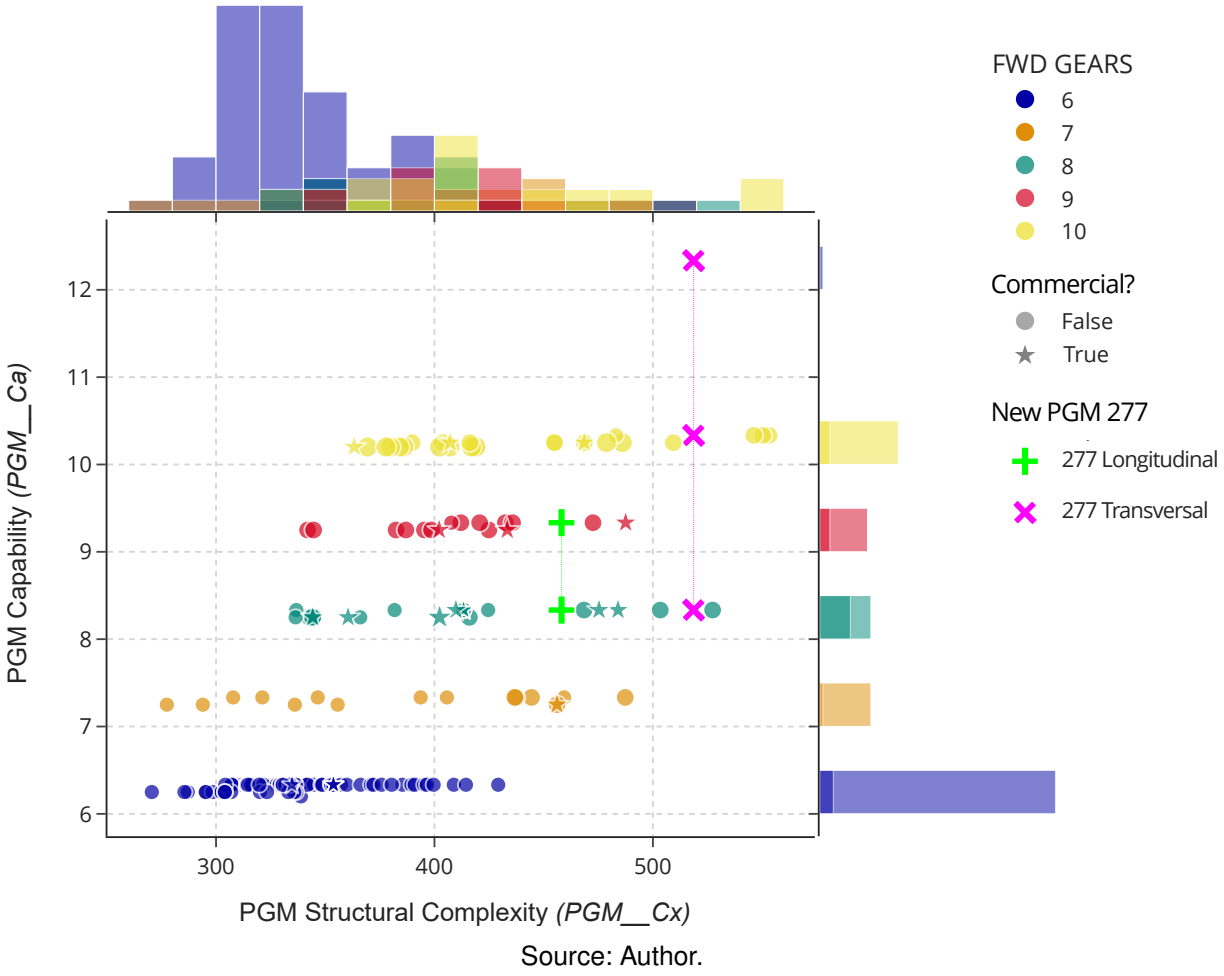

Source: Author.

This chapter successfully achieved its objective by demonstrating how the analysis of innovation sets derived from patent database gaps can support the generation of potentially novel planetary gear mechanisms in automotive transmissions. The methodology's effectiveness was demonstrated by identifying two novel PGMs with promising characteristics for automotive applications.

7 CONCLUSIONS AND FUTURE WORK

This chapter provides a comprehensive summary of the conclusions drawn from the research conducted in this thesis, along with the identification of future research directions. The conclusions address the research questions in relation to the objectives and hypotheses, while also offering recommendations and suggestions for future work. The following sections highlight the objective attainment, acknowledge the scientific contributions made in this thesis, discuss the challenges and limitations encountered, and outline potential topics for future research and development.

7.1 ANALYSIS OF OBJECTIVE ATTAINMENT

This section provides an analysis of the attainment of the specific objectives outlined in the introduction (Section 1.1). A summary of the results is presented in Table 51.

Table 51: Analysis of Objective Attainment

Objective	Attainment	Evidence
1. Investigate analysis and synthesis processes of PGMs	★	Chapters 2 and 3
2. Construct a comprehensive database of PGMs	•	Section 5.3.3
3. Establish a systematic process to identify relevant features	★	Section 4.4
4. Develop an analysis method for identifying innovative gaps	✓	Section 4.5
5. Implement the proposed process in a case study of PGMs	★	Chapters 5 and 6

Legend: ★ exceeded expectations, ✓ complete, • partial, ✗ not achieved.
Source: Author.

Objective 1, the *investigation of pertinent analysis and synthesis processes* for planetary gear mechanisms, exceeded expectations. This was evidenced by an exhaustive analysis of planetary gear mechanisms, as detailed in Chapters 2 and 3. A comprehensive review of the planetary gear mechanism graph model facilitated the development of a revised mobility equation. This equation, an enhancement of the Grübler-Kutzbach criterion, accurately accounts for redundant and virtual constraints in complex planetary gear mechanisms. Its efficacy was validated through several case studies, significantly enhancing the understanding of kinematics in planetary gear mechanisms. Additionally, new metrics for evaluating mechanism performance, focusing on topological characteristics such as the complexity and capability of PGMs, were introduced, laying a foundation for innovative planetary gear mechanism design.

Objective 2, the *construction of a comprehensive database*, was partially achieved as detailed in Section 5.3.3. The diversity aspect of the database was fulfilled with 186 features, which were later reduced to 143 following data cleansing. However, the extensiveness aspect, essential for fostering innovation, did not fully meet expectations. Out of over 3,500 patents identified as having potential planetary gear mechanisms,

only 160 mechanisms were initially included, and this number was further reduced to 155 due to isomorphism. With this number of instances, although the process is validated, it is not possible to assert that the identified gaps are indeed innovative. Despite falling short of the ideal, the rigorous and time-consuming manual process of dataset generation for each mechanism is noteworthy.

Objective 3, *establishing a systematic approach to identify relevant features*, was exceptionally achieved. In Phase 3 of the process, detailed in Section 4.4, a comprehensive feature analysis was conducted. Through link analysis, complexity metrics, and a technological boundary map, a robust approach for identifying relevant features was established.

Objective 4, *developing an analysis method for innovative gaps*, was successfully achieved on the Phase 4 of the process outlined in Section 4.5. The method identified gaps and provided precise criteria for selecting the most promising innovative sets for design requirements.

Objective 5, *the implementation of the proposed process in a case study*, was successfully achieved as detailed in Chapters 5 and 6. Applied to automatic planetary gear mechanisms, the process generated at least thirteen distinct innovation sets with multiple PGSs sequences, providing essential structural requirements for the creation of novel designs. This effort highlighted essential gaps and provided detailed information for guiding design decisions throughout the synthesis process. By focusing on gaps in structural properties on the local context of 10 forward speeds, it was possible to design two potentially new PGMs, emphasizing the value of the comprehensive database and its analyses.

Regarding the overall objective, it can be concluded that it was fully accomplished. This is evident through the identification of innovative requirements that can enable the discovery of potentially new mechanisms not present in the database. The attainment of these innovative requirements demonstrates the successful fulfillment of the general objective.

7.2 SCIENTIFIC CONTRIBUTIONS

The following scientific contributions have been acknowledged in this thesis:

- **Mobility Equation Review**: A comprehensive analysis of the mobility equation, addressing redundant j_Q and virtual j_V constraints, solves the issue of understanding the mobility within planetary gear mechanisms (PGMs) when analyzing the non-actuated mechanisms.
- **Complexity and capability Metrics**: The proposed metrics enable for more accurate comparison between PGMs, providing valuable insights for evaluating technological boundary maps, supporting decision-making during the synthesis process.

- **Process for Identifying Innovation Sets**: A systematic process is devised for identifying innovation sets, integrating the PGM Dataset Template, Attribute Analysis, Gap Analysis, and the application of non-trivial Graph Theory metrics (e.g., Largest Loop, Eccentricity, Centrality). This comprehensive approach enables in-depth analysis of PGMs for determining innovative design requirements.
- **Innovation Sets Concept**: The Introduction of Innovation Sets, aids in identifying and categorizing innovative PGM configurations. This facilitates a structured exploration of potential advancements within the domain of planetary gear mechanisms.
- **Synthesis of New PGMs**: Two potentially novel PGMs were designed in a synthesis process based on innovation sets, demonstrating the effectiveness of the database analysis and discovery process outlined in this thesis.

These scientific contributions enhance the understanding of planetary gear mechanisms and provide valuable insights into their mobility, complexity, and capability. The process developed in this thesis offers a structured approach for identifying and analyzing innovative configurations, contributing to the advancement of planetary gear mechanism research and design.

7.3 CHALLENGES AND LIMITATIONS

This section has highlighted some limitations and challenges encountered during the course of this thesis effort. These limitations include:

- *Limited instances in the database*: The database used in this study contains a relatively small number of instances due to meticulous and time-consuming manual process of converting patents into mechanisms into model datasets. This limitation may impact the generalization of the findings and necessitates caution when interpreting the results.
- *Scope of the solution*: Although the process developed in this thesis is designed to be applicable to various types of mechanisms, the implemented solution presented in this study is specifically limited to Planetary Gear Trains (PGTs). Further adaptations and modifications would be required to tailor the process to other types of mechanisms under investigation.
- *Technical expertise required*: The analysis and characterization of PGMs demand a high level of technical knowledge, which may limit the widespread adoption and use of the process. The successful application of the process relies on individuals with a deep understanding of the technical aspects of gear trains.

These limitations and challenges provide valuable insights into the boundaries and potential areas for improvement in this research. Addressing these limitations will contribute to the refinement and further development of the process, enhancing its

applicability and expanding its utility to a broader range of mechanisms.

7.4 FUTURE WORK

The following list outlines potential avenues for future research and development:

1. **Automate Data Collection**: To enhance the comprehensiveness and representativeness of the database, future work should focus on automating data collection processes. Specifically, improvements can be made in patent search accuracy and the conversion of patent designs into model datasets. Patent search is a labor-intensive task that requires significant manual effort and time for researchers to filter relevant results and convert images and claims into mechanism representations. The use of techniques such as classification models using KDD (WOLSKI et al., 2023) and image and claim conversion automation can help expedite this process with accuracy. By automating these tasks, a larger number of instances can be included in the database, facilitating more robust analyses and improving the scalability of the mechanism survey.
2. **Expand the characterization of PGMs**: In addition to the existing features considered for PGM characterization, future studies could include additional metrics such as efficiency analysis (LAUS et al., 2012). Incorporating efficiency measurements would provide a more comprehensive understanding of the performance characteristics of PGMs and enable more precise comparisons and evaluations.
3. **Designing new PGMs**: Expanding the PGM database to identify innovation sets with greater innovation potential and synthesizing new automatic transmissions.
4. **Enhance complexity metrics**: To further refine the complexity assessment of PGMs, future work should consider including detailed project information such as dimensions, manufacturing processes, costs, and other relevant factors. This additional information would provide a more nuanced evaluation of the complexity of PGMs and aid in decision-making processes related to design and optimization.
5. **Improve capability metrics**: The capability analysis of PGMs can be enhanced by incorporating efficiency as a metric. Efficiency measurements would capture the energy losses and power transmission capabilities of PGMs, enabling a more comprehensive assessment of their overall performance.
6. **Automation of innovation set analysis using matroids**: Future research could explore the use of matroids, a mathematical framework, to automate the analysis of innovation sets. Matroids can provide a systematic and efficient approach to identify innovative configurations within the design space, streamlining the innovation discovery process.
7. **Generalize the process to other complex mechanisms**: The developed pro-

cess has the potential to be extended to the synthesis and analysis of other complex mechanisms beyond PGMs. Future studies could explore its application to diverse systems such as hybrid gearboxes, robot parallel manipulators, or any other mechanical devices. This expansion would further validate the process's effectiveness and broaden its practical utility.

8. **Utilize graph representation learning (GRL)**: Instead of converting the graph representation of mechanisms into conventional data structures, employ specific methods designed for graph data structures in knowledge discovery and data mining (KDD). GRL models (HAMILTON, 2020) facilitate the computation of graph embeddings that capture the topological, structural, and semantic relationships of the graph. This enables various tasks, including visualization, clustering, and prediction of node and edge labels. State-of-the-art algorithms in GRL, such as GRAPE (CAPPELLETTI et al., 2023), have demonstrated their effectiveness in diverse domains such as sociology, biology, medicine, and others.

These future research directions aim to enhance the process, broaden its scope, and enable its application to a wider range of complex mechanisms. By addressing these areas, researchers can further advance the field and uncover new insights and innovations in mechanism design and analysis.

REFERENCES

ABU-AISHEH, Z.; RAVEAUX, R.; RAMEL, J.-Y.; MARTINEAU, P. “An Exact Graph Edit Distance Algorithm for Solving Pattern Recognition Problems ”. In: p. 271–278. Cit. on p. 115.

ALI, T. N.; ESMAIL, E. L.; NAFEH, H. “A Graph-Based Approach for Detection Degenerate Structures in Multi-Planet Gear Trains ”. **Cogent Engineering**, Cogent OA, v. 9, 1 2022. Cit. on p. 73.

ALTSHULLER, G. S.; SHULYAK, L.; RODMAN, S. *The Innovation Algorithm: TRIZ, Systematic Innovation and Technical Creativity* . Technical Innovation Center, 1999. Cit. on p. 40.

ANFAVEA. *Brazilian Automotive Industry Yearbook 2023* . Feb. 2023. Cit. on p. 33.

AOKI, T.; KATO, H.; KATO, N.; MASARU, M. “The World’s First Transverse 8-Speed Automatic Transmission ”. **SAE Technical Papers**, SAE International, v. 2, 2013. Cit. on pp. 135, 136.

ARISTODEMOU, L.; TIETZE, F. “The State-Of-The-Art on Intellectual Property Analytics (ipa): A Literature Review on Artificial Intelligence, Machine Learning and Deep Learning Methods for Analysing Intellectual Property (ip) Data ”. **World Patent Information**, Pergamon, v. 55, p. 37–51, Dec. 2018. Cit. on pp. 40, 104.

ARTELT, B.; BRIX, T.; DÖRING, U. Thedi – the First Online Editor for the IFToMM Dictionary. In: ed. by Tadeusz Uhl. IFToMM WC 2019: Springer International Publishing, June 2019. v. 73, p. 3511–3519. Cit. on p. 51.

BACK, N.; OGLIARI, A.; DIAS, A.; SILVA, J. *Projeto Integrado De Produtos: Planejamento, Concepção E Modelagem* . Manole, 2008. Cit. on p. 69.

BARABÁSI, A.-L.; PÓSFAI, M. *Network Science* . Cambridge University Press, 2016. Cit. on p. 111.

BENFORD, H. L.; LEISING, M. B. “The Lever Analogy: A New Tool in Transmission Analysis ”. In. Cit. on pp. 58, 78, 184.

BERA, P. "A Design Method of Selecting Gear Ratios in Manual Transmissions of Modern Passenger Cars ". **Mechanism and Machine Theory**, Pergamon, v. 132, p. 133–153, Feb. 2019. Cit. on p. 50.

BISONG, E. Google Colaboratory. In: BUILDING Machine Learning and Deep Learning Models on Google Cloud Platform: A Comprehensive Guide for Beginners. Berkeley, CA: Apress, 2019. P. 59–64. Cit. on p. 138.

BOLÓN-CANEDO, V.; ALONSO-BETANZOS, A. *Recent Advances in Ensembles for Feature Selection* . Springer International Publishing, 2018. v. 147, p. 171. Cit. on pp. 119, 121.

BOSCH, R. *Bosch Automotive Handbook, 9th Edition* . Robert Bosch, Oct. 2014. Cit. on p. 46.

BRUCE, P.; BRUCE, A.; GEDECK, P.; O'REILLY MEDIA COMPANY. SAFARI, an. *Practical Statistics for Data Scientists* . 2. ed.: O'Reilly, May 2020. Cit. on p. 117.

BUCHSBAUM, F.; FREUDENSTEIN, F. "Synthesis of Kinematic Structure of Geared Kinematic Chains and Other Mechanisms ". **Journal of Mechanisms**, Pergamon Press, v. 5, p. 357–392, 3 Sept. 1970. Cit. on pp. 58, 59, 66, 73, 74, 87.

CAI, J.; LUO, J.; WANG, S.; YANG, S. "Feature Selection in Machine Learning: A New Perspective ". **Neurocomputing**, Elsevier B.V., v. 300, p. 70–79, July 2018. Cit. on pp. 120, 121.

CAPPELLETTI, L.; FONTANA, T.; CASIRAGHI, E.; RAVANMEHR, V.; CALLAHAN, T. J.; CANO, C.; JOACHIMIAK, M. P.; MUNGALL, C. J.; ROBINSON, P. N.; REESE, J.; VALENTINI, G. "Grape for Fast and Scalable Graph Processing and Random-Walk-Based Embedding ". **Nature Computational Science 2023 3:6**, Nature Publishing Group, v. 3, p. 552–568, 6 June 2023. Cit. on p. 197.

CARBONNELLE, P. *Pypl Popularity of Programming Language* . 2023. Available from: `https://pypl.github.io/PYPL.html`. Visited on: 26 June 2023. Cit. on p. 113.

CASTILLO, J. M. del. "Enumeration of 1-Dof Planetary Gear Train Graphs Based on Functional Constraints ". **Journal of Mechanical Design**, v. 124, p. 723–732, 4 Dec. 2002. Cit. on p. 62.

CAZANGI, H. R. "Aplicacão Do Método De Davies Para Análise Cinemática E Estática De Mecanismos De Múltiplos Graus De Liberdade ", p. 219, 2008. Cit. on p. 59.

CAZANGI, H. R.; MARTINS, D. "Kinematic Analysis of Automotive Gearbox Mechanisms Using Davies' Method ". In. Cit. on pp. 59, 80.

CHANDRASHEKAR, G.; SAHIN, F. "A Survey on Feature Selection Methods ". **Computers & Electrical Engineering**, v. 40, p. 16–28, 1 Jan. 2014. Cit. on p. 120.

CHATTERJEE, G.; TSAI, L.-W. "Enumeration of Epicyclic-Type Automatic Transmission Gear Trains ". In. Cit. on pp. 39, 62, 68.

CHEN, R.-C.; DEWI, C.; HUANG, S.-W.; CARAKA, R. E. "Selecting Critical Features for Data Classification Based on Machine Learning Methods ". **Journal of Big Data**, Springer, v. 7, p. 52, 1 Dec. 2020. Cit. on p. 120.

CHEN, Y. *Automotive Transmissions* . Springer Singapore, 2021. Cit. on pp. 33, 35, 37, 38, 40, 46.

CROSSLEY, F. R. E. "The Permutations of Kinematic Chains of Eight Member or Less from the Graph-Theoretic Viewpoint ". **Developments in Theoretical and Applied Mechanisms**, v. 2, p. 467–486, 1965. Cit. on p. 59.

DAVIES, T. H. "Circuit actions attributable to active couplings ". **Mechanism and Machine Theory**, Pergamon, v. 30, p. 1001–1012, 7 Oct. 1995. Cit. on p. 59.

DAVIES, T. H. "Couplings, Coupling Networks and Their Graphs ". **Mechanism and Machine Theory**, Pergamon, v. 30, p. 991–1000, 7 Oct. 1995. Cit. on pp. 51, 59.

DEGASPERI, D. *Audi kills off multitronic CVT automatic* . Drive. 22 July 2014. Available from: https://www.drive.com.au/news/audi-kills-off-multitronic-cvt-automatic-forever/. Visited on: 9 Feb. 2023. Cit. on p. 36.

DEMŠAR, J.; CURK, T.; ERJAVEC, A.; GORUP, Č.; HOČEVAR, T.; MILUTINOVIČ, M.; MOŽINA, M.; POLAJNAR, M.; TOPLAK, M.; STARIČ, A.; ŠTAJDOHAR, M.; UMEK, L.; ŽAGAR, L.; ŽBONTAR, J.; ŽITNIK, M.; ZUPAN, B. "Orange: Data Mining Toolbox in Python ". **Journal of Machine Learning Research**, v. 14, p. 2349–2353, 2013. Cit. on p. 114.

DING, H. “Automatic Structural Synthesis of Planar Mechanisms and Its Application to Creative Design ”, Feb. 2015. Cit. on pp. 39, 74.

DING, H.; CAI, C. “Patent Analysis and Structural Synthesis of Epicyclic Gear Trains Used in Automatic Transmissions ”. **Applied Sciences**, Multidisciplinary Digital Publishing Institute, v. 10, p. 82, 1 Dec. 2019. Cit. on pp. 40, 77.

DING, H.; CAI, C.; CHEN, Z.; KE, T.; MAO, B. “Configuration Synthesis and Performance Analysis of 9-Speed Automatic Transmissions ”. **Chinese Journal of Mechanical Engineering**, v. 33, p. 50, 1 Dec. 2020. Cit. on pp. 75, 184, 185.

DING, H.; HUANG, Z. “Isomorphism Identification of Graphs: Especially for the Graphs of Kinematic Chains ”. **Mechanism and Machine Theory**, v. 44, p. 122–139, 1 Jan. 2009. Cit. on p. 115.

DING, H.; YANG, W.; HUANG, P.; KECSKEMÉTHY, A. “Automatic Structural Synthesis of Planar Multiple Joint Kinematic Chains ”. **Journal of Mechanical Design**, v. 135, p. 091007, 9 2013. Cit. on p. 39.

DING, H.; YANG, W.; KECSKEMÉTHY, A. *Automatic Structural Synthesis and Creative Design of Mechanisms* . Springer Nature Singapore, 2022. Cit. on pp. 58, 73, 80.

DOBRJANSKYJ, L.; FREUDENSTEIN, F. “Some Applications of Graph Theory to the Structural Analysis of Mechanisms ”. **Journal of Engineering for Industry**, American Society of Mechanical Engineers, v. 89, p. 153, 1 Feb. 1967. Cit. on pp. 59, 73.

DONG, P.; ZUO, S.; LIU, T.; XU, X.; GUO, W.; LIU, Y.; WU, H.; WANG, S. “A Matrix-Based Method for Searching Configurations of Planetary Gear Trains ”. **Mechanism and Machine Theory**, Elsevier BV, v. 180, p. 105161, Feb. 2023. Cit. on p. 75.

DÖRR, C.; KALCZYNSKI, H.; RINK, A.; SOMMER, M. “Nine-Speed Automatic Transmission 9g-Tronic by Mercedes-Benz ”. **ATZ worldwide**, Springer Science and Business Media LLC, v. 116, p. 20–25, 1 Jan. 2014. Cit. on p. 35.

DVORNIKOV, L. T.; ZHUKOV, I. A. “Fundamentals of a Unified Theory of Planetary Gears ”. **Russian Engineering Research**, © Allerton Press, Inc, v. 42, p. 541–547, 6 June 2022. Cit. on p. 64.

ELMARAGHY, W.; ELMARAGHY, H.; TOMIYAMA, T.; MONOSTORI, L. "Complexity in Engineering Design and Manufacturing ". **CIRP Annals - Manufacturing Technology**, v. 61, p. 793–814, 2 2012. Cit. on p. 91.

ESMAIL, E. L. "Teaching Planetary Gear Trains with the Aid of Nomographs ". **Advances in Mechanical Engineering**, Hindawi Publishing Corporation, v. 5, p. 978418, Jan. 2013. Cit. on p. 58.

F. COSTA, L. da; RODRIGUES, F. A.; TRAVIESO, G.; BOAS, P. R. V. "Characterization of Complex Networks: A Survey of Measurements ". **Advances in Physics**, v. 56, p. 167–242, 1 Jan. 2007. Cit. on p. 109.

FAYYAD, U. M. "Data Mining and Knowledge Discovery: Making Sense Out of Data ". **IEEE Expert**, v. 11, p. 20–25, 5 Oct. 1996. Cit. on pp. 101–103.

FELK, Y.; MASSON, P. L.; WEIL, B.; COGEZ, P.; HATCHUEL, A. "DESIGNING PATENT PORTFOLIO FOR DISRUPTIVE INNOVATION - A NEW METHODOLOGY BASED ON C-K THEORY ". In. Cit. on p. 40.

FISCHER, R.; KÜÇÜKAY, F.; JÜRGENS, G.; NAJORK, R.; POLLAK, B. *The Automotive Transmission Book* . Springer International Publishing, 2015. Cit. on pp. 33, 36, 46.

FOLKSON, R.; SAPSFORD, S. (Eds.). *Alternative Fuels and Advanced Vehicle Technologies for Improved Environmental Performance* . 2. ed.: Elsevier, 2022. Cit. on pp. 33, 38.

FOUNDATION, P. S. *Python* . 2023. Available from: `https://python.org`. Visited on: 26 June 2023. Cit. on p. 113.

FREUDENSTEIN, F.; MAKI, E. R. "The Creation of Mechanisms According to Kinematic Structure and Function ". **Environment and Planning B: Planning and Design**, v. 6, p. 375–391, 4 Dec. 1979. Cit. on pp. 39, 71, 92, 105.

FREUDENSTEIN, F. "An Application of Boolean Algebra to the Motion of Epicyclic Drives ". **Journal of Engineering for Industry**, v. 93, p. 176–182, 1 Feb. 1971. Cit. on pp. 61, 66, 73.

GAERTNER, L.; EBENHOCH, M. “The Zf Automatic Transmission 9hp48 Transmission System, Design and Mechanical Parts ”. **SAE International Journal of Passenger Cars - Mechanical Systems**, SAE International, v. 6, p. 2013-01–1276, 2 Apr. 2013. Cit. on p. 35.

GEORGES, N.; MHIRI, I.; REKIK, I. “Identifying the Best Data-Driven Feature Selection Method for Boosting Reproducibility in Classification Tasks ”. **Pattern Recognition**, Elsevier Ltd, v. 101, p. 107183, May 2020. Cit. on p. 121.

GHOSH, A.; NASHAAT, M.; MILLER, J.; QUADER, S.; MARSTON, C. “A Comprehensive Review of Tools for Exploratory Analysis of Tabular Industrial Datasets ”. **Visual Informatics**, Elsevier B.V., v. 2, p. 235–253, 4 Dec. 2018. Cit. on p. 116.

GOGU, G. “Mobility of Mechanisms: A Critical Review ”. **Mechanism and Machine Theory**, Pergamon, v. 40, p. 1068–1097, 9 Sept. 2005. Cit. on p. 64.

GOLESKI, G. D.; BALDWIN, R. A. *Us8545362b1 - Multi-Speed Transmission* . Oct. 2013. Cit. on p. 148.

GRÜBLER, M. *Getriebelehre* . Springer Berlin Heidelberg, 1917. Cit. on p. 64.

GUYON, I.; ELISSEEFF, A. “An Introduction to Variable and Feature Selection ”. **J. Mach. Learn. Res.**, JMLR.org, v. 3, p. 1157–1182, Mar. 2003. Cit. on p. 118.

HAGBERG, A. A.; SCHULT, D. A.; SWART, P. J. “Exploring Network Structure, Dynamics, and Function Using Networkx ”. In: VAROQUAUX, G.; VAUGHT, T.; MILLMAN, J. (Eds.), p. 11–15. Cit. on p. 113.

HAIR, J. F.; BLACK, W. C.; BABIN, B. J.; ANDERSON, R. E. *Multivariate Data Analysis Eighth Edition* . 8. ed.: Cengage Learning, 2019. Cit. on pp. 115, 118.

HALDERMAN, J. D.; BIRCH, T. W. *Automatic Transmissions and Transaxles* . 7. ed.: Pearson, 2017. P. 290. Cit. on pp. 45, 46, 48, 57.

HAMILTON, W. L. *Graph Representation Learning* . Springer International Publishing, 2020. v. 46. Cit. on p. 197.

HAN, J.; KAMBER, M.; PEI, J. *Data Mining* . 3. ed.: Elsevier, 2012. Cit. on pp. 102, 114, 115.

HAN, Y.-H.; LEE, K. "A Case-Based Framework for Reuse of Previous Design Concepts in Conceptual Synthesis of Mechanisms ". **Computers in Industry**, v. 57, p. 305–318, 4 May 2006. Cit. on p. 71.

HARRIS, C. R.; MILLMAN, K. J.; WALT, S. J. van der; GOMMERS, R.; VIRTANEN, P.; COURNAPEAU, D.; WIESER, E.; TAYLOR, J.; BERG, S.; SMITH, N. J.; KERN, R.; PICUS, M.; HOYER, S.; KERKWIJK, M. H. van; BRETT, M.; HALDANE, A.; RÍO, J. F. del; WIEBE, M.; PETERSON, P.; GÉRARD-MARCHANT, P.; SHEPPARD, K.; REDDY, T.; WECKESSER, W.; ABBASI, H.; GOHLKE, C.; OLIPHANT, T. E. "Array Programming with Numpy ". **Nature**, Springer Science and Business Media LLC, v. 585, p. 357–362, 7825 Sept. 2020. Cit. on p. 113.

HART, J. M. "General Motors Rear Wheel Drive Eight Speed Automatic Transmission ". **SAE International Journal of Passenger Cars - Mechanical Systems**, SAE International, v. 7, p. 289–294, 1 2014. Cit. on p. 78.

HARTENBERG, R. S.; DENAVIT, J. *Kinematic Synthesis of Linkages (mechanical Engineering Series)* . McGraw-Hill, 1964. Cit. on pp. 39, 70.

HE, B.; HUANG, S. "Functional Synthesis of Mechanisms under Cost Consideration ". **Proceedings of the Institution of Mechanical Engineers, Part B: Journal of Engineering Manufacture**, SAGE PublicationsSage UK: London, England, v. 230, p. 91–99, 1 Jan. 2016. Cit. on p. 39.

HENNIG, A.; TOPCU, T. G.; SZAJNFARBER, Z. "So You Think Your System Is Complex?: Why and How Existing Complexity Measures Rarely Agree ". **Journal of Mechanical Design, Transactions of the ASME**, American Society of Mechanical Engineers (ASME), v. 144, 4 Apr. 2022. Cit. on p. 91.

HENRY, I. *Daimler-Renault-Nissan – The alliance in action* . We conclude our review of Daimler's partnership with Renault and Nissan with a look at platform and production sharing projects. en. 29 July 2015. Available from: `https://www.automotivemanufacturingsolutions.com/daimler-renault-nissan-the-alliance-in-action/6319.article`. Visited on: 8 Feb. 2023. Cit. on p. 35.

HERNÁNDEZ, J. M.; MIEGHEM, P. V. *Classification of Graph Metrics* . Nov. 2011. Cit. on p. 109.

HINTZE, J. L.; NELSON, R. D. "Violin Plots: A Box Plot-Density Trace Synergism ". **The American Statistician**, Taylor & Francis, v. 52, n. 2, p. 181–184, 1998. Cit. on pp. 389, 390.

HO, T.-T.; HWANG, S.-J. "Configuration Synthesis of Novel Hybrid Transmission Systems Using a Combination of a Ravigneaux Gear Train and a Simple Planetary Gear Train ". **Energies**, v. 13, p. 2333, 9 May 2020. Cit. on p. 75.

HOELTGEBAUM, T.; SIMONI, R.; MARTINS, D. "Reconfigurability of Engines: A Kinematic Approach to Variable Compression Ratio Engines ". **Mechanism and Machine Theory**, Pergamon, v. 96, p. 308–322, Feb. 2016. Cit. on p. 40.

HOELTGEBAUM, T.; SOUZA VIEIRA, R. de; MARTINS, D. "A Patent Survey Methodology Focused on Automotive Mechanisms ". In. Cit. on pp. 40, 76, 105, 106.

HSIEH, H.-I.; TSAI, L.-W. "A Methodology for Enumeration of Clutching Sequences Associated with Epicyclic-Type Automatic Transmission Mechanisms ". In: p. 151–159. Cit. on p. 78.

HSIEH, H.-I.; TSAI, L.-W. "Kinematic Analysis of Epicyclic-Type Transmission Mechanisms Using the Concept of Fundamental Geared Entities ". **Journal of Mechanical Design**, ASME International, v. 118, n. 2, p. 294–299, 2 June 1996. Cit. on p. 53.

HSU, C.-H.; HSU, J.-J. "Epicyclic Gear Trains for Automotive Automatic Transmissions ". **Proceedings of the Institution of Mechanical Engineers, Part D: Journal of Automobile Engineering**, Prof Eng Publ Ltd, v. 214, p. 523–532, 5 May 2000. Cit. on p. 74.

HSU, C.-H.; LAM, K.-T. "A New Graph Representation for the Automatic Kinematic Analysis of Planetary Spur-Gear Trains ". **Journal of Mechanical Design**, v. 114, p. 196–200, 1 Mar. 1992. Cit. on pp. 62, 68.

HU, J.; MA, J.; FENG, J. F.; PENG, Y. H. "Research on New Creative Conceptual Design System Using Adapted Case-Based Reasoning Technique ". **Artificial Intelligence for Engineering Design, Analysis and Manufacturing: AIEDAM**, v. 31, p. 16–29, 1 2017. Cit. on pp. 39, 71.

HUNT, K. H. *Kinematic Geometry of Mechanisms* . Bookcraft, 1990. Cit. on p. 51.

HUNTER, J. D. "Matplotlib: A 2d Graphics Environment ". **Computing in Science & Engineering**, Ieee Computer Soc, v. 9, p. 90–95, 3 2007. Cit. on p. 113.

HWANG, W.-M.; HUANG, Y.-L. "Connecting Clutch Elements to Planetary Gear Trains for Automotive Automatic Transmissions Via Coded Sketches ". **Mechanism and Machine Theory**, v. 46, p. 44–52, 1 Jan. 2011. Cit. on p. 75.

HWANG, W.-M.; HUANG, Y.-L. "Configuration Design of Six-Speed Automatic Transmissions with Two-Degree-Of-Freedom Planetary Gear Trains ". **Transactions of the Canadian Society for Mechanical Engineering**, v. 29, p. 41–55, 1 Mar. 2005. Cit. on p. 75.

IEA. *Global Ev Outlook 2023* . Mar. 2023. Cit. on p. 33.

IKEMURA, M.; OTA, H.; HAGINO, Y.; TOYODA, M.; MICHIKOSHI, Y. *Vehicular Automatic Transmission* . June 2016. Cit. on pp. 132, 133, 135.

IONESCU, T. "Standardization of Terminology ". **Mechanism and Machine Theory**, Pergamon, v. 38, p. 597–1112, 7-10 July 2003. Cit. on p. 51.

JEONG, C.; KIM, K. "Creating Patents on the New Technology Using Analogy-Based Patent Mining ". **Expert Systems with Applications**, Pergamon, v. 41, p. 3605–3614, 8 June 2014. Cit. on p. 40.

JOHNSON, R. C.; TOWFIGH, K. "Creative Design of Epicyclic Gear Trains Using Number Synthesis ". **Journal of Engineering for Industry**, v. 89, p. 309–314, 2 May 1967. Cit. on p. 58.

JUBER, A. H.; ESMAIL, E. L.; ALI, T. N. "Graph Representation of Planetary Gear Trains: A Review ". **Al-Qadisiyah Journal for Engineering Sciences**, Al-Qadisiyah Journal for Engineering Sciences (QJES), v. 14, p. 227–231, 4 May 2022. Cit. on p. 59.

JÜTTNER, A.; MADARASI, P. "Vf2++—An Improved Subgraph Isomorphism Algorithm ". **Discrete Applied Mathematics**, Elsevier B.V., v. 242, p. 69–81, June 2018. Cit. on p. 115.

KARHULA, H.; NICOLAI, M. "Towards Automated Synthesis of Automatic Automated Transmission Designs ". **International Journal of Automotive Engineering**, v. 9, p. 20184115, 4 2018. Cit. on pp. 59, 71, 72, 76, 77, 91, 92, 118, 141.

KARHULA, H.; NICOLAI, M.; DESMET, W. “Exhaustive Synthesis and Analysis of Automotive 2-Stage Planetary Transmission Designs ”. In. Cit. on pp. 71, 72, 92.

KE, T.; DING, H.; GONG, C.; GENG, M. “Configuration Synthesis of Nine-Speed Automatic Transmissions Based on Structural Decomposition ”. **Mechanism and Machine Theory**, Elsevier Ltd, v. 164, 104421 Oct. 2021. Cit. on p. 75.

KHALID, S.; KHALIL, T.; NASREEN, S. “A Survey of Feature Selection and Feature Extraction Techniques in Machine Learning ”. **Proceedings of 2014 Science and Information Conference, SAI 2014**, The Science and Information (SAI) Organization, p. 372–378, 2014. Cit. on p. 120.

KHAN, W. A.; CARO, S.; ANGELES, J.; PASINI, D.; DAMIANO, P. A. “A Formulation of Complexity-Based Rules for the Preliminary Design Stage of Robotic Architectures ”. In: p. 1–11. Cit. on p. 96.

KHULIEF, Y. A. *Resolving the Misinterpretation of the Gear Joint in Mobility Calculations* . 2013. Cit. on pp. 64, 80.

KIZILOZ, H. E. “Classifier Ensemble Methods in Feature Selection ”. **Neurocomputing**, Elsevier B.V., v. 419, p. 97–107, Jan. 2021. Cit. on p. 121.

KÖLLER, S.; SCHMITZ, V. “Systematic Synthesis and Multi-Criteria Evaluation of Transmission Topologies for Electric Vehicles ”. **Automotive and Engine Technology**, Springer Science and Business Media LLC, v. 7, p. 65–79, 1-2 June 2022. Cit. on pp. 71, 73, 91, 92.

KOMOROWSKI, M.; MARSHALL, D. C.; SALCICCIOLI, J. D.; CRUTAIN, Y. Exploratory Data Analysis. In: Springer International Publishing, Jan. 2016. P. 185–203. Cit. on p. 116.

KOTA, S.; CHIOU, S.-J. “Conceptual Design of Mechanisms Based on Computational Synthesis and Simulation of Kinematic Building Blocks ”. **Research in Engineering Design**, v. 4, p. 75–87, 2 June 1992. Cit. on pp. 39, 59, 71.

KOZA, J. R.; KEANE, M. A.; STREETER, M. J.; ADAMS, T. P.; JONES, L. W. “Invention and creativity in automated design by means of genetic programming ”. **Artificial Intelligence for Engineering Design, Analysis and Manufacturing**, Cambridge University Press (CUP), v. 18, n. 3, p. 245–269, Aug. 2004. Cit. on p. 40.

KUTZBACH, K. "Mechanische Leitungsverzweigung, Ihre Gesetze Und Anwendungen ". **Maschinenbau der Betrieb**, v. 8, p. 710–716, 21 1929. Cit. on p. 64.

LAR. *Laboratório De Robótica Aplicada (lar)* . 2018. Available from: http://robotica.ufsc.br/. Visited on: 12 Aug. 2022. Cit. on p. 76.

LAUS, L. P.; SIMAS, H.; MARTINS, D. "Efficiency of Gear Trains Determined Using Graph and Screw Theories ". **Mechanism and Machine Theory**, v. 52, p. 296–325, APRIL 2012. Cit. on p. 196.

LEWICKI, P.; HILL, T. *Statistics: Methods and Applications: A Comprehensive Reference for Science, Industry, and Data Mining* . 1. ed.: StatSoft, Inc., 2006. Cit. on p. 117.

LIU, H.; MOTODA, H. *Feature Extraction, Construction and Selection* . Ed. by Huan Liu and Hiroshi Motoda. Springer US, 1998. Cit. on p. 119.

LIU, H.; MOTODA, H. *Feature Selection for Knowledge Discovery and Data Mining* . Springer US, 1998. Cit. on p. 118.

LIU, H.; YU, L. "Toward Integrating Feature Selection Algorithms for Classification and Clustering ". **IEEE Transactions on Knowledge and Data Engineering**, v. 17, p. 491–502, 4 Apr. 2005. Cit. on pp. 119, 120.

MARSHALL, H. A. Advanced Transmission Systems for New Propulsion Technologies. In: 2. ed.: Woodhead Publishing, 2022. P. 413–429. Cit. on p. 35.

MARTIN, T.; HENDRICKSON, J. "General Motors Hydra-Matic 9t50 Automatic Transaxle ". In: 2018-April. Cit. on p. 35.

MARTINS, D.; FRANK, T.; SIMAS, H.; SOUZA VIEIRA, R. de; SIMONI, R.; MURAI, E. H.; HOELTGEBAUM, T. "Structural Analysis, Survey and Classification of Kinematic Chains for Atkinson Cycle Engines ". **Journal of the Brazilian Society of Mechanical Sciences and Engineering**, Springer Berlin Heidelberg, v. 40, p. 52, 2 Feb. 2018. Cit. on p. 40.

MATA, A. S.; TORRAS, A. B.; CARRILLO, J. A. C.; JUANCO, F. E.; FERNÁNDEZ, A. J. G.; MARTINEZ, F. N.; FERNÁNDEZ, A. O. *Fundamentals of Machine Theory and Mechanisms* . Springer International, 2016. v. 40. Cit. on pp. 51, 70.

MCKAY, B. D.; PIPERNO, A. “Practical Graph Isomorphism, Ii ”. **Journal of Symbolic Computation**, Academic Press, v. 60, p. 94–112, Jan. 2014. Cit. on p. 68.

MCKINNEY, W. “Data Structures for Statistical Computing in Python ”. In: WALT, S. van der; MILLMAN, J. (Eds.), p. 56–61. Cit. on p. 113.

MISHRA, P.; PANDEY, C. M.; SINGH, U.; GUPTA, A.; SAHU, C.; KESHRI, A. “Descriptive Statistics and Normality Tests for Statistical Data. ” **Annals of cardiac anaesthesia**, Wolters Kluwer Medknow Publications, v. 22, p. 67–72, 1 Jan. 2019. Cit. on p. 116.

MOLIAN, S. “Kinematics of Compound Differential Mechanisms ”. **Proceedings of the Institution of Mechanical Engineers**, v. 185, p. 733–739, 1 June 1970. Cit. on p. 58.

MRUTHYUNJAYA, T. S. “Kinematic Structure of Mechanisms Revisited ”. **Mechanism and Machine Theory**, v. 38, p. 279–320, 4 2003. Cit. on pp. 59, 73.

MURAI, E. H.; MARTINS, D.; SIMAS, H. “Number and Type Syntheses for an One-Side Stitching Device ”. In: v. 6, p. 6121–6132. Cit. on p. 76.

MURAI, E. H. *Number Synthesis Methods for Mechanism Design: An Alternative Approach* . 11 Feb. 2019. 266 pp. PhD thesis – Universidade Federal de Santa Catarina, Florianópolis. Cit. on pp. 39, 73, 76.

MURAI, E. H.; SIMAS, H.; MARTINS, D. “New Kinematic Structures for One-Side Stitching Devices ”. In. Cit. on p. 76.

MUSTAFA, J.; HASAN, A.; KHAN, R. A. “An Innovative Approach for Detection of Isomorphism of Epicyclic Gear Trains ”. **Materials Today: Proceedings**, Elsevier Ltd, v. 25, p. 862–867, 2019. Cit. on p. 68.

MUSTAFA, J.; HASAN, A.; KHAN, R. A. “Identification of Isomorphism in Epicyclic Gear Trains - a Bocher’s Approach ”. **Materials Today: Proceedings**, Elsevier Ltd, v. 25, p. 881–887, 2019. Cit. on p. 68.

NAUNHEIMER, H.; BERTSCHE, B.; RYBORZ, J.; NOVAK, W. *Automotive Transmissions* . Springer Berlin Heidelberg, 2011. Cit. on pp. 33, 46, 47.

NAUNHEIMER, H.; BERTSCHE, B.; RYBORZ, J.; NOVAK, W.; FIETKAU, P. *Fahrzeuggetriebe* . Springer Berlin Heidelberg, 2019. Cit. on pp. 34, 35, 37, 38, 46, 49.

NEWMAN, M. E. J. (E. J. *Networks : An Introduction* . Oxford University Press, 2010. P. 772. Cit. on p. 111.

NORTON, R. L. *Machine Design : An Integrated Approach* . Pearson Prentice Hall, 2006. P. 984. Cit. on p. 69.

OEHLERS, M.; FABIAN, B. "Graph Metrics for Network Robustness—A Survey ". **Mathematics**, MDPI AG, v. 9, p. 895, 8 Apr. 2021. Cit. on p. 109.

OLIVEIRA E COSTA, M. V. de; MURAI, E. H.; SILVA ROSA, F. da; MARTINS, D. "Review and Classification of Workpiece Toggle Clamping Devices ". In: CARVALHO, J. C. M.; MARTINS, D.; SIMONI, R.; SIMAS, H. (Eds.). v. 54, p. 74–84. Cit. on p. 40.

OLSON, D. G.; ERDMAN, A. G.; RILEY, D. R. "Topological Analysis of Single-Degree-Of-Freedom Planetary Gear Trains ". **Journal of Mechanical Design**, v. 113, p. 10–16, 1 Mar. 1991. Cit. on p. 61.

OU, F.-M.; YAN, H.-S.; TANG, M.-F. "The Synthesis of Mechanism Systems Using a Mechanism Concept Library ". **Transactions of the Canadian Society for Mechanical Engineering**, v. 34, p. 151–163, 1 2010. Cit. on pp. 39, 71.

OVERSCHIE, J. G. S.; ALSAHAF, A.; AZZOPARDI, G. "Fseval: A Benchmarking Framework for Feature Selection and Feature Ranking Algorithms ". **Journal of Open Source Software**, The Open Journal, v. 7, p. 4611, 79 Nov. 2022. Cit. on p. 121.

PAHL, G.; BEITZ, W.; FELDHUSEN, J.; GROTE, K.-H. *Engineering Design* . Springer London, 2007. Cit. on p. 69.

PEDREGOSA, F.; VAROQUAUX, G.; GRAMFORT, A.; MICHEL, V.; THIRION, B.; GRISEL, O.; BLONDEL, M.; MÜLLER, A.; NOTHMAN, J.; LOUPPE, G.; PRETTENHOFER, P.; WEISS, R.; DUBOURG, V.; VANDERPLAS, J.; PASSOS, A.; COURNAPEAU, D.; BRUCHER, M.; PERROT, M.; DUCHESNAY, É. "Scikit-Learn: Machine Learning in Python ". **Journal of Machine Learning Research**, v. 12, p. 2825–2830, Jan. 2012. Cit. on p. 113.

PENNESTRI, E.; CAVACECE, M.; VITA, L. “On the Computation of Degrees-Of-Freedom: A Didactic Perspective ”. In: v. 6 C, p. 1733–1741. Cit. on p. 64.

PENNESTRI, E.; BELFIORE, N. P. “On Crossley’s Contribution to the Development of Graph Based Algorithms for the Analysis of Mechanisms and Gear Trains ”. **Mechanism and Machine Theory**, v. 89, p. 92–106, 2015. Cit. on p. 59.

POLDER, J. “A Network Theory for Variable Epicyclic Gear Trains ”, June 1969. Cit. on p. 58.

RAGHAVAN, M. “Synthesis of Transmissions with Four Planetary Gearsets ”. In: p. 605–609. Cit. on p. 78.

RAGHAVAN, M. A Short Story on Long Pinions. In: Springer Netherlands, 2013. v. 14, p. 177–188. Cit. on p. 78.

RAGHAVAN, M. *Long Pinions for Alternative Transmission Mechanizations* . v. 9. 2018. P. 32–37. Cit. on p. 78.

RAGHAVAN, M. Role of Mms and IFToMM in the Creation of Novel Automotive Transmissions and Hybrids. In: Springer Netherlands, 2011. v. 1, p. 191–202. Cit. on p. 78.

RAGHAVAN, M. “The Analysis of Planetary Gear Trains ”. **Journal of Mechanisms and Robotics**, v. 2, 2 2010. Cit. on p. 78.

RAGHAVAN, M.; BUCKNOR, N.; MAGUIRE, J.; HENDRICKSON, J.; SINGH, T. “The Algebraic Design of Transmissions & Evts ”. **SAE Technical Papers**, SAE International, 2007. Cit. on p. 78.

RAGHAVAN, M.; USORO, P. B. *Us6422969b1 - Powertrain with a Six Speed Planetary Transmission Having Three Planetary Gear Sets - Google Patents* . 2000. Cit. on p. 50.

RAVISANKAR, R.; MRUTHYUNJAYA, T. “Computerized Synthesis of the Structure of Geared Kinematic Chains ”. **Mechanism and Machine Theory**, v. 20, p. 367–387, 5 Jan. 1985. Cit. on pp. 61, 80.

REULEAUX, F. *Kinematics of Machinery: Outlines of a Theory of Machines*. MACMILLAN and CO., 1876. Cit. on pp. 51, 64.

RODRIGUES, F. A. "Network Centrality: An Introduction ". **arXiv**, Jan. 2019. Cit. on p. 110.

ROSS, C. S.; ROUTE, W. D. "A Method for Selecting Parallel-Connected, Planetary Gear Train Arrangements for Automotive Automatic Transmissions ". In. Cit. on p. 75.

RUSSO, M. "Measuring Performance: Metrics for Manipulator Design, Control, and Optimization ". **Robotics**, MDPI, v. 12, p. 4, 1 Dec. 2022. Cit. on p. 97.

S., R. V.; GHOSE, D. "Degrees of Freedom Analysis of Mechanisms Using the New Zebra Crossing Method ". **ArXiv**, abs/2201.02352, Jan. 2022. Cit. on p. 59.

DEVELOPERS, T. S. *Sagemath, the Sage Mathematics Software System (version 10.0)* . 2023. Cit. on pp. 113, 138.

SAHU, B.; DEHURI, S.; JAGADEV, A. "A Study on the Relevance of Feature Selection Methods in Microarray Data ". **The Open Bioinformatics Journal**, v. 11, p. 117–139, 1 July 2018. Cit. on p. 119.

SCHIRMER, M. *Gm and Ford to Jointly Develop Advanced Automatic Transmissions* . Apr. 2013. Available from: `https://news.gm.com/newsroom.detail.html/Pages/news/us/en/2013/Apr/0415-transmission.html`. Visited on: 16 Mar. 2021. Cit. on p. 148.

SEABOLD, S.; PERKTOLD, J. "Statsmodels: Econometric and Statistical Modeling with Python ". In: 9^{th} Python in Science Conference. 2010. Cit. on p. 113.

SHANMUKHASUNDARAM, V. R.; RAO, Y. V. D.; REGALLA, S. P. "Enumeration of Displacement Graphs of Epicyclic Gear Train from a Given Rotation Graph Using Concept of Building of Kinematic Units ". **Mechanism and Machine Theory**, Pergamon, v. 134, p. 393–424, Apr. 2019. Cit. on p. 74.

SHANMUKHASUNDARAM, V. R.; RAO, Y. V. D.; REGALLA, S. P. "Review of Structural Synthesis Algorithms for Epicyclic Gear Trains ". **Lecture Notes in Mechanical Engineering**, Springer, Singapore, p. 351–375, 2021. Cit. on pp. 73, 80.

SHERVASHIDZE, N.; SCHWEITZER, P.; LEEUWEN, E. J. van; MEHLHORN, K.; BORGWARDT, K. M. "Weisfeiler-Lehman Graph Kernels ". **J. Mach. Learn. Res.**, JMLR.org, v. 12, p. 2539–2561, Nov. 2011. Cit. on p. 115.

SHIXIN, L. *Exploratory Data Analysis for Feature Selection in Machine Learning Contents* . Jan. 2020. Cit. on p. 117.

SIMONI, R.; CARBONI, A. P.; SIMAS, H.; MARTINS, D. "Enumeration of Kinematic Chains and Mechanisms Review ". In: p. 19–25. Cit. on p. 73.

SINGH, J.; SRINIVASA, K. V.; SINGH, J. "Selection of Gear Ratio for Smooth Gear Shifting ". In: v. 8. Cit. on p. 50.

SINGH, T.; OLENZEK, R. "General Motors Small Front Wheel Drive Six Speed Automatic Transmission Family ". In. Cit. on pp. 58, 85.

SINHA, K. "Structural Complexity and Its Implications for Design of Cyber-Physical Systems ", Feb. 2014. Cit. on pp. 93, 95, 97.

SINHA, K.; SUH, E. S. "Pareto-Optimization of Complex System Architecture for Structural Complexity and Modularity ". **Research in Engineering Design**, Springer London, v. 29, p. 123–141, 1 Jan. 2018. Cit. on pp. 91, 93.

SINHA, K.; WECK, O. L. D. "Structural Complexity Quantification for Engineered Complex Systems and Implications on System Architecture and Design ". In: 3 A. Cit. on p. 92.

SKIENA, S. S. *The Algorithm Design Manual* . Springer London, 2008. P. 103–144. Cit. on p. 90.

SPOONER, A.; MOHAMMADI, G.; SACHDEV, P. S.; BRODATY, H.; SOWMYA, A. "Ensemble Feature Selection with Data-Driven Thresholding for Alzheimer's Disease Biomarker Discovery ". **BMC Bioinformatics**, BioMed Central Ltd, v. 24, 1 Dec. 2023. Cit. on p. 121.

STANDARDIZATION OF TERMINOLOGY, I. P. C. (for. *IFToMM Dictionaries Online* . 2014. Available from: https://iftomm-terminology.antonkb.nl/. Visited on: 20 Jan. 2023. Cit. on p. 51.

STARZHINSKY, V. E.; GOLDFARB, V. I.; SHILKO, S. V.; SHALOBAEV, E. V.; TESKER, E. I. "Development of Terminology in Gearing and Power Transmissions. Part 1. Development of the Gearing Terminology by IFToMM Permanent Commission Standard-

ization of Terminology on Tmm ". **Intellekt. Sist. Proizv.**, Kalashnikov Izhevsk State Technical University, v. 15, p. 30, 1 Mar. 2017. Cit. on p. 51.

STEEN, M. van. *Graph Theory and Complex Networks: An Introduction* . Maarten van Steen, 2010. P. 285. Cit. on p. 111.

SUBRAMANIAN, D.; WANG, C.-S. "Kinematic Synthesis with Configuration Spaces ". **Research in Engineering Design**, Springer-Verlag, v. 7, p. 193–213, 3 Sept. 1995. Cit. on pp. 39, 71.

SUH, N. P. "Complexity in Engineering ". **CIRP Annals**, v. 54, p. 46–63, 2 2005. Cit. on p. 91.

SUN, W.; LI, R.; KONG, J.; LI, A. "A New Method for Isomorphism Identification of Planetary Gear Trains ". **Mechanical Sciences**, Copernicus GmbH, v. 12, p. 193–202, 1 Feb. 2021. Cit. on p. 68.

SUZUKI, T.; SUGIURA, H.; NIINOMI, A.; MAEZUKA, S.; MIYAZAKI, T.; HABATA, Y. "New RWD 10 Speed Automatic Transmission for Passenger Vehicles ". **SAE International Journal of Engines**, SAE International, v. 10, n. 2, p. 695–700, 2 Mar. 2017. Cit. on p. 35.

TOYOTA. *New 8-Speed and 10-Speed Automatic Transmissions* . 2016. Cit. on p. 132.

TSAI, L.-W.; MAKI, E. R.; LIU, T.; KAPIL, N. G. "The Categorization of Planetary Gear Trains for Automatic Transmissions According to Kinematic Topology ". In. Cit. on pp. 63, 67.

TSAI, L.-W. "An Application of the Linkage Characteristic Polynomial to the Topological Synthesis of Epicyclic Gear Trains ". **Journal of Mechanisms, Transmissions, and Automation in Design**, v. 109, p. 329–336, 3 Sept. 1987. Cit. on p. 74.

TSAI, L.-W. *Mechanism Design: Enumeration of Kinematic Structures According to Function* . CRC Press, 2001. v. 31. Cit. on pp. 39, 47, 51, 53, 56, 58, 59, 62, 64, 67–70, 73, 76, 80, 92.

TSAI, M. C.; HUANG, C. C.; LIN, B. J. "Kinematic Analysis of Planetary Gear Systems Using Block Diagrams ". **Journal of Mechanical Design, Transactions of the ASME**, v. 132, p. 0650011–06500110, 6 June 2010. Cit. on p. 39.

VENKATESH, B.; ANURADHA, J. "A Review of Feature Selection and Its Methods ". **Cybernetics and Information Technologies**, Sciendo, v. 19, p. 3–26, 1 Mar. 2019. Cit. on p. 119.

VIRTANEN, P. et al. "Scipy 1.0: Fundamental Algorithms for Scientific Computing in Python ". **Nature Methods**, v. 17, p. 261–272, 3 Mar. 2020. Cit. on p. 113.

VOLKSWAGEN. *Dual-clutch gearbox (DSG)* . en. Volkswagen AG. Available from: https://www.volkswagen-newsroom.com/en/dual-clutch-gearbox-dsg-3651. Visited on: 27 May 2023. Cit. on p. 35.

WASKOM, M. "Seaborn: Statistical Data Visualization ". **Journal of Open Source Software**, The Open Journal, v. 6, p. 3021, 60 Apr. 2021. Cit. on p. 113.

WIPO. *Finding Technology Using Patents* . World Intellectual Property Organization, 2015. WIPO Publication No. L434/2E. Cit. on pp. 40, 104, 105.

WIPO. *Wipo Patent Drafting Manual* . 2011. Cit. on p. 104.

WITTEN, I. H.; FRANK, E.; HALL, M. A.; PAL, C. J. *Data Mining Practical Machine Learning Tools and Techniques Fourth Edition* . 2017. Cit. on p. 101.

WOLSKI, L.; PIZONI, W. A.; GONÇALVES, A. L. "Modelo De ClassificaÇÃo De Patentes Baseado Em TÉcnicas De Engenharia De Conhecimento ". In. Cit. on p. 196.

XU, X.; DONG, P.; LIU, Y.; ZHANG, H. "Progress in Automotive Transmission Technology ". **Automotive Innovation**, v. 1, p. 187–210, 3 July 2018. Cit. on p. 39.

XU, X.; SUN, H.; LIU, Y.; DONG, P. "Matrix-Based Operation Method for Detecting Structural Isomorphism of Planetary Gear Train Structures ". **Journal of Mechanical Design, Transactions of the ASME**, American Society of Mechanical Engineers (ASME), v. 142, 6 June 2020. Cit. on p. 68.

XUE, B.; ZHANG, M.; BROWNE, W. N.; YAO, X. "A Survey on Evolutionary Computation Approaches to Feature Selection ". **IEEE Transactions on Evolutionary Computation**, v. 20, p. 606–626, 4 Aug. 2016. Cit. on p. 120.

XUE, H.-L.; LIU, G.; YANG, X.-H. "A Review of Graph Theory Application Research in Gears ". **Proceedings of the Institution of Mechanical Engineers, Part C: Journal**

of Mechanical Engineering Science, SAGE Publications Ltd, v. 230, p. 1697–1714, 10 June 2016. Cit. on pp. 59, 62.

YAN, H. sen. "A Methodology for Creative Mechanism Design ". **Mechanism and Machine Theory**, Pergamon, v. 27, p. 235–242, 3 May 1992. Cit. on pp. 39, 73.

YAN, H. S.; CHIU, Y. T. "On the Number Synthesis of Kinematic Chains ". **Mechanism and Machine Theory**, Elsevier Ltd, v. 89, p. 128–144, 2015. Cit. on p. 73.

YAN, H.-S. *Creative Design of Mechanical Devices* . Springer-Verlag Singapore Pte. Ltd., 1998. P. 244. Cit. on pp. 39, 54, 69, 70, 74, 76.

YAN, H.-S.; OU, F.-M. "An Approach for the Enumeration of Combined Configurations of Kinematic Building Blocks ". **Mechanism and Machine Theory**, Pergamon, v. 40, p. 1240–1257, 11 Nov. 2005. Cit. on p. 71.

YANG, W.; DING, H. "The Complete Set of One-Degree-Of-Freedom Planetary Gear Trains with up to Nine Links ". **Journal of Mechanical Design**, v. 141, 4 Apr. 2019. Cit. on p. 68.

YANG, W.; DING, H. "The Perimeter Loop-Based Method for the Automatic Isomorphism Detection in Planetary Gear Trains ". **Journal of Mechanical Design**, American Society of Mechanical Engineers (ASME), v. 140, 12 Dec. 2018. Cit. on pp. 68, 145.

YANG, W.; DING, H.; ZI, B.; ZHANG, D. "New Graph Representation for Planetary Gear Trains ". **Journal of Mechanical Design**, American Society of Mechanical Engineers (ASME), v. 140, 1 Jan. 2018. Cit. on pp. 62, 68, 69.

YANG, W.; LI, C. "Symmetry Detection and Topological Synthesis of Mechanisms of Powertrains ". **Energies**, MDPI, v. 15, 13 July 2022. Cit. on p. 68.

YANG, X.; YU, W.; SHAO, Y.; XU, Z.; ZENG, Q.; NIE, C.; PENG, D. "An Augmented Lever Analogy Method for Kinematic Analysis of Dual-Input Planetary/epicyclic Gear Sets Involving Planet Gear ". **IEEE Access**, Institute of Electrical and Electronics Engineers Inc., v. 10, p. 101137–101148, 2022. Cit. on p. 184.

YU, L.; LIU, H. "Efficient Feature Selection Via Analysis of Relevance and Redundancy ". **Journal of Machine Learning Research**, v. 5, p. 1205–1224, Oct 2004. Cit. on p. 119.

ZHANG, Y.; MI, C. *Automotive Power Transmission Systems* . Wiley, Aug. 2018. Cit. on pp. 33, 35, 46.

Appendix

APPENDIX A – PLANETARY GEAR MECHANISMS DATABASE

This appendix is dedicated to presenting the construction of the database using the PGM dataset template and details each of the 159 PGM datasets used throughout the thesis to demonstrate the application of the process proposed in the Chapter 4.

A link to the Google Drive folder containing all datasets is available at PGM Datasets folder.

The complete database can be found in the PGM Complete Database Spreadsheet.

A.1 PGM DATASET TEMPLATE

As described in the Section 4.2.3 section, each PGM collected data was input into a worksheet template that automatically generated its corresponding dataset information. For reasons of space, the dataset template for the sample of Figure 45 is detailed in 15 sectors, arranged in a Google Sheets spreadsheet according to the map shown in Figure 64. This dataset is available at US10563738B2___20230618.

Figure 64 – PGM Dataset Template Map.

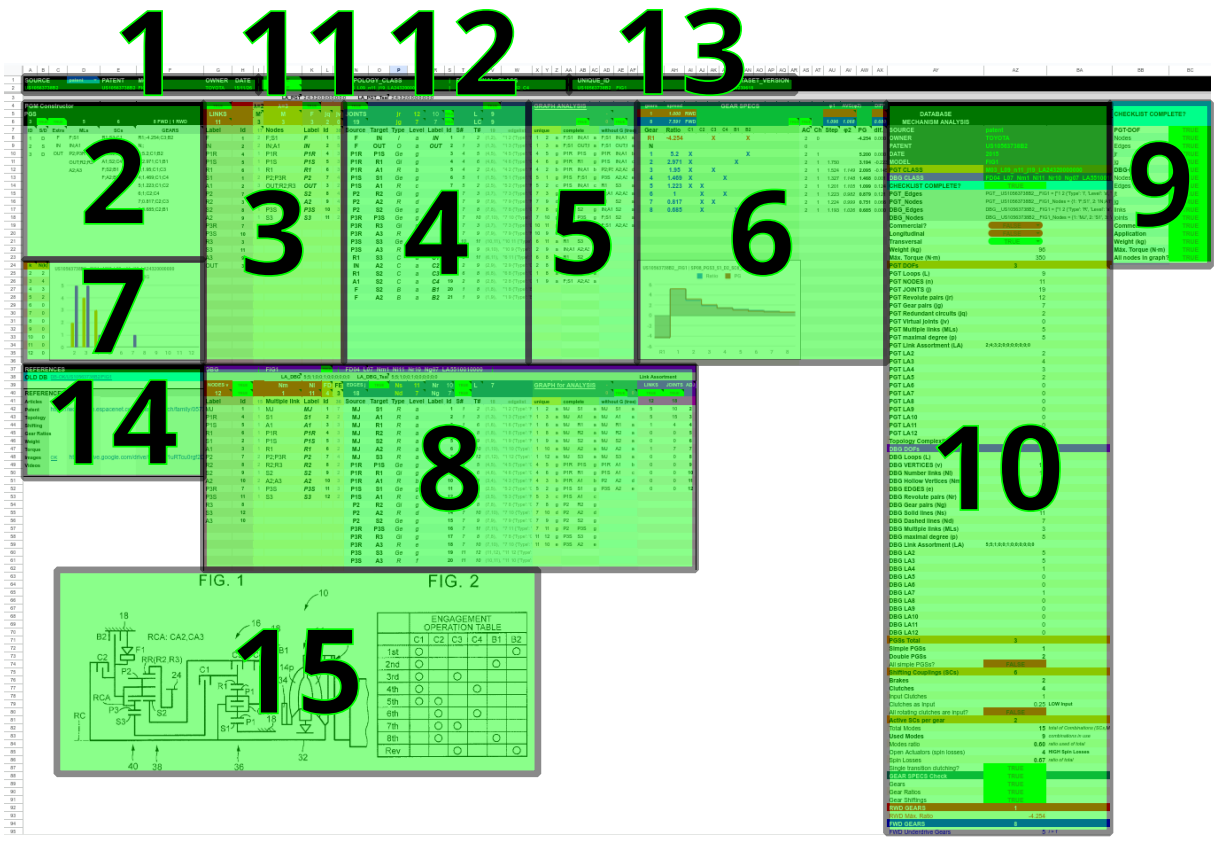

Source: Author.

Figure 65 – Sector 1: Dataset Identification (manual)

SOURCE	patent	PATENT	MODEL	OWNER	DATE	
US10563738B2		US10563738B2	FIG1	TOYOTA	15/11/26	

Source: Author.

Figure 66 – Sector 2: Topological and functional data input (manual)

PGM Constructor PGSs					
3	TRUE	TRUE	5	6	8 FWD | 1 RWD
ID	S/D	Extra	CLs	SCs	GEARS
1	D	F	F;S1	R1;S3;C1	R1;-4.254;C3;B2
2	S	IN	IN;A1	IN;A2;C2	N;;
3	D	OUT	P2;P3R	R1;S2;C3	1;5.2;C1;B2
			OUT;R2;R3	A1;S2;C4	2;2.971;C1;B1
			A2;A3	F;S2;B1	3;1.95;C1;C3
				F;A2;B2	4;1.469;C1;C4
					5;1.223;C1;C2
					6;1;C2;C4
					7;0.817;C2;C3
					8;0.685;C2;B1

Source: Author.

Figure 67 – Sector 3: Links creation (automatic)

LINKS (n) 11		M' 3	M 3	F 3	jQ 2	jV 0
elementar	Id	17	Links	Label	Id	38
F	1	2	F;S1	***F***	1	5
IN	2	2	IN;A1	***IN***	2	5
P1R	4	1	P1R	***P1R***	4	3
P1S	5	1	P1S	***P1S***	5	3
R1	6	1	R1	***R1***	6	3
S1	1	2	P2;P3R	***P2***	7	4
A1	2	3	OUT;R2;R3	***OUT***	3	2
P2	7	1	S2	***S2***	8	4
R2	3	2	A2;A3	***A2***	9	4
S2	8	1	P3S	***P3S***	10	3
A2	9	1	S3	***S3***	11	2
P3R	7					
P3S	10					
R3	3					
S3	11					
A3	9					
OUT	3					

Source: Author.

Figure 68 – Sector 4: Joints creation (automatic)

TRUE								TRUE	
JOINTS (j)		jR	12	10	TRUE		L	9	
19		jG	7	7	TRUE		LC	9	
Source	Target	Type	Level	Label	Id	S#	T#	19	edgelist
F	IN	*I*	*a*	***IN***	1	*1*	*2*	(1,2),	"1 2 {'Type': 'I', 'Level': 'a', 'Label': 'IN'}"
F	OUT	*O*	*a*	***OUT***	2	*1*	*3*	(1,3),	"1 3 {'Type': 'O', 'Level': 'a', 'Label': 'OUT'}"
P1R	P1S	*Ge*	*g*		3	*4*	*5*	(4,5),	"4 5 {'Type': 'Ge', 'Level': 'g', 'Label': ''}"
P1R	R1	*Gi*	*g*		4	*4*	*6*	(4,6),	"4 6 {'Type': 'Gi', 'Level': 'g', 'Label': ''}"
P1R	A1	*R*	*b*		5	*4*	*2*	(2,4),	"4 2 {'Type': 'R', 'Level': 'b', 'Label': ''}"
P1S	S1	*Ge*	*g*		6	*5*	*1*	(1,5),	"5 1 {'Type': 'Ge', 'Level': 'g', 'Label': ''}"
P1S	A1	*R*	*c*		7	*5*	*2*	(2,5),	"5 2 {'Type': 'R', 'Level': 'c', 'Label': ''}"
P2	R2	*Gi*	*g*		8	*7*	*3*	(3,7),	"7 3 {'Type': 'Gi', 'Level': 'g', 'Label': ''}"
P2	A2	*R*	*d*		9	*7*	*9*	(7,9),	"7 9 {'Type': 'R', 'Level': 'd', 'Label': ''}"
P2	S2	*Ge*	*g*		10	*7*	*8*	(7,8),	"7 8 {'Type': 'Ge', 'Level': 'g', 'Label': ''}"
P3R	P3S	*Ge*	*g*		11	*7*	*10*	(7,10),	"7 10 {'Type': 'Ge', 'Level': 'g', 'Label': ''}"
P3R	R3	*Gi*	*g*		12	*7*	*3*	(3,7),	"7 3 {'Type': 'Gi', 'Level': 'g', 'Label': ''}"
P3R	A3	*R*	*e*		13	*7*	*9*	(7,9),	"7 9 {'Type': 'R', 'Level': 'e', 'Label': ''}"
P3S	S3	*Ge*	*g*		14	*10*	*11*	(10,11),	"10 11 {'Type': 'Ge', 'Level': 'g', 'Label': ''}"
P3S	A3	*R*	*f*		15	*10*	*9*	(9,10),	"10 9 {'Type': 'R', 'Level': 'f', 'Label': ''}"
R1	S3	*C*	*a*	***C1***	16	*6*	*11*	(6,11),	"6 11 {'Type': 'C', 'Level': 'a', 'Label': 'C1'}"
IN	A2	*C*	*a*	***C2***	17	*2*	*9*	(2,9),	"2 9 {'Type': 'C', 'Level': 'a', 'Label': 'C2'}"
R1	S2	*C*	*a*	***C3***	18	*6*	*8*	(6,8),	"6 8 {'Type': 'C', 'Level': 'a', 'Label': 'C3'}"
A1	S2	*C*	*a*	***C4***	19	*2*	*8*	(2,8),	"2 8 {'Type': 'C', 'Level': 'a', 'Label': 'C4'}"
F	S2	*B*	*a*	***B1***	20	*1*	*8*	(1,8),	"1 8 {'Type': 'B', 'Level': 'a', 'Label': 'B1'}"
F	A2	*B*	*a*	***B2***	21	*1*	*9*	(1,9),	"1 9 {'Type': 'B', 'Level': 'a', 'Label': 'B2'}"

Source: Author.

Figure 69 – Sector 5: PGM Graph analysis (automatic)

GRAPH ANALYSIS								
				TRUE		- 0	TRUE	
unique			complete			without G (tree)		
1	2	a	F;S1	IN;A1	a	F;S1	IN;A1	a
1	3	a	F;S1	OUT;R2;R3	a	F;S1	OUT;R2;R3	a
4	5	g	P1R	P1S	g	P1R	IN;A1	b
4	6	g	P1R	R1	g	P1S	IN;A1	c
4	2	b	P1R	IN;A1	b	P2;P3R	A2;A3	d
5	1	g	P1S	F;S1	g	P3S	A2;A3	e
5	2	c	P1S	IN;A1	c	R1	S3	a
7	3	g	P2;P3R	OUT;R2;R3	g	IN;A1	A2;A3	a
7	9	d	P2;P3R	A2;A3	d	R1	S2	a
7	8	g	P2;P3R	S2	g	IN;A1	S2	a
7	10	g	P2;P3R	P3S	g	F;S1	S2	a
10	11	g	P3S	S3	g	F;S1	A2;A3	a
10	9	e	P3S	A2;A3	e			
6	11	a	R1	S3	a			
2	9	a	IN;A1	A2;A3	a			
6	8	a	R1	S2	a			
2	8	a	IN;A1	S2	a			
1	8	a	F;S1	S2	a			
1	9	a	F;S1	A2;A3	a			

Source: Author.

Figure 70 – Sector 6: Gear specifications (automatic)

gears	spread		GEAR SPECS							φ1	AVG(φ2)		DIFF
1	1.000	RWD											
8	7.591	FWD						TRUE	TRUE	1.096	1.068		0.680
Gear	Ratio	C1	C2	C3	C4	B1	B2						
R1	-4.254			X			X						
N													
1	5.2	X					X						
2	2.971	X				X							
3	1.95	X		X									
4	1.469	X			X								
5	1.223	X	X										
6	1		X		X								
7	0.817		X	X									
8	0.685		X			X							

AC	Ch	Step	φ2	PG	dif.
2	0			-4.254	0.000
0					
2	1			5.200	0.000
2	1	1.750		3.194	-0.223
2	1	1.524	1.149	2.095	-0.145
2	1	1.327	1.148	1.468	0.001
2	1	1.201	1.105	1.099	0.124
2	1	1.223	0.982	0.879	0.121
2	1	1.224	0.999	0.751	0.066
2	1	1.193	1.026	0.685	0.000

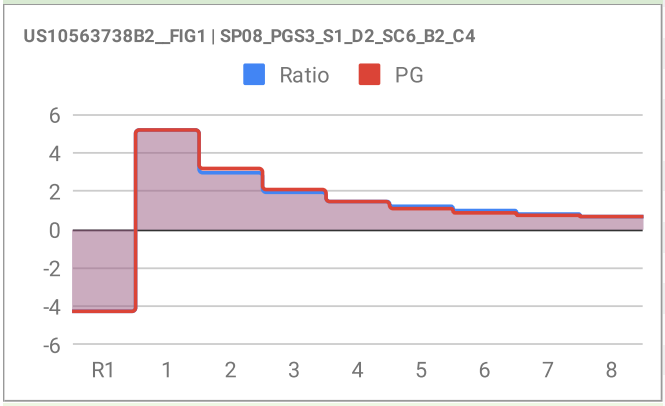

Source: Author.

Figure 71 – Sector 7: PGM Graph link assortment (automatic)

k	N(k)
2	2
3	4
4	3
5	2
6	0
7	0
8	0
9	0
10	0
11	0
12	0

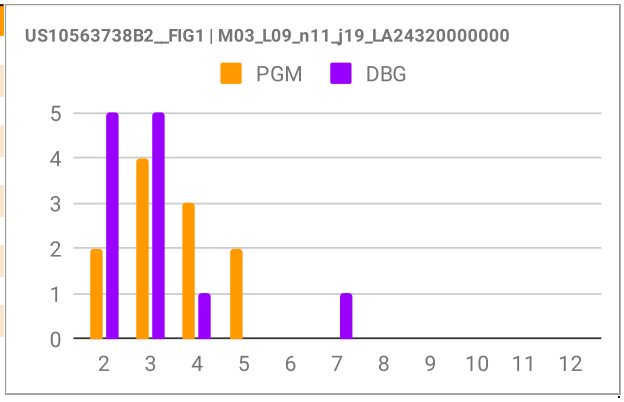

Source: Author.

Figure 72 – Sector 8: PGT Kinematic chain - DBG graph creation (automatic)

DBG		FIG1		TRUE	FD04_L07_Nm1_Nl11_Nr10_Ng07_LA55100100000																										
				LA_DBG	5;5;1;0;0;1;0;0;0;0;0;0			LA_DBG_Tsai	5;5;1;0;0;1;0;0;0;0;0;0																					Link Assortment	
LINKS (v)	TRUE	Nm	Nl	FD	FE	JOINTS (e)	TRUE	Ns	11	Nr	10	TRUE	L	7							GRAPH for ANALYSIS						-			LINKS	JOINTS	ADJ
12	TRUE	1	11	4	3	18		Nd	7	Ng	7	TRUE															0	TRUE	3	TRUE	TRUE	
elementar	Id	15	Links	Label	Id	36	Source	Target	Type	Level	Label	Id	S#	T#	18	edgelist					unique			complete			without G (tree)			12	18	
MJ	1	1	MJ	*MJ*	1	7	**MJ**	**S1**	*R*	*a*		1	*1*	*2*	(1,2),	"1 2 {'Type': 'R', 'Level': 'a', 'Lab	1	2	a	MJ	S1	a	MJ	S1	a	5	10	**2**			
P1R	4	1	S1	*S1*	2	2	**MJ**	**A1**	*R*	*a*		2	*1*	*3*	(1,3),	"1 3 {'Type': 'R', 'Level': 'a', 'Lab	1	3	a	MJ	A1	a	MJ	A1	a	5	15	**3**			
P1S	5	1	A1	*A1*	3	3	**MJ**	**R1**	*R*	*a*		3	*1*	*6*	(1,6),	"1 6 {'Type': 'R', 'Level': 'a', 'Lab	1	6	a	MJ	R1	a	MJ	R1	a	1	4	**4**			
R1	6	1	P1R	*P1R*	4	3	**MJ**	**R2**	*R*	*a*		4	*1*	*8*	(1,8),	"1 8 {'Type': 'R', 'Level': 'a', 'Lab	1	8	a	MJ	R2;R3	a	MJ	R2;R3	a	0	0	**5**			
S1	2	1	P1S	*P1S*	5	3	**MJ**	**S2**	*R*	*a*		5	*1*	*9*	(1,9),	"1 9 {'Type': 'R', 'Level': 'a', 'Lab	1	9	a	MJ	S2	a	MJ	S2	a	0	0	**6**			
A1	3	1	R1	*R1*	6	2	**MJ**	**A2**	*R*	*a*		6	*1*	*10*	(1,10),	"1 10 {'Type': 'R', 'Level': 'a', 'Lal	1	10	a	MJ	A2;A3	a	MJ	A2;A3	a	1	7	**7**			
P2	7	2	P2;P3R	*P2*	7	4	**MJ**	**S3**	*R*	*a*		7	*1*	*12*	(1,12),	"1 12 {'Type': 'R', 'Level': 'a', 'Lal	1	12	a	MJ	S3	a	MJ	S3	a	0	0	**8**			
R2	8	2	R2;R3	*R2*	8	2	**P1R**	**P1S**	*Ge*	*g*		8	*4*	*5*	(4,5),	"4 5 {'Type': 'Ge', 'Level': 'g', 'La	4	5	g	P1R	P1S	g	P1R	A1	b	0	0	**9**			
S2	9	1	S2	*S2*	9	2	**P1R**	**R1**	*Gi*	*g*		9	*4*	*6*	(4,6),	"4 6 {'Type': 'Gi', 'Level': 'g', 'Lab	4	6	g	P1R	R1	g	P1S	A1	c	0	0	**10**			
A2	10	2	A2;A3	*A2*	10	3	**P1R**	**A1**	*R*	*b*		10	*4*	*3*	(3,4),	"4 3 {'Type': 'R', 'Level': 'b', 'Lab	4	3	b	P1R	A1	b	P2;P3R	A2;A3	d	0	0	**11**			
P3R	7	1	P3S	*P3S*	11	3	**P1S**	**S1**	*Ge*	*g*		11	*5*	*2*	(2,5),	"5 2 {'Type': 'Ge', 'Level': 'g', 'La	5	2	g	P1S	S1	g	P3S	A2;A3	e	0	0	**12**			
P3S	11	1	S3	*S3*	12	2	**P1S**	**A1**	*R*	*c*		12	*5*	*3*	(3,5),	"5 3 {'Type': 'R', 'Level': 'c', 'Labe	5	3	c	P1S	A1	c									
R3	8						**P2**	**R2**	*Gi*	*g*		13	*7*	*8*	(7,8),	"7 8 {'Type': 'Gi', 'Level': 'g', 'Lab	7	8	g	P2;P3R	R2;R3	g									
S3	12						**P2**	**A2**	*R*	*d*		14	*7*	*10*	(7,10),	"7 10 {'Type': 'R', 'Level': 'd', 'Lal	7	10	d	P2;P3R	A2;A3	d									
A3	10						**P2**	**S2**	*Ge*	*g*		15	*7*	*9*	(7,9),	"7 9 {'Type': 'Ge', 'Level': 'g', 'La	7	9	g	P2;P3R	S2	g									
							P3R	**P3S**	*Ge*	*g*		16	*7*	*11*	(7,11),	"7 11 {'Type': 'Ge', 'Level': 'g', 'L	7	11	g	P2;P3R	P3S	g									
							P3R	**R3**	*Gi*	*g*		17	*7*	*8*	(7,8),	"7 8 {'Type': 'Gi', 'Level': 'g', 'Lab	11	12	g	P3S	S3	g									
							P3R	**A3**	*R*	*e*		18	*7*	*10*	(7,10),	"7 10 {'Type': 'R', 'Level': 'e', 'Lal	11	10	e	P3S	A2;A3	e									
							P3S	**S3**	*Ge*	*g*		19	*11*	*12*	(11,12),	"11 12 {'Type': 'Ge', 'Level': 'g', 'l															
							P3S	**A3**	*R*	*f*		20	*11*	*10*	(10,11),	"11 10 {'Type': 'R', 'Level': 'f', 'La															

Source: Author.

Figure 73 – Sector 9: Validators checklist (automatic)

CHECKLIST COMPLETE?	
PGT-DOF	TRUE
Links (n)	TRUE
Joints (j)	TRUE
jR	TRUE
jG	TRUE
DBG-DOF	TRUE
Links (v)	TRUE
Joints (e)	TRUE
Nr	TRUE
Ng	TRUE
LINKS	TRUE
JOINTS	TRUE
Commercial?	TRUE
Application	TRUE
Weight (kg)	TRUE
Máx. Torque (N·m)	TRUE
All nodes in graph?	TRUE

Source: Author.

Figure 74 – Sector 10: Dataset summary (automatic) - 1 of 2

DATASET SUMMARY	
PGM INFO	
SOURCE	patent
OWNER	TOYOTA
PATENT	US10563738B2
DATE	2015
MODEL	FIG1
PGM CLASS	M03_L09_n11_j19_LA24320000000
DBG CLASS	FD04_L07_Nm1_Nl11_Nr10_Ng07_LA55100100000
CHECKLIST COMPLETE?	TRUE
PGM_Edges	PGM__US10563738B2__FIG1 = ["1 2 {'Type': 'I', 'Level': 'a', 'Label':
PGM_Nodes	PGM__US10563738B2__FIG1_Nodes = {1: 'F;S1', 2: 'IN;A1', 4: 'P1
DBG_Edges	DBG__US10563738B2__FIG1 = ["1 2 {'Type': 'R', 'Level': 'a', 'Label':
DBG_Nodes	DBG__US10563738B2__FIG1_Nodes = {1: 'MJ', 2: 'S1', 3: 'A1', 4: 'P
Commercial?	FALSE
Longitudinal	FALSE
Transversal	TRUE
Weight (kg)	96
Máx. Torque (N·m)	350
PGM DOFs	3
PGM Loops (L)	9
PGM LINKS (n)	11
PGM JOINTS (j)	19
PGM Revolute pairs (jR)	12
PGM Gear pairs (jG)	7
PGM Redundant circuits (jQ)	2
PGM Virtual joints (jV)	0
PGM Compound links (CL)	5
PGM Maximal degree (p)	8
PGM Link Assortment (LA)	2;4;3;2;0;0;0;0;0;0
PGM LA n2	2
PGM LA n3	4
PGM LA n4	3
PGM LA n5	2
PGM LA n6	0
PGM LA n7	0
PGM LA n8	0
PGM LA n9	0
PGM LA n10	0
PGM LA n11	0
PGM LA n12	0
PGM Complexity Karhula	13

Source: Author.

Figure 75 – Sector 10: Dataset summary (automatic) - 2 of 2

DBG DOFs	**4**		
DBG Loops (L)		7	
DBG LINKS (v)		12	
DBG Number links (Nl)		11	
DBG Hollow Vertices (Nm)		1	
DBG JOINTS (e)		18	
DBG Revolute pairs (Nr)		10	
DBG Gear pairs (Ng)		7	
DBG Solid lines (Ns)		11	
DBG Dashed lines (Nd)		7	
DBG Compound links (CL)		3	
DBG Maximal degree (p)		8	
DBG Link Assortment (LA)	5;5;1;0;0;1;0;0;0;0;0;0		
DBG LA n2		5	
DBG LA n3		5	
DBG LA n4		1	
DBG LA n5		0	
DBG LA n6		0	
DBG LA n7		1	
DBG LA n8		0	
DBG LA n9		0	
DBG LA n10		0	
DBG LA n11		0	
DBG LA n12		0	
PGSs Total	**3**		
Simple PGSs		**1**	
Double PGSs		**2**	
All simple PGSs?	FALSE		
Shifting Couplings (SC)	**6**		
Brakes (B)		**2**	
Clutches (C)		**4**	
Input Clutches		1	
Clutches as Input		0.25	**LOW Input**
All clutches are input?	FALSE		
Active SCs per gear	**2**		
Total Modes		**15**	*total of Combinations (SCs,M-1)*
Used Modes		**9**	*combinations in use*
Modes ratio		**0.60**	*ratio used of total*
Open Actuators		**4**	**HIGH Spin Losses**
Spin Losses		**0.67**	*ratio of total*
Single transition?	TRUE		
GEAR SPECS Check	TRUE		
Gears	TRUE		
Gear Ratios	TRUE		
Gear Shiftings	TRUE		
RWD GEARS	**1**		
RWD Máx. Ratio		-4.254	
FWD GEARS	**8**		
FWD Underdrive Gears		5	*i > 1*
FWD Direct Drive Ratio		1	*i = 1*
FWD Overdrive Gears		2	*i < 1*
FWD Overall Ratio		7.591	
FWD Base ratio change (φ1)		1.096	*1.1 to 1.7 (Naunheimer, 2011)*
FWD Avg Progression Factor (φ2)		1.068	*1.0 to 1.2 (Newman2016)*
FWD φ2 STDEV		0.075	**LOW Dispersion**
FWD φ2 VAR COEF		0.070	**LOW Dispersion**
FWD Reference diff		0.680	
Direct drive?	TRUE		

Source: Author.

Figure 76 – Sector 11: PGM and DBG General validation (automatic)

TRUE	PGM Check
TRUE	DBG Check

Source: Author.

Figure 77 – Sector 12: Topological and Functional classification (automatic)

TOPOLOGY_CLASS	FUNCTIONAL_CLASS
M03_L09_n11_j19_LA24320000000	SP08_PGS3_S1_D2_SC6_B2_C4

Source: Author.

Figure 78 – Sector 13: Unique dataset identifier and version control (automatic)

UNIQUE_ID	DATASET_VERSION
US10563738B2__FIG1	20230618

Source: Author.

Figure 79 – Sector 14: Dataset references (manual)

REFERENCES		
OLD DB	DB-OK/US10563738B2/FIG1	

REFERENCES		
Articles		
Patent	https://worldwide.espacenet.com/patent/search/family/057396365/publicati	
Topology		
Shifting		
Gear Ratios		
Weight		
Torque		
Images	OK	https://drive.google.com/drive/folders/1uRTcu0rgf2D3uGHNd32k4
Videos		

Source: Author.

Figure 80 – Sector 15: PGM Figures (manual)

FIG. 1

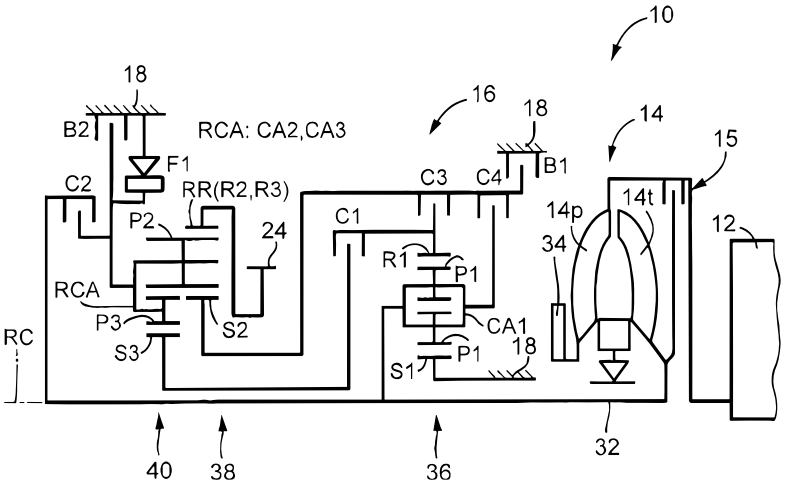

FIG. 2

	ENGAGEMENT OPERATION TABLE					
	C1	C2	C3	C4	B1	B2
1st	○					○
2nd	○				○	
3rd	○		○			
4th	○			○		
5th	○	○				
6th		○		○		
7th		○	○			
8th		○			○	
Rev			○			○

Source: Author.

A.2 PGM COMPLETE DATABASE

The complete database employed for this thesis is comprised of 159 PGMs of automatic transmission. For each model is presented the identification, topological, and functional data, besides the mechanism functional diagram, the PGM graph, and the DBG graph. Following, the instances are presented and identified by their respective *UNIQUE_ID*.

Table 52 – AISIN_TOYOTA__AT_6_speed_L dataset information.

IDENTIFICATION		TOPOLOGY					GEARS SPECS		
UNIQUE_ID	**AISIN_TOYOTA__AT_6_speed_L**	**PGS**	**S/D**	**+/-**	**CLs**	**SCs**	**GEARS**	**Ratios**	**Engaged SCs**
Source	industry	1	S	F	F;S1	B1: F;S2	R1		
Owner	AISIN_TOYOTA	2	S	IN	IN;R1	B2: F;A3	1		
Patent		3	D	OUT	P2;P3R	C1: A1;S2	2		
Date					OUT;R2;R3	C2: A1;S3	3		
Model	AT_6_speed_L				A2;A3	C3: IN;A3	4		
Commercial?	true						5		
Longitudinal	true						6		
Transversal	false								
Weight (kg)									
Máx. Torque (N·m)									

Figure 81 – AISIN_TOYOTA__AT_6_speed_L representations.

(a) Functional diagram

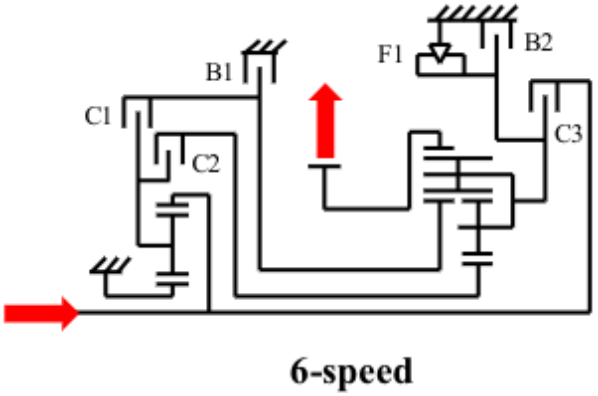

(b) PGM Graph

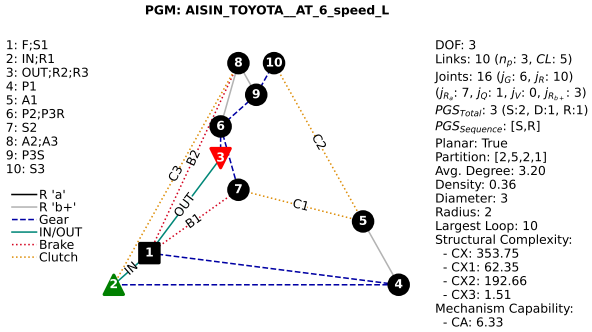

(c) DBG Graph

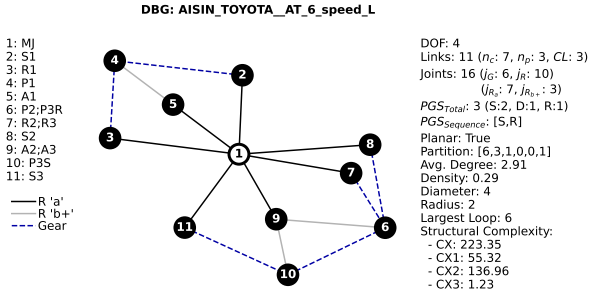

Table 53 – AISIN_TOYOTA__AT_8_speed_L dataset information.

IDENTIFICATION		TOPOLOGY					GEARS SPECS		
UNIQUE_ID	**AISIN_TOYOTA__AT_8_speed_L**	**PGS**	**S/D**	**+/-**	**CLs**	**SCs**	**GEARS**	**Ratios**	**Engaged SCs**
Source	industry	1	D	F	F;S1	B1-B1: F;S2	R1	-2.18	B2-B2;C1-C4
Owner	AISIN_TOYOTA	2	S	IN	IN;A1	B2-B2: F;A3	1	4.6	B2-B2;C3-C1
Patent		3	D	OUT	P2;P3R	C1-C4: S2;A1	2	2.72	B1-B1;C3-C1
Date					OUT;R2;R3	C2-C3: S2;R1	3	1.86	C2-C3;C3-C1
Model	AT_8_speed_L				A2;A3	C3-C1: R1;S3	4	1.46	C1-C4;C3-C1
Commercial?	true					C4-C2: IN;A3	5	1.23	C3-C1;C4-C2
Longitudinal	true						6	1	C1-C4;C4-C2
Transversal	false						7	0.82	C2-C3;C4-C2
Weight (kg)							8	0.69	B1-B1;C4-C2
Máx. Torque (N·m)									

Figure 82 – AISIN_TOYOTA__AT_8_speed_L representations.

(a) Functional diagram

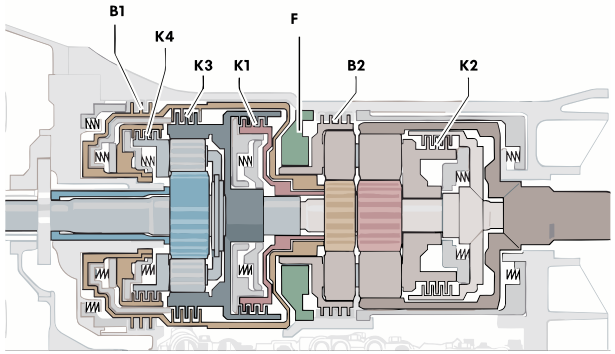

(b) PGM Graph

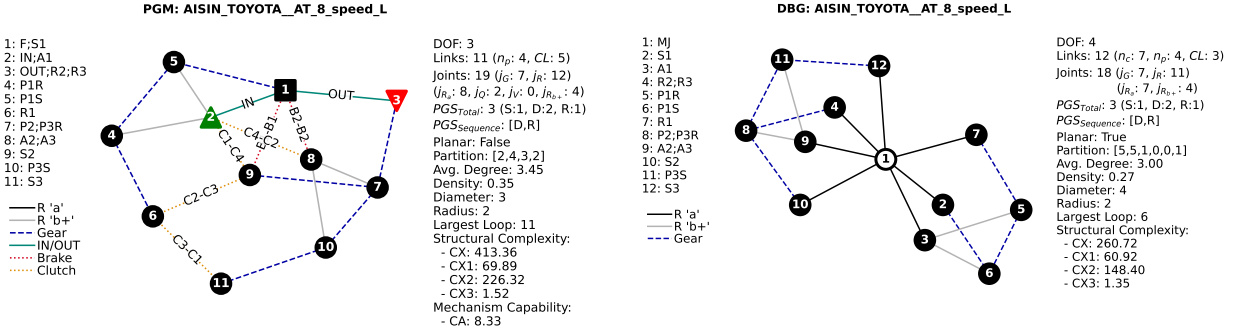

(c) DBG Graph

Table 54 – AISIN_TOYOTA__AT_10_speed_L dataset information.

IDENTIFICATION		TOPOLOGY					GEARS SPECS		
UNIQUE_ID	**AISIN_TOYOTA__AT_10_speed_L**	**PGS**	**S/D**	**+/-**	**CLs**	**SCs**	**GEARS**	**Ratios**	**Engaged SCs**
Source	industry	1	S	F	IN;A1;A2;A4	B1-B-1: F;S1	R1	-5.17	B2-B-2;C2-C-2;C4-C-3
Owner	AISIN_TOYOTA	2	D	IN	P1;P2R	B2-B-2: F;R3	1	4.923	B2-B-2;C1-C-1;C2-C-2
Patent		3	S	OUT	R1;R2	C1-C-1: R1;S3	2	3.153	B1-B-1;B2-B-2;C1-C-1
Date		4	S		S3;S4	C2-C-2: S2;S3	3	2.349	B1-B-1;B2-B-2;C2-C-2
Model	AT_10_speed_L				OUT;A3	C3-C-4: A3;R4	4	1.879	B1-B-1;B2-B-2;C3-C-4
Commercial?	true					C4-C-3: R1;R3	5	1.462	B1-B-1;C2-C-2;C3-C-4
Longitudinal	true						6	1.193	B1-B-1;C1-C-1;C3-C-4
Transversal	false						7	1	C1-C-1;C3-C-4;C4-C-3
Weight (kg)							8	0.792	B1-B-1;C3-C-4;C4-C-3
Máx. Torque (N·m)							9	0.64	B1-B-1;C1-C-1;C4-C-3
							10	0.598	B1-B-1;C2-C-2;C4-C-3

Figure 83 – AISIN_TOYOTA__AT_10_speed_L representations.

(a) Functional diagram

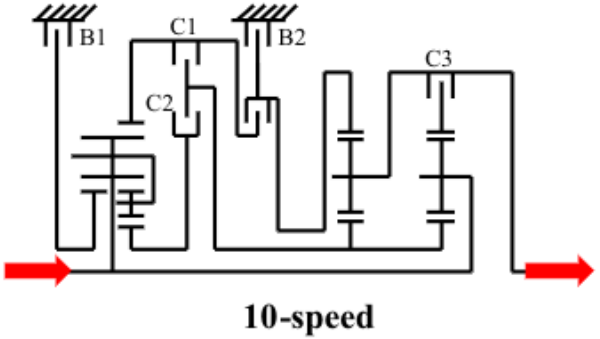

(b) PGM Graph

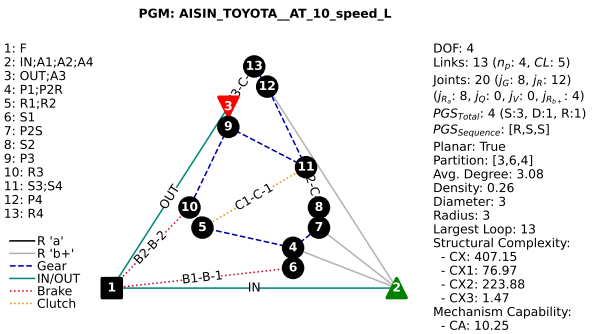

(c) DBG Graph

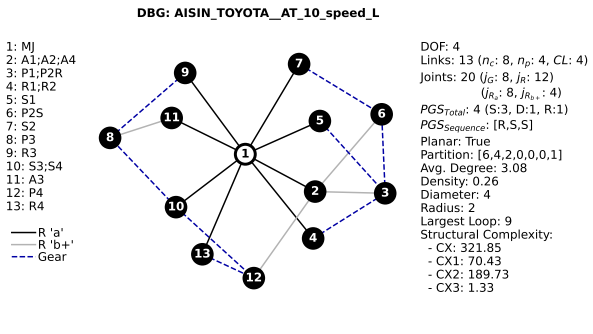

Table 55 – AISIN_TOYOTA__AT_6_speed_FT dataset information.

IDENTIFICATION		TOPOLOGY					GEARS SPECS		
UNIQUE_ID	**AISIN_TOYOTA__AT_6_speed_FT**	**PGS**	**S/D**	**+/-**	**CLs**	**SCs**	**GEARS**	**Ratios**	**Engaged SCs**
Source	industry	1	S	F	F;S1	B1: F;S2	R1	-3.394	B2;C1
Owner	AISIN_TOYOTA	2	S	IN	IN;R1	B2: F;A2	1	4.044	B2;C2
Patent		3	D	OUT	P2;P3R	C1: A1;S2	2	2.37	B1;C2
Date					OUT;R2;R3	C2: A1;S3	3	1.556	C1;C2
Model	AT_6_speed_FT				A2;A3	C3: IN;A2	4	1.159	C2;C3
Commercial?	true						5	0.852	C1;C3
Longitudinal	false						6	0.672	B1;C3
Transversal	true								
Weight (kg)									
Máx. Torque (N·m)									

Figure 84 – AISIN_TOYOTA__AT_6_speed_FT representations.

(a) Functional diagram

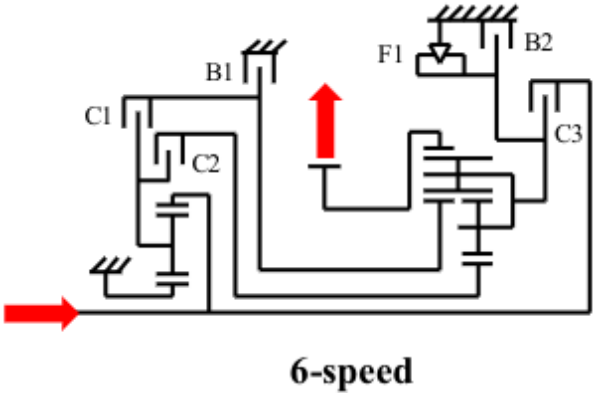

(b) PGM Graph

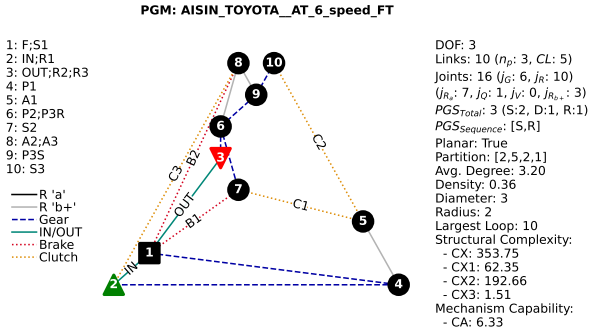

(c) DBG Graph

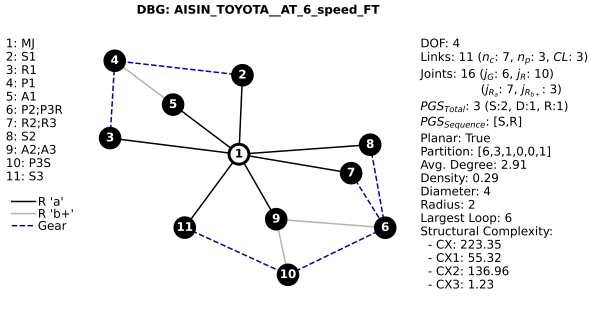

Table 56 – AISIN_TOYOTA__AT_8_speed_FT dataset information.

IDENTIFICATION		TOPOLOGY					GEARS SPECS		
UNIQUE_ID	**AISIN_TOYOTA__AT_8_speed_FT**	**PGS**	**S/D**	**+/-**	**CLs**	**SCs**	**GEARS**	**Ratios**	**Engaged SCs**
Source	industry	1	D	F	F;S1	B1-B-1: F;S2	R1	-4.221	B2-B-2;C1-C-3
Owner	AISIN_TOYOTA	2	S	IN	IN;A1	B2-B-2: F;A2	1	5.2	B2-B-2;C2-C-1
Patent		3	D	OUT	P2;P3R	C1-C-3: R1;S2	2	2.971	B1-B-1;C2-C-1
Date					OUT;R2;R3	C2-C-1: R1;S3	3	1.95	C1-C-3;C2-C-1
Model	AT_8_speed_FT				A2;A3	C3-C-2: IN;A2	4	1.47	C2-C-1;C4-C-4
Commercial?	true					C4-C-4: A1;S2	5	1.224	C2-C-1;C3-C-2
Longitudinal	false						6	1	C3-C-2;C4-C-4
Transversal	true						7	0.818	C1-C-3;C3-C-2
Weight (kg)							8	0.686	B1-B-1;C3-C-2
Máx. Torque (N·m)									

Figure 85 – AISIN_TOYOTA__AT_8_speed_FT representations.

(a) Functional diagram

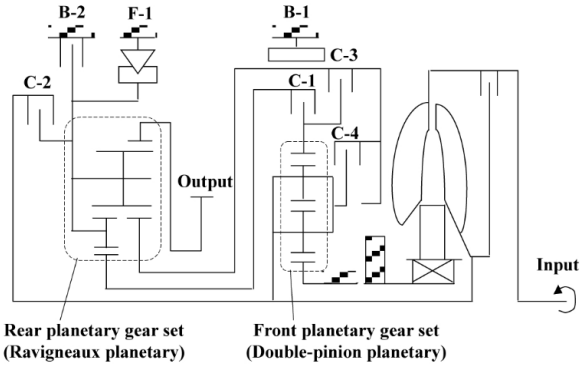

Fig. 2. Gear train schematic

(b) PGM Graph

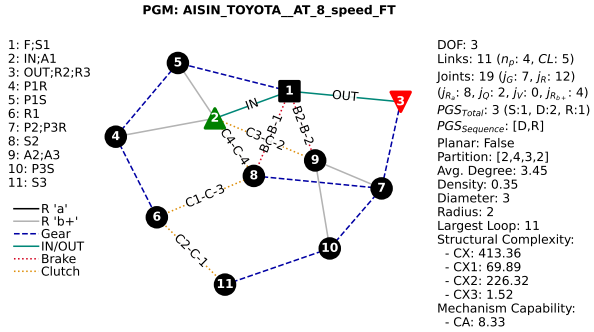

(c) DBG Graph

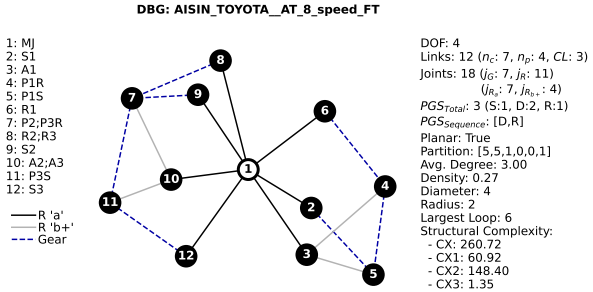

Table 57 – CN100480537C__FIG1 dataset information.

IDENTIFICATION		TOPOLOGY					GEARS SPECS		
UNIQUE_ID	**CN100480537C__FIG1**	**PGS**	**S/D**	**+/-**	**CLs**	**SCs**	**GEARS**	**Ratios**	**Engaged SCs**
Source	industry	1	S	F	F;S1	C1: A1;S3	R		C3;B1
Owner	HYUNDAI	2	S	IN	IN;R1	C2: A1;S2	1		C1;B1
Patent	CN100480537C	3	D	OUT	P2;P3R	C3: IN;A3	2		C1;B2
Date	2021				A2;A3	B1: F;A2	3		C2;B2
Model	FIG1				OUT;R2;R3	B2: F;S2	4		C1;C2
Commercial?	false						5		C2;C3
Longitudinal	true						6		C1;C3
Transversal	false								
Weight (kg)									
Máx. Torque (N·m)									

Figure 86 – CN100480537C__FIG1 representations.

(a) Functional diagram

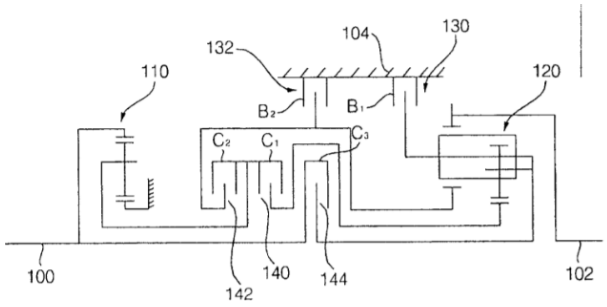

图1

(b) PGM Graph

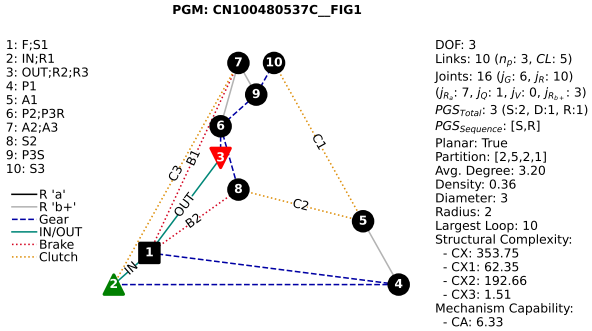

(c) DBG Graph

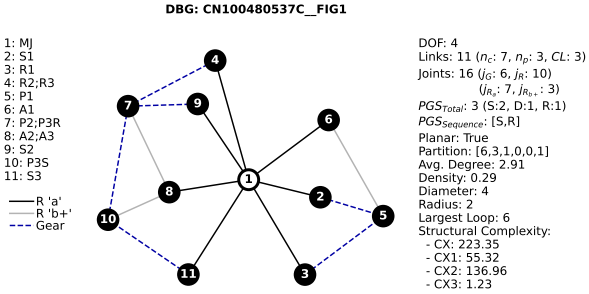

Table 58 – CN100480537C__FIG3 dataset information.

IDENTIFICATION		TOPOLOGY					GEARS SPECS		
UNIQUE_ID	**CN100480537C__FIG3**	**PGS**	**S/D**	**+/-**	**CLs**	**SCs**	**GEARS**	**Ratios**	**Engaged SCs**
Source	patent	1	D	F	F;S1	C1: R1;S2	R		C3;B1
Owner	HYUNDAI	2	S	IN	IN;A1	C2: R1;S3	1		C1;B1
Patent	CN100480537C	3	S	OUT	P2;P3	C3: A1;R2	2		C2;B1
Date	2021				OUT;A2;A3	B1: F;R3	3		C1;B2
Model	FIG3					B2: F;R2	4		C2;B2
Commercial?	false						5		C1;C2
Longitudinal	true						6		C2;C3
Transversal	false						7		C1;C3
Weight (kg)									
Máx. Torque (N·m)									

Figure 87 – CN100480537C__FIG3 representations.

(a) Functional diagram

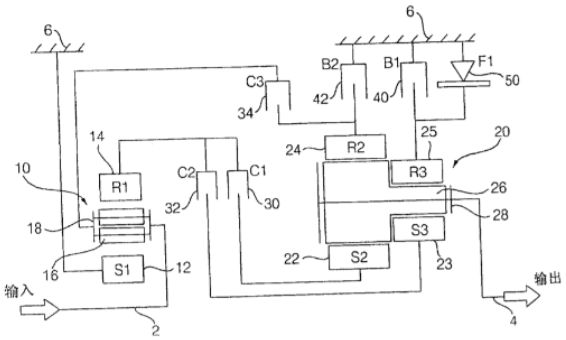

图3

(b) PGM Graph

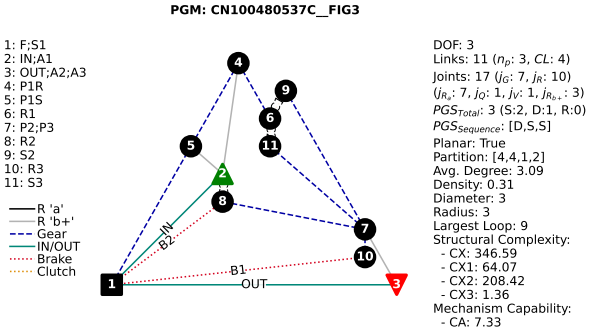

(c) DBG Graph

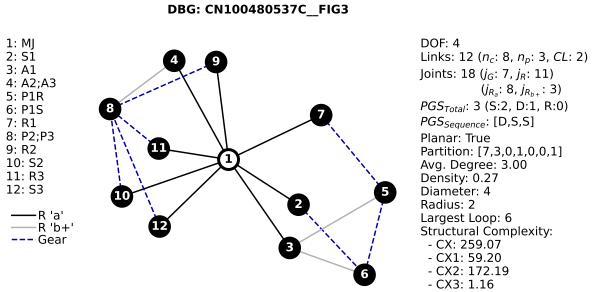

Table 59 – CN101036001A__FIG1 dataset information.

IDENTIFICATION		TOPOLOGY					GEARS SPECS		
UNIQUE_ID	**CN101036001A__FIG1**	**PGS**	**S/D**	**+/-**	**CLs**	**SCs**	**GEARS**	**Ratios**	**Engaged SCs**
Source	patent	1	D	F	F;S1	C1-A: R1;S3	R2		B2-D;B3-F
Owner	ZF	2	S	IN	IN;A1	C2-B: R1;S2	R1		C2-B;B2-D
Patent	CN101036001A	3	D	OUT	P2;P3R	B1-C: F;S2	1		C1-A;B2-D
Date	2004				OUT;R2;R3	B2-D: F;A2	2		C1-A;B1-C
Model	FIG1				A2;A3	C3-E: IN;A2	3		C1-A;C2-B
Commercial?	false					B3-F: IN;S2	4		C1-A;B3-F
Longitudinal	true						5		C1-A;C3-E
Transversal	false						6		C3-E;B3-F
Weight (kg)							7		C2-B;C3-E
Máx. Torque (N·m)							8		B1-C;C3-E

Figure 88 – CN101036001A__FIG1 representations.

(a) Functional diagram

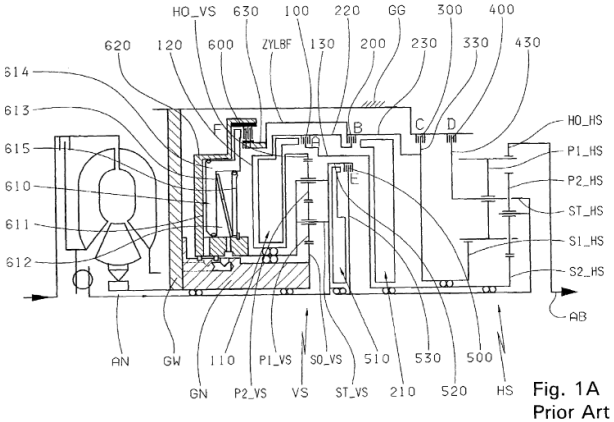

Fig. 1A
Prior Art

(b) PGM Graph

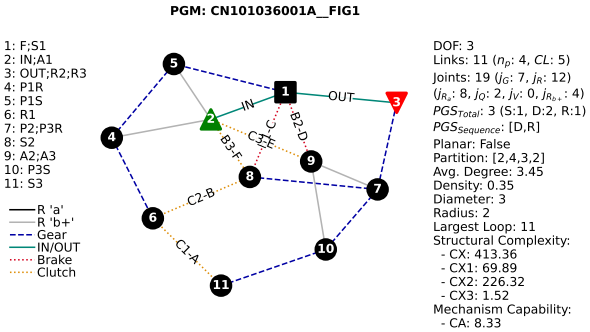

(c) DBG Graph

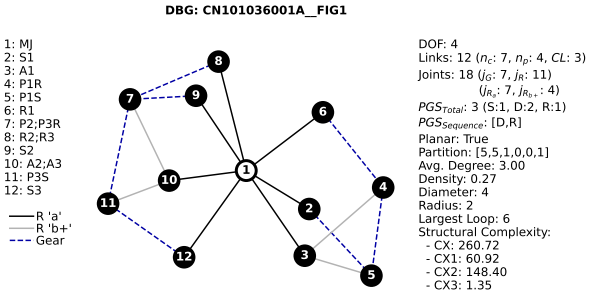

Table 60 – CN113503344A__FIG1 dataset information.

IDENTIFICATION		TOPOLOGY					GEARS SPECS		
UNIQUE_ID	**CN113503344A__FIG1**	**PGS**	**S/D**	**+/-**	**CLs**	**SCs**	**GEARS**	**Ratios**	**Engaged SCs**
Source	patent	1	S	F	F;S1	C1: A1;S3	R1		C3;B2
Owner	GRC AUTOMOBILE	2	S	IN	IN;R1	C2: IN;A2	1		C1;B2
Patent	CN113503344A	3	D	OUT	P2;P3R	C3: A1;S2	2		C1;B1
Date	2021				OUT;R2	C4: IN;R3	3		C1;C3
Model	FIG1				A2;A3	B1: F;S2	4		C1;C2
Commercial?	false					B2: F;A2	5		C1;C4
Longitudinal	false						6		C2;C4
Transversal	true						7		C3;C4
Weight (kg)							8		C4;B1
Máx. Torque (N·m)							9		C4;B2

Figure 89 – CN113503344A__FIG1 representations.

(a) Functional diagram

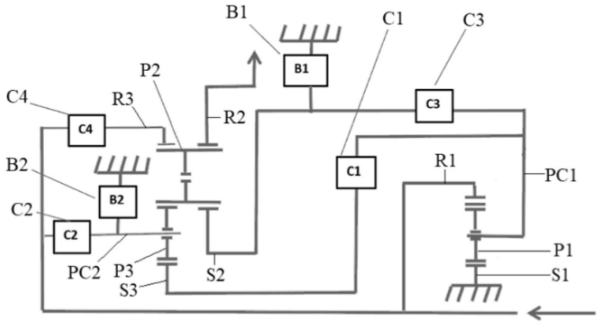

(b) PGM Graph

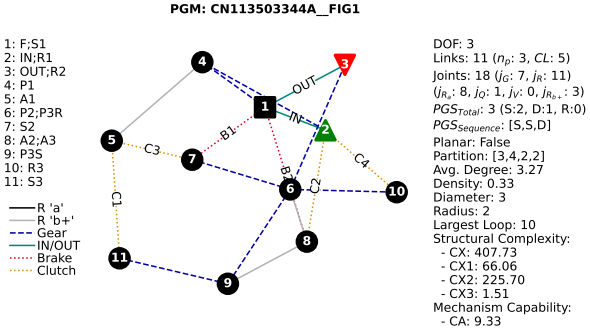

(c) DBG Graph

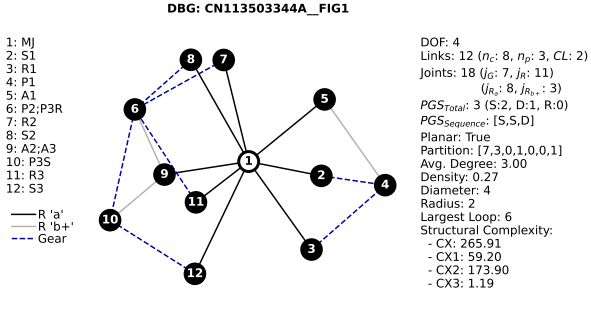

Table 61 – CN113503347A__FIG1 dataset information.

IDENTIFICATION		TOPOLOGY					GEARS SPECS		
UNIQUE_ID	**CN113503347A__FIG1**	**PGS**	**S/D**	**+/-**	**CLs**	**SCs**	**GEARS**	**Ratios**	**Engaged SCs**
Source	patent	1	D	F	F;S1	C1: R1;S3	R2		C4;B2
Owner	GRC AUTOMOBILE	2	S	IN	IN;A1	C2: IN;A2	R1		C3;B2
Patent	CN113503347A	3	D	OUT	P2;P3R	C3: R1;S2	1		C1;B2
Date	2021				OUT;R2	C4: A1;S2	2		C1;B1
Model	FIG1				A2;A3	C5: IN;R3	3		C1;C3
Commercial?	false					B1: F;S2	4		C1;C4
Longitudinal	false					B2: F;A2	5		C1;C2
Transversal	true						6		C1;C5
Weight (kg)							7		C2;C5
Máx. Torque (N·m)							8		C3;C5
							9		C5;B1
							10		C5;B2

Figure 90 – CN113503347A__FIG1 representations.

(a) Functional diagram

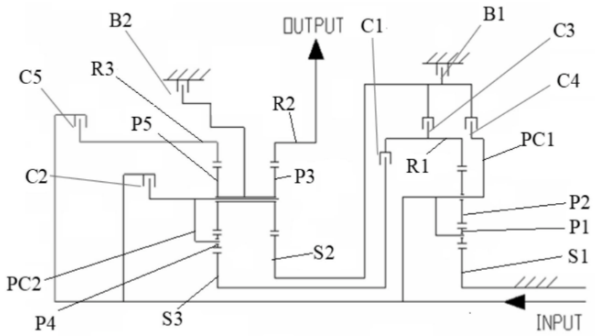

图1

(b) PGM Graph

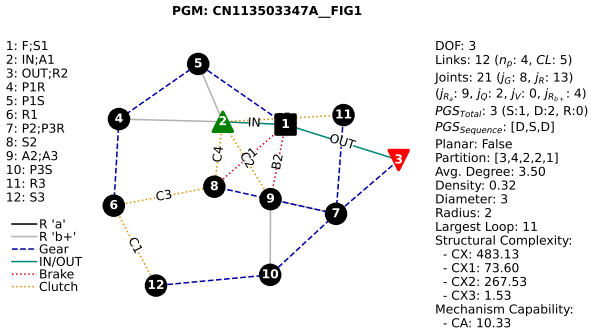

(c) DBG Graph

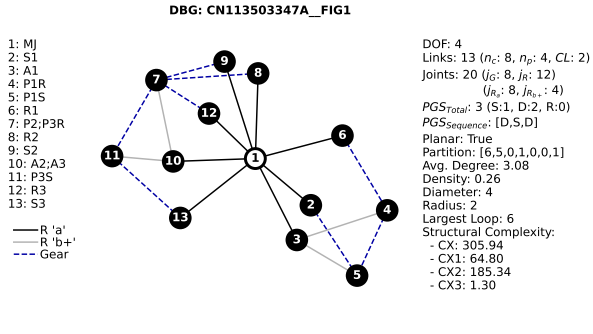

Table 62 – CN114810958A__FIG1 dataset information.

IDENTIFICATION		TOPOLOGY					GEARS SPECS		
UNIQUE_ID	**CN114810958A__FIG1**	**PGS**	**S/D**	**+/-**	**CLs**	**SCs**	**GEARS**	**Ratios**	**Engaged SCs**
Source	patent	1	S	F	IN;A2	B1: F;S1	R1	-4.179	B1;B2;C3
Owner	CAI FANGXING	2	S	IN	S1;S2	B2: F;R1	1	5.2	B1;B2;C1
Patent	CN114810958A	3	S	OUT	A1;R3;R4	C1: IN;S4	2	3.343	B1;B2;C2
Date	2022	4	S		OUT;A3;A4	C2: R2;S4	3	2.167	B2;C1;C2
Model	FIG1					C3: R2;S3	4	1.714	B2;C2;C3
Commercial?	false						5	1.297	B2;C1;C3
Longitudinal	true						6	1	C1;C2;C3
Transversal	true						7	0.834	B1;C1;C3
Weight (kg)							8	0.643	B1;C2;C3
Máx. Torque (N·m)									

Figure 91 – CN114810958A__FIG1 representations.

(a) Functional diagram

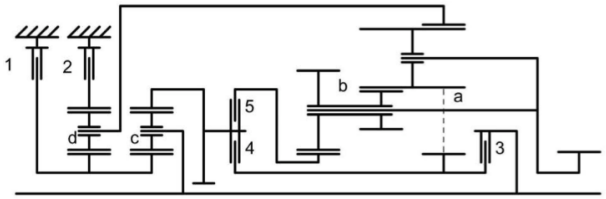

(b) PGM Graph

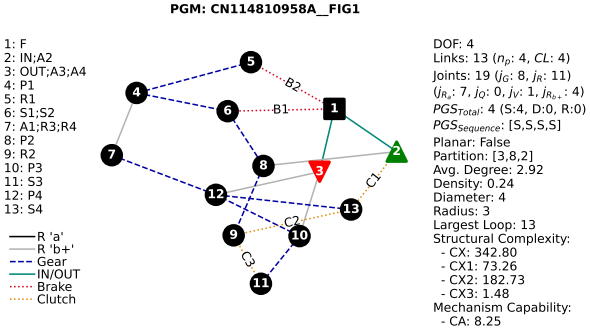

(c) DBG Graph

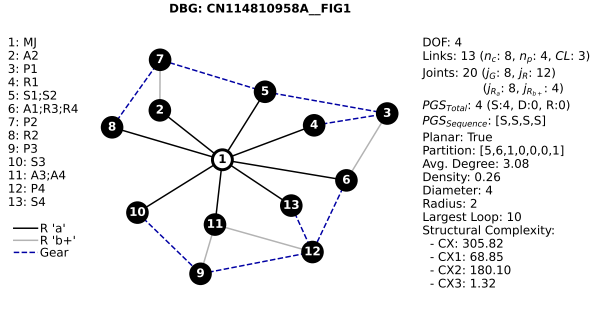

Table 63 – JP3519037B2__7GTronic dataset information.

IDENTIFICATION		TOPOLOGY					GEARS SPECS		
UNIQUE_ID	**JP3519037B2__7GTronic**	**PGS**	**S/D**	**+/-**	**CLs**	**SCs**	**GEARS**	**Ratios**	**Engaged SCs**
Source	industry	1	D	F	IN;R2	B1-B1: F;S1	R2	-2.23	B1-B1;B3-BR;C3-C3
Owner	DAIMLER	2	S	IN	P1S;P2	B2-B3: F;R1	R1	-3.42	B2-B3;B3-BR;C3-C3
Patent	JP3519037B2	3	S	OUT	S1;S2	B3-BR: F;A4	1	4.377	B2-B3;B4-B2;C3-C3
Date	1999	4	S		A1;A2;R4	B4-B2: F;S3	2	2.859	B1-B1;B4-B2;C3-C3
Model	7GTronic				R3;A4	C1-C1: S1;R1	3	1.921	B4-B2;C1-C1;C3-C3
Commercial?	true				OUT;A3	C2-C2: R2;R3	4	1.368	B4-B2;C1-C1;C2-C2
Longitudinal	true					C3-C3: S3;S4	5	1	C1-C1;C2-C2;C3-C3
Transversal	false						6	0.821	B1-B1;C2-C2;C3-C3
Weight (kg)	82						7	0.728	B2-B3;C2-C2;C3-C3
Máx. Torque (N·m)	700								

Figure 92 – JP3519037B2__7GTronic representations.

(a) Functional diagram

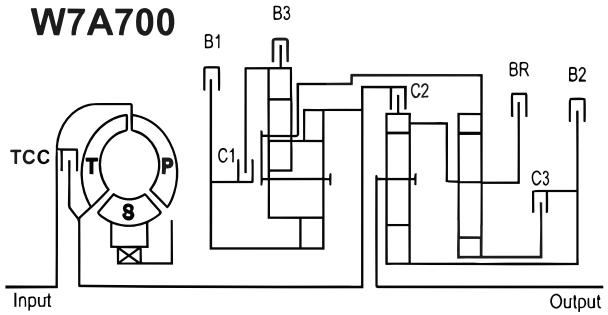

(b) PGM Graph

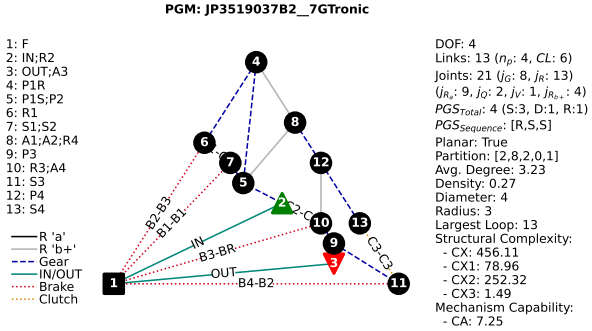

(c) DBG Graph

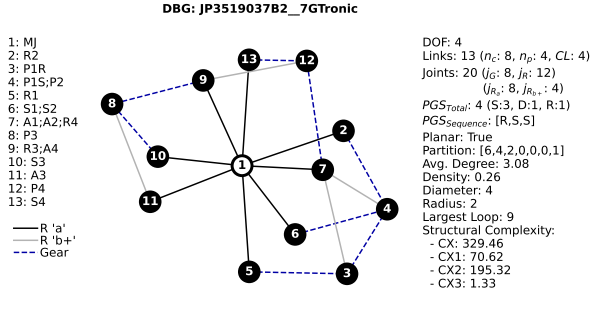

Table 64 – CN105229337B__9GTronic dataset information.

IDENTIFICATION		TOPOLOGY					GEARS SPECS		
UNIQUE_ID	**CN105229337B__9GTronic**	**PGS**	**S/D**	**+/-**	**CLs**	**SCs**	**GEARS**	**Ratios**	**Engaged SCs**
Source	industry	1	S	F	IN;S1;A4	B1-C: F;A1	R1	-4.8	B1-C;B2-A;B3-B
Owner	DAIMLER	2	S	IN	R1;A2	B2-A: F;S2	1	5.35	B2-A;B3-B;C2-E
Patent	CN105229337B	3	S	OUT	R2;S3;S4	B3-B: F;R3	2	3.24	B3-B;C1-F;C2-E
Date	2013	4	S		OUT;A3	C1-F: IN;A1	3	2.25	B2-A;B3-B;C1-F
Model	9GTronic					C2-E: A1;R2	4	1.64	B2-A;B3-B;C3-D
Commercial?	true					C3-D: A3;R4	5	1.21	B2-A;C1-F;C3-D
Longitudinal	true						6	1	C1-F;C2-E;C3-D
Transversal	false						7	0.87	B2-A;C2-E;C3-D
Weight (kg)	94.8						8	0.72	B1-C;C2-E;C3-D
Máx. Torque (N·m)	700						9	0.6	B1-C;B2-A;C3-D

Figure 93 – CN105229337B__9GTronic representations.

(a) Functional diagram

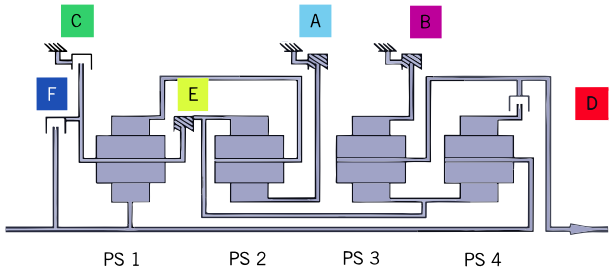

(b) PGM Graph

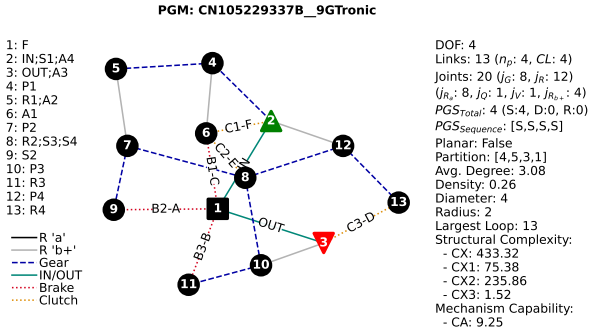

DOF: 4
Links: 13 (n_p: 4, CL: 4)
Joints: 20 (j_G: 8, j_R: 12)
(j_{R_a}: 8, j_O: 1, j_V: 1, $j_{R_{a+}}$: 4)
PGS_{Total}: 4 (S:4, D:0, R:0)
$PGS_{Sequence}$: [S,S,S,S]
Planar: False
Partition: [4,5,3,1]
Avg. Degree: 3.08
Density: 0.26
Diameter: 4
Radius: 2
Largest Loop: 13
Structural Complexity:
- CX: 433.32
- CX1: 75.38
- CX2: 235.86
- CX3: 1.52
Mechanism Capability:
- CA: 9.25

(c) DBG Graph

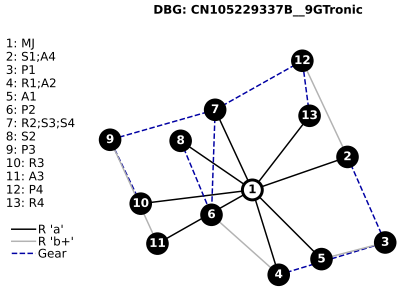

DOF: 4
Links: 13 (n_c: 8, n_p: 4, CL: 3)
Joints: 20 (j_G: 8, j_R: 12)
(j_{R_a}: 8, $j_{R_{a+}}$: 4)
PGS_{Total}: 4 (S:4, D:0, R:0)
$PGS_{Sequence}$: [S,S,S,S]
Planar: True
Partition: [5,6,1,0,0,0,1]
Avg. Degree: 3.08
Density: 0.26
Diameter: 4
Radius: 2
Largest Loop: 10
Structural Complexity:
- CX: 322.78
- CX1: 69.05
- CX2: 189.47
- CX3: 1.34

Table 65 – EP2655929B1__FIG1 dataset information.

IDENTIFICATION		TOPOLOGY					GEARS SPECS		
UNIQUE_ID	**EP2655929B1__FIG1**	**PGS**	**S/D**	**+/-**	**CLs**	**SCs**	**GEARS**	**Ratios**	**Engaged SCs**
Source	patent	1	S	F	A1;R3	B1: F;S1	R	-1	C1;C2;C3
Owner	ZF	2	S	IN	R1;R2	B2: F;S3	1	2.228	B1;B2;C3
Patent	EP2655929B1	3	S	OUT	IN;A2	C1: R1;A3	2	1.882	B1;B2;C2
Date	2020				OUT;A3	C2: S1;S2	3	1.555	B2;C2;C3
Model	FIG1					C3: A1;S2	4	1.346	B2;C1;C2
Commercial?	false						5	1.123	B2;C1;C3
Longitudinal	true						6	0.921	B1;C1;C3
Transversal	false						7	0.778	B1;C1;C2
Weight (kg)									
Máx. Torque (N·m)									

Figure 94 – EP2655929B1__FIG1 representations.

(a) Functional diagram

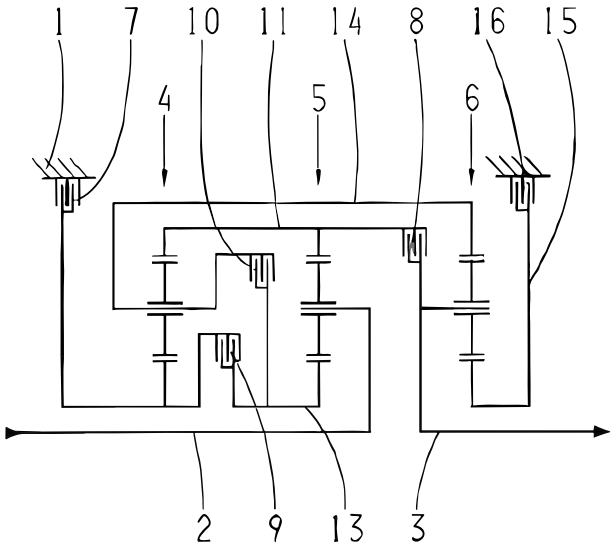

(b) PGM Graph

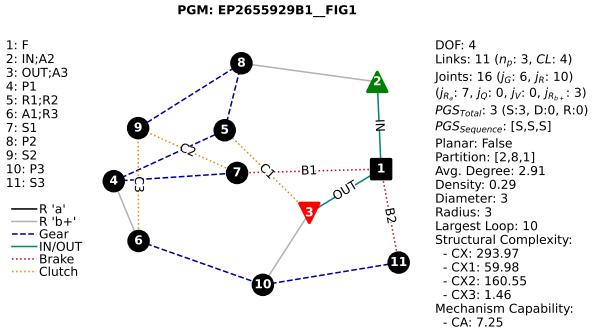

(c) DBG Graph

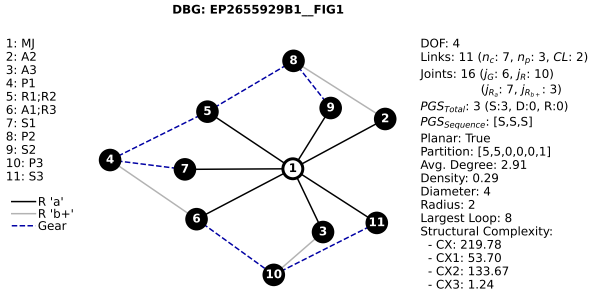

Table 66 – EP2655929B1__FIG5 dataset information.

IDENTIFICATION		TOPOLOGY					GEARS SPECS		
UNIQUE_ID	**EP2655929B1__FIG5**	**PGS**	**S/D**	**+/-**	**CLs**	**SCs**	**GEARS**	**Ratios**	**Engaged SCs**
Source	patent	1	S	F	A1;R3	B1: F;S1	R	-1	C1;C2;C3
Owner	ZF	2	S	IN	R1;R2	B2: F;S3	1	2.228	B1;B2;C3
Patent	EP2655929B1	3	S	OUT	IN;A2	C1: R1;A3	2	1.882	B1;B2;C2
Date	2020				OUT;A3	C2: S1;S2	3	1.555	B2;C2;C3
Model	FIG5					C3: A1;S2	4	1.346	B2;C1;C2
Commercial?	false					C4: A1;A2	5	1.123	B2;C1;C3
Longitudinal	true						6	0.921	B1;C1;C3
Transversal	false						7	0.778	B1;C1;C2
Weight (kg)							8	0.643	B1;C1;C4
Máx. Torque (N·m)									

Figure 95 – EP2655929B1__FIG5 representations.

(a) Functional diagram

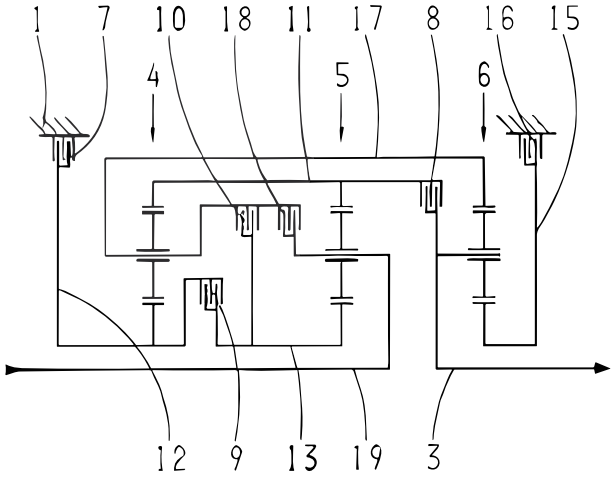

(b) PGM Graph

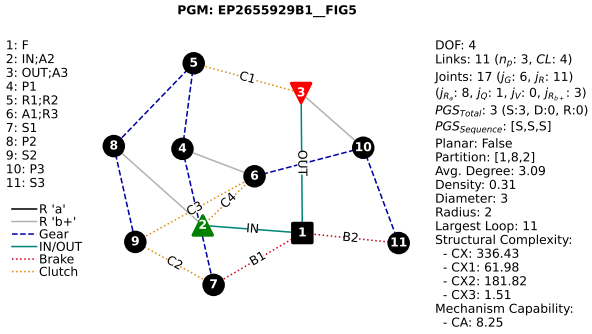

(c) DBG Graph

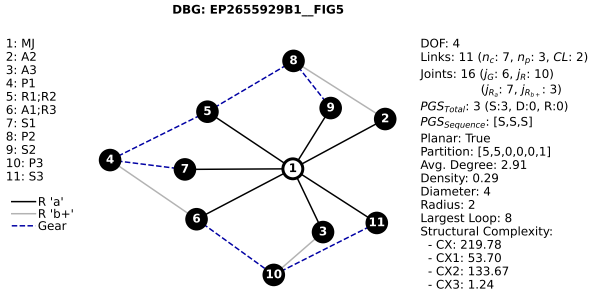

Table 67 – FORD__AT_8_speed_FT_8F24 dataset information.

IDENTIFICATION		TOPOLOGY					GEARS SPECS		
UNIQUE_ID	**FORD__AT_8_speed_FT_8F24**	**PGS**	**S/D**	**+/-**	**CLs**	**SCs**	**GEARS**	**Ratios**	**Engaged SCs**
Source	industry	1	S	F	IN;S2	B1-A: F;S1	R1	-4.293	B2-D;C1-B
Owner	FORD	2	S	IN	R1;A2;R4	B2-D: F;A3	1	5.324	B1-A;B2-D
Patent		3	S	OUT	OUT;A1;R3	B3-F: F;S3	2	3.417	B1-A;B3-F
Date	2018	4	S		R2;A3	B4-C: F;S4	3	2.645	B1-A;B4-C
Model	AT_8_speed_FT_8F24				S3;A4	C1-B: IN;S4	4	2.036	B1-A;C1-B
Commercial?	true					C2-E: IN;R4	5	1.42	B1-A;C2-E
Longitudinal	false						6	1	C1-B;C2-E
Transversal	true						7	0.864	B4-C;C2-E
Weight (kg)							8	0.694	B3-F;C2-E
Máx. Torque (N·m)									

Figure 96 – FORD__AT_8_speed_FT_8F24 representations.

(a) Functional diagram

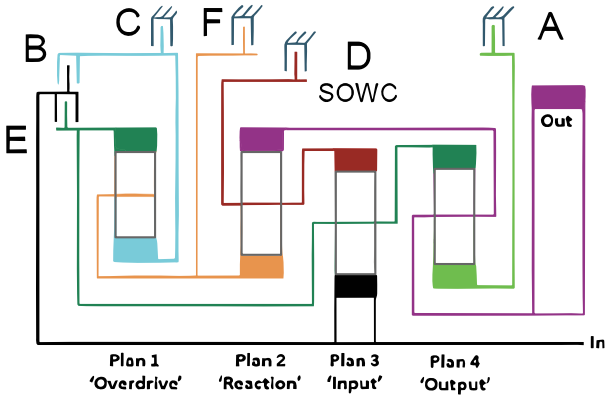

(b) PGM Graph

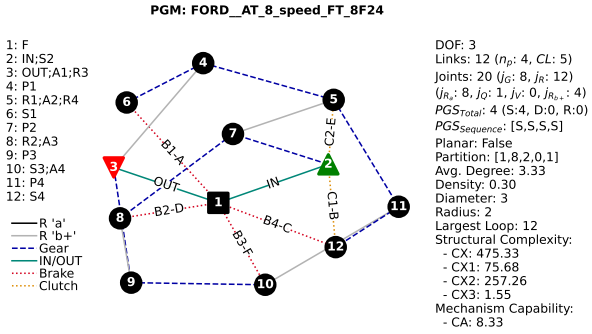

(c) DBG Graph

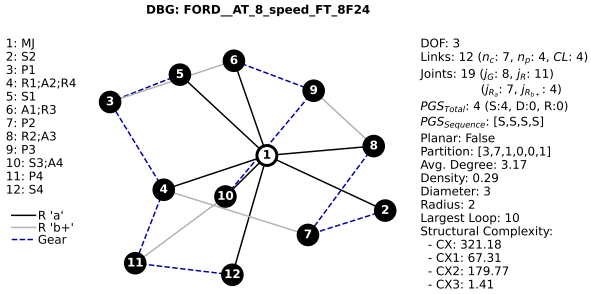

Table 68 – FORD__AT_8_speed_FT_8F35 dataset information.

IDENTIFICATION		TOPOLOGY					GEARS SPECS		
UNIQUE_ID	**FORD__AT_8_speed_FT_8F35**	**PGS**	**S/D**	**+/-**	**CLs**	**SCs**	**GEARS**	**Ratios**	**Engaged SCs**
Source	industry	1	S	F	IN;S2	B1-A: F;S1	R1	-2.88	C1-B;B4-D
Owner	FORD	2	S	IN	R1;A2	B2-F: F;S4	1	4.48	B1-A;B4-D
Patent		3	S	OUT	OUT;A1;R3	B3-C: F;S3	2	3.15	B1-A;B2-F
Date	2018	4	S	-R4	R2;A3;A4	C1-B: IN;S3	3	2.87	B1-A;B3-C
Model	AT_8_speed_FT_8F35				P3;P4	C2-E: IN;A3	4	1.84	B1-A;C1-B
Commercial?	true					B4-D: F;A4	5	1.41	B1-A;C2-E
Longitudinal	false						6	1	C1-B;C2-E
Transversal	true						7	0.74	B3-C;C2-E
Weight (kg)							8	0.62	B2-F;C2-E
Máx. Torque (N·m)									

Figure 97 – FORD__AT_8_speed_FT_8F35 representations.

(a) Functional diagram

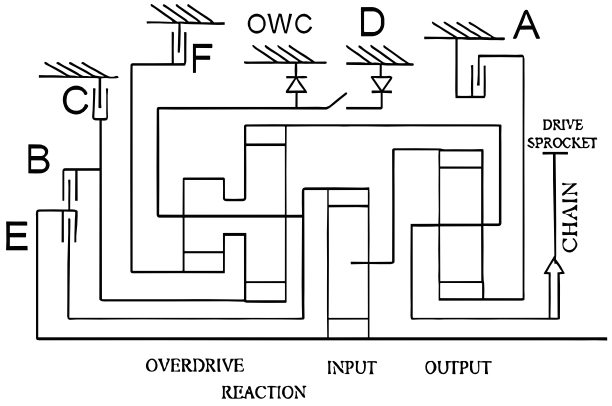

(b) PGM Graph

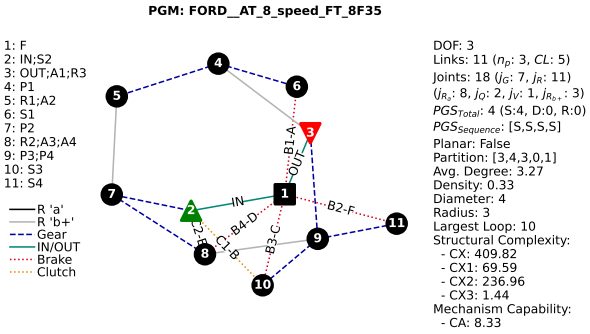

(c) DBG Graph

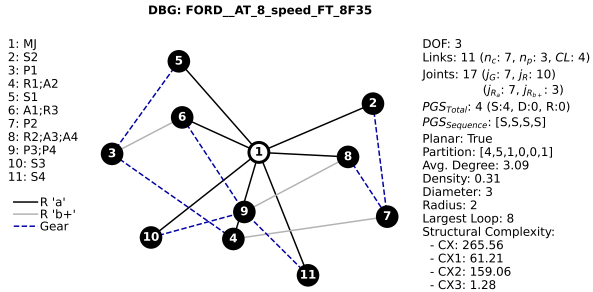

Table 69 – FORD__AT_8_speed_FT_8F57 dataset information.

IDENTIFICATION		TOPOLOGY					GEARS SPECS		
UNIQUE_ID	**FORD__AT_8_speed_FT_8F57**	**PGS**	**S/D**	**+/-**	**CLs**	**SCs**	**GEARS**	**Ratios**	**Engaged SCs**
Source	industry	1	S	F	IN;S2	B1-A: F;S1	R1	-2.88	B2-D;C1-B
Owner	FORD	2	S	IN	R1;A2	B2-D: F;A4	1	4.48	B1-A;B2-D
Patent		3	S	OUT	OUT;A1;R3;R4	B3-F: F;S4	2	3.15	B1-A;B3-F
Date	2018	4	S		R2;A3;A4	B4-C: F;S3	3	2.87	B1-A;B4-C
Model	AT_8_speed_FT_8F57					C1-B: IN;S3	4	1.84	B1-A;C1-B
Commercial?	true					C2-E: IN;A3	5	1.41	B1-A;C2-E
Longitudinal	false						6	1	C1-B;C2-E
Transversal	true						7	0.74	B4-C;C2-E
Weight (kg)							8	0.62	B3-F;C2-E
Máx. Torque (N·m)									

Figure 98 – FORD__AT_8_speed_FT_8F57 representations.

(a) Functional diagram

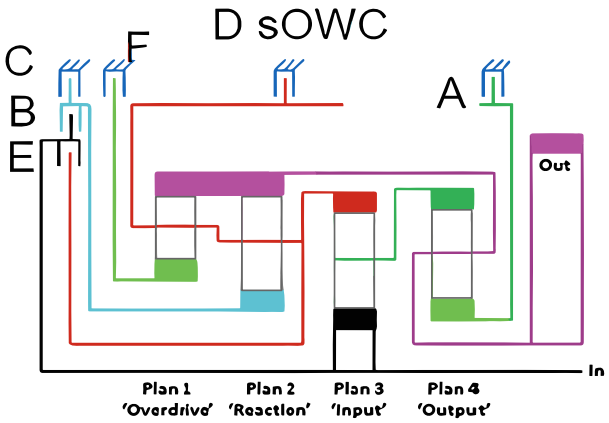

(b) PGM Graph

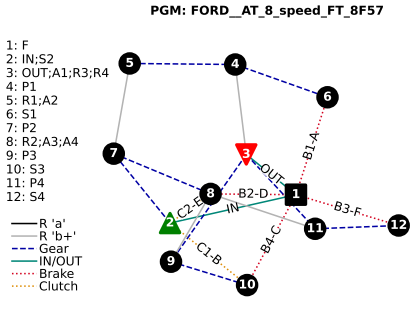

(c) DBG Graph

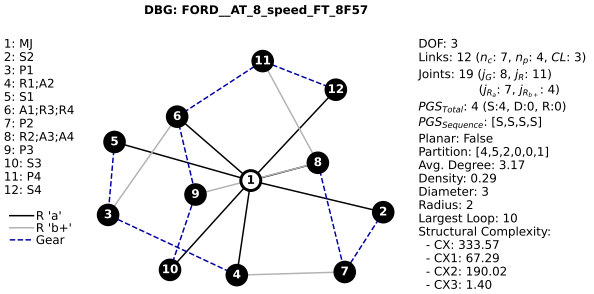

Table 70 – US8545362B1__AT_10_speed_L_10R80 dataset information.

IDENTIFICATION		TOPOLOGY					GEARS SPECS		
UNIQUE_ID	**US8545362B1__AT_10_speed_L_10R80**	**PGS**	**S/D**	**+/-**	**CLs**	**SCs**	**GEARS**	**Ratios**	**Engaged SCs**
Source	industry	1	S	F	IN;A2	B1-B: F;S1	R1	-4.786	B1-B;B2-A;C2-F;C3-D
Owner	FORD	2	S	IN	S1;S2	B2-A: F;R1	1	4.696	B1-B;B2-A;C3-D;C4-E
Patent	US8545362B1	3	S	L1	A1;R4	C1-C: L1;R2	2	2.985	B1-B;B2-A;C1-C;C3-D
Date	2018	4	S	OUT	R2;S3	C2-F: L1;A1	3	2.179	B2-A;C1-C;C3-D;C4-E
Model	AT_10_speed_L_10R80				R3;S4	C3-D: L1;A3	4	1.801	B2-A;C1-C;C2-F;C3-D
Commercial?	true				OUT;A4	C4-E: IN;R3	5	1.539	B2-A;C1-C;C2-F;C4-E
Longitudinal	true						6	1.288	B2-A;C2-F;C3-D;C4-E
Transversal	false						7	1	C1-C;C2-F;C3-D;C4-E
Weight (kg)							8	0.852	B1-B;C2-F;C3-D;C4-E
Máx. Torque (N·m)	800						9	0.689	B1-B;C1-C;C2-F;C4-E
							10	0.636	B1-B;C1-C;C2-F;C3-D

Figure 99 – US8545362B1__AT_10_speed_L_10R80 representations.

(a) Functional diagram

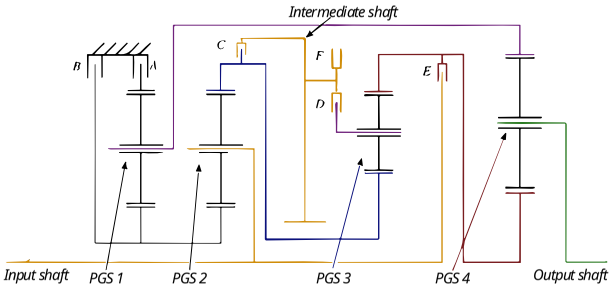

(b) PGM Graph

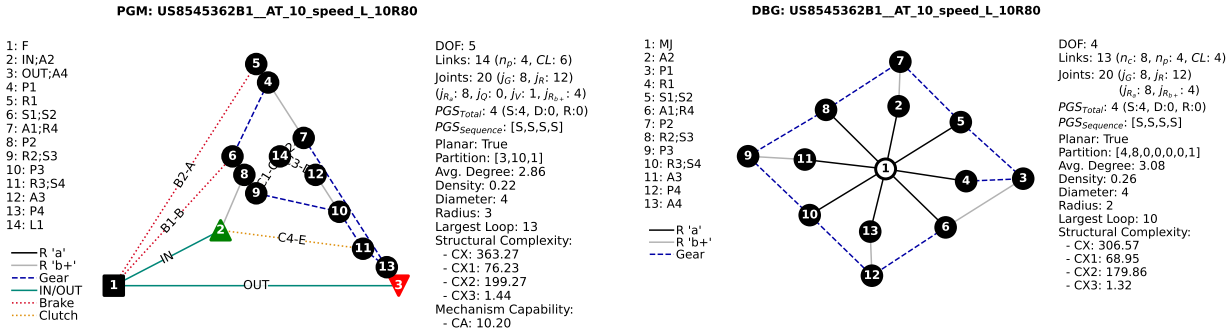

(c) DBG Graph

Table 71 – GM__AT_8_speed_L dataset information.

IDENTIFICATION		TOPOLOGY					GEARS SPECS		
UNIQUE_ID	**GM__AT_8_speed_L**	**PGS**	**S/D**	**+/-**	**CLs**	**SCs**	**GEARS**	**Ratios**	**Engaged SCs**
Source	industry	1	S	F	IN;A2	B1: F;S2	R1	-3.905	B1;B2;C3
Owner	GM	2	S	IN	S1;R2	B2: F;R3	1	4.552	B1;B2;C1
Patent		3	S	OUT	OUT;A1;A4	C1: IN;S4	2	2.959	B1;B2;C2
Date		4	S		S2;S3	C2: R2;S4	3	2.074	B2;C1;C2
Model	AT_8_speed_L				A3;R4	C3: R1;S4	4	1.691	B2;C2;C3
Commercial?	true						5	1.268	B2;C1;C3
Longitudinal	true						6	1	C1;C2;C3
Transversal	false						7	0.847	B1;C1;C3
Weight (kg)	99						8	0.65	B1;C2;C3
Máx. Torque (N·m)	100								

Figure 100 – GM__AT_8_speed_L representations.

(a) Functional diagram

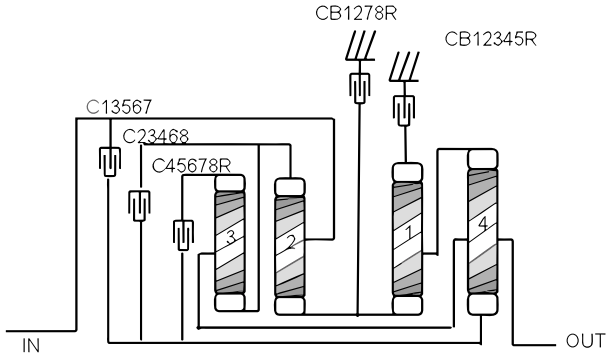

(b) PGM Graph

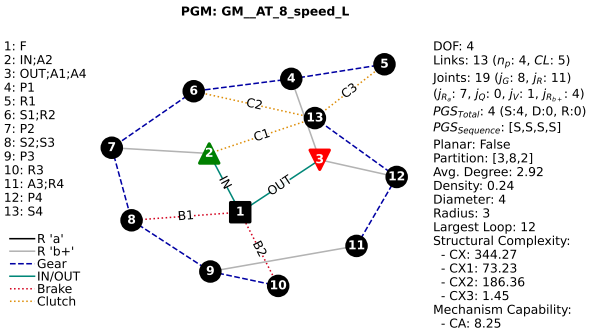

(c) DBG Graph

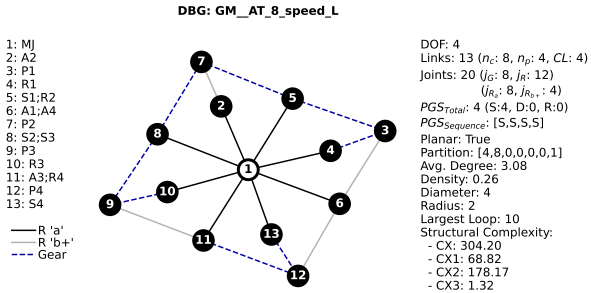

Table 72 – GM__AT_10_speed_L dataset information.

IDENTIFICATION		TOPOLOGY					GEARS SPECS		
UNIQUE_ID	**GM__AT_10_speed_L**	**PGS**	**S/D**	**+/-**	**CLs**	**SCs**	**GEARS**	**Ratios**	**Engaged SCs**
Source	industry	1	S	F	IN;A2	B1: F;S1	R1	-4.866	B1;B2;C2;C3
Owner	GM	2	S	IN	S1;S2	B2: F;R1	1	4.696	B1;B2;C3;C4
Patent		3	S	L1	A1;R4	C1: L1;R2	2	2.985	B1;B2;C1;C3
Date		4	S	OUT	R2;S3	C2: L1;A1	3	2.146	B2;C1;C3;C4
Model	AT_10_speed_L				R3;S4	C3: L1;A3	4	1.769	B2;C1;C2;C3
Commercial?	true				OUT;A4	C4: IN;R3	5	1.52	B2;C1;C2;C4
Longitudinal	true						6	1.27	B2;C2;C3;C4
Transversal	false						7	1	C1;C2;C3;C4
Weight (kg)							8	0.854	B1;C2;C3;C4
Máx. Torque (N·m)	900						9	0.689	B1;C1;C2;C4
							10	0.636	B1;C1;C2;C3

Figure 101 – GM__AT_10_speed_L representations.

(a) Functional diagram

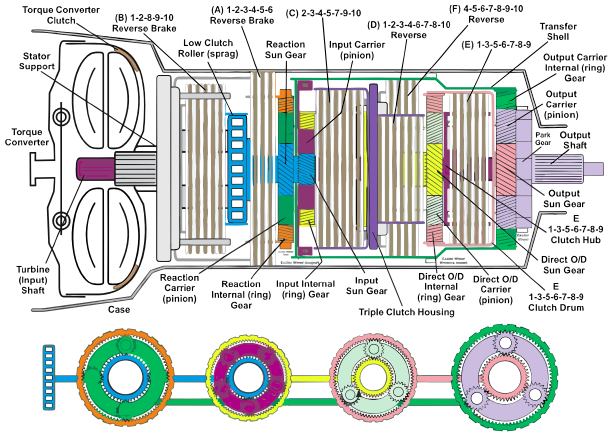

(b) PGM Graph

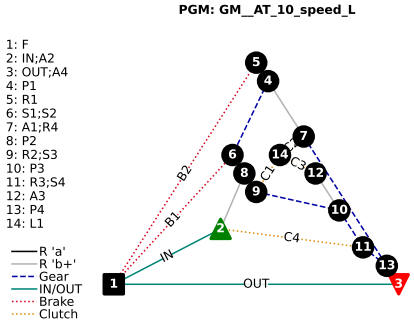

1: F
2: IN;A2
3: OUT;A4
4: P1
5: R1
6: S1;S2
7: A1;R4
8: P2
9: R2;S3
10: P3
11: R3;S4
12: A3
13: P4
14: L1

R 'a'
R 'b+'
Gear
IN/OUT
Brake
Clutch

DOF: 5
Links: 14 (n_p: 4, CL: 6)
Joints: 20 (j_G: 8, j_R: 12)
(j_{R_a}: 8, j_O: 0, j_V: 1, $j_{R_{b+}}$: 4)
PGS_{Total}: 4 (S:4, D:0, R:0)
$PGS_{Sequence}$: [S,S,S,S]
Planar: True
Partition: [3,10,1]
Avg. Degree: 2.86
Density: 0.22
Diameter: 4
Radius: 3
Largest Loop: 13
Structural Complexity:
- CX: 363.27
- CX1: 76.23
- CX2: 199.27
- CX3: 1.44
Mechanism Capability:
- CA: 10.20

(c) DBG Graph

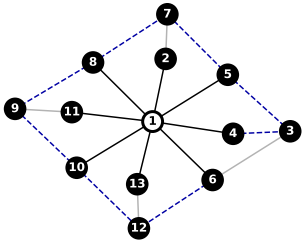

1: MJ
2: A2
3: P1
4: R1
5: S1;S2
6: A1;R4
7: P2
8: R2;S3
9: P3
10: R3;S4
11: A3
12: P4
13: A4

R 'a'
R 'b+'
Gear

DOF: 4
Links: 13 (n_C: 8, n_P: 4, CL: 4)
Joints: 20 (j_C: 8, j_R: 12)
(j_{R_a}: 8, $j_{R_{b+}}$: 4)
PGS_{Total}: 4 (S:4, D:0, R:0)
$PGS_{Sequence}$: [S,S,S,S]
Planar: True
Partition: [4,8,0,0,0,0,1]
Avg. Degree: 3.08
Density: 0.26
Diameter: 4
Radius: 2
Largest Loop: 10
Structural Complexity:
- CX: 306.57
- CX1: 68.95
- CX2: 179.86
- CX3: 1.32

Table 73 – GM__AT_6_speed_FT dataset information.

IDENTIFICATION		TOPOLOGY					GEARS SPECS		
UNIQUE_ID	**GM__AT_6_speed_FT**	**PGS**	**S/D**	**+/-**	**CLs**	**SCs**	**GEARS**	**Ratios**	**Engaged SCs**
Source	industry	1	S	F	IN;S2	B1: F;S1	R1	-2.94	B2;C1
Owner	GM	2	S	IN	R1;A2	B2: F;A3	1	4.584	B1;B2
Patent		3	S	OUT	OUT;A1;R3	B3: F;S3	2	2.964	B1;B3
Date					R2;A3	C1: IN;S3	3	1.912	B1;C1
Model	AT_6_speed_FT					C2: IN;A3	4	1.446	B1;C2
Commercial?	true						5	1	C1;C2
Longitudinal	false						6	0.746	B3;C2
Transversal	true								
Weight (kg)									
Máx. Torque (N·m)									

Figure 102 – GM__AT_6_speed_FT representations.

(a) Functional diagram

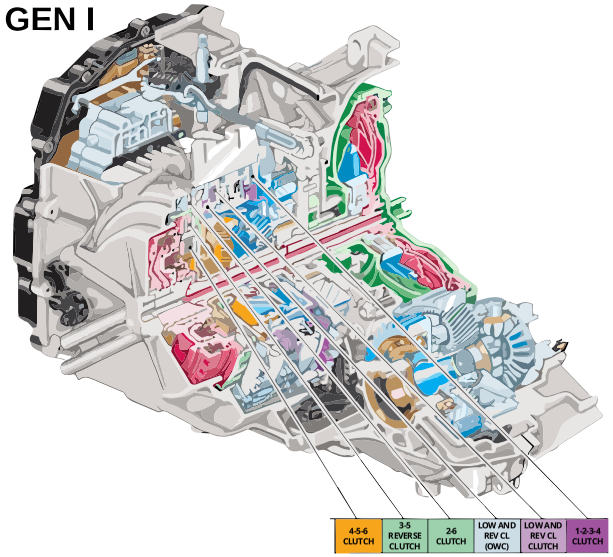

(b) PGM Graph

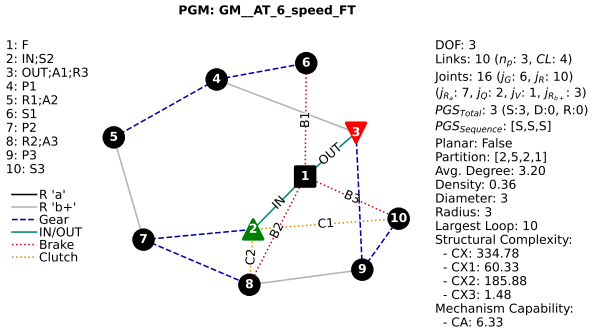

(c) DBG Graph

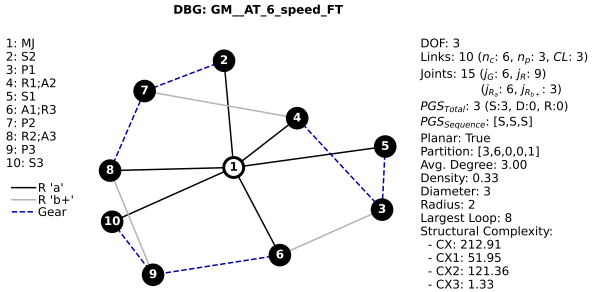

Table 74 – GM__AT_9_speed_FT dataset information.

IDENTIFICATION		TOPOLOGY					GEARS SPECS		
UNIQUE_ID	**GM__AT_9_speed_FT**	**PGS**	**S/D**	**+/-**	**CLs**	**SCs**	**GEARS**	**Ratios**	**Engaged SCs**
Source	industry	1	S	F	IN;S2	B1: F;S1	R1	-2.96	C2;B4-S1
Owner	GM	2	S	IN	R1;A2	B2: F;S4	1	4.689	B1;B4-S1
Patent		3	S	OUT	OUT;A1;R3;R4	B3: F;S3	2	3.306	B1;B2
Date		4	S		R2;A3;A4	C1: S4;A4	3	3.012	B1;B3
Model	AT_9_speed_FT				P3;P4	C2: IN;S3	4	2.446	B1;C1
Commercial?	true					C3: IN;R2	5	1.923	B1;C2
Longitudinal	false					B4-S1: F;A4	6	1.446	B1;C3
Transversal	true						7	1	C2;C3
Weight (kg)	95.9						8	0.747	B3;C3
Máx. Torque (N·m)	400						9	0.617	B2;C3

Figure 103 – GM__AT_9_speed_FT representations.

(a) Functional diagram

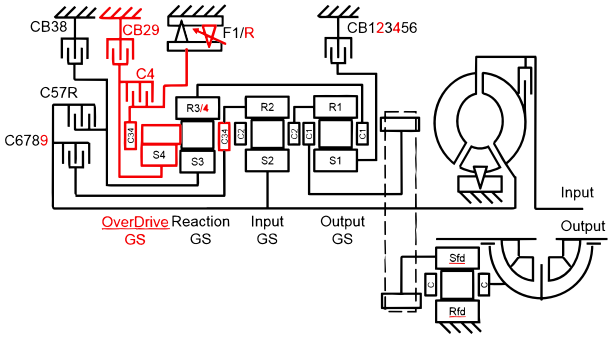

(b) PGM Graph

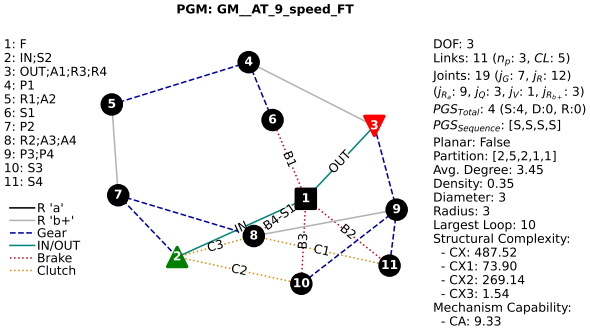

DOF: 3
Links: 11 (n_p: 3, CL: 5)
Joints: 19 (j_G: 7, j_R: 12)
(j_{R_a}: 9, j_O: 3, j_V: 1, $j_{R_{b+}}$: 3)
PGS_{Total}: 4 (S:4, D:0, R:0)
$PGS_{Sequence}$: [S,S,S,S]
Planar: False
Partition: [2,5,2,1,1]
Avg. Degree: 3.45
Density: 0.35
Diameter: 3
Radius: 3
Largest Loop: 10
Structural Complexity:
- CX: 487.52
- CX1: 73.90
- CX2: 269.14
- CX3: 1.54
Mechanism Capability:
- CA: 9.33

(c) DBG Graph

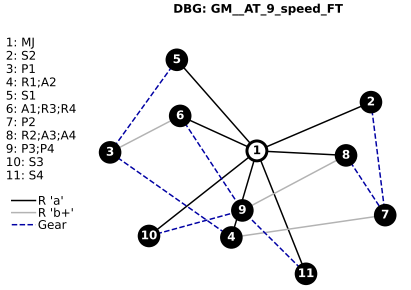

DOF: 3
Links: 11 (n_c: 7, n_p: 3, CL: 4)
Joints: 17 (j_G: 7, j_R: 10)
(j_{R_a}: 7, $j_{R_{b+}}$: 3)
PGS_{Total}: 4 (S:4, D:0, R:0)
$PGS_{Sequence}$: [S,S,S,S]
Planar: True
Partition: [4,5,1,0,0,1]
Avg. Degree: 3.09
Density: 0.31
Diameter: 3
Radius: 2
Largest Loop: 8
Structural Complexity:
- CX: 275.54
- CX1: 63.39
- CX2: 165.14
- CX3: 1.28

Table 75 – CN108691965A__AT_10_speed_FT dataset information.

IDENTIFICATION		TOPOLOGY					GEARS SPECS		
UNIQUE_ID	**CN108691965A__AT_10_speed_FT**	**PGS**	**S/D**	**+/-**	**CLs**	**SCs**	**GEARS**	**Ratios**	**Engaged SCs**
Source	industry	1	S	F	IN;S3	B1: F;S1	R1	-3.97	B2;C3;B4-S1
Owner	HONDA	2	S	IN	R1;A3;A4	B2: F;S4	1	5.25	B1;B2;B4-S1
Patent	CN108691965A	3	S	OUT	A1;A2	B3: F;R4	2	3.27	B1;B2;C2
Date	2017	4	S		OUT;R2	C1: IN;A1	3	2.19	B1;B2;C3
Model	AT_10_speed_FT				S2;R3	C2: R3;S4	4	1.6	B1;C2;C3
Commercial?	true					C3: IN;R4	5	1.3	B1;C1;C3
Longitudinal	false					B4-S1: F;A1	6	1	C1;C2;C3
Transversal	true						7	0.78	B2;C1;C3
Weight (kg)	100						8	0.65	B2;C1;C2
Máx. Torque (N·m)							9	0.58	B2;B3;C1
							10	0.52	B3;C1;C2

Figure 104 – CN108691965A__AT_10_speed_FT representations.

(a) Functional diagram

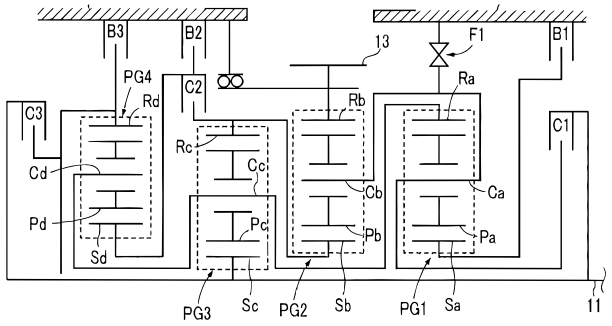

FIG. 2

(b) PGM Graph

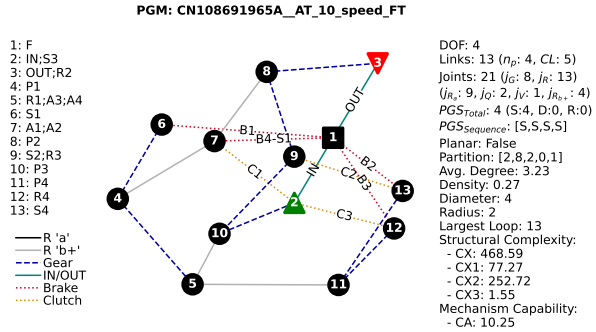

(c) DBG Graph

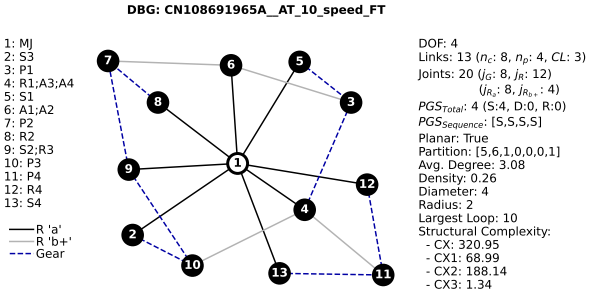

Table 76 – CN105179615A__MECH1 dataset information.

IDENTIFICATION		TOPOLOGY					GEARS SPECS		
UNIQUE_ID	**CN105179615A__MECH1**	**PGS**	**S/D**	**+/-**	**CLs**	**SCs**	**GEARS**	**Ratios**	**Engaged SCs**
Source	academic	1	S	F	IN;S1;S2	A: IN;S4	R1	-5.6	D;F
Owner	HUAFENG_DING	2	S	IN	R1;R2	B: IN;R4	1	4.9	C;F
Patent	CN105179615A	3	S	OUT	A2;S3	C: F;A1	2	3.2	A;F
Date	2015	4	S		OUT;R3;A4	D: F;R1	3	2.6	A;C
Model	MECH1				A3;R4	E: F;A2	4	1.92	A;E
Commercial?	false					F: F;A3	5	1.56	A;D
Longitudinal	true						6	1	A;B
Transversal	false						7	0.65	B;D
Weight (kg)							8	0.58	B;E
Máx. Torque (N·m)							9	0.52	B;C

Figure 105 – CN105179615A__MECH1 representations.

(a) Functional diagram

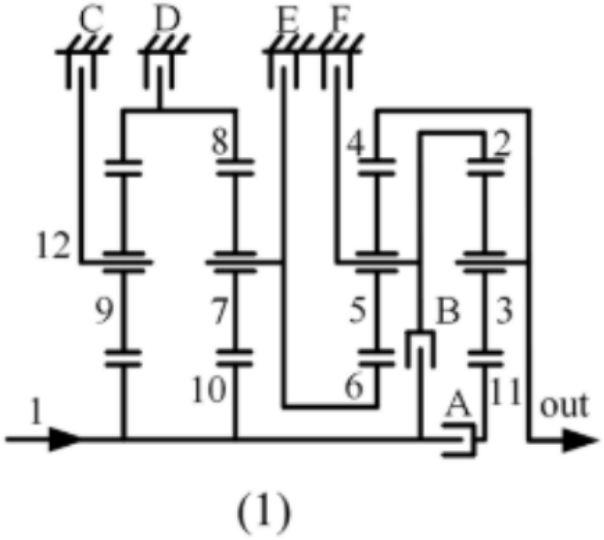

(b) PGM Graph

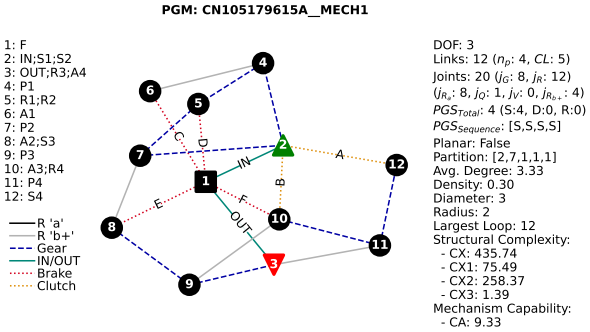

(c) DBG Graph

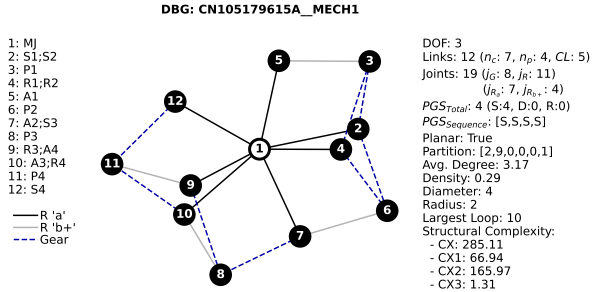

Table 77 – CN105090394A__MECH2 dataset information.

IDENTIFICATION		TOPOLOGY					GEARS SPECS		
UNIQUE_ID	**CN105090394A__MECH2**	**PGS**	**S/D**	**+/-**	**CLs**	**SCs**	**GEARS**	**Ratios**	**Engaged SCs**
Source	academic	1	S	F	IN;S1	A: IN;S4	R1	-9.32	D;F
Owner	HUAFENG_DING	2	S	IN	R1;R2	B: IN;A3	1	4.51	C;F
Patent	CN105090394A	3	S	OUT	A1;S2	C: F;A1	2	2.9	A;F
Date	2015	4	S		A2;S3	D: F;R1	3	2.36	A;C
Model	MECH2				OUT;R3;A4	E: F;A2	4	1.76	A;E
Commercial?	false				A3;R4	F: F;A3	5	1.57	A;D
Longitudinal	true						6	1	A;B
Transversal	false						7	0.64	B;D
Weight (kg)							8	0.6	B;E
Máx. Torque (N·m)							9	0.53	B;C

Figure 106 – CN105090394A__MECH2 representations.

(a) Functional diagram

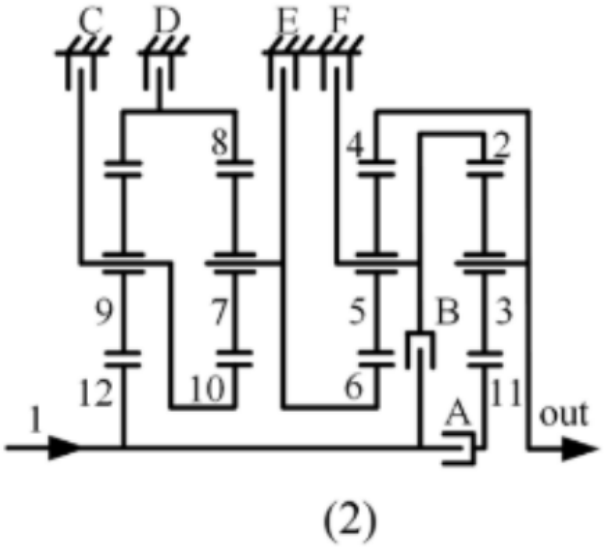

(b) PGM Graph

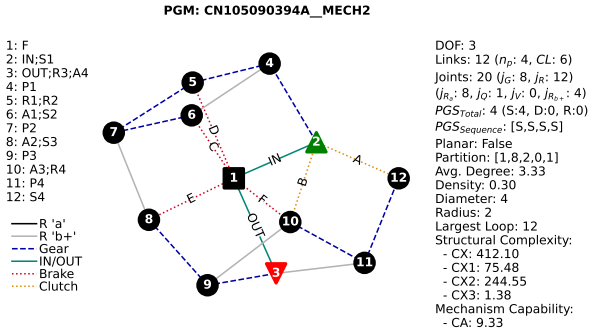

(c) DBG Graph

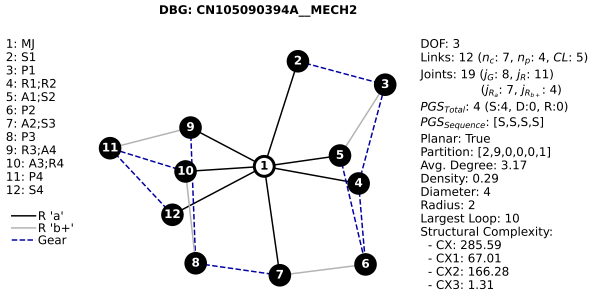

Table 78 – CN109764095A__MECH3 dataset information.

IDENTIFICATION		TOPOLOGY					GEARS SPECS		
UNIQUE_ID	**CN109764095A__MECH3**	**PGS**	**S/D**	**+/-**	**CLs**	**SCs**	**GEARS**	**Ratios**	**Engaged SCs**
Source	academic	1	S	F	IN;S1	A: IN;S3	R1	-3	B;E
Owner	HUAFENG_DING	2	S	IN	R1;R2	B: IN;S4	1	5.57	B;D
Patent	CN109764095A	3	S	OUT	A1;S2	C: F;A1	2	3.3	A;E
Date	2019	4	D		A2;R3;R4	D: F;R1	3	1.95	D;F
Model	MECH3				P3;P4R	E: F;A2	4	1.75	A;D
Commercial?	false				OUT;A3;A4	F: F;S4	5	1.58	A;F
Longitudinal	false						6	1	A;B
Transversal	true						7	0.8	A;C
Weight (kg)							8	0.67	B;C
Máx. Torque (N·m)							9	0.55	C;F

Figure 107 – CN109764095A__MECH3 representations.

(a) Functional diagram

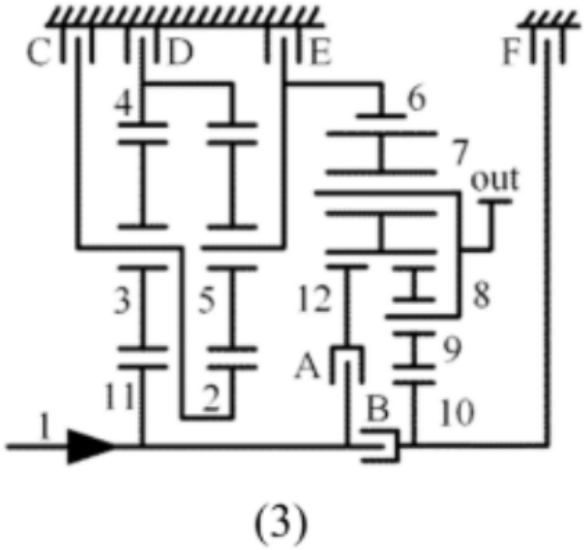

(b) PGM Graph

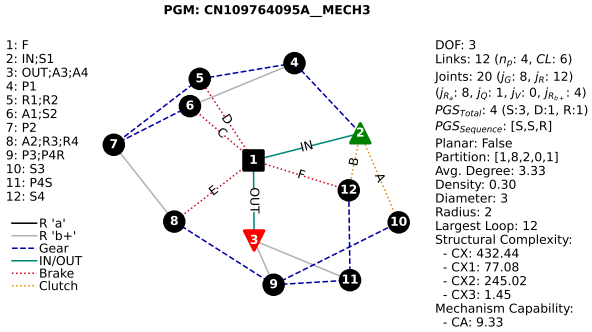

(c) DBG Graph

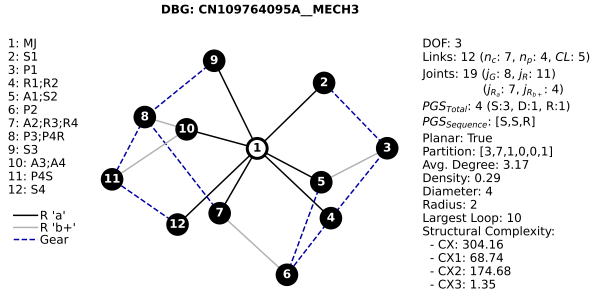

Table 79 – CN109798334A__MECH4 dataset information.

IDENTIFICATION		TOPOLOGY					GEARS SPECS		
UNIQUE_ID	**CN109798334A__MECH4**	**PGS**	**S/D**	**+/-**	**CLs**	**SCs**	**GEARS**	**Ratios**	**Engaged SCs**
Source	academic	1	S	F	IN;S1	A: IN;S4	R1	-9.67	D;F
Owner	HUAFENG_DING	2	S	IN	R1;R2	B: IN;R4	1	4.68	C;F
Patent	CN109798334A	3	D	OUT	A1;S2	C: F;A1	2	2.8	A;F
Date	2019	4	S		A2;S3	D: F;R1	3	2.228	A;C
Model	MECH4				P3R;P4	E: F;A2	4	1.78	A;E
Commercial?	false				R3;R4	F: F;R4	5	1.61	A;D
Longitudinal	false				OUT;A3;A4	:	6	1	A;B
Transversal	true						7	0.6	B;D
Weight (kg)							8	0.57	B;E
Máx. Torque (N·m)							9	0.5	B;C

Figure 108 – CN109798334A__MECH4 representations.

(a) Functional diagram

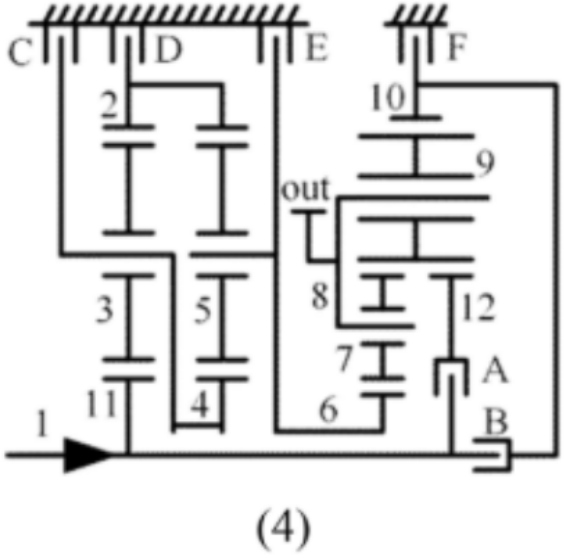

(b) PGM Graph

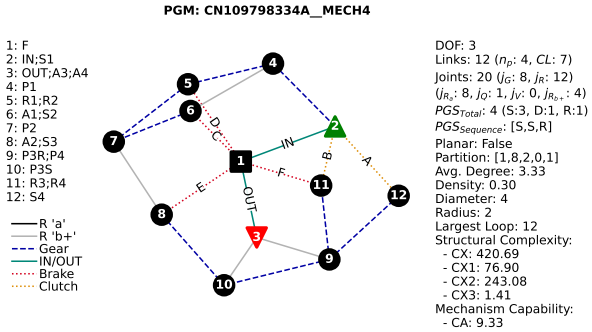

(c) DBG Graph

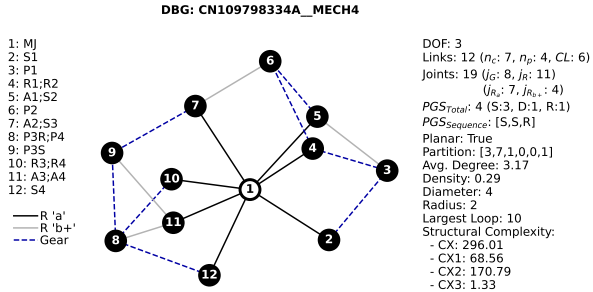

Table 80 – JP3519037B2__FIG1 dataset information.

IDENTIFICATION		TOPOLOGY					GEARS SPECS		
UNIQUE_ID	**JP3519037B2__FIG1**	**PGS**	**S/D**	**+/-**	**CLs**	**SCs**	**GEARS**	**Ratios**	**Engaged SCs**
Source	patent	1	S	F	IN;R1	C1: S1;R3	R2		C1;C3;C4;B3
Owner	DAIMLER	2	S	IN	OUT;A2	C2: IN;R2	R1		C3;C4;B1;B3
Patent	JP3519037B2	3	S	OUT	R2;A3	C3: S2;S3	1		C3;C4;B1;B2
Date	1999					C4: A1;R3	2		C1;C3;C4;B2
Model	FIG1					B1: F;S1	3		C1;C2;C4;B2
Commercial?	false					B2: F;S2	4		C1;C2;C3;C4
Longitudinal	true					B3: F;A3	5		C2;C3;C4;B1
Transversal	false						6		C1;C2;C3;B1
Weight (kg)									
Máx. Torque (N·m)									

Figure 109 – JP3519037B2__FIG1 representations.

(a) Functional diagram

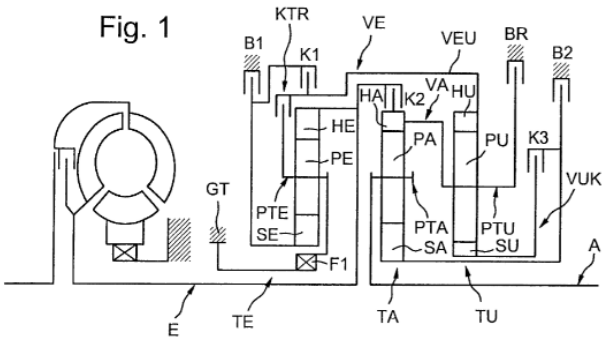

(b) PGM Graph

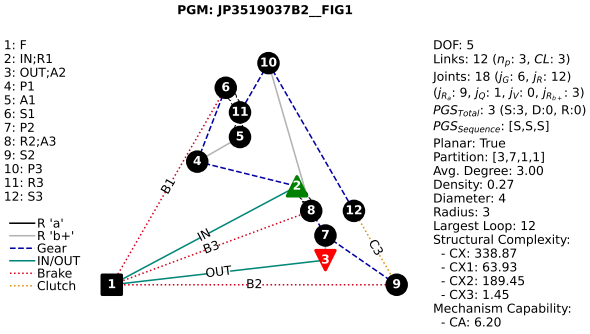

(c) DBG Graph

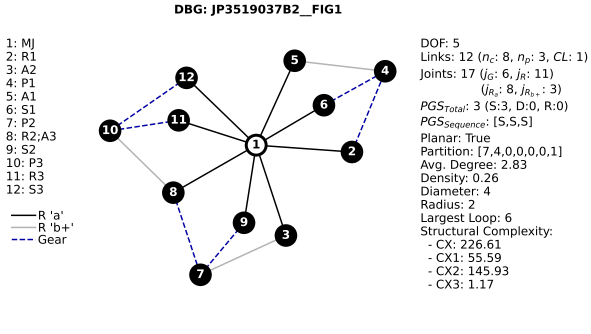

Table 81 – JP3519037B2__FIG3 dataset information.

IDENTIFICATION		TOPOLOGY					GEARS SPECS		
UNIQUE_ID	**JP3519037B2__FIG3**	**PGS**	**S/D**	**+/-**	**CLs**	**SCs**	**GEARS**	**Ratios**	**Engaged SCs**
Source	patent	1	S	F	IN;R1	C1: S1;R3	R2		C1;C3;B3
Owner	DAIMLER	2	S	IN	OUT;A2	C2: IN;R2	R1		C3;B1;B3
Patent	JP3519037B2	3	S	OUT	R2;A3	C3: A1;R3	1		C3;B1;B2
Date	1999				S2;S3	B1: F;S1	2		C1;C3;B2
Model	FIG3					B2: F;S2	3		C1;C2;B2
Commercial?	false					B3: F;A3	4		C1;C2;C3
Longitudinal	true						5		C2;C3;B1
Transversal	false						6		C1;C2;B1
Weight (kg)									
Máx. Torque (N·m)									

Figure 110 – JP3519037B2__FIG3 representations.

(a) Functional diagram

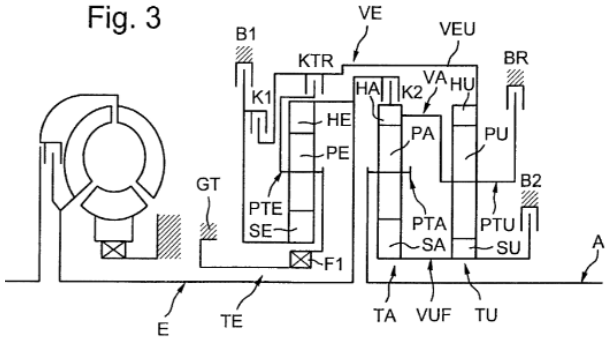

(b) PGM Graph

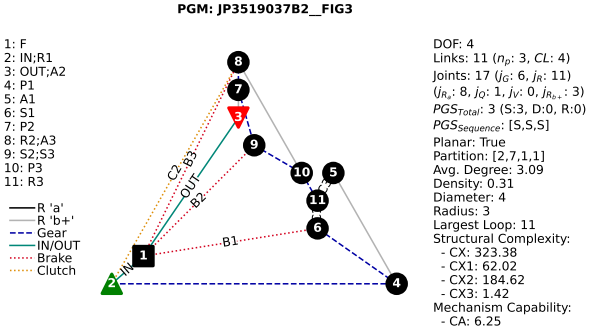

(c) DBG Graph

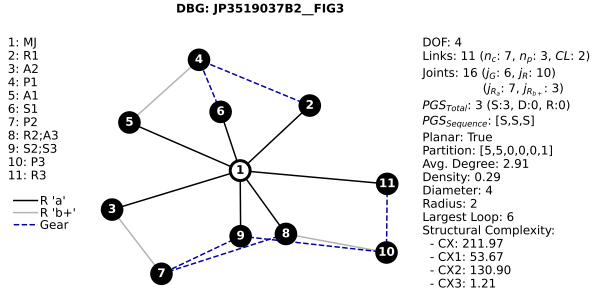

Table 82 – JP3519037B2__FIG5 dataset information.

IDENTIFICATION		TOPOLOGY					GEARS SPECS		
UNIQUE_ID	**JP3519037B2__FIG5**	**PGS**	**S/D**	**+/-**	**CLs**	**SCs**	**GEARS**	**Ratios**	**Engaged SCs**
Source	patent	1	D	F	IN;R1	C1: S1;R1	R3		C3;B3;B4
Owner	DAIMLER	2	S	IN	OUT;A2	C2: IN;R2	R2		C1;C3;B4
Patent	JP3519037B2	3	S	OUT	R2;A3	C3: S2;S3	R1		C3;B1;B4
Date	1999				A1;R3	B1: F;S1	1		C3;B2;B3
Model	FIG5					B2: F;S2	2		C3;B1;B2
Commercial?	false					B3: F;R1	3		C1;C3;B2
Longitudinal	true					B4: F;A3	4		C1;C2;B2
Transversal	false						5		C1;C2;C3
Weight (kg)							6		C2;C3;B1
Máx. Torque (N·m)							7		C3;B1;B3

Figure 111 – JP3519037B2__FIG5 representations.

(a) Functional diagram

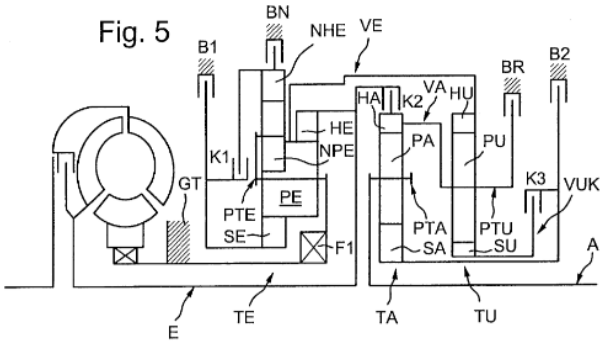

(b) PGM Graph

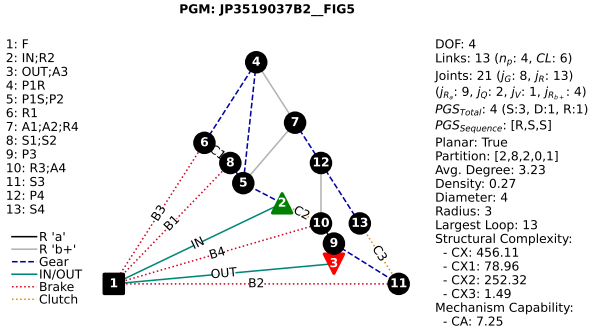

(c) DBG Graph

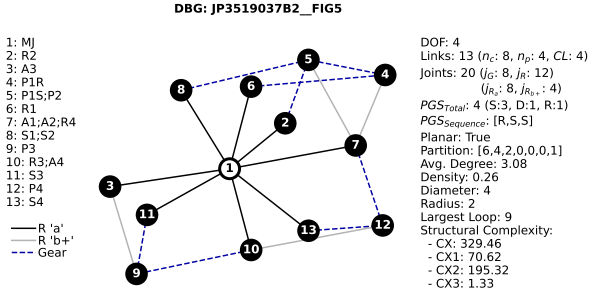

Table 83 – JP3519037B2__FIG7 dataset information.

IDENTIFICATION		TOPOLOGY					GEARS SPECS		
UNIQUE_ID	**JP3519037B2__FIG7**	**PGS**	**S/D**	**+/-**	**CLs**	**SCs**	**GEARS**	**Ratios**	**Engaged SCs**
Source	patent	1	D	F	IN;R1	C1: S1;R1	R3		B3;B4
Owner	DAIMLER	2	S	IN	OUT;A2	C2: IN;R2	R2		C1;B4
Patent	JP3519037B2	3	S	OUT	R2;A3	B1: F;S1	R1		B1;B4
Date	1999				A1;R3	B2: F;S2	1		B2;B3
Model	FIG7				S2;S3	B3: F;R1	2		B1;B2
Commercial?	false					B4: F;A3	3		C1;B2
Longitudinal	true						4		C2;B2
Transversal	false						5		C1;C2
Weight (kg)							6		C2;B1
Máx. Torque (N·m)							7		C2;B3

Figure 112 – JP3519037B2__FIG7 representations.

(a) Functional diagram

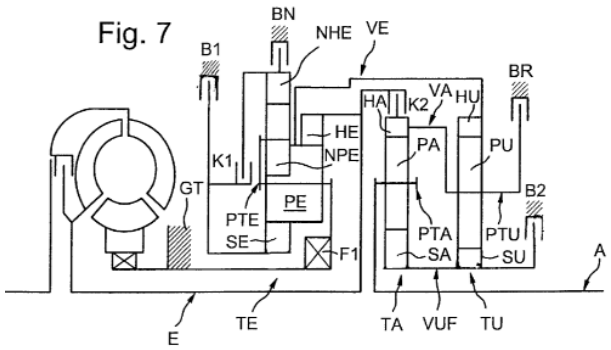

(b) PGM Graph

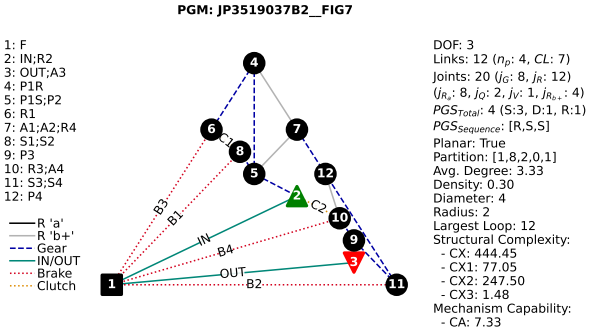

(c) DBG Graph

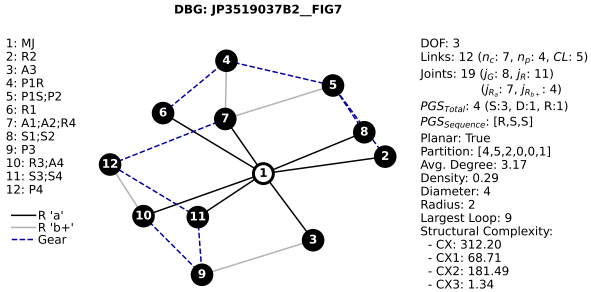

Table 84 – JP3710180B2__FIG2 dataset information.

IDENTIFICATION		TOPOLOGY					GEARS SPECS		
UNIQUE_ID	**JP3710180B2__FIG2**	**PGS**	**S/D**	**+/-**	**CLs**	**SCs**	**GEARS**	**Ratios**	**Engaged SCs**
Source	patent	1	S	F	A1;R2	C1: A1;A3	R1	-2.37	C1;B1;B3
Owner	JATCO	2	S	IN	R1;S2	C2: IN;S1	1	3.33	C1;C2;B1
Patent	JP3710180B2	3	S	OUT	A2;R3	C3: IN;A3	2	2.4	C1;C2;B2
Date	1995				OUT;S3	B1: F;A3	3	1.73	C1;C2;B3
Model	FIG2					B2: F;A2	4	1	C1;C2;C3
Commercial?	false					B3: F;S2	5	0.69	C1;C3;B3
Longitudinal	true						6	0.4	C2;C3;B3
Transversal	false								
Weight (kg)									
Máx. Torque (N·m)									

Figure 113 – JP3710180B2__FIG2 representations.

(a) Functional diagram

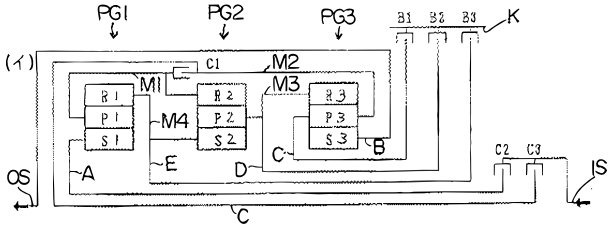

(b) PGM Graph

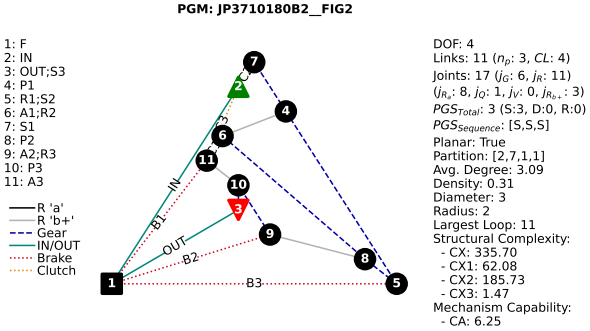

(c) DBG Graph

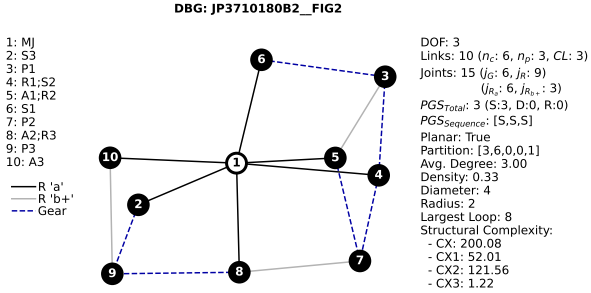

Table 85 – JP3710180B2__FIG5 dataset information.

IDENTIFICATION		TOPOLOGY					GEARS SPECS		
UNIQUE_ID	**JP3710180B2__FIG5**	**PGS**	**S/D**	**+/-**	**CLs**	**SCs**	**GEARS**	**Ratios**	**Engaged SCs**
Source	patent	1	S	F	S1;S2	C1: R2;A3	R1	-2.5	C3;B1;B3
Owner	JATCO	2	S	IN	A1;R2	C2: IN;R1	1	3.67	C1;C2;B1
Patent	JP3710180B2	3	S	OUT	A2;S3	C3: IN;A1	2	1.98	C1;C2;B2
Date	1995				OUT;R3	B1: F;A3	3	1.41	C1;C2;B3
Model	FIG5					B2: F;S3	4	1	C1;C2;C3
Commercial?	false					B3: F;S1	5	0.85	C1;C3;B3
Longitudinal	true						6	0.75	C1;C3;B2
Transversal	false								
Weight (kg)									
Máx. Torque (N·m)									

Figure 114 – JP3710180B2__FIG5 representations.

(a) Functional diagram

【図5】

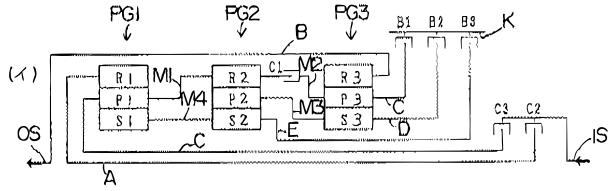

(b) PGM Graph

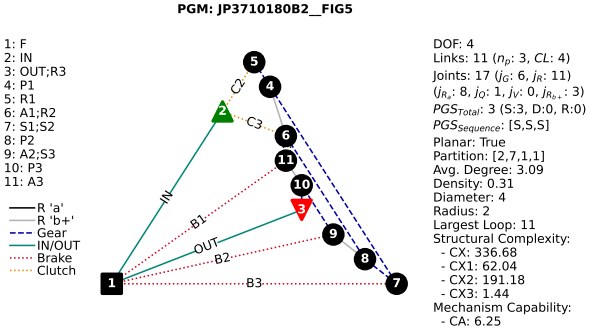

(c) DBG Graph

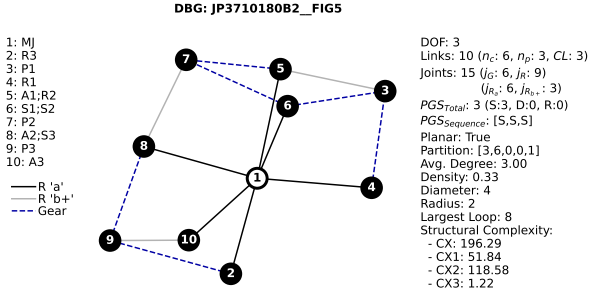

Table 86 – JP3710180B2__FIG8 dataset information.

IDENTIFICATION		TOPOLOGY					GEARS SPECS		
UNIQUE_ID	**JP3710180B2__FIG8**	**PGS**	**S/D**	**+/-**	**CLs**	**SCs**	**GEARS**	**Ratios**	**Engaged SCs**
Source	patent	1	S	F	S1;S2	C1: R2;A3	R1	-4.24	C1;C4;B2
Owner	JATCO	2	S	IN	A1;R2	C2: IN;A3	1	3.58	C1;C4;B1
Patent	JP3710180B2	3	S	OUT	A2;S3	C3: IN;A2	2	2.24	C1;C3;B1
Date	1995				OUT;R3	C4: IN;S2	3	1.49	C1;C2;B1
Model	FIG8					B1: F;R1	4	1	C1;C2;C4
Commercial?	false					B2: F;A1	5	0.8	C2;C4;B1
Longitudinal	true						6	0.6	C2;B1;B2
Transversal	false								
Weight (kg)									
Máx. Torque (N·m)									

Figure 115 – JP3710180B2__FIG8 representations.

(a) Functional diagram

【図8】

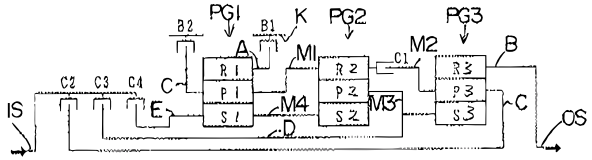

(b) PGM Graph

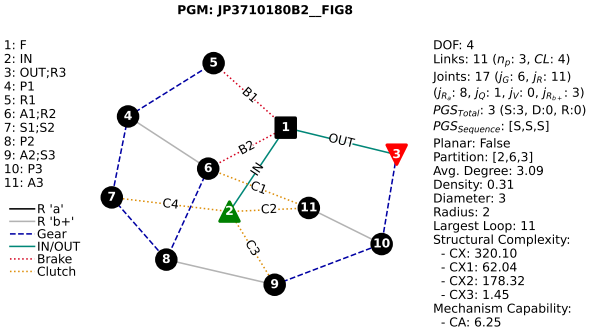

(c) DBG Graph

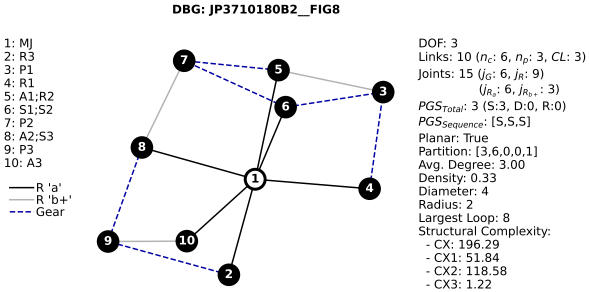

Table 87 – JP3710180B2__FIG23 dataset information.

IDENTIFICATION		TOPOLOGY					GEARS SPECS		
UNIQUE_ID	**JP3710180B2__FIG23**	**PGS**	**S/D**	**+/-**	**CLs**	**SCs**	**GEARS**	**Ratios**	**Engaged SCs**
Source	patent	1	S	F	S1;S2	C1: A1;A3	R1	-2.28	C1;C4;B2
Owner	JATCO	2	S	IN	R1;A2;R3	C2: IN;A3	1	4.26	C1;C4;B1
Patent	JP3710180B2	3	S	OUT	OUT;S3	C3: IN;R3	2	2.68	C1;C3;B1
Date	1995					C4: IN;R2	3	2	C1;C2;B1
Model	FIG23					B1: F;S1	4	1	C1;C2;C4
Commercial?	false					B2: F;A1	5	0.64	C2;C4;B1
Longitudinal	true						6	0.48	C2;C4;B2
Transversal	false						7	0.4	C2;B1;B2
Weight (kg)									
Máx. Torque (N·m)									

Figure 116 – JP3710180B2__FIG23 representations.

(a) Functional diagram

【図23】

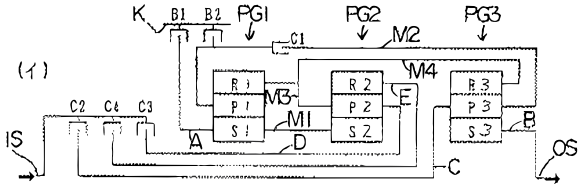

(b) PGM Graph

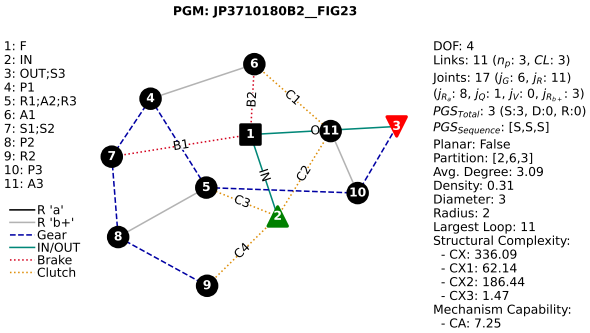

(c) DBG Graph

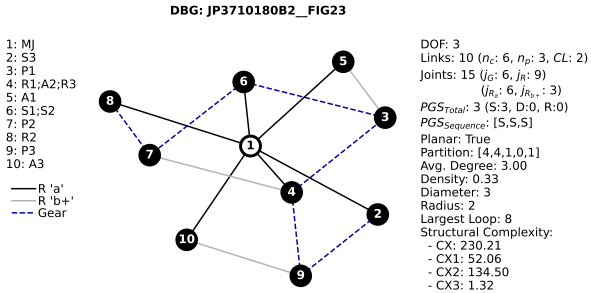

Table 88 – JP3710180B2__FIG44 dataset information.

IDENTIFICATION		TOPOLOGY					GEARS SPECS		
UNIQUE_ID	**JP3710180B2__FIG44**	**PGS**	**S/D**	**+/-**	**CLs**	**SCs**	**GEARS**	**Ratios**	**Engaged SCs**
Source	patent	1	S	F	A1;R2	C1: A1;A3	R1	-1.76	C1;C4;B2
Owner	JATCO	2	S	IN	R1;A2;R3	C2: IN;A3	1	3.78	C1;C4;B1
Patent	JP3710180B2	3	S	OUT	OUT;S3	C3: IN;A2	2	2.69	C1;C3;B1
Date	1995					C4: IN;S2	3	2	C1;C2;B1
Model	FIG44					B1: F;S1	4	1	C1;C2;C4
Commercial?	false					B2: F;A1	5	0.69	C2;C4;B1
Longitudinal	true						6	0.51	C2;C4;B2
Transversal	false						7	0.4	C2;B1;B2
Weight (kg)									
Máx. Torque (N·m)									

Figure 117 – JP3710180B2__FIG44 representations.

(a) Functional diagram

【図44】

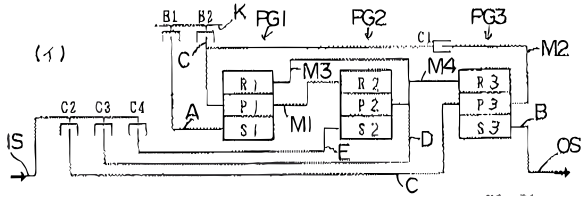

(b) PGM Graph

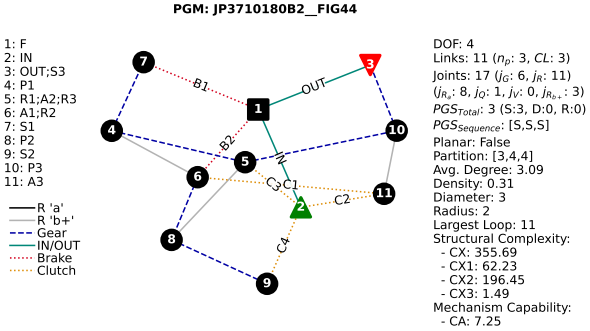

(c) DBG Graph

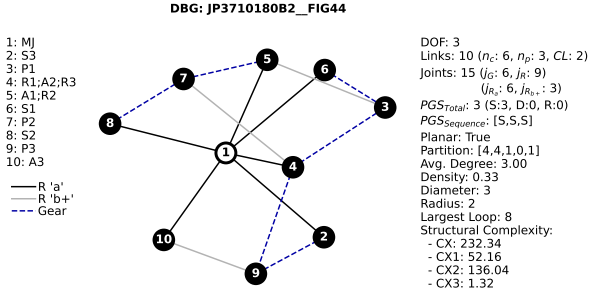

Table 89 – KR101154689B1__FIG1 dataset information.

IDENTIFICATION		TOPOLOGY					GEARS SPECS		
UNIQUE_ID	**KR101154689B1__FIG1**	**PGS**	**S/D**	**+/-**	**CLs**	**SCs**	**GEARS**	**Ratios**	**Engaged SCs**
Source	patent	1	S	F	F;S1	C1: A1;R2	R3		C1;C4
Owner	HYUNDAI	2	S	IN	IN;R1	C2: R1;S2	R2		B1;C3
Patent	KR101154689B1	3	S	OUT	S2;S3;S4	C3: R1;A2	R1		B1;C4
Date	2010	4	S		A2;R3	B1: F;R2	1		B2;C4
Model	FIG1				OUT;A3;A4	B2: F;R3	2		B2;C3
Commercial?	false					B3: F;R4	3		B2;C2
Longitudinal	true						4		B1;B2
Transversal	false						5		B2;C1
Weight (kg)							6		B1;C1
Máx. Torque (N·m)							7		C1;C2

Figure 118 – KR101154689B1__FIG1 representations.

(a) Functional diagram

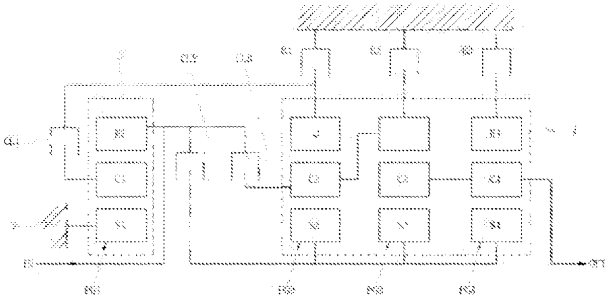

(b) PGM Graph

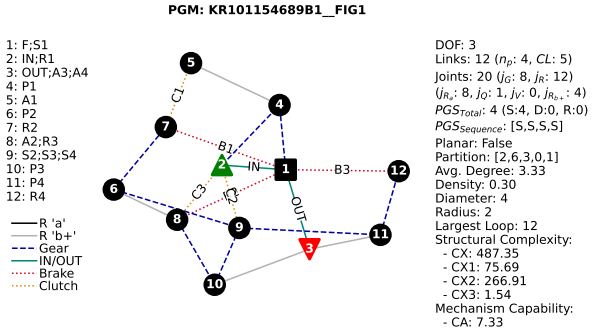

(c) DBG Graph

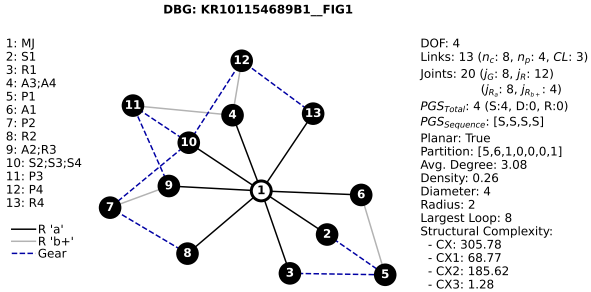

Table 90 – KR102417360B1__FIG1 dataset information.

IDENTIFICATION		TOPOLOGY					GEARS SPECS		
UNIQUE_ID	**KR102417360B1__FIG1**	**PGS**	**S/D**	**+/-**	**CLs**	**SCs**	**GEARS**	**Ratios**	**Engaged SCs**
Source	patent	1	S	F	R1;S3	C1: IN;S1	R1	-2.76	C1;C4;B1
Owner	HYUNDAI/KIA	2	S	IN	S1;S2	C2: IN;R2	1	5.673	C1;B2
Patent	KR102417360B1	3	S	OUT	A2;R3;R4	C3: S1;A1	2	3.507	C1;C4;B2
Date	2017	4	S		OUT;A3;A4	C4: A1;A2	3	2.467	C1;C3;B2
Model	FIG1					B1: F;A1	4	1.667	C1;C2;B2
Commercial?	false					B2: F;S4	5	1.424	C2;C3;B2
Longitudinal	true						6	1.109	C2;C4;B2
Transversal	false						7	1	C2;C3;C4
Weight (kg)							8	0.836	C2;C4;B1
Máx. Torque (N·m)							9	0.711	C2;C3;B1
							10	0.68	C1;C2;B1

Figure 119 – KR102417360B1__FIG1 representations.

(a) Functional diagram

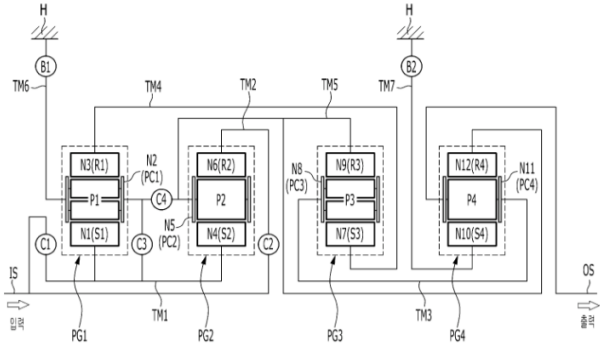

(b) PGM Graph

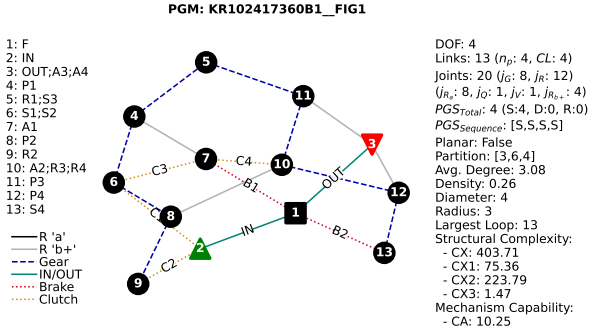

(c) DBG Graph

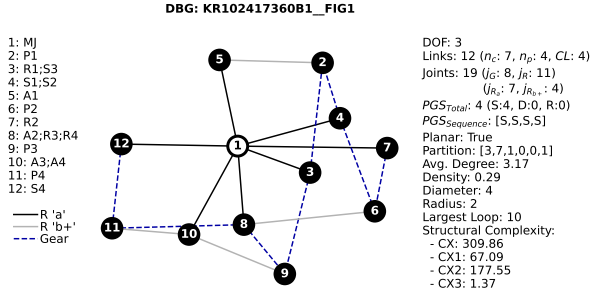

Table 91 – KR20090096701A__FIG1 dataset information.

IDENTIFICATION		TOPOLOGY					GEARS SPECS		
UNIQUE_ID	**KR20090096701A__FIG1**	**PGS**	**S/D**	**+/-**	**CLs**	**SCs**	**GEARS**	**Ratios**	**Engaged SCs**
Source	patent	1	S	F	F;S1	B1: F;R2	R3	-1.7	B2;C1
Owner	ZF	2	S	IN	R1;A2;S3	B2: F;A3	R2	-2.525	B2;C3
Patent	KR20090096701A	3	S	OUT	IN;S2	C1: R2;A2	R1	-4.589	B1;B2
Date	2006				OUT;R3	C2: IN;A3	1	4.941	B1;C4
Model	FIG1					C3: A1;R2	2	2.719	C3;C4
Commercial?	false					C4: A1;A3	3	1.83	C1;C4
Longitudinal	true						4	1.308	C2;C4
Transversal	false						5	1	C1;C2
Weight (kg)							6	0.839	C2;C3
Máx. Torque (N·m)									

Figure 120 – KR20090096701A__FIG1 representations.

(a) Functional diagram

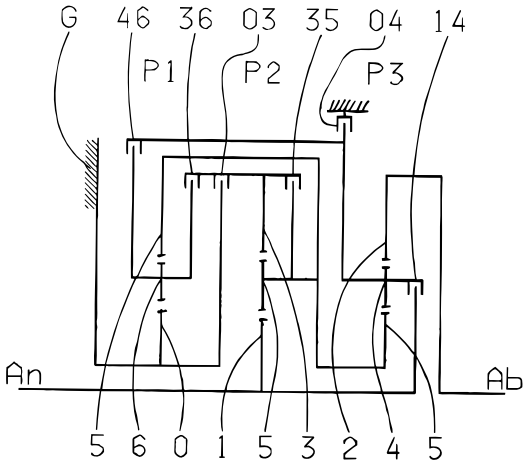

Fig. 1

(b) PGM Graph

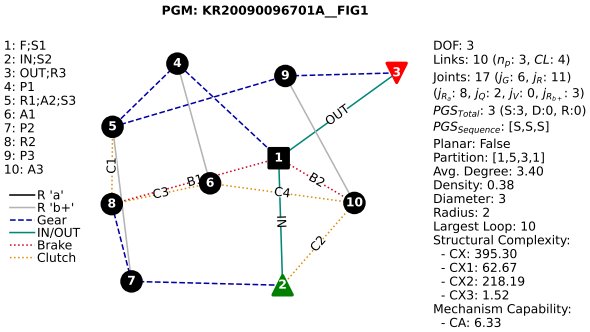

(c) DBG Graph

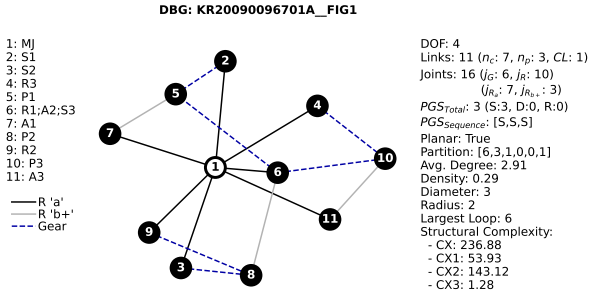

Table 92 – KR20090096701A__FIG1A dataset information.

IDENTIFICATION		TOPOLOGY					GEARS SPECS		
UNIQUE_ID	**KR20090096701A__FIG1A**	**PGS**	**S/D**	**+/-**	**CLs**	**SCs**	**GEARS**	**Ratios**	**Engaged SCs**
Source	patent	1	S	F	F;S1	B1: F;R2	R3	-1.7	B2;C1
Owner	ZF	2	S	IN	R1;A2;R2;S3	B2: F;A3	R2	-2.525	B2;C3
Patent	KR20090096701A	3	S	OUT	IN;S2	C1: IN;R2	R1	-4.589	B1;B2
Date	2006				OUT;R3	C2: IN;A3	1	4.941	B1;C4
Model	FIG1A					C3: A1;R2	2	2.719	C3;C4
Commercial?	false					C4: A1;A3	3	1.83	C1;C4
Longitudinal	true						4	1.308	C2;C4
Transversal	false						5	1	C1;C2
Weight (kg)							6	0.839	C2;C3
Máx. Torque (N·m)							7	0.73	B1;C2

Figure 121 – KR20090096701A__FIG1A representations.

(a) Functional diagram

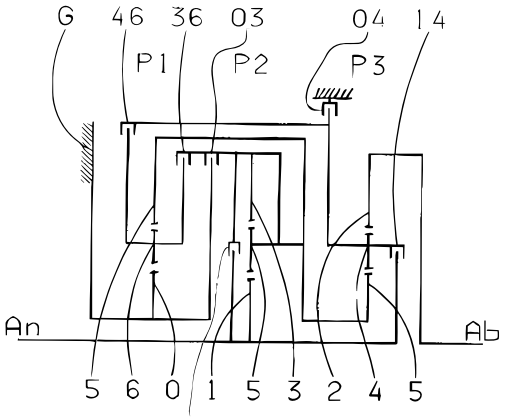

Fig. 1A

(b) PGM Graph

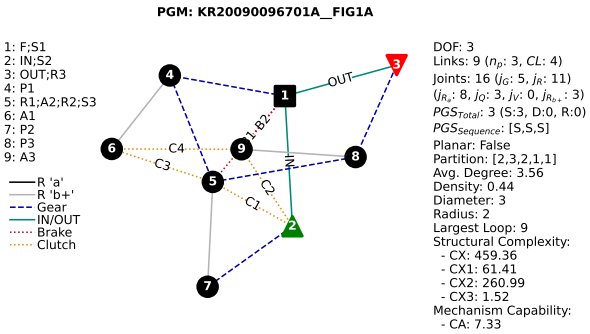

(c) DBG Graph

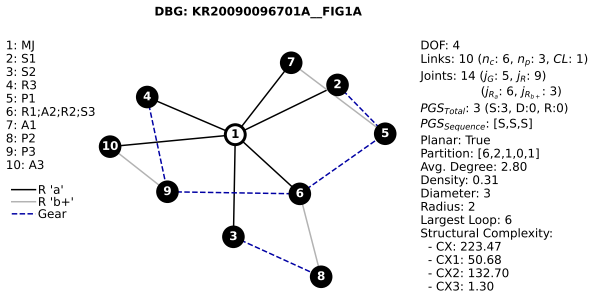

Table 93 – PIGAMARTINS__FIG2 dataset information.

IDENTIFICATION		TOPOLOGY					GEARS SPECS		
UNIQUE_ID	**PIGAMARTINS__FIG2**	**PGS**	**S/D**	**+/-**	**CLs**	**SCs**	**GEARS**	**Ratios**	**Engaged SCs**
Source	academic	1	S	F	IN;S1;R2	B1: F;A3	R1	-4.495	B1;C2;C3
Owner	PIGAMARTINS	2	S	IN	A1;R4	B2: F;S3	1	4.504	B1;B2;C1
Patent		3	S	OUT	S2;R3	C1: A3;R1	2	2.242	B1;B2;C3
Date	2009	4	S		S3;S4	C2: A2;R1	3	1.966	B1;B2;C2
Model	FIG2				OUT;A4	C3: A1;A2	4	1.609	B2;C2;C3
Commercial?	false						5	1.414	B2;C1;C2
Longitudinal	false						6	1.193	B2;C1;C3
Transversal	true						7	1	C1;C2;C3
Weight (kg)							8	0.77	B1;C1;C3
Máx. Torque (N·m)							9	0.423	B1;C1;C2

Figure 122 – PIGAMARTINS__FIG2 representations.

(a) Functional diagram

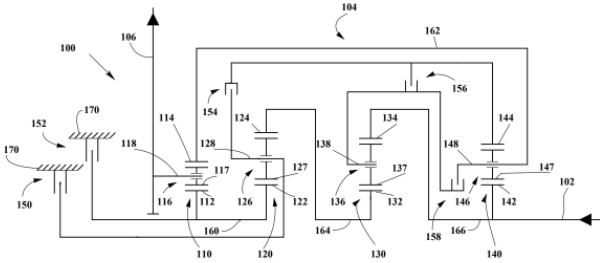

(b) PGM Graph

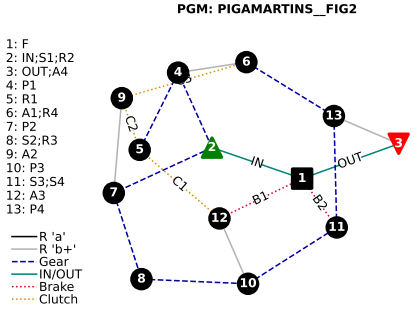

(c) DBG Graph

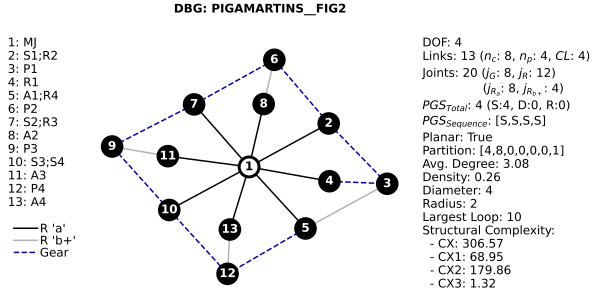

Table 94 – PIGAMARTINS__FIG3 dataset information.

IDENTIFICATION		TOPOLOGY					GEARS SPECS		
UNIQUE_ID	**PIGAMARTINS__FIG3**	**PGS**	**S/D**	**+/-**	**CLs**	**SCs**	**GEARS**	**Ratios**	**Engaged SCs**
Source	academic	1	S	F	IN;S1	B1: F;R1	R1	-4.495	B1;C2;C3
Owner	PIGAMARTINS	2	S	IN	OUT;A3	B2: F;S4	1	4.504	B1;B2;C1
Patent		3	S	OUT	R1;R2	C1: A1;A2	2	2.242	B1;B2;C3
Date	2009	4	S		A1;R4	C2: A2;A4	3	1.966	B1;B2;C2
Model	FIG3				S2;S3	C3: A3;A4	4	1.609	B2;C2;C3
Commercial?	false				R3;S4	:	5	1.414	B2;C1;C2
Longitudinal	false						6	1.193	B2;C1;C3
Transversal	true						7	1	C1;C2;C3
Weight (kg)							8	0.77	B1;C1;C3
Máx. Torque (N·m)							9	0.423	B1;C1;C2

Figure 123 – PIGAMARTINS__FIG3 representations.

(a) Functional diagram

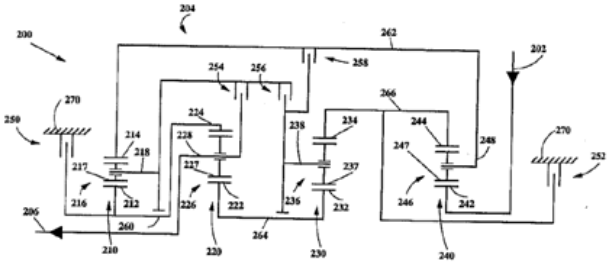

Figure 3:

(b) PGM Graph

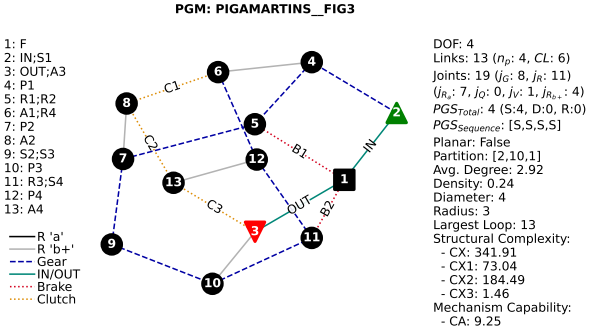

(c) DBG Graph

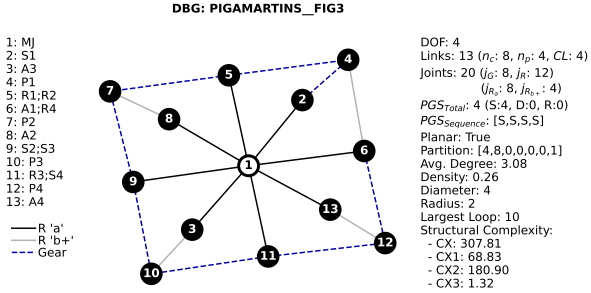

Table 95 – US10161483B2__FIG2 dataset information.

IDENTIFICATION		TOPOLOGY					GEARS SPECS		
UNIQUE_ID	**US10161483B2__FIG2**	**PGS**	**S/D**	**+/-**	**CLs**	**SCs**	**GEARS**	**Ratios**	**Engaged SCs**
Source	patent	1	S	F	IN;S1	C1: IN;S2	R2	-7	B3;B5
Owner	ALLISON	2	S	IN	A1;R2	C2: IN;A2	R1	-20	B3;B6
Patent	US10161483B2	3	S	OUT	S2;S3	B3: F;R1	1	9	C1;B6
Date	2011	4	S		A2;R3;S4	B4: F;R2	2	6	C1;B5
Model	FIG2				OUT;A3;R4	B5: F;R3	3	4.5	C1;B4
Commercial?	false					B6: F;A4	4	3	C1;B3
Longitudinal	true						5	1.1	C1;C2
Transversal	false						6	0.99	C2;B3
Weight (kg)							7	0.25	C2;B4
Máx. Torque (N·m)									

Figure 124 – US10161483B2__FIG2 representations.

(a) Functional diagram

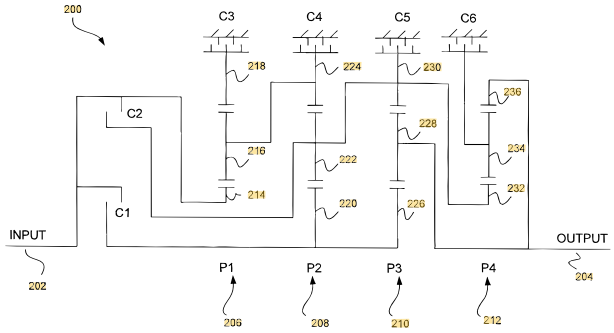

FIG. 2

(b) PGM Graph

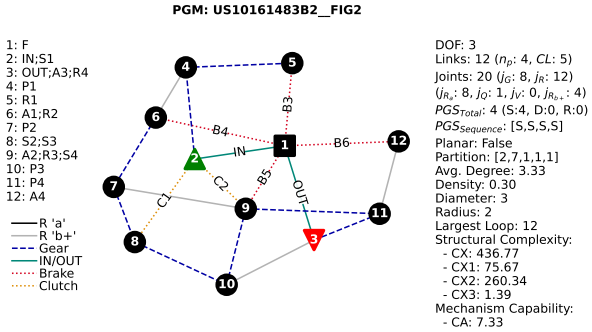

(c) DBG Graph

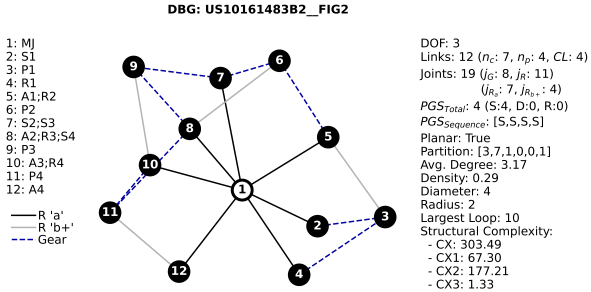

Table 96 – US10161483B2__FIG3 dataset information.

IDENTIFICATION		TOPOLOGY					GEARS SPECS		
UNIQUE_ID	**US10161483B2__FIG3**	**PGS**	**S/D**	**+/-**	**CLs**	**SCs**	**GEARS**	**Ratios**	**Engaged SCs**
Source	patent	1	S	F	IN;S1	C1: IN;S2	R2	-7	B3;B5
Owner	ALLISON	2	S	IN	OUT;A3;S4	C2: IN;A2	R1	-20	B3;B6
Patent	US10161483B2	3	S	OUT	A1;R2	B3: F;R1	1	9	C1;B6
Date	2011	4	S		A2;R3;R4	B4: F;R2	2	6	C1;B5
Model	FIG3				S2;S3	B5: F;R3	3	4.5	C1;B4
Commercial?	false					B6: F;A4	4	3	C1;B3
Longitudinal	true						5	1.1	C1;C2
Transversal	false						6	0.99	C2;B3
Weight (kg)							7	0.25	C2;B4
Máx. Torque (N·m)									

Figure 125 – US10161483B2__FIG3 representations.

(a) Functional diagram

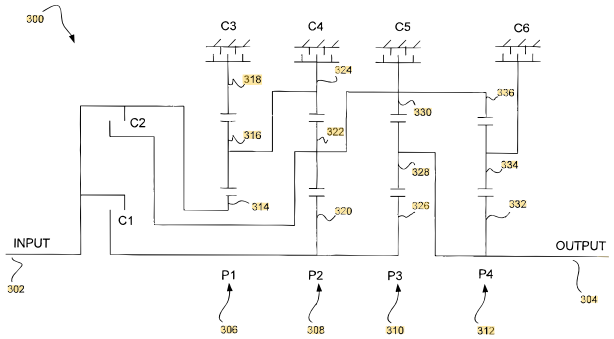

FIG. 3

(b) PGM Graph

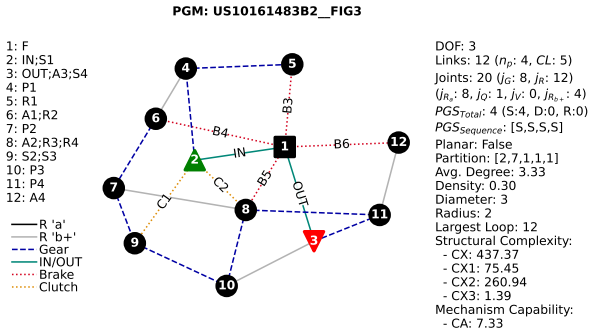

(c) DBG Graph

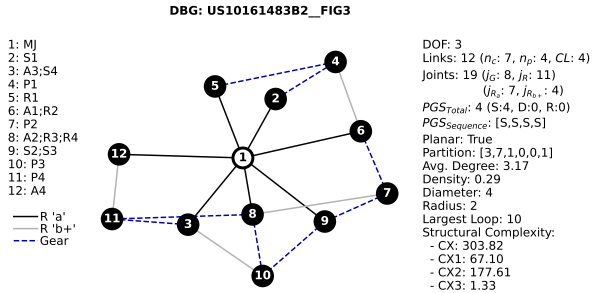

Table 97 – US10323726B2__FIG1 dataset information.

IDENTIFICATION		TOPOLOGY					GEARS SPECS		
UNIQUE_ID	**US10323726B2__FIG1**	**PGS**	**S/D**	**+/-**	**CLs**	**SCs**	**GEARS**	**Ratios**	**Engaged SCs**
Source	patent	1	S	F	IN;R4	C1: R3;R4	R1	-2.071	C1;C4;B1
Owner	HYUNDAI	2	S	IN	S1;A4	C2: S3;A4	1	5.453	C1;C4;B2
Patent	US10323726B2	3	S	OUT	OUT;A1;A2;A3	C3: S3;S4	2	3.259	C2;C4;B2
Date	2017	4	S		R2;R3	C4: S2;S4	3	2.968	C3;C4;B2
Model	FIG1					B1: F;S1	4	2.45	C2;C3;B2
Commercial?	false					B2: F;R1	5	1.988	C1;C3;B2
Longitudinal	false						6	1.522	C1;C2;B2
Transversal	true						7	1	C1;C2;C3
Weight (kg)							8	0.64	C1;C2;B1
Máx. Torque (N·m)							9	0.319	C1;C3;B1

Figure 126 – US10323726B2__FIG1 representations.

(a) Functional diagram

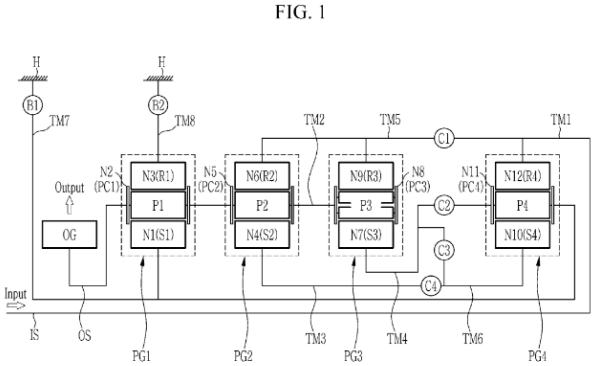

(b) PGM Graph

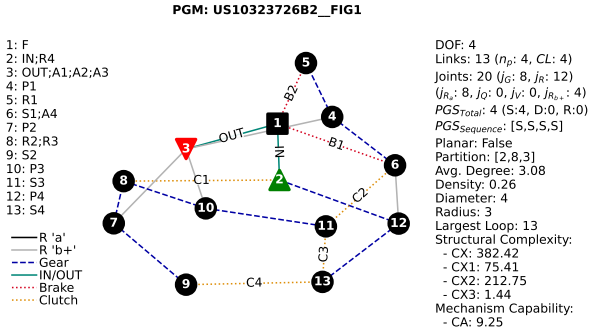

(c) DBG Graph

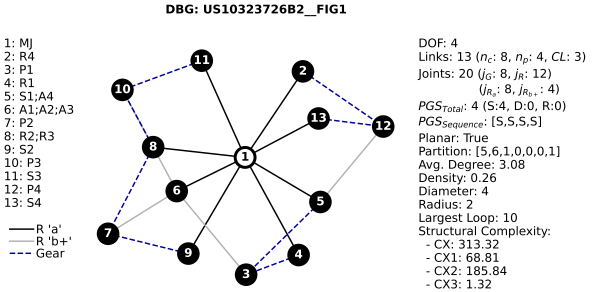

Table 98 – US10323726B2__FIG4 dataset information.

IDENTIFICATION		TOPOLOGY					GEARS SPECS		
UNIQUE_ID	**US10323726B2__FIG4**	**PGS**	**S/D**	**+/-**	**CLs**	**SCs**	**GEARS**	**Ratios**	**Engaged SCs**
Source	patent	1	S	F	IN;R4	C1: R3;R4	R1	-2.071	C1;C4;B1
Owner	HYUNDAI	2	S	IN	S1;A4	C2: S3;A4	1	5.453	C1;C4;B2
Patent	US10323726B2	3	D	OUT	OUT;A1;A2;A3	C3: S3;S4	2	3.259	C2;C4;B2
Date	2017	4	S		P2;P3R	C4: S2;S4	3	2.968	C3;C4;B2
Model	FIG4				R2;R3	B1: F;S1	4	2.45	C2;C3;B2
Commercial?	false					B2: F;R1	5	1.988	C1;C3;B2
Longitudinal	false						6	1.522	C1;C2;B2
Transversal	true						7	1	C1;C2;C3
Weight (kg)							8	0.64	C1;C2;B1
Máx. Torque (N·m)							9	0.319	C1;C3;B1

Figure 127 – US10323726B2__FIG4 representations.

(a) Functional diagram

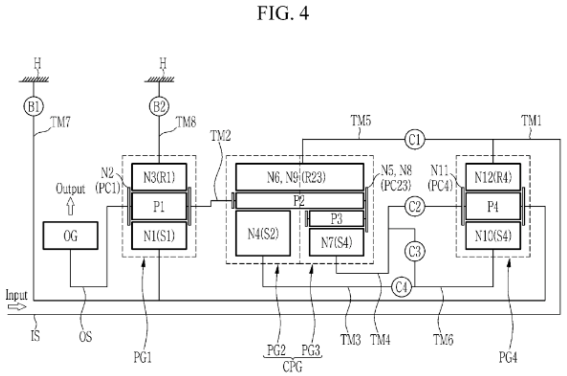

(b) PGM Graph

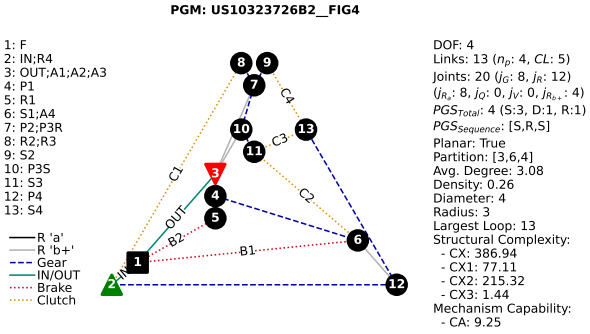

(c) DBG Graph

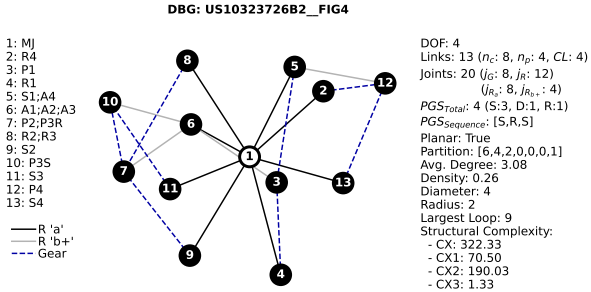

Table 99 – US10563738B2__FIG1 dataset information.

IDENTIFICATION		TOPOLOGY					GEARS SPECS		
UNIQUE_ID	**US10563738B2__FIG1**	**PGS**	**S/D**	**+/-**	**CLs**	**SCs**	**GEARS**	**Ratios**	**Engaged SCs**
Source	patent	1	D	F	F;S1	C1: R1;S3	R1	-4.254	C3;B2
Owner	TOYOTA	2	S	IN	IN;A1	C2: IN;A2	1	5.2	C1;B2
Patent	US10563738B2	3	D	OUT	P2;P3R	C3: R1;S2	2	2.971	C1;B1
Date	2015				OUT;R2;R3	C4: A1;S2	3	1.95	C1;C3
Model	FIG1				A2;A3	B1: F;S2	4	1.469	C1;C4
Commercial?	false					B2: F;A2	5	1.223	C1;C2
Longitudinal	false						6	1	C2;C4
Transversal	true						7	0.817	C2;C3
Weight (kg)	96						8	0.685	C2;B1
Máx. Torque (N·m)	350								

Figure 128 – US10563738B2__FIG1 representations.

(a) Functional diagram

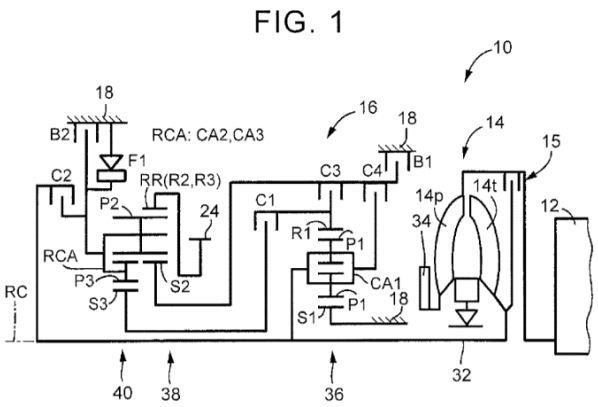

(b) PGM Graph

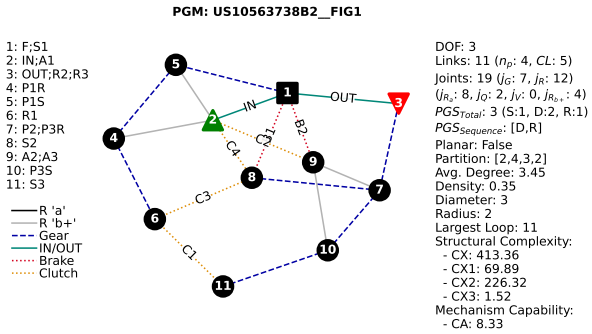

(c) DBG Graph

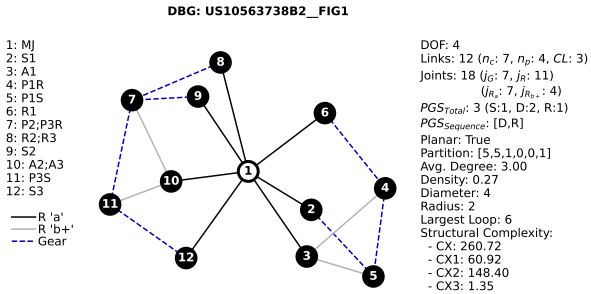

Table 100 – US10612627B2__FIG1 dataset information.

IDENTIFICATION		TOPOLOGY					GEARS SPECS		
UNIQUE_ID	**US10612627B2__FIG1**	**PGS**	**S/D**	**+/-**	**CLs**	**SCs**	**GEARS**	**Ratios**	**Engaged SCs**
Source	patent	1	S	F	S1;S2	C1: A2;R3	R1	-4.921	B1;B2;C3;C4
Owner	HYUNDAI	2	S	IN	A1;R4	B1: F;S1	1	5.1	C1;B1;B2;C4
Patent	US10612627B2	3	S	OUT	IN;A2	B2: F;R1	2	3.211	B1;B2;C2;C4
Date	2017	4	S	-S5	R3;S4	C2: R2;A3	3	2.113	C1;B2;C2;C4
Model	FIG1	5	S		P4;P5	C3: A3;R5	4	1.704	B2;C2;C3;C4
Commercial?	false				OUT;A4;A5	C4: R2;S3	5	1.488	C1;B2;C2;C3
Longitudinal	true						6	1.269	C1;B2;C3;C4
Transversal	false						7	1	C1;C2;C3;C4
Weight (kg)							8	0.843	C1;B1;C3;C4
Máx. Torque (N·m)							9	0.686	C1;B1;C2;C3
							10	0.63	B1;C2;C3;C4

Figure 129 – US10612627B2__FIG1 representations.

(a) Functional diagram

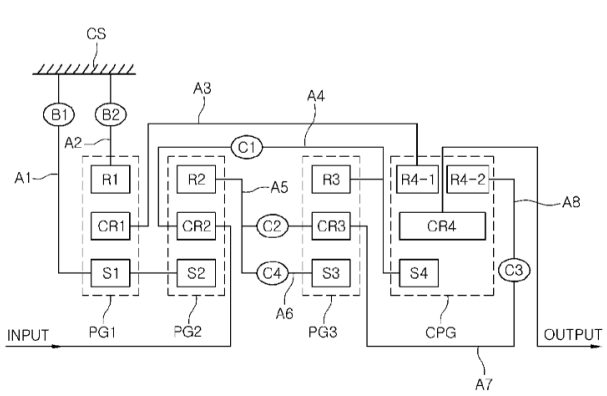

(b) PGM Graph

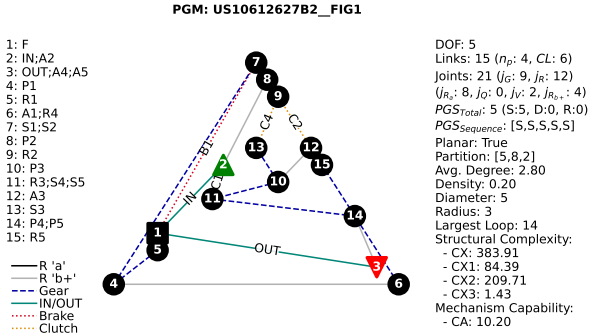

(c) DBG Graph

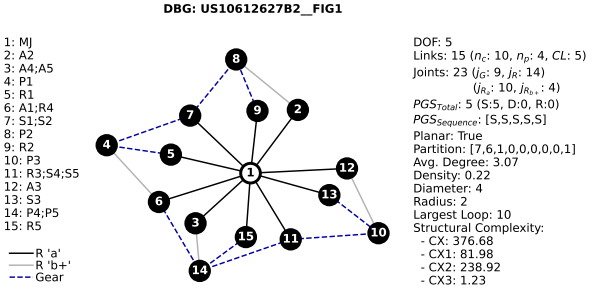

Table 101 – US10612627B2__FIG2 dataset information.

IDENTIFICATION		TOPOLOGY					GEARS SPECS		
UNIQUE_ID	**US10612627B2__FIG2**	**PGS**	**S/D**	**+/-**	**CLs**	**SCs**	**GEARS**	**Ratios**	**Engaged SCs**
Source	patent	1	S	F	S1;S2	C1: A2;R3	R1	-4.921	B1;B2;C3;C4
Owner	HYUNDAI	2	S	IN	A1;R4	B1: F;S1	1	5.1	C1;B1;B2;C4
Patent	US10612627B2	3	S	OUT	IN;A2	B2: F;R1	2	3.211	B1;B2;C2;C4
Date	2017	4	S		R3;S4;S5	C2: R2;A3	3	2.113	C1;B2;C2;C4
Model	FIG2	5	S		OUT;A4;A5	C3: A3;R5	4	1.704	B2;C2;C3;C4
Commercial?	false					C4: R2;S3	5	1.488	C1;B2;C2;C3
Longitudinal	true						6	1.269	C1;B2;C3;C4
Transversal	false						7	1	C1;C2;C3;C4
Weight (kg)							8	0.843	C1;B1;C3;C4
Máx. Torque (N·m)							9	0.686	C1;B1;C2;C3
							10	0.63	B1;C2;C3;C4

Figure 130 – US10612627B2__FIG2 representations.

(a) Functional diagram

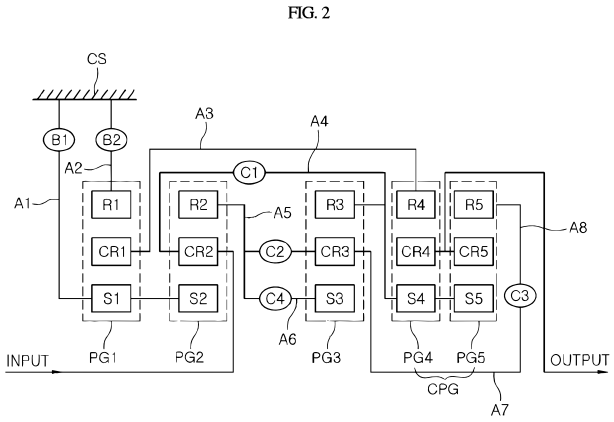

(b) PGM Graph

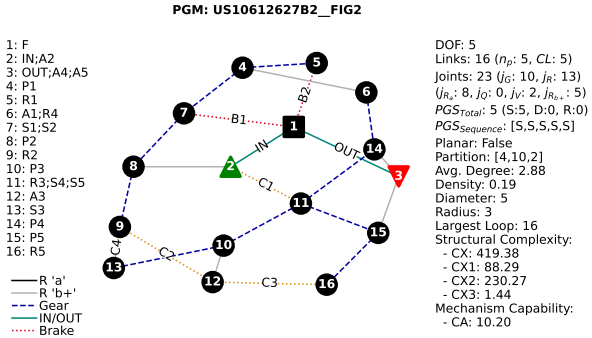

(c) DBG Graph

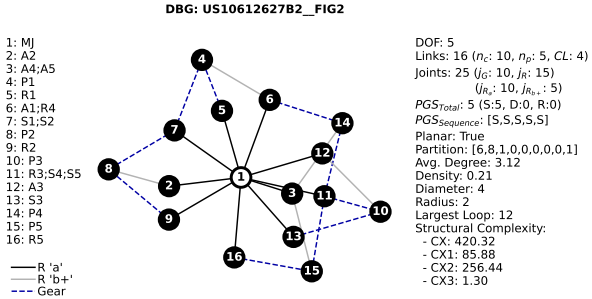

Table 102 – US10612627B2__FIG3 dataset information.

IDENTIFICATION		TOPOLOGY					GEARS SPECS		
UNIQUE_ID	**US10612627B2__FIG3**	**PGS**	**S/D**	**+/-**	**CLs**	**SCs**	**GEARS**	**Ratios**	**Engaged SCs**
Source	patent	1	S	F	S1;S2	C1: A2;R3	R1	-4.921	B1;B2;C3;C4
Owner	HYUNDAI	2	S	IN	A1;R4	B1: F;S1	1	5.1	C1;B1;B2;C4
Patent	US10612627B2	3	S	OUT	IN;A2	B2: F;R1	2	3.211	B1;B2;C2;C4
Date	2017	4	S	-S5	R2;S3	C2: R2;A3	3	2.113	C1;B2;C2;C4
Model	FIG3	5	S		P4;P5	C3: A3;R5	4	1.704	B2;C2;C3;C4
Commercial?	false				OUT;A4;A5	C4: R3;S4	5	1.488	C1;B2;C2;C3
Longitudinal	true						6	1.269	C1;B2;C3;C4
Transversal	false						7	1	C1;C2;C3;C4
Weight (kg)							8	0.843	C1;B1;C3;C4
Máx. Torque (N·m)							9	0.686	C1;B1;C2;C3
							10	0.63	B1;C2;C3;C4

Figure 131 – US10612627B2__FIG3 representations.

(a) Functional diagram

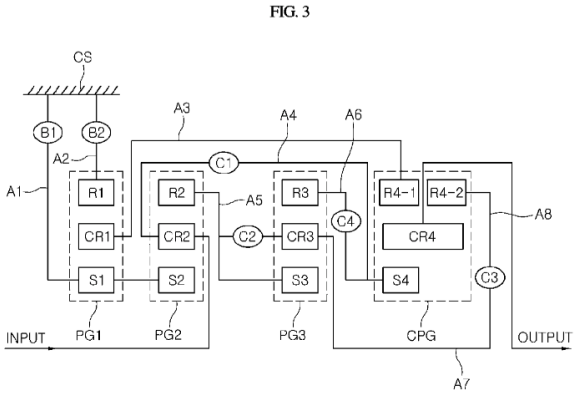

(b) PGM Graph

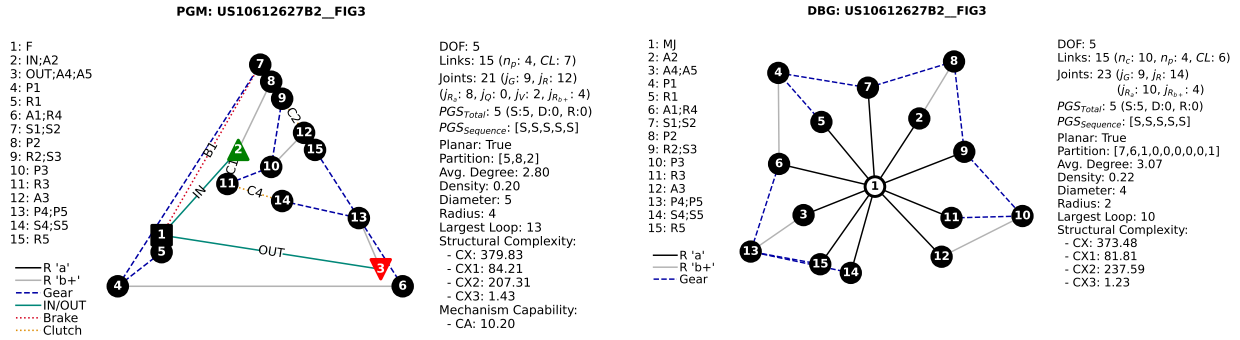

(c) DBG Graph

Table 103 – US10612627B2__FIG4 dataset information.

IDENTIFICATION		TOPOLOGY					GEARS SPECS		
UNIQUE_ID	**US10612627B2__FIG4**	**PGS**	**S/D**	**+/-**	**CLs**	**SCs**	**GEARS**	**Ratios**	**Engaged SCs**
Source	patent	1	S	F	S1;S2	C1: A2;S4	R1	-4.921	B1;B2;C3;C4
Owner	HYUNDAI	2	S	IN	A1;R4	B1: F;S1	1	5.1	C1;B1;B2;C4
Patent	US10612627B2	3	S	OUT	IN;A2	B2: F;R1	2	3.211	B1;B2;C2;C4
Date	2017	4	S		S4;S5	C2: R2;A3	3	2.113	C1;B2;C2;C4
Model	FIG4	5	S		OUT;A4;A5	C3: A3;R5	4	1.704	B2;C2;C3;C4
Commercial?	false				R2;S3	C4: R3;S4	5	1.488	C1;B2;C2;C3
Longitudinal	true						6	1.269	C1;B2;C3;C4
Transversal	false						7	1	C1;C2;C3;C4
Weight (kg)							8	0.843	C1;B1;C3;C4
Máx. Torque (N·m)							9	0.686	C1;B1;C2;C3
							10	0.63	B1;C2;C3;C4

Figure 132 – US10612627B2__FIG4 representations.

(a) Functional diagram

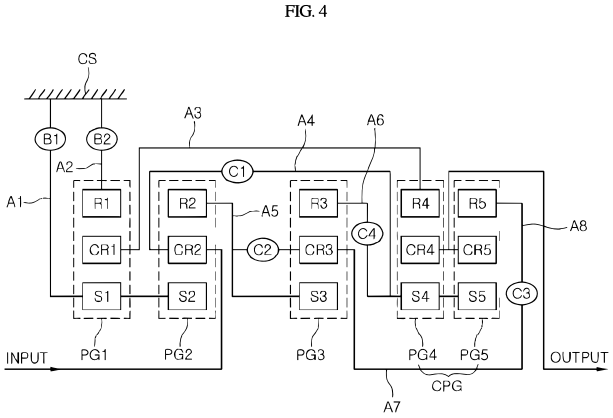

(b) PGM Graph

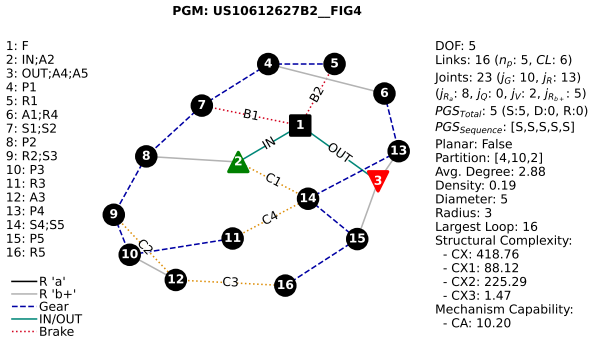

(c) DBG Graph

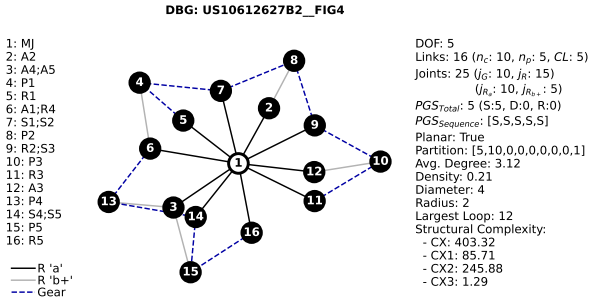

Table 104 – US10612627B2__FIG5 dataset information.

IDENTIFICATION		TOPOLOGY					GEARS SPECS		
UNIQUE_ID	**US10612627B2__FIG5**	**PGS**	**S/D**	**+/-**	**CLs**	**SCs**	**GEARS**	**Ratios**	**Engaged SCs**
Source	patent	1	S	F	S1;S2	C1: A2;S4	R1	-4.921	B1;B2;C3;C4
Owner	HYUNDAI	2	S	IN	A1;R4	B1: F;S1	1	5.1	C1;B1;B2;C4
Patent	US10612627B2	3	S	OUT	IN;A2	B2: F;R1	2	3.211	B1;B2;C2;C4
Date	2017	4	S	-S5	R2;S3	C2: R2;R3	3	2.113	C1;B2;C2;C4
Model	FIG5	5	S		P4;P5	C3: A3;R5	4	1.704	B2;C2;C3;C4
Commercial?	false				OUT;A4;A5	C4: R3;S4	5	1.488	C1;B2;C2;C3
Longitudinal	true						6	1.269	C1;B2;C3;C4
Transversal	false						7	1	C1;C2;C3;C4
Weight (kg)							8	0.843	C1;B1;C3;C4
Máx. Torque (N·m)							9	0.686	C1;B1;C2;C3
							10	0.63	B1;C2;C3;C4

Figure 133 – US10612627B2__FIG5 representations.

(a) Functional diagram

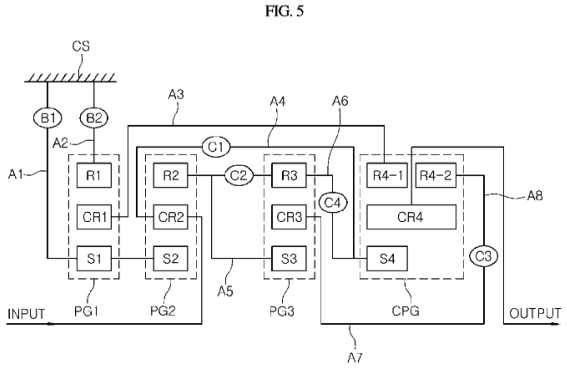

(b) PGM Graph

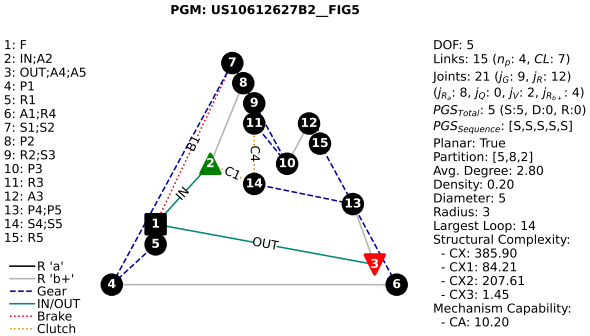

(c) DBG Graph

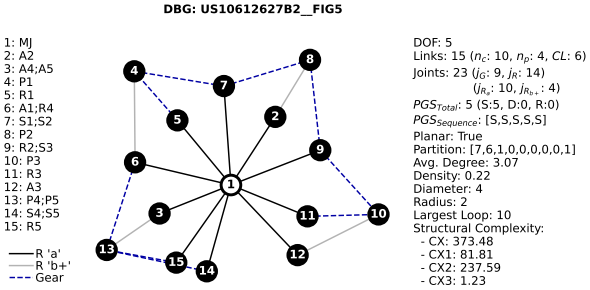

Table 105 – US10612627B2__FIG6 dataset information.

IDENTIFICATION		TOPOLOGY					GEARS SPECS		
UNIQUE_ID	**US10612627B2__FIG6**	**PGS**	**S/D**	**+/-**	**CLs**	**SCs**	**GEARS**	**Ratios**	**Engaged SCs**
Source	patent	1	S	F	S1;S2	C1: A2;S4	R1	-4.921	B1;B2;C3;C4
Owner	HYUNDAI	2	S	IN	A1;R4	B1: F;S1	1	5.100	C1;B1;B2;C4
Patent	US10612627B2	3	S	OUT	IN;A2	B2: F;R1	2	3.211	B1;B2;C2;C4
Date	2017	4	S		S4;S5	C2: R2;A3	3	2.113	C1;B2;C2;C4
Model	FIG6	5	S		OUT;A4;A5	C3: A3;R5	4	1.704	B2;C2;C3;C4
Commercial?	false				R2;S3	C4: R3;S4	5	1.488	C1;B2;C2;C3
Longitudinal	true						6	1.269	C1;B2;C3;C4
Transversal	false						7	1.000	C1;C2;C3;C4
Weight (kg)							8	0.843	C1;B1;C3;C4
Máx. Torque (N·m)							9	0.686	C1;B1;C2;C3
							10	0.630	B1;C2;C3;C4

Figure 134 – US10612627B2__FIG6 representations.

(a) Functional diagram

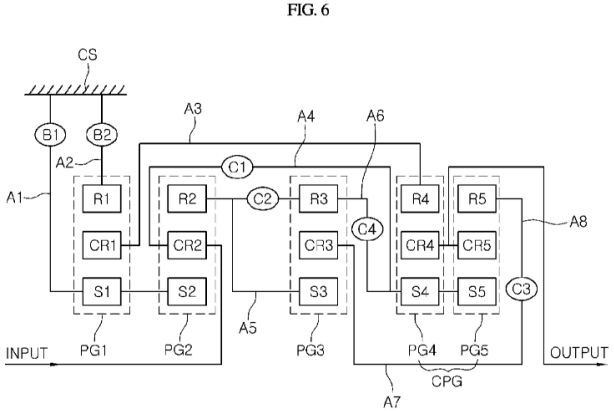

(b) PGM Graph

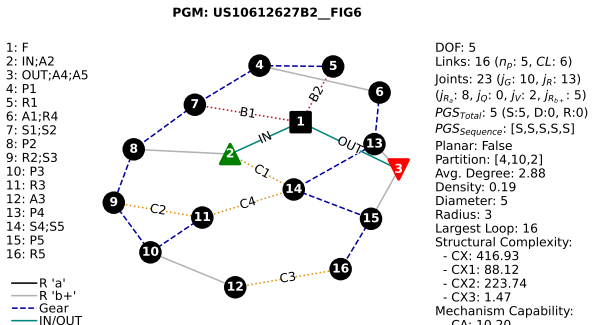

(c) DBG Graph

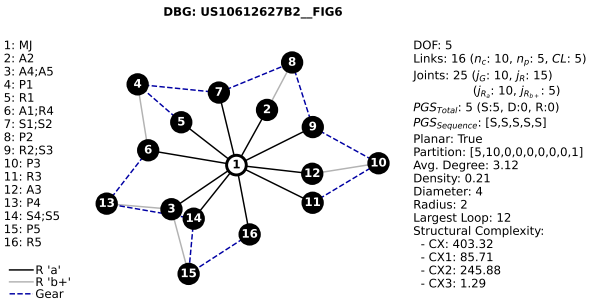

Table 106 – US10612627B2__FIG7 dataset information.

IDENTIFICATION		TOPOLOGY					GEARS SPECS		
UNIQUE_ID	**US10612627B2__FIG7**	**PGS**	**S/D**	**+/-**	**CLs**	**SCs**	**GEARS**	**Ratios**	**Engaged SCs**
Source	patent	1	S	F	S1;S2	C1: A2;S4	R1	-4.921	B1;B2;C3;C4
Owner	HYUNDAI	2	S	IN	A1;R4	B1: F;S1	1	5.1	C1;B1;B2;C4
Patent	US10612627B2	3	S	OUT	IN;A2	B2: F;R1	2	3.211	B1;B2;C2;C4
Date	2017	4	S	-S5	R2;S3	C2: A3;R3	3	2.113	C1;B2;C2;C4
Model	FIG7	5	S		P4;P5	C3: A3;R5	4	1.704	B2;C2;C3;C4
Commercial?	false				OUT;A4;A5	C4: R3;S4	5	1.488	C1;B2;C2;C3
Longitudinal	true						6	1.269	C1;B2;C3;C4
Transversal	false						7	1	C1;C2;C3;C4
Weight (kg)							8	0.843	C1;B1;C3;C4
Máx. Torque (N·m)							9	0.686	C1;B1;C2;C3
							10	0.63	B1;C2;C3;C4

Figure 135 – US10612627B2__FIG7 representations.

(a) Functional diagram

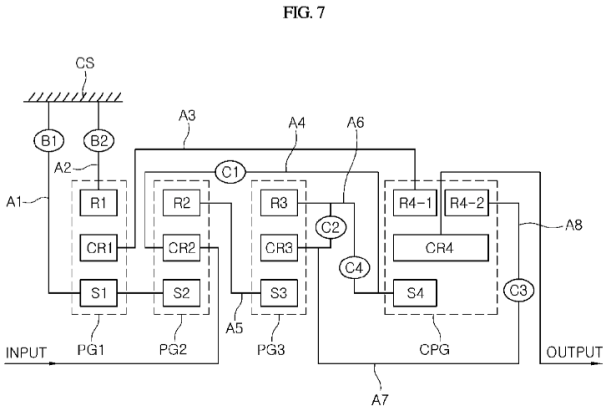

(b) PGM Graph

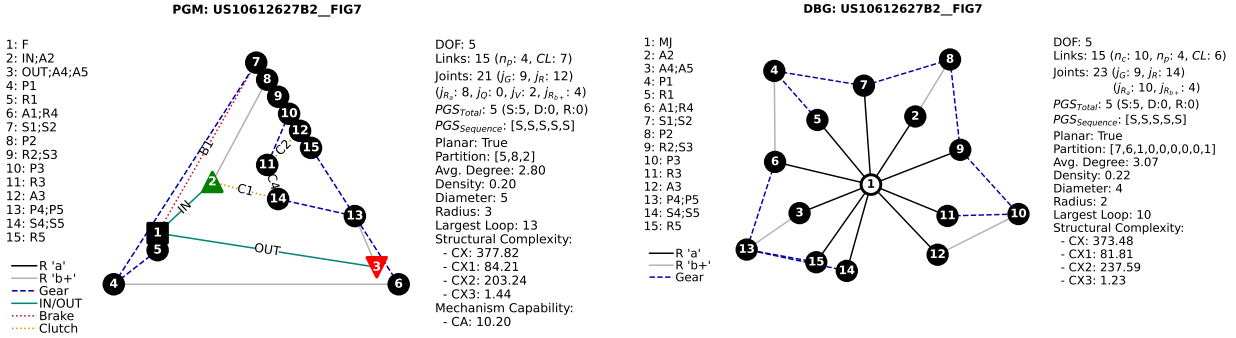

(c) DBG Graph

Table 107 – US10612627B2__FIG8 dataset information.

IDENTIFICATION		TOPOLOGY					GEARS SPECS		
UNIQUE_ID	**US10612627B2__FIG8**	**PGS**	**S/D**	**+/-**	**CLs**	**SCs**	**GEARS**	**Ratios**	**Engaged SCs**
Source	patent	1	S	F	S1;S2	C1: A2;S4	R1	-4.921	B1;B2;C3;C4
Owner	HYUNDAI	2	S	IN	A1;R4	B1: F;S1	1	5.1	C1;B1;B2;C4
Patent	US10612627B2	3	S	OUT	IN;A2	B2: F;R1	2	3.211	B1;B2;C2;C4
Date	2017	4	S		S4;S5	C2: A3;R3	3	2.113	C1;B2;C2;C4
Model	FIG8	5	S		OUT;A4;A5	C3: A3;R5	4	1.704	B2;C2;C3;C4
Commercial?	false				R2;S3	C4: R3;S4	5	1.488	C1;B2;C2;C3
Longitudinal	true						6	1.269	C1;B2;C3;C4
Transversal	false						7	1	C1;C2;C3;C4
Weight (kg)							8	0.843	C1;B1;C3;C4
Máx. Torque (N·m)							9	0.686	C1;B1;C2;C3
							10	0.63	B1;C2;C3;C4

Figure 136 – US10612627B2__FIG8 representations.

(a) Functional diagram

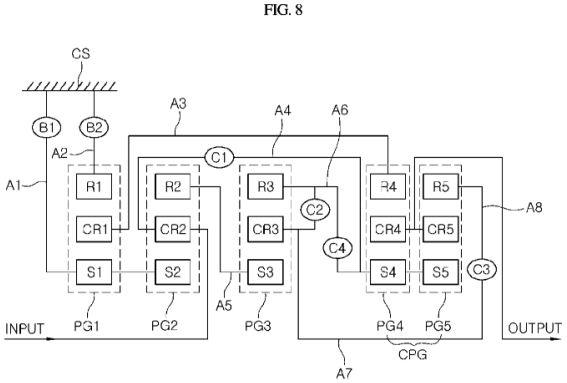

(b) PGM Graph

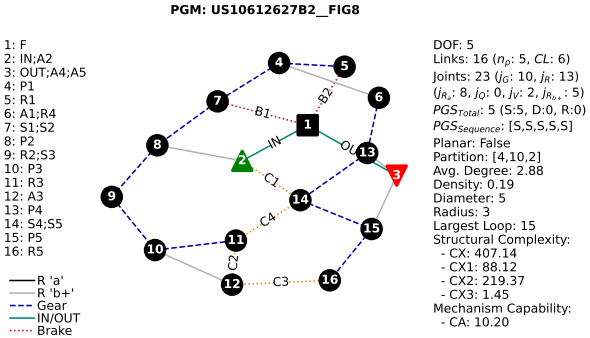

(c) DBG Graph

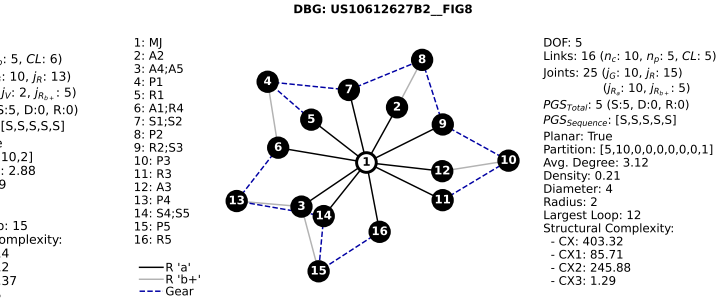

Table 108 – US10612627B2__FIG9 dataset information.

IDENTIFICATION		TOPOLOGY					GEARS SPECS		
UNIQUE_ID	**US10612627B2__FIG9**	**PGS**	**S/D**	**+/-**	**CLs**	**SCs**	**GEARS**	**Ratios**	**Engaged SCs**
Source	patent	1	S	F	S1;S2	C1: A2;S4	R1	-4.921	B1;B2;C3;C4
Owner	HYUNDAI	2	S	IN	A1;R4	B1: F;S1	1	5.1	C1;B1;B2;C4
Patent	US10612627B2	3	S	OUT	IN;A2	B2: F;R1	2	3.211	B1;B2;C2;C4
Date	2017	4	S	-S5	A3;R5	C2: R2;R3	3	2.113	C1;B2;C2;C4
Model	FIG9	5	S		P4;P5	C3: R2;S3	4	1.704	B2;C2;C3;C4
Commercial?	false				OUT;A4;A5	C4: R3;S4	5	1.488	C1;B2;C2;C3
Longitudinal	true						6	1.269	C1;B2;C3;C4
Transversal	false						7	1	C1;C2;C3;C4
Weight (kg)							8	0.843	C1;B1;C3;C4
Máx. Torque (N·m)							9	0.686	C1;B1;C2;C3
							10	0.63	B1;C2;C3;C4

Figure 137 – US10612627B2__FIG9 representations.

(a) Functional diagram

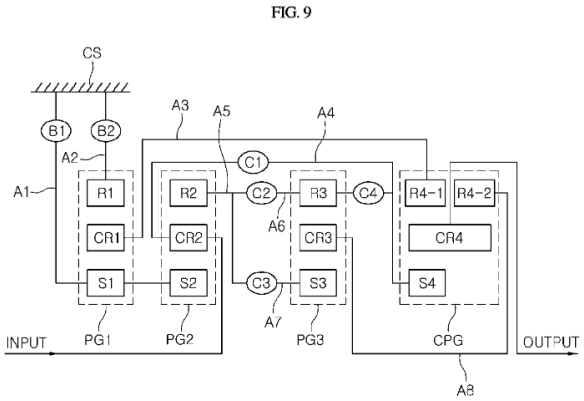

(b) PGM Graph

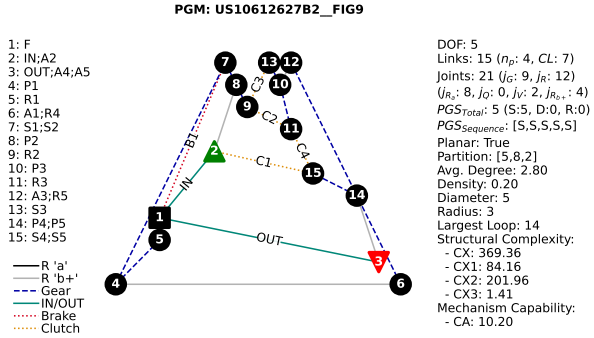

(c) DBG Graph

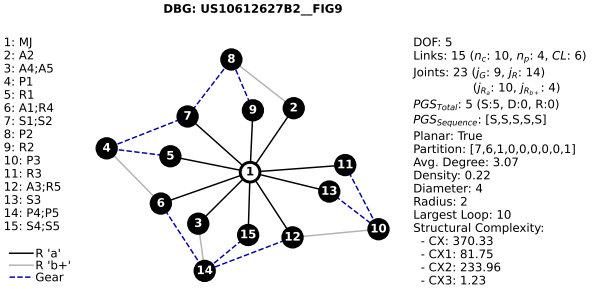

Table 109 – US10612627B2__FIG10 dataset information.

IDENTIFICATION		TOPOLOGY					GEARS SPECS		
UNIQUE_ID	**US10612627B2__FIG10**	**PGS**	**S/D**	**+/-**	**CLs**	**SCs**	**GEARS**	**Ratios**	**Engaged SCs**
Source	patent	1	S	F	S1;S2	C1: A2;S4	R1	-4.921	B1;B2;C3;C4
Owner	HYUNDAI	2	S	IN	A1;R4	B1: F;S1	1	5.1	C1;B1;B2;C4
Patent	US10612627B2	3	S	OUT	IN;A2	B2: F;R1	2	3.211	B1;B2;C2;C4
Date	2017	4	S		A3;R5	C2: R2;R3	3	2.113	C1;B2;C2;C4
Model	FIG10	5	S		S4;S5	C3: R2;S3	4	1.704	B2;C2;C3;C4
Commercial?	false				OUT;A4;A5	C4: R3;S4	5	1.488	C1;B2;C2;C3
Longitudinal	true						6	1.269	C1;B2;C3;C4
Transversal	false						7	1	C1;C2;C3;C4
Weight (kg)							8	0.843	C1;B1;C3;C4
Máx. Torque (N·m)							9	0.686	C1;B1;C2;C3
							10	0.63	B1;C2;C3;C4

Figure 138 – US10612627B2__FIG10 representations.

(a) Functional diagram

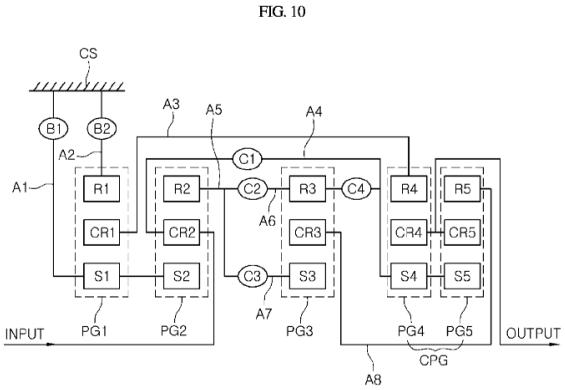

(b) PGM Graph

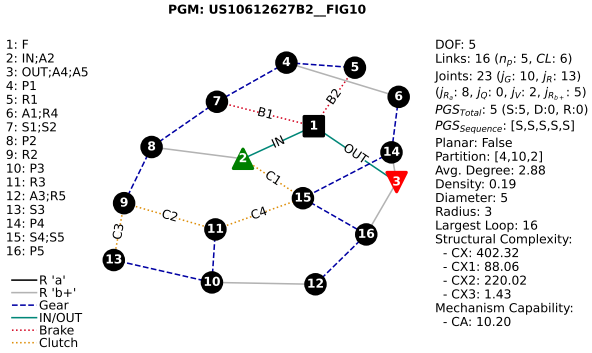

(c) DBG Graph

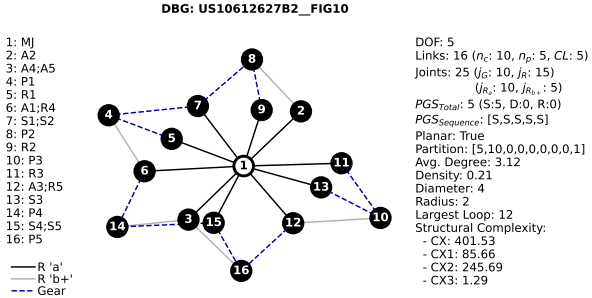

Table 110 – US11199246B2__FIG1 dataset information.

IDENTIFICATION		TOPOLOGY					GEARS SPECS		
UNIQUE_ID	**US11199246B2__FIG1**	**PGS**	**S/D**	**+/-**	**CLs**	**SCs**	**GEARS**	**Ratios**	**Engaged SCs**
Source	patent	1	S	F	IN;A1;A2	C1: A1;S4	R1	-4.034	C3;B1;B2
Owner	MAZDA	2	S	IN	P1;P2	C2: R1;S4	1	5.258	C1;B1;B2
Patent	US11199246B2	3	S	OUT	R1;R2;S3	C3: R2;S4	2	3.303	C2;B1;B2
Date	2019	4	S		S2;S5	B1: F;S1	3	2.129	C1;C2;B2
Model	FIG1	5	S		OUT;A3;A5	B2: F;R4	4	1.705	C2;C3;B2
Commercial?	true				A4;R5		5	1.3	C1;C3;B2
Longitudinal	true						6	1	C1;C2;C3
Transversal	false						7	0.822	C1;C3;B1
Weight (kg)							8	0.628	C2;C3;B1
Máx. Torque (N·m)									

Figure 139 – US11199246B2__FIG1 representations.

(a) Functional diagram

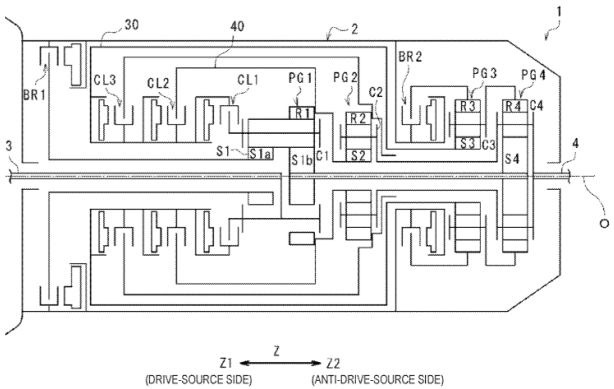

FIG. 1

(b) PGM Graph

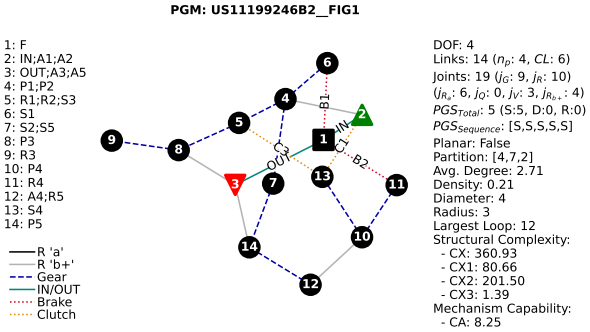

(c) DBG Graph

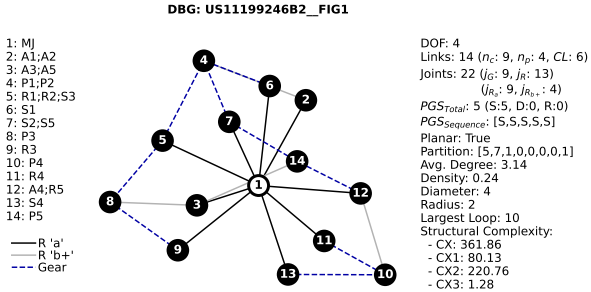

Table 111 – US11231105B2__FIG2 dataset information.

IDENTIFICATION		TOPOLOGY					GEARS SPECS		
UNIQUE_ID	**US11231105B2__FIG2**	**PGS**	**S/D**	**+/-**	**CLs**	**SCs**	**GEARS**	**Ratios**	**Engaged SCs**
Source	patent	1	D	F	F;S1	C1: R1;S3	R2		C4;B2
Owner	TOYOTA	2	S	IN	IN;A1	C2: IN;A3	R1		C3;B2
Patent	US11231105B2	3	D	OUT	P2;P3R	C3: S2;R1	1		C1;B2
Date	2018				OUT;R2;R3	C4: IN;S2	2		C1;B1
Model	FIG2				A2;A3	B1: F;S2	3		C1;C3
Commercial?	false					B2: F;A3	4		C1;C4
Longitudinal	false						5		C1;C2
Transversal	true						6		C2;C4
Weight (kg)							7		C2;C3
Máx. Torque (N·m)							8		C2;B2

Figure 140 – US11231105B2__FIG2 representations.

(a) Functional diagram

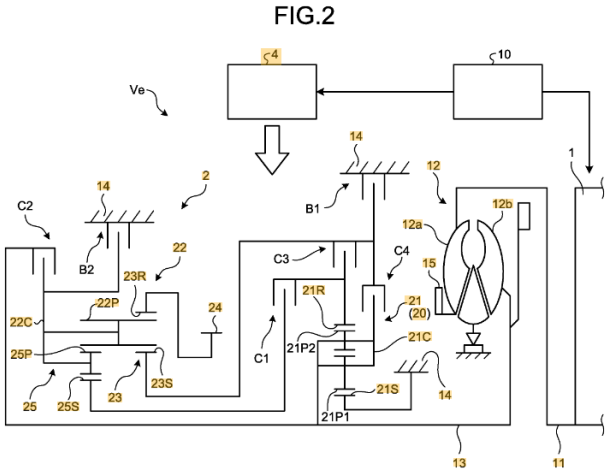

(b) PGM Graph

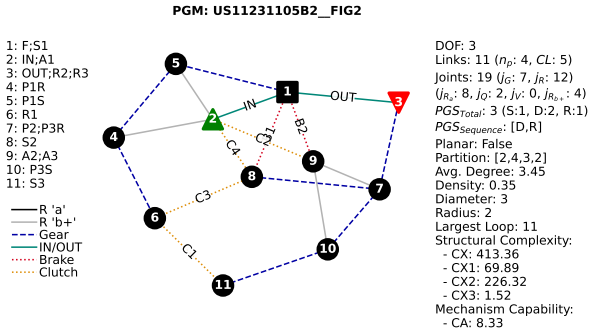

(c) DBG Graph

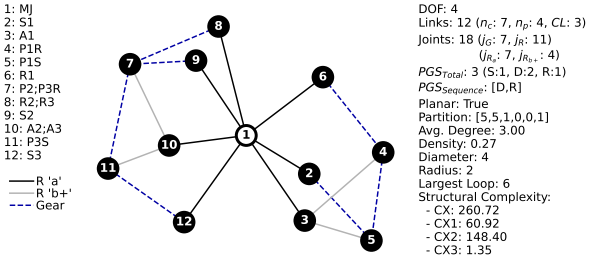

Table 112 – US11248699B2__FIG_1 dataset information.

IDENTIFICATION		TOPOLOGY					GEARS SPECS		
UNIQUE_ID	**US11248699B2__FIG_1**	**PGS**	**S/D**	**+/-**	**CLs**	**SCs**	**GEARS**	**Ratios**	**Engaged SCs**
Source	patent	1	S	F	IN;S1	C1: IN;S5	R1	-5	C3;B1;B3
Owner	HYUNDAI	2	S	IN	A1;S2;S3	C2: IN;A3	1	5.863	C1;B1;B3
Patent	US11248699B2	3	S	OUT	R1;S4	C3: R2;A4	2	3.646	C2;B1;B3
Date	2018	4	S		A4;R5	B1: F;A1	3	2.616	C2;B2;B3
Model	FIG_1	5	S		A2;R3;S5	B2: F;R1	4	1.801	C1;C2;B3
Commercial?	false				OUT;A5	B3: F;R4	5	1.442	C2;C3;B3
Longitudinal	true						6	1.195	C1;C3;B3
Transversal	false						7	1	C1;C2;C3
Weight (kg)							8	0.879	C1;C3;B2
Máx. Torque (N·m)							9	0.724	C2;C3;B2
							10	0.617	C2;C3;B1

Figure 141 – US11248699B2__FIG_1 representations.

(a) Functional diagram

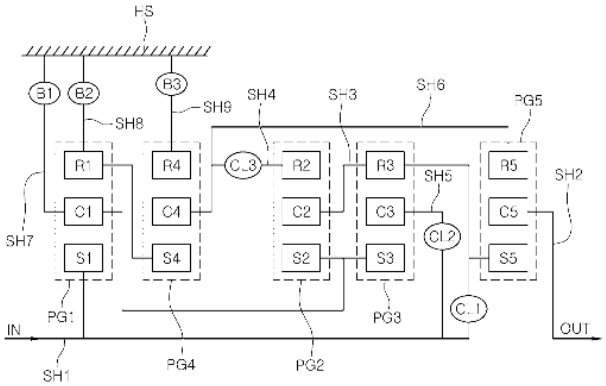

(b) PGM Graph

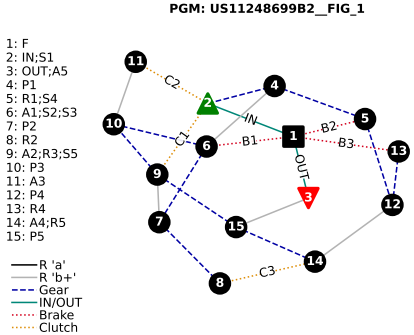

(c) DBG Graph

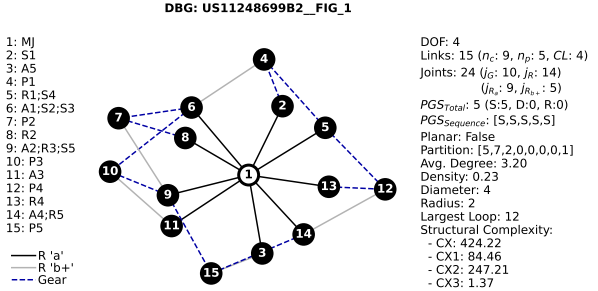

Table 113 – US11248699B2__FIG_3 dataset information.

IDENTIFICATION		TOPOLOGY					GEARS SPECS		
UNIQUE_ID	**US11248699B2__FIG_3**	**PGS**	**S/D**	**+/-**	**CLs**	**SCs**	**GEARS**	**Ratios**	**Engaged SCs**
Source	patent	1	S	F	IN;S1	C1: IN;S5	R1	-5	C3;B1;B3
Owner	HYUNDAI	2	S	IN	A1;S2;S3	C2: IN;A3	1	5.863	C1;B1;B3
Patent	US11248699B2	3	S	OUT	R1;S4	C3: R2;A5	2	3.646	C2;B1;B3
Date	2018	4	S		A4;R5	B1: F;A1	3	2.616	C2;B2;B3
Model	FIG_3	5	S		A2;R3;S5	B2: F;R1	4	1.801	C1;C2;B3
Commercial?	false				OUT;A5	B3: F;R4	5	1.442	C2;C3;B3
Longitudinal	true						6	1.195	C1;C3;B3
Transversal	false						7	1	C1;C2;C3
Weight (kg)							8	0.879	C1;C3;B2
Máx. Torque (N·m)							9	0.724	C2;C3;B2
							10	0.617	C2;C3;B1

Figure 142 – US11248699B2__FIG_3 representations.

(a) Functional diagram

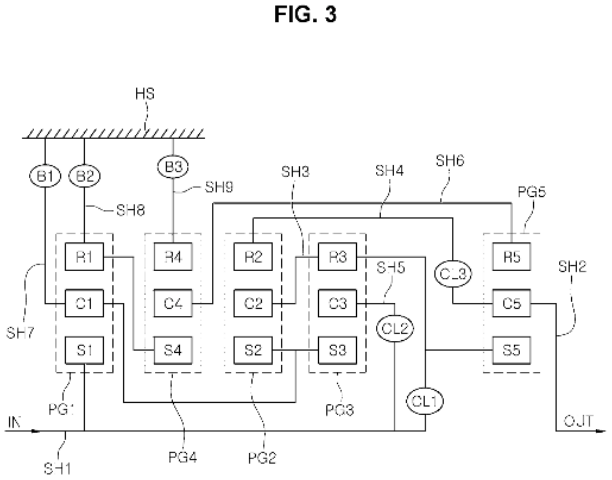

(b) PGM Graph

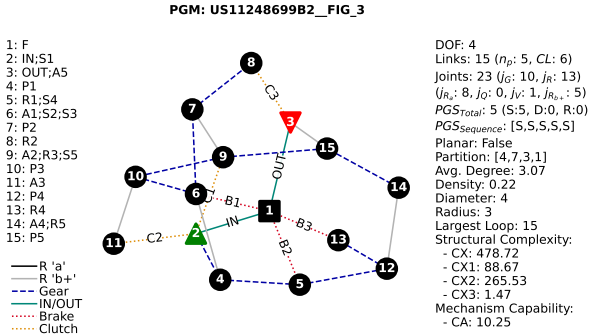

(c) DBG Graph

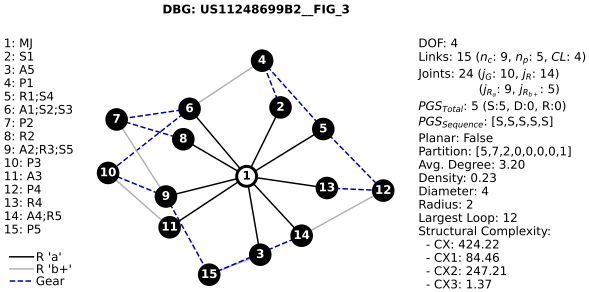

Table 114 – US5599251A__FIG1 dataset information.

IDENTIFICATION		TOPOLOGY					GEARS SPECS		
UNIQUE_ID	**US5599251A__FIG1**	**PGS**	**S/D**	**+/-**	**CLs**	**SCs**	**GEARS**	**Ratios**	**Engaged SCs**
Source	patent	1	S	F	A1;S2	B1: F;S3	R2		C1;B3
Owner	FORD	2	S	IN	IN;R1	B2: F;S1	R1		B3
Patent	US5599251A	3	S	OUT	A2;R3	C1: S1;R1	1		B1;B2
Date	1995				OUT;R2;A3	C2: R1;A2	2		B1;C1
Model	FIG1					B3: F;A2	3		B1;C2
Commercial?	false					B4: F;A1	4		C1;C2
Longitudinal	true						5		B2;C2
Transversal	false						6		C2;B4
Weight (kg)									
Máx. Torque (N·m)									

Figure 143 – US5599251A__FIG1 representations.

(a) Functional diagram

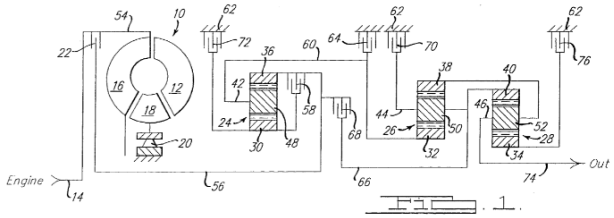

(b) PGM Graph

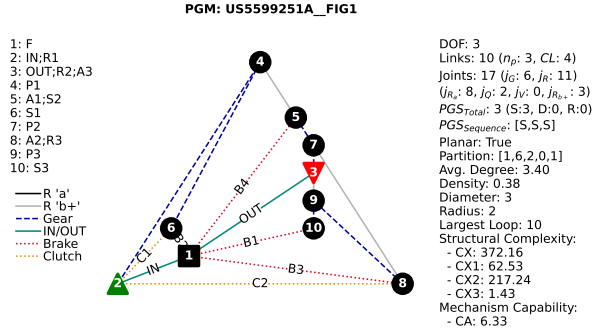

(c) DBG Graph

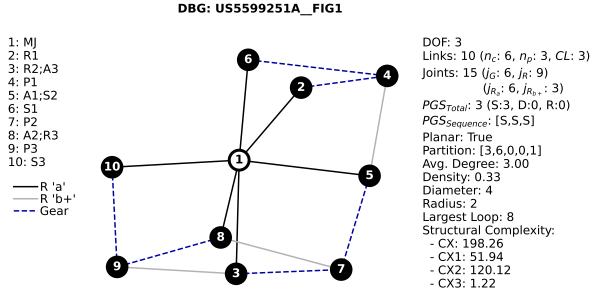

Table 115 – US6422969B1__FIG1 dataset information.

IDENTIFICATION		TOPOLOGY					GEARS SPECS		
UNIQUE_ID	**US6422969B1__FIG1**	**PGS**	**S/D**	**+/-**	**CLs**	**SCs**	**GEARS**	**Ratios**	**Engaged SCs**
Source	patent	1	S	F	IN;R1;S2	B1: F;S1	R1	-3.46	B1;B3
Owner	GM	2	S	IN	A1;A2	B2: F;R2	1	3.94	B3;C2
Patent	US6422969B1	3	S	OUT	R2;S3	B3: F;A3	2	2.05	B2;C2
Date	2000				OUT;R3	C1: S2;A3	3	1.33	B1;C2
Model	FIG1					C2: A2;A3	4	1	C1;C2
Commercial?	false						5	0.78	B1;C1
Longitudinal	true						6	0.64	B2;C1
Transversal	false								
Weight (kg)									
Máx. Torque (N·m)									

Figure 144 – US6422969B1__FIG1 representations.

(a) Functional diagram

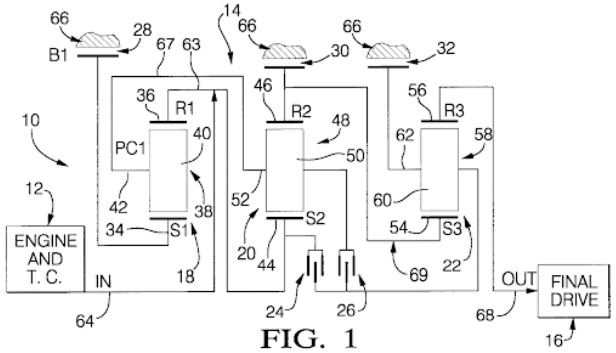

FIG. 1

(b) PGM Graph

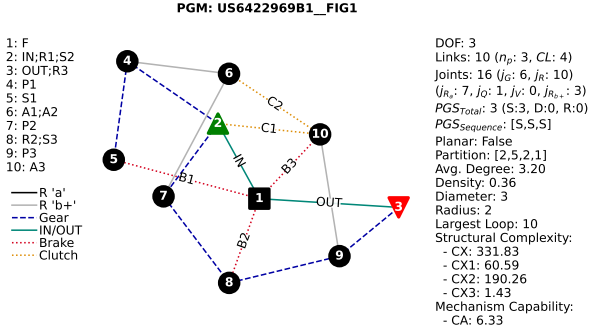

(c) DBG Graph

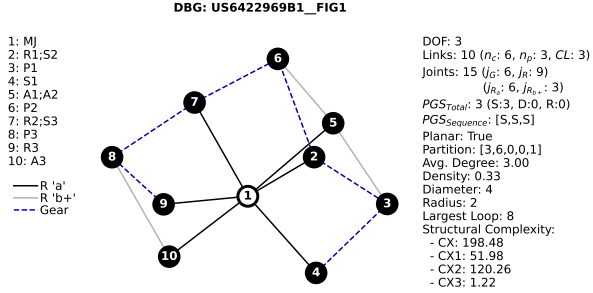

Table 116 – US6422969B1__FIG3 dataset information.

IDENTIFICATION		TOPOLOGY					GEARS SPECS		
UNIQUE_ID	**US6422969B1__FIG3**	**PGS**	**S/D**	**+/-**	**CLs**	**SCs**	**GEARS**	**Ratios**	**Engaged SCs**
Source	patent	1	S	F	IN;R1;A2	B1: F;S1	R1	-2.87	B1;B3
Owner	GM	2	D	IN	A1;R2	B2: F;A3	1	4.14	B3;C2
Patent	US6422969B1	3	D	OUT	S2;A3	B3: F;R3	2	2.4	B2;C2
Date	2000				OUT;S3	C1: A2;R3	3	1.5	B1;C2
Model	FIG3					C2: A1;OUT	4	1	C1;C2
Commercial?	false						5	0.68	B1;C1
Longitudinal	true						6	0.55	B2;C1
Transversal	false								
Weight (kg)									
Máx. Torque (N·m)									

Figure 145 – US6422969B1__FIG3 representations.

(a) Functional diagram

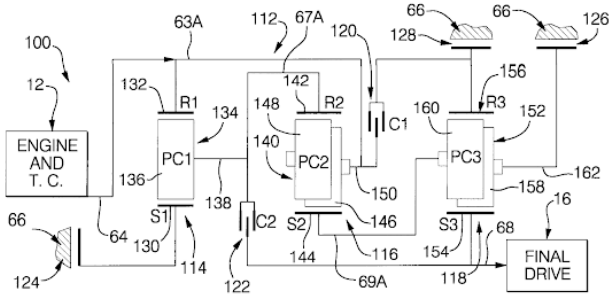

FIG. 3

(b) PGM Graph

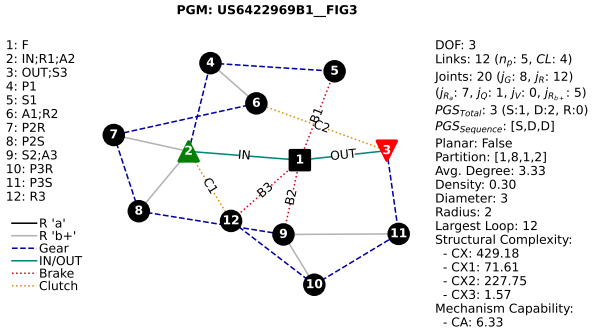

(c) DBG Graph

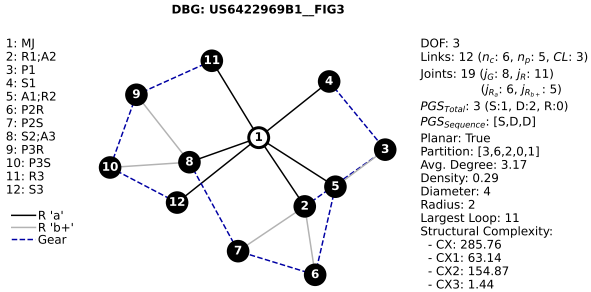

Table 117 – US6422969B1__FIG5 dataset information.

IDENTIFICATION		TOPOLOGY					GEARS SPECS		
UNIQUE_ID	**US6422969B1__FIG5**	**PGS**	**S/D**	**+/-**	**CLs**	**SCs**	**GEARS**	**Ratios**	**Engaged SCs**
Source	patent	1	D	F	IN;A1;R2	B1: F;R1	R1	-2.68	B1;C2
Owner	GM	2	S	IN	R1;A2	B2: F;S1	1	2.88	B2;C2
Patent	US6422969B1	3	S	OUT	S2;S3	B3: F;S2	2	1.58	B3;C2
Date	2000				OUT;R3	C1: A1;A3	3	1	C1;C2
Model	FIG5					C2: S1;A3	4	0.69	B3;C1
Commercial?	false						5	0.55	B2;C1
Longitudinal	true						6	0.37	B1;C1
Transversal	false								
Weight (kg)									
Máx. Torque (N·m)									

Figure 146 – US6422969B1__FIG5 representations.

(a) Functional diagram

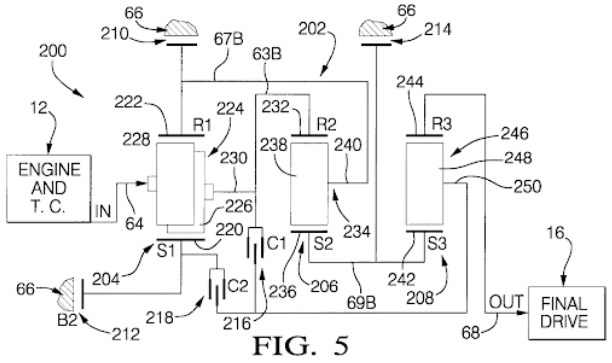

FIG. 5

(b) PGM Graph

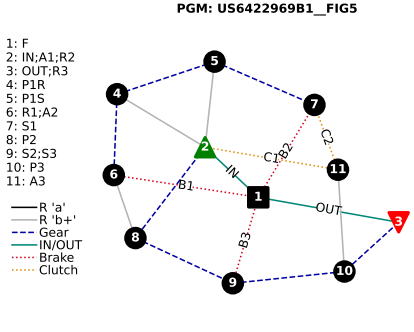

(c) DBG Graph

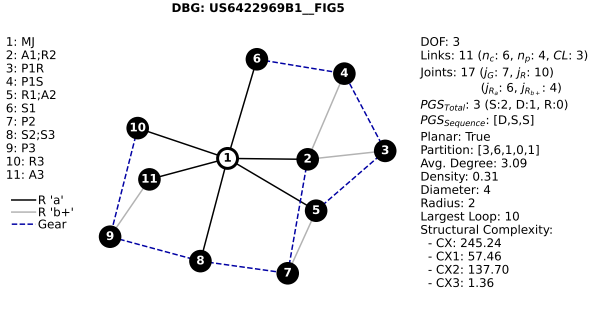

Table 118 – US6422969B1__FIG7 dataset information.

IDENTIFICATION		TOPOLOGY					GEARS SPECS		
UNIQUE_ID	**US6422969B1__FIG7**	**PGS**	**S/D**	**+/-**	**CLs**	**SCs**	**GEARS**	**Ratios**	**Engaged SCs**
Source	patent	1	D	F	IN;R1;A2	B1: F;A1	R1	-2.65	B2;C2
Owner	GM	2	S	IN	A1;R2	B2: F;S1	1	3.04	B2;C1
Patent	US6422969B1	3	D	OUT	S2;S3	B3: F;S2	2	2.02	B3;C2
Date	2000				OUT;R3	C1: A1;A3	3	1.32	B3;C1
Model	FIG7					C2: A2;A3	4	1	C1;C2
Commercial?	false						5	0.68	B1;C1
Longitudinal	true						6	0.5	B1;C2
Transversal	false								
Weight (kg)									
Máx. Torque (N·m)									

Figure 147 – US6422969B1__FIG7 representations.

(a) Functional diagram

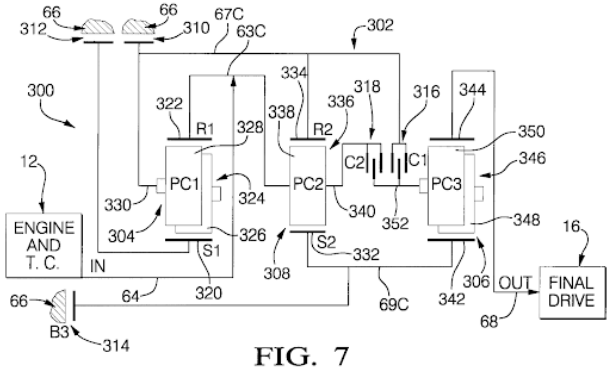

FIG. 7

(b) PGM Graph

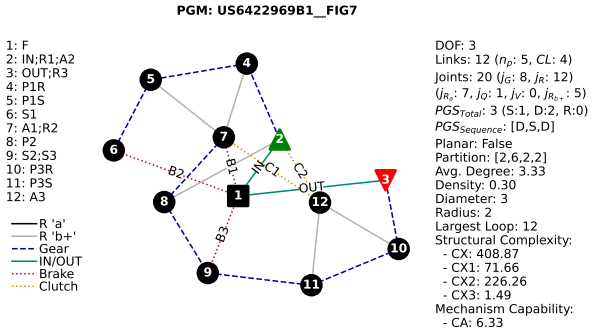

(c) DBG Graph

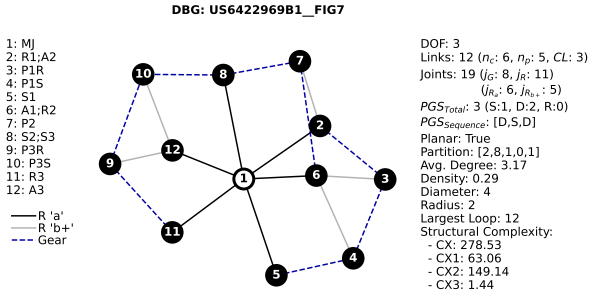

Table 119 – US6422969B1__FIG9 dataset information.

IDENTIFICATION		TOPOLOGY					GEARS SPECS		
UNIQUE_ID	**US6422969B1__FIG9**	**PGS**	**S/D**	**+/-**	**CLs**	**SCs**	**GEARS**	**Ratios**	**Engaged SCs**
Source	patent	1	S	F	IN;A1;R2	B1: F;A2	R1	-1.9	B3;C2
Owner	GM	2	D	IN	R1;A2	B2: F;S1	1	3.22	B3;C1
Patent	US6422969B1	3	S	OUT	S2;R3	B3: F;S2	2	2.3	B2;C2
Date	2000				OUT;A3	C1: A1;S3	3	1.34	B2;C1
Model	FIG9					C2: S1;S3	4	1	C1;C2
Commercial?	false						5	0.67	B1;C1
Longitudinal	true						6	0.48	B1;C2
Transversal	false								
Weight (kg)									
Máx. Torque (N·m)									

Figure 148 – US6422969B1__FIG9 representations.

(a) Functional diagram

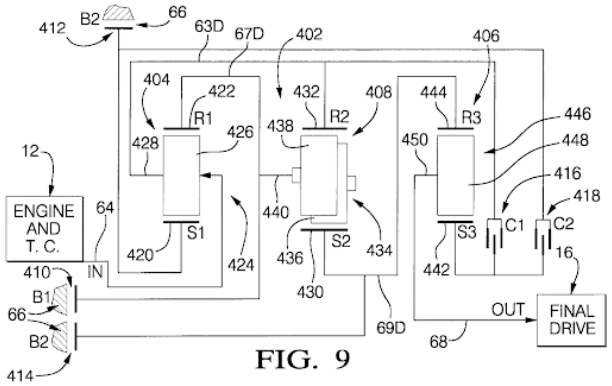

FIG. 9

(b) PGM Graph

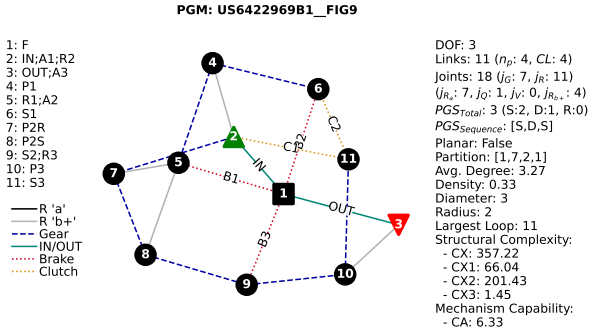

(c) DBG Graph

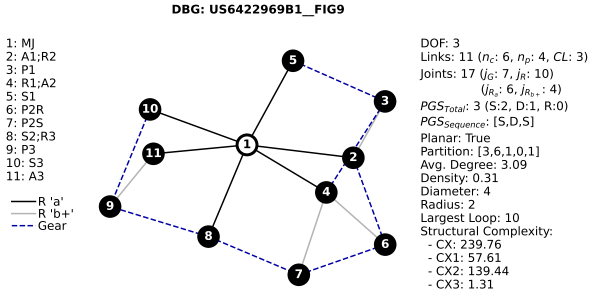

Table 120 – US6514170B1__FIG1 dataset information.

IDENTIFICATION		TOPOLOGY					GEARS SPECS		
UNIQUE_ID	**US6514170B1__FIG1**	**PGS**	**S/D**	**+/-**	**CLs**	**SCs**	**GEARS**	**Ratios**	**Engaged SCs**
Source	patent	1	S	F	F;S1	C1: A1;S2	R1	-1.82	C2;C5
Owner	GM	2	S	IN	IN;S3	C2: A1;R2	1	3.5	C1;C2
Patent	US6514170B1	3	S	OUT	R1;A2	C3: IN;A1	2	2.02	C1;C5
Date	2001				S2;R3	C4: IN;R2	3	1.41	C1;C4
Model	FIG1				OUT;A3	C5: R2;A3	4	1	C1;C3
Commercial?	false						5	0.73	C3;C5
Longitudinal	true						6	0.55	C2;C3
Transversal	false								
Weight (kg)									
Máx. Torque (N·m)									

Figure 149 – US6514170B1__FIG1 representations.

(a) Functional diagram

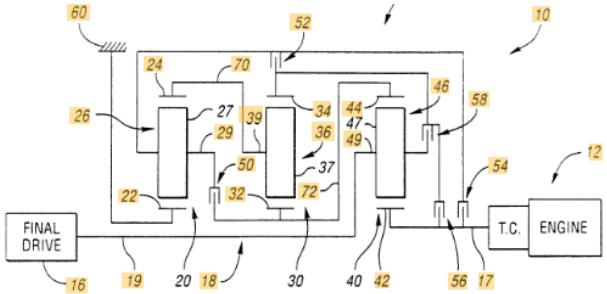

Fig. 1a

(b) PGM Graph

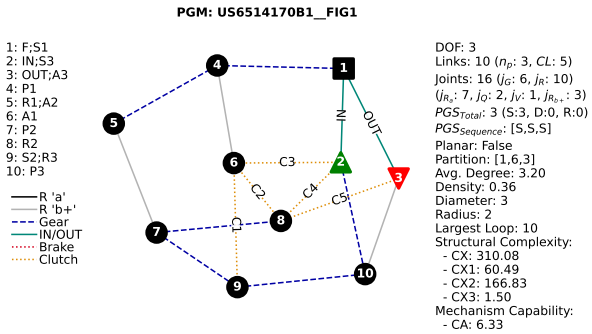

(c) DBG Graph

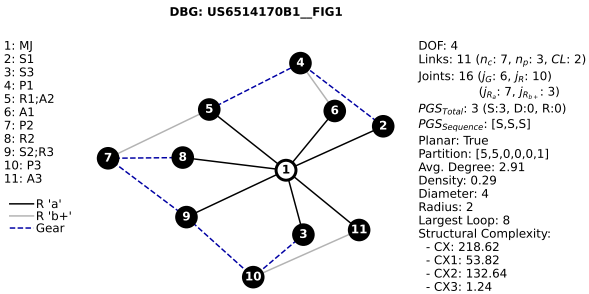

Table 121 – US6514170B1__FIG2 dataset information.

IDENTIFICATION		TOPOLOGY					GEARS SPECS		
UNIQUE_ID	**US6514170B1__FIG2**	**PGS**	**S/D**	**+/-**	**CLs**	**SCs**	**GEARS**	**Ratios**	**Engaged SCs**
Source	patent	1	S	F	F;S1	C1: A1;A2	R1	-1.73	C1;C5
Owner	GM	2	S	IN	IN;A2;S3	C2: A1;R3	1	3.4	C2;C3
Patent	US6514170B1	3	S	OUT	R1;R2	C3: R2;R3	2	1.96	C2;C4
Date	2001				OUT;A3	C4: R2;A3	3	1.31	C2;C5
Model	FIG2					C5: S2;A3	4	1	C3;C5
Commercial?	false						5	0.68	C1;C3
Longitudinal	true						6	0.6	C1;C4
Transversal	false								
Weight (kg)									
Máx. Torque (N·m)									

Figure 150 – US6514170B1__FIG2 representations.

(a) Functional diagram

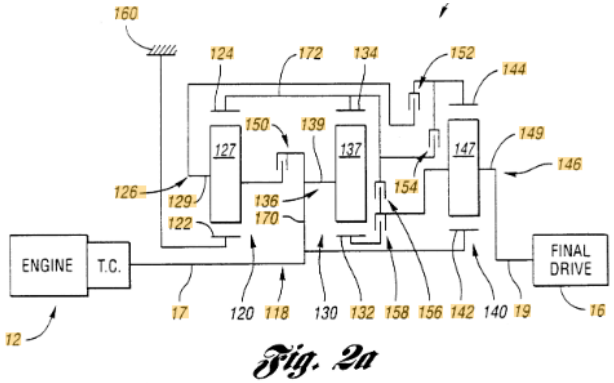

Fig. 2a

(b) PGM Graph

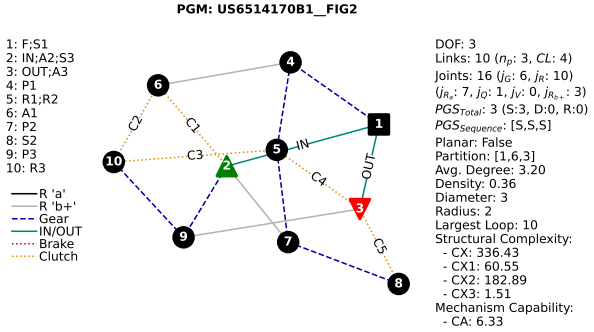

DOF: 3
Links: 10 (n_p: 3, CL: 4)
Joints: 16 (j_C: 6, j_R: 10)
(j_{R_a}: 7, j_O: 1, j_V: 0, $j_{R_{a+}}$: 3)
PGS_{Total}: 3 (S:3, D:0, R:0)
$PGS_{Sequence}$: [S,S,S]
Planar: False
Partition: [1,6,3]
Avg. Degree: 3.20
Density: 0.36
Diameter: 3
Radius: 2
Largest Loop: 10
Structural Complexity:
- CX: 336.43
- CX1: 60.55
- CX2: 182.89
- CX3: 1.51
Mechanism Capability:
- CA: 6.33

(c) DBG Graph

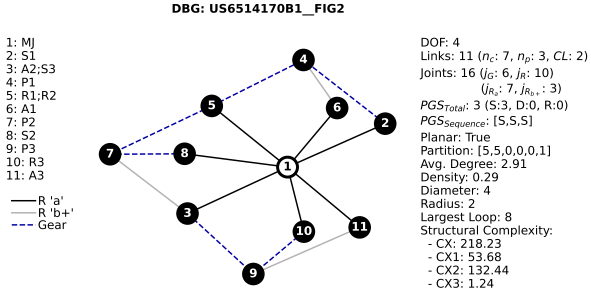

DOF: 4
Links: 11 (n_c: 7, n_p: 3, CL: 2)
Joints: 16 (j_C: 6, j_R: 10)
(j_{R_a}: 7, $j_{R_{a+}}$: 3)
PGS_{Total}: 3 (S:3, D:0, R:0)
$PGS_{Sequence}$: [S,S,S]
Planar: True
Partition: [5,5,0,0,0,1]
Avg. Degree: 2.91
Density: 0.29
Diameter: 4
Radius: 2
Largest Loop: 8
Structural Complexity:
- CX: 218.23
- CX1: 53.68
- CX2: 132.44
- CX3: 1.24

Table 122 – US6514170B1__FIG3 dataset information.

IDENTIFICATION		TOPOLOGY					GEARS SPECS		
UNIQUE_ID	**US6514170B1__FIG3**	**PGS**	**S/D**	**+/-**	**CLs**	**SCs**	**GEARS**	**Ratios**	**Engaged SCs**
Source	patent	1	S	F	F;S1	C1: A1;A2	R1	-1.88	C1;C4
Owner	GM	2	S	IN	IN;S2	C2: A1;R2	1	3.62	C1;C3
Patent	US6514170B1	3	S	OUT	R1;A2	C3: A1;A3	2	2.23	C3;C4
Date	2001				R2;S3	C4: R2;A3	3	1.52	C3;C5
Model	FIG3				OUT;R3	C5: IN;A3	4	1	C4;C5
Commercial?	false						5	0.78	C2;C5
Longitudinal	true						6	0.56	C1;C5
Transversal	false								
Weight (kg)									
Máx. Torque (N·m)									

Figure 151 – US6514170B1__FIG3 representations.

(a) Functional diagram

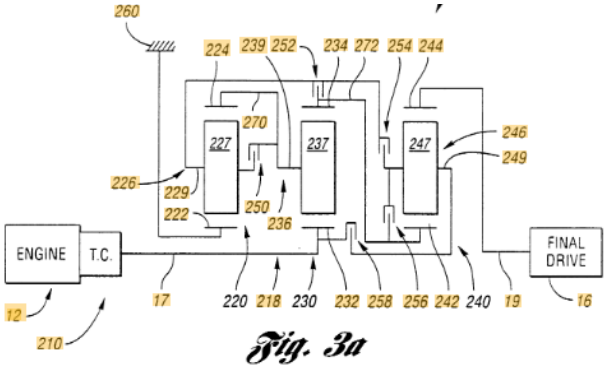

Fig. 3a

(b) PGM Graph

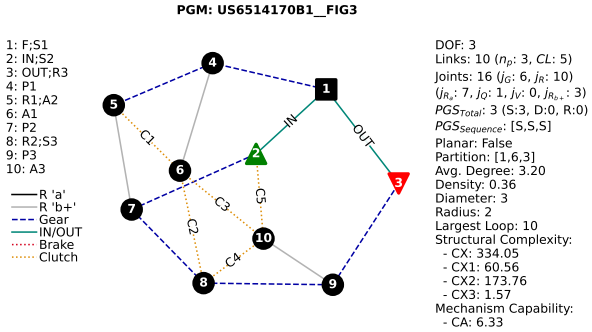

(c) DBG Graph

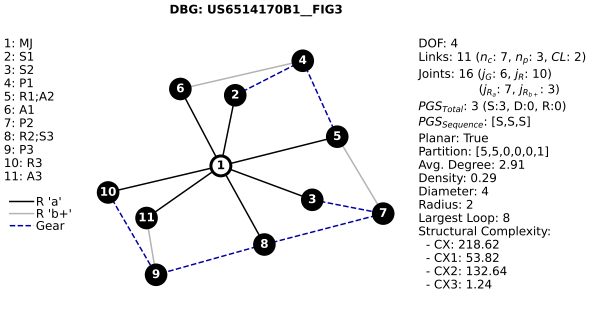

Table 123 – US6514170B1__FIG4 dataset information.

IDENTIFICATION		TOPOLOGY					GEARS SPECS		
UNIQUE_ID	**US6514170B1__FIG4**	**PGS**	**S/D**	**+/-**	**CLs**	**SCs**	**GEARS**	**Ratios**	**Engaged SCs**
Source	patent	1	S	F	F;S1	C1: A1;S2	R1	-4.02	C2;C3
Owner	GM	2	S	IN	IN;S3	C2: A1;A2	1	4.33	C2;C5
Patent	US6514170B1	3	S	OUT	R1;R2	C3: IN;A1	2	2.67	C1;C2
Date	2001				S2;R3	C4: A2;R1	3	1.56	C1;C5
Model	FIG4				OUT;A3	C5: A2;A3	4	1	C4;C5
Commercial?	false						5	0.71	C3;C4
Longitudinal	true						6	0.55	C3;C5
Transversal	false								
Weight (kg)									
Máx. Torque (N·m)									

Figure 152 – US6514170B1__FIG4 representations.

(a) Functional diagram

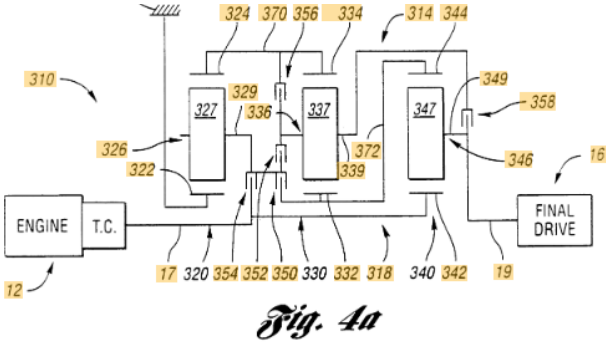

Fig. 4a

(b) PGM Graph

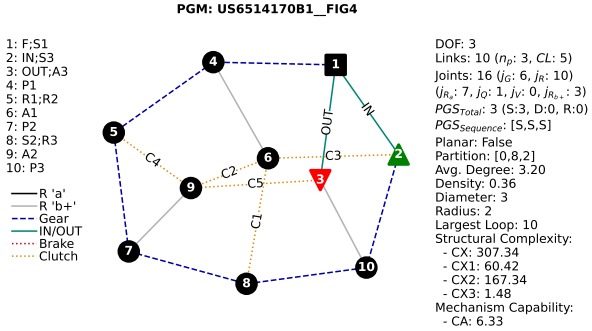

(c) DBG Graph

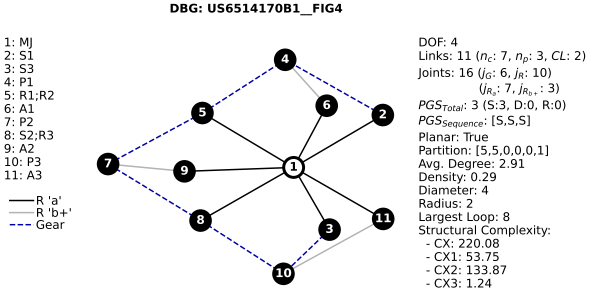

Table 124 – US6514170B1__FIG5 dataset information.

IDENTIFICATION		TOPOLOGY					GEARS SPECS		
UNIQUE_ID	**US6514170B1__FIG5**	**PGS**	**S/D**	**+/-**	**CLs**	**SCs**	**GEARS**	**Ratios**	**Engaged SCs**
Source	patent	1	S	F	F;A1	C1: R1;S1	R1	-1.28	C3;C5
Owner	GM	2	S	IN	IN;S3	C2: R1;A2	1	2.49	C2;C5
Patent	US6514170B1	3	S	OUT	S1;S2	C3: R1;R3	2	1.5	C1;C5
Date	2001				OUT;R2;A3	C4: A2;R3	3	1	C4;C5
Model	FIG5					C5: IN;A2	4	0.67	C1;C4
Commercial?	false						5	0.53	C3;C4
Longitudinal	true						6	0.4	C1;C3
Transversal	false								
Weight (kg)									
Máx. Torque (N·m)									

Figure 153 – US6514170B1__FIG5 representations.

(a) Functional diagram

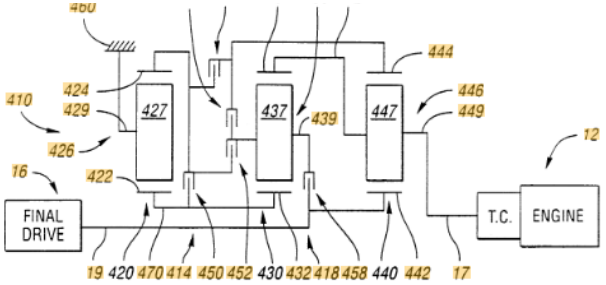

Fig. 5a

(b) PGM Graph

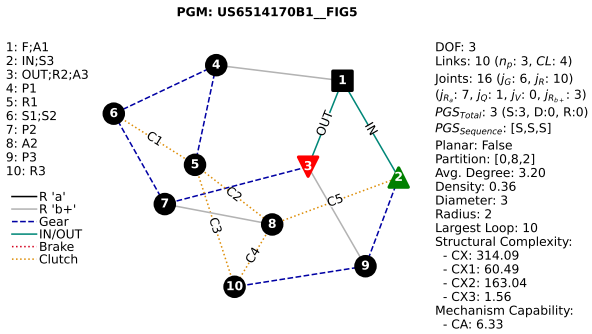

(c) DBG Graph

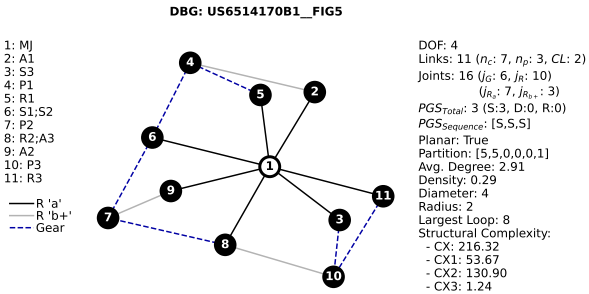

Table 125 – US6514170B1__FIG6 dataset information.

IDENTIFICATION		TOPOLOGY					GEARS SPECS		
UNIQUE_ID	**US6514170B1__FIG6**	**PGS**	**S/D**	**+/-**	**CLs**	**SCs**	**GEARS**	**Ratios**	**Engaged SCs**
Source	patent	1	S	F	F;S1	C1: R1;A1	R1	-1.53	C1;C3
Owner	GM	2	S	IN	IN;S2	C2: R1;A2	1	2.88	C1;C5
Patent	US6514170B1	3	S	OUT	A1;R2	C3: R1;A3	2	1.73	C3;C5
Date	2001				A2;R3	C4: IN;A3	3	1	C4;C5
Model	FIG6				OUT;S3	C5: A3;OUT	4	0.68	C3;C4
Commercial?	false						5	0.56	C2;C4
Longitudinal	true						6	0.45	C1;C4
Transversal	false								
Weight (kg)									
Máx. Torque (N·m)									

Figure 154 – US6514170B1__FIG6 representations.

(a) Functional diagram

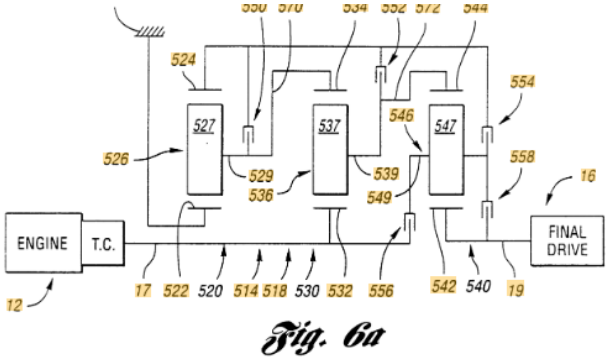

Fig. 6a

(b) PGM Graph

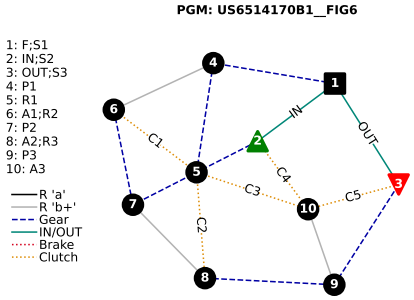

(c) DBG Graph

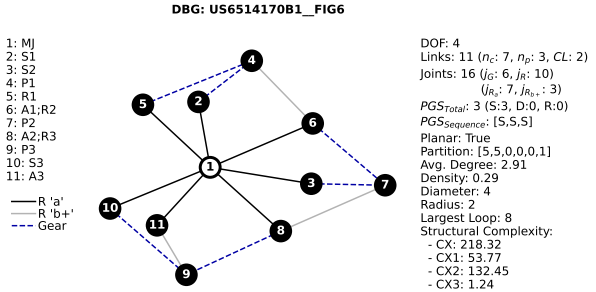

Table 126 – US6514170B1__FIG7 dataset information.

IDENTIFICATION		TOPOLOGY					GEARS SPECS		
UNIQUE_ID	**US6514170B1__FIG7**	**PGS**	**S/D**	**+/-**	**CLs**	**SCs**	**GEARS**	**Ratios**	**Engaged SCs**
Source	patent	1	S	F	F;R1	C1: A1;A2	R1	-2.05	C2;C5
Owner	GM	2	S	IN	IN;A3	C2: A1;R3	1	2.86	C2;C3
Patent	US6514170B1	3	S	OUT	S1;R2	C3: IN;S1	2	1.5	C2;C4
Date	2001				S2;S3	C4: S2;A2	3	1	C3;C4
Model	FIG7				OUT;R3	C5: A2;A3	4	0.73	C1;C4
Commercial?	false						5	0.61	C1;C3
Longitudinal	true						6	0.46	C1;C5
Transversal	false								
Weight (kg)									
Máx. Torque (N·m)									

Figure 155 – US6514170B1__FIG7 representations.

(a) Functional diagram

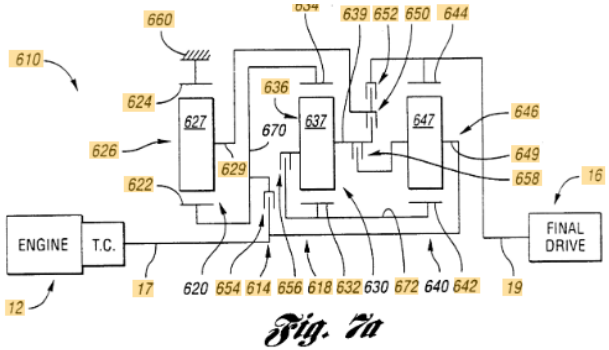

Fig. 7a

(b) PGM Graph

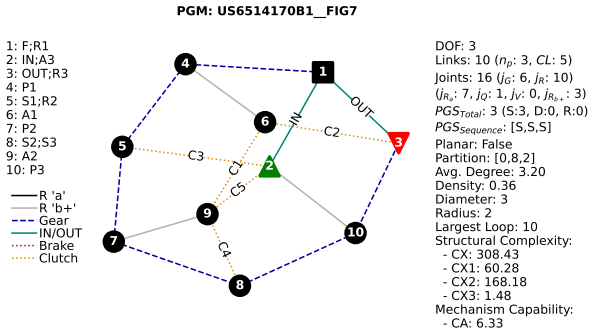

(c) DBG Graph

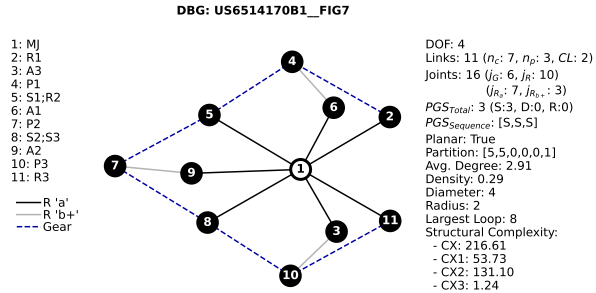

Table 127 – US6514170B1__FIG8 dataset information.

IDENTIFICATION		TOPOLOGY					GEARS SPECS		
UNIQUE_ID	**US6514170B1__FIG8**	**PGS**	**S/D**	**+/-**	**CLs**	**SCs**	**GEARS**	**Ratios**	**Engaged SCs**
Source	patent	1	S	F	F;S1	C1: A1;R1	R1	-2.3	C3;C5
Owner	GM	2	S	IN	IN;S2;S3	C2: R1;R2	1	2.9	C1;C4
Patent	US6514170B1	3	S	OUT	A1;A2	C3: R1;A3	2	1.48	C3;C4
Date	2001				OUT;A3	C4: A2;R3	3	1	C4;C5
Model	FIG8					C5: R2;R3	4	0.59	C2;C4
Commercial?	false						5	0.47	C2;C5
Longitudinal	true						6	0.36	C2;C3
Transversal	false								
Weight (kg)									
Máx. Torque (N·m)									

Figure 156 – US6514170B1__FIG8 representations.

(a) Functional diagram

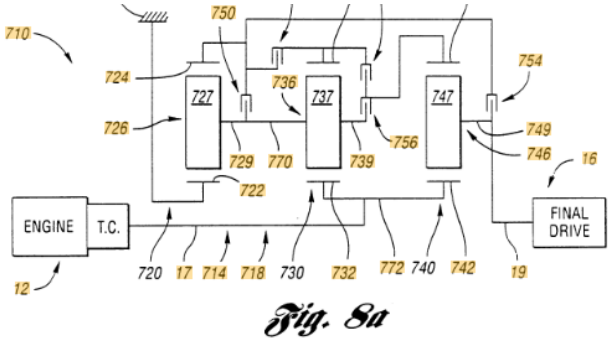

Fig. 8a

(b) PGM Graph

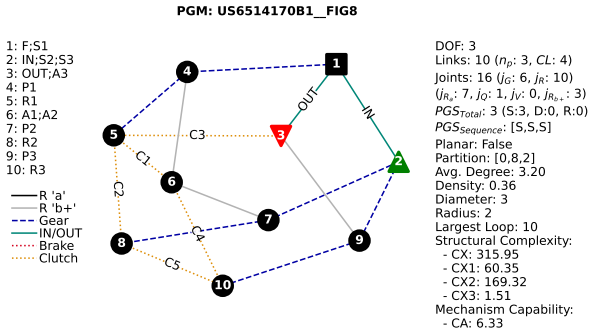

(c) DBG Graph

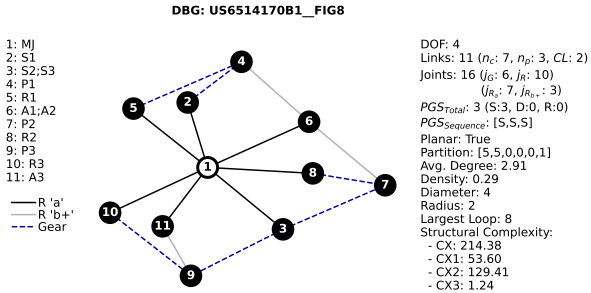

Table 128 – US6514170B1__FIG9 dataset information.

IDENTIFICATION		TOPOLOGY					GEARS SPECS		
UNIQUE_ID	**US6514170B1__FIG9**	**PGS**	**S/D**	**+/-**	**CLs**	**SCs**	**GEARS**	**Ratios**	**Engaged SCs**
Source	patent	1	S	F	F;S1	C1: A1;R1	R1	-1.7	C1;C5
Owner	GM	2	S	IN	IN;R2;S3	C2: R1;S2	1	2.6	C1;C4
Patent	US6514170B1	3	S	OUT	A1;A2	C3: R1;OUT	2	1.56	C3;C4
Date	2001				OUT;A3	C4: A2;R3	3	1	C4;C5
Model	FIG9					C5: S2;R3	4	0.76	C2;C4
Commercial?	false						5	0.55	C2;C5
Longitudinal	true						6	0.43	C2;C3
Transversal	false								
Weight (kg)									
Máx. Torque (N·m)									

Figure 157 – US6514170B1__FIG9 representations.

(a) Functional diagram

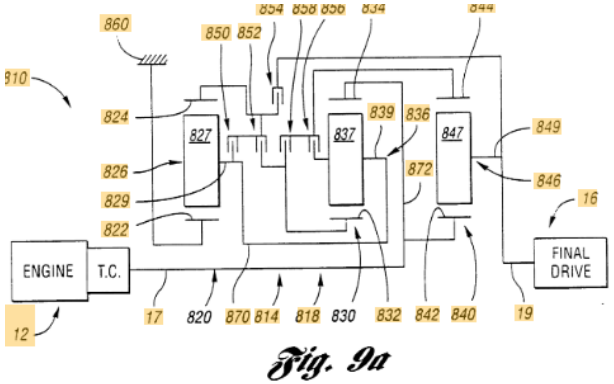

Fig. 9a

(b) PGM Graph

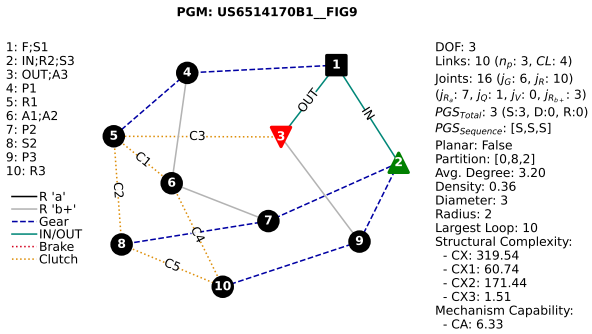

(c) DBG Graph

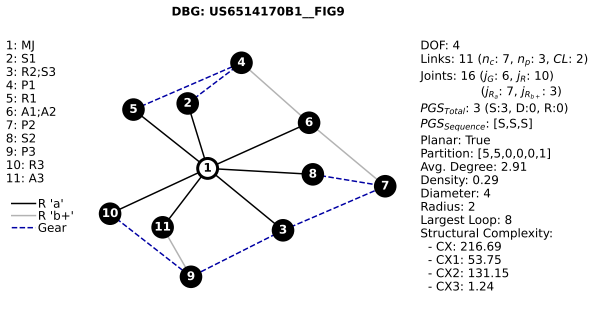

Table 129 – US6514170B1__FIG10 dataset information.

IDENTIFICATION		TOPOLOGY					GEARS SPECS		
UNIQUE_ID	**US6514170B1__FIG10**	**PGS**	**S/D**	**+/-**	**CLs**	**SCs**	**GEARS**	**Ratios**	**Engaged SCs**
Source	patent	1	D	F	F;R1	C1: S1;S2	R1	-1.51	C2;C5
Owner	GM	2	S	IN	IN;A3	C2: IN;S1	1	2.68	C1;C4
Patent	US6514170B1	3	S	OUT	A1;A2	C3: A2;S2	2	1.43	C1;C5
Date	2001				R2;S3	C4: A1;A3	3	1	C3;C5
Model	FIG10				OUT;R3	C5: A1;R3	4	0.68	C1;C3
Commercial?	false						5	0.56	C2;C3
Longitudinal	true						6	0.46	C1;C2
Transversal	false								
Weight (kg)									
Máx. Torque (N·m)									

Figure 158 – US6514170B1__FIG10 representations.

(a) Functional diagram

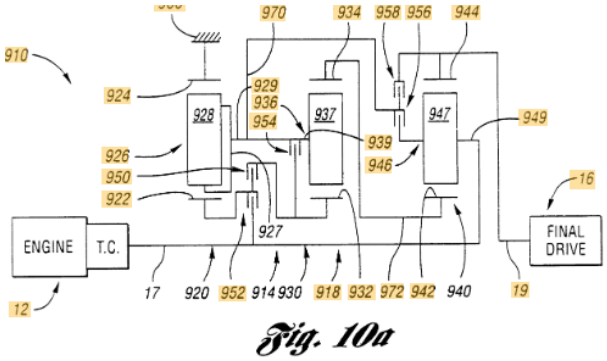

Fig. 10a

(b) PGM Graph

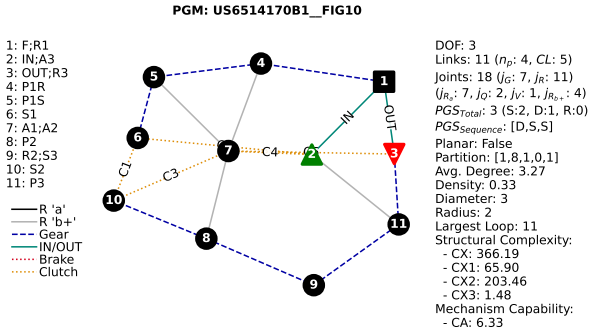

(c) DBG Graph

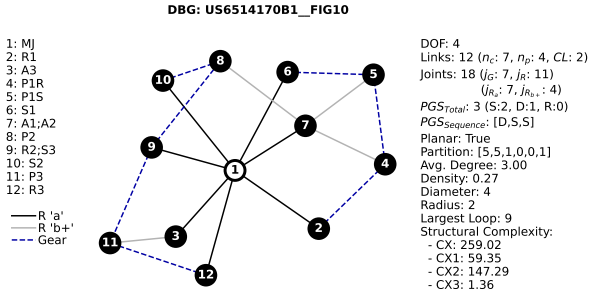

Table 130 – US6514170B1__FIG11 dataset information.

IDENTIFICATION		TOPOLOGY					GEARS SPECS		
UNIQUE_ID	**US6514170B1__FIG11**	**PGS**	**S/D**	**+/-**	**CLs**	**SCs**	**GEARS**	**Ratios**	**Engaged SCs**
Source	patent	1	S	F	F;A1	C1: S1;S3	R1	-2.31	C3;C4
Owner	GM	2	S	IN	IN;R3	C2: A1;S1	1	4.3	C2;C4
Patent	US6514170B1	3	S	OUT	R1;S2	C3: IN;S1	2	3.07	C1;C4
Date	2001				R2;S3	C4: R1;OUT	3	1.63	C1;C2
Model	FIG11				OUT;A3	C5: A2;OUT	4	1	C1;C3
Commercial?	false						5	0.75	C2;C3
Longitudinal	true						6	0.54	C3;C5
Transversal	false						7	0.46	C2;C5
Weight (kg)							8	0.28	C1;C5
Máx. Torque (N·m)									

Figure 159 – US6514170B1__FIG11 representations.

(a) Functional diagram

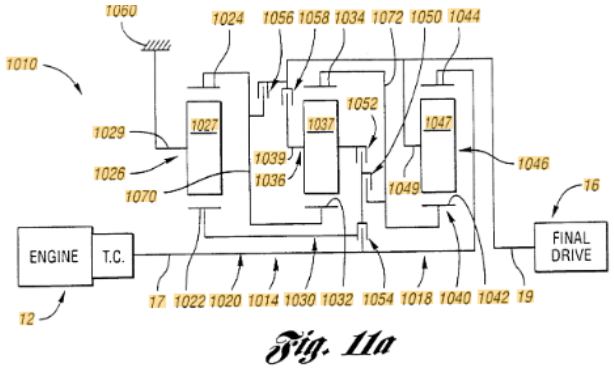

Fig. 11a

(b) PGM Graph

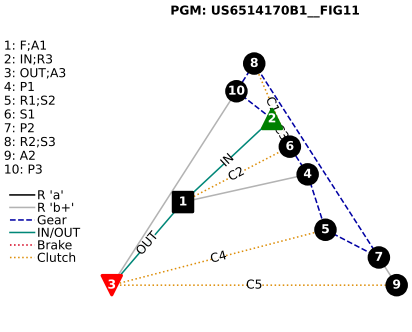

(c) DBG Graph

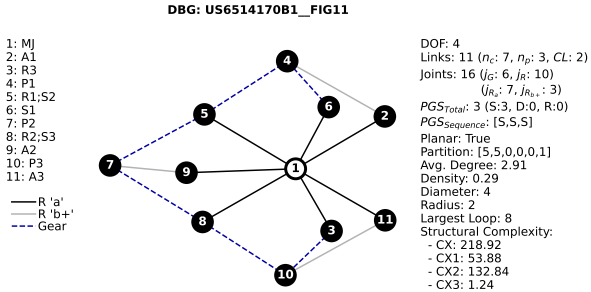

Table 131 – US6514170B1__FIG12 dataset information.

IDENTIFICATION		TOPOLOGY					GEARS SPECS		
UNIQUE_ID	**US6514170B1__FIG12**	**PGS**	**S/D**	**+/-**	**CLs**	**SCs**	**GEARS**	**Ratios**	**Engaged SCs**
Source	patent	1	S	F	F;S1	C1: R1;A3	R1	-1.85	C1;C2
Owner	GM	2	S	IN	IN;S3	C2: R1;S2	1	2.81	C1;C5
Patent	US6514170B1	3	S	OUT	A1;R2	C3: R1;OUT	2	1.63	C2;C5
Date	2001				A2;A3	C4: IN;A1	3	1	C4;C5
Model	FIG12				OUT;R3	C5: A1;OUT	4	0.75	C2;C4
Commercial?	false						5	0.61	C3;C4
Longitudinal	true						6	0.51	C1;C4
Transversal	false						7	0.28	C2;C3
Weight (kg)									
Máx. Torque (N·m)									

Figure 160 – US6514170B1__FIG12 representations.

(a) Functional diagram

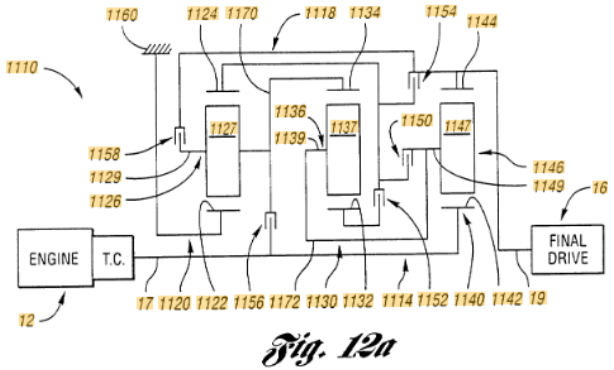

Fig. 12a

(b) PGM Graph

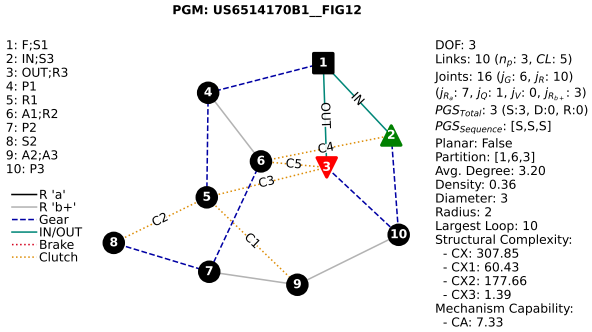

(c) DBG Graph

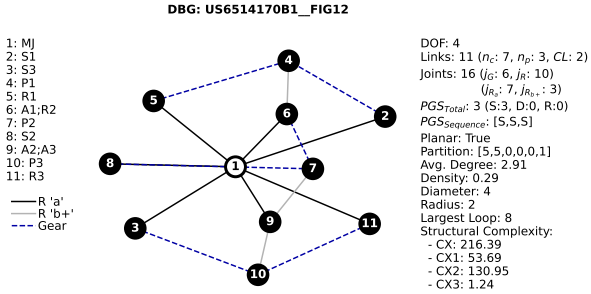

Table 132 – US6530858B1__FIG1 dataset information.

IDENTIFICATION		TOPOLOGY					GEARS SPECS		
UNIQUE_ID	**US6530858B1__FIG1**	**PGS**	**S/D**	**+/-**	**CLs**	**SCs**	**GEARS**	**Ratios**	**Engaged SCs**
Source	patent	1	S	F	F;A3	C1: IN;A2	R1	-1.92	C1;C2;C3
Owner	GM	2	S	IN	IN;R1	C2: S1;S3	1	3.53	C2;C3;C5
Patent	US6530858B1	3	S	OUT	OUT;A1;R2	C3: A2;R3	2	2.37	C2;C3;C4
Date	2001					C4: S2;S3	3	1.67	C2;C4;C5
Model	FIG1					C5: S2;R3	4	1	C1;C2;C4
Commercial?	false						5	0.7	C1;C4;C5
Longitudinal	true						6	0.51	C1;C2;C5
Transversal	false						7	0.38	C1;C3;C4
Weight (kg)									
Máx. Torque (N·m)									

Figure 161 – US6530858B1__FIG1 representations.

(a) Functional diagram

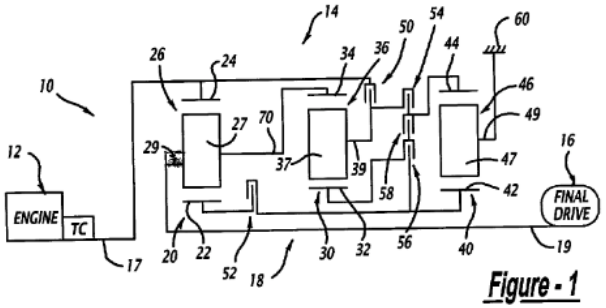

(b) PGM Graph

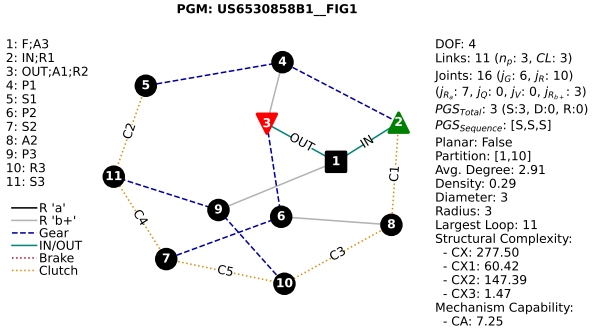

(c) DBG Graph

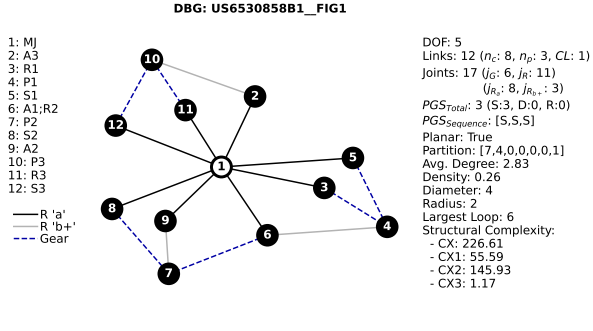

Table 133 – US6530858B1__FIG3 dataset information.

IDENTIFICATION		TOPOLOGY					GEARS SPECS		
UNIQUE_ID	**US6530858B1__FIG3**	**PGS**	**S/D**	**+/-**	**CLs**	**SCs**	**GEARS**	**Ratios**	**Engaged SCs**
Source	patent	1	S	F	F;R3	C1: S1;A2	R1	-1.86	C3;C4;C5
Owner	GM	2	S	IN	IN;R1	C2: S1;S3	1	3.46	C2;C4;C5
Patent	US6530858B1	3	S	OUT	OUT;A1;R2	C3: IN;A3	2	1.95	C1;C4;C5
Date	2001					C4: A2;A3	3	1.33	C1;C2;C4
Model	FIG3					C5: S2;S3	4	1	C1;C2;C5
Commercial?	false						5	0.78	C1;C3;C5
Longitudinal	true						6	0.62	C1;C2;C3
Transversal	false								
Weight (kg)									
Máx. Torque (N·m)									

Figure 162 – US6530858B1__FIG3 representations.

(a) Functional diagram

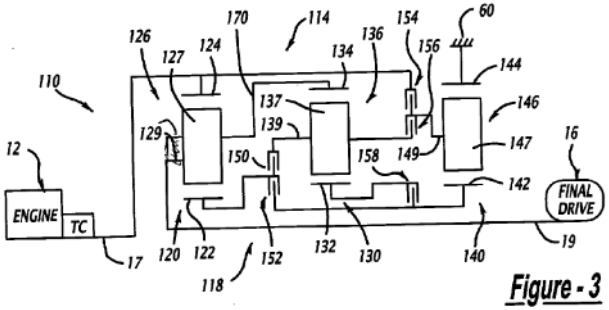

(b) PGM Graph

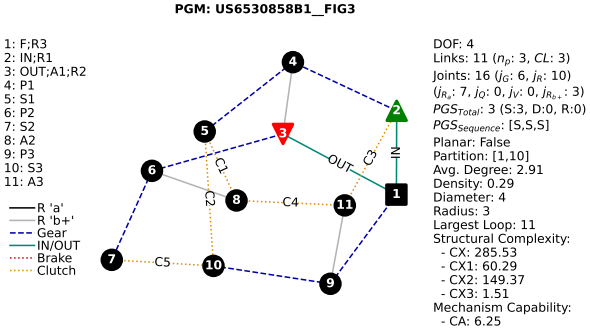

(c) DBG Graph

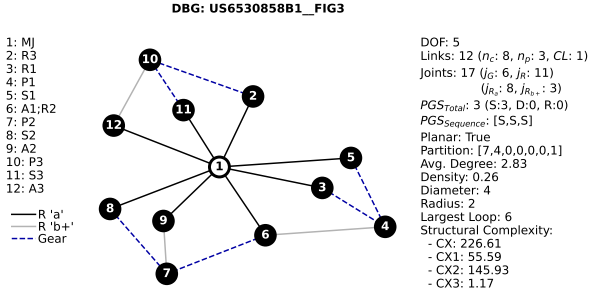

Table 134 – US6530858B1__FIG5 dataset information.

IDENTIFICATION		TOPOLOGY					GEARS SPECS		
UNIQUE_ID	**US6530858B1__FIG5**	**PGS**	**S/D**	**+/-**	**CLs**	**SCs**	**GEARS**	**Ratios**	**Engaged SCs**
Source	patent	1	S	F	F;R3	C1: OUT;A3	R1	-1.59	C2;C3;C5
Owner	GM	2	S	IN	IN;A1;R2	C2: S1;A2	1	3.13	C1;C4;C5
Patent	US6530858B1	3	S	OUT	OUT;R1	C3: S1;A3	2	1.85	C1;C2;C4
Date	2001					C4: A2;S3	3	1.3	C1;C2;C5
Model	FIG5					C5: S2;S3	4	1	C2;C4;C5
Commercial?	false						5	0.69	C3;C4;C5
Longitudinal	true						6	0.6	C2;C3;C4
Transversal	false								
Weight (kg)									
Máx. Torque (N·m)									

Figure 163 – US6530858B1__FIG5 representations.

(a) Functional diagram

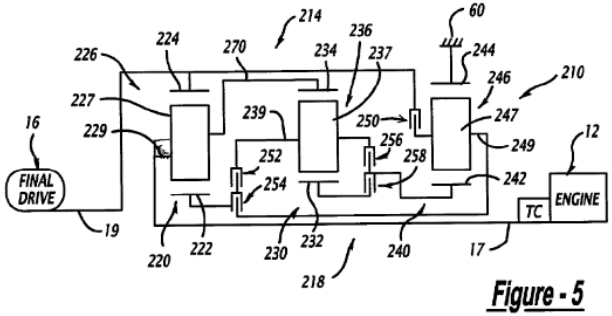

(b) PGM Graph

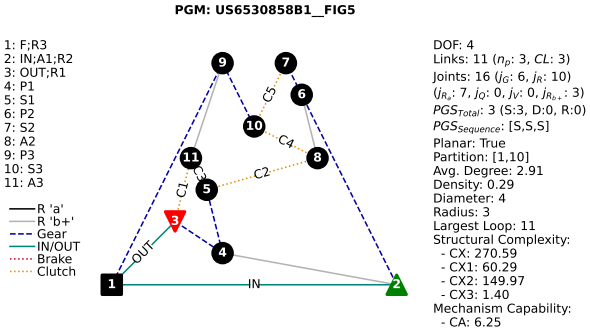

(c) DBG Graph

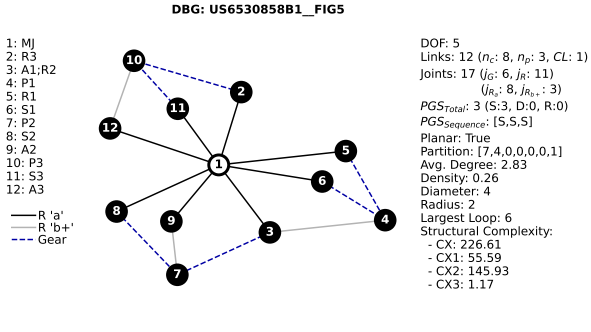

Table 135 – US6530858B1__FIG7 dataset information.

IDENTIFICATION		TOPOLOGY					GEARS SPECS		
UNIQUE_ID	**US6530858B1__FIG7**	**PGS**	**S/D**	**+/-**	**CLs**	**SCs**	**GEARS**	**Ratios**	**Engaged SCs**
Source	patent	1	S	F	F;S3	C1: A2;A3	R1	-1.83	C1;C2;C5
Owner	GM	2	S	IN	IN;A1	C2: A1;S2	1	2.61	C1;C2;C4
Patent	US6530858B1	3	S	OUT	R1;A2	C3: S1;A3	2	1.57	C1;C3;C4
Date	2001				OUT;R2	C4: S2;R3	3	1	C1;C2;C3
Model	FIG7					C5: R3;A3	4	0.75	C2;C3;C4
Commercial?	false						5	0.55	C2;C3;C5
Longitudinal	true						6	0.42	C3;C4;C5
Transversal	false								
Weight (kg)									
Máx. Torque (N·m)									

Figure 164 – US6530858B1__FIG7 representations.

(a) Functional diagram

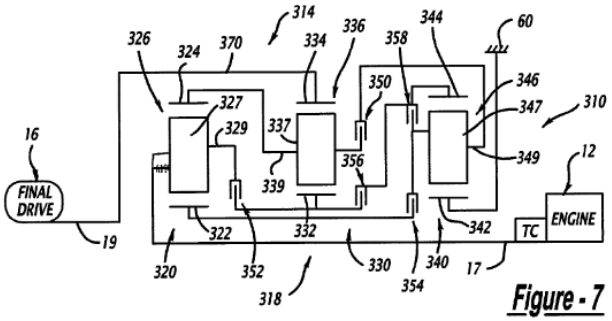

(b) PGM Graph

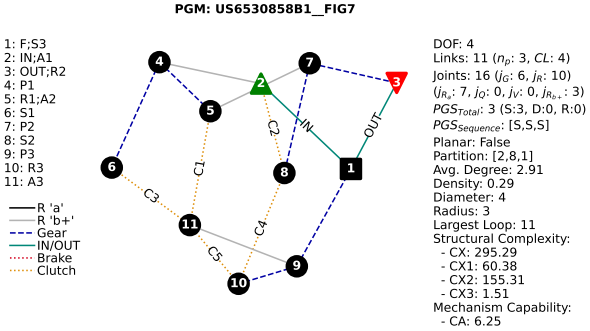

(c) DBG Graph

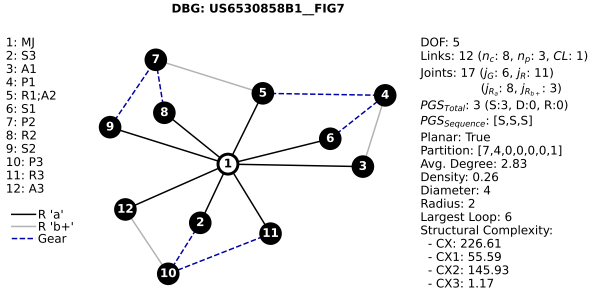

Table 136 – US6530858B1__FIG9 dataset information.

IDENTIFICATION		TOPOLOGY					GEARS SPECS		
UNIQUE_ID	**US6530858B1__FIG9**	**PGS**	**S/D**	**+/-**	**CLs**	**SCs**	**GEARS**	**Ratios**	**Engaged SCs**
Source	patent	1	S	F	F;A3	C1: A1;R2	R1	-2.78	C2;C4;C5
Owner	GM	2	S	IN	IN;R1;A2	C2: S1;S3	1	3.08	C1;C2;C4
Patent	US6530858B1	3	S	OUT	OUT;A1	C3: R2;S3	2	1.53	C2;C3;C4
Date	2001					C4: R2;R3	3	1	C1;C2;C3
Model	FIG9					C5: S2;R3	4	0.76	C2;C3;C5
Commercial?	false						5	0.53	C1;C3;C5
Longitudinal	true						6	0.39	C1;C2;C5
Transversal	false								
Weight (kg)									
Máx. Torque (N·m)									

Figure 165 – US6530858B1__FIG9 representations.

(a) Functional diagram

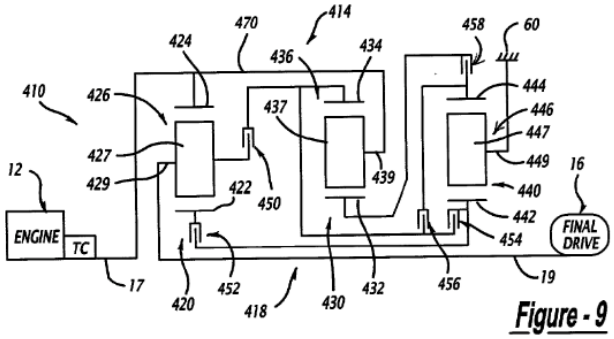

(b) PGM Graph

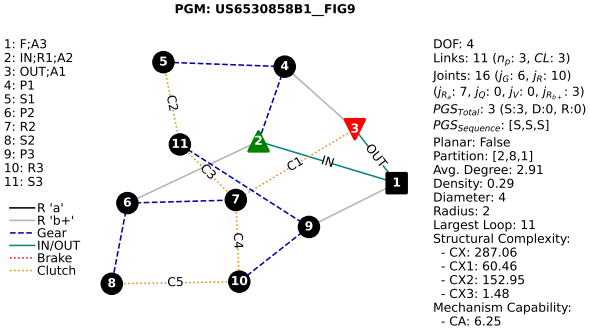

(c) DBG Graph

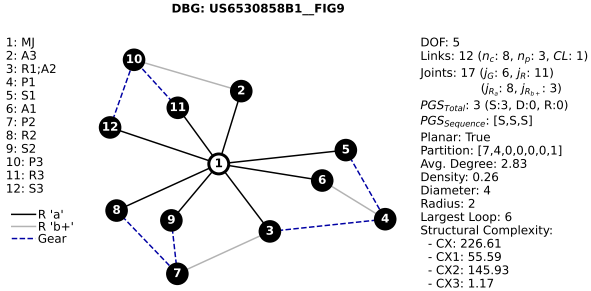

Table 137 – US6530858B1__FIG11 dataset information.

IDENTIFICATION		TOPOLOGY					GEARS SPECS		
UNIQUE_ID	**US6530858B1__FIG11**	**PGS**	**S/D**	**+/-**	**CLs**	**SCs**	**GEARS**	**Ratios**	**Engaged SCs**
Source	patent	1	S	F	F;S3	B1: F;A2	R1	-2.01	B1;C1;C3
Owner	GM	2	S	IN	IN;S2	C1: R2;A3	1	3.69	B1;C3;C4
Patent	US6530858B1	3	S	OUT	OUT;R1	C2: IN;A1	2	2.28	C1;C3;C4
Date	2001				S1;R2	C3: A1;A3	3	1.53	C2;C3;C4
Model	FIG11					C4: A2;R3	4	1	C1;C2;C3
Commercial?	false						5	0.77	C1;C2;C4
Longitudinal	true						6	0.55	B1;C1;C2
Transversal	false								
Weight (kg)									
Máx. Torque (N·m)									

Figure 166 – US6530858B1__FIG11 representations.

(a) Functional diagram

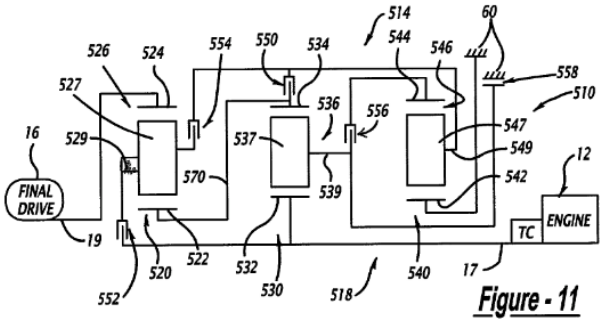

(b) PGM Graph

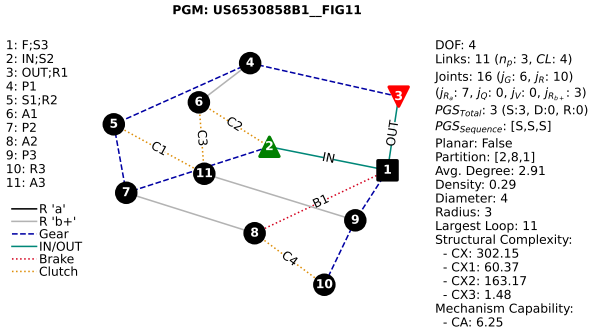

(c) DBG Graph

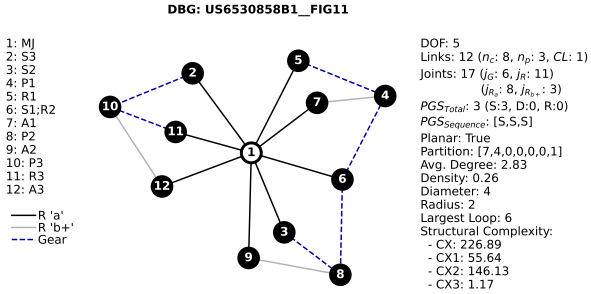

Table 138 – US6530858B1__FIG13 dataset information.

IDENTIFICATION		TOPOLOGY					GEARS SPECS		
UNIQUE_ID	**US6530858B1__FIG13**	**PGS**	**S/D**	**+/-**	**CLs**	**SCs**	**GEARS**	**Ratios**	**Engaged SCs**
Source	patent	1	S	F	F;S3	B1: F;S2	R1	-1.72	B1;C2;C4
Owner	GM	2	S	IN	IN;A2	C1: OUT;S1	1	3.32	B1;C2;C3
Patent	US6530858B1	3	S	OUT	OUT;R1	C2: A1;A3	2	2.23	C2;C3;C4
Date	2001				S1;R2	C3: A2;R3	3	1.54	C1;C2;C3
Model	FIG13					C4: S2;A3	4	1	C1;C2;C4
Commercial?	false						5	0.82	C1;C3;C4
Longitudinal	true						6	0.61	B1;C1;C4
Transversal	false								
Weight (kg)									
Máx. Torque (N·m)									

Figure 167 – US6530858B1__FIG13 representations.

(a) Functional diagram

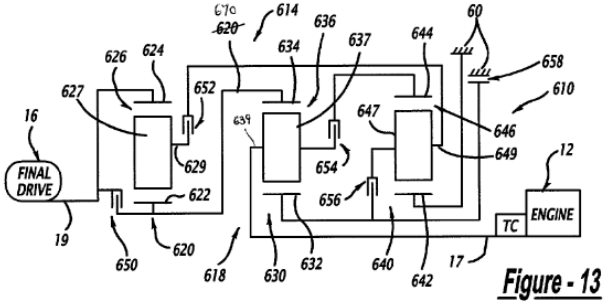

(b) PGM Graph

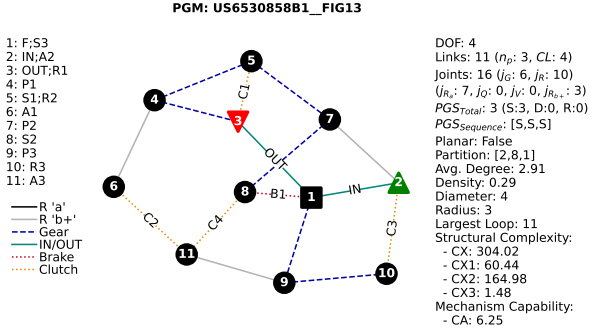

(c) DBG Graph

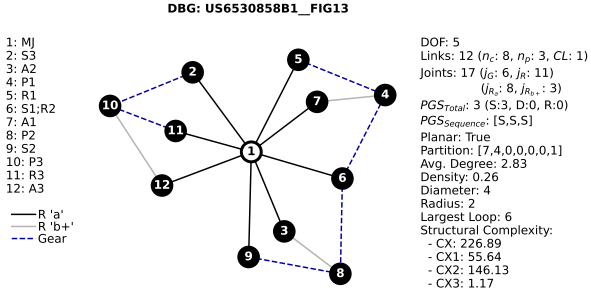

Table 139 – US6530858B1__FIG15 dataset information.

IDENTIFICATION		TOPOLOGY					GEARS SPECS		
UNIQUE_ID	**US6530858B1__FIG15**	**PGS**	**S/D**	**+/-**	**CLs**	**SCs**	**GEARS**	**Ratios**	**Engaged SCs**
Source	patent	1	S	F	F;S3	B1: F;S1	R1	-1.73	B1;C2;C4
Owner	GM	2	S	IN	IN;A1	C1: A1;R3	1	3.23	B1;C1;C4
Patent	US6530858B1	3	S	OUT	R1;S2	C2: S1;A3	2	2.2	C1;C2;C4
Date	2001				OUT;R2	C3: R2;A2	3	1.53	C1;C3;C4
Model	FIG15					C4: A2;A3	4	1	C2;C3;C4
Commercial?	false						5	0.82	C1;C2;C3
Longitudinal	true						6	0.61	B1;C1;C3
Transversal	false								
Weight (kg)									
Máx. Torque (N·m)									

Figure 168 – US6530858B1__FIG15 representations.

(a) Functional diagram

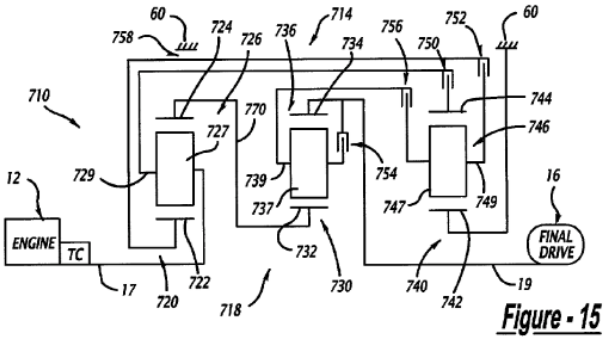

(b) PGM Graph

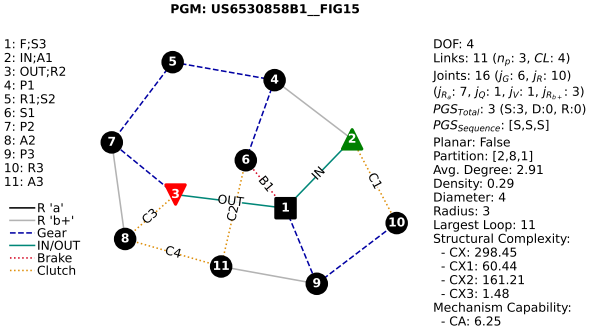

(c) DBG Graph

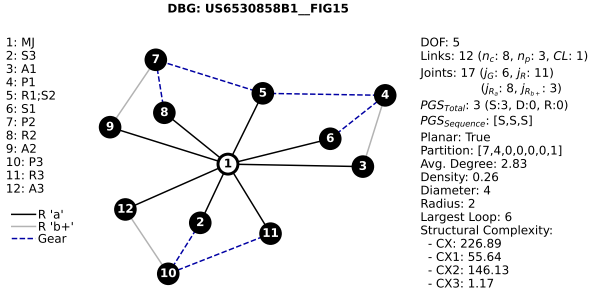

Table 140 – US6530858B1__FIG17 dataset information.

IDENTIFICATION		TOPOLOGY					GEARS SPECS		
UNIQUE_ID	**US6530858B1__FIG17**	**PGS**	**S/D**	**+/-**	**CLs**	**SCs**	**GEARS**	**Ratios**	**Engaged SCs**
Source	patent	1	S	F	F;S3	B1: F;S1	R1	-2.56	B1;C3;C4
Owner	GM	2	S	IN	IN;R1	C1: S2;R3	1	4.89	B1;C1;C4
Patent	US6530858B1	3	S	OUT	A1;S2	C2: R1;A2	2	2.93	C1;C3;C4
Date	2001				OUT;R2	C3: S1;R3	3	1.76	C1;C2;C4
Model	FIG17					C4: A2;A3	4	1.21	C2;C3;C4
Commercial?	false						5	1	C1;C2;C3
Longitudinal	true						6	0.79	B1;C2;C3
Transversal	false								
Weight (kg)									
Máx. Torque (N·m)									

Figure 169 – US6530858B1__FIG17 representations.

(a) Functional diagram

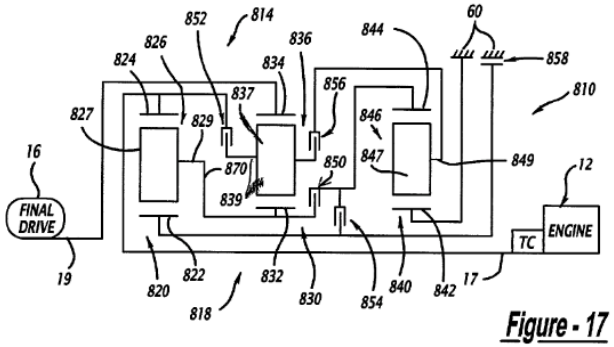

(b) PGM Graph

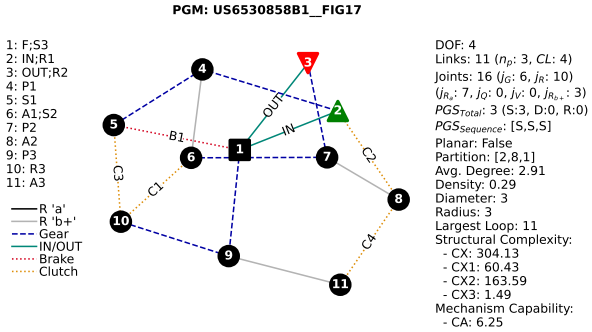

(c) DBG Graph

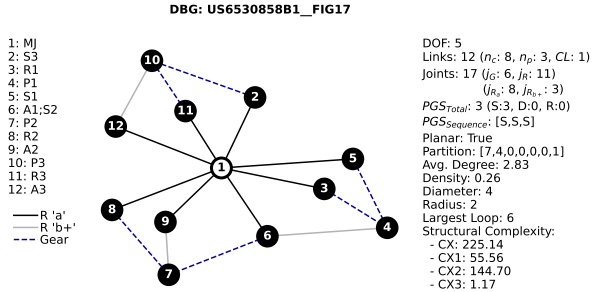

Table 141 – US6530858B1__FIG19 dataset information.

IDENTIFICATION		TOPOLOGY					GEARS SPECS		
UNIQUE_ID	**US6530858B1__FIG19**	**PGS**	**S/D**	**+/-**	**CLs**	**SCs**	**GEARS**	**Ratios**	**Engaged SCs**
Source	patent	1	S	F	F;S3	B1: F;R1	R1	-1.52	B1;C3;C4
Owner	GM	2	S	IN	IN;S1	C1: R2;R3	1	2.86	B1;C1;C4
Patent	US6530858B1	3	S	OUT	A1;R2	C2: IN;A2	2	1.64	C1;C3;C4
Date	2001				OUT;S2	C3: R1;A3	3	1	C1;C2;C4
Model	FIG19					C4: A2;R3	4	0.7	C2;C3;C4
Commercial?	false						5	0.58	C1;C2;C3
Longitudinal	true						6	0.45	B1;C2;C3
Transversal	false								
Weight (kg)									
Máx. Torque (N·m)									

Figure 170 – US6530858B1__FIG19 representations.

(a) Functional diagram

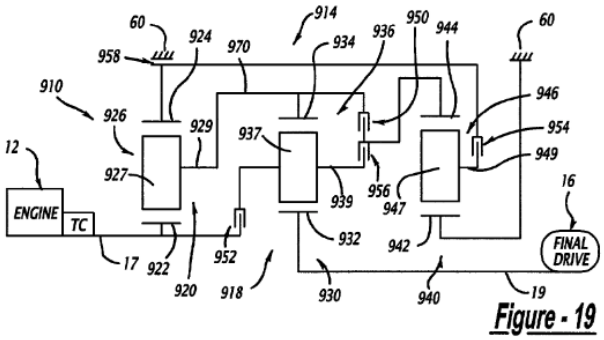

(b) PGM Graph

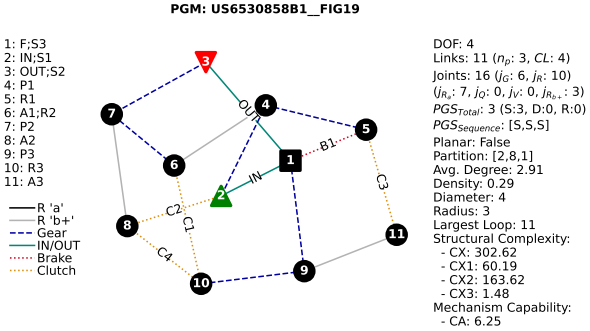

(c) DBG Graph

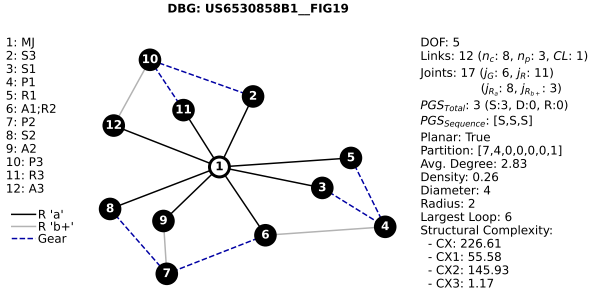

Table 142 – US6530858B1__FIG21 dataset information.

IDENTIFICATION		TOPOLOGY					GEARS SPECS		
UNIQUE_ID	**US6530858B1__FIG21**	**PGS**	**S/D**	**+/-**	**CLs**	**SCs**	**GEARS**	**Ratios**	**Engaged SCs**
Source	patent	1	S	F	F;A3	B1: F;S2	R1	-1.98	C1;C2;C3
Owner	GM	2	S	IN	IN;A1;R2	C1: S1;A2	1	2.59	C1;C3;C4
Patent	US6530858B1	3	S	OUT	OUT;S1	C2: R1;R3	2	1.59	B1;C1;C4
Date	2001					C3: S2;S3	3	1	C1;C2;C4
Model	FIG21					C4: A2;R3	4	0.59	B1;C2;C4
Commercial?	false						5	0.46	C2;C3;C4
Longitudinal	true						6	0.35	B1;C2;C3
Transversal	false								
Weight (kg)									
Máx. Torque (N·m)									

Figure 171 – US6530858B1__FIG21 representations.

(a) Functional diagram

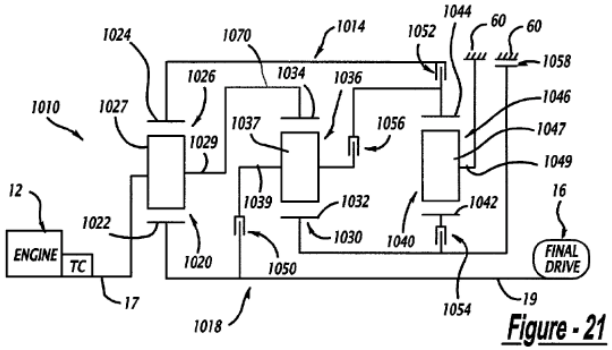

(b) PGM Graph

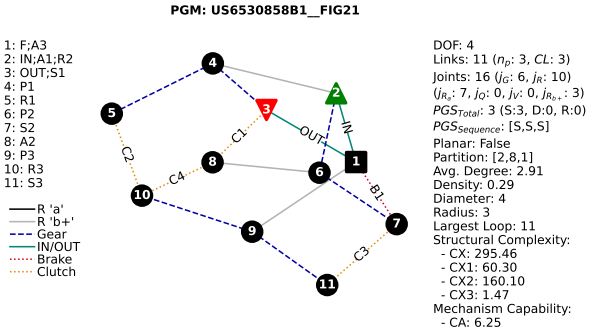

(c) DBG Graph

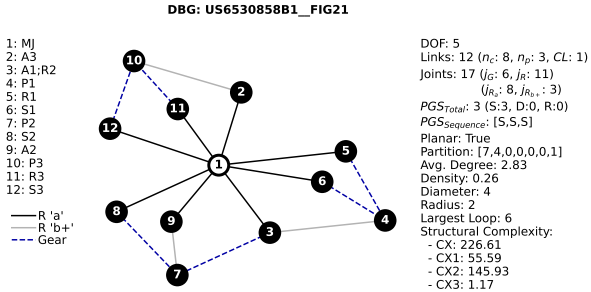

Table 143 – US6530858B1__FIG23 dataset information.

IDENTIFICATION		TOPOLOGY					GEARS SPECS		
UNIQUE_ID	**US6530858B1__FIG23**	**PGS**	**S/D**	**+/-**	**CLs**	**SCs**	**GEARS**	**Ratios**	**Engaged SCs**
Source	patent	1	S	F	F;S3	B1: F;A3	R1	-1.83	B1;C1;C2
Owner	GM	2	S	IN	IN;A1	C1: A2;A3	1	2.61	C1;C2;C4
Patent	US6530858B1	3	S	OUT	R1;A2	C2: A1;S2	2	1.57	C1;C3;C4
Date	2001				OUT;R2	C3: S1;A3	3	1	C1;C2;C3
Model	FIG23					C4: S2;R3	4	0.75	C2;C3;C4
Commercial?	false						5	0.55	B1;C2;C3
Longitudinal	true						6	0.42	B1;C3;C4
Transversal	false								
Weight (kg)									
Máx. Torque (N·m)									

Figure 172 – US6530858B1__FIG23 representations.

(a) Functional diagram

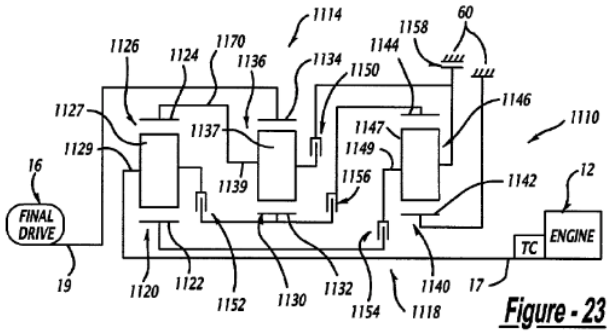

(b) PGM Graph

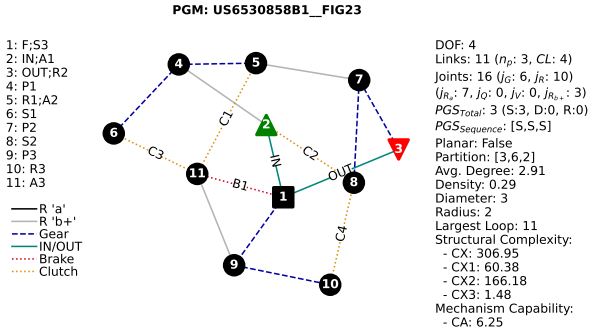

(c) DBG Graph

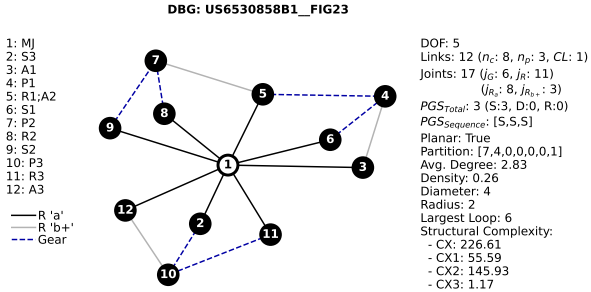

Table 144 – US6530858B1__FIG25 dataset information.

IDENTIFICATION		TOPOLOGY					GEARS SPECS		
UNIQUE_ID	**US6530858B1__FIG25**	**PGS**	**S/D**	**+/-**	**CLs**	**SCs**	**GEARS**	**Ratios**	**Engaged SCs**
Source	patent	1	S	F	F;R3	B1: F;R2	R1	-1.6	C1;C2;C4
Owner	GM	2	S	IN	IN;A1	C1: IN;S3	1	2.61	C1;C2;C3
Patent	US6530858B1	3	D	OUT	OUT;R1	C2: R1;A2	2	1.61	B1;C2;C3
Date	2001				S1;S2	C3: R2;A3	3	1	C2;C3;C4
Model	FIG25					C4: A2;A3	4	0.66	B1;C3;C4
Commercial?	false						5	0.54	C1;C3;C4
Longitudinal	true						6	0.41	B1;C1;C4
Transversal	false								
Weight (kg)									
Máx. Torque (N·m)									

Figure 173 – US6530858B1__FIG25 representations.

(a) Functional diagram

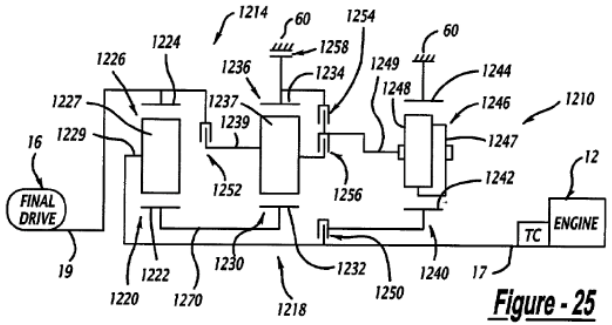

(b) PGM Graph

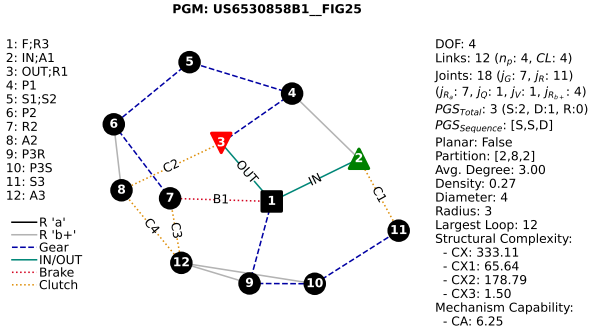

(c) DBG Graph

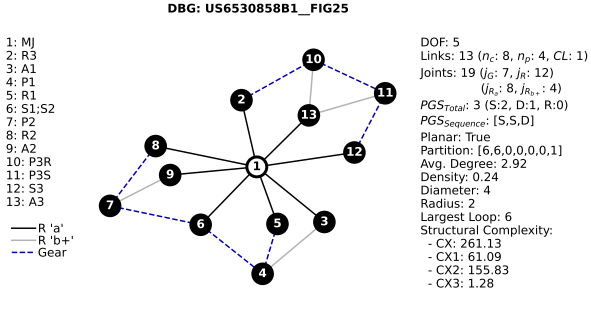

Table 145 – US6595892B2__FIG1 dataset information.

IDENTIFICATION		TOPOLOGY					GEARS SPECS		
UNIQUE_ID	**US6595892B2__FIG1**	**PGS**	**S/D**	**+/-**	**CLs**	**SCs**	**GEARS**	**Ratios**	**Engaged SCs**
Source	patent	1	S	F	F;S1	C1: S2;S3	R1	-2.13	C2;C5
Owner	GM	2	S	IN	IN;S3	C2: A2;A3	1	4.2	C1;C5
Patent	US6595892B2	3	S	OUT	R1;S2	C3: A2;R3	2	2.32	C1;C2
Date	2001				A1;A2	C4: R2;S3	3	1.63	C1;C3
Model	FIG1				OUT;R3	C5: R2;A3	4	1	C2;C3
Commercial?	false						5	0.78	C3;C4
Longitudinal	true						6	0.71	C2;C4
Transversal	false								
Weight (kg)									
Máx. Torque (N·m)									

Figure 174 – US6595892B2__FIG1 representations.

(a) Functional diagram

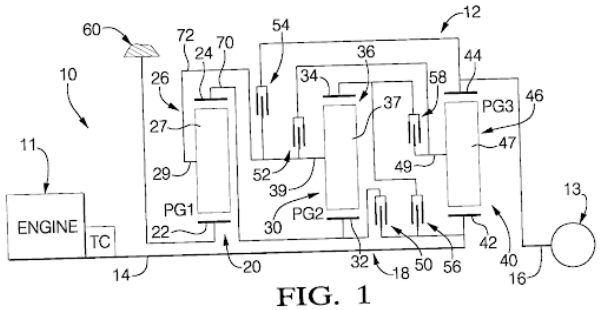

FIG. 1

(b) PGM Graph

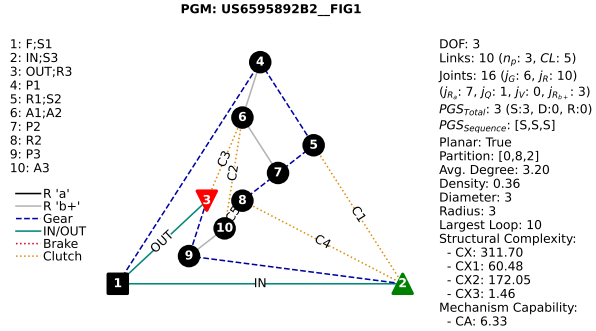

(c) DBG Graph

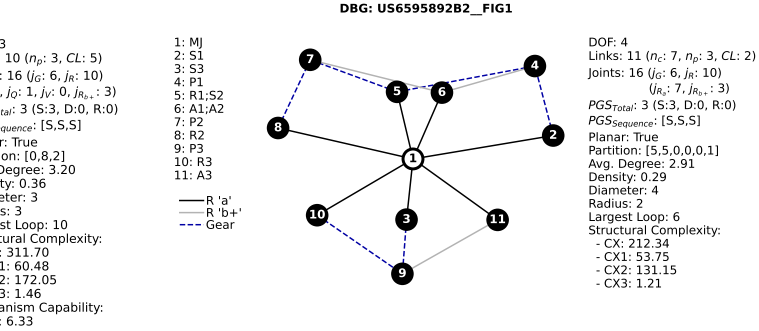

Table 146 – US6595892B2__FIG3 dataset information.

IDENTIFICATION		TOPOLOGY					GEARS SPECS		
UNIQUE_ID	**US6595892B2__FIG3**	**PGS**	**S/D**	**+/-**	**CLs**	**SCs**	**GEARS**	**Ratios**	**Engaged SCs**
Source	patent	1	S	F	F;S1	C1: S2;A3	R1	-1.93	C1;C4
Owner	GM	2	S	IN	IN;S3	C2: S2;R3	1	3.76	C1;C5
Patent	US6595892B2	3	S	OUT	R1;S2	C3: IN;A1	2	2.05	C4;C5
Date	2001				A1;A2	C4: A1;A3	3	1.36	C3;C5
Model	FIG3				OUT;R3	C5: R2;R3	4	1	C3;C4
Commercial?	false						5	0.71	C2;C3
Longitudinal	true						6	0.6	C1;C3
Transversal	false								
Weight (kg)									
Máx. Torque (N·m)									

Figure 175 – US6595892B2__FIG3 representations.

(a) Functional diagram

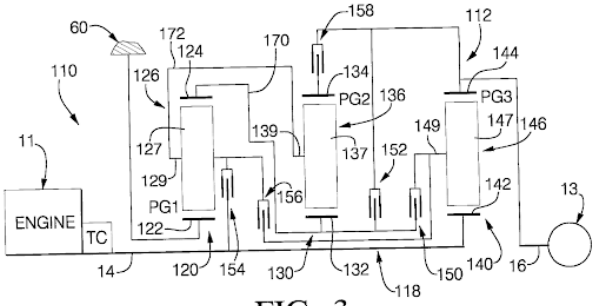

FIG. 3

(b) PGM Graph

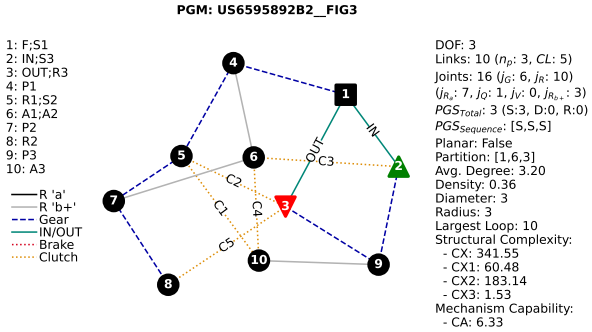

(c) DBG Graph

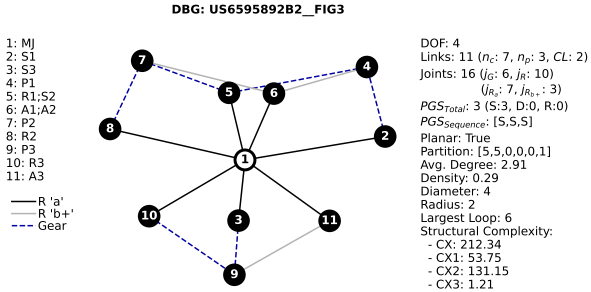

Table 147 – US6595892B2__FIG5 dataset information.

IDENTIFICATION		TOPOLOGY					GEARS SPECS		
UNIQUE_ID	**US6595892B2__FIG5**	**PGS**	**S/D**	**+/-**	**CLs**	**SCs**	**GEARS**	**Ratios**	**Engaged SCs**
Source	patent	1	S	F	F;R1	C1: R2;S3	R1	-1.44	C4;C5
Owner	GM	2	S	IN	IN;A3	C2: A2;S3	1	2.7	C1;C3
Patent	US6595892B2	3	S	OUT	S1;R2	C3: A1;A3	2	1.45	C1;C4
Date	2001				A1;A2	C4: A1;R3	3	1	C2;C4
Model	FIG5				OUT;R3	C5: IN;S2	4	0.71	C1;C2
Commercial?	false						5	0.59	C2;C5
Longitudinal	true						6	0.47	C1;C5
Transversal	false								
Weight (kg)									
Máx. Torque (N·m)									

Figure 176 – US6595892B2__FIG5 representations.

(a) Functional diagram

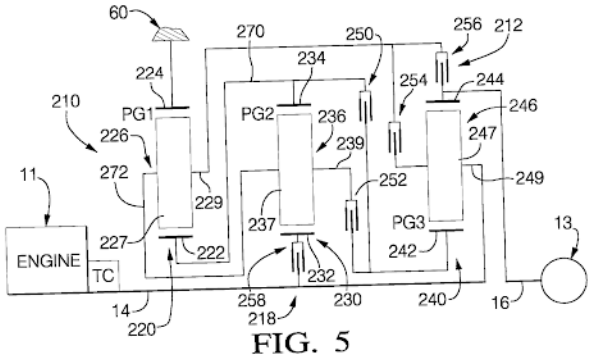

FIG. 5

(b) PGM Graph

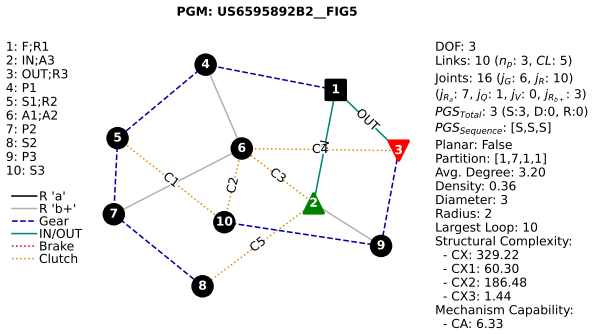

(c) DBG Graph

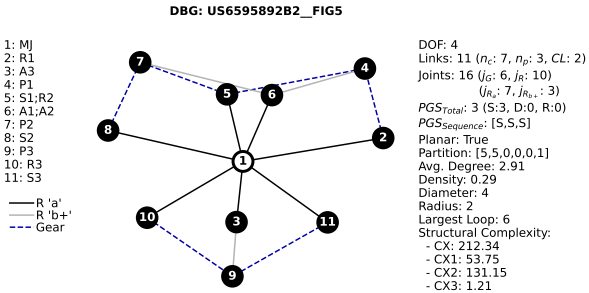

Table 148 – US6595892B2__FIG7 dataset information.

IDENTIFICATION		TOPOLOGY					GEARS SPECS		
UNIQUE_ID	**US6595892B2__FIG7**	**PGS**	**S/D**	**+/-**	**CLs**	**SCs**	**GEARS**	**Ratios**	**Engaged SCs**
Source	patent	1	S	F	F;A1	C1: R1;A3	R1	-1.65	C3;C4
Owner	GM	2	S	IN	IN;A3	C2: R1;S3	1	2.66	C1;C5
Patent	US6595892B2	3	S	OUT	R1;A2	C3: R1;R3	2	1.4	C3;C5
Date	2001				S1;S2	C4: IN;S1	3	1	C2;C3
Model	FIG7				OUT;R3	C5: R2;S3	4	0.65	C2
Commercial?	false						5	0.54	C2;C4
Longitudinal	true						6	0.45	C4;C5
Transversal	false								
Weight (kg)									
Máx. Torque (N·m)									

Figure 177 – US6595892B2__FIG7 representations.

(a) Functional diagram

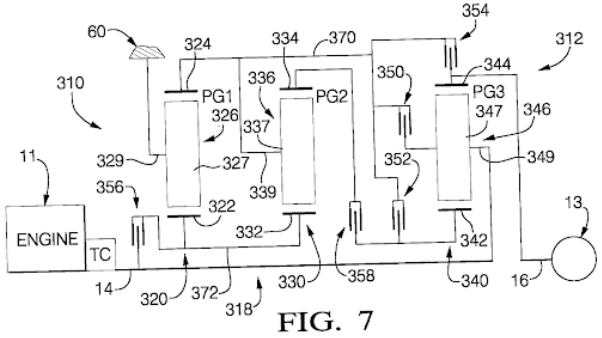

FIG. 7

(b) PGM Graph

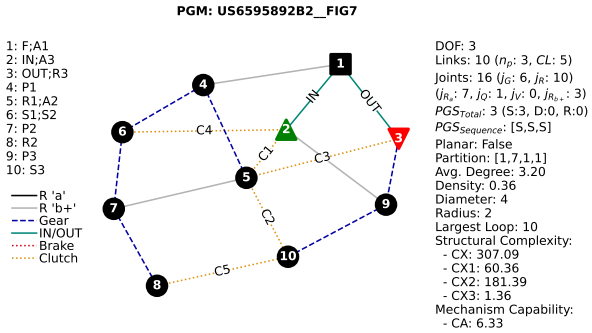

(c) DBG Graph

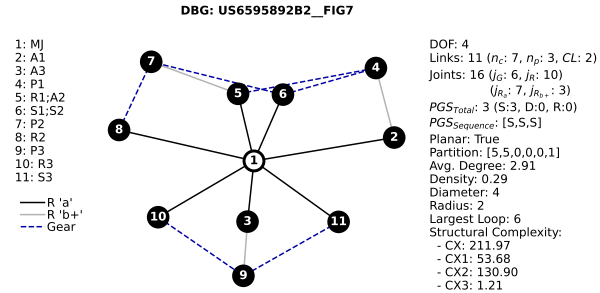

Table 149 – US6595892B2__FIG9 dataset information.

IDENTIFICATION		TOPOLOGY					GEARS SPECS		
UNIQUE_ID	**US6595892B2__FIG9**	**PGS**	**S/D**	**+/-**	**CLs**	**SCs**	**GEARS**	**Ratios**	**Engaged SCs**
Source	patent	1	S	F	F;S1	C1: IN;A1	R1	-2.13	C2;C3
Owner	GM	2	S	IN	IN;S3	C2: A1;A3	1	3.71	C3;C5
Patent	US6595892B2	3	S	OUT	R1;S2	C3: S2;A3	2	1.96	C2;C5
Date	2001				A1;A2	C4: S2;R3	3	1.31	C1;C5
Model	FIG9				OUT;R3	C5: R2;R3	4	1	C1;C2
Commercial?	false						5	0.7	C1;C4
Longitudinal	true						6	0.61	C1;C3
Transversal	false								
Weight (kg)									
Máx. Torque (N·m)									

Figure 178 – US6595892B2__FIG9 representations.

(a) Functional diagram

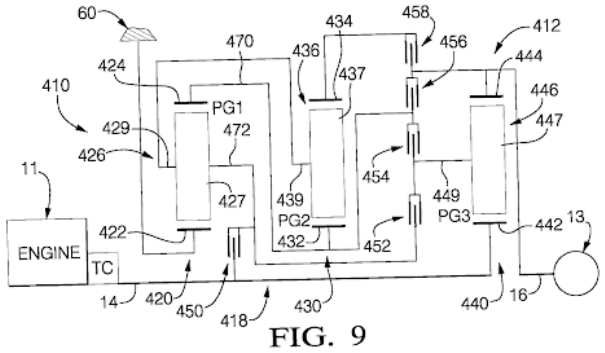

FIG. 9

(b) PGM Graph

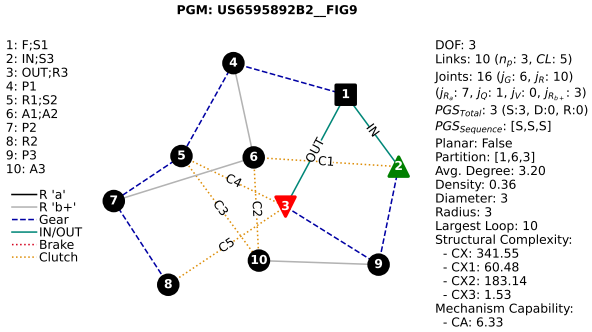

(c) DBG Graph

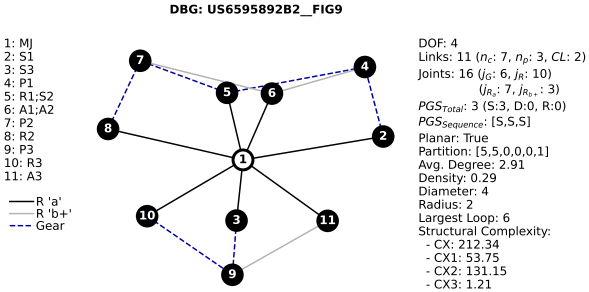

Table 150 – US6595892B2__FIG11 dataset information.

IDENTIFICATION		TOPOLOGY					GEARS SPECS		
UNIQUE_ID	**US6595892B2__FIG11**	**PGS**	**S/D**	**+/-**	**CLs**	**SCs**	**GEARS**	**Ratios**	**Engaged SCs**
Source	patent	1	S	F	F;S1	C1: IN;R1	R1	-2.33	C2;C4
Owner	GM	2	S	IN	IN;S3	C2: R1;A3	1	3.91	C3;C4
Patent	US6595892B2	3	S	OUT	R1;A2	C3: A1;R3	2	2.12	C2;C3
Date	2001				A1;R2	C4: S2;A3	3	1.34	C1;C3
Model	FIG11				OUT;R3	C5: S2;R3	4	1	C1;C2
Commercial?	false						5	0.72	C1;C5
Longitudinal	true						6	0.65	C1;C4
Transversal	false								
Weight (kg)									
Máx. Torque (N·m)									

Figure 179 – US6595892B2__FIG11 representations.

(a) Functional diagram

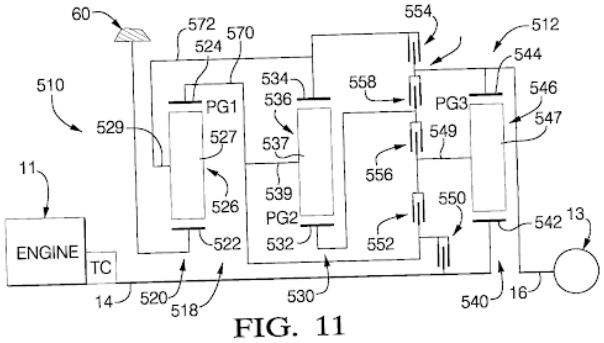

FIG. 11

(b) PGM Graph

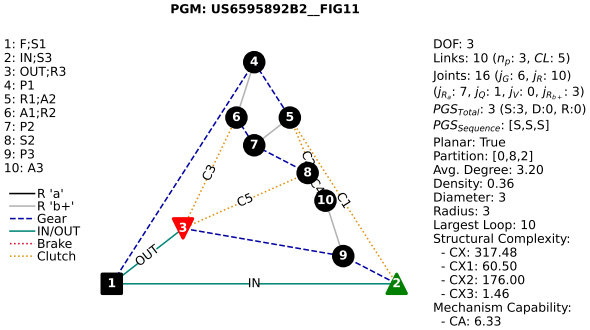

(c) DBG Graph

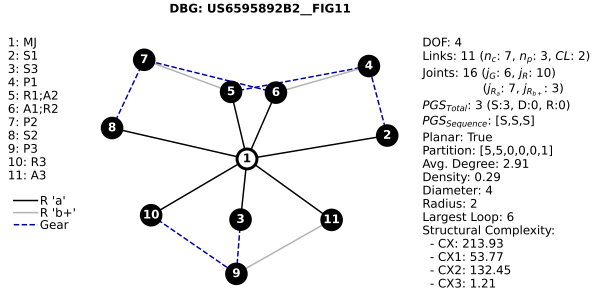

Table 151 – US6595892B2__FIG13 dataset information.

IDENTIFICATION		TOPOLOGY					GEARS SPECS		
UNIQUE_ID	**US6595892B2__FIG13**	**PGS**	**S/D**	**+/-**	**CLs**	**SCs**	**GEARS**	**Ratios**	**Engaged SCs**
Source	patent	1	S	F	F;S1	C1: S2;OUT	R1	-2.4	C2;C5
Owner	GM	2	S	IN	IN;S3	C2: S2;A3	1	3.16	C2;C4
Patent	US6595892B2	3	S	OUT	R1;S2	C3: R2;S3	2	1.77	C4;C5
Date	2001				A1;R2	C4: A1;OUT	3	1	C3;C4
Model	FIG13				OUT;R3	C5: A2;A3	4	0.76	C3;C5
Commercial?	false						5	0.61	C1;C3
Longitudinal	true						6	0.53	C2;C3
Transversal	false								
Weight (kg)									
Máx. Torque (N·m)									

Figure 180 – US6595892B2__FIG13 representations.

(a) Functional diagram

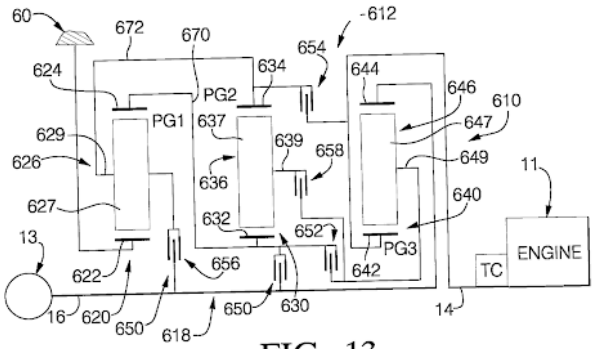

FIG. 13

(b) PGM Graph

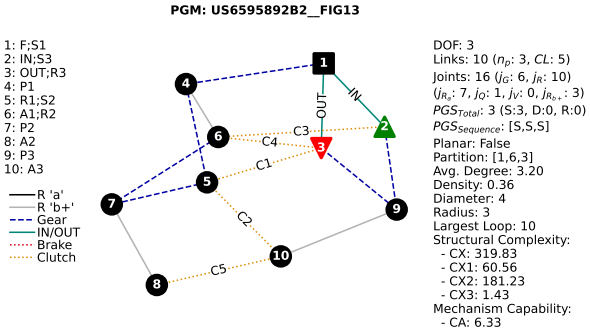

(c) DBG Graph

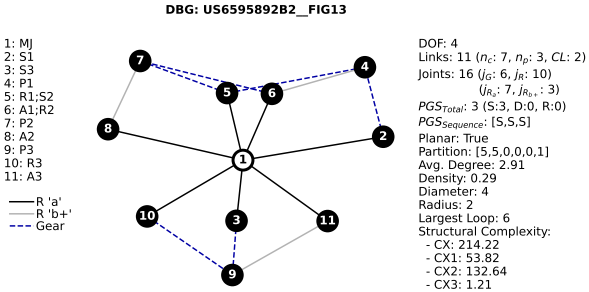

Table 152 – US6595892B2__FIG15 dataset information.

IDENTIFICATION		TOPOLOGY					GEARS SPECS		
UNIQUE_ID	**US6595892B2__FIG15**	**PGS**	**S/D**	**+/-**	**CLs**	**SCs**	**GEARS**	**Ratios**	**Engaged SCs**
Source	patent	1	S	F	F;A1	C1: R1;OUT	R1	-1.98	C1;C2
Owner	GM	2	S	IN	IN;R3	C2: S1;R3	1	3.95	C1;C5
Patent	US6595892B2	3	S	OUT	R1;S2	C3: A2;S3	2	2.79	C1;C3
Date	2001				S1;A2	C4: R2;R3	3	1.6	C3;C5
Model	FIG15				OUT;A3	C5: R2;S3	4	1.23	C3;C4
Commercial?	false						5	1	C2;C3
Longitudinal	true						6	0.73	C2;C5
Transversal	false								
Weight (kg)									
Máx. Torque (N·m)									

Figure 181 – US6595892B2__FIG15 representations.

(a) Functional diagram

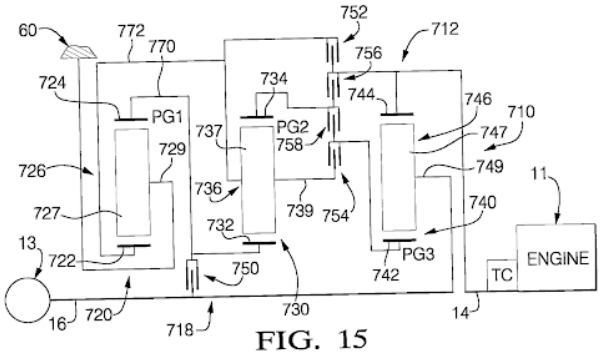

FIG. 15

(b) PGM Graph

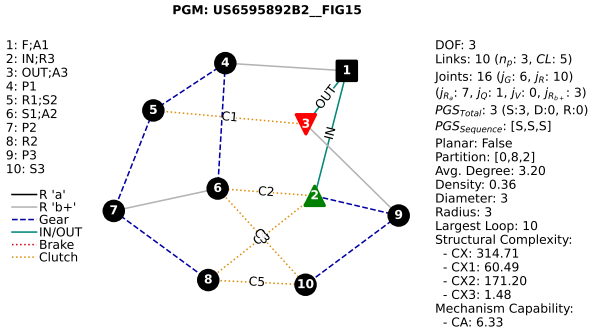

(c) DBG Graph

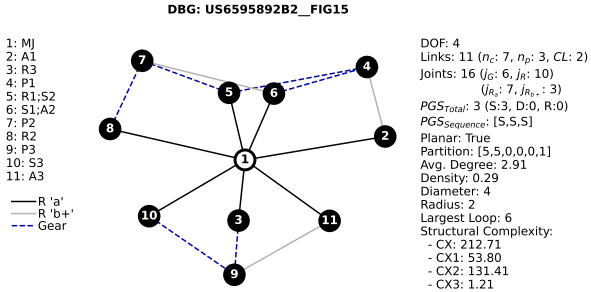

Table 153 – US6595892B2__FIG17 dataset information.

IDENTIFICATION		TOPOLOGY					GEARS SPECS		
UNIQUE_ID	**US6595892B2__FIG17**	**PGS**	**S/D**	**+/-**	**CLs**	**SCs**	**GEARS**	**Ratios**	**Engaged SCs**
Source	patent	1	S	F	F;A1	C1: R1;OUT	R1	-2.47	C1;C3
Owner	GM	2	S	IN	IN;R3	C2: S1;S3	1	3.73	C1;C5
Patent	US6595892B2	3	S	OUT	R1;S2	C3: IN;S1	2	2.65	C1;C2
Date	2001				S1;A2	C4: S1;A3	3	1.48	C2;C5
Model	FIG17				OUT;A3	C5: R2;S3	4	1	C2;C3
Commercial?	false						5	0.77	C3;C5
Longitudinal	true						6	0.56	C4;C5
Transversal	false								
Weight (kg)									
Máx. Torque (N·m)									

Figure 182 – US6595892B2__FIG17 representations.

(a) Functional diagram

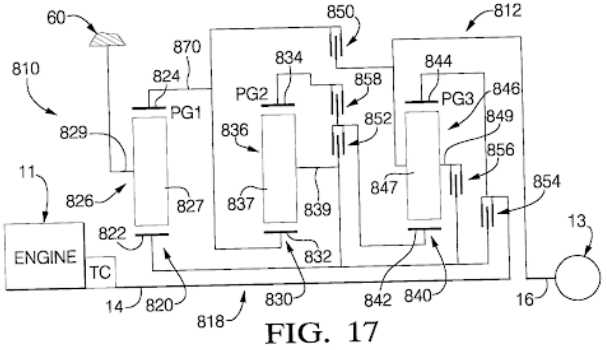

FIG. 17

(b) PGM Graph

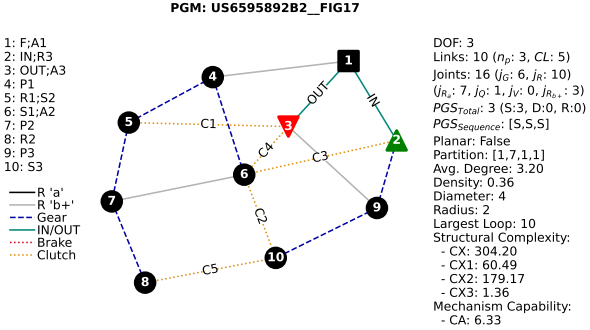

(c) DBG Graph

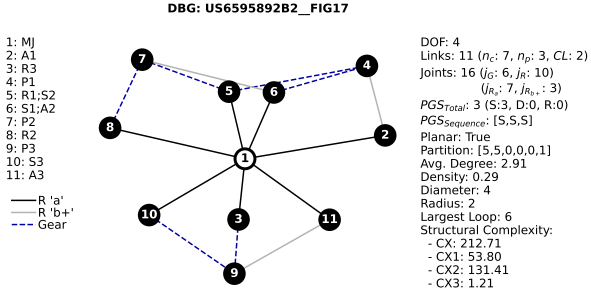

Table 154 – US6595892B2__FIG19 dataset information.

IDENTIFICATION		TOPOLOGY					GEARS SPECS		
UNIQUE_ID	**US6595892B2__FIG19**	**PGS**	**S/D**	**+/-**	**CLs**	**SCs**	**GEARS**	**Ratios**	**Engaged SCs**
Source	patent	1	D	F	F;S1	C1: A1;OUT	R1	-2.86	C3;C5
Owner	GM	2	S	IN	IN;S3	C2: A1;R3	1	3.62	C1;C5
Patent	US6595892B2	3	S	OUT	R1;A2	C3: IN;R1	2	2.53	C5
Date	2001				A1;R2	C4: A2;R3	3	1.65	C1;C4
Model	FIG19				OUT;A3	C5: S2;R3	4	1	C3;C4
Commercial?	false						5	0.69	C2;C3
Longitudinal	true						6	0.58	C1;C3
Transversal	false								
Weight (kg)									
Máx. Torque (N·m)									

Figure 183 – US6595892B2__FIG19 representations.

(a) Functional diagram

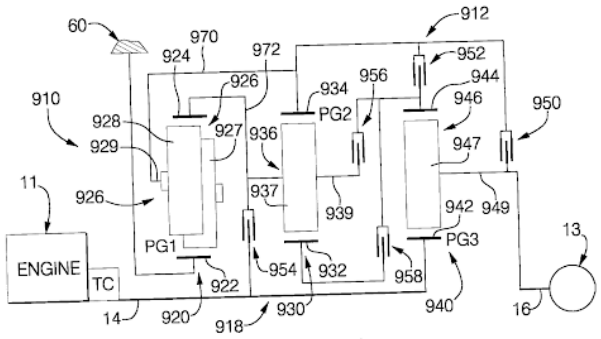

FIG. 19

(b) PGM Graph

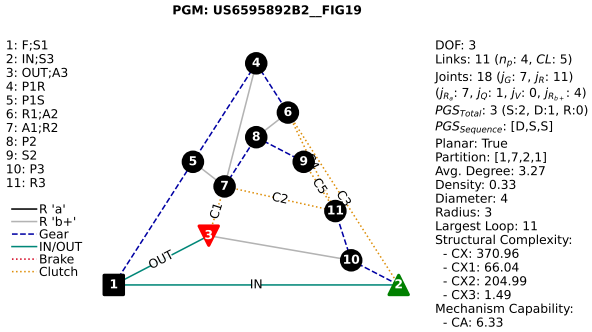

(c) DBG Graph

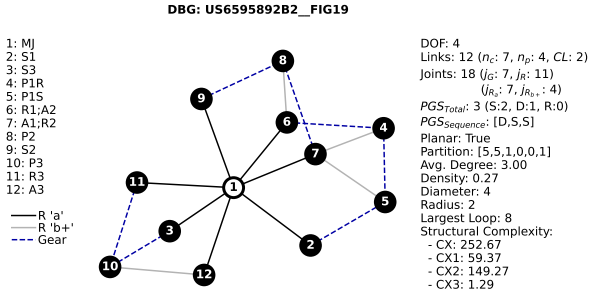

Table 155 – US6595892B2__FIG21 dataset information.

IDENTIFICATION		TOPOLOGY					GEARS SPECS		
UNIQUE_ID	**US6595892B2__FIG21**	**PGS**	**S/D**	**+/-**	**CLs**	**SCs**	**GEARS**	**Ratios**	**Engaged SCs**
Source	patent	1	S	F	F;S1	C1: S2;R3	R1	-1.53	C1;C3
Owner	GM	2	S	IN	IN;S3	C2: S2;A3	1	2.76	C1;C5
Patent	US6595892B2	3	D	OUT	R1;S2	C3: A2;R3	2	1.47	C3;C5
Date	2001				A1;A2	C4: IN;R2	3	1	C4;C5
Model	FIG21				OUT;A3	C5: R2;A3	4	0.76	C3;C4
Commercial?	false						5	0.59	C2;C4
Longitudinal	true						6	0.46	C1;C4
Transversal	false								
Weight (kg)									
Máx. Torque (N·m)									

Figure 184 – US6595892B2__FIG21 representations.

(a) Functional diagram

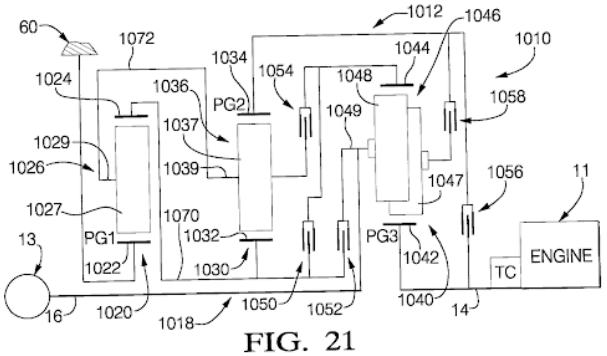

FIG. 21

(b) PGM Graph

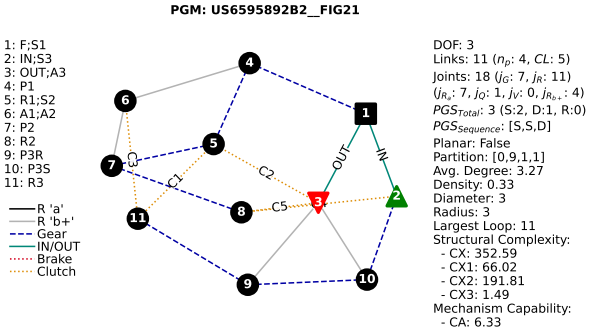

(c) DBG Graph

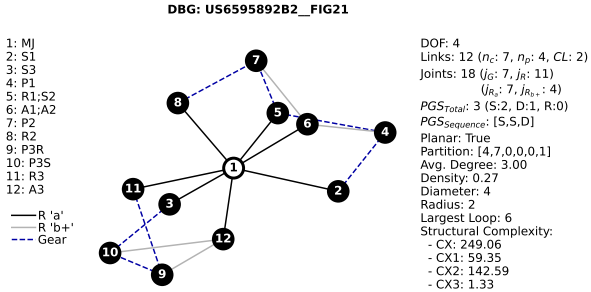

Table 156 – US6595892B2__FIG23 dataset information.

IDENTIFICATION		TOPOLOGY					GEARS SPECS		
UNIQUE_ID	**US6595892B2__FIG23**	**PGS**	**S/D**	**+/-**	**CLs**	**SCs**	**GEARS**	**Ratios**	**Engaged SCs**
Source	patent	1	S	F	F;S1	C1: R1;A3	R1	-1.67	C1;C5
Owner	GM	2	S	IN	IN;S3	C2: A1;R3	1	3.25	C2;C5
Patent	US6595892B2	3	S	OUT	R1;A2	C3: IN;A1	2	1.89	C1;C2
Date	2001				A1;R2	C4: S2;R3	3	1	C2;C3
Model	FIG23				OUT;R3	C5: S2;A3	4	0.65	C1;C3
Commercial?	false						5	0.54	C3;C4
Longitudinal	true						6	0.43	C3;C5
Transversal	false						7	0.26	C1;C4
Weight (kg)									
Máx. Torque (N·m)									

Figure 185 – US6595892B2__FIG23 representations.

(a) Functional diagram

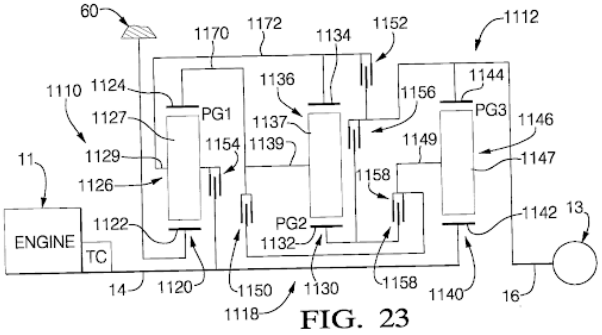

FIG. 23

(b) PGM Graph

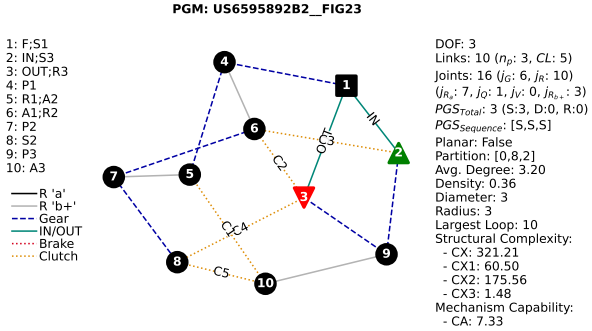

(c) DBG Graph

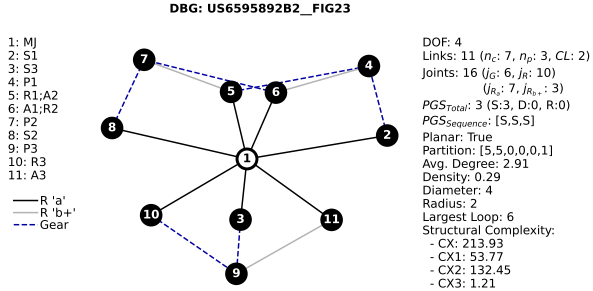

Table 157 – US6595892B2__FIG25 dataset information.

IDENTIFICATION		TOPOLOGY					GEARS SPECS		
UNIQUE_ID	**US6595892B2__FIG25**	**PGS**	**S/D**	**+/-**	**CLs**	**SCs**	**GEARS**	**Ratios**	**Engaged SCs**
Source	patent	1	S	F	F;R1	C1: A2;A3	R1	-1.6	C4;C5
Owner	GM	2	D	IN	IN;R3	C2: A2;R3	1	2.63	C2;C4
Patent	US6595892B2	3	D	OUT	S1;A2	C3: A1;A3	2	1.73	C1;C4
Date	2001				A1;R2	C4: A1;OUT	3	1	C3;C4
Model	FIG25				OUT;S3	C5: S2;R3	4	0.66	C2;C3
Commercial?	false						5	0.55	C1;C3
Longitudinal	true						6	0.43	C3;C5
Transversal	false						7	0.32	C1;C5
Weight (kg)									
Máx. Torque (N·m)									

Figure 186 – US6595892B2__FIG25 representations.

(a) Functional diagram

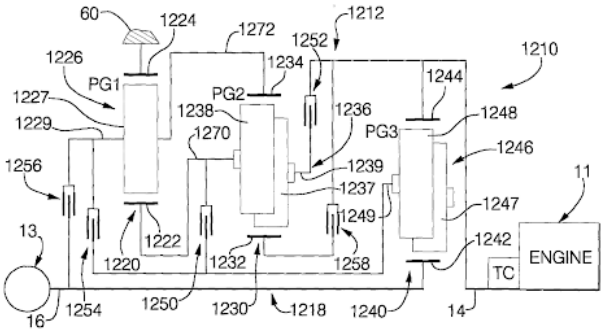

FIG. 25

(b) PGM Graph

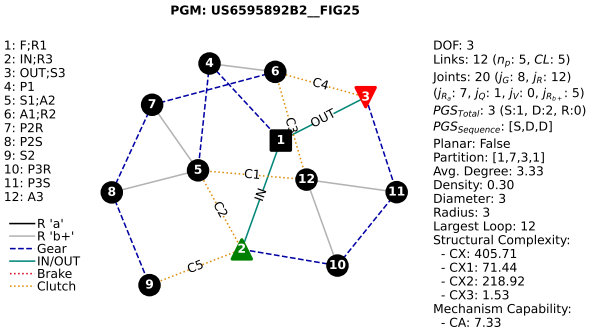

(c) DBG Graph

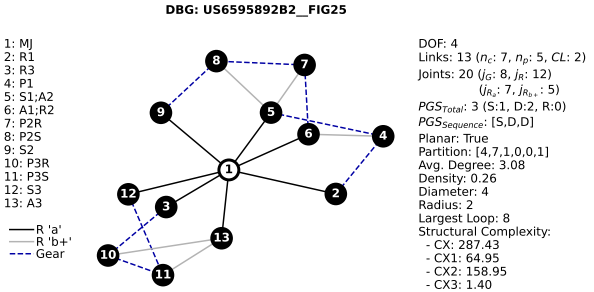

Table 158 – US6595892B2__FIG27 dataset information.

IDENTIFICATION		TOPOLOGY					GEARS SPECS		
UNIQUE_ID	**US6595892B2__FIG27**	**PGS**	**S/D**	**+/-**	**CLs**	**SCs**	**GEARS**	**Ratios**	**Engaged SCs**
Source	patent	1	D	F	F;S1	C1: S2;S3	R1	-2.42	C1;C3
Owner	GM	2	S	IN	IN;R3	C2: A1;R3	1	3.13	C2;C5
Patent	US6595892B2	3	D	OUT	R1;A2	C3: R1;R3	2	2.23	C1;C5
Date	2001				A1;S2	C4: R2;S3	3	1.54	C3;C5
Model	FIG27				OUT;A3	C5: R2;A3	4	1	C4;C5
Commercial?	false						5	0.67	C3;C4
Longitudinal	true						6	0.52	C2;C4
Transversal	false						7	0.42	C1;C4
Weight (kg)									
Máx. Torque (N·m)									

Figure 187 – US6595892B2__FIG27 representations.

(a) Functional diagram

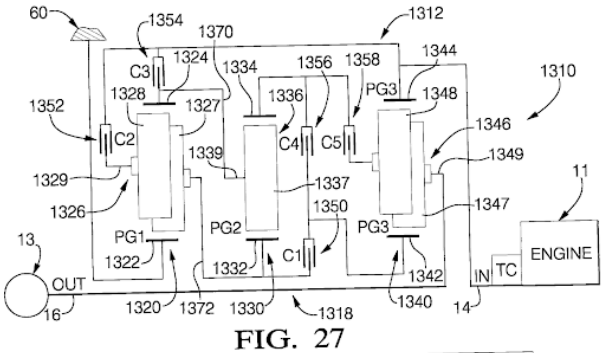

FIG. 27

(b) PGM Graph

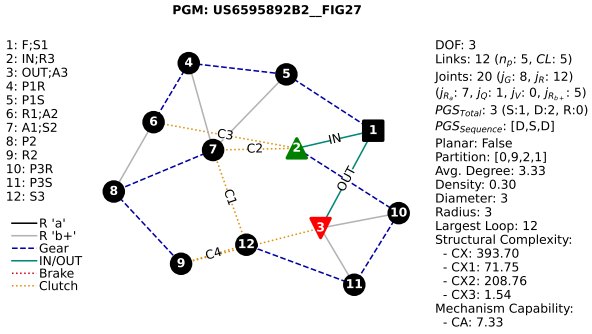

(c) DBG Graph

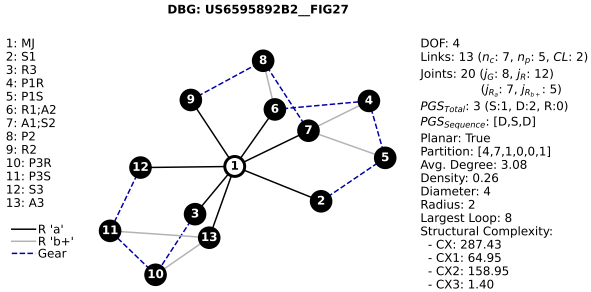

Table 159 – US6623398B2__FIG1 dataset information.

IDENTIFICATION		TOPOLOGY					GEARS SPECS		
UNIQUE_ID	**US6623398B2__FIG1**	**PGS**	**S/D**	**+/-**	**CLs**	**SCs**	**GEARS**	**Ratios**	**Engaged SCs**
Source	patent	1	S	F	F;R3	C1: A2;S3	R1	-2.99	C2;C5
Owner	GM	2	S	IN	IN;A1	C2: A2;A3	1	3.63	C3;C4
Patent	US6623398B2	3	S	OUT	OUT;R1;R2	C3: OUT;A3	2	2.05	C1;C3
Date	2001				S1;A2	C4: IN;S3	3	1.31	C3;C5
Model	FIG1					C5: S2;S3	4	1	C4;C5
Commercial?	false						5	0.67	C2;C4
Longitudinal	true						6	0.67	C1;C2
Transversal	false								
Weight (kg)									
Máx. Torque (N·m)									

Figure 188 – US6623398B2__FIG1 representations.

(a) Functional diagram

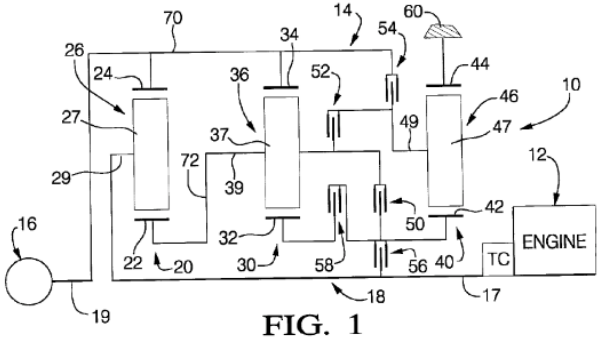

FIG. 1

(b) PGM Graph

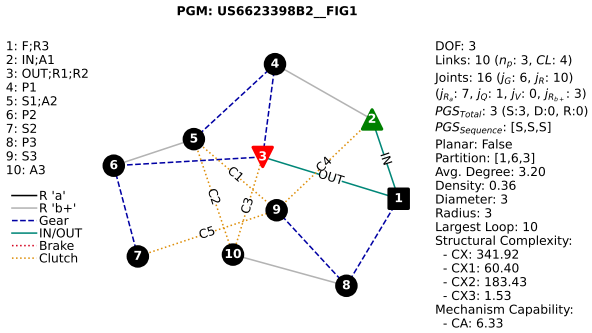

(c) DBG Graph

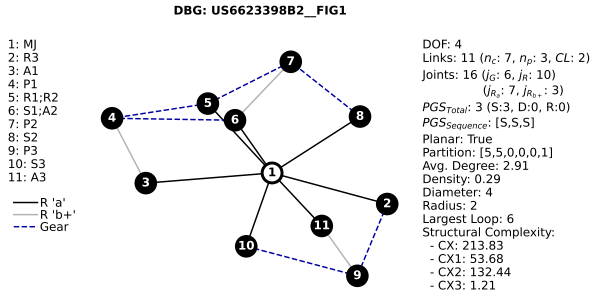

Table 160 – US6623398B2__FIG3 dataset information.

IDENTIFICATION		TOPOLOGY					GEARS SPECS		
UNIQUE_ID	**US6623398B2__FIG3**	**PGS**	**S/D**	**+/-**	**CLs**	**SCs**	**GEARS**	**Ratios**	**Engaged SCs**
Source	patent	1	S	F	F;R3	C1: A1;S3	R1	-1.77	C2;C5
Owner	GM	2	S	IN	IN;A1;S2	C2: R2;S3	1	2.63	C1;C5
Patent	US6623398B2	3	S	OUT	S1;R2	C3: R1;S3	2	1.88	C3;C5
Date	2001				OUT;A2	C4: R1;A3	3	1	C2;C3
Model	FIG3					C5: A3;OUT	4	0.7	C2;C4
Commercial?	false						5	0.58	C1;C4
Longitudinal	true						6	0.46	C3;C4
Transversal	false								
Weight (kg)									
Máx. Torque (N·m)									

Figure 189 – US6623398B2__FIG3 representations.

(a) Functional diagram

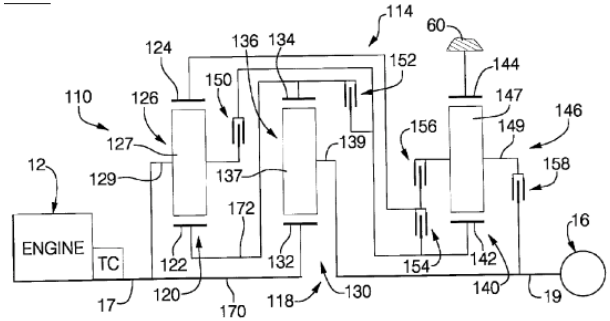

(b) PGM Graph

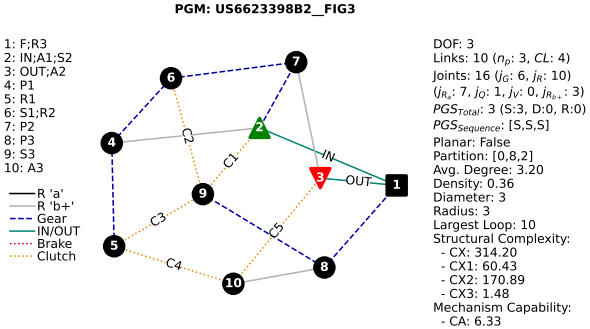

(c) DBG Graph

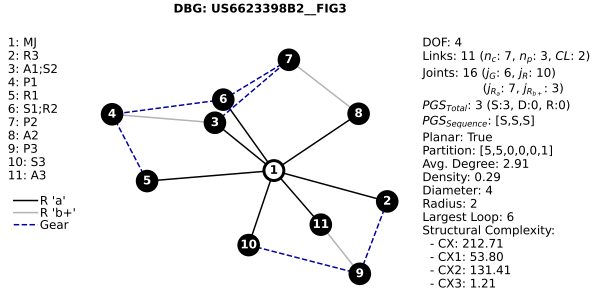

Table 161 – US6623398B2__FIG5 dataset information.

IDENTIFICATION		TOPOLOGY					GEARS SPECS		
UNIQUE_ID	**US6623398B2__FIG5**	**PGS**	**S/D**	**+/-**	**CLs**	**SCs**	**GEARS**	**Ratios**	**Engaged SCs**
Source	patent	1	S	F	F;S3	C1: A2;A3	R1	-1.9	C1;C5
Owner	GM	2	S	IN	IN;A2;S1	C2: A1;R3	1	3.64	C3;C4
Patent	US6623398B2	3	S	OUT	OUT;A1;S2	C3: R1;A3	2	2.05	C2;C3
Date	2001					C4: R1;R3	3	1.32	C3;C5
Model	FIG5					C5: R2;R3	4	1	C1;C3
Commercial?	false						5	0.68	C1;C4
Longitudinal	true						6	0.6	C1;C2
Transversal	false								
Weight (kg)									
Máx. Torque (N·m)									

Figure 190 – US6623398B2__FIG5 representations.

(a) Functional diagram

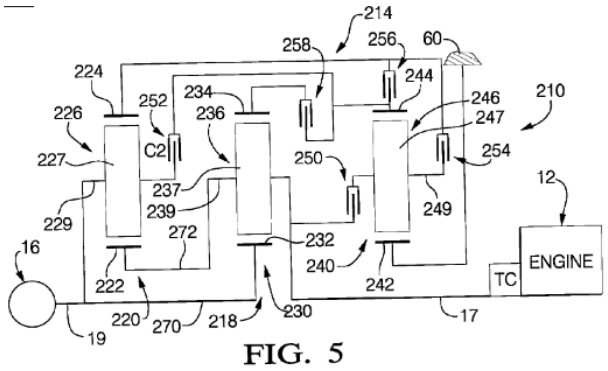

FIG. 5

(b) PGM Graph

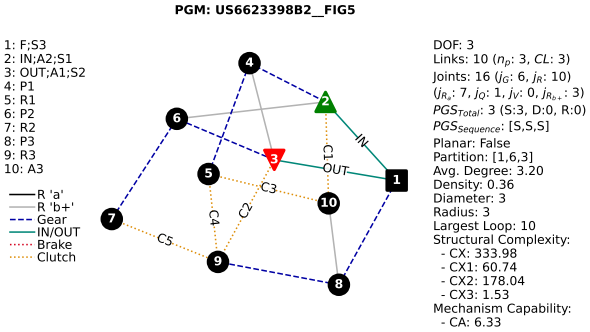

(c) DBG Graph

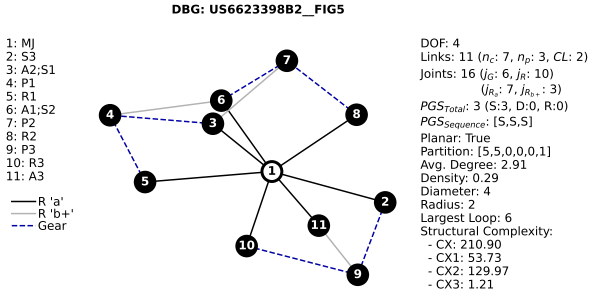

Table 162 – US6623398B2__FIG7 dataset information.

IDENTIFICATION		TOPOLOGY					GEARS SPECS		
UNIQUE_ID	**US6623398B2__FIG7**	**PGS**	**S/D**	**+/-**	**CLs**	**SCs**	**GEARS**	**Ratios**	**Engaged SCs**
Source	patent	1	D	F	F;R3	C1: A2;S3	R1	-2.99	C2;C5
Owner	GM	2	S	IN	IN;R1	C2: A2;A3	1	3.63	C3;C4
Patent	US6623398B2	3	S	OUT	S1;A2	C3: R2;A3	2	2.05	C1;C3
Date	2001				OUT;A1;R2	C4: IN;S3	3	1.31	C3;C5
Model	FIG7					C5: S2;S3	4	1	C4;C5
Commercial?	false						5	0.67	C2;C4
Longitudinal	true						6	0.6	C1;C2
Transversal	false								
Weight (kg)									
Máx. Torque (N·m)									

Figure 191 – US6623398B2__FIG7 representations.

(a) Functional diagram

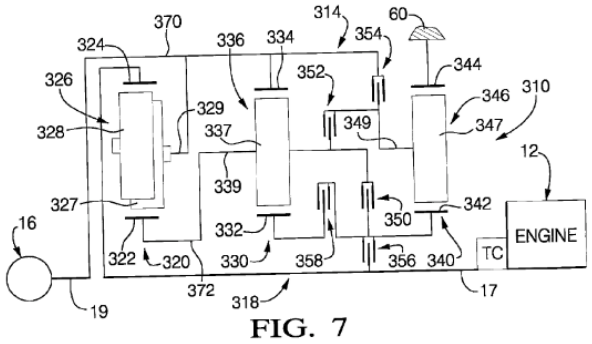

FIG. 7

(b) PGM Graph

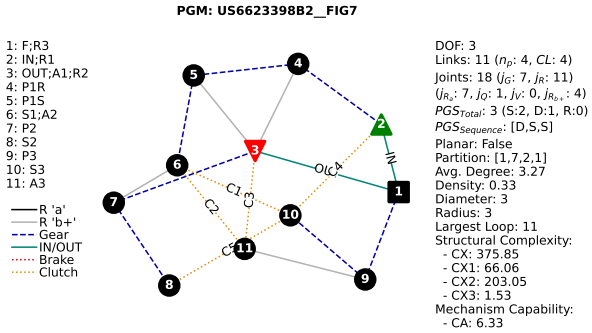

(c) DBG Graph

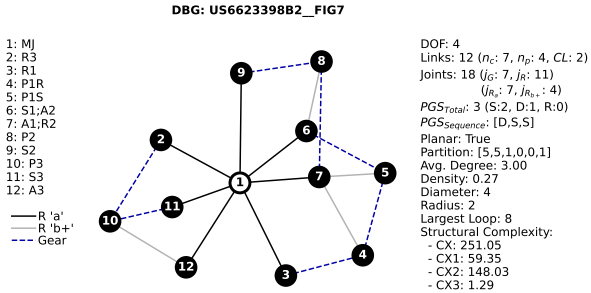

Table 163 – US6623398B2__FIG9 dataset information.

IDENTIFICATION		TOPOLOGY					GEARS SPECS		
UNIQUE_ID	**US6623398B2__FIG9**	**PGS**	**S/D**	**+/-**	**CLs**	**SCs**	**GEARS**	**Ratios**	**Engaged SCs**
Source	patent	1	S	F	F;R3	C1: S2;S3	R1	-2.4	C2;C4
Owner	GM	2	D	IN	IN;R2	C2: A1;A3	1	3.63	C3;C5
Patent	US6623398B2	3	S	OUT	OUT;R1;A2	C3: OUT;A3	2	2.01	C1;C3
Date	2001				A1;S2	C4: S1;S3	3	1.3	C3;C4
Model	FIG9					C5: R2;S3	4	1	C4;C5
Commercial?	false						5	0.69	C2;C5
Longitudinal	true						6	0.61	C1;C2
Transversal	false								
Weight (kg)									
Máx. Torque (N·m)									

Figure 192 – US6623398B2__FIG9 representations.

(a) Functional diagram

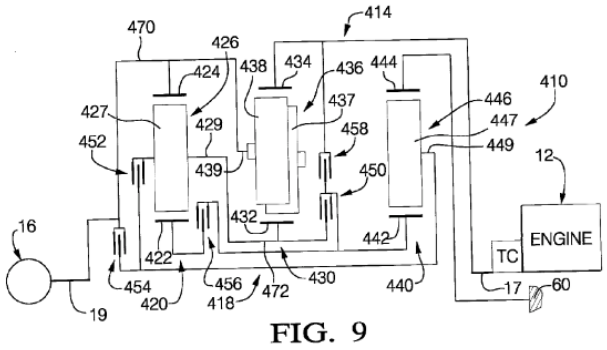

FIG. 9

(b) PGM Graph

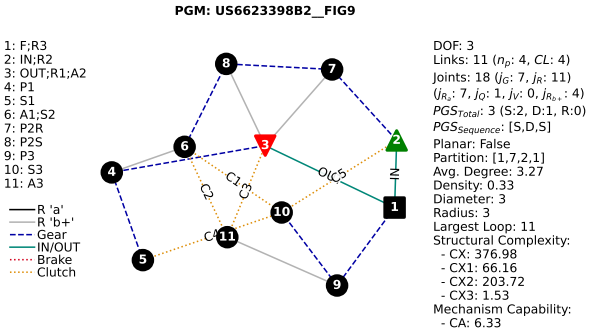

(c) DBG Graph

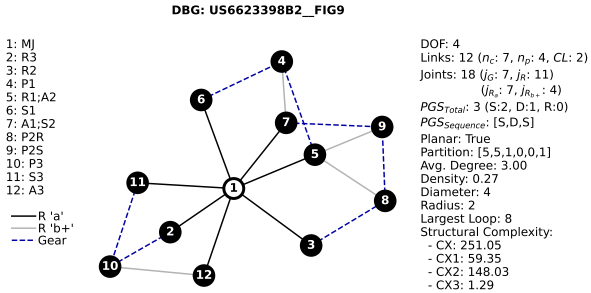

Table 164 – US6623398B2__FIG11 dataset information.

IDENTIFICATION		TOPOLOGY					GEARS SPECS		
UNIQUE_ID	**US6623398B2__FIG11**	**PGS**	**S/D**	**+/-**	**CLs**	**SCs**	**GEARS**	**Ratios**	**Engaged SCs**
Source	patent	1	S	F	F;A3	B1: F;A2	R1	-2.83	B1;C1
Owner	GM	2	S	IN	IN;S3	C1: S2;S3	1	4.67	B1;C4
Patent	US6623398B2	3	D	OUT	S1;S2	C2: S2;A3	2	3.09	C2;C4
Date	2001				A1;A2	C3: A2;S3	3	1.98	C1;C4
Model	FIG11				OUT;R2	C4: R1;R3	4	1.49	C3;C4
Commercial?	false						5	1	C1;C3
Longitudinal	true						6	0.74	C2;C3
Transversal	false								
Weight (kg)									
Máx. Torque (N·m)									

Figure 193 – US6623398B2__FIG11 representations.

(a) Functional diagram

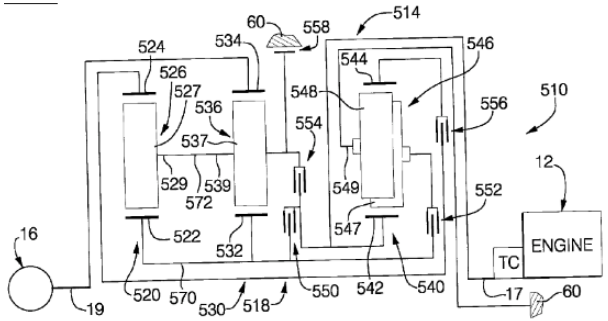

FIG. 11

(b) PGM Graph

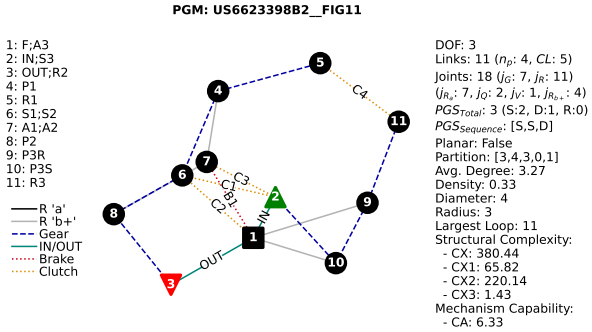

(c) DBG Graph

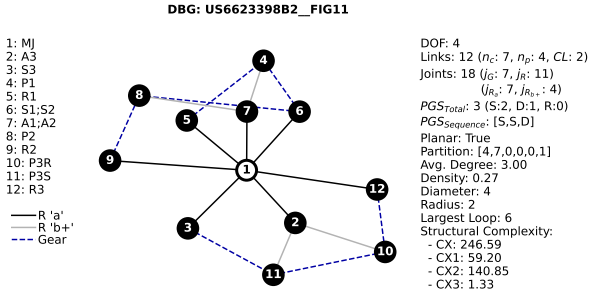

Table 165 – US6623398B2__FIG13 dataset information.

IDENTIFICATION		TOPOLOGY					GEARS SPECS		
UNIQUE_ID	**US6623398B2__FIG13**	**PGS**	**S/D**	**+/-**	**CLs**	**SCs**	**GEARS**	**Ratios**	**Engaged SCs**
Source	patent	1	S	F	F;A3	B1: F;A2	R1	-2.33	B1;C1
Owner	GM	2	S	IN	IN;S3	C1: R1;R3	1	3.71	B1;C4
Patent	US6623398B2	3	D	OUT	R1;S2	C2: R1;A3	2	2.39	C2;C4
Date	2001				A1;A2	C3: IN;A2	3	1.58	C1;C4
Model	FIG13				OUT;R2	C4: S1;R3	4	1.17	C3;C4
Commercial?	false						5	0.82	C1;C3
Longitudinal	true						6	0.6	C2;C3
Transversal	false								
Weight (kg)									
Máx. Torque (N·m)									

Figure 194 – US6623398B2__FIG13 representations.

(a) Functional diagram

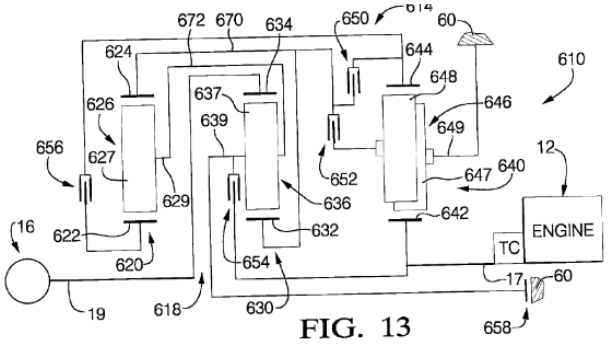

FIG. 13

(b) PGM Graph

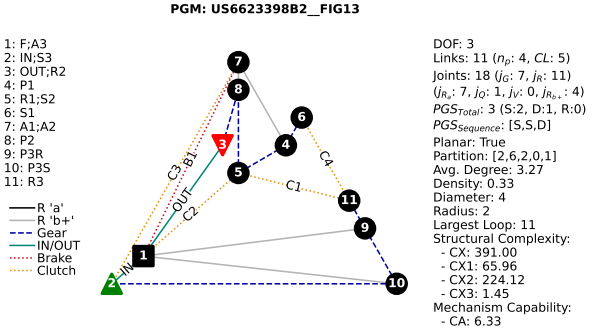

(c) DBG Graph

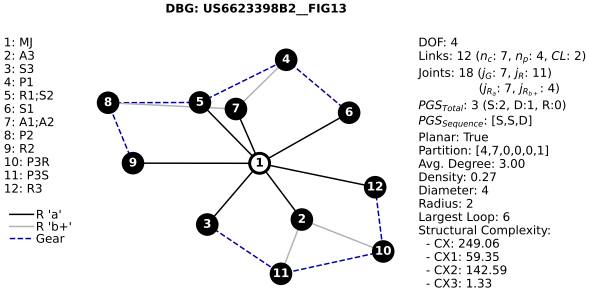

Table 166 – US6623398B2__FIG15 dataset information.

IDENTIFICATION		TOPOLOGY					GEARS SPECS		
UNIQUE_ID	**US6623398B2__FIG15**	**PGS**	**S/D**	**+/-**	**CLs**	**SCs**	**GEARS**	**Ratios**	**Engaged SCs**
Source	patent	1	S	F	F;A3	B1: F;A1	R1	-3.46	B1;C1
Owner	GM	2	S	IN	IN;S3	C1: S2;R3	1	3.78	B1;C4
Patent	US6623398B2	3	D	OUT	R1;S2	C2: S2;A3	2	2.06	C2;C4
Date	2001				A1;A2	C3: IN;A1	3	1.38	C1;C4
Model	FIG15				OUT;R2	C4: IN;S1	4	1	C3;C4
Commercial?	false						5	0.75	C1;C3
Longitudinal	true						6	0.62	C2;C3
Transversal	false								
Weight (kg)									
Máx. Torque (N·m)									

Figure 195 – US6623398B2__FIG15 representations.

(a) Functional diagram

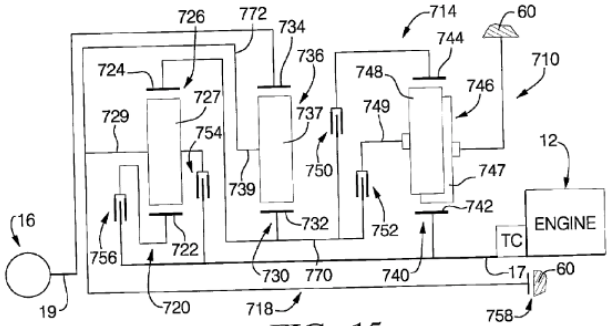

FIG. 15

(b) PGM Graph

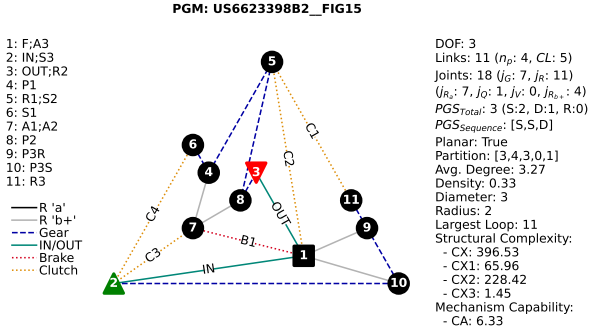

(c) DBG Graph

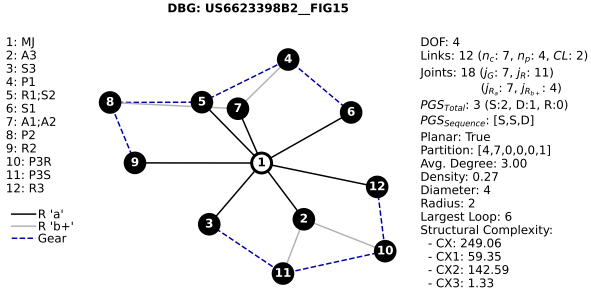

Table 167 – US6623398B2__FIG17 dataset information.

IDENTIFICATION		TOPOLOGY					GEARS SPECS		
UNIQUE_ID	**US6623398B2__FIG17**	**PGS**	**S/D**	**+/-**	**CLs**	**SCs**	**GEARS**	**Ratios**	**Engaged SCs**
Source	patent	1	S	F	F;A3	B1: F;A2	R1	-1.12	B1;C1
Owner	GM	2	S	IN	IN;R3	C1: S2;S3	1	1.85	B1;C4
Patent	US6623398B2	3	D	OUT	S1;S2	C2: S2;A3	2	1.22	C2;C4
Date	2001				A1;A2	C3: A2;S3	3	0.78	C1;C4
Model	FIG17				OUT;R2	C4: IN;R1	4	0.59	C3;C4
Commercial?	false						5	0.4	C1;C3
Longitudinal	true						6	0.29	C2;C3
Transversal	false								
Weight (kg)									
Máx. Torque (N·m)									

Figure 196 – US6623398B2__FIG17 representations.

(a) Functional diagram

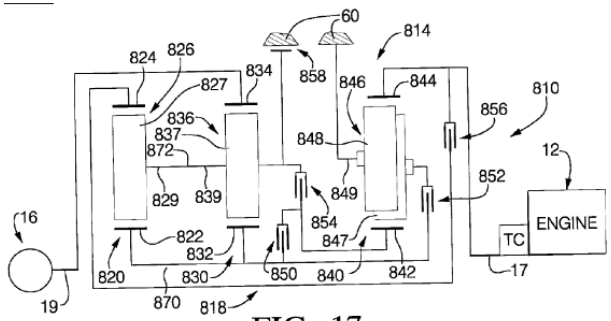

FIG. 17

(b) PGM Graph

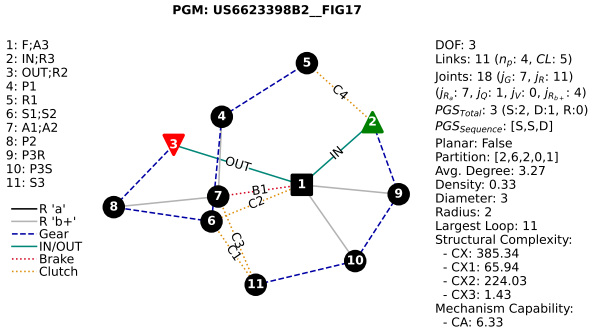

(c) DBG Graph

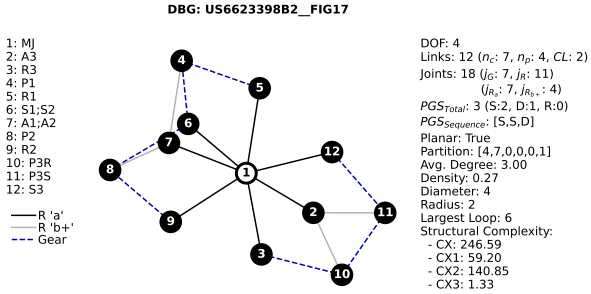

Table 168 – US6623398B2__FIG19 dataset information.

IDENTIFICATION		TOPOLOGY					GEARS SPECS		
UNIQUE_ID	**US6623398B2__FIG19**	**PGS**	**S/D**	**+/-**	**CLs**	**SCs**	**GEARS**	**Ratios**	**Engaged SCs**
Source	patent	1	S	F	F;A3	B1: F;A2	R1	-1.53	B1;C1
Owner	GM	2	S	IN	IN;R3	C1: IN;S2	1	2.42	B1;C4
Patent	US6623398B2	3	D	OUT	R1;S2	C2: R1;A3	2	1.56	C2;C4
Date	2001				A1;A2	C3: A2;S3	3	1	C1;C4
Model	FIG19				OUT;R2	C4: IN;S1	4	0.76	C3;C4
Commercial?	false						5	0.53	C1;C3
Longitudinal	true						6	0.4	C2;C3
Transversal	false								
Weight (kg)									
Máx. Torque (N·m)									

Figure 197 – US6623398B2__FIG19 representations.

(a) Functional diagram

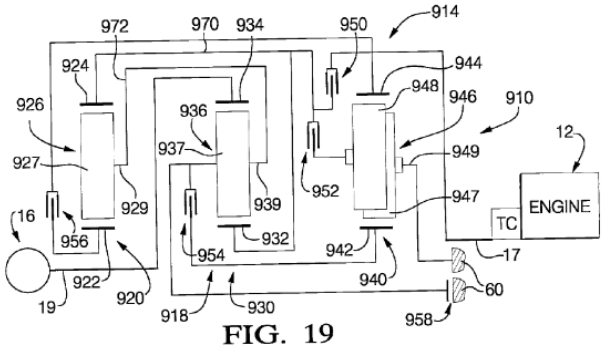

FIG. 19

(b) PGM Graph

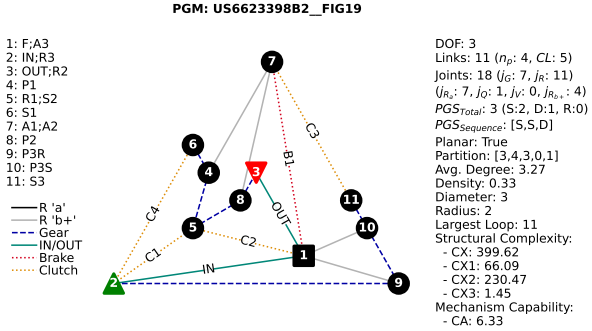

(c) DBG Graph

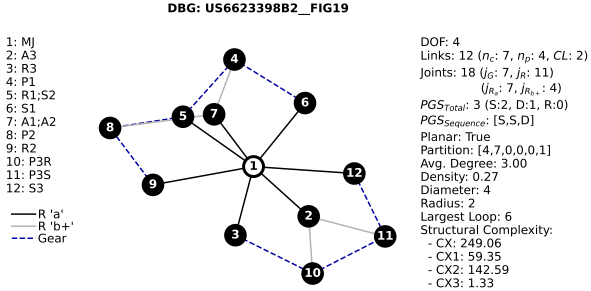

Table 169 – US6705967B2__FIG1 dataset information.

IDENTIFICATION		TOPOLOGY					GEARS SPECS		
UNIQUE_ID	**US6705967B2__FIG1**	**PGS**	**S/D**	**+/-**	**CLs**	**SCs**	**GEARS**	**Ratios**	**Engaged SCs**
Source	patent	1	S	F	IN;S1;S2	B1: F;R1	R1	-3.77	B1;B3
Owner	GM	2	S	IN	A1;R2;S3	B2: F;A1	1	3.97	B3;C2
Patent	US6705967B2	3	S	OUT	OUT;R3	B3: F;A3	2	2.18	B2;C2
Date	2001					C1: IN;A3	3	1.48	B1;C2
Model	FIG1					C2: A2;A3	4	1	C1;C2
Commercial?	false						5	0.72	B1;C1
Longitudinal	true						6	0.6	B2;C1
Transversal	false								
Weight (kg)									
Máx. Torque (N·m)									

Figure 198 – US6705967B2__FIG1 representations.

(a) Functional diagram

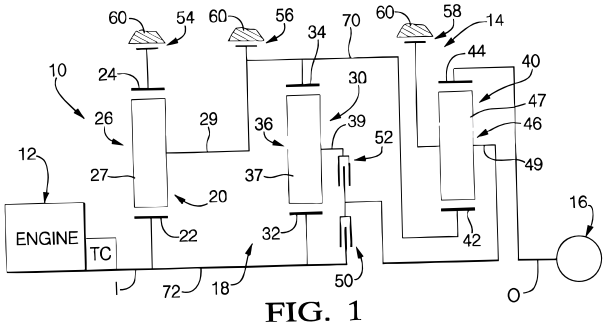

FIG. 1

(b) PGM Graph

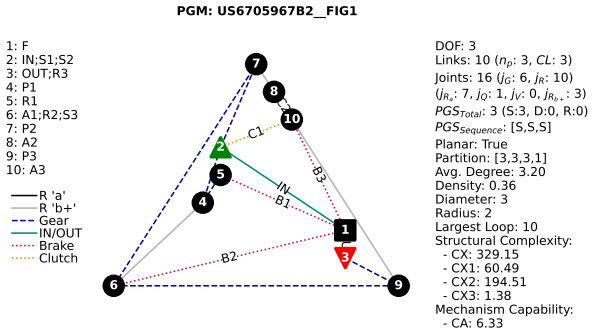

(c) DBG Graph

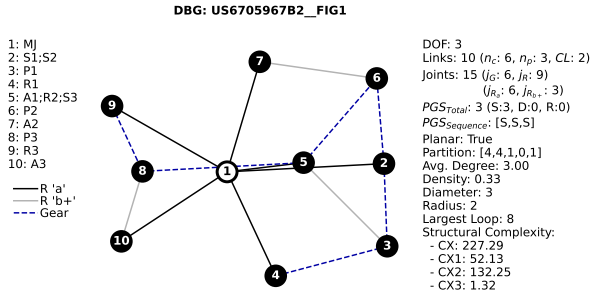

Table 170 – US6705967B2__FIG3 dataset information.

IDENTIFICATION		TOPOLOGY					GEARS SPECS		
UNIQUE_ID	**US6705967B2__FIG3**	**PGS**	**S/D**	**+/-**	**CLs**	**SCs**	**GEARS**	**Ratios**	**Engaged SCs**
Source	patent	1	S	F	IN;S3	B1: F;A1	R1	-3.9	B1;B3
Owner	GM	2	S	IN	OUT;R1	B2: F;R2	1	4.43	B1;C2
Patent	US6705967B2	3	S	OUT	S1;R2;A3	B3: F;R3	2	2.37	B2;C2
Date	2001				A1;A2	C1: IN;A2	3	1.55	B3;C2
Model	FIG3					C2: IN;S2	4	1	C1;C2
Commercial?	false						5	0.71	B3;C1
Longitudinal	true						6	0.6	B2;C1
Transversal	false								
Weight (kg)									
Máx. Torque (N·m)									

Figure 199 – US6705967B2__FIG3 representations.

(a) Functional diagram

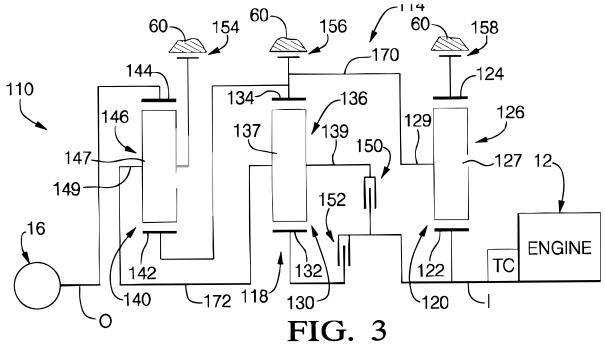

FIG. 3

(b) PGM Graph

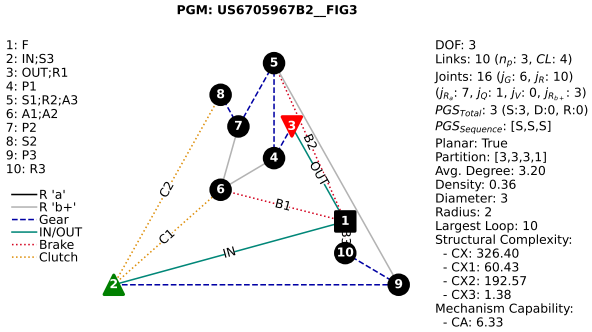

(c) DBG Graph

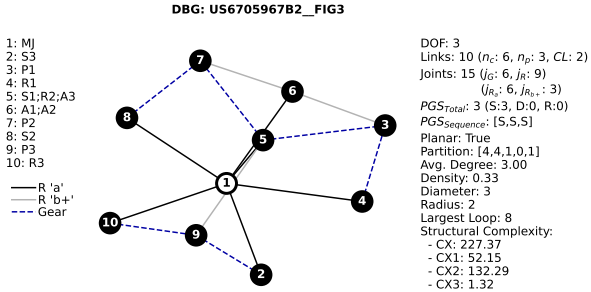

Table 171 – US6705967B2__FIG5 dataset information.

IDENTIFICATION		TOPOLOGY					GEARS SPECS		
UNIQUE_ID	**US6705967B2__FIG5**	**PGS**	**S/D**	**+/-**	**CLs**	**SCs**	**GEARS**	**Ratios**	**Engaged SCs**
Source	patent	1	S	F	IN;S3	B1: F;A1	R1	-3.9	B1;B3
Owner	GM	2	S	IN	OUT;R1	B2: F;A2	1	4.54	B1;C2
Patent	US6705967B2	3	S	OUT	S1;A2;A3	B3: F;R3	2	2.42	B2;C2
Date	2001				A1;R2	C1: IN;A1	3	1.56	B3;C2
Model	FIG5					C2: S2;R3	4	1	C1;C2
Commercial?	false						5	0.71	B3;C1
Longitudinal	true						6	0.6	B2;C1
Transversal	false								
Weight (kg)									
Máx. Torque (N·m)									

Figure 200 – US6705967B2__FIG5 representations.

(a) Functional diagram

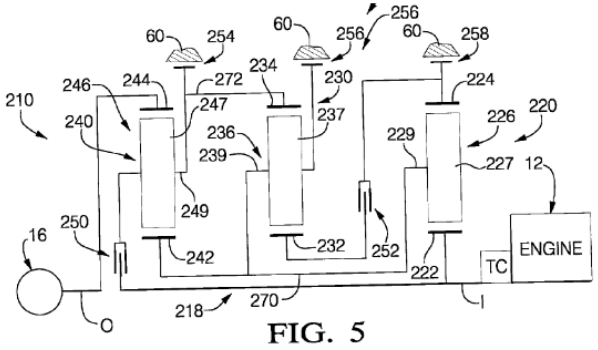

FIG. 5

(b) PGM Graph

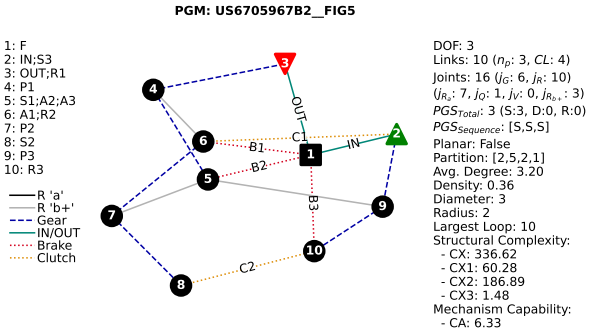

(c) DBG Graph

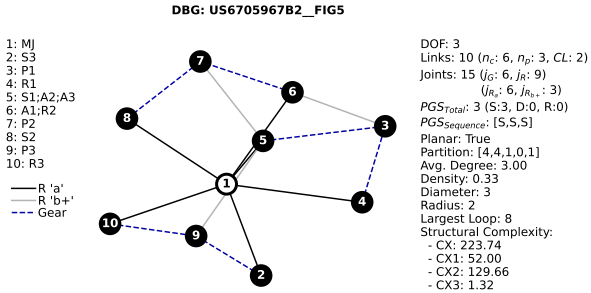

Table 172 – US6705967B2__FIG7 dataset information.

IDENTIFICATION		TOPOLOGY					GEARS SPECS		
UNIQUE_ID	**US6705967B2__FIG7**	**PGS**	**S/D**	**+/-**	**CLs**	**SCs**	**GEARS**	**Ratios**	**Engaged SCs**
Source	patent	1	S	F	IN;S2	B1: F;S1	R1	-3.89	B1;B3
Owner	GM	2	S	IN	R1;A2	B2: F;A1	1	4.45	B3;C1
Patent	US6705967B2	3	S	OUT	A1;R2;S3	B3: F;A3	2	2.38	B2;C1
Date	2001				OUT;R3	C1: A2;A3	3	1.55	B1;C1
Model	FIG7					C2: IN;A3	4	1	C1;C2
Commercial?	false						5	0.71	B1;C2
Longitudinal	true						6	0.6	B2;C2
Transversal	false								
Weight (kg)									
Máx. Torque (N·m)									

Figure 201 – US6705967B2__FIG7 representations.

(a) Functional diagram

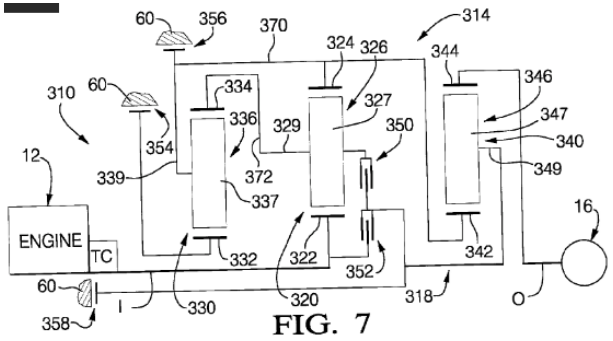

FIG. 7

(b) PGM Graph

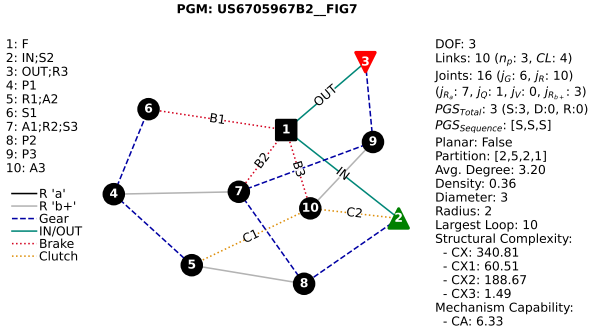

(c) DBG Graph

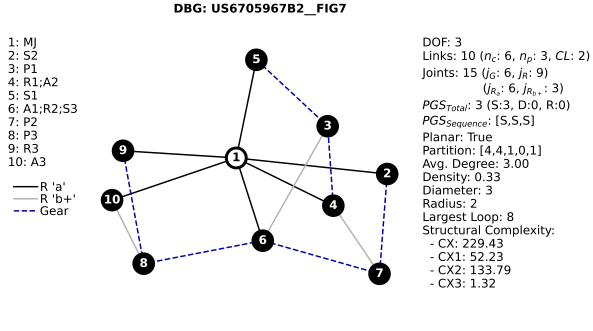

Table 173 – US6705967B2__FIG9 dataset information.

IDENTIFICATION		TOPOLOGY					GEARS SPECS		
UNIQUE_ID	**US6705967B2__FIG9**	**PGS**	**S/D**	**+/-**	**CLs**	**SCs**	**GEARS**	**Ratios**	**Engaged SCs**
Source	patent	1	S	F	IN;S1	B1: F;R1	R1	-3.5	B2;B3
Owner	GM	2	S	IN	R1;A2;S3	B2: F;S2	1	3.51	B3;C1
Patent	US6705967B2	3	S	OUT	A1;R2	B3: F;A3	2	2	B1;C1
Date	2001				OUT;R3	C1: A1;A3	3	1.4	B2;C1
Model	FIG9					C2: IN;A3	4	1	C1;C2
Commercial?	false						5	0.73	B2;C2
Longitudinal	true						6	0.6	B1;C2
Transversal	false								
Weight (kg)									
Máx. Torque (N·m)									

Figure 202 – US6705967B2__FIG9 representations.

(a) Functional diagram

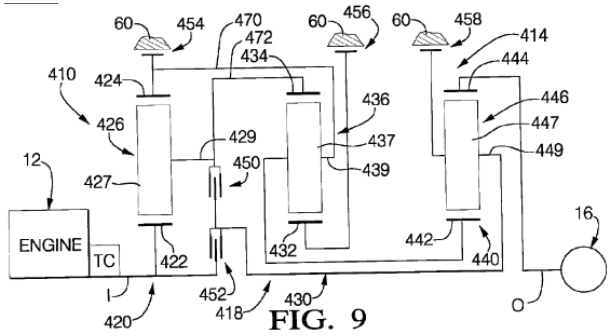

FIG. 9

(b) PGM Graph

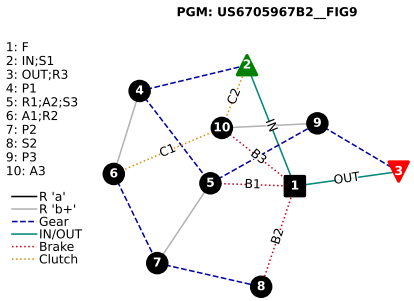

(c) DBG Graph

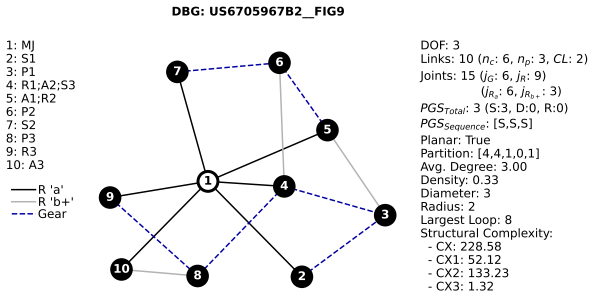

Table 174 – US6705967B2__FIG11 dataset information.

IDENTIFICATION		TOPOLOGY					GEARS SPECS		
UNIQUE_ID	**US6705967B2__FIG11**	**PGS**	**S/D**	**+/-**	**CLs**	**SCs**	**GEARS**	**Ratios**	**Engaged SCs**
Source	patent	1	S	F	IN;S2	B1: F;S1	R1	-4.24	B1;B3
Owner	GM	2	S	IN	S1;R2	B2: F;A1	1	4.26	B3;C1
Patent	US6705967B2	3	S	OUT	A1;A2;S3	B3: F;A3	2	2.26	B2;C1
Date	2001				OUT;R3	C1: R1;A3	3	1.54	B1;C1
Model	FIG11					C2: IN;A3	4	1	C1;C2
Commercial?	false						5	0.72	B1;C2
Longitudinal	true						6	0.61	B2;C2
Transversal	false								
Weight (kg)									
Máx. Torque (N·m)									

Figure 203 – US6705967B2__FIG11 representations.

(a) Functional diagram

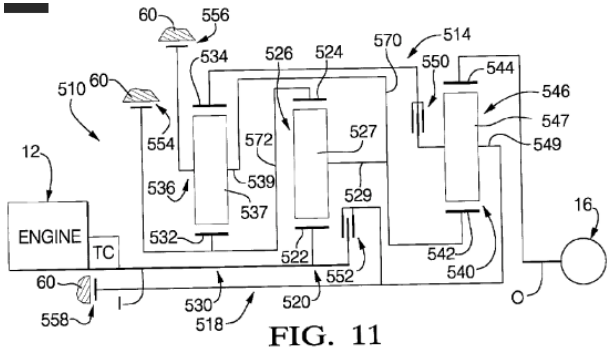

FIG. 11

(b) PGM Graph

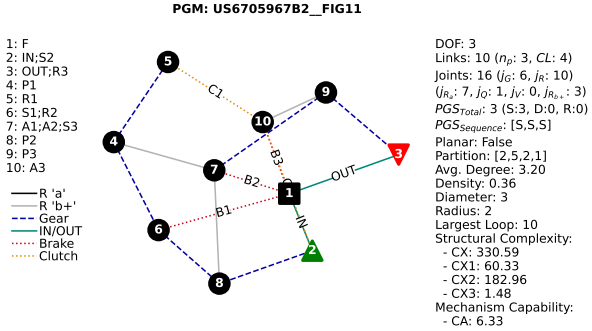

(c) DBG Graph

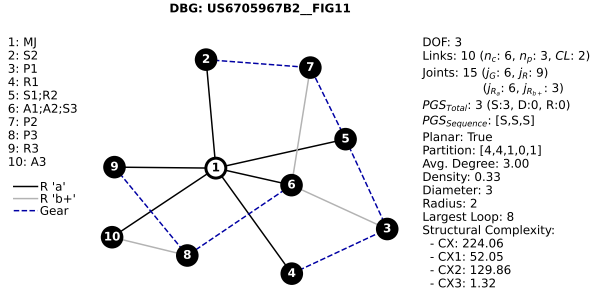

Table 175 – US6705967B2__FIG13 dataset information.

IDENTIFICATION		TOPOLOGY					GEARS SPECS		
UNIQUE_ID	**US6705967B2__FIG13**	**PGS**	**S/D**	**+/-**	**CLs**	**SCs**	**GEARS**	**Ratios**	**Engaged SCs**
Source	patent	1	S	F	IN;A1;S2	B1: F;S1	R1	-1.8	B2;C1
Owner	GM	2	S	IN	R1;R2;A3	B2: F;A3	1	2.53	B2;C2
Patent	US6705967B2	3	S	OUT	OUT;R3	B3: F;S3	2	1.55	B3;C2
Date	2001					C1: A1;S3	3	1	C1;C2
Model	FIG13					C2: A2;R3	4	0.75	B1;C2
Commercial?	false						5	0.54	B1;C1
Longitudinal	true						6	0.42	B1;B3
Transversal	false								
Weight (kg)									
Máx. Torque (N·m)									

Figure 204 – US6705967B2__FIG13 representations.

(a) Functional diagram

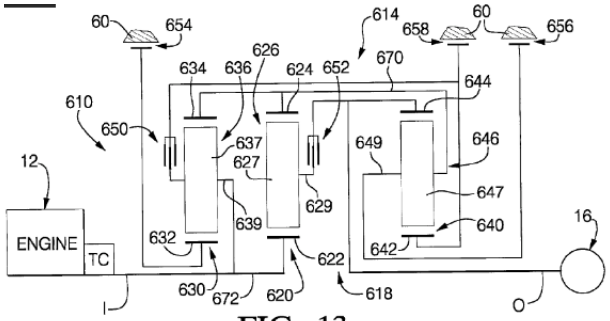

FIG. 13

(b) PGM Graph

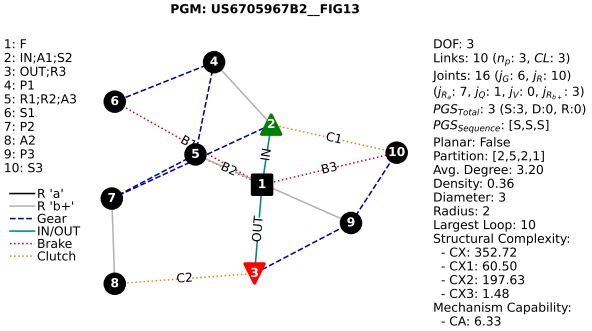

(c) DBG Graph

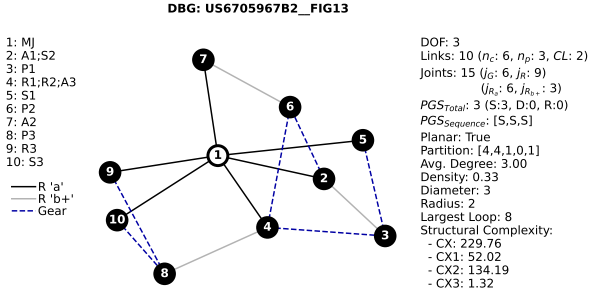

Table 176 – US6705967B2__FIG15 dataset information.

IDENTIFICATION		TOPOLOGY					GEARS SPECS		
UNIQUE_ID	**US6705967B2__FIG15**	**PGS**	**S/D**	**+/-**	**CLs**	**SCs**	**GEARS**	**Ratios**	**Engaged SCs**
Source	patent	1	S	F	IN;A3	B1: F;R2	R1	-1.5	B2;C1
Owner	GM	2	S	IN	OUT;R1	B2: F;A1	1	2.51	B2;C2
Patent	US6705967B2	3	S	OUT	S1;R2	B3: F;S3	2	1.61	B1;C2
Date	2001				A1;A2;R3	C1: R2;A3	3	1	C1;C2
Model	FIG15					C2: S2;A3	4	0.75	B3;C2
Commercial?	false						5	0.53	B3;C1
Longitudinal	true						6	0.39	B1;B3
Transversal	false								
Weight (kg)									
Máx. Torque (N·m)									

Figure 205 – US6705967B2__FIG15 representations.

(a) Functional diagram

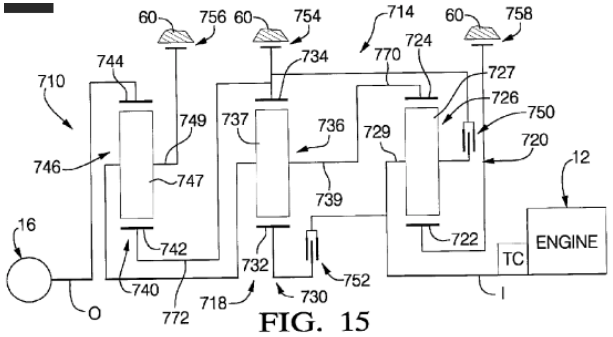

FIG. 15

(b) PGM Graph

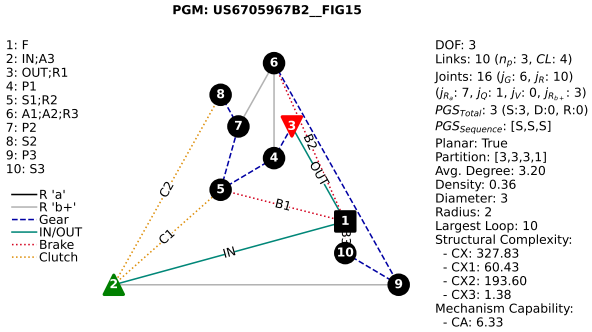

(c) DBG Graph

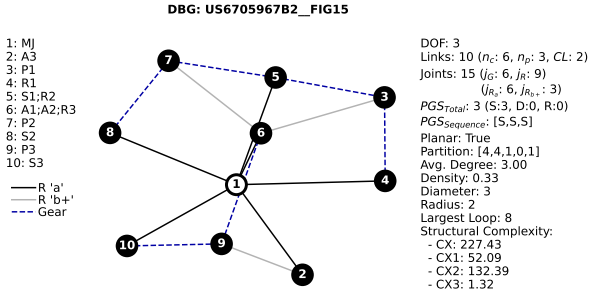

Table 177 – US6705967B2__FIG17 dataset information.

IDENTIFICATION		TOPOLOGY					GEARS SPECS		
UNIQUE_ID	**US6705967B2__FIG17**	**PGS**	**S/D**	**+/-**	**CLs**	**SCs**	**GEARS**	**Ratios**	**Engaged SCs**
Source	patent	1	S	F	IN;A2;S1	B1: F;A1	R1	-1.6	B1;C1
Owner	GM	2	S	IN	A1;R2;A3	B2: F;S2	1	2.4	B1;C2
Patent	US6705967B2	3	S	OUT	OUT;R3	B3: F;S3	2	1.54	B3;C2
Date	2001					C1: A2;S3	3	1	C1;C2
Model	FIG17					C2: R1;S3	4	0.76	B2;C2
Commercial?	false						5	0.53	B2;C1
Longitudinal	true						6	0.4	B2;B3
Transversal	false								
Weight (kg)									
Máx. Torque (N·m)									

Figure 206 – US6705967B2__FIG17 representations.

(a) Functional diagram

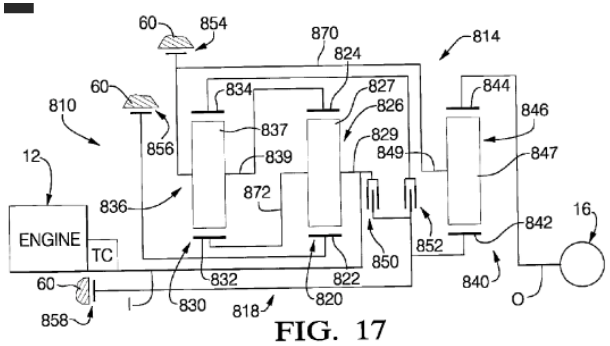

FIG. 17

(b) PGM Graph

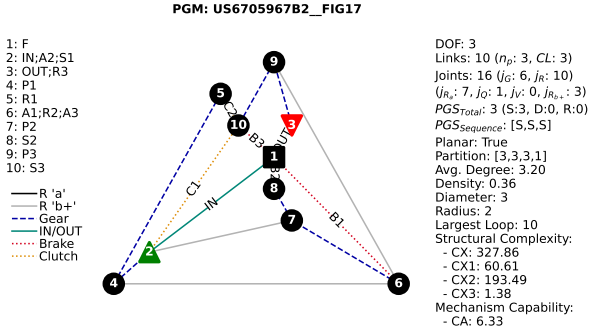

(c) DBG Graph

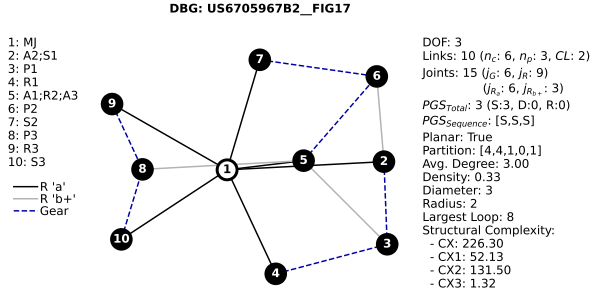

Table 178 – US6705967B2__FIG19 dataset information.

IDENTIFICATION		TOPOLOGY					GEARS SPECS		
UNIQUE_ID	**US6705967B2__FIG19**	**PGS**	**S/D**	**+/-**	**CLs**	**SCs**	**GEARS**	**Ratios**	**Engaged SCs**
Source	patent	1	S	F	IN;A1	B1: F;S1	R1	-2.2	B2;C1
Owner	GM	2	S	IN	R1;A2;A3	B2: F;A3	1	2.51	B2;C2
Patent	US6705967B2	3	S	OUT	S1;S2	B3: F;S3	2	1.47	B3;C2
Date	2001				OUT;R3	C1: IN;S3	3	1	C1;C2
Model	FIG19					C2: R2;S3	4	0.72	B1;C2
Commercial?	false						5	0.51	B1;C1
Longitudinal	true						6	0.42	B1;B3
Transversal	false								
Weight (kg)									
Máx. Torque (N·m)									

Figure 207 – US6705967B2__FIG19 representations.

(a) Functional diagram

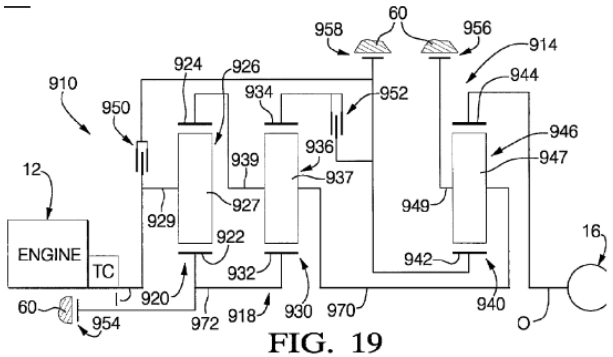

FIG. 19

(b) PGM Graph

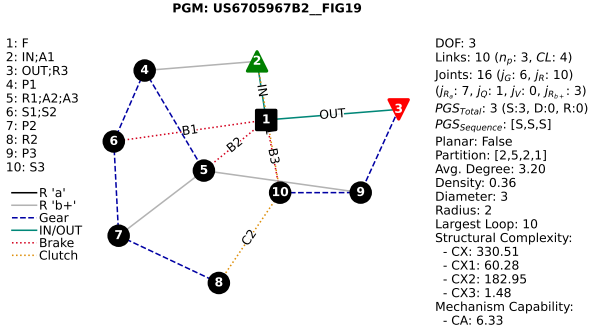

(c) DBG Graph

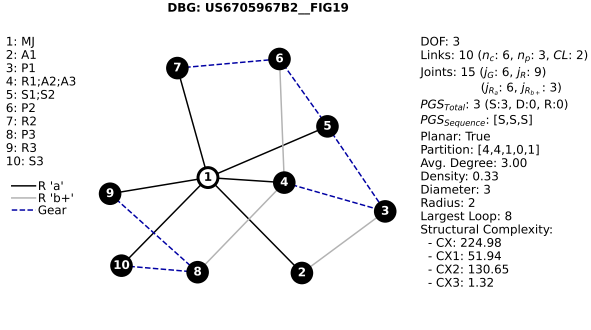

Table 179 – US6705967B2__FIG21 dataset information.

IDENTIFICATION		TOPOLOGY					GEARS SPECS		
UNIQUE_ID	**US6705967B2__FIG21**	**PGS**	**S/D**	**+/-**	**CLs**	**SCs**	**GEARS**	**Ratios**	**Engaged SCs**
Source	patent	1	S	F	IN;A3	B1: F;S1	R1	-2.5	B2;C1
Owner	GM	2	S	IN	OUT;R1;A2	B2: F;A1	1	2.83	B2;C2
Patent	US6705967B2	3	S	OUT	A1;R2;R3	B3: F;S3	2	1.52	B1;C2
Date	2001					C1: S1;A3	3	1	C1;C2
Model	FIG21					C2: S2;A3	4	0.74	B3;C2
Commercial?	false						5	0.57	B3;C1
Longitudinal	true						6	0.46	B1;B3
Transversal	false								
Weight (kg)									
Máx. Torque (N·m)									

Figure 208 – US6705967B2__FIG21 representations.

(a) Functional diagram

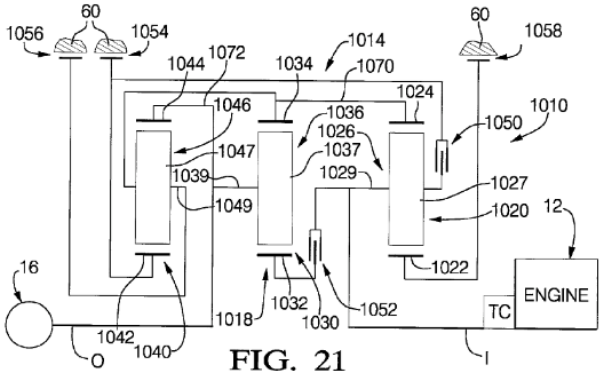

FIG. 21

(b) PGM Graph

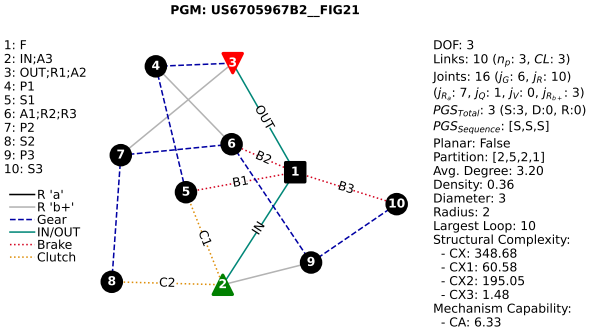

(c) DBG Graph

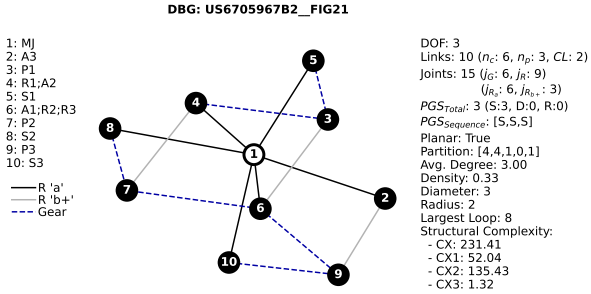

Table 180 – US6705967B2__FIG23 dataset information.

IDENTIFICATION		TOPOLOGY					GEARS SPECS		
UNIQUE_ID	**US6705967B2__FIG23**	**PGS**	**S/D**	**+/-**	**CLs**	**SCs**	**GEARS**	**Ratios**	**Engaged SCs**
Source	patent	1	S	F	IN;A3	B1: F;A1	R1	-2.57	B1;C1
Owner	GM	2	D	IN	R1;A2	B2: F;S3	1	4.85	B1;C2
Patent	US6705967B2	3	S	OUT	S1;S2;R3	B3: A2;S3	2	2.93	B1;B2
Date	2001				OUT;R2	C1: A2;A3	3	1.92	B1;B3
Model	FIG23					C2: S1;A3	4	1.26	B2;B3
Commercial?	false						5	1	B3;C1
Longitudinal	true						6	0.76	B2;C1
Transversal	false								
Weight (kg)									
Máx. Torque (N·m)									

Figure 209 – US6705967B2__FIG23 representations.

(a) Functional diagram

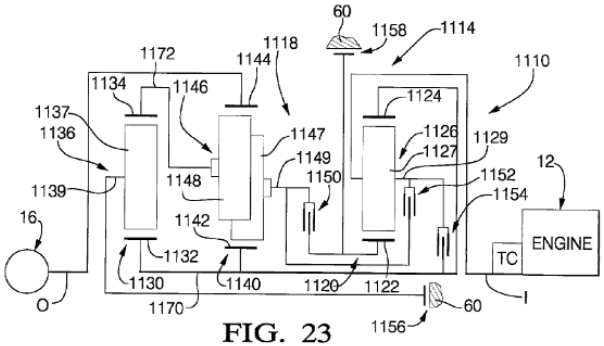

FIG. 23

(b) PGM Graph

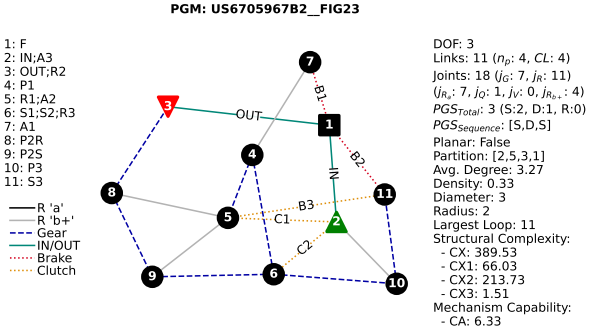

(c) DBG Graph

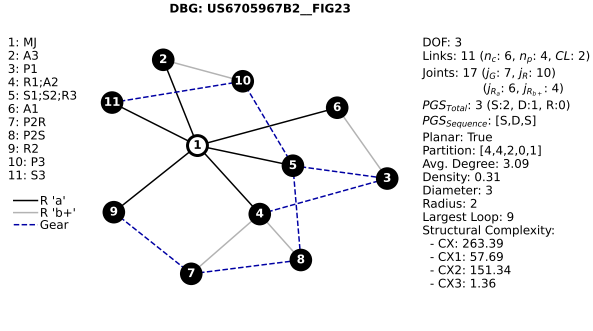

Table 181 – US6705967B2__FIG25 dataset information.

IDENTIFICATION		TOPOLOGY					GEARS SPECS		
UNIQUE_ID	**US6705967B2__FIG25**	**PGS**	**S/D**	**+/-**	**CLs**	**SCs**	**GEARS**	**Ratios**	**Engaged SCs**
Source	patent	1	D	F	IN;R3	B1: F;A2	R1	-2.44	B1;C3
Owner	GM	2	S	IN	OUT;R1	B2: F;A3	1	3.15	B1;B2
Patent	US6705967B2	3	D	OUT	S1;S2;S3	C1: A1;OUT	2	2.05	B1;C2
Date	2001				A1;R2	C2: A1;A3	3	1.31	B2;C2
Model	FIG25					C3: A1;IN	4	1	C2;C3
Commercial?	false						5	0.74	B2;C3
Longitudinal	true						6	0.55	B2;C1
Transversal	false								
Weight (kg)									
Máx. Torque (N·m)									

Figure 210 – US6705967B2__FIG25 representations.

(a) Functional diagram

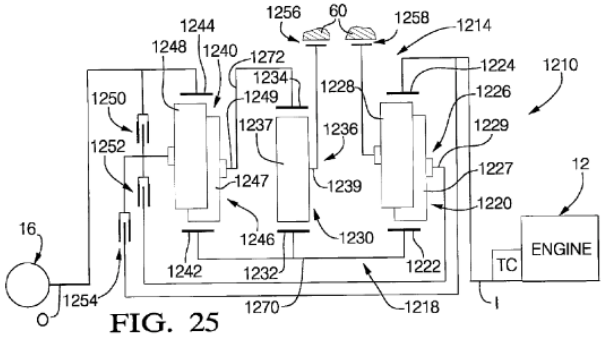

FIG. 25

(b) PGM Graph

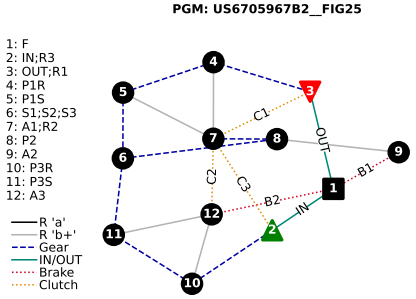

DOF: 3
Links: 12 (n_p: 5, CL: 4)
Joints: 20 (j_G: 8, j_R: 12)
(j_{R_a}: 7, j_O: 2, j_V: 1, $j_{R_{b+}}$: 5)
PGS_{Total}: 3 (S:1, D:2, R:0)
$PGS_{Sequence}$: [D,S,D]
Planar: False
Partition: [1,8,2,0,1]
Avg. Degree: 3.33
Density: 0.30
Diameter: 3
Radius: 2
Largest Loop: 12
Structural Complexity:
- CX: 414.42
- CX1: 71.47
- CX2: 229.75
- CX3: 1.49
Mechanism Capability:
- CA: 6.33

(c) DBG Graph

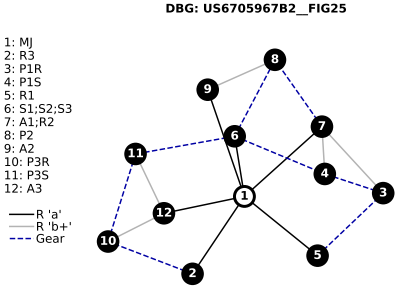

DOF: 3
Links: 12 (n_c: 6, n_p: 5, CL: 2)
Joints: 19 (j_G: 8, j_R: 11)
(j_{R_a}: 6, $j_{R_{b+}}$: 5)
PGS_{Total}: 3 (S:1, D:2, R:0)
$PGS_{Sequence}$: [D,S,D]
Planar: True
Partition: [3,6,2,0,1]
Avg. Degree: 3.17
Density: 0.29
Diameter: 4
Radius: 2
Largest Loop: 11
Structural Complexity:
- CX: 292.30
- CX1: 63.06
- CX2: 158.92
- CX3: 1.44

Table 182 – US6705967B2__FIG27 dataset information.

IDENTIFICATION		TOPOLOGY					GEARS SPECS		
UNIQUE_ID	**US6705967B2__FIG27**	**PGS**	**S/D**	**+/-**	**CLs**	**SCs**	**GEARS**	**Ratios**	**Engaged SCs**
Source	patent	1	S	F	IN;S3	B1: F;S1	R1	-4.89	B2;C2
Owner	GM	2	S	IN	R1;S2;A3	B2: F;R3	1	5.6	B1;B2
Patent	US6705967B2	3	S	OUT	A1;A2	C1: IN;A1	2	3.36	B1;C2
Date	2001				OUT;R2	C2: A2;R3	3	2.16	B1;C3
Model	FIG27					C3: IN;A3	4	1.4	B1;C1
Commercial?	false						5	1	C1;C2
Longitudinal	true						6	0.75	B2;C1
Transversal	false								
Weight (kg)									
Máx. Torque (N·m)									

Figure 211 – US6705967B2__FIG27 representations.

(a) Functional diagram

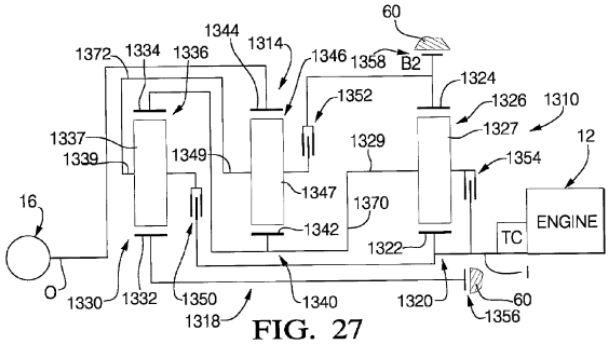

FIG. 27

(b) PGM Graph

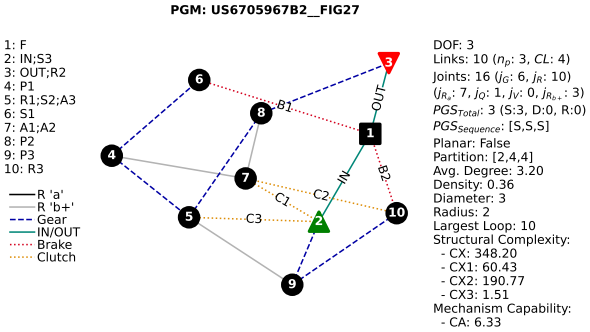

(c) DBG Graph

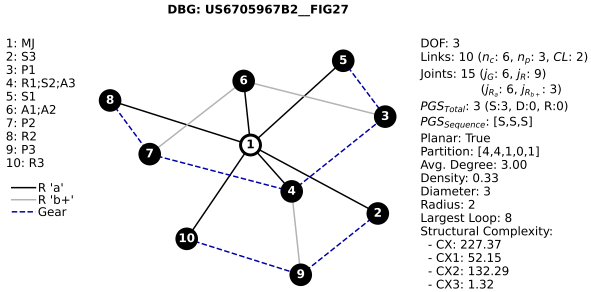

Table 183 – US6705967B2__FIG29 dataset information.

IDENTIFICATION		TOPOLOGY					GEARS SPECS		
UNIQUE_ID	**US6705967B2__FIG29**	**PGS**	**S/D**	**+/-**	**CLs**	**SCs**	**GEARS**	**Ratios**	**Engaged SCs**
Source	patent	1	S	F	IN;A3	B1: F;R1	R1	-1.59	B1;C2
Owner	GM	2	S	IN	R1;A2;R3	B2: F;R2	1	2.54	B1;C1
Patent	US6705967B2	3	S	OUT	S1;S2	B3: F;S3	2	1.59	B2;C1
Date	2001				OUT;A1	C1: S1;A3	3	1	C1;C2
Model	FIG29					C2: R2;A3	4	0.75	B3;C1
Commercial?	false						5	0.53	B3;C2
Longitudinal	true						6	0.4	B2;B3
Transversal	false								
Weight (kg)									
Máx. Torque (N·m)									

Figure 212 – US6705967B2__FIG29 representations.

(a) Functional diagram

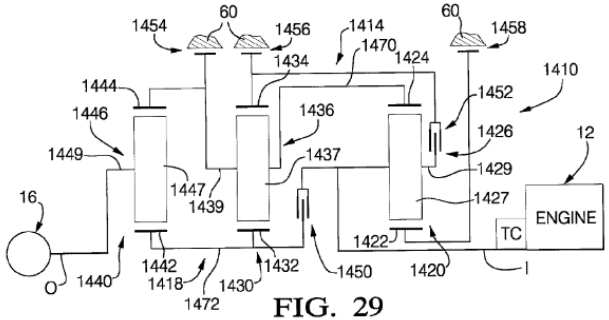

FIG. 29

(b) PGM Graph

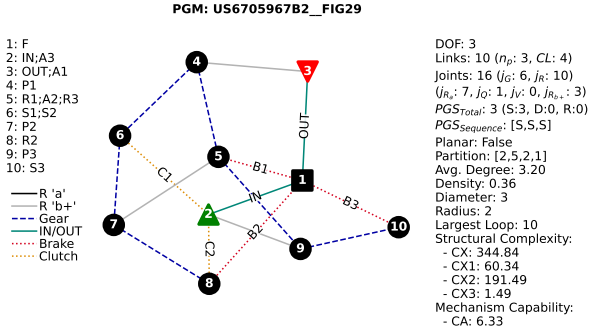

(c) DBG Graph

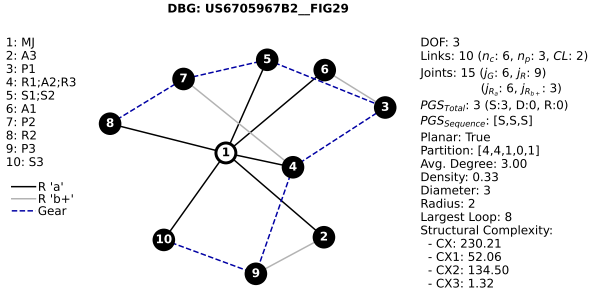

Table 184 – US6705967B2__FIG31 dataset information.

IDENTIFICATION		TOPOLOGY					GEARS SPECS		
UNIQUE_ID	**US6705967B2__FIG31**	**PGS**	**S/D**	**+/-**	**CLs**	**SCs**	**GEARS**	**Ratios**	**Engaged SCs**
Source	patent	1	S	F	IN;S3	B1: F;S2	R1	-4.83	B2;C2
Owner	GM	2	S	IN	OUT;R1	B2: F;R3	1	4.87	B1;B2
Patent	US6705967B2	3	S	OUT	S1;R2;A3	C1: IN;A2	2	2.78	B1;C2
Date	2001				A1;A2	C2: A1;R3	3	1.87	B1;C3
Model	FIG31					C3: IN;A3	4	1.31	B1;C1
Commercial?	false						5	1	C1;C3
Longitudinal	true						6	0.75	B2;C1
Transversal	false								
Weight (kg)									
Máx. Torque (N·m)									

Figure 213 – US6705967B2__FIG31 representations.

(a) Functional diagram

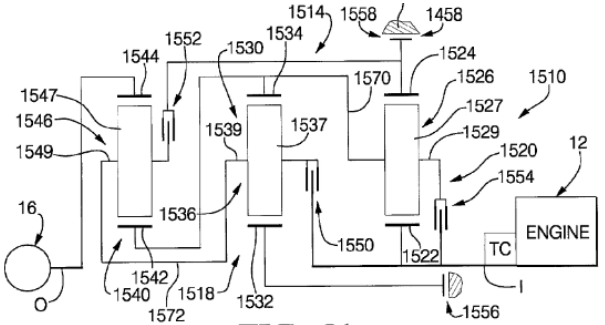

FIG. 31

(b) PGM Graph

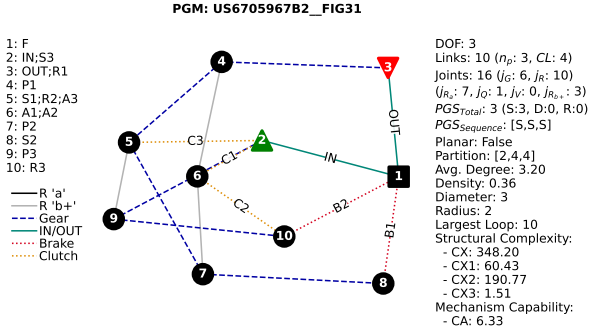

(c) DBG Graph

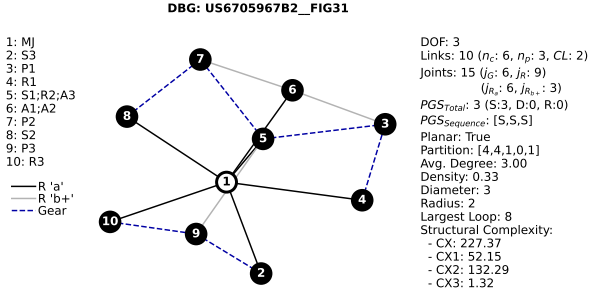

Table 185 – US6705967B2__FIG33 dataset information.

IDENTIFICATION		TOPOLOGY					GEARS SPECS		
UNIQUE_ID	**US6705967B2__FIG33**	**PGS**	**S/D**	**+/-**	**CLs**	**SCs**	**GEARS**	**Ratios**	**Engaged SCs**
Source	patent	1	S	F	IN;A3	B1: F;R1	R1	-2.12	B1;C3
Owner	GM	2	S	IN	R1;A2	B2: F;S3	1	3.99	B1;C1
Patent	US6705967B2	3	S	OUT	S1;S2;R3	C1: S1;A3	2	2.47	B1;B2
Date	2001				OUT;A1	C2: R2;S3	3	1.67	B1;C2
Model	FIG33					C3: R2;A3	4	1.21	B2;C2
Commercial?	false						5	1	C2;C3
Longitudinal	true						6	0.76	B2;C3
Transversal	false								
Weight (kg)									
Máx. Torque (N·m)									

Figure 214 – US6705967B2__FIG33 representations.

(a) Functional diagram

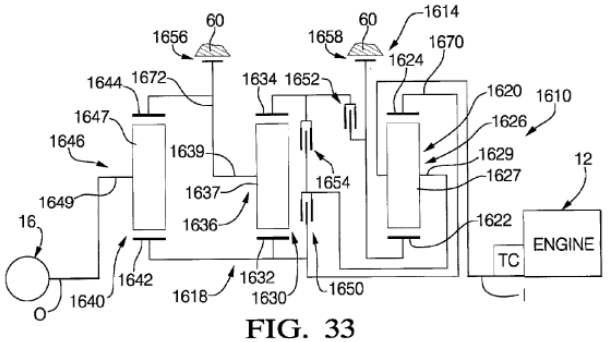

FIG. 33

(b) PGM Graph

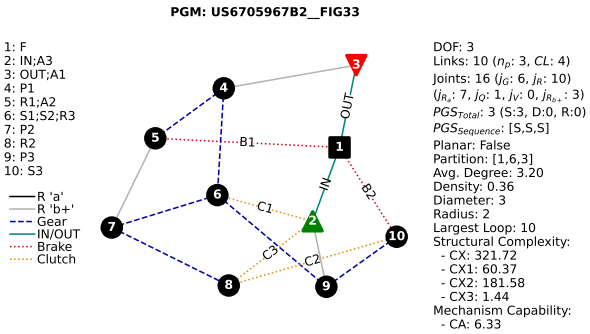

(c) DBG Graph

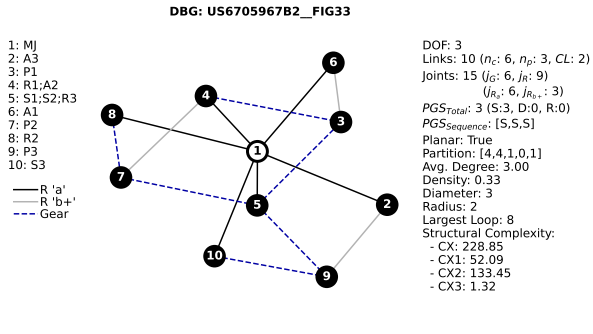

Table 186 – US7621841B2__FIG1 dataset information.

IDENTIFICATION		TOPOLOGY					GEARS SPECS		
UNIQUE_ID	**US7621841B2__FIG1**	**PGS**	**S/D**	**+/-**	**CLs**	**SCs**	**GEARS**	**Ratios**	**Engaged SCs**
Source	patent	1	S	F	F;S1	C1: S2;S4	R1		C4;B1
Owner	HYUNDAI	2	S	IN	IN;R1	C2: A1;A2	1		C1;B1
Patent	US7621841B2	3	S	OUT	OUT;R3;R4	C3: IN;A4	2		C1;B2
Date	2006	4	D		A1;S2	C4: S3;R3	3		C1;C4
Model	FIG1				R2;S3	B1: F;A2	4		C1;C3
Commercial?	false				A3;A4	B2: F;R2	5		C3;C4
Longitudinal	true				P3;P4R	:	6		C2;C3
Transversal	false						7		C3;B2
Weight (kg)							8		C3;B1
Máx. Torque (N·m)									

Figure 215 – US7621841B2__FIG1 representations.

(a) Functional diagram

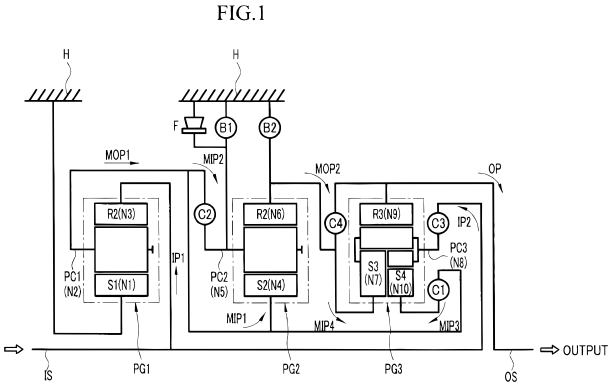

(b) PGM Graph

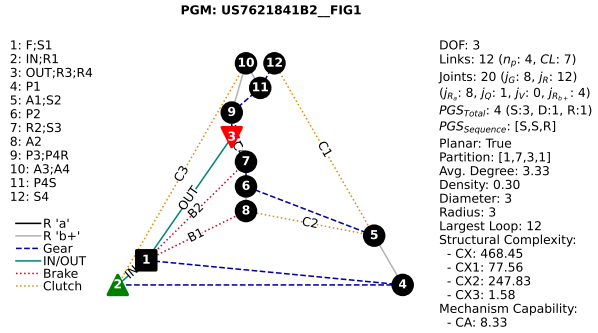

(c) DBG Graph

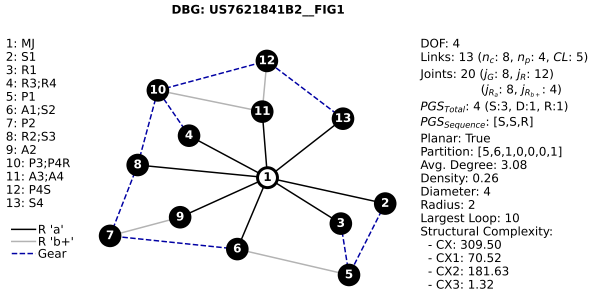

Table 187 – US7621841B2__FIG4 dataset information.

IDENTIFICATION		TOPOLOGY					GEARS SPECS		
UNIQUE_ID	**US7621841B2__FIG4**	**PGS**	**S/D**	**+/-**	**CLs**	**SCs**	**GEARS**	**Ratios**	**Engaged SCs**
Source	patent	1	S	F	F;S1	C1: S2;S4	R1		C4;B2
Owner	HYUNDAI	2	D	IN	IN;R1	C2: A1;A2	1		C1;B2
Patent	US7621841B2	3	S	OUT	A1;S2	C3: IN;A4	2		C1;B1
Date	2006	4	D		A2;S3	C4: S3;R3	3		C1;C4
Model	FIG4				A3;A4	B1: F;R2	4		C1;C3
Commercial?	false				OUT;R3;R4	B2: F;A2	5		C3;C4
Longitudinal	true				P3;P4R	:	6		C2;C3
Transversal	false						7		C3;B1
Weight (kg)							8		C3;B2
Máx. Torque (N·m)									

Figure 216 – US7621841B2__FIG4 representations.

(a) Functional diagram

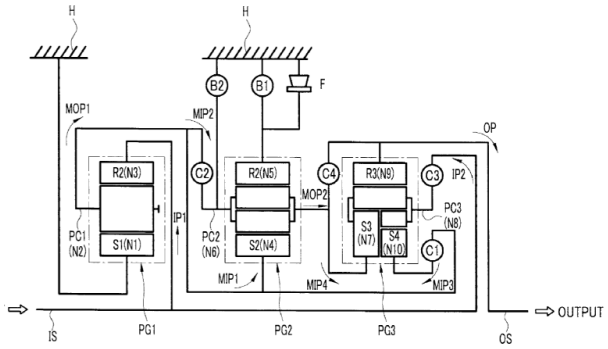

(b) PGM Graph

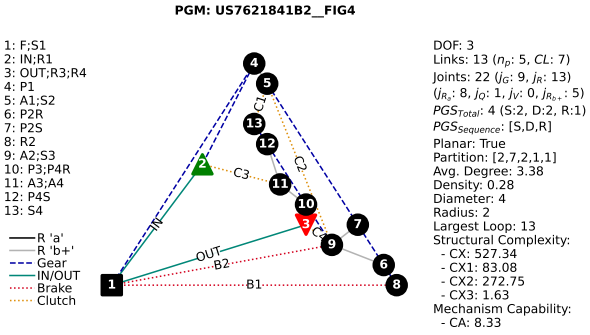

(c) DBG Graph

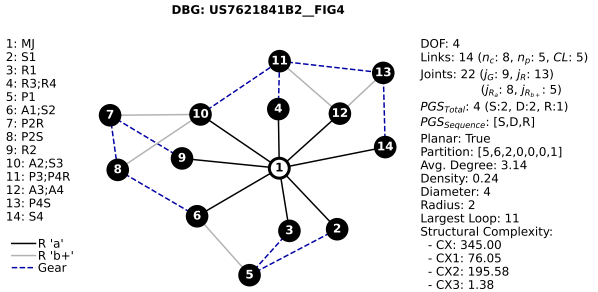

Table 188 – US7621841B2__FIG5 dataset information.

IDENTIFICATION		TOPOLOGY					GEARS SPECS		
UNIQUE_ID	**US7621841B2__FIG5**	**PGS**	**S/D**	**+/-**	**CLs**	**SCs**	**GEARS**	**Ratios**	**Engaged SCs**
Source	patent	1	S	F	F;S1	C1: S2;S4	R1		C4;B2
Owner	HYUNDAI	2	D	IN	IN;R1	C2: A1;R2	1		C1;B2
Patent	US7621841B2	3	S	OUT	A1;S2	C3: IN;A4	2		C1;B1
Date	2006	4	D		A2;S3	C4: S3;R3	3		C1;C4
Model	FIG5				A3;A4	B1: F;R2	4		C1;C3
Commercial?	false				OUT;R3;R4	B2: F;A2	5		C3;C4
Longitudinal	true				P3;P4R	:	6		C2;C3
Transversal	false						7		C3;B1
Weight (kg)							8		C3;B2
Máx. Torque (N·m)									

Figure 217 – US7621841B2__FIG5 representations.

(a) Functional diagram

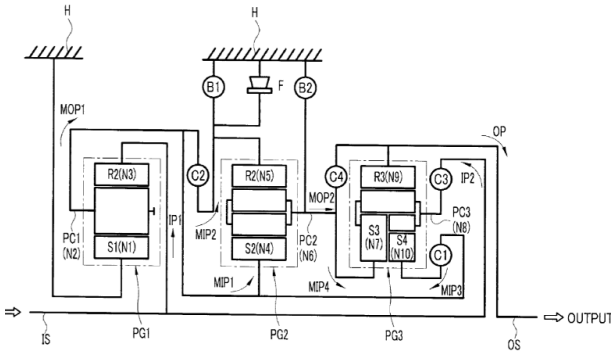

(b) PGM Graph

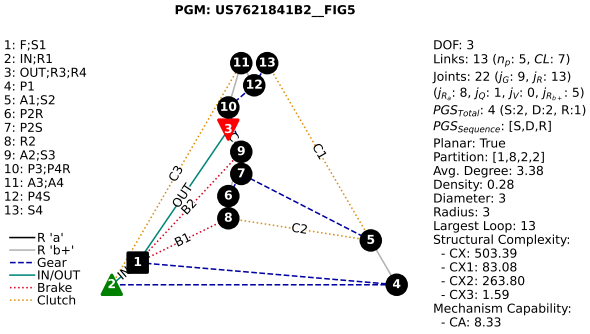

(c) DBG Graph

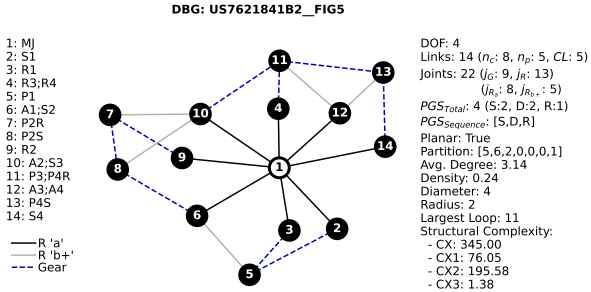

Table 189 – US7628726B2__FIG1 dataset information.

IDENTIFICATION		TOPOLOGY					GEARS SPECS		
UNIQUE_ID	**US7628726B2__FIG1**	**PGS**	**S/D**	**+/-**	**CLs**	**SCs**	**GEARS**	**Ratios**	**Engaged SCs**
Source	patent	1	D	F	F;S1	C1: R1;S3	R2		C4;B2
Owner	AISIN	2	S	IN	IN;A1	C2: IN;A3	R1		C3;B2
Patent	US7628726B2	3	D	OUT	P2;P3R	C3: R1;S2	1		C1;B2
Date	2004				OUT;R2;R3	C4: A1;S2	2		C1;B1
Model	FIG1				A2;A3	B1: F;S2	3		C1;C3
Commercial?	true					B2: F;A3	4		C1;C4
Longitudinal	true						5		C1;C2
Transversal	false						6		C2;C4
Weight (kg)							7		C2;C3
Máx. Torque (N·m)							8		C2;B1

Figure 218 – US7628726B2__FIG1 representations.

(a) Functional diagram

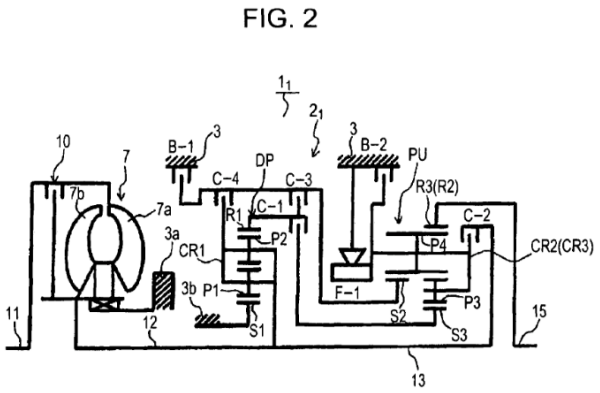

(b) PGM Graph

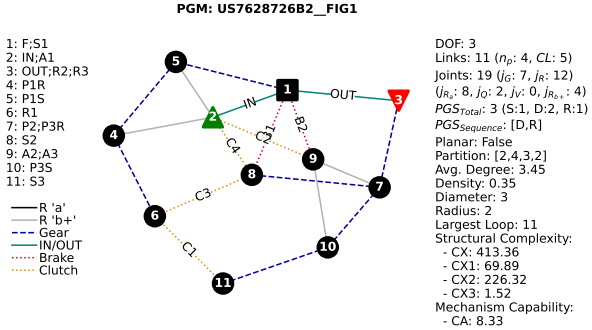

(c) DBG Graph

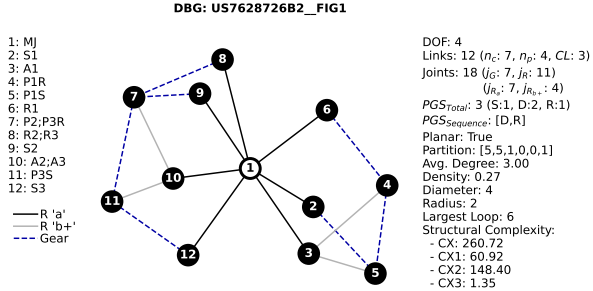

Table 190 – US7967716B2__FIG2 dataset information.

IDENTIFICATION		TOPOLOGY					GEARS SPECS		
UNIQUE_ID	**US7967716B2__FIG2**	**PGS**	**S/D**	**+/-**	**CLs**	**SCs**	**GEARS**	**Ratios**	**Engaged SCs**
Source	patent	1	D	F	F;S1	C1: R1;S2	R2		C4;B2
Owner	AISIN	2	D	IN	IN;A1	C2: IN;A2	R1		C3;B2
Patent	US7967716B2	3	S	OUT	P2R;P3	C3: R1;S3	1		C1;B2
Date	2005				OUT;R2;R3	C4: IN;S2	2		C1;B1
Model	FIG2				A2;A3	B1: F;S2	3		C1;C3
Commercial?	false					B2: F;A2	4		C1;C4
Longitudinal	false						5		C1;C2
Transversal	true						6		C2;C4
Weight (kg)							7		C2;C3
Máx. Torque (N·m)							8		C2;B1

Figure 219 – US7967716B2__FIG2 representations.

(a) Functional diagram

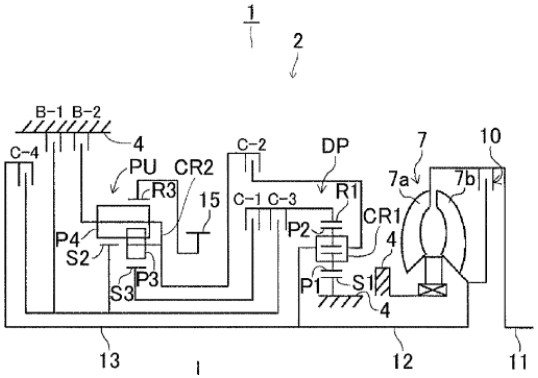

(b) PGM Graph

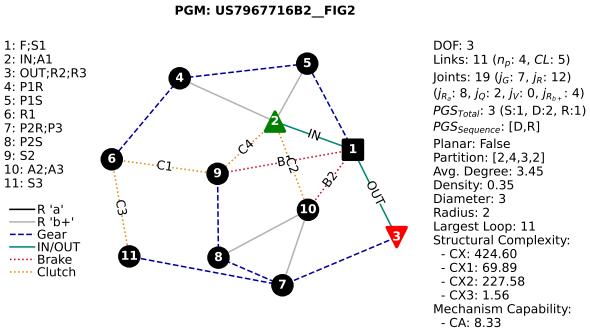

(c) DBG Graph

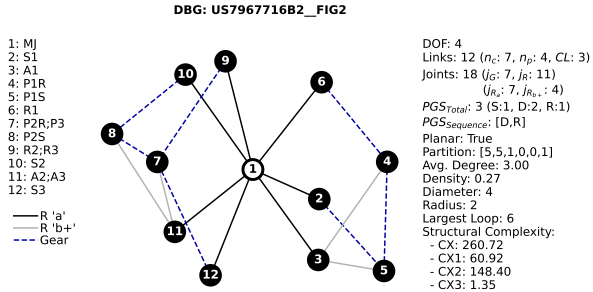

Table 191 – US7985160B2__FIG1 dataset information.

IDENTIFICATION		TOPOLOGY					GEARS SPECS		
UNIQUE_ID	**US7985160B2__FIG1**	**PGS**	**S/D**	**+/-**	**CLs**	**SCs**	**GEARS**	**Ratios**	**Engaged SCs**
Source	patent	1	S	F	A1;R2	C1: IN;A3	R1	-2.846	C2;B1
Owner	HYUNDAI	2	S	IN	IN;S2	C2: IN;S1	1	4.91	C4;B1
Patent	US7985160B2	3	S	OUT	A2;R3	C3: S1;A1	2	2.804	C4;B2
Date	2008				F;S3	C4: R1;A3	3	2.064	C3;C4
Model	FIG1				OUT;R1	B1: F;A1	4	1.611	C2;C4
Commercial?	false					B2: F;S1	5	1	C2;C3
Longitudinal	false						6	0.728	C1;C3
Transversal	true						7	0.664	C1;C2
Weight (kg)							8	0.539	C1;B2
Máx. Torque (N·m)									

Figure 220 – US7985160B2__FIG1 representations.

(a) Functional diagram

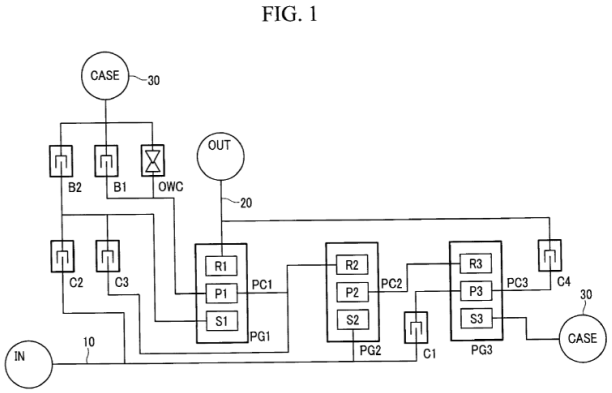

(b) PGM Graph

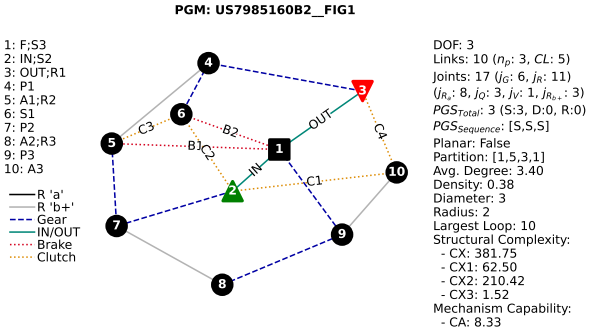

(c) DBG Graph

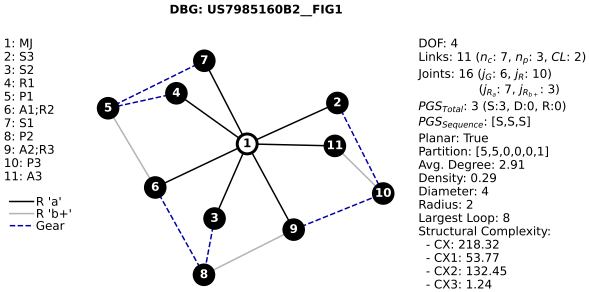

Table 192 – US8012059B2__FIG1 dataset information.

IDENTIFICATION		TOPOLOGY					GEARS SPECS		
UNIQUE_ID	**US8012059B2__FIG1**	**PGS**	**S/D**	**+/-**	**CLs**	**SCs**	**GEARS**	**Ratios**	**Engaged SCs**
Source	patent	1	S	F	S1;S2	B1: F;S1	R1	-3.653	B1;B2;C3
Owner	GM	2	S	IN	IN;A2	B2: F;R1	1	4.6	B1;B2
Patent	US8012059B2	3	S	OUT	A1;R4	C1: S3;S4	2	3.067	B1;B2;C1
Date	2007	4	S		R2;S3	C2: A2;S4	3	2.013	B2;C1;C2
Model	FIG1				OUT;A3;A4	C3: R3;S4	4	1.6	B2;C1;C3
Commercial?	false						5	1.244	B2;C2;C3
Longitudinal	true						6	1	C1;C2;C3
Transversal	false						7	0.848	B1;C2;C3
Weight (kg)							8	0.667	B1;C1;C3
Máx. Torque (N·m)									

Figure 221 – US8012059B2__FIG1 representations.

(a) Functional diagram

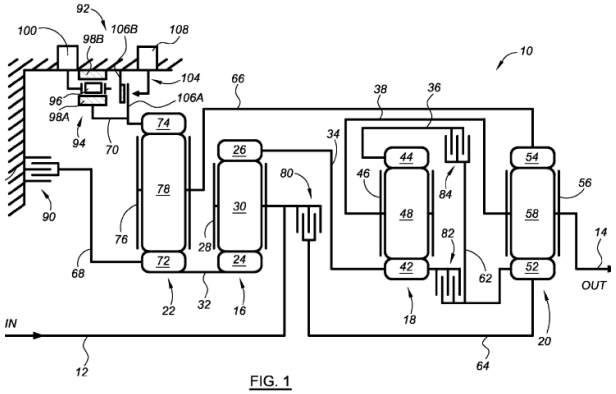

FIG. 1

(b) PGM Graph

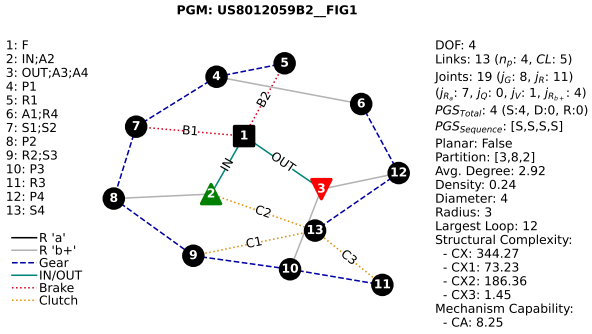

(c) DBG Graph

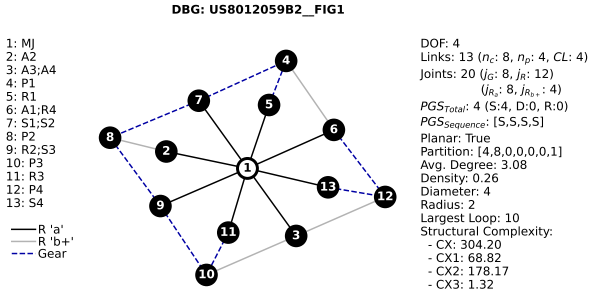

Table 193 – US8029405B2__FIG1 dataset information.

IDENTIFICATION		TOPOLOGY					GEARS SPECS		
UNIQUE_ID	**US8029405B2__FIG1**	**PGS**	**S/D**	**+/-**	**CLs**	**SCs**	**GEARS**	**Ratios**	**Engaged SCs**
Source	patent	1	D	F	F;S1	C1: S2;S4	R3		C3;B1
Owner	HYUNDAI	2	S	IN	IN;A1	C2: A2;R2	R2		C2;B1
Patent	US8029405B2	3	S	OUT	R1;S2	C3: A1;R2	R1		B1;B3
Date	2008	4	D		A2;S3	C4: IN;A3	1		C1;B1
Model	FIG1				P3;P4R	B1: F;A3	2		C1;B2
Commercial?	false				OUT;R3;R4	B2: F;A2	3		C1;B3
Longitudinal	true				A3;A4	B3: F;R2	4		C1;C2
Transversal	false						5		C1;C3
Weight (kg)							6		C1;C4
Máx. Torque (N·m)							7		C3;C4
							8		C2;C4
							9		C4;B3
							10		C4;B2

Figure 222 – US8029405B2__FIG1 representations.

(a) Functional diagram

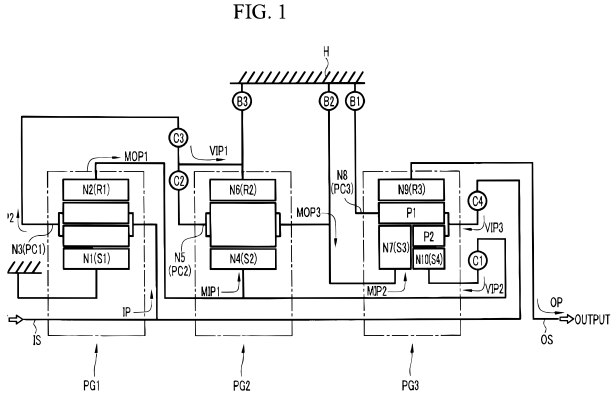

(b) PGM Graph

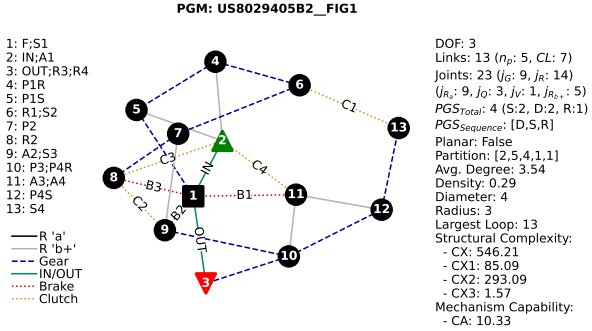

(c) DBG Graph

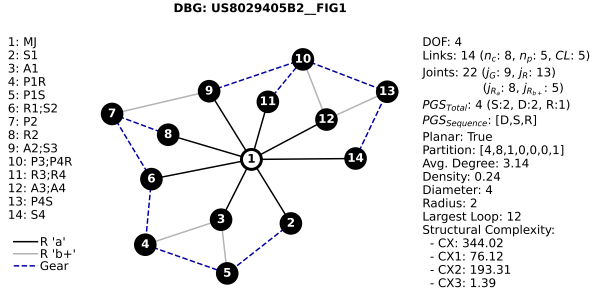

Table 194 – US8029405B2__FIG4 dataset information.

IDENTIFICATION		TOPOLOGY					GEARS SPECS		
UNIQUE_ID	**US8029405B2__FIG4**	**PGS**	**S/D**	**+/-**	**CLs**	**SCs**	**GEARS**	**Ratios**	**Engaged SCs**
Source	patent	1	D	F	F;S1	C1: S2;S4	R3		C3;B1
Owner	HYUNDAI	2	S	IN	IN;A1	C2: A2;S2	R2		C2;B1
Patent	US8029405B2	3	S	OUT	R1;S2	C3: A1;R2	R1		B1;B3
Date	2008	4	D		A2;S3	C4: IN;A3	1		C1;B1
Model	FIG4				P3;P4R	B1: F;A3	2		C1;B2
Commercial?	false				OUT;R3;R4	B2: F;A2	3		C1;B3
Longitudinal	true				A3;A4	B3: F;R2	4		C1;C2
Transversal	false						5		C1;C3
Weight (kg)							6		C1;C4
Máx. Torque (N·m)							7		C3;C4
							8		C2;C4
							9		C4;B3
							10		C4;B2

Figure 223 – US8029405B2__FIG4 representations.

(a) Functional diagram

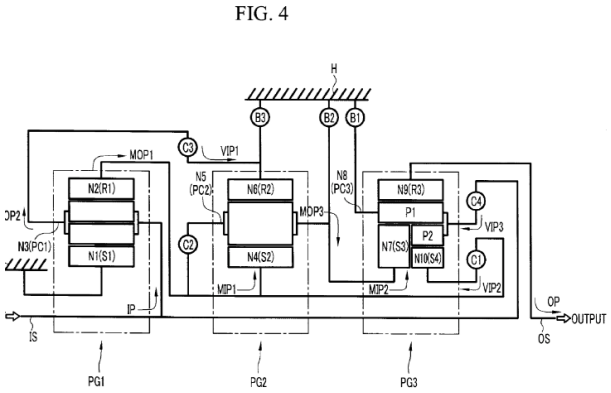

(b) PGM Graph

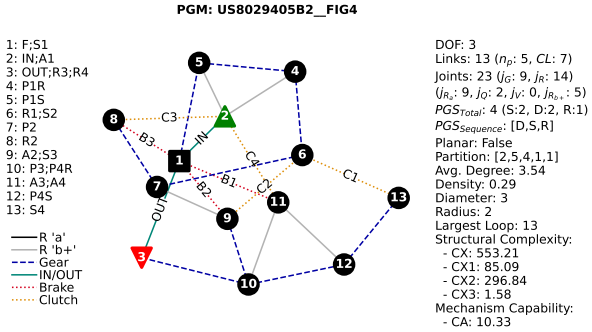

(c) DBG Graph

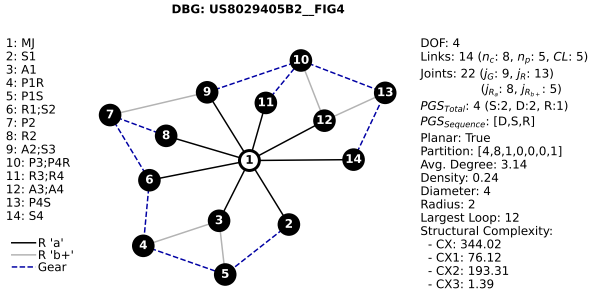

Table 195 – US8029405B2__FIG5 dataset information.

IDENTIFICATION		TOPOLOGY					GEARS SPECS		
UNIQUE_ID	**US8029405B2__FIG5**	**PGS**	**S/D**	**+/-**	**CLs**	**SCs**	**GEARS**	**Ratios**	**Engaged SCs**
Source	patent	1	D	F	F;S1	C1: S2;S4	R3		C3;B1
Owner	HYUNDAI	2	S	IN	IN;A1	C2: S2;R2	R2		C2;B1
Patent	US8029405B2	3	S	OUT	R1;S2	C3: A1;R2	R1		B1;B3
Date	2008	4	D		A2;S3	C4: IN;A3	1		C1;B1
Model	FIG5				P3;P4R	B1: F;A3	2		C1;B2
Commercial?	false				OUT;R3;R4	B2: F;A2	3		C1;B3
Longitudinal	true				A3;A4	B3: F;R2	4		C1;C2
Transversal	false						5		C1;C3
Weight (kg)							6		C1;C4
Máx. Torque (N·m)							7		C3;C4
							8		C2;C4
							9		C4;B3
							10		C4;B2

Figure 224 – US8029405B2__FIG5 representations.

(a) Functional diagram

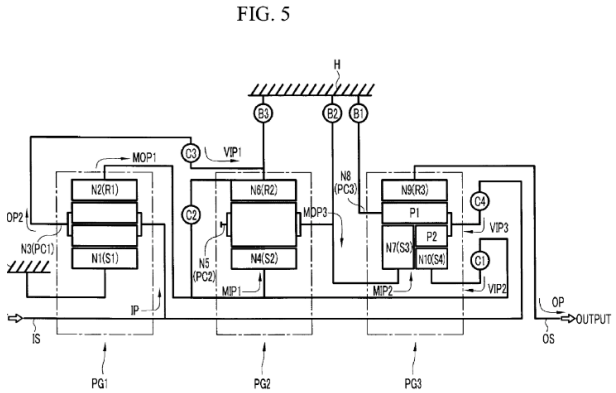

(b) PGM Graph

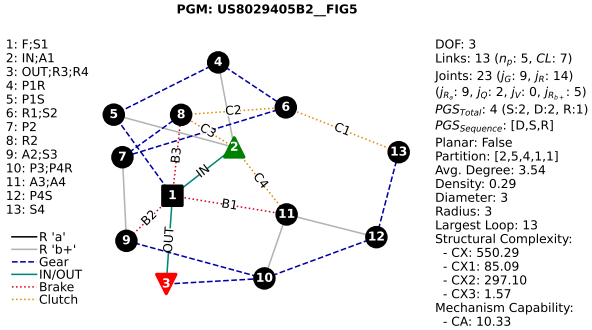

(c) DBG Graph

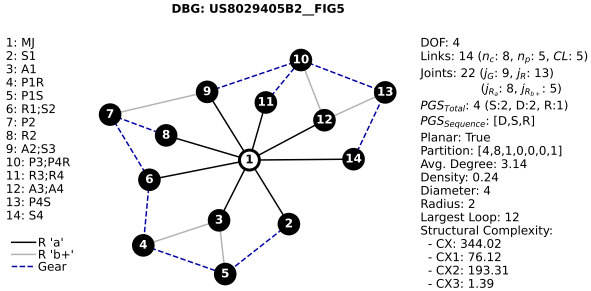

Table 196 – US8123650B2__FIG1 dataset information.

IDENTIFICATION		TOPOLOGY					GEARS SPECS		
UNIQUE_ID	**US8123650B2__FIG1**	**PGS**	**S/D**	**+/-**	**CLs**	**SCs**	**GEARS**	**Ratios**	**Engaged SCs**
Source	patent	1	S	F	S1;S2	B1: F;S1	R1		
Owner	GM	2	S	IN	A1;R4	B2: F;R1	1		
Patent	US8123650B2	3	S	OUT	IN;A2	C1: A2;S4	2		
Date	2008	4	S		R2;S3	C2: R2;S4	3		
Model	FIG1				OUT;A3;A4	C3: R3;S4	4		
Commercial?	false						5		
Longitudinal	false						6		
Transversal	true						7		
Weight (kg)							8		
Máx. Torque (N·m)									

Figure 225 – US8123650B2__FIG1 representations.

(a) Functional diagram

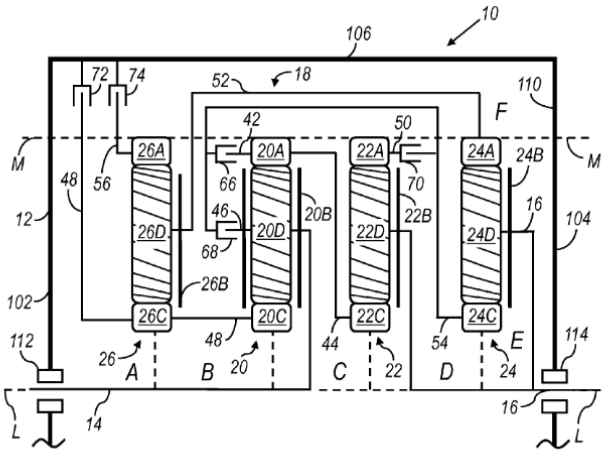

FIG. 1A

(b) PGM Graph

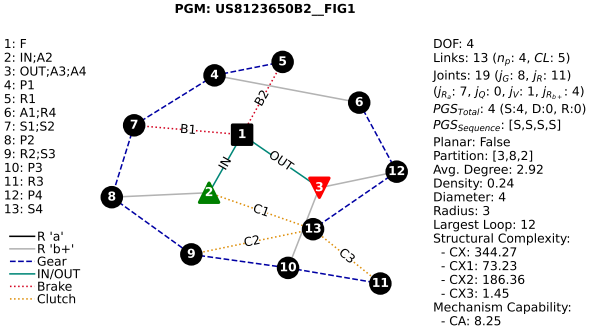

(c) DBG Graph

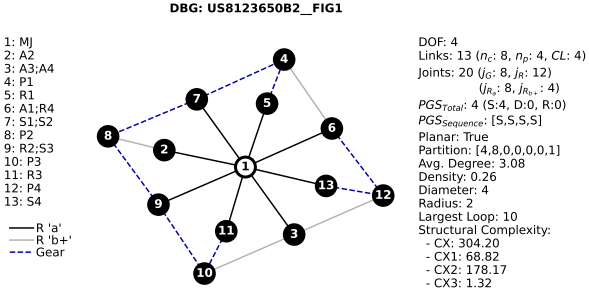

Table 197 – US8202192B2__FIG1 dataset information.

IDENTIFICATION		TOPOLOGY					GEARS SPECS		
UNIQUE_ID	**US8202192B2__FIG1**	**PGS**	**S/D**	**+/-**	**CLs**	**SCs**	**GEARS**	**Ratios**	**Engaged SCs**
Source	patent	1	S	F	S1;S3	C1: IN;R3	R1	-2.101	C2;C3;B1
Owner	HONDA	2	D	IN	IN;A1	C2: S3;A2	1	3.416	C3;B1;B2
Patent	US8202192B2	3	S	OUT	OUT;R2;A3	C3: R1;S2	2	2.203	C2;C3;B2
Date	2009					B1: F;R3	3	1.823	C1;C3;B2
Model	FIG1					B2: F;A2	4	1.388	C1;C2;B2
Commercial?	false					B3: F;S2	5	1	C1;C2;C3
Longitudinal	false						6	0.834	C1;C2;B3
Transversal	true						7	0.647	C1;C3;B3
Weight (kg)							8	0.484	C2;C3;B3
Máx. Torque (N·m)									

Figure 226 – US8202192B2__FIG1 representations.

(a) Functional diagram

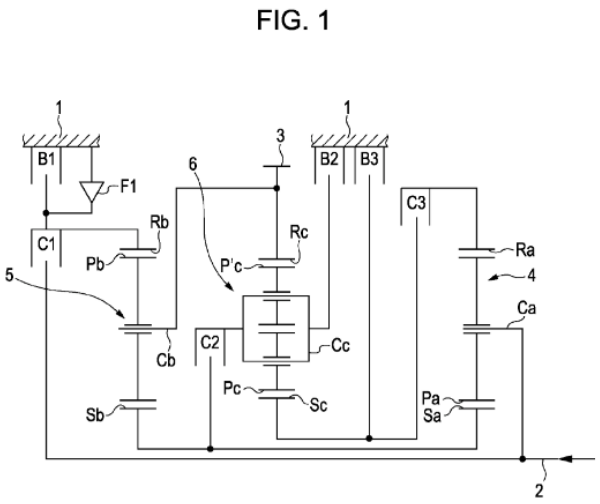

(b) PGM Graph

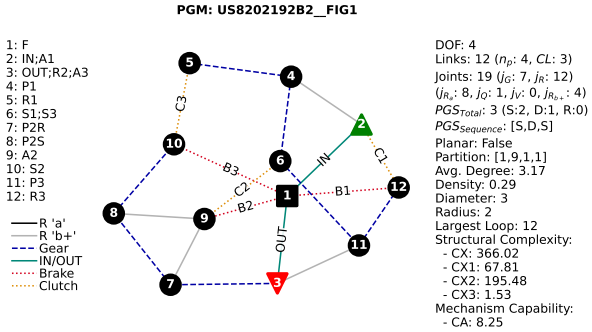

(c) DBG Graph

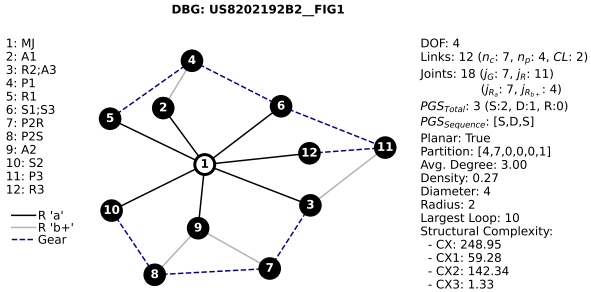

Table 198 – US8506443B2__FIG1 dataset information.

IDENTIFICATION		TOPOLOGY					GEARS SPECS		
UNIQUE_ID	**US8506443B2__FIG1**	**PGS**	**S/D**	**+/-**	**CLs**	**SCs**	**GEARS**	**Ratios**	**Engaged SCs**
Source	patent	1	S	F	R1;A2;S3	C1: IN;S2	R4		C2;B2;B3
Owner	HYUNDAI	2	S	IN	A1;R2	C2: IN;A1	R3		C1;C2;B3
Patent	US8506443B2	3	S	OUT	OUT;R3;A4	C3: IN;A3	R2		C1;B2;B3
Date	2011	4	S		A3;R4	B1: F;A1	R1		C1;B1;B3
Model	FIG1					B2: F;S1	1		C1;B1;B4
Commercial?	false					B3: F;A3	2		C1;B2;B4
Longitudinal	true					B4: F;S4	3		C1;C2;B4
Transversal	false						4		C2;B2;B4
Weight (kg)							5		C3;B2;B4
Máx. Torque (N·m)							6		C2;C3;B2
							7		C1;C2;C3
							8		C1;C3;B2
							9		C1;C3;B1
							10		C3;B1;B2

Figure 227 – US8506443B2__FIG1 representations.

(a) Functional diagram

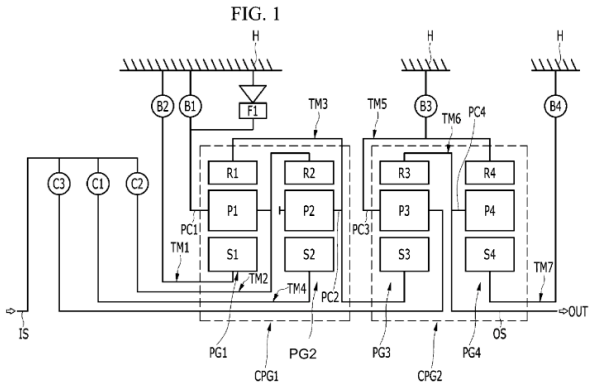

(b) PGM Graph

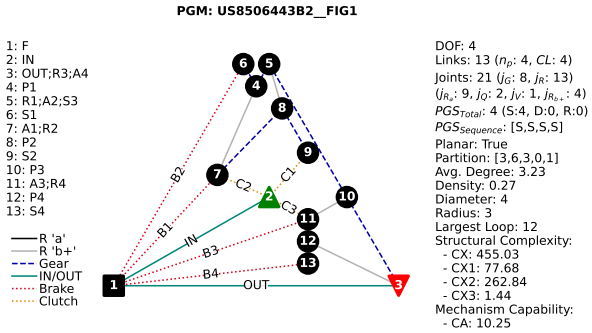

(c) DBG Graph

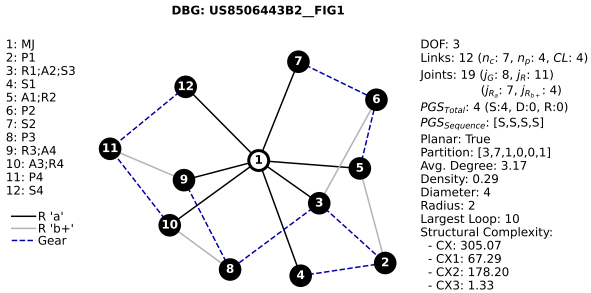

Table 199 – US8597153B2__FIG1 dataset information.

IDENTIFICATION		TOPOLOGY					GEARS SPECS		
UNIQUE_ID	**US8597153B2__FIG1**	**PGS**	**S/D**	**+/-**	**CLs**	**SCs**	**GEARS**	**Ratios**	**Engaged SCs**
Source	patent	1	S	F	IN;S1	B1: F;S2	R1	-3.318	B2;B3;C3
Owner	HONDA	2	S	IN	A1;S2	B2: F;A3	1	4.766	B2;B3;C2
Patent	US8597153B2	3	S	OUT	OUT;R2	B3: F;R1	2	3.332	B1;B2;C2
Date	2010	4	S		A2;R4	C1: IN;A3	3	2.334	B2;C2;C3
Model	FIG1				R3;S4	C2: IN;S3	4	1.67	B1;C2;C3
Commercial?	false				A3;A4	C3: S2;R3	5	1.392	B3;C2;C3
Longitudinal	false						6	1	C1;C2;C3
Transversal	true						7	0.825	B3;C1;C2
Weight (kg)							8	0.585	B3;C1;C3
Máx. Torque (N·m)							9	0.498	B1;C1;C3

Figure 228 – US8597153B2__FIG1 representations.

(a) Functional diagram

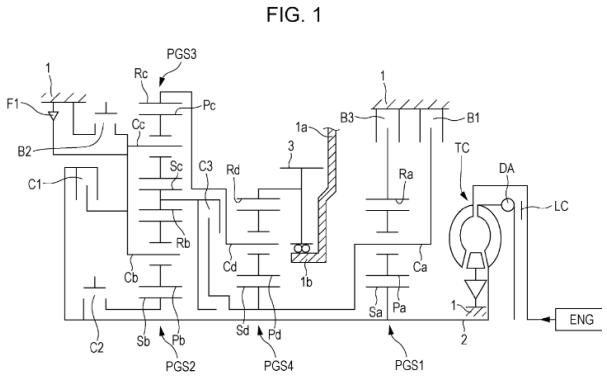

(b) PGM Graph

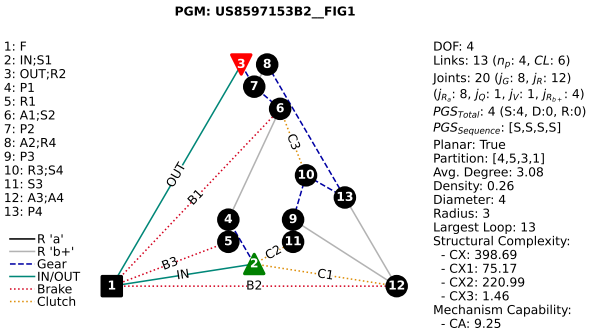

(c) DBG Graph

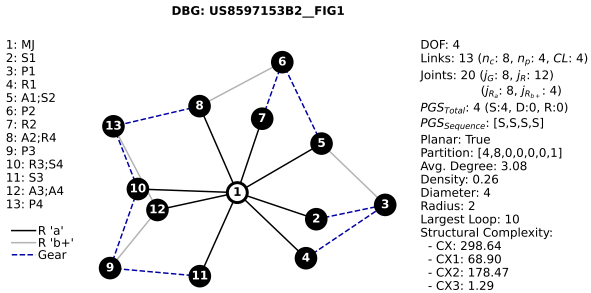

Table 200 – US8597153B2__FIG4 dataset information.

IDENTIFICATION		TOPOLOGY					GEARS SPECS		
UNIQUE_ID	**US8597153B2__FIG4**	**PGS**	**S/D**	**+/-**	**CLs**	**SCs**	**GEARS**	**Ratios**	**Engaged SCs**
Source	patent	1	S	F	IN;S1;S3	B1: F;S2	R1	-3.317	B2;B3;C3
Owner	HONDA	2	S	IN	A1;S2	B2: F;A4	1	4.767	B2;B3;C2
Patent	US8597153B2	3	S	OUT	OUT;R2	B3: F;R1	2	3.332	B1;B2;C2
Date	2010	4	S		A2;R4	C1: IN;A4	3	2.334	B2;C2;C3
Model	FIG4				R3;S4	C2: A3;A4	4	1.67	B1;C2;C3
Commercial?	false					C3: S2;R3	5	1.392	B3;C2;C3
Longitudinal	false						6	1	C1;C2;C3
Transversal	true						7	0.825	B3;C1;C2
Weight (kg)							8	0.586	B3;C1;C3
Máx. Torque (N·m)							9	0.498	B1;C1;C3

Figure 229 – US8597153B2__FIG4 representations.

(a) Functional diagram

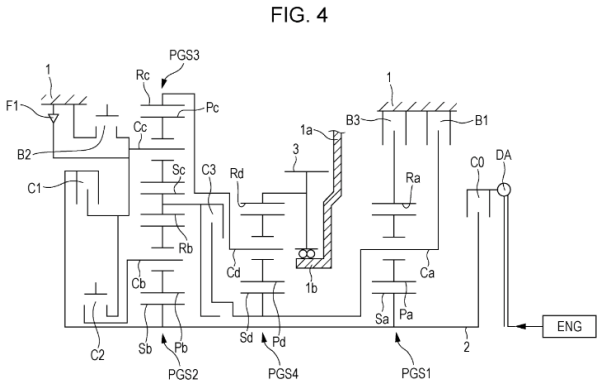

(b) PGM Graph

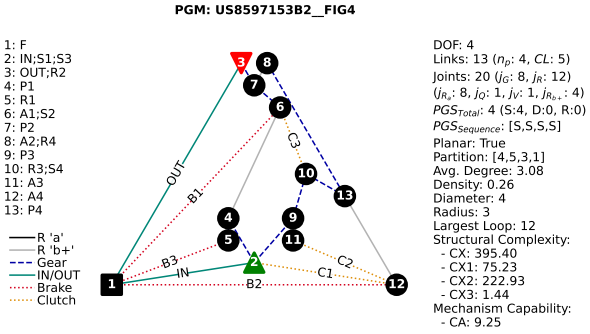

(c) DBG Graph

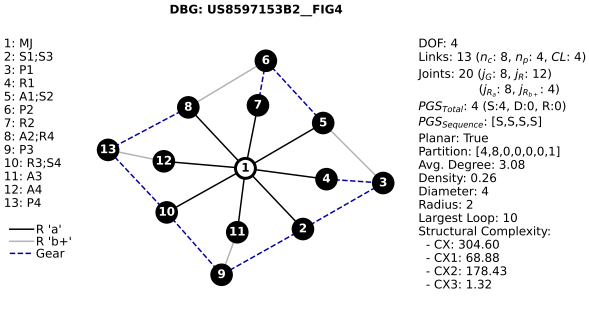

Table 201 – US8657718B2__FIG1 dataset information.

IDENTIFICATION		TOPOLOGY					GEARS SPECS		
UNIQUE_ID	**US8657718B2__FIG1**	**PGS**	**S/D**	**+/-**	**CLs**	**SCs**	**GEARS**	**Ratios**	**Engaged SCs**
Source	patent	1	S	F	IN;S3	B1: F;S1	R1	-2.765	B2;B3;C4
Owner	HONDA	2	S	IN	R1;A3;A4	B2: F;S4	1	5.176	B1;B2;B3
Patent	US8657718B2	3	S	OUT	A1;A2	B3: F;R4	2	3.244	B1;B2;C3
Date	2012	4	S		OUT;R2	C1: IN;A1	3	2.181	B1;B2;C2
Model	FIG1				S2;R3	C2: IN;R4	4	1.597	B1;C2;C3
Commercial?	false					C3: R3;S4	5	1.306	B1;C1;C2
Longitudinal	false					C4: A2;R2	6	1	C1;C2;C3
Transversal	true					: R1;IN	7	0.78	C1;C2
Weight (kg)							8	0.652	C1;C3
Máx. Torque (N·m)							9	0.579	B3;C1
							10	0.515	B3;C1;C3

Figure 230 – US8657718B2__FIG1 representations.

(a) Functional diagram

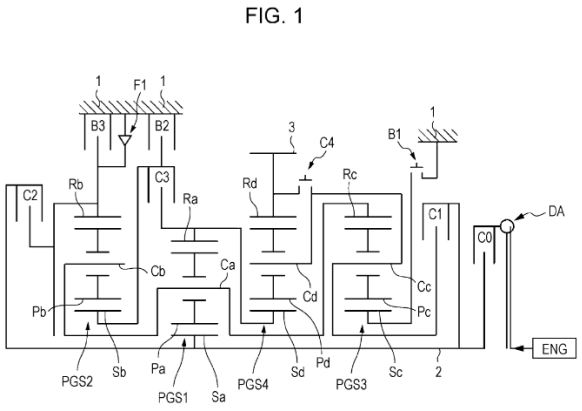

(b) PGM Graph

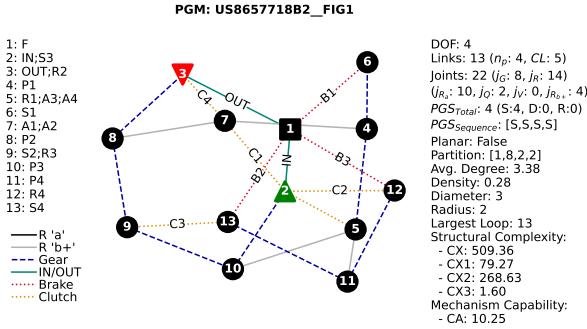

(c) DBG Graph

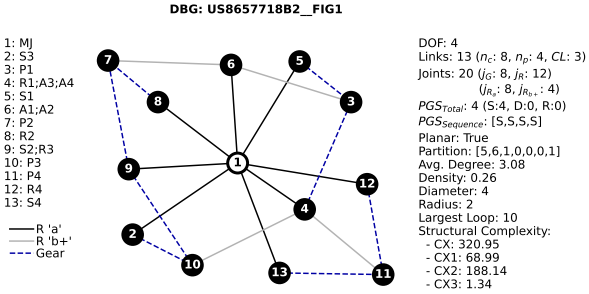

Table 202 – US8663055B2__FIG1 dataset information.

IDENTIFICATION		TOPOLOGY					GEARS SPECS		
UNIQUE_ID	**US8663055B2__FIG1**	**PGS**	**S/D**	**+/-**	**CLs**	**SCs**	**GEARS**	**Ratios**	**Engaged SCs**
Source	patent	1	S	F	S1;S2	B1-A: F;S1	R2	-3.28	B1-A;B2-B;C2-D
Owner	ZF	2	S	IN	A1;R4	B2-B: F;R1	R1	-5.013	B1-A;B2-B;C4-F
Patent	US8663055B2	3	S	OUT	IN;A2	C1-C: IN;S4	1	4.699	B1-A;B2-B;C1-C
Date	2007	4	S		R2;S3	C2-D: A3;A4	2	3.134	B1-A;B2-B;C3-E
Model	FIG1				R3;S4	C3-E: S3;S4	3	2.104	B2-B;C1-C;C3-E
Commercial?	false				OUT;A4	C4-F: A1;A3	4	1.667	B2-B;C2-D;C3-E
Longitudinal	true						5	1.285	B2-B;C1-C;C2-D
Transversal	false						6	1.238	B2-B;C1-C;C4-F
Weight (kg)							7	1	C1-C;C3-E;C4-F
Máx. Torque (N·m)							8	0.869	B1-A;C1-C;C4-F
							9	0.839	B1-A;C1-C;C2-D
							10	0.667	B1-A;C2-D;C3-E

Figure 231 – US8663055B2__FIG1 representations.

(a) Functional diagram

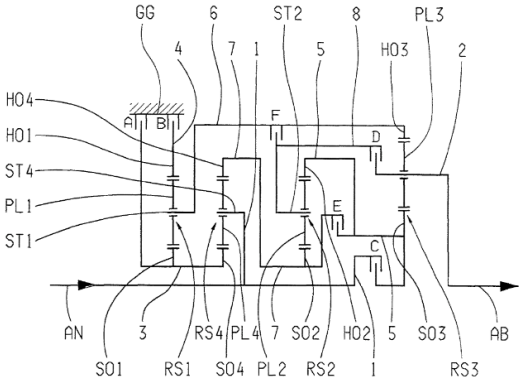

Fig. 1

(b) PGM Graph

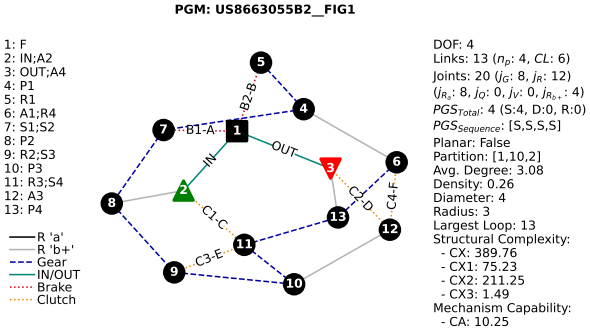

(c) DBG Graph

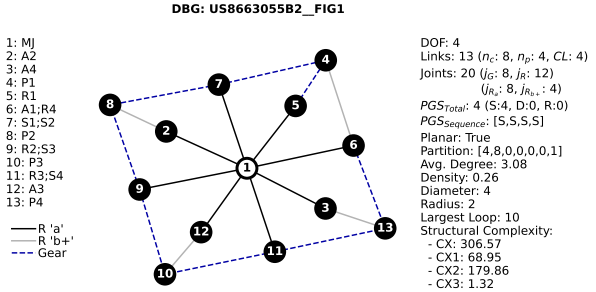

Table 203 – US8678973B2__FIG1 dataset information.

IDENTIFICATION		TOPOLOGY					GEARS SPECS		
UNIQUE_ID	**US8678973B2__FIG1**	**PGS**	**S/D**	**+/-**	**CLs**	**SCs**	**GEARS**	**Ratios**	**Engaged SCs**
Source	patent	1	S	F	IN;S1	B1: F;R1	R1	-3.989	B1;B2;C2
Owner	HONDA	2	S	IN	R1;S2	B2: F;R4	1	5.147	B1;B2;C3
Patent	US8678973B2	3	S	OUT	OUT;R2	B3: F;A1	2	3.38	B2;B3;C3
Date	2012	4	S		A2;A4	B4: F;R3	3	2.342	B2;C2;C3
Model	FIG1				R3;S4	C1: IN;A3	4	1.656	B3;C2;C3
Commercial?	false				A3;R4	C2: IN;S3	5	1.349	B1;C2;C3
Longitudinal	false					C3: A1;R3	6	1	C1;C2;C3
Transversal	true						7	0.839	B1;C1;C3
Weight (kg)							8	0.642	B1;C1;C2
Máx. Torque (N·m)							9	0.539	B3;C1;C2
							10	0.475	B3;B4;C1

Figure 232 – US8678973B2__FIG1 representations.

(a) Functional diagram

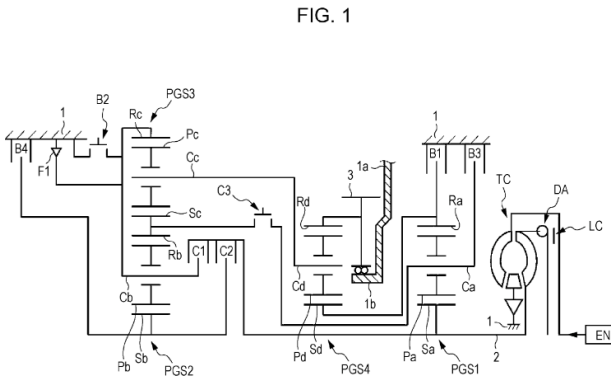

(b) PGM Graph

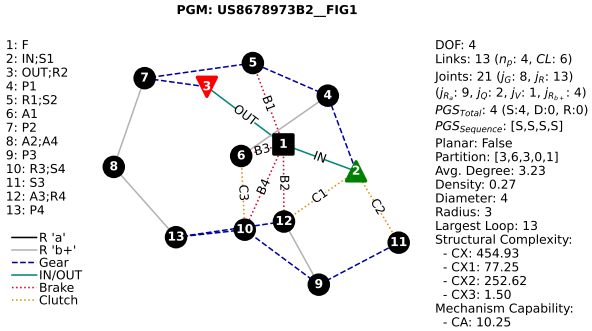

(c) DBG Graph

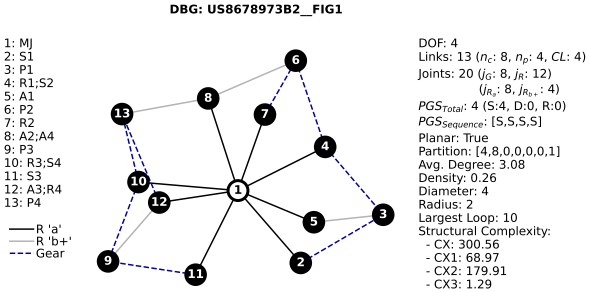

Table 204 – US8992374B2__FIG1 dataset information.

IDENTIFICATION		TOPOLOGY					GEARS SPECS		
UNIQUE_ID	**US8992374B2__FIG1**	**PGS**	**S/D**	**+/-**	**CLs**	**SCs**	**GEARS**	**Ratios**	**Engaged SCs**
Source	patent	1	S	F	IN;S3	B1: F;S1	R1	-4.008	B2;B3;C3
Owner	HONDA	2	S	IN	R1;A3;A4	B2: F;A1	1	5.233	B1;B2;B3
Patent	US8992374B2	3	S	OUT	A1;A2	B3: F;S4	2	3.367	B1;C2
Date	2013	4	S		OUT;R2	C1: IN;A1	3	2.298	B1;C3
Model	FIG1				S2;R3	C2: R3;S4	4	1.705	B1;C2;C3
Commercial?	false					C3: IN;R4	5	1.363	B1;C1;C3
Longitudinal	false						6	1	C1;C2;C3
Transversal	true						7	0.786	B3;C1;C3
Weight (kg)							8	0.657	B3;C1;C2
Máx. Torque (N·m)									

Figure 233 – US8992374B2__FIG1 representations.

(a) Functional diagram

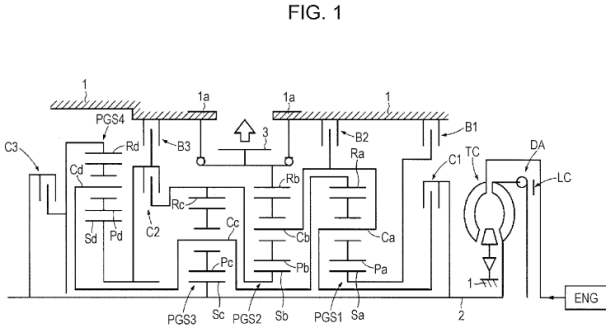

(b) PGM Graph

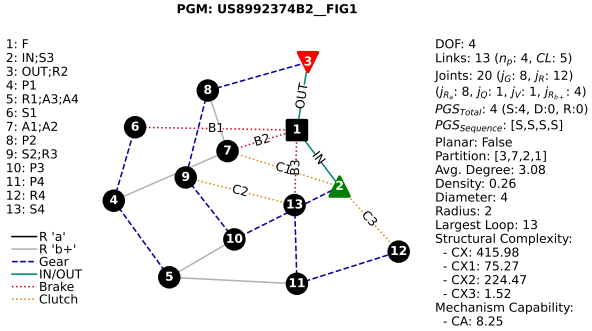

(c) DBG Graph

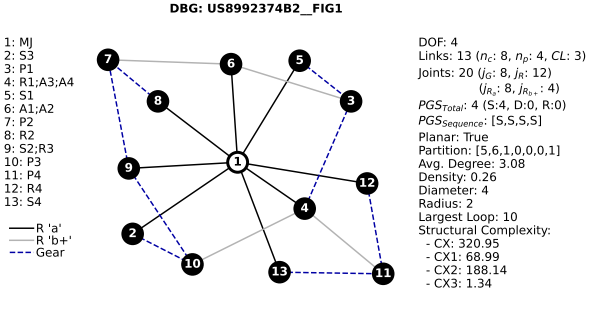

Table 205 – US8992374B2__FIG5 dataset information.

IDENTIFICATION		TOPOLOGY					GEARS SPECS		
UNIQUE_ID	**US8992374B2__FIG5**	**PGS**	**S/D**	**+/-**	**CLs**	**SCs**	**GEARS**	**Ratios**	**Engaged SCs**
Source	patent	1	S	F	IN;S3	B1: F;S1	R1	-4.008	B2;B3;C3
Owner	HONDA	2	S	IN	R1;A3;A4	B2: F;A1	1	5.233	B1;B2;B3
Patent	US8992374B2	3	S	OUT	A1;A2	B3: F;S4	2	3.367	B1;C2
Date	2013	4	S		OUT;R2	B4: F;R4	3	2.298	B1;C3
Model	FIG5				S2;R3	C1: IN;A1	4	1.705	B1;C2;C3
Commercial?	false					C2: R3;S4	5	1.363	B1;C1;C3
Longitudinal	false					C3: IN;R4	6	1	C1;C2;C3
Transversal	true						7	0.786	B3;C1;C3
Weight (kg)							8	0.657	B3;C1;C2
Máx. Torque (N·m)							9	0.584	B3;B4;C1
							10	0.52	B4;C1;C2

Figure 234 – US8992374B2__FIG5 representations.

(a) Functional diagram

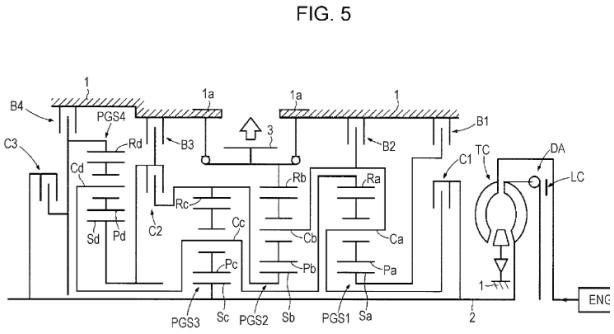

(b) PGM Graph

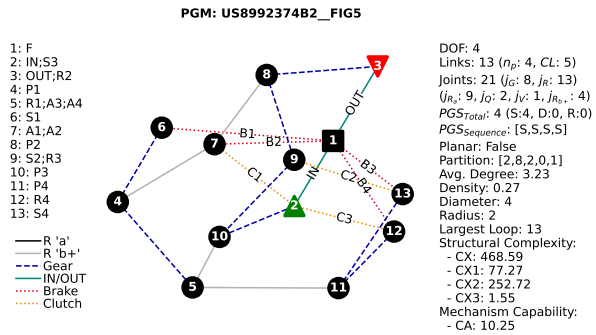

(c) DBG Graph

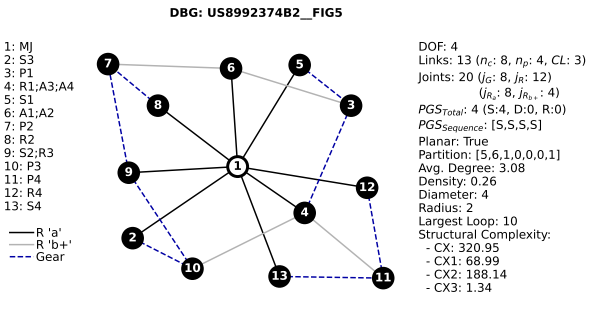

Table 206 – US9587716B1__FIG1 dataset information.

IDENTIFICATION		TOPOLOGY					GEARS SPECS		
UNIQUE_ID	**US9587716B1__FIG1**	**PGS**	**S/D**	**+/-**	**CLs**	**SCs**	**GEARS**	**Ratios**	**Engaged SCs**
Source	patent	1	S	F	F;S1	B1: F;A2	R1	-3.755	B1;B2;C4
Owner	HYUNDAI	2	S	IN	IN;R1	B2: F;R3	1	6.045	B2;C3;C4
Patent	US9587716B1	3	S	OUT	S2;S3;S4	C1: IN;A2	2	3.72	B2;C1;C3
Date	2015	4	S		OUT;A3;R4	C2: IN;A4	3	2.297	B2;C1;C4
Model	FIG1					C3: R2;A2	4	1.563	B2;C1;C2
Commercial?	false					C4: A1;R2	5	1.193	C1;C2;C4
Longitudinal	true						6	1	C1;C2;C3
Transversal	false						7	0.909	C2;C3;C4
Weight (kg)							8	0.793	B1;C2;C3
Máx. Torque (N·m)							9	0.658	B1;C2;C4

Figure 235 – US9587716B1__FIG1 representations.

(a) Functional diagram

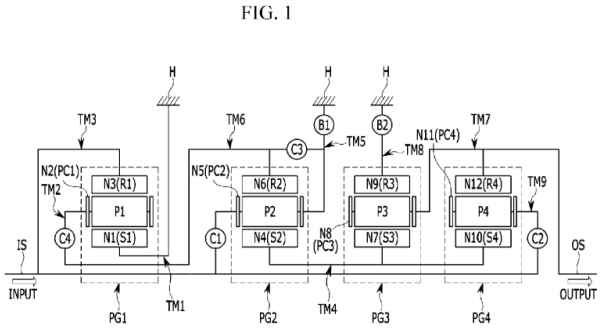

(b) PGM Graph

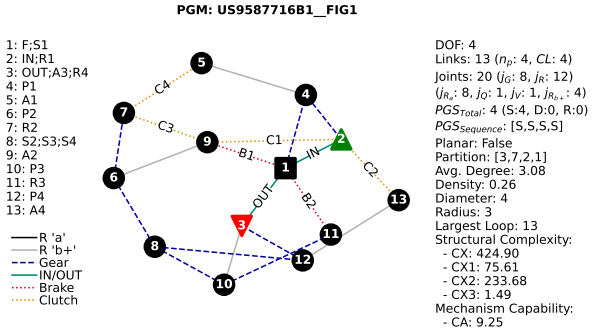

(c) DBG Graph

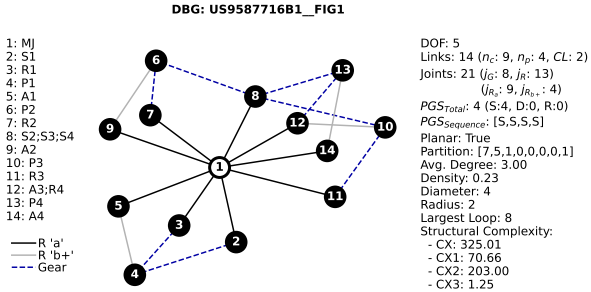

Table 207 – US9726262B1__FIG1 dataset information.

IDENTIFICATION		TOPOLOGY					GEARS SPECS		
UNIQUE_ID	**US9726262B1__FIG1**	**PGS**	**S/D**	**+/-**	**CLs**	**SCs**	**GEARS**	**Ratios**	**Engaged SCs**
Source	patent	1	S	F	A1;A2	C1: IN;A2	R1	-3.091	C3;B1;B3
Owner	HYUNDAI	2	S	IN	R1;A3	C2: OUT;A3	1	5.415	C3;B1;B2
Patent	US9726262B1	3	S	OUT	IN;S2;S3	C3: A1;S4	2	3.687	B1;B2;B3
Date	2016	4	S		R3;A4	B1: F;S1	3	2.72	C2;B1;B2
Model	FIG1				OUT;R4	B2: F;R2	4	1.909	C2;B2;B3
Commercial?	false					B3: F;S4	5	1.506	C2;C3;B2
Longitudinal	true						6	1.182	C2;C3;B1
Transversal	false						7	1	C1;C2;C3
Weight (kg)							8	0.8	C1;C2;B1
Máx. Torque (N·m)							9	0.712	C1;C3;B1
							10	0.589	C1;B1;B3

Figure 236 – US9726262B1__FIG1 representations.

(a) Functional diagram

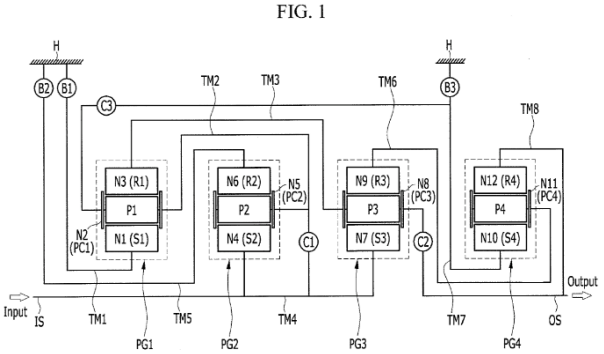

(b) PGM Graph

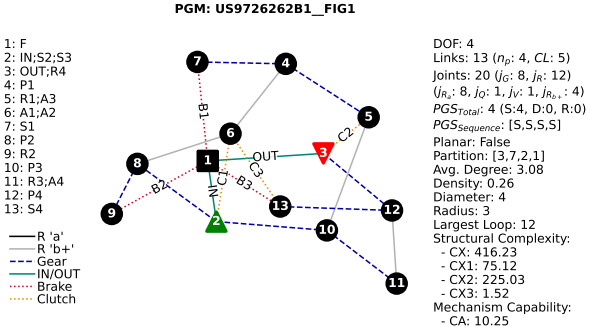

(c) DBG Graph

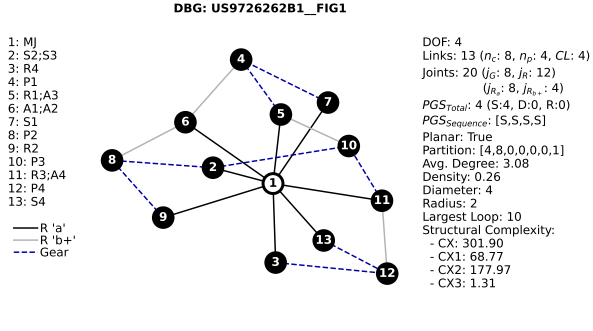

Table 208 – US9841085B2__FIG1 dataset information.

IDENTIFICATION		TOPOLOGY					GEARS SPECS		
UNIQUE_ID	**US9841085B2__FIG1**	**PGS**	**S/D**	**+/-**	**CLs**	**SCs**	**GEARS**	**Ratios**	**Engaged SCs**
Source	patent	1	S	F	F;S1	C1: IN;R2	R1	-3.667	C1;B3
Owner	HYUNDAI	2	S	IN	A1;R3	C2: IN;S3	1	5.5	B2;B3
Patent	US9841085B2	3	S	OUT	R1;R2	C3: IN;A3	2	3.3	C2;B3
Date	2016	4	S		IN;S2	B1: F;A1	3	2.412	C2;B2
Model	FIG1				S3;S4	B2: F;A2	4	1.719	C2;B1
Commercial?	false				A3;R4	B3: F;R4	5	1.201	C1;C2
Longitudinal	true				OUT;A4	:	6	1	C2;C3
Transversal	false						7	0.846	C1;C3
Weight (kg)							8	0.688	C3;B1
Máx. Torque (N·m)							9	0.611	C3;B2

Figure 237 – US9841085B2__FIG1 representations.

(a) Functional diagram

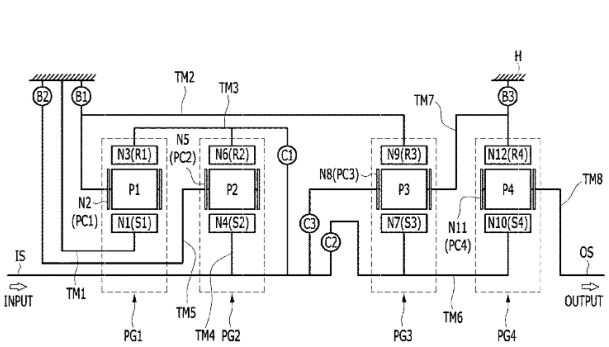

(b) PGM Graph

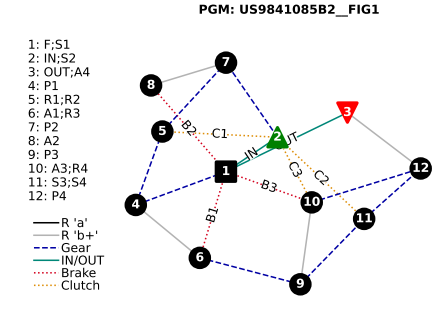

(c) DBG Graph

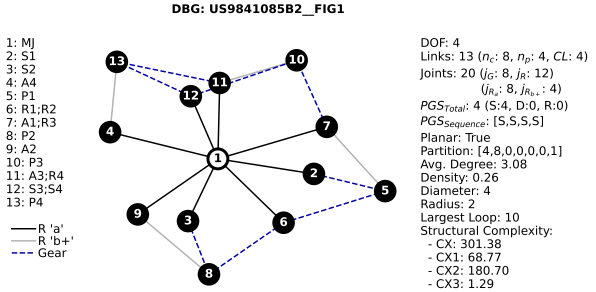

Table 209 – DE10140424A1__6HP dataset information.

IDENTIFICATION		TOPOLOGY					GEARS SPECS		
UNIQUE_ID	**DE10140424A1__6HP**	**PGS**	**S/D**	**+/-**	**CLs**	**SCs**	**GEARS**	**Ratios**	**Engaged SCs**
Source	industry	1	S	F	F;S1	B1-C: F;S2	R1	-3.4	B2-D;C3-B
Owner	ZF	2	S	IN	IN;R1	B2-D: F;A2	1	4.17	B2-D;C2-A
Patent	DE10140424A1	3	D	OUT	P2;P3R	C1-E: IN;A3	2	2.34	B1-C;C2-A
Date	2001				OUT;R2;R3	C2-A: A1;S3	3	1.52	C2-A;C3-B
Model	6HP				A2;A3	C3-B: A1;S2	4	1.14	C1-E;C2-A
Commercial?	true						5	0.87	C1-E;C3-B
Longitudinal	true						6	0.69	B1-C;C1-E
Transversal	false								
Weight (kg)	92.5								
Máx. Torque (N·m)	700								

Figure 238 – DE10140424A1__6HP representations.

(a) Functional diagram

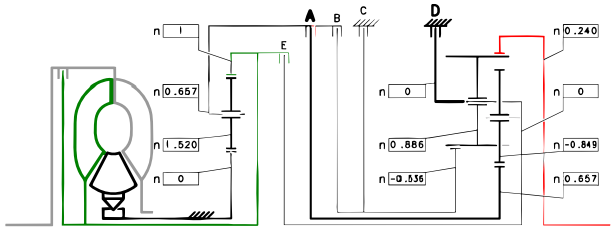

(b) PGM Graph

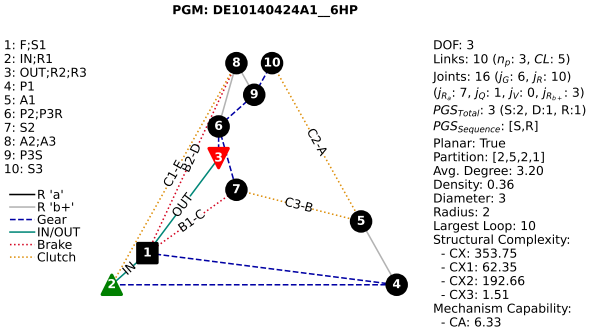

(c) DBG Graph

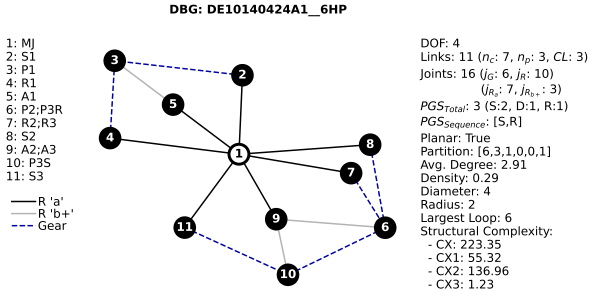

Table 210 – ZF__8HP dataset information.

IDENTIFICATION		TOPOLOGY					GEARS SPECS		
UNIQUE_ID	**ZF__8HP**	**PGS**	**S/D**	**+/-**	**CLs**	**SCs**	**GEARS**	**Ratios**	**Engaged SCs**
Source	industry	1	S	F	IN;A2	B1-A: F;S1	R1	-3.456	B1-A;B2-B;C2-D
Owner	ZF	2	S	IN	S1;S2	B2-B: F;R1	1	5	B1-A;B2-B;C3-C
Patent		3	S	OUT	A1;R4	C1-E: S3;S4	2	3.2	B1-A;B2-B;C1-E
Date	2018	4	S		R2;S3	C2-D: A3;A4	3	2.143	B2-B;C1-E;C3-C
Model	8HP				R3;S4	C3-C: IN;S4	4	1.72	B2-B;C1-E;C2-D
Commercial?	true				OUT;A4	:	5	1.314	B2-B;C2-D;C3-C
Longitudinal	true						6	1	C1-E;C2-D;C3-C
Transversal	false						7	0.822	B1-A;C2-D;C3-C
Weight (kg)	87						8	0.64	B1-A;C1-E;C2-D
Máx. Torque (N·m)	750								

Figure 239 – ZF__8HP representations.

(a) Functional diagram

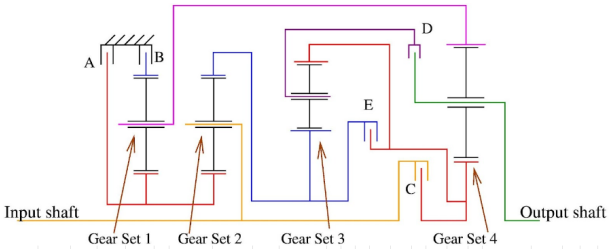

(b) PGM Graph

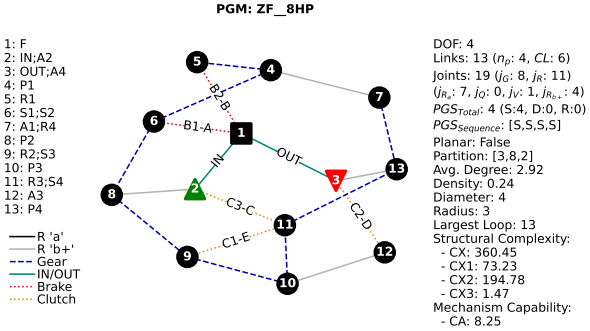

(c) DBG Graph

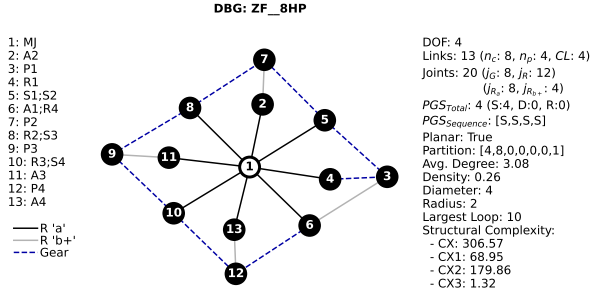

Table 211 – US8398522B2__9HP dataset information.

IDENTIFICATION		TOPOLOGY					GEARS SPECS		
UNIQUE_ID	**US8398522B2__9HP**	**PGS**	**S/D**	**+/-**	**CLs**	**SCs**	**GEARS**	**Ratios**	**Engaged SCs**
Source	industry	1	S	F	R1;A2	B1-D: F;R3	R1	-3.8	B1-D;B3-F;C2-B
Owner	ZF	2	S	IN	S1;S2	B2-C: F;S4	1	4.7	B1-D;B3-F;C3-A
Patent	US8398522B2	3	S	OUT	OUT;A1	B3-F: F;S1	2	2.84	B2-C;B3-F;C3-A
Date	2008	4	S		R2;A3;A4	C1-E: IN;A2	3	1.91	B3-F;C2-B;C3-A
Model	9HP				S3;R4	C2-B: IN;S4	4	1.38	B3-F;C1-E;C3-A
Commercial?	true					C3-A: IN;S3	5	1	C1-E;C2-B;C3-A
Longitudinal	false						6	0.81	B2-C;C1-E;C3-A
Transversal	true						7	0.7	B1-D;C1-E;C3-A
Weight (kg)	86						8	0.58	B1-D;B2-C;C1-E
Máx. Torque (N·m)	480						9	0.48	B1-D;C1-E;C2-B

Figure 240 – US8398522B2__9HP representations.

(a) Functional diagram

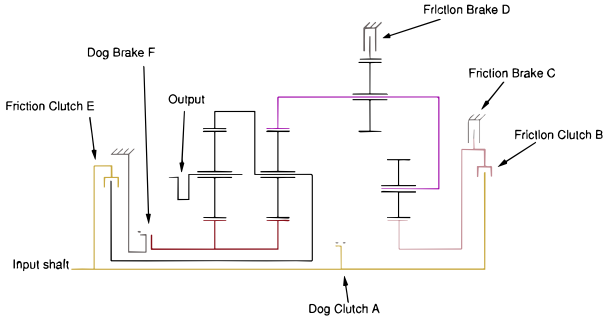

(b) PGM Graph

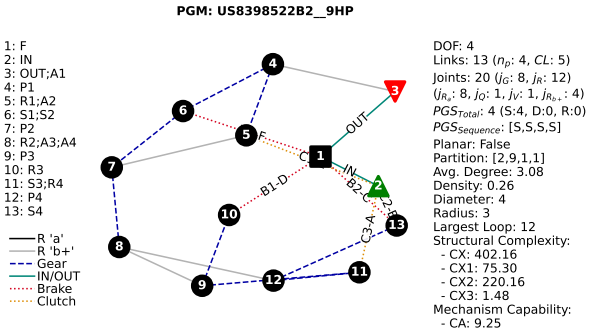

(c) DBG Graph

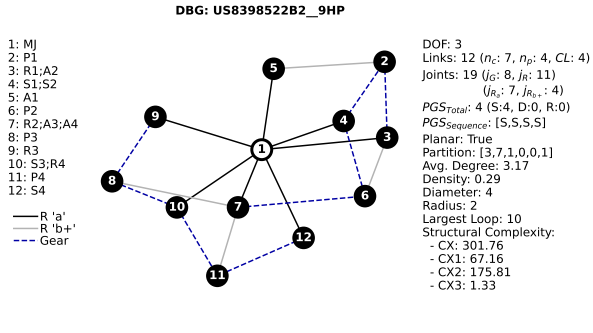

APPENDIX B – VISUAL RESULTS FROM THE PROCESS APPLICATION

In the journey of scientific exploration, visual representations often bridge the gap between complex data interpretations and a clear understanding of the underlying phenomena. This appendix is dedicated to presenting a comprehensive collection of charts resulting from the application of the process in Chapter 5. Each chart serves as a visual testament to the intricate processes, analyses, and findings detailed in the preceding sections. Readers are encouraged to refer to these visual aids to enhance their comprehension and appreciation of the data science techniques employed and the insights gathered from them.

The database containing all PGM data after cleansing (Section 5.4.1) is available in PGM Prepared Database Spreadsheet.

The PGM correlation matrix of the database, containing all correlations (Section 5.4.2), is available in PGM Database Correlation Matrix Spreadsheet.

In the following pages, the results of the univariate, bivariate and multivariate data analysis of PGMs (Section 5.4.2) are presented in corresponding sections.

B.1 RESULTS OF UNIVARIATE DATA ANALYSIS

The results of the univariate data analysis discussed in Section 5.4.2 are presented in representative graphs according to each feature data type.

For numerical values, it was utilized the violin plots that merges the characteristics of a boxplot with a smoothed probability density function, offering an unbiased visualization of data distributions (HINTZE; NELSON, 1998). It highlights key statistical markers like the median, quartiles, and extremes, making it ideal for graphically examining and comparing multiple data sets as shown in Figure 241.

The features analyzed were segmented by three main characteristics: number of forward gears, number of total PGSs, and the commercial status.

Figure 241 – Violin plot explanation

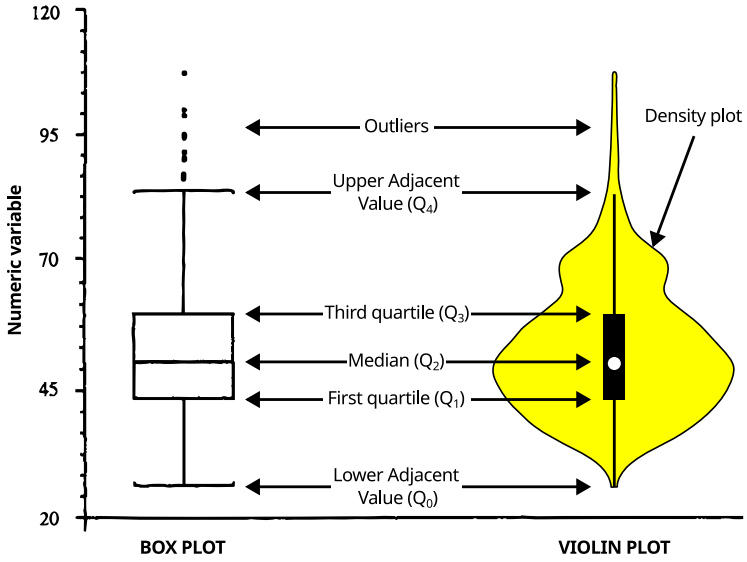

Source: Adapted from Hintze and Nelson (1998).

B.1.1 Features Distribution Segmented by *FWD GEARS*

Figure 242 – Violin plots of numerical features - *FWD GEARS* (1 of 8)

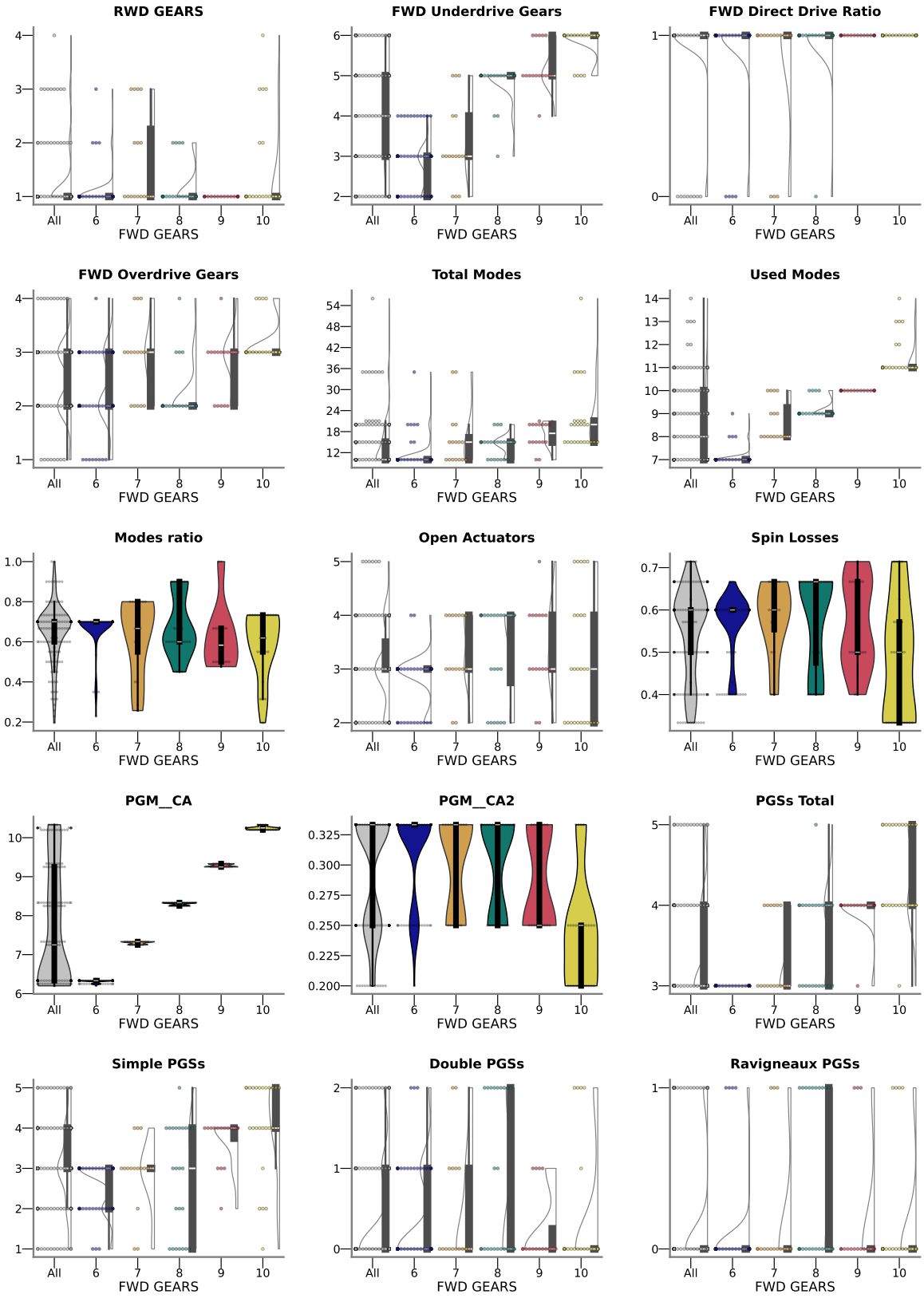

Source: Author.

Figure 243 – Violin plots of numerical features - *FWD GEARS* (2 of 8)

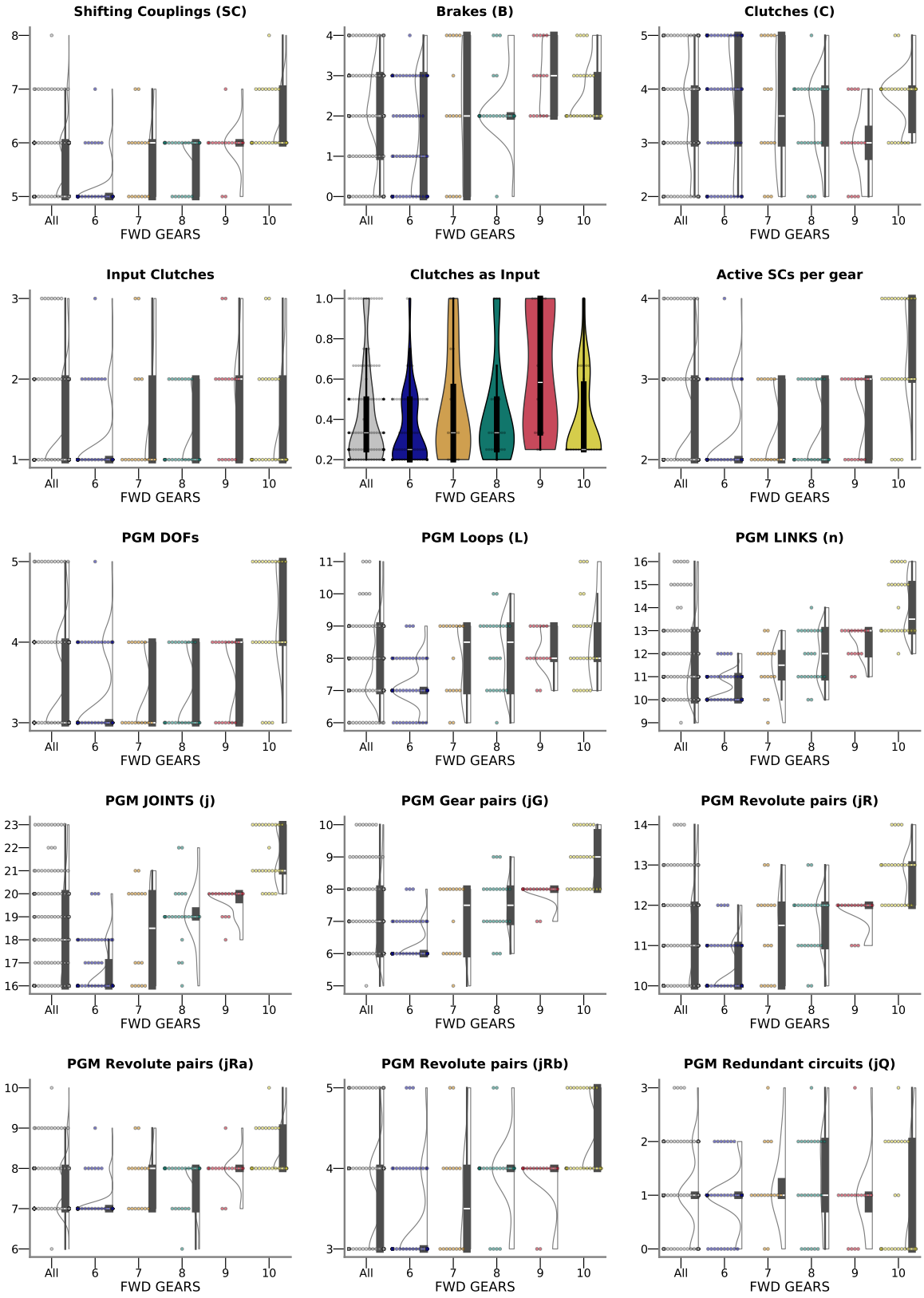

Source: Author.

Figure 244 – Violin plots of numerical features - *FWD GEARS* (3 of 8)

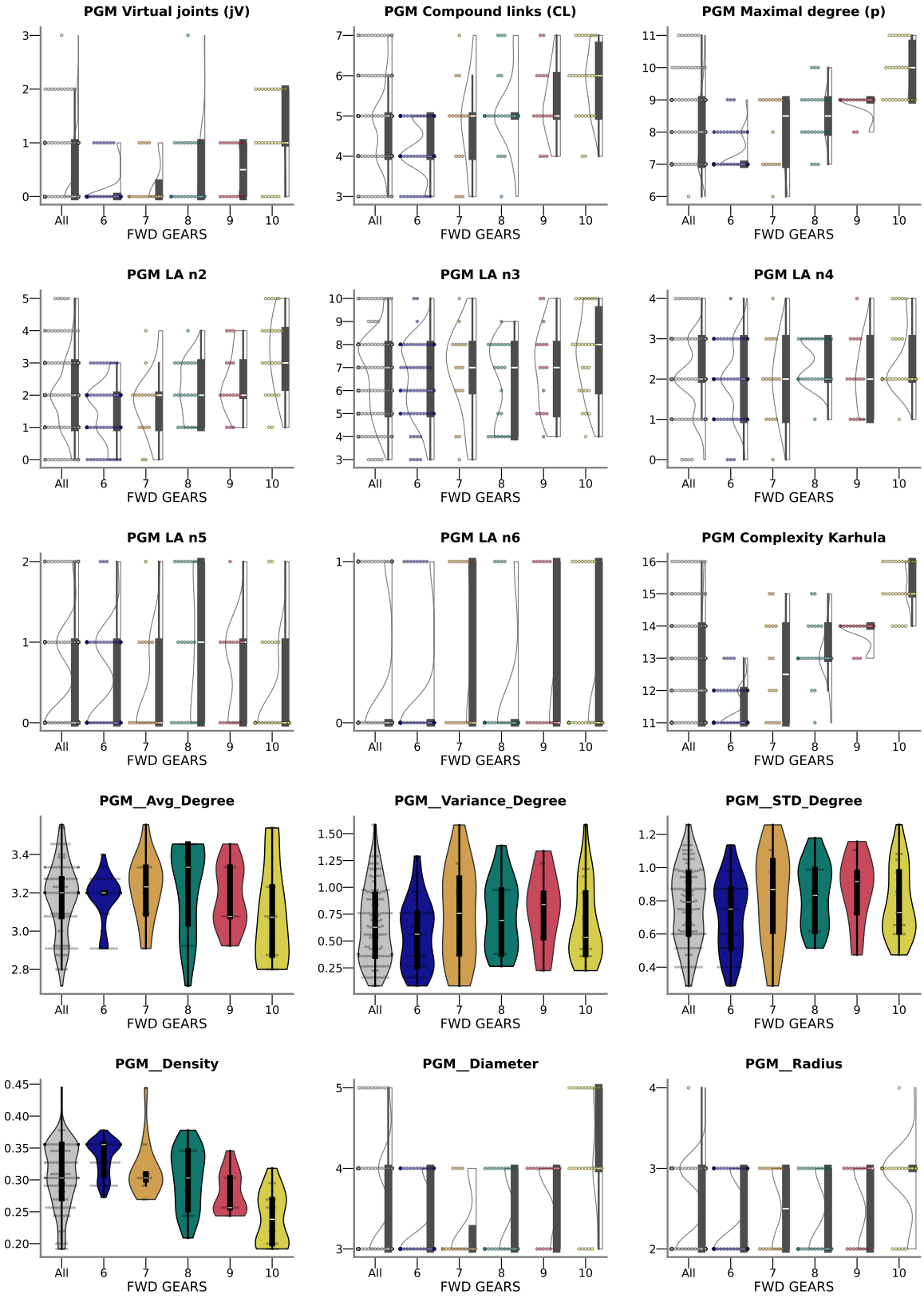

Source: Author.

Figure 245 – Violin plots of numerical features - *FWD GEARS* (4 of 8)

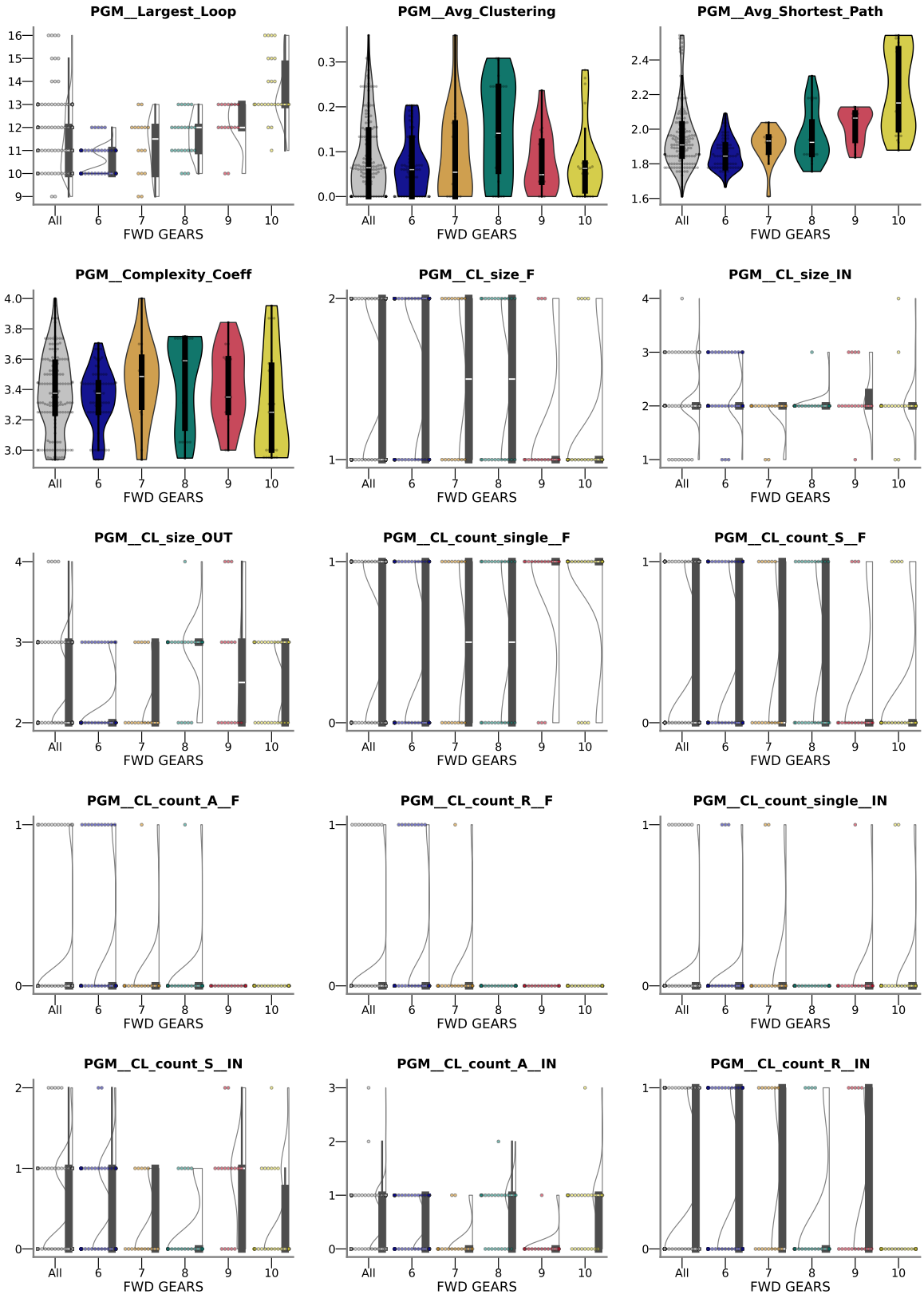

Source: Author.

Figure 246 – Violin plots of numerical features - *FWD GEARS* (5 of 8)

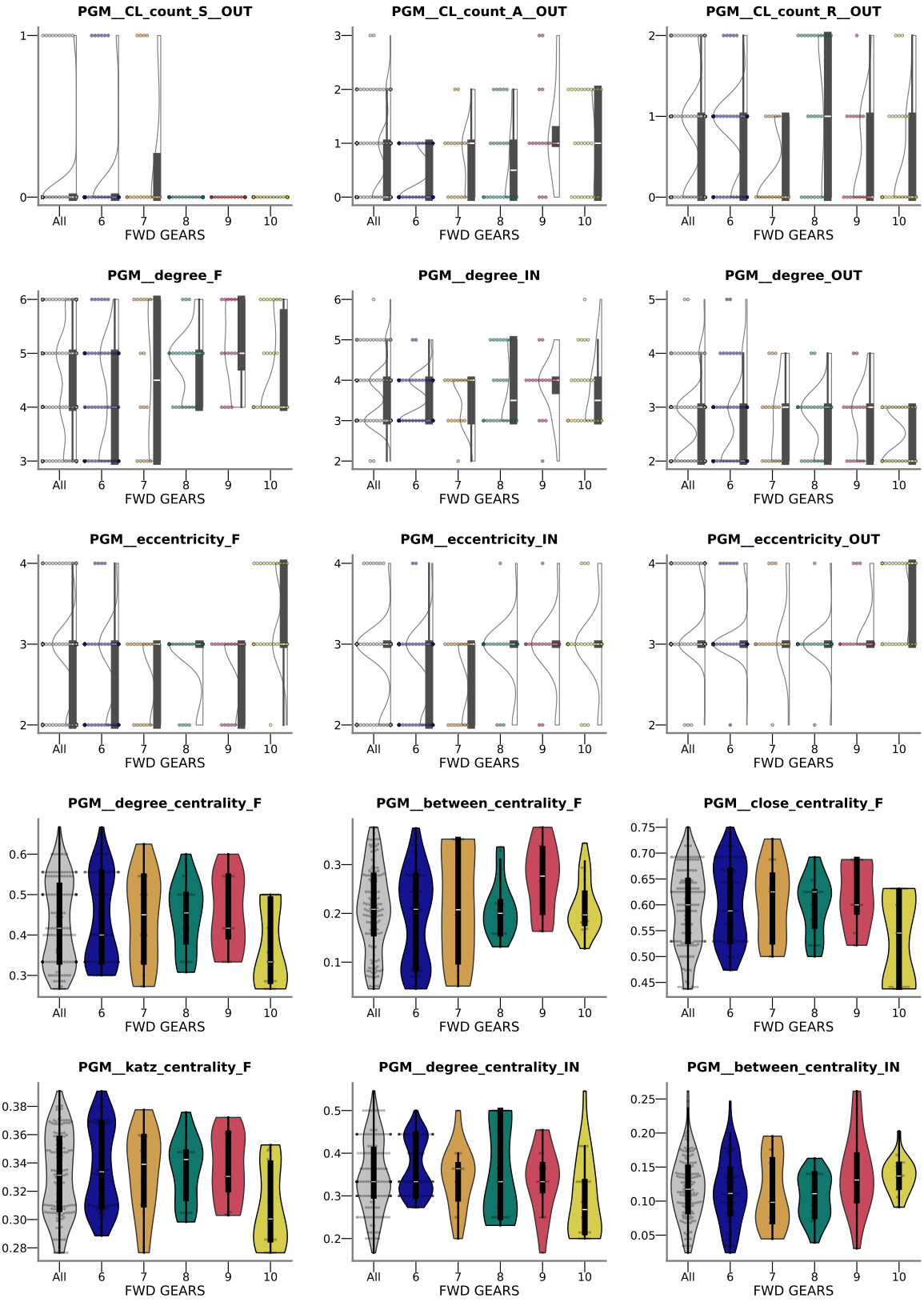

Source: Author.

Figure 247 – Violin plots of numerical features - *FWD GEARS* (6 of 8)

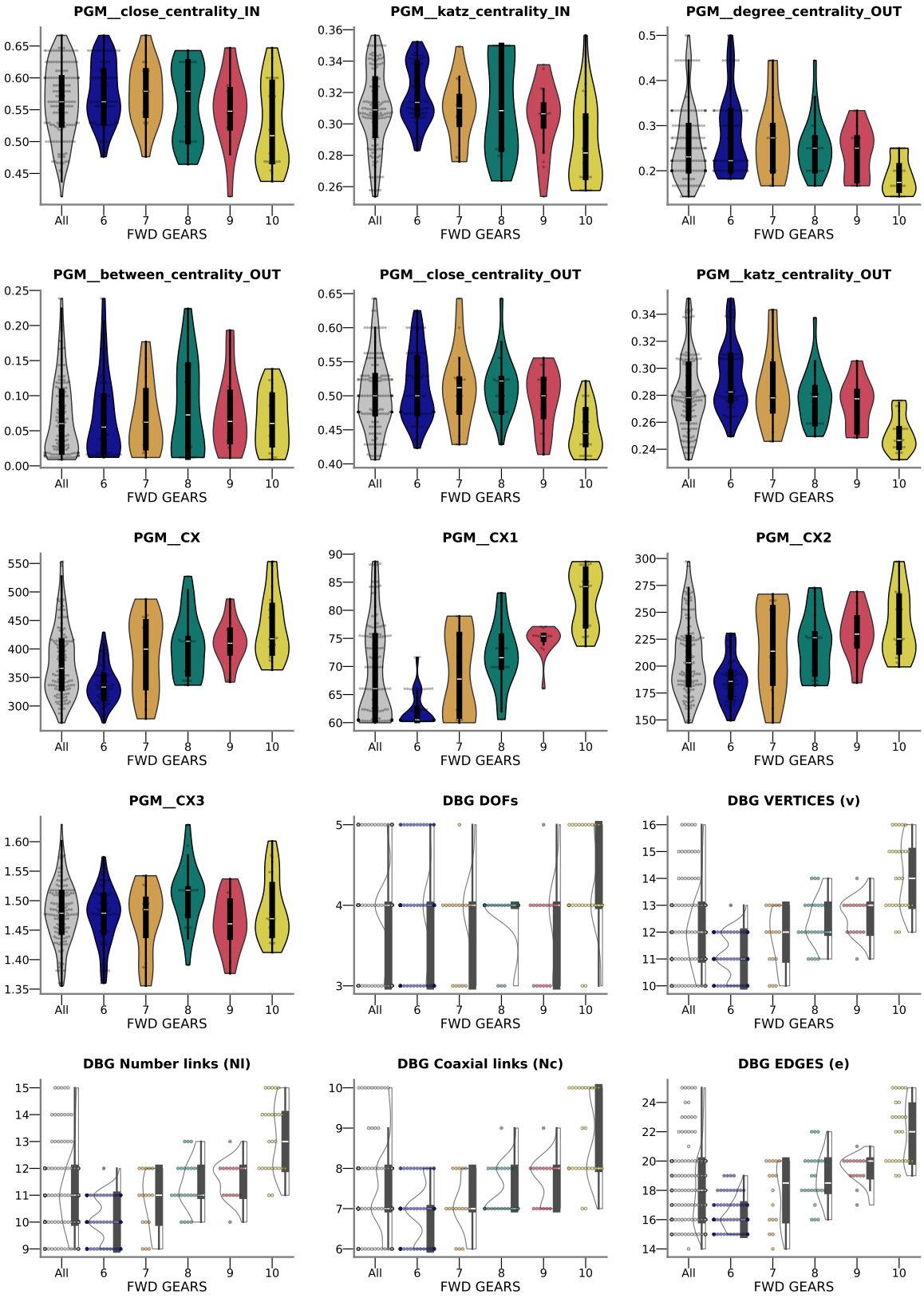

Source: Author.

Figure 248 – Violin plots of numerical features - *FWD GEARS* (7 of 8)

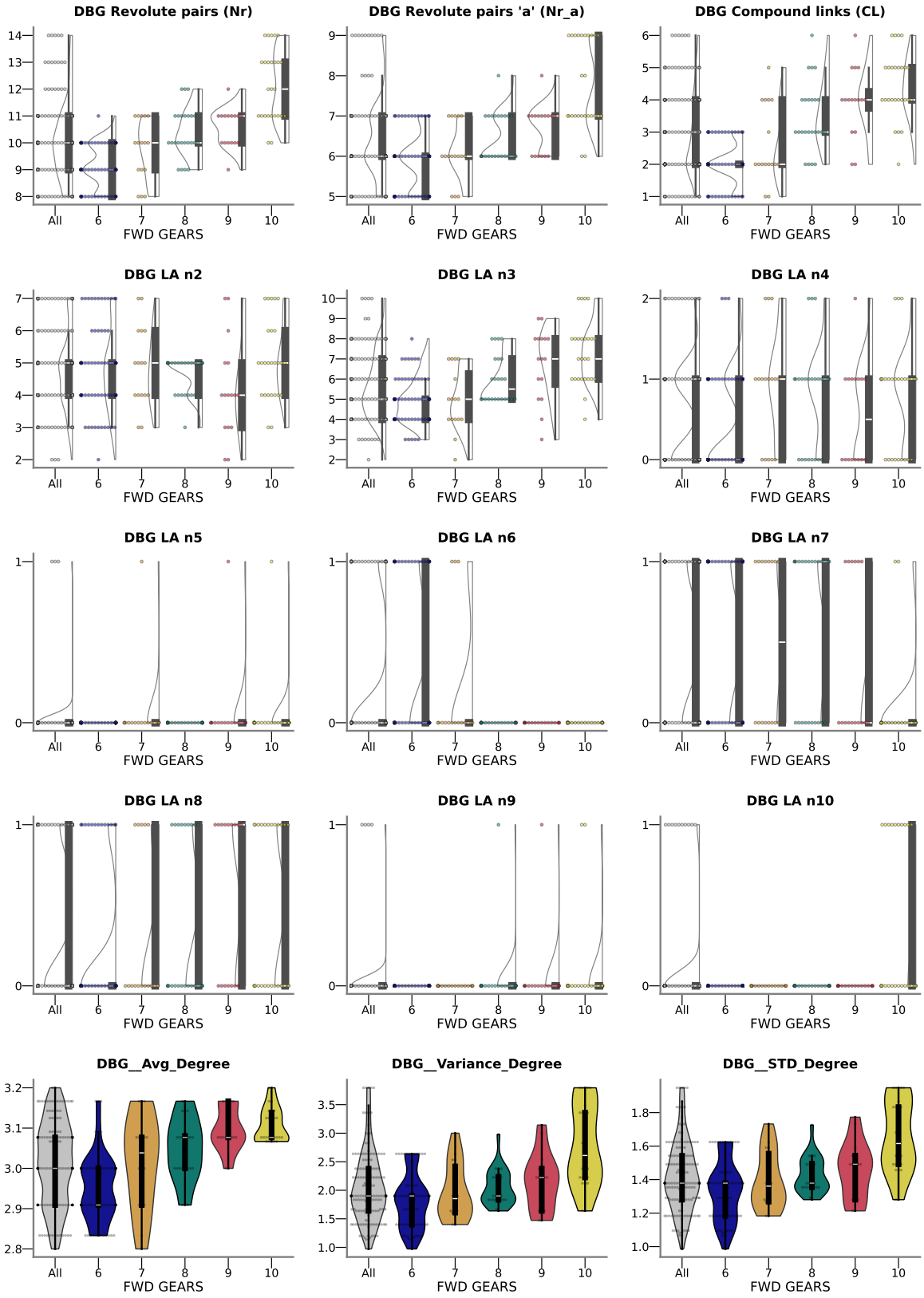

Source: Author.

Figure 249 – Violin plots of numerical features - *FWD GEARS* (8 of 8)

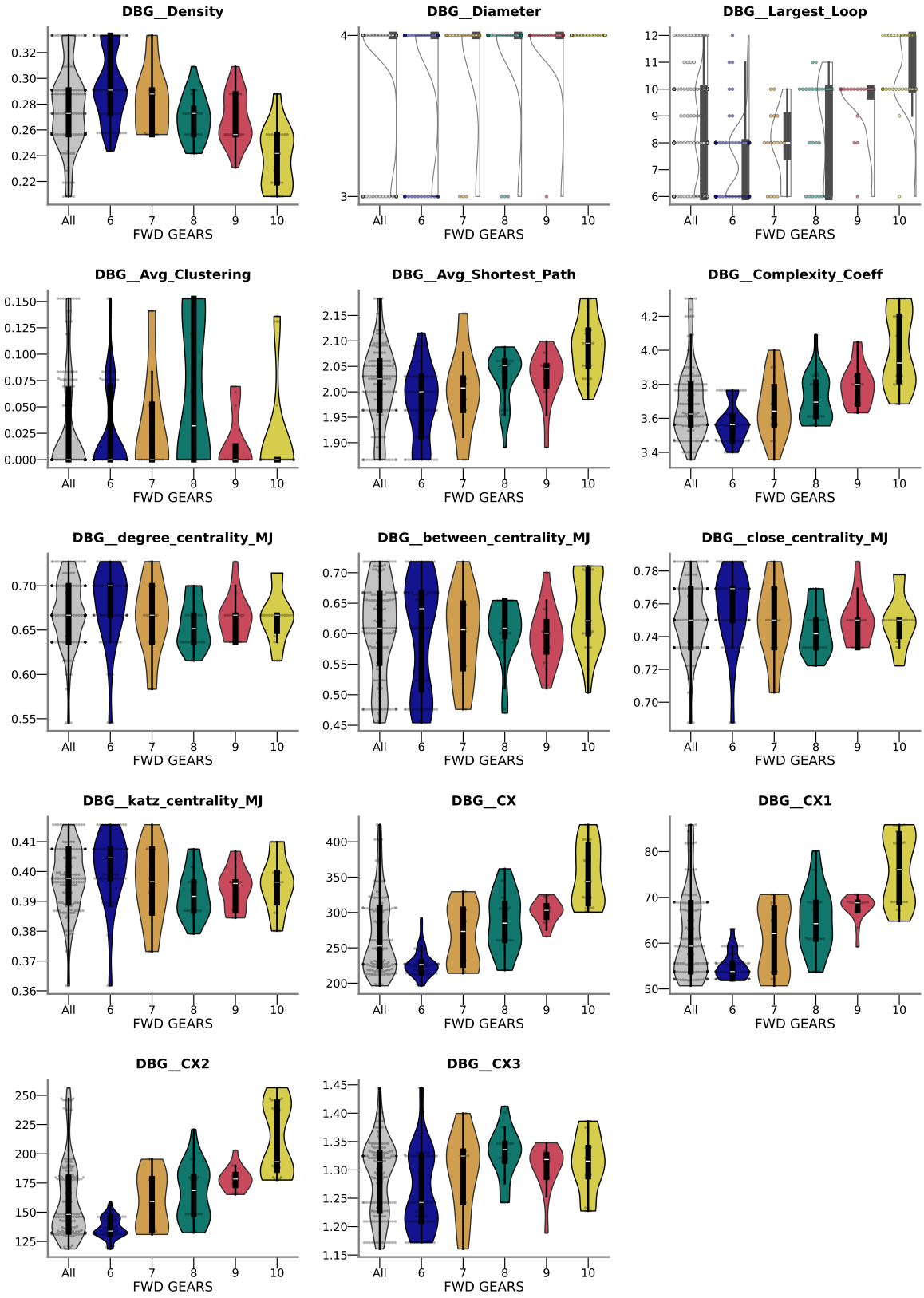

Source: Author.

Figure 250 – Charts of boolean features - *FWD GEARS*

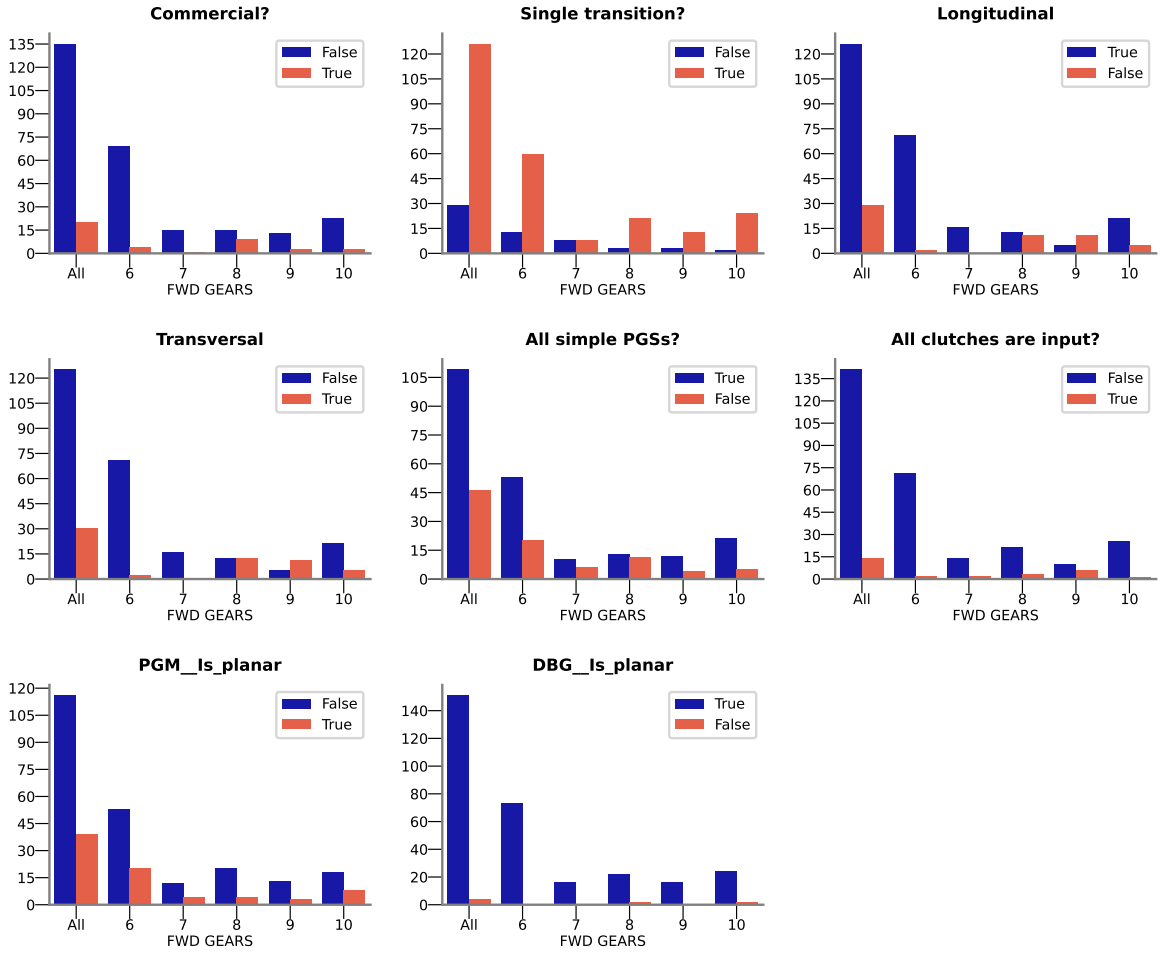

Source: Author.

Figure 251 – Charts of categorical feature - Unique Sources ID - *FWD GEARS*

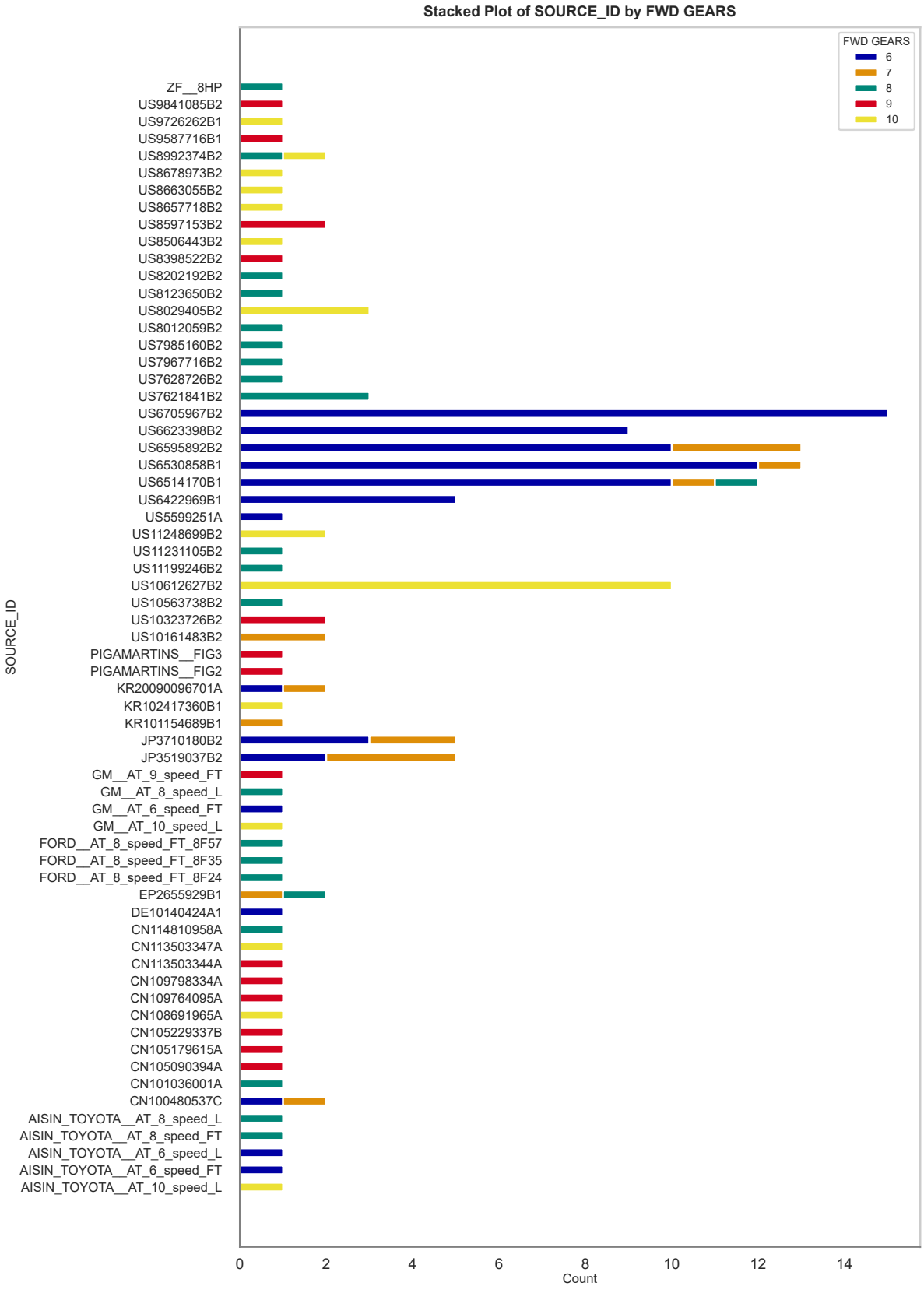

Source: Author.

Figure 252 – Charts of categorical feature - PGSs Sequences - *FWD GEARS*

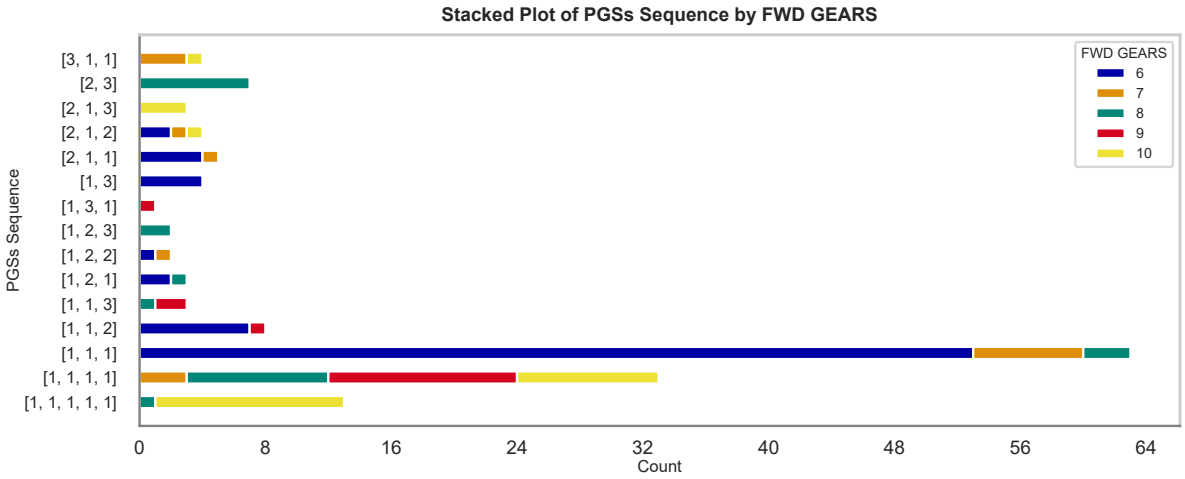

Source: Author.

Figure 253 – Charts of categorical feature - DBG Classification - *FWD GEARS*

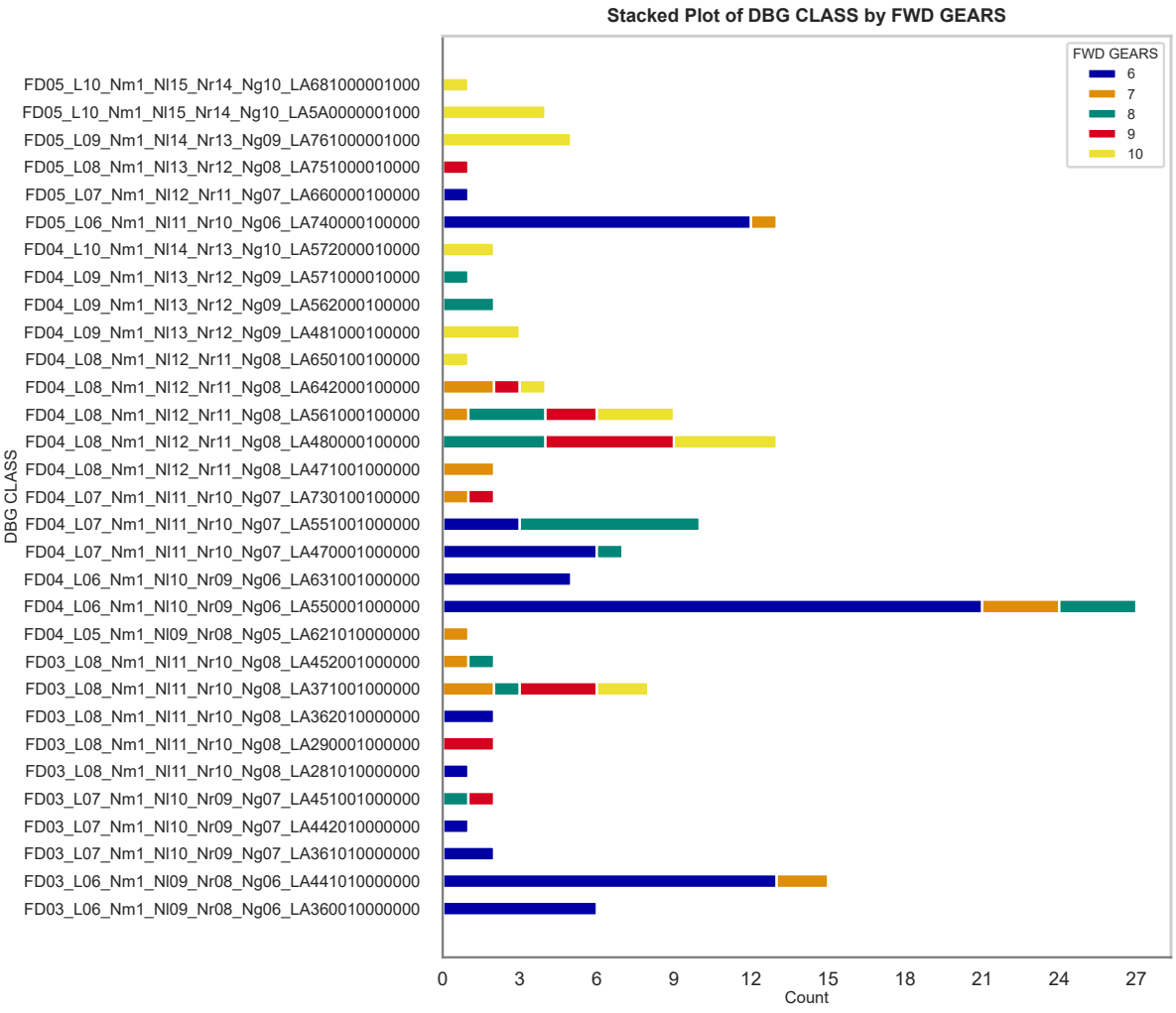

Source: Author.

Figure 254 – Charts of categorical feature - DBG Link Assortments - *FWD GEARS*

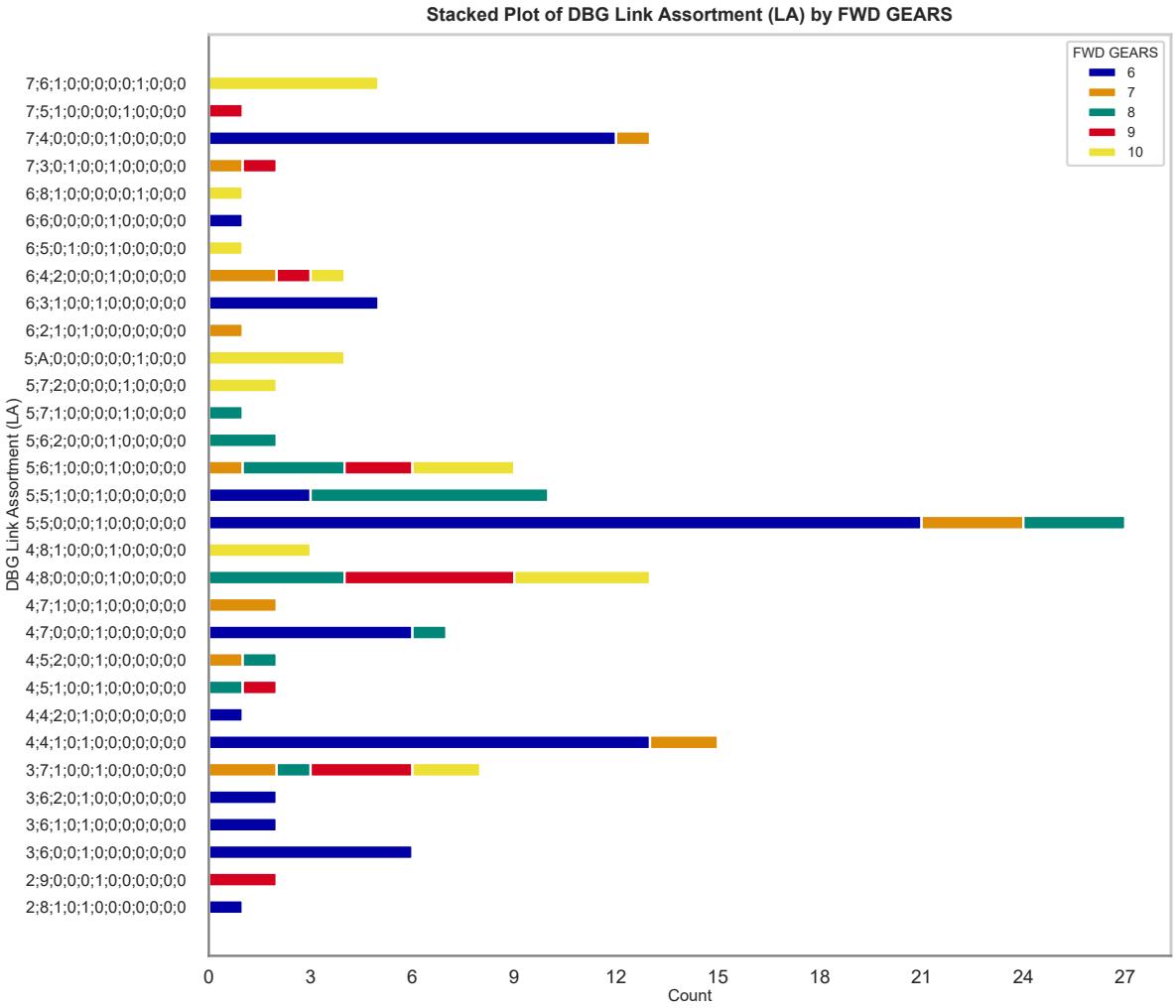

Source: Author.

Figure 255 – Charts of categorical feature - PGM Classification - *FWD GEARS*

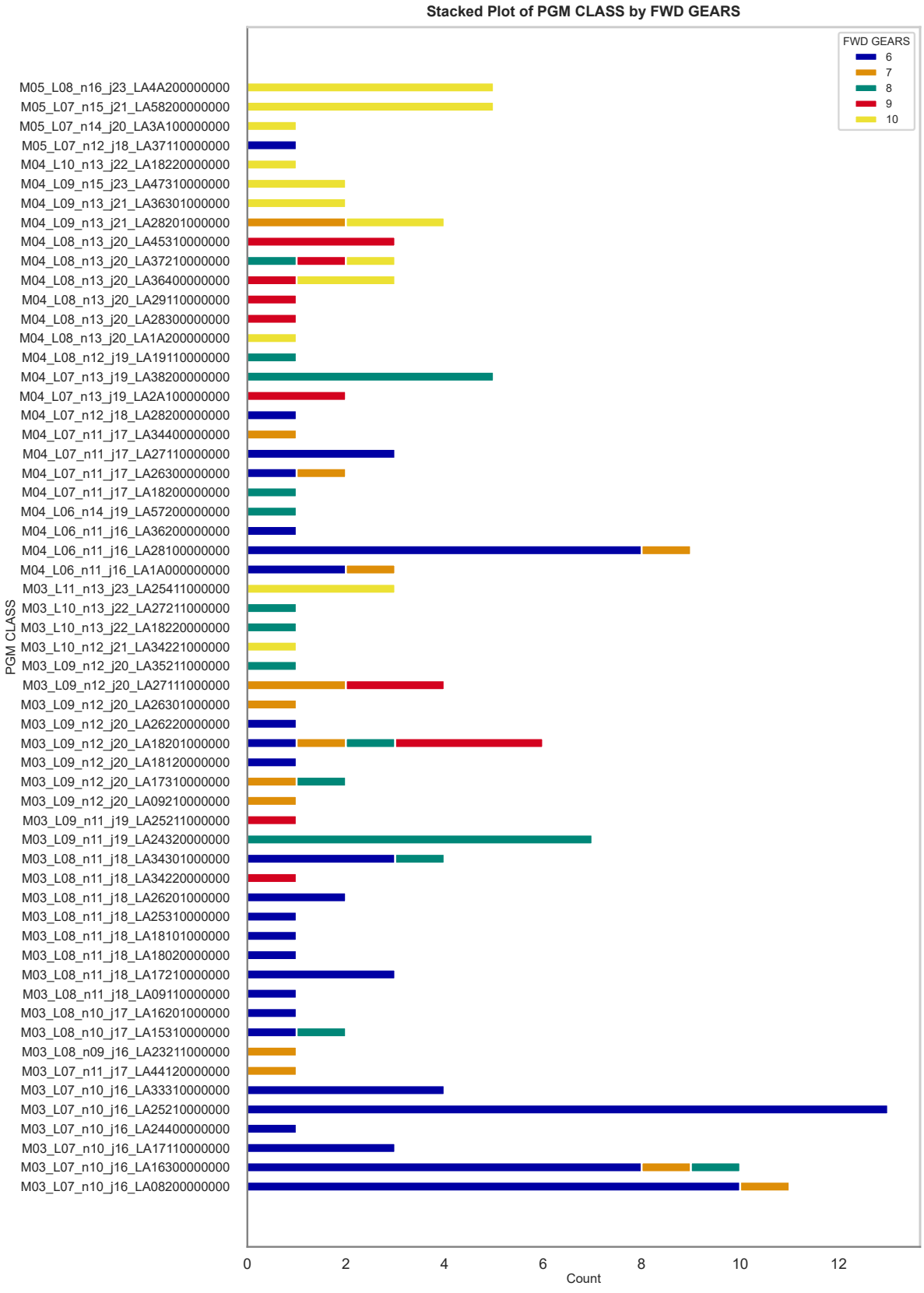

Source: Author.

Figure 256 – Charts of categorical feature - PGM Link Assortments - *FWD GEARS*

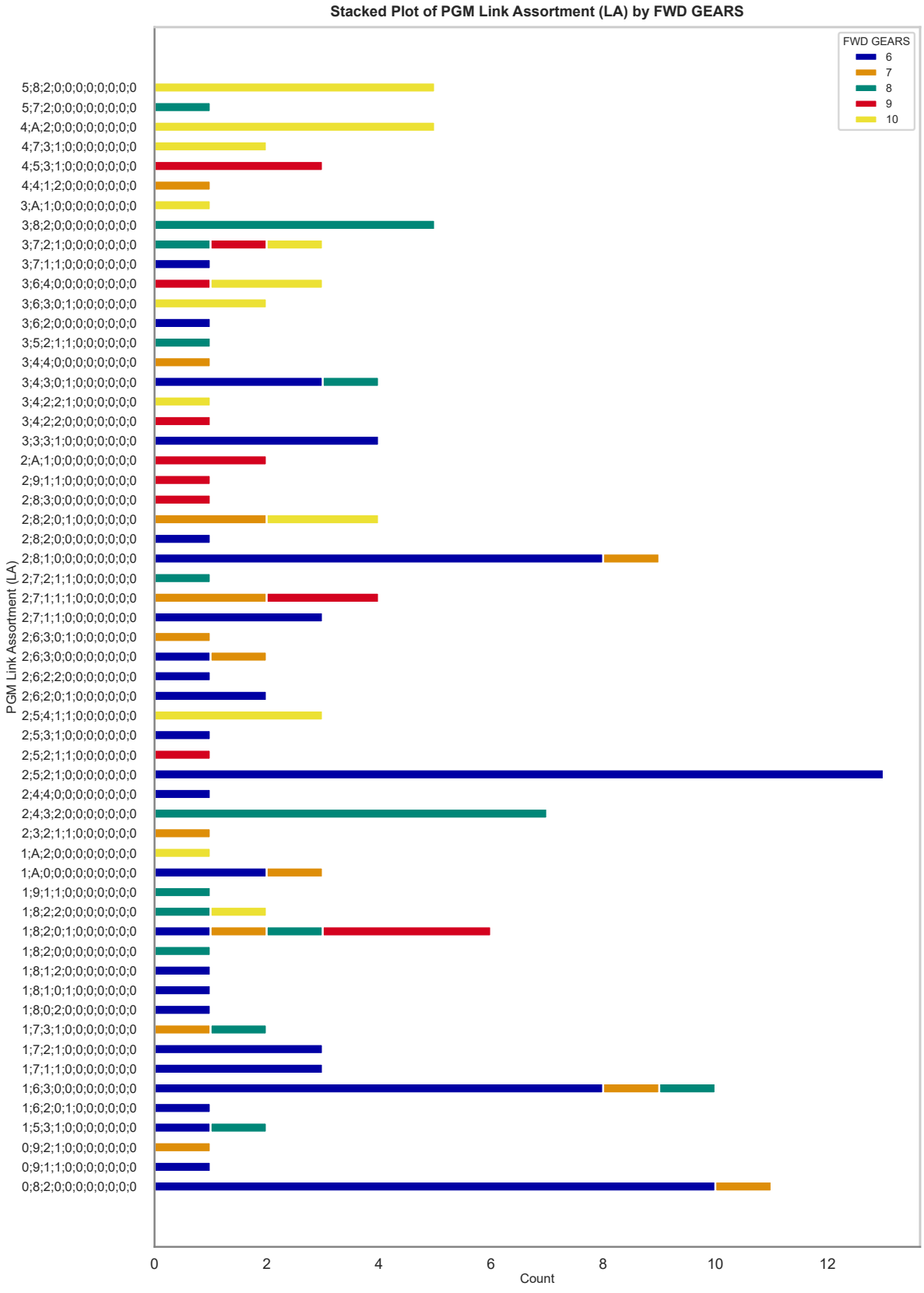

Source: Author.

B.1.2 Features Distribution Segmented by *PGSs Total*

Figure 257 – Violin plots of numerical features - *PGSs Total* (1 of 8)

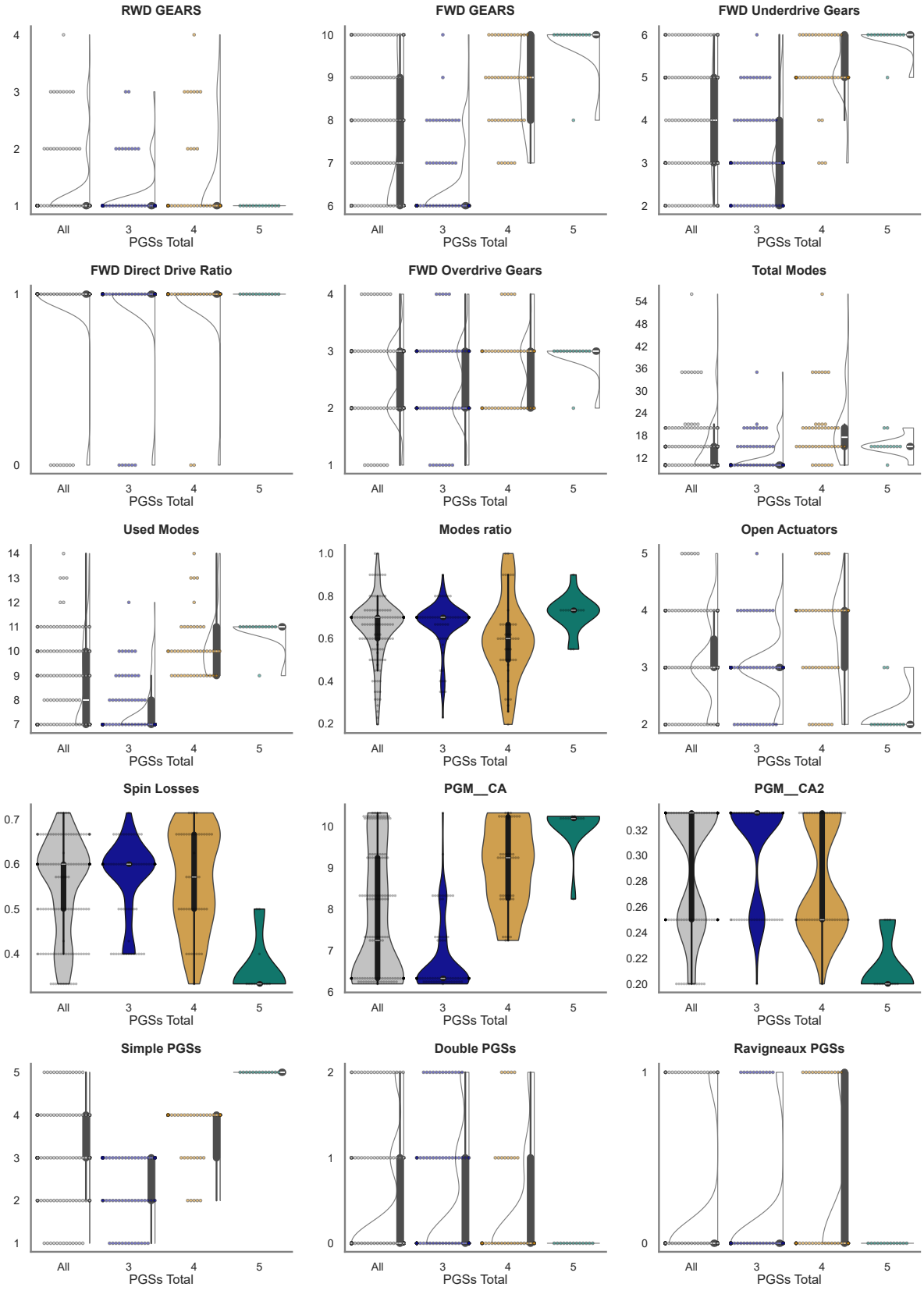

Source: Author.

Figure 258 – Violin plots of numerical features - *PGSs Total* (2 of 8)

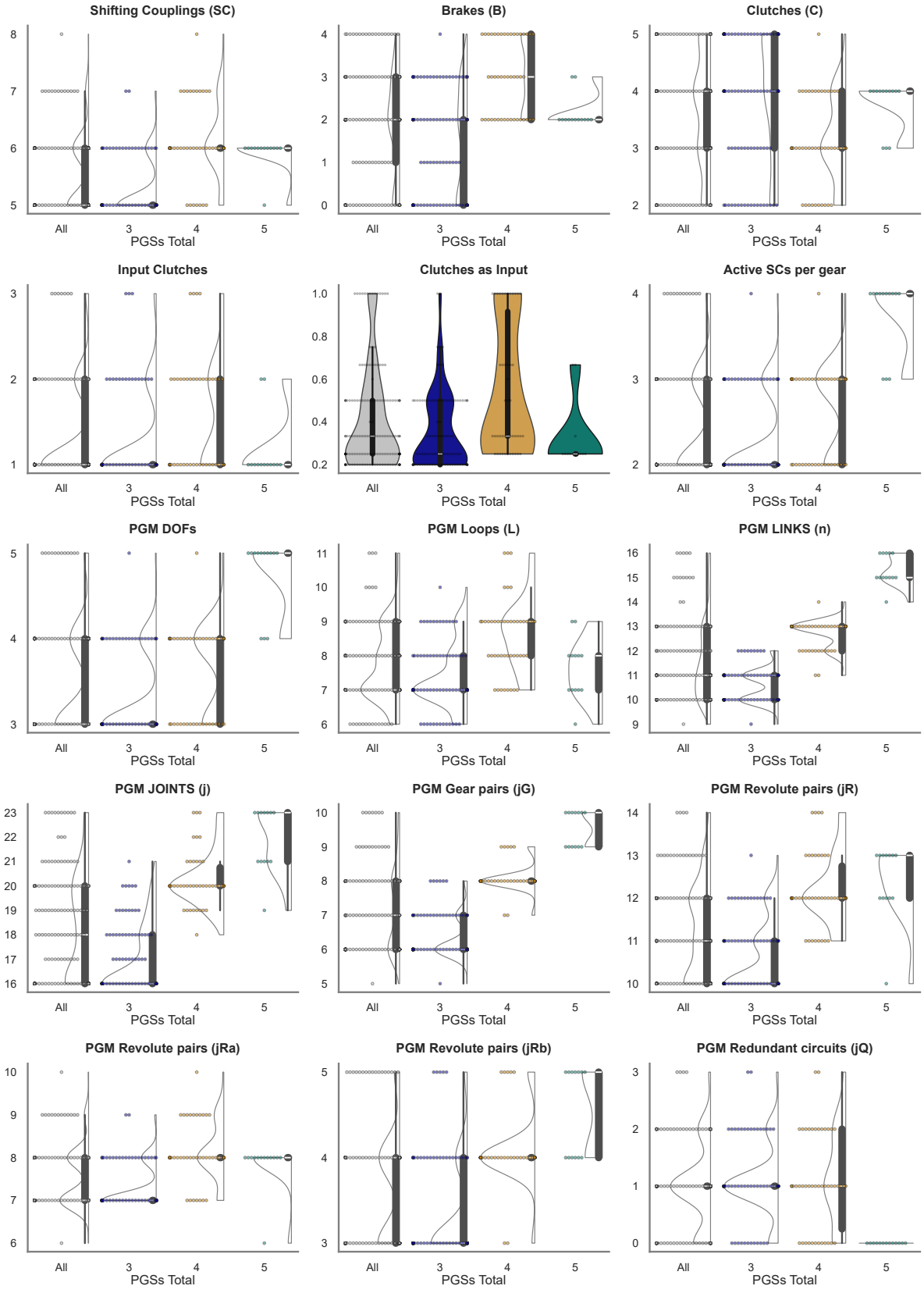

Source: Author.

Figure 259 – Violin plots of numerical features - *PGSs Total* (3 of 8)

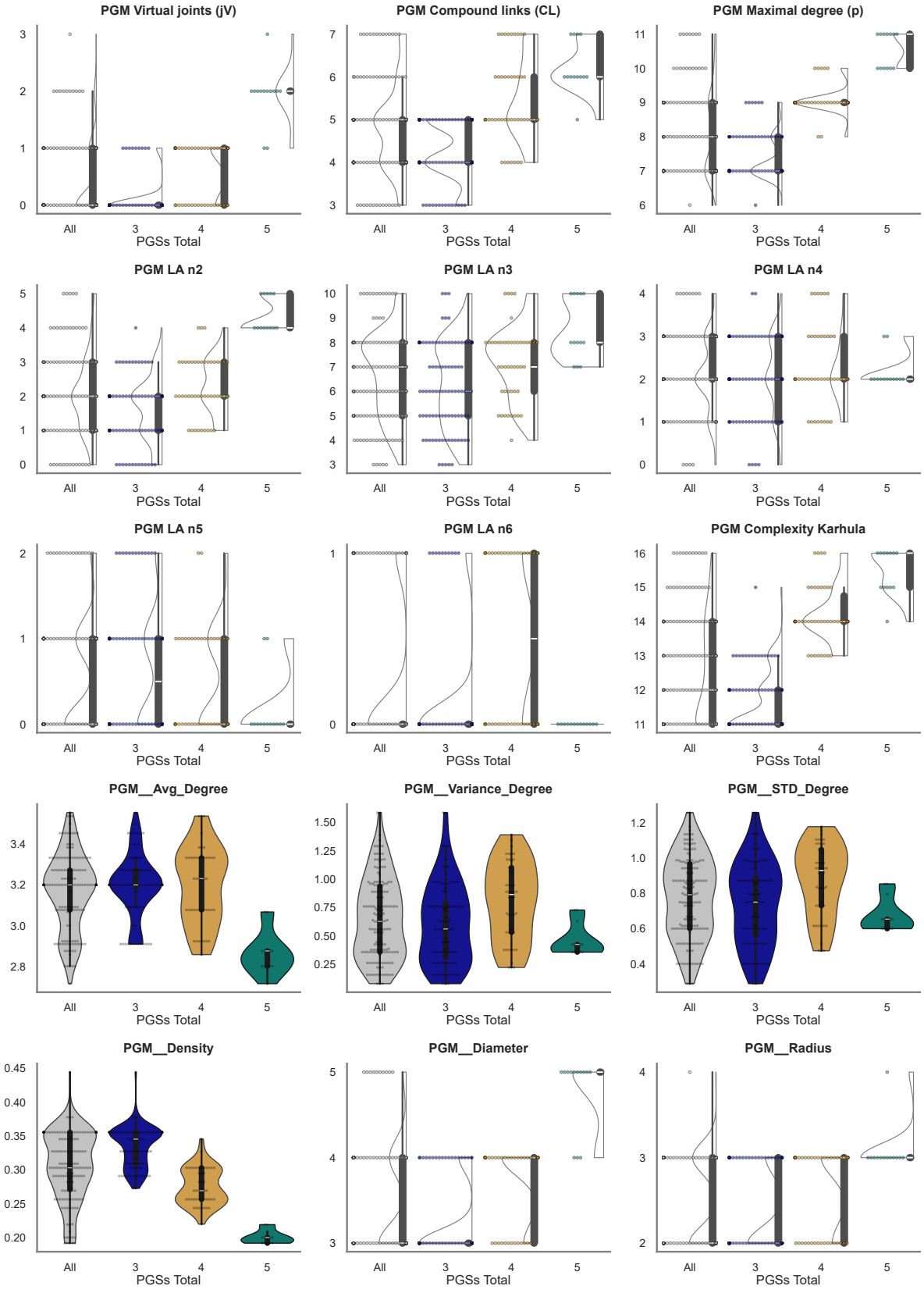

Source: Author.

Figure 260 – Violin plots of numerical features - *PGSs Total* (4 of 8)

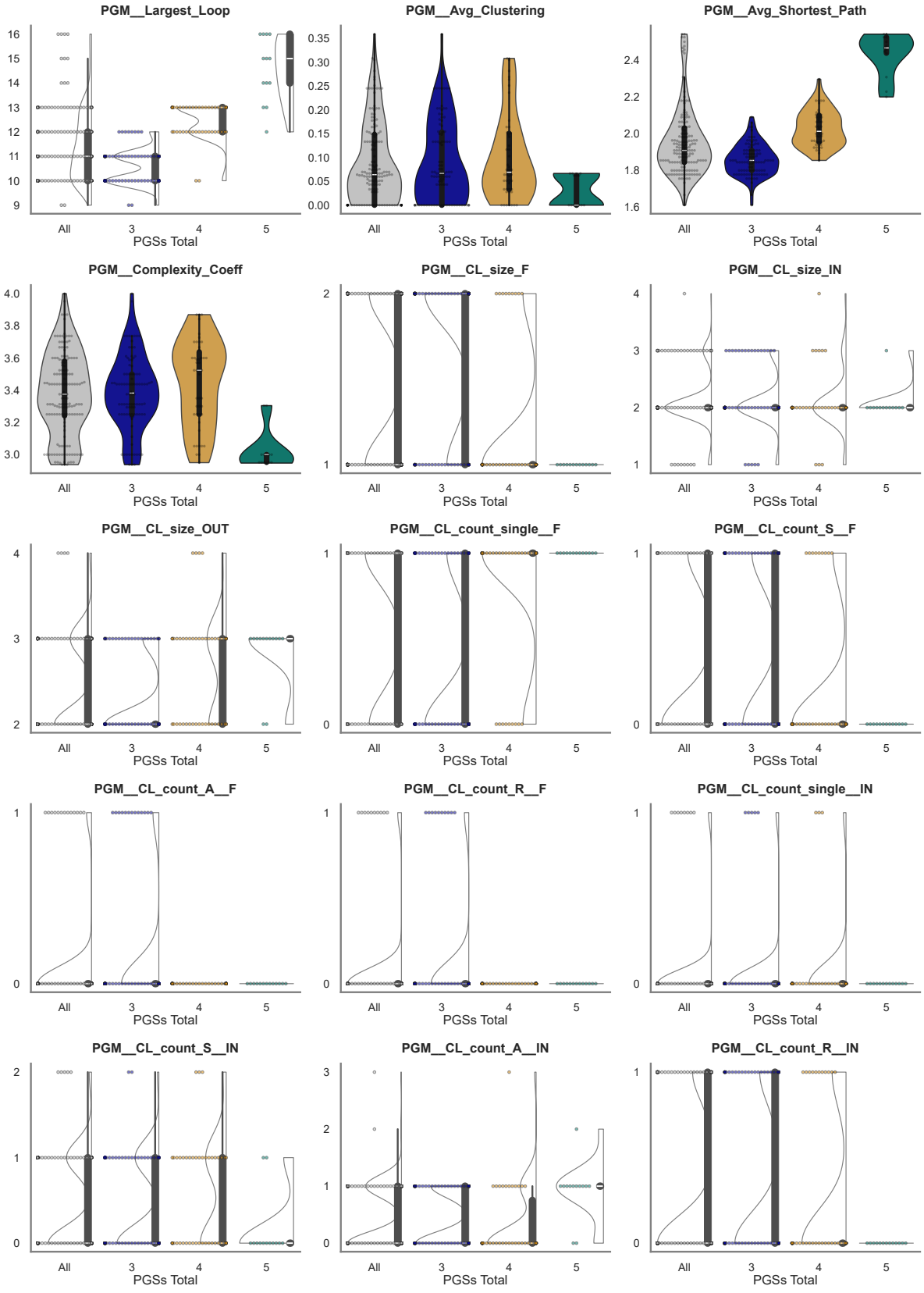

Source: Author.

Figure 261 – Violin plots of numerical features - *PGSs Total* (5 of 8)

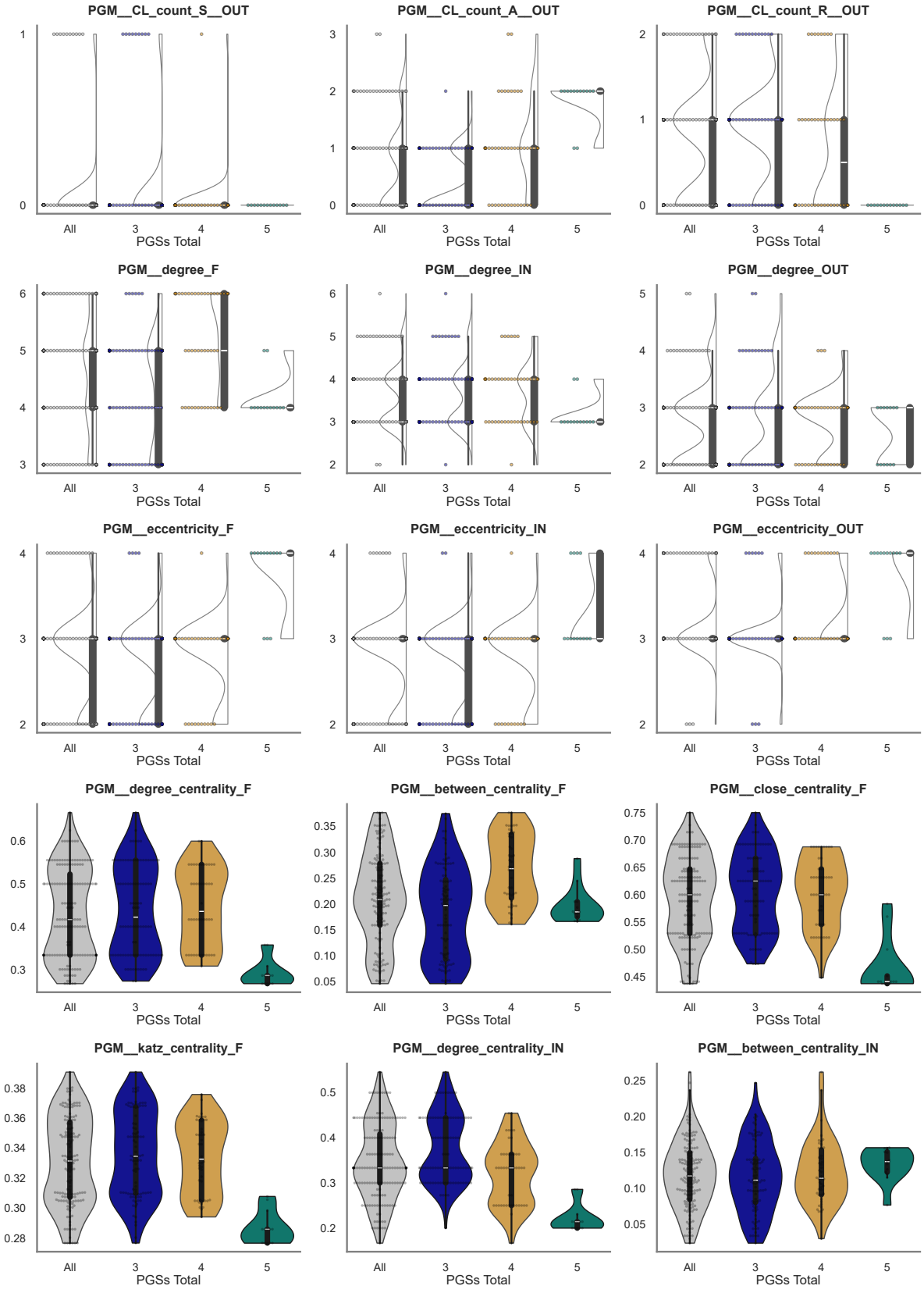

Source: Author.

Figure 262 – Violin plots of numerical features - *PGSs Total* (6 of 8)

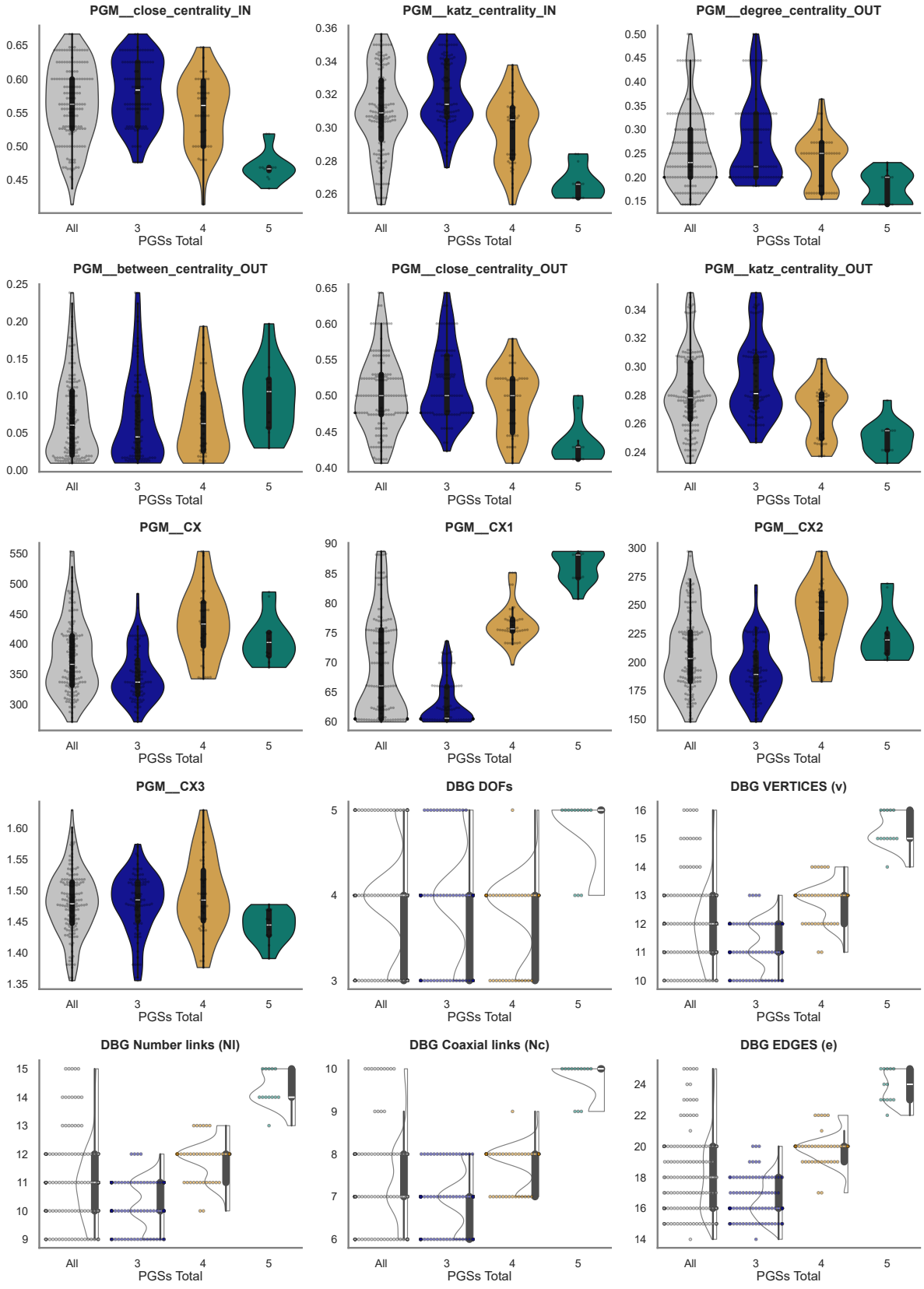

Source: Author.

Figure 263 – Violin plots of numerical features - *PGSs Total* (7 of 8)

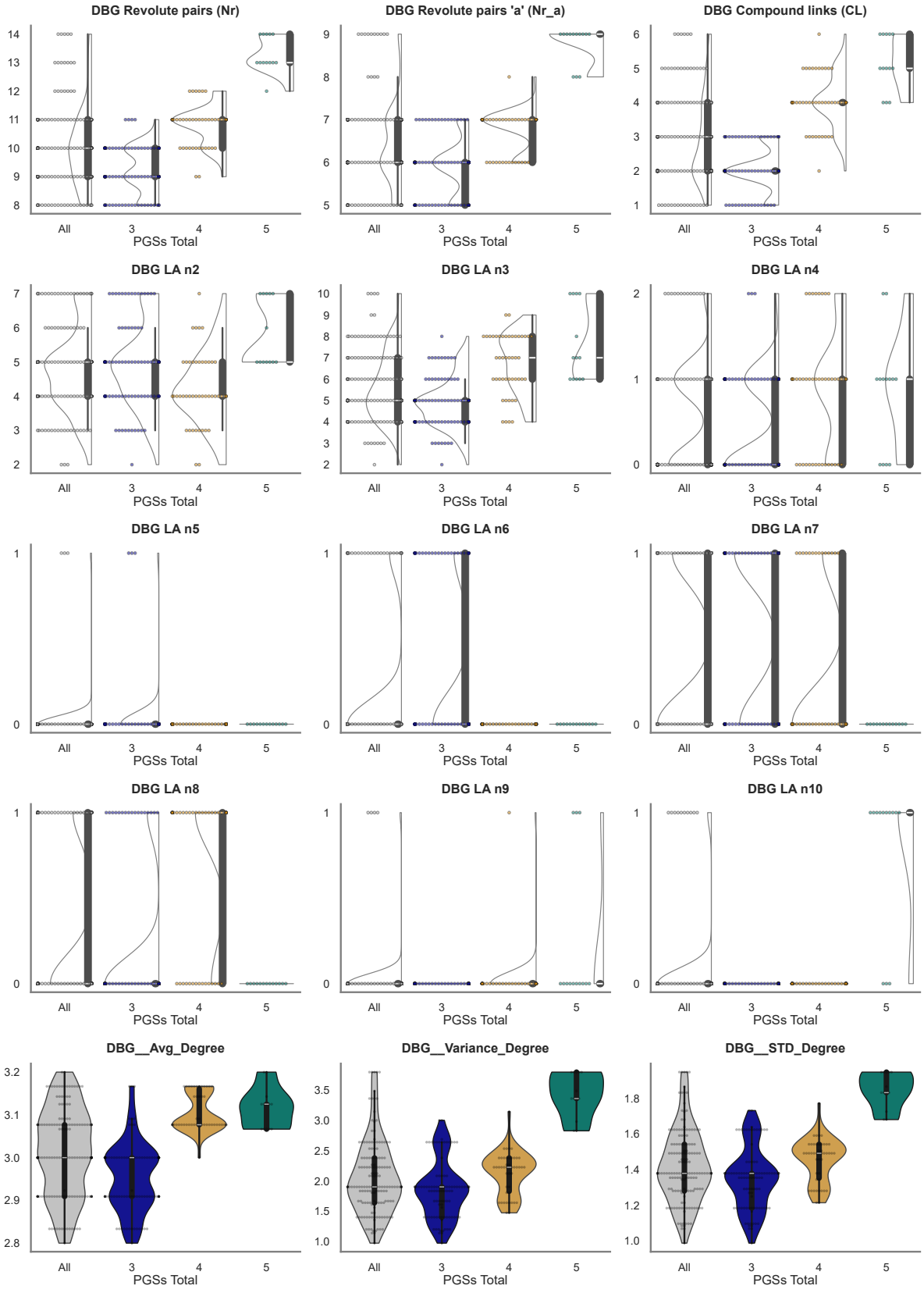

Source: Author.

Figure 264 – Violin plots of numerical features - *PGSs Total* (8 of 8)

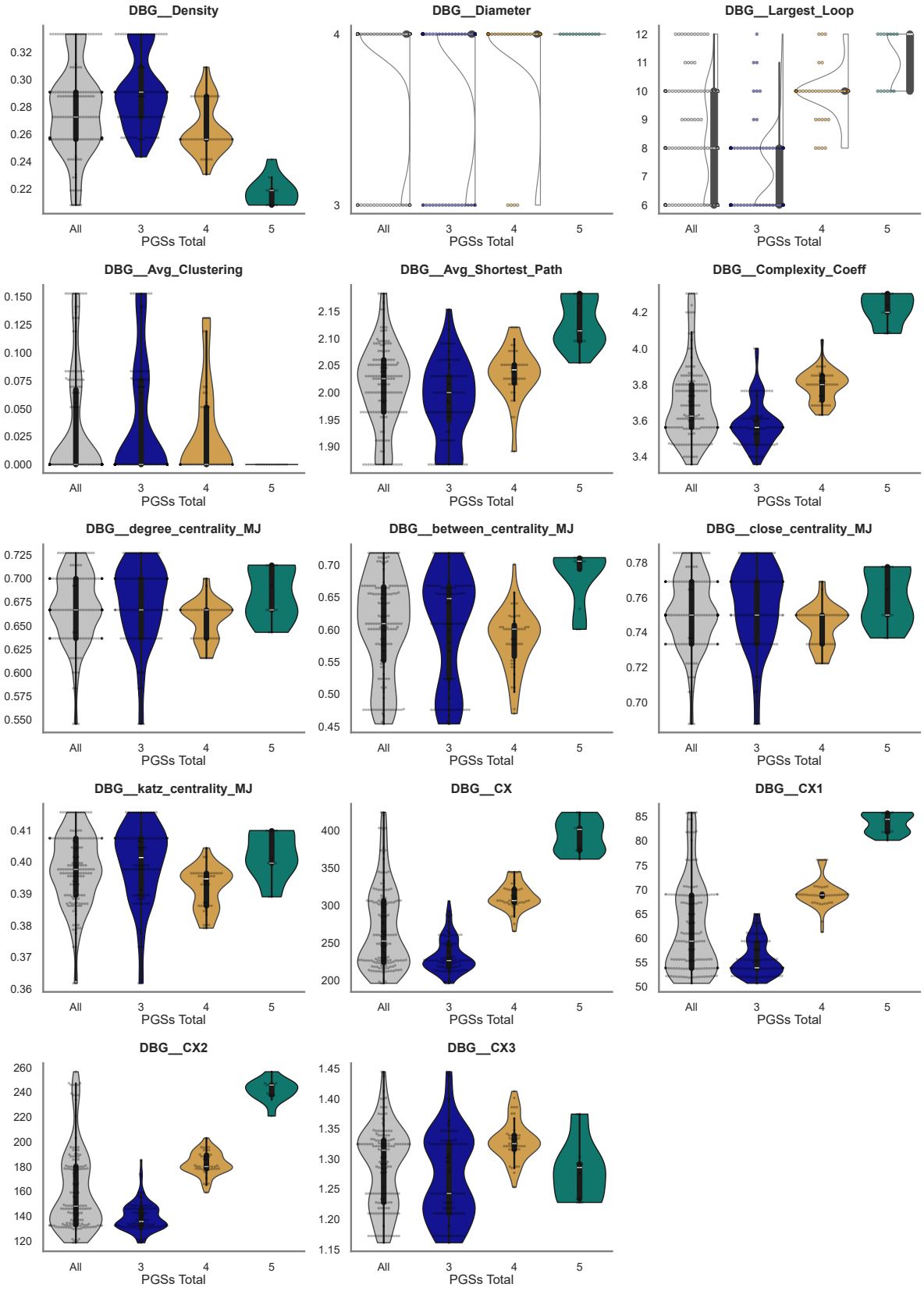

Source: Author.

Figure 265 – Charts of boolean features - *PGSs Total*

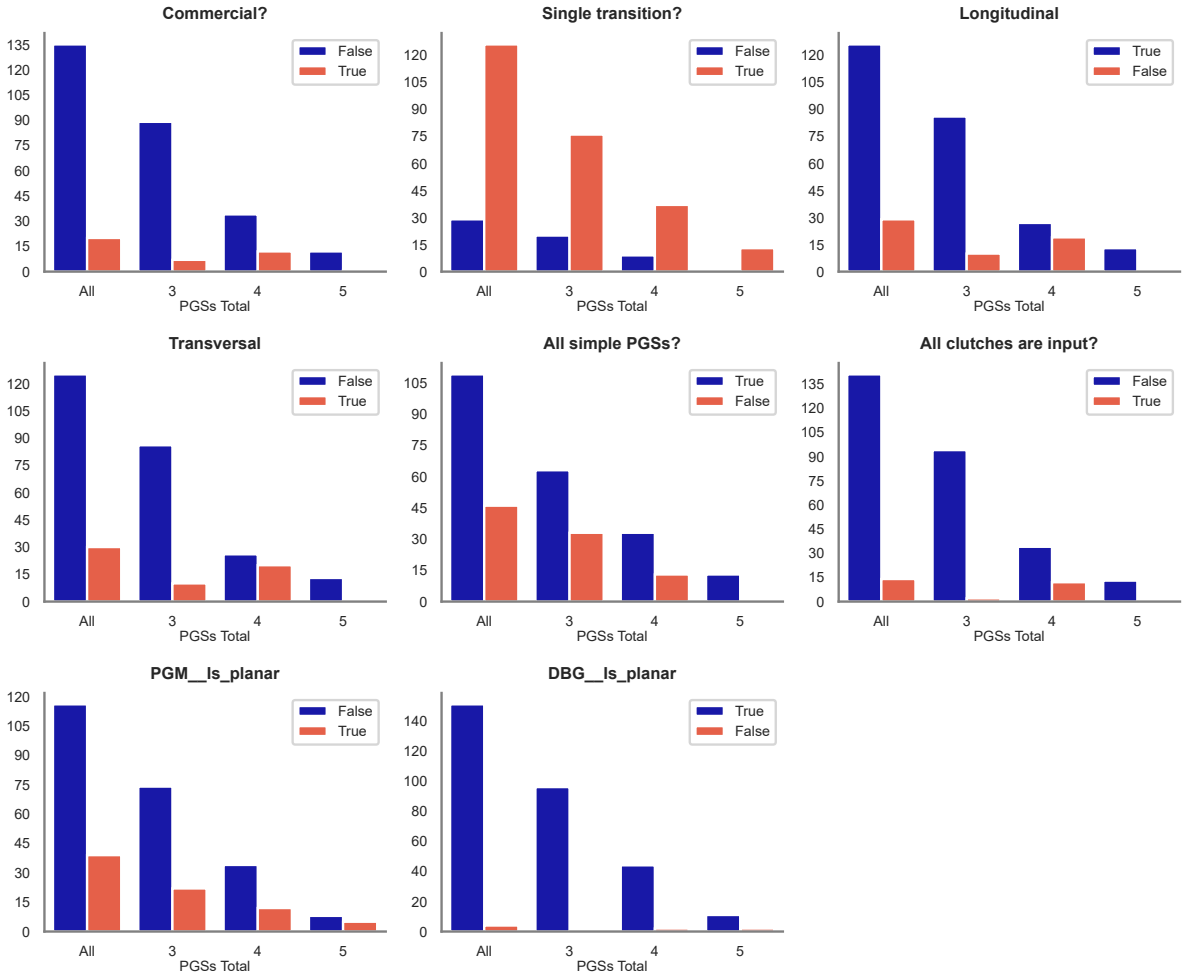

Source: Author.

Figure 266 – Charts of categorical feature - Unique Sources ID - *PGSs Total*

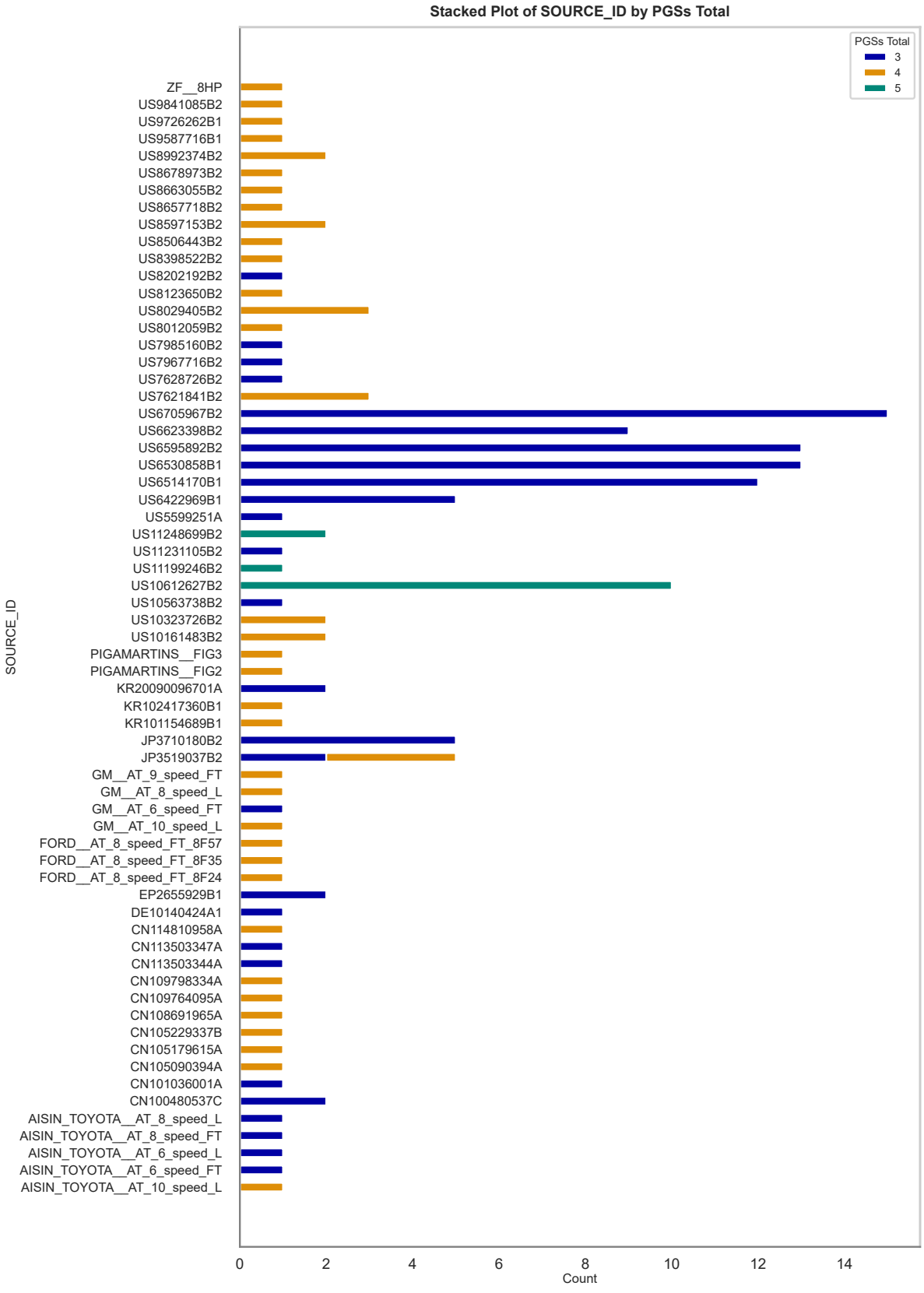

Source: Author.

Figure 267 – Charts of categorical feature - PGSs Sequences - *PGSs Total*

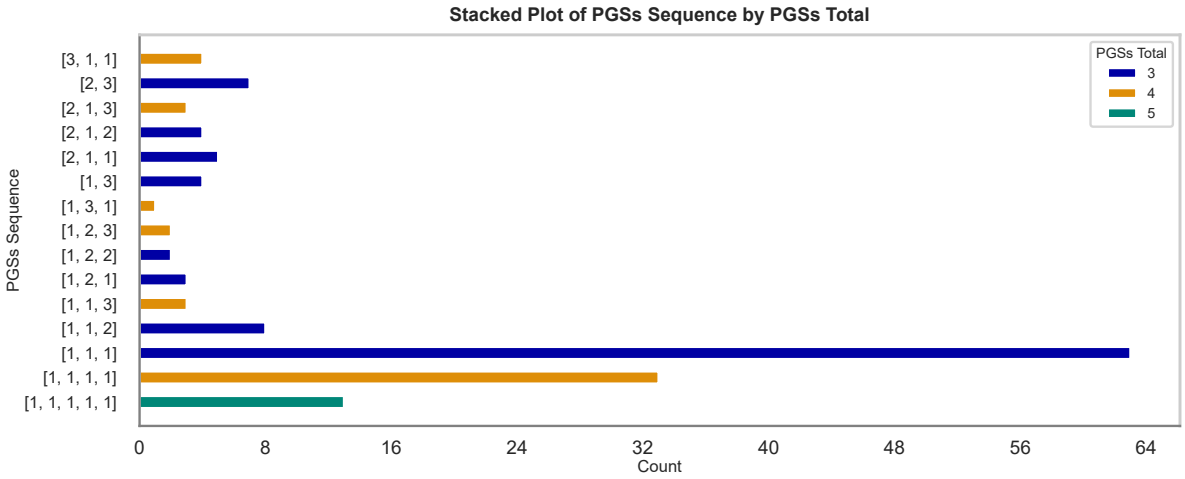

Source: Author.

Figure 268 – Charts of categorical feature - DBG Classification - *PGSs Total*

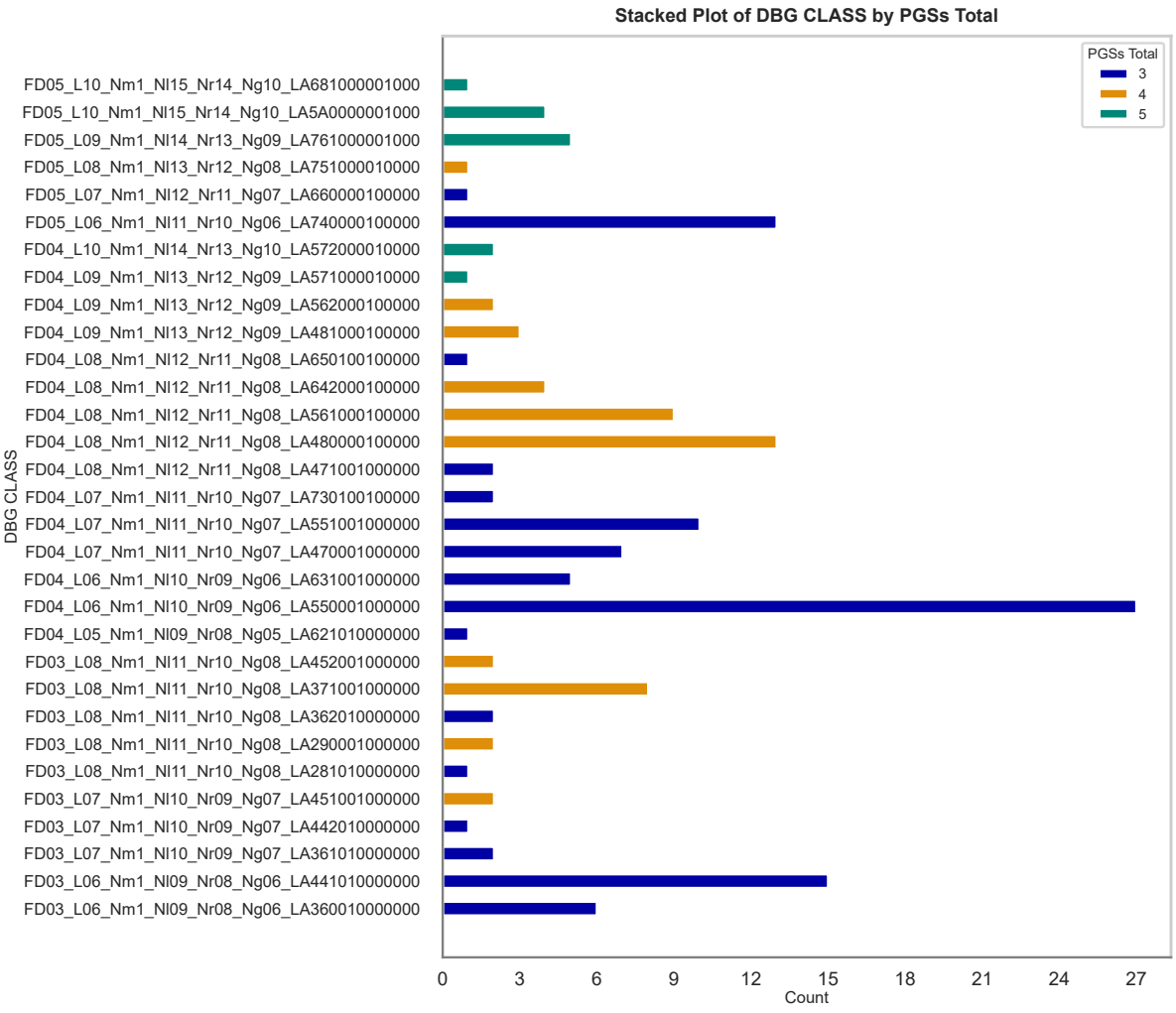

Source: Author.

Figure 269 – Charts of categorical feature - DBG Link Assortments - *PGSs Total*

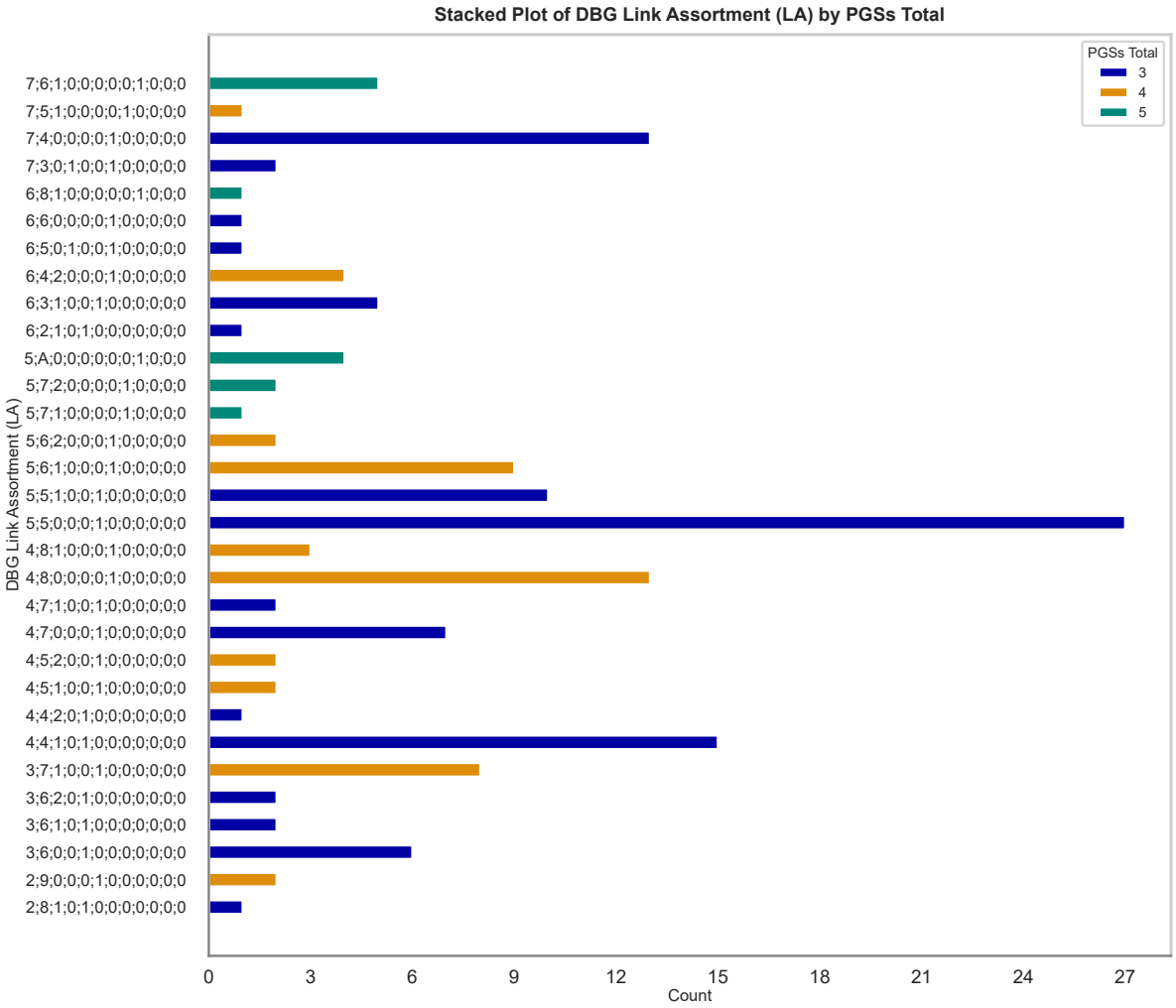

Source: Author.

Figure 270 – Charts of categorical feature - PGM Classification - *PGSs Total*

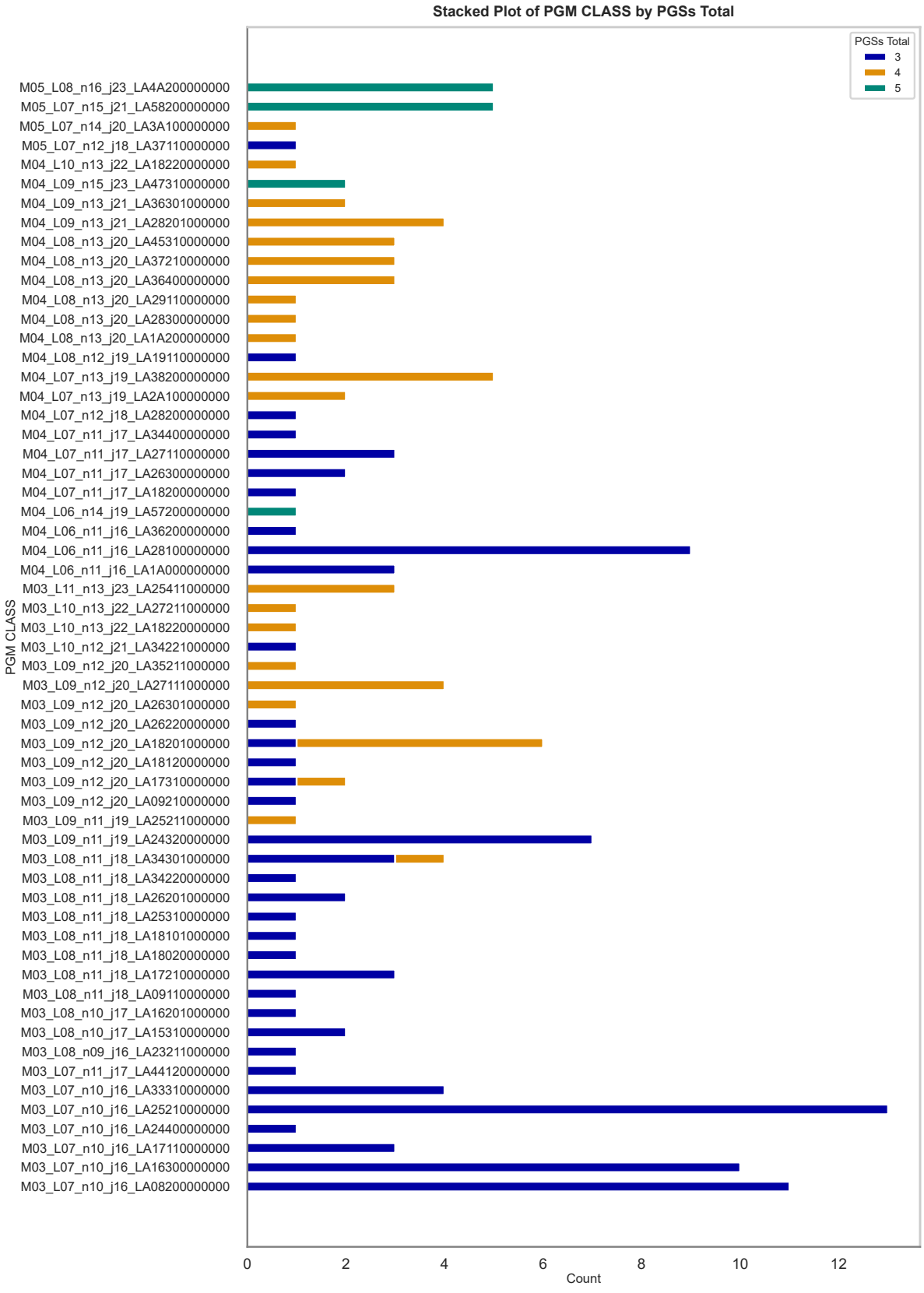

Source: Author.

Figure 271 – Charts of categorical feature - PGM Link Assortments - *PGSs Total*

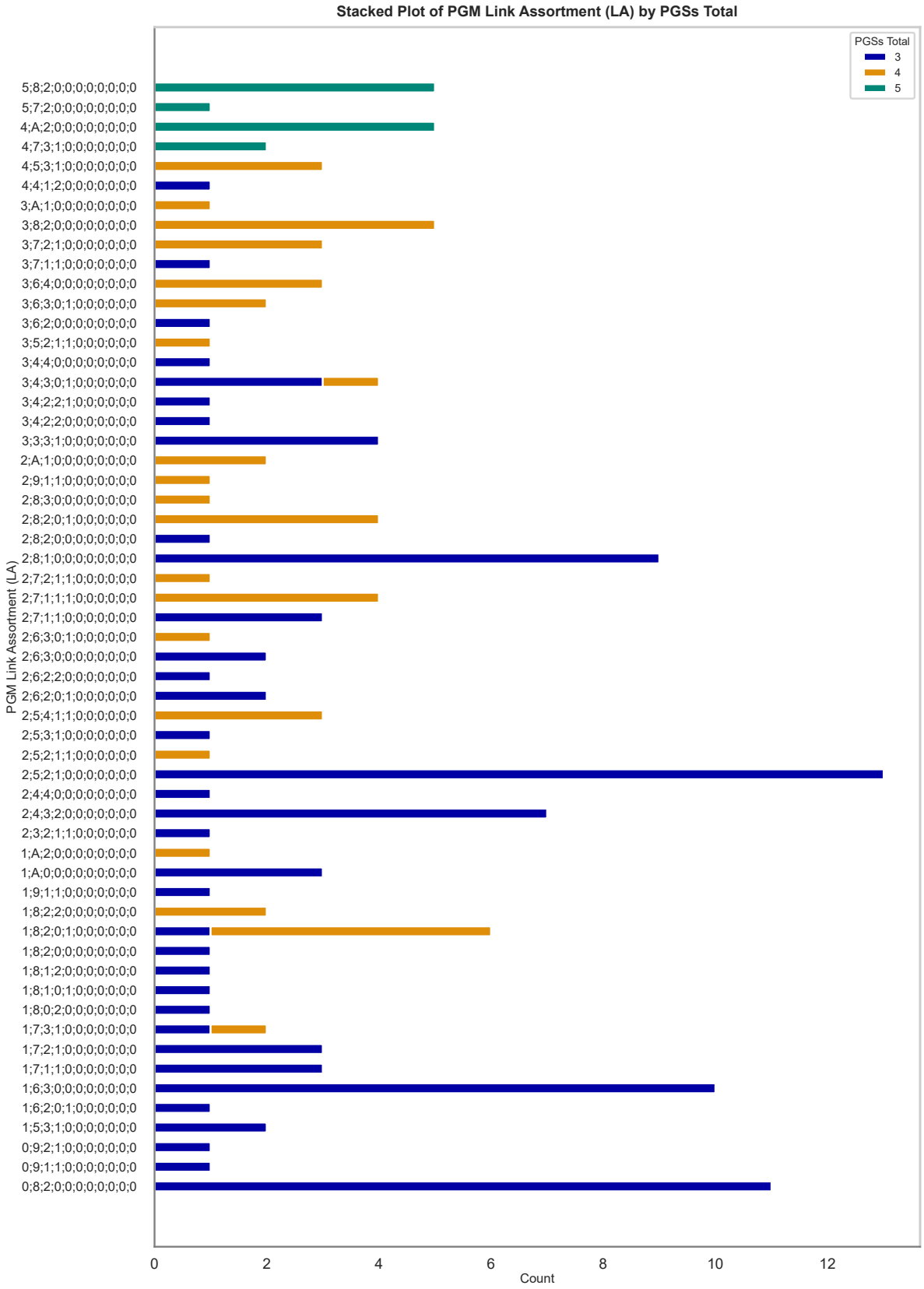

Source: Author.

B.1.3 Features Distribution Segmented by *Commercial?*

Figure 272 – Violin plots of numerical features - *Commercial?* (1 of 8)

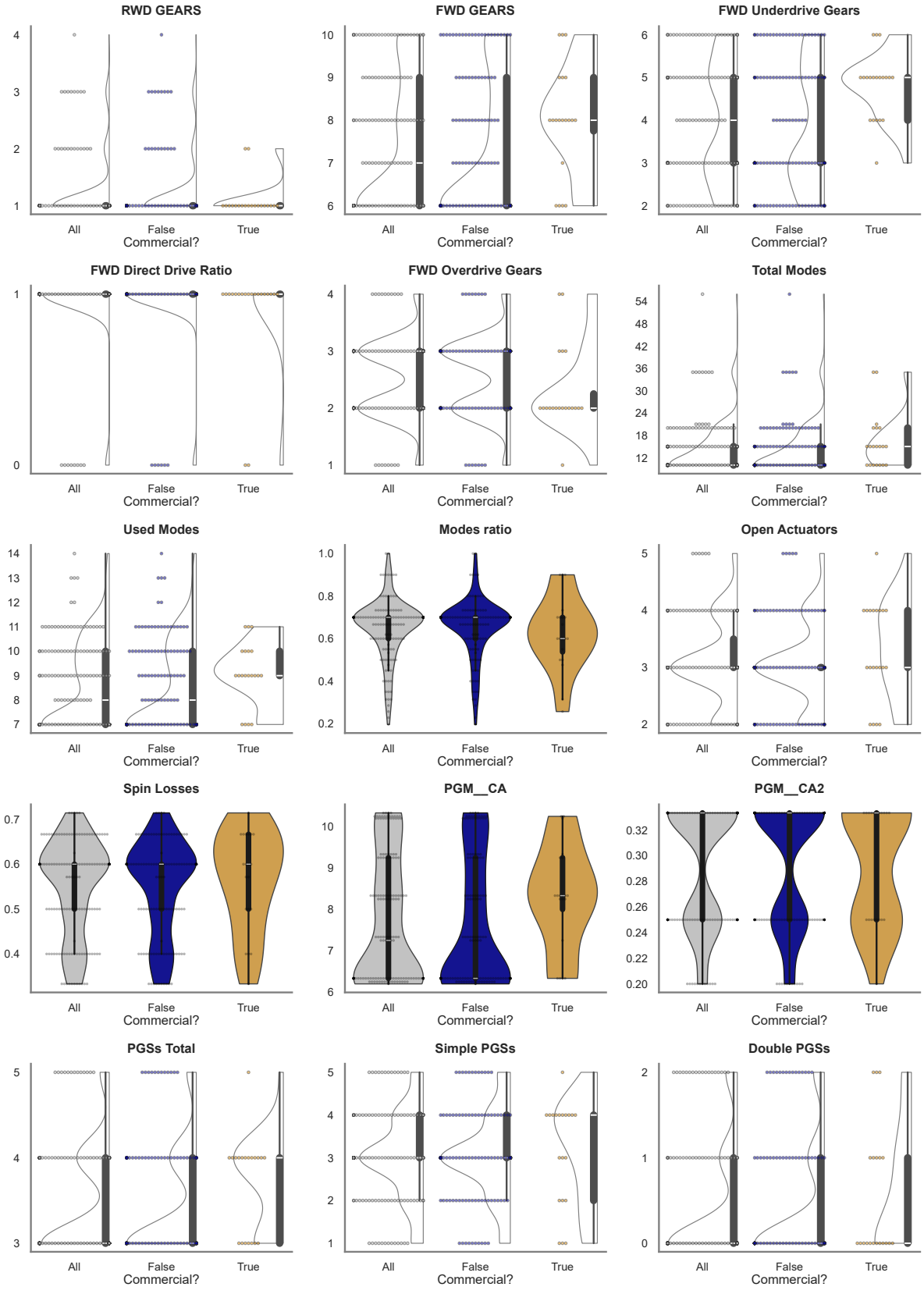

Source: Author.

Figure 273 – Violin plots of numerical features - *Commercial?* (2 of 8)

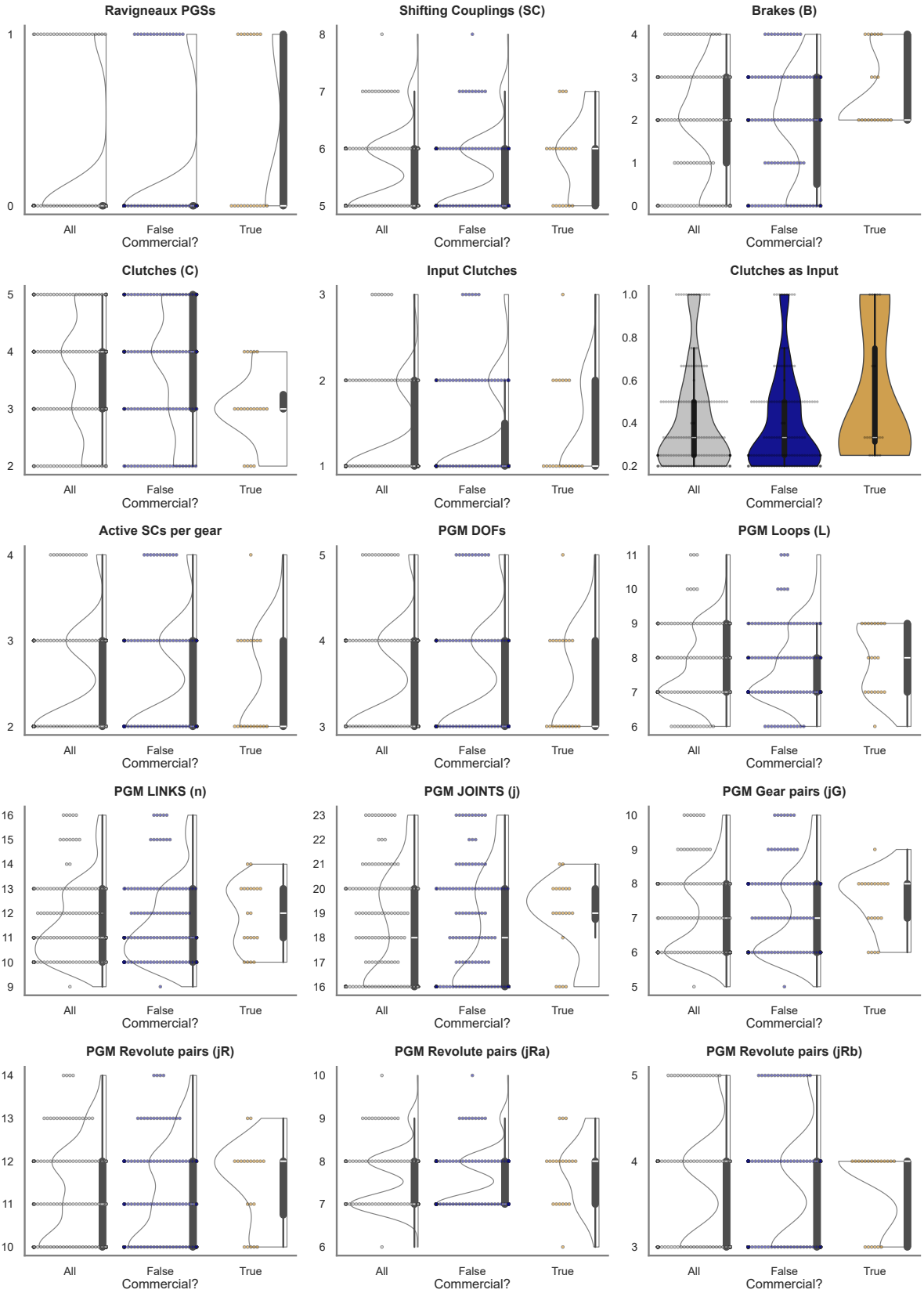

Source: Author.

Figure 274 – Violin plots of numerical features - *Commercial?* (3 of 8)

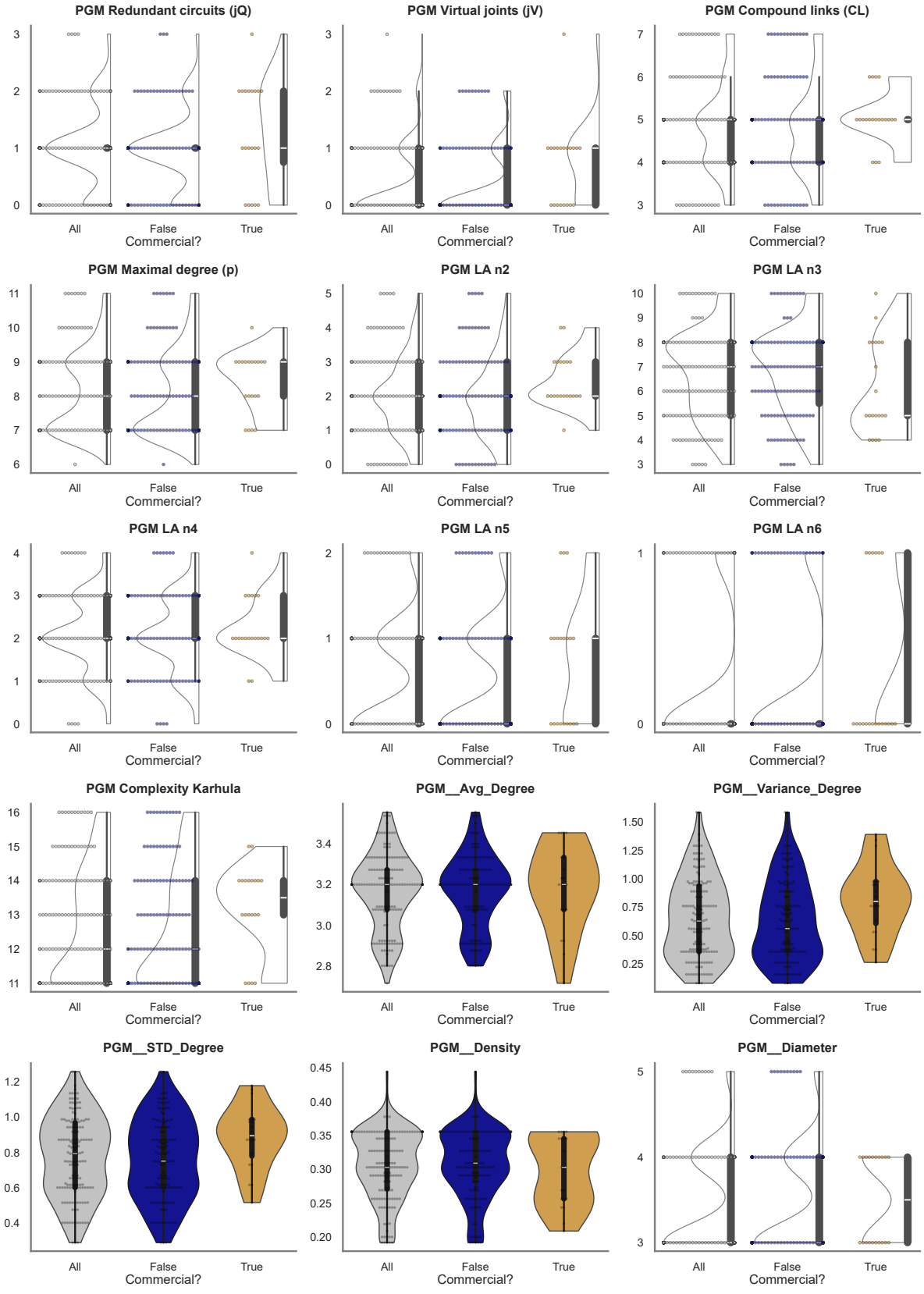

Source: Author.

Figure 275 – Violin plots of numerical features - *Commercial?* (4 of 8)

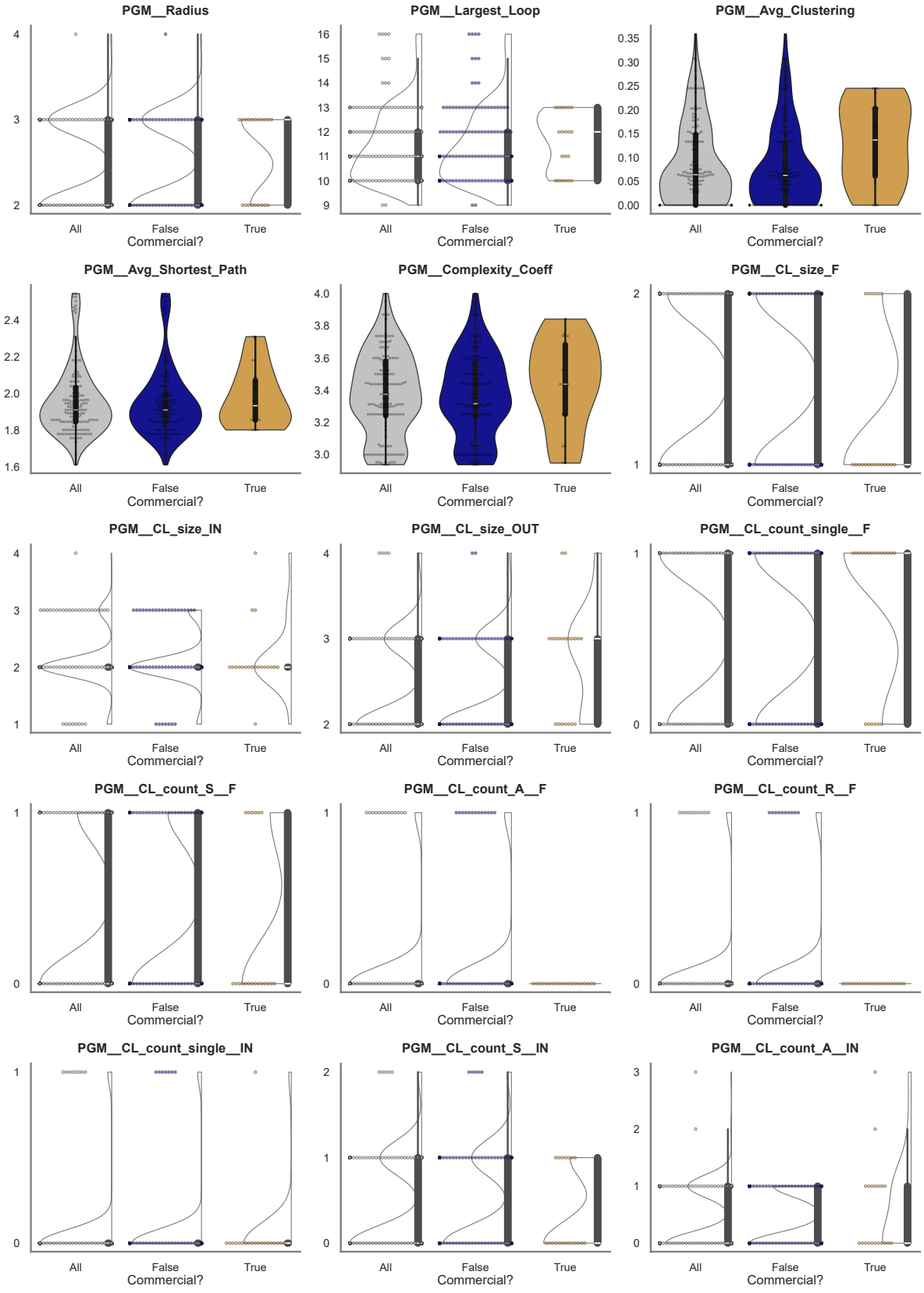

Source: Author.

Figure 276 – Violin plots of numerical features - *Commercial?* (5 of 8)

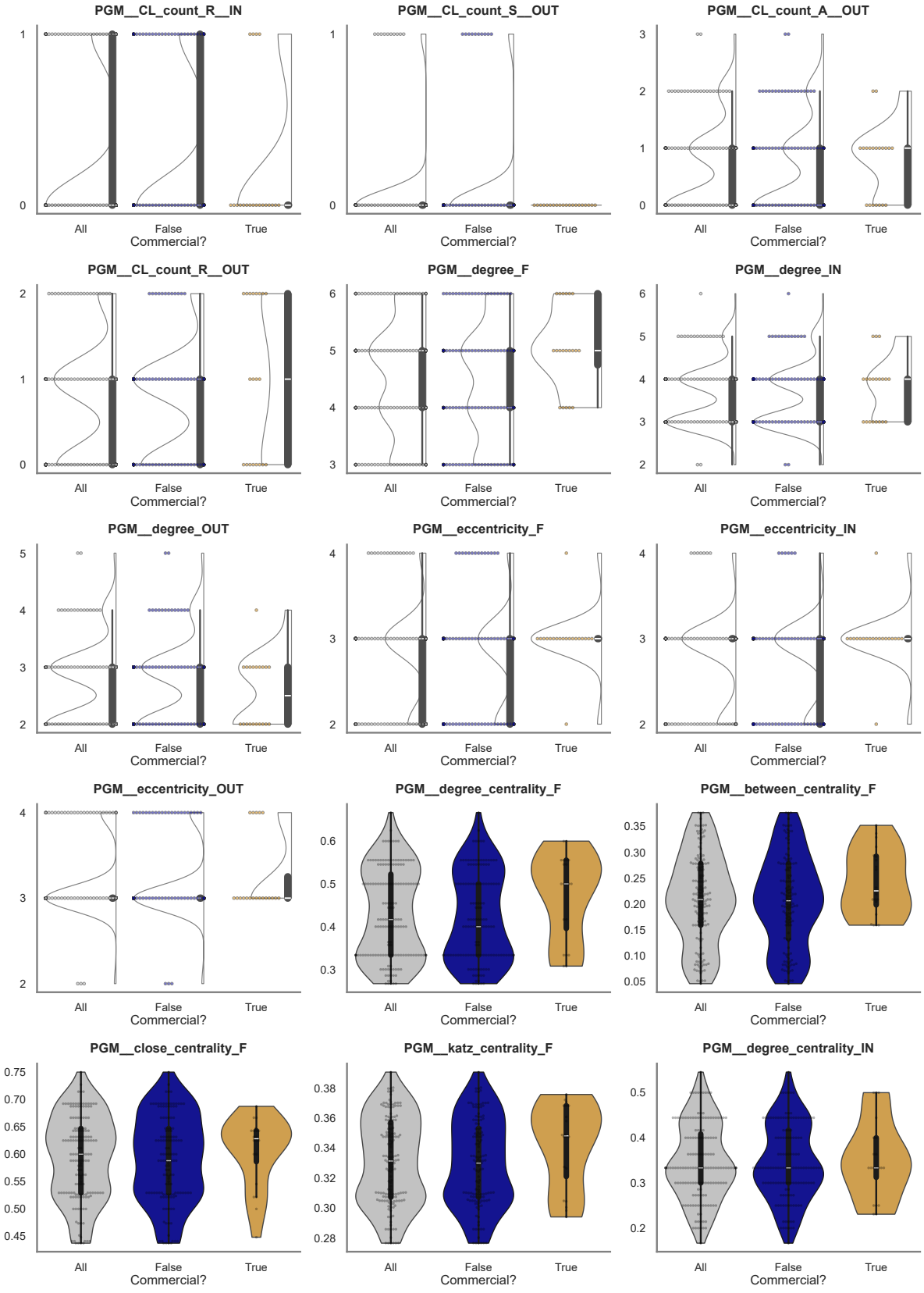

Source: Author.

Figure 277 – Violin plots of numerical features - *Commercial?* (6 of 8)

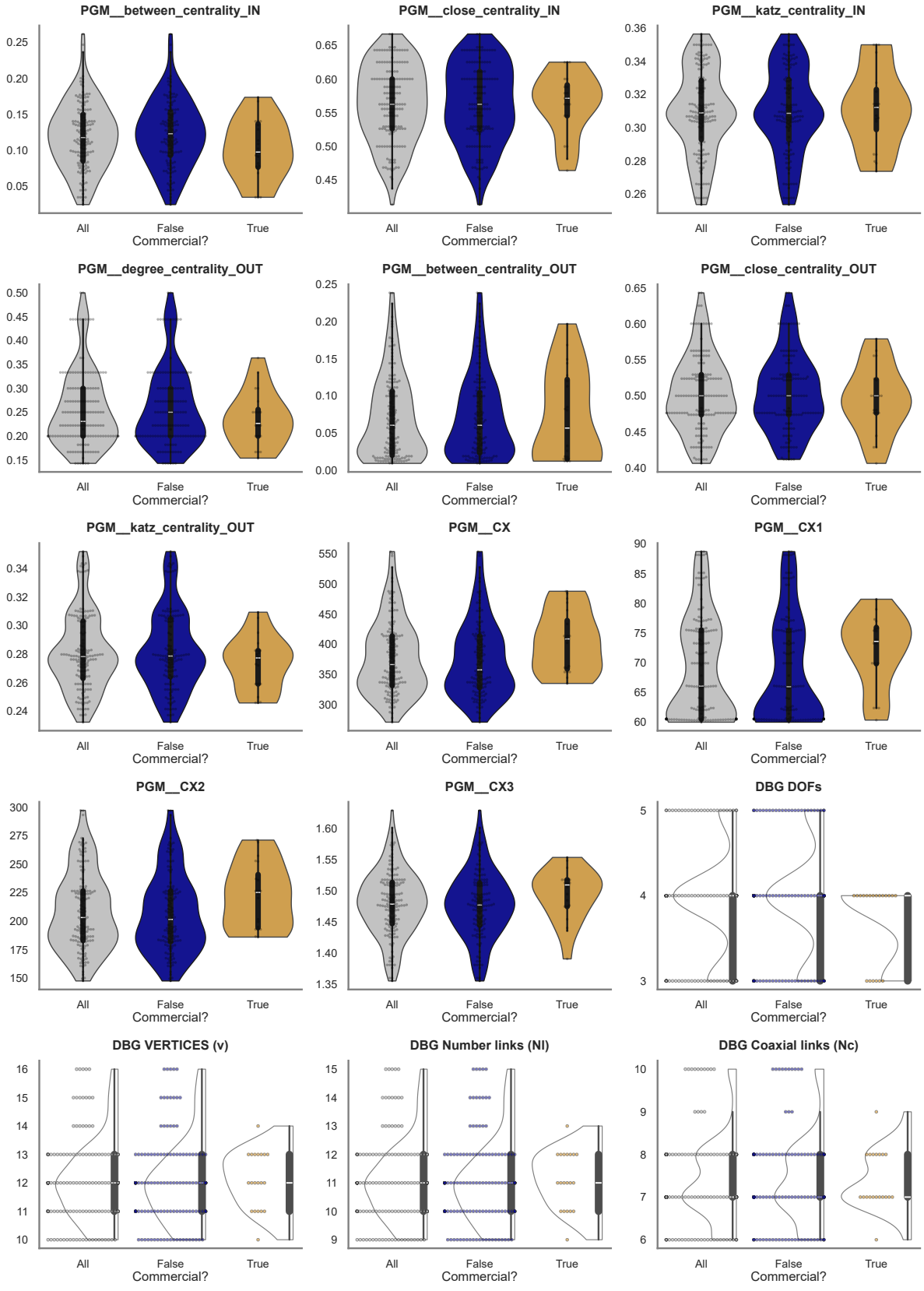

Source: Author.

Figure 278 – Violin plots of numerical features - *Commercial?* (7 of 8)

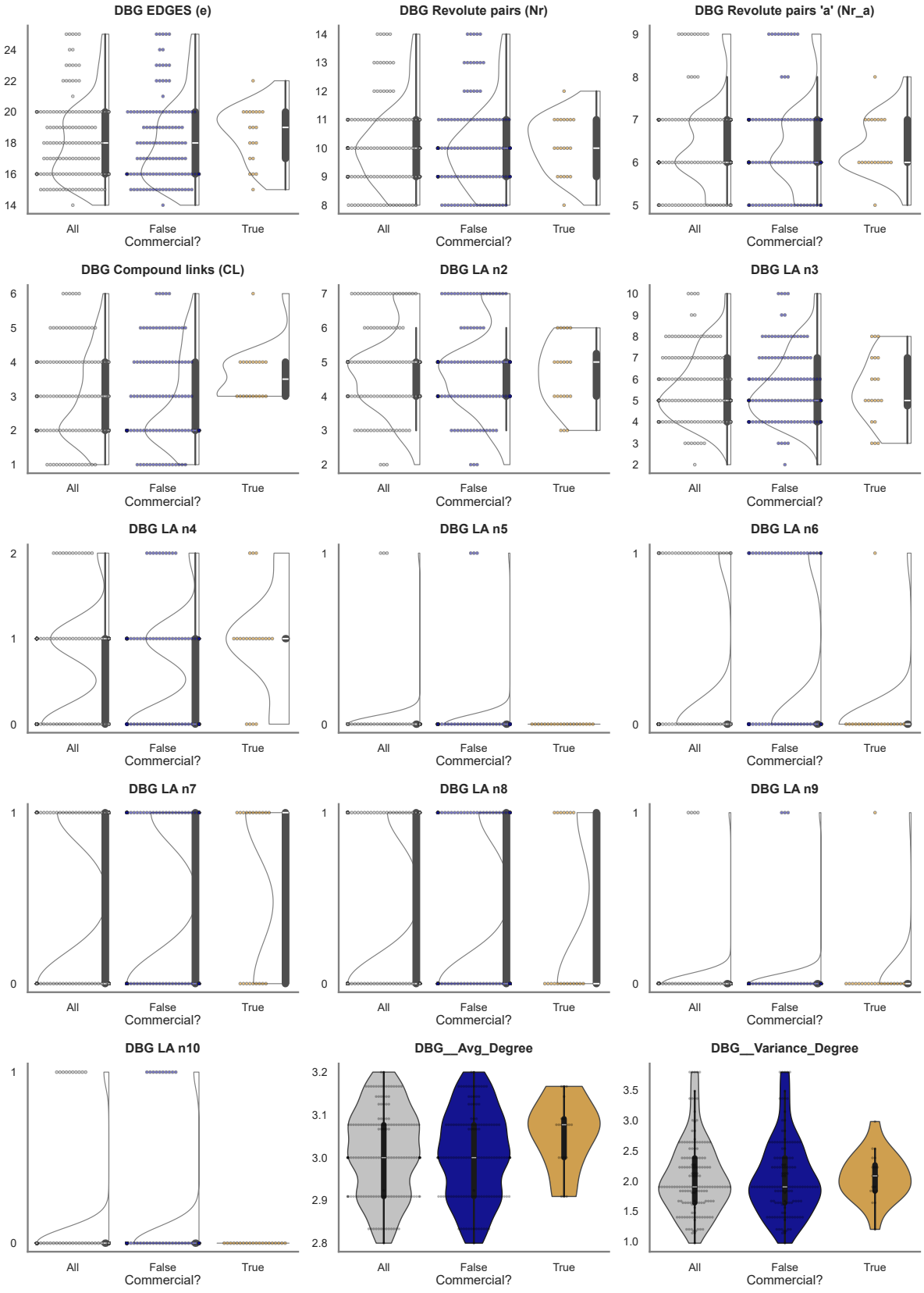

Source: Author.

Figure 279 – Violin plots of numerical features - *Commercial?* (8 of 8)

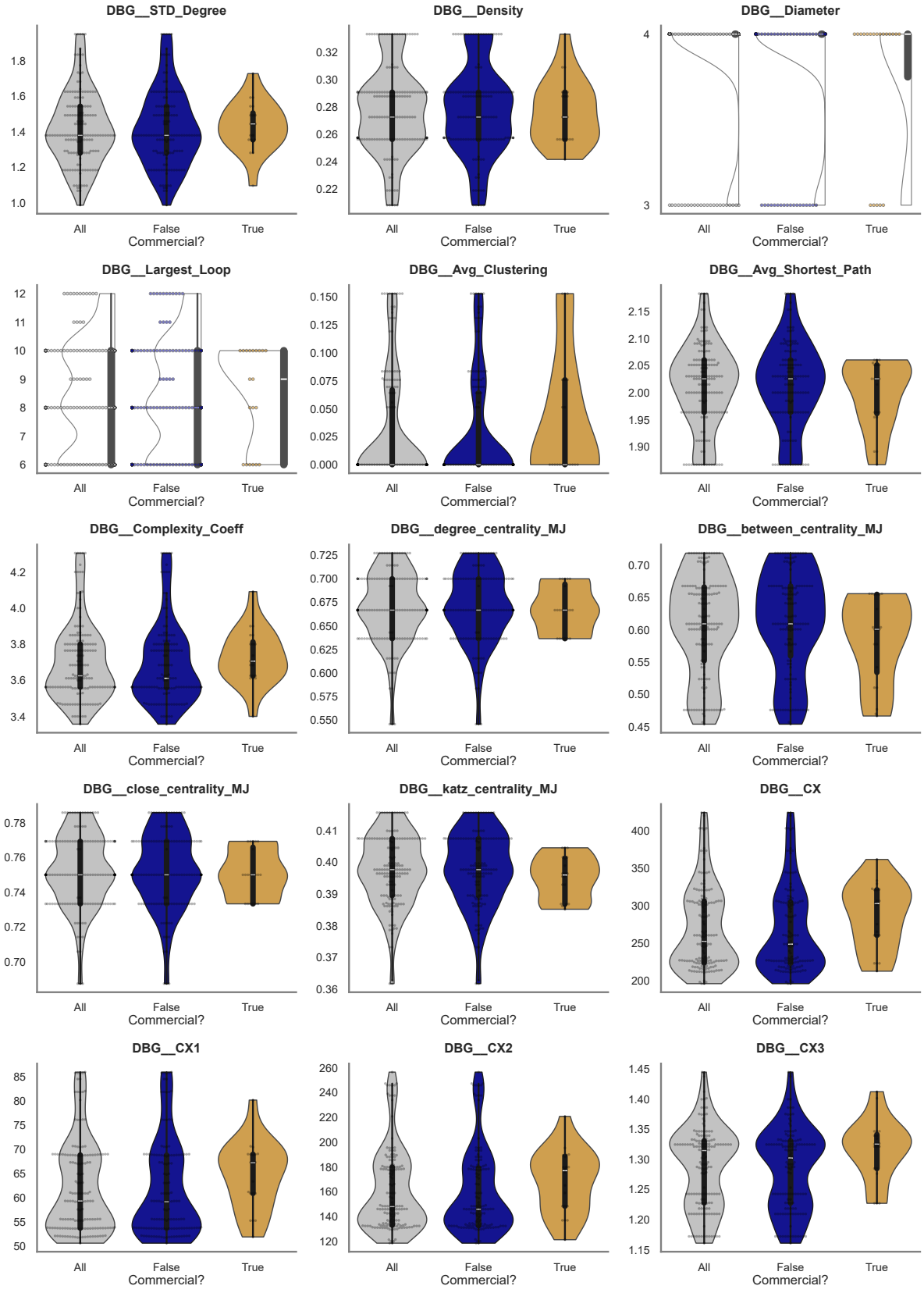

Source: Author.

Figure 280 – Charts of boolean features - *Commercial?*

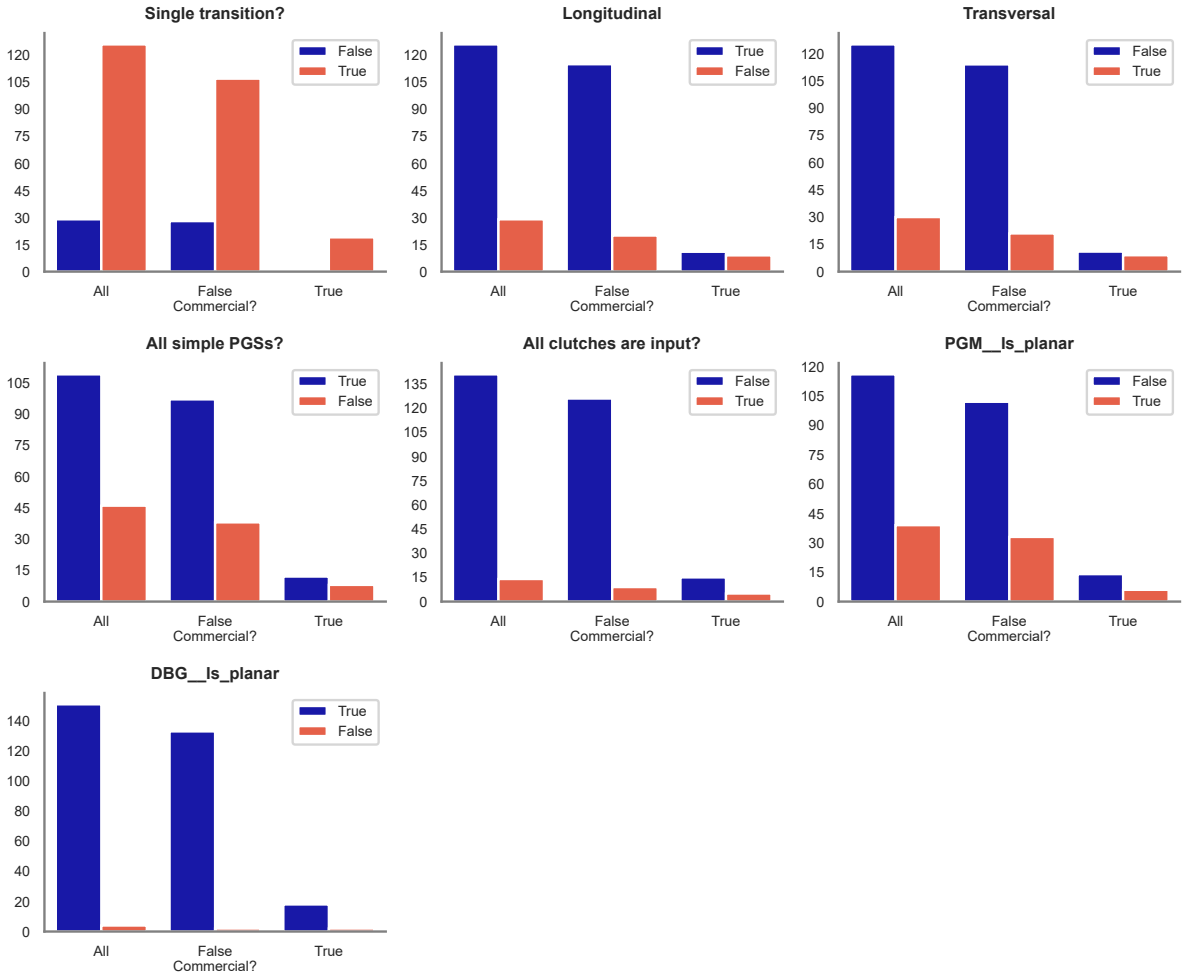

Source: Author.

Figure 281 – Charts of categorical feature - Unique Sources ID - *Commercial?*

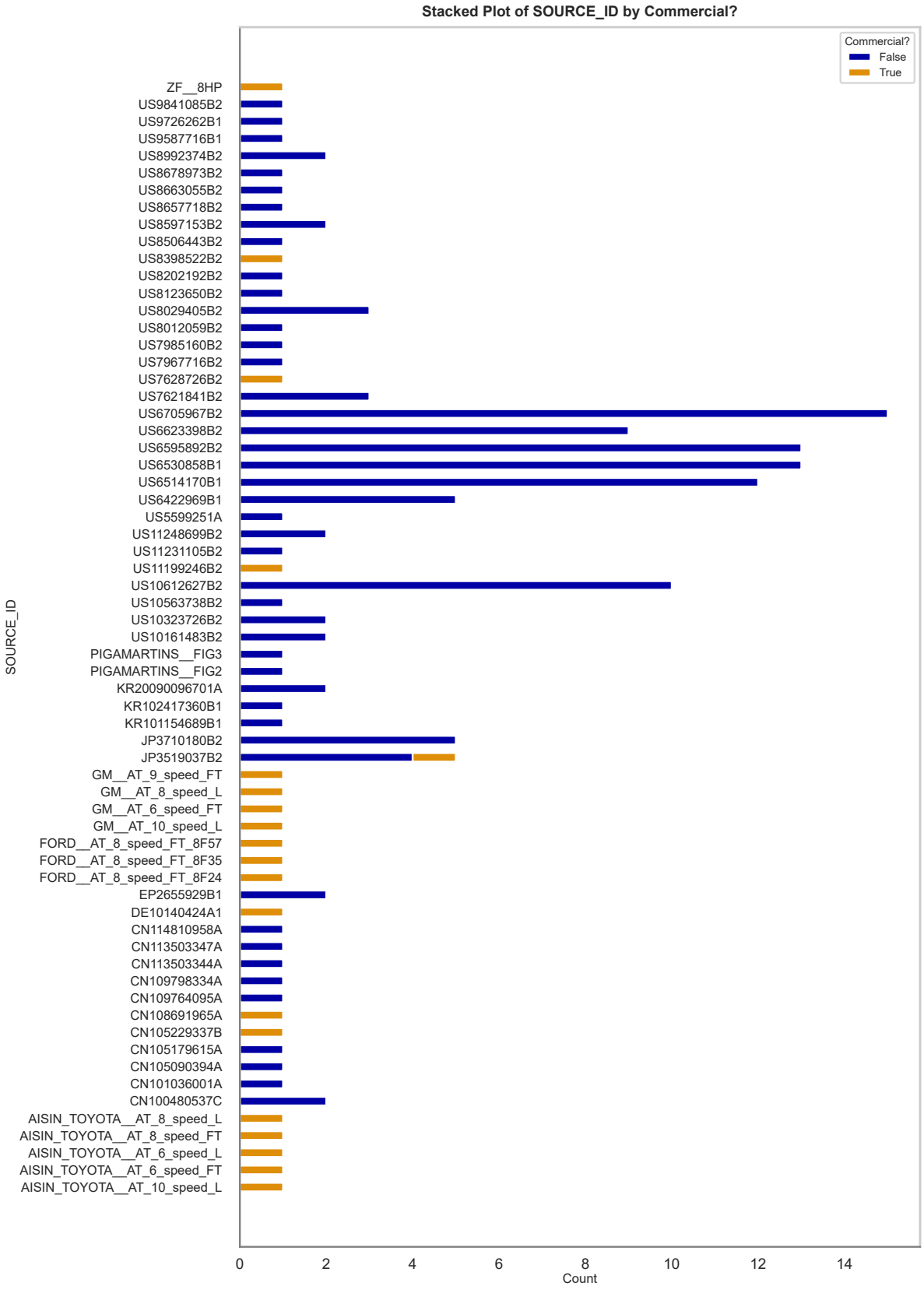

Source: Author.

Figure 282 – Charts of categorical feature - PGSs Sequences - *Commercial?*

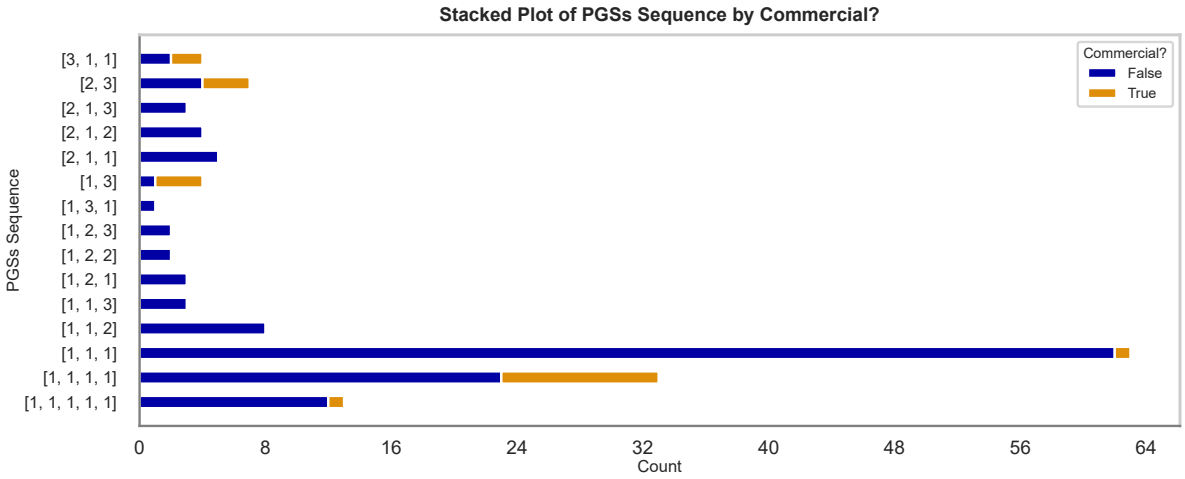

Source: Author.

Figure 283 – Charts of categorical feature - DBG Classification - *Commercial?*

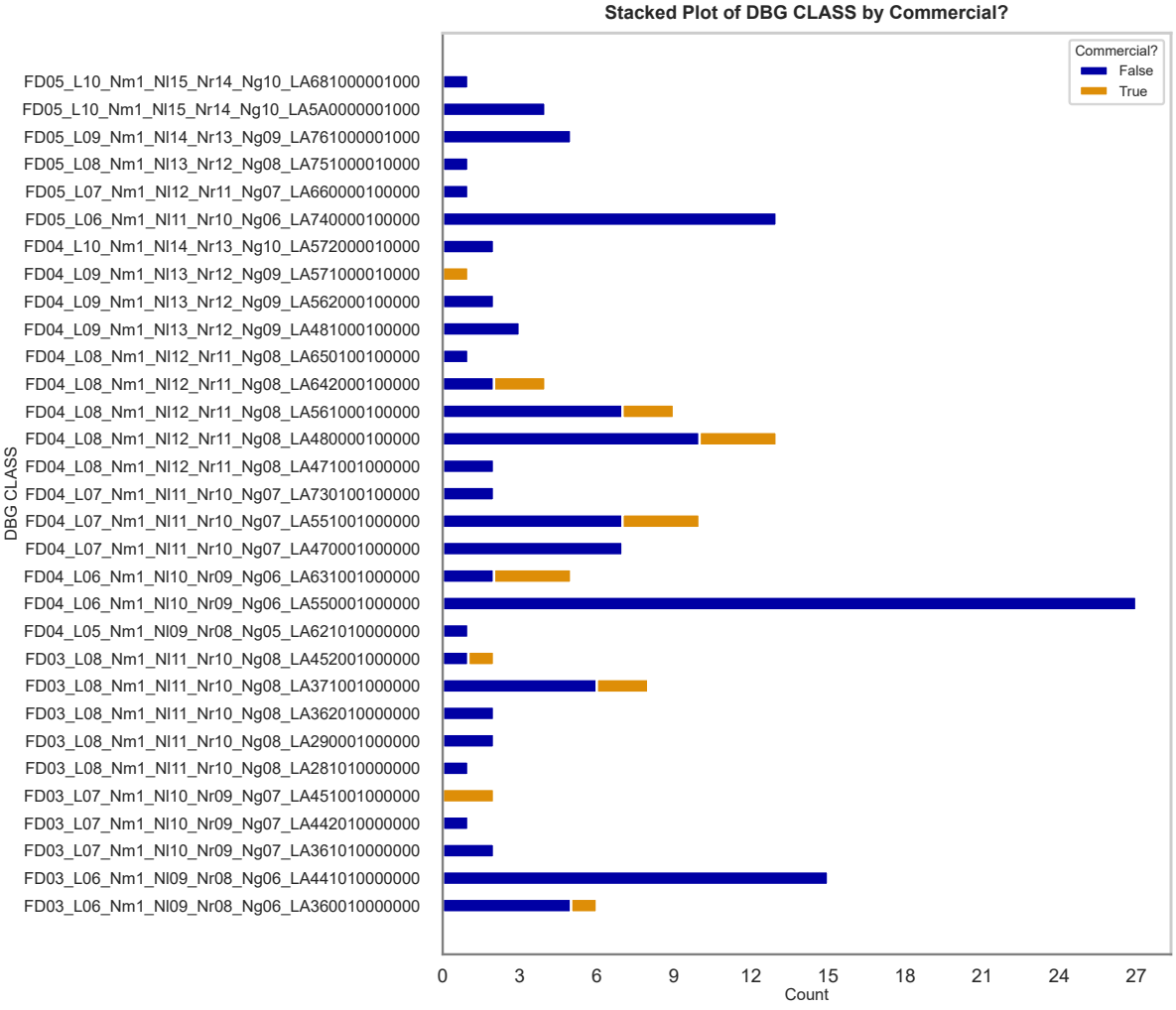

Source: Author.

Figure 284 – Charts of categorical feature - DBG Link Assortments - *Commercial?*

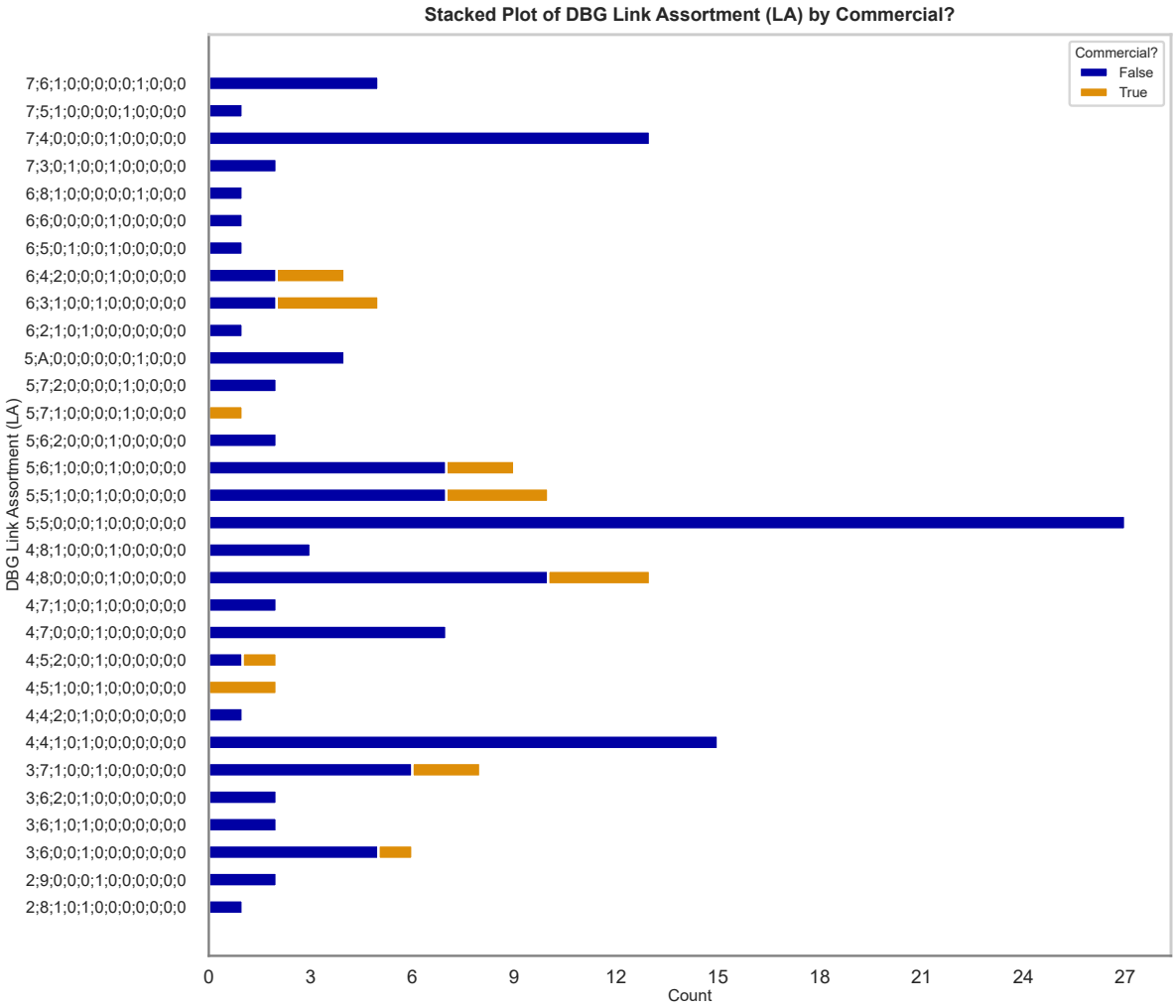

Source: Author.

Figure 285 – Charts of categorical feature - PGM Classification - *Commercial?*

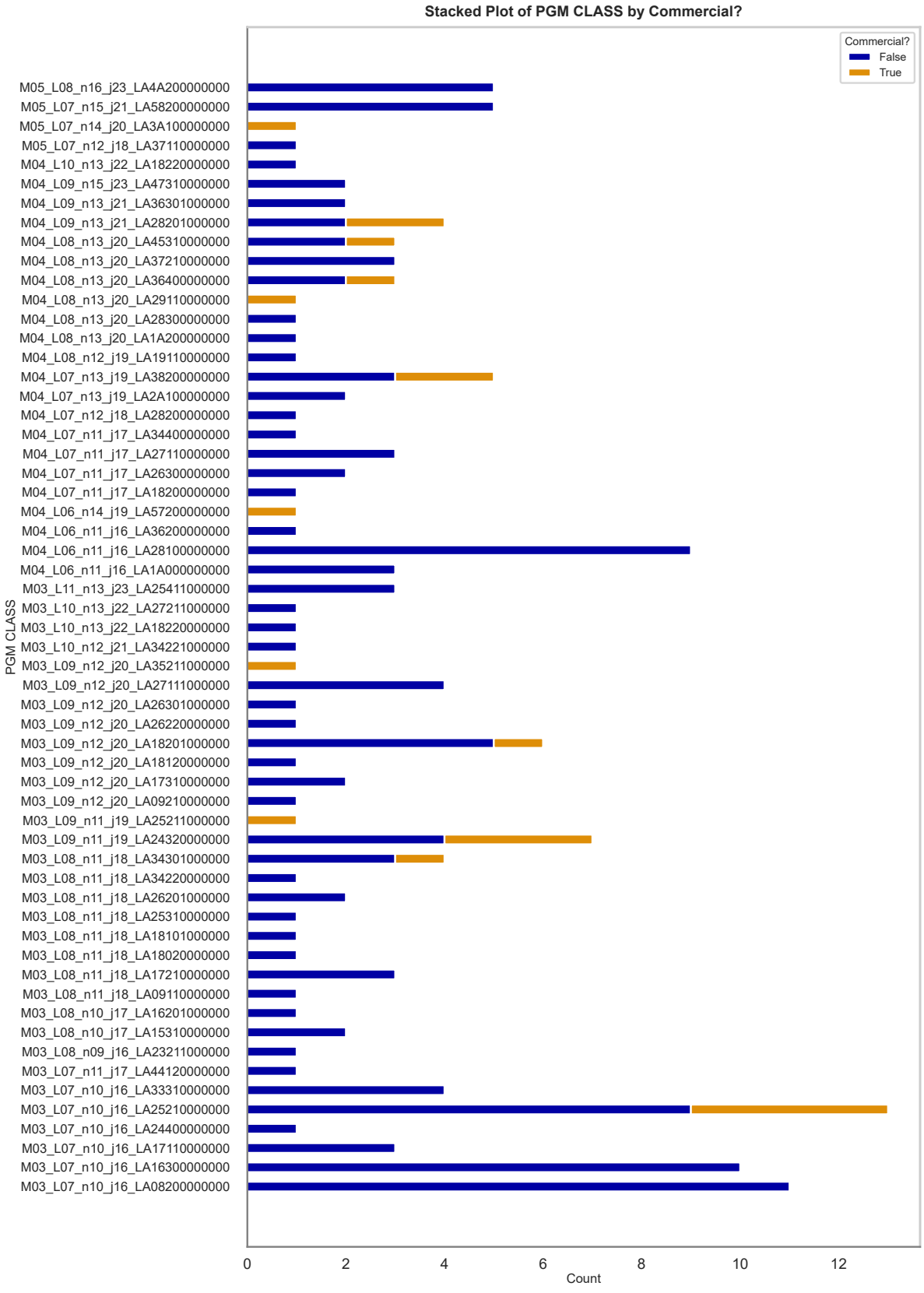

Source: Author.

Figure 286 – Charts of categorical feature - PGM Link Assortments - *Commercial?*

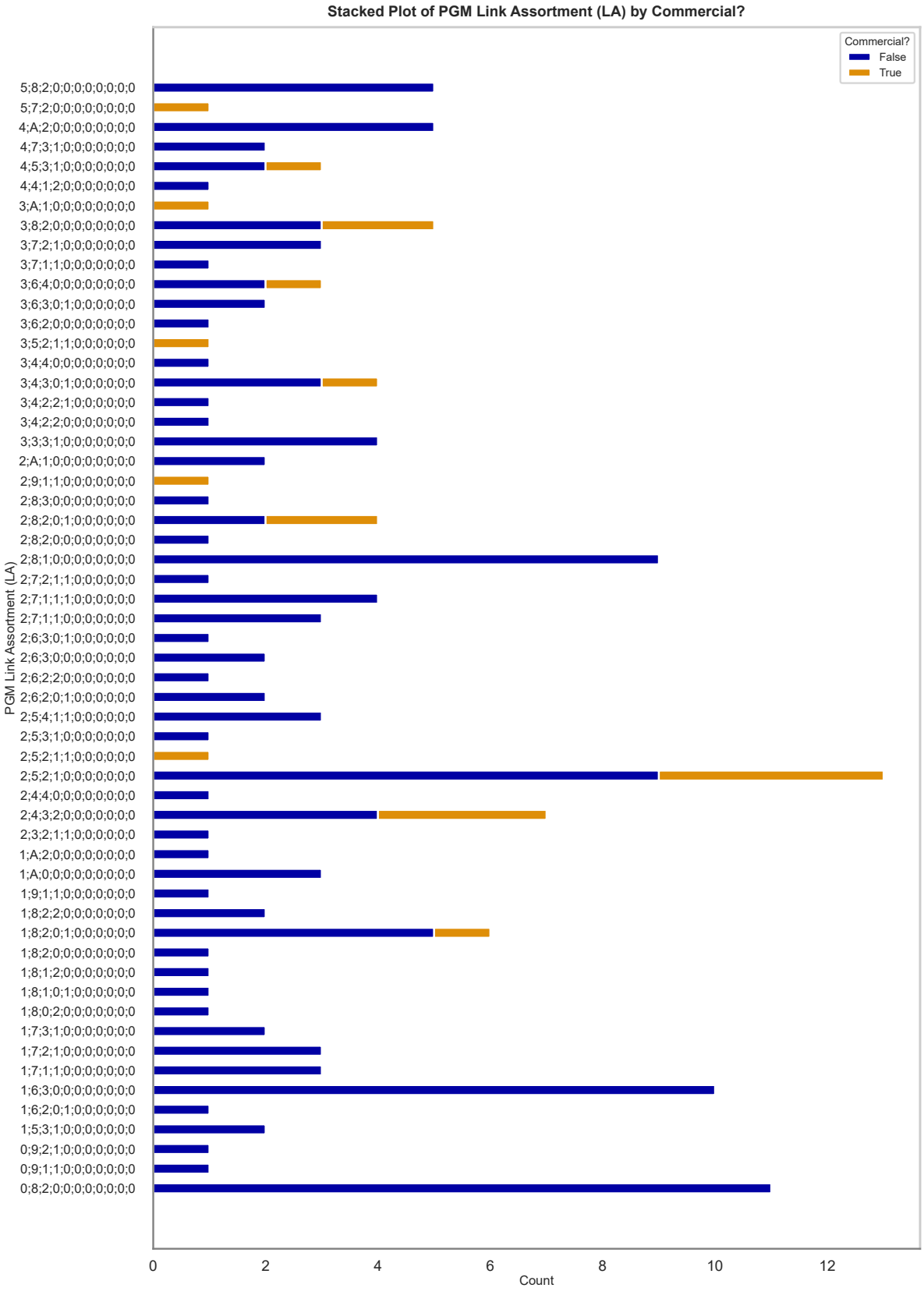

Source: Author.

B.1.4 Univariate Normality Results

In the following pages, the results of the normality tests discussed in Section 5.4.2 are presented for the numerical features in representative graphs.

Figure 287 – Normality Tests Results (1 of 24)

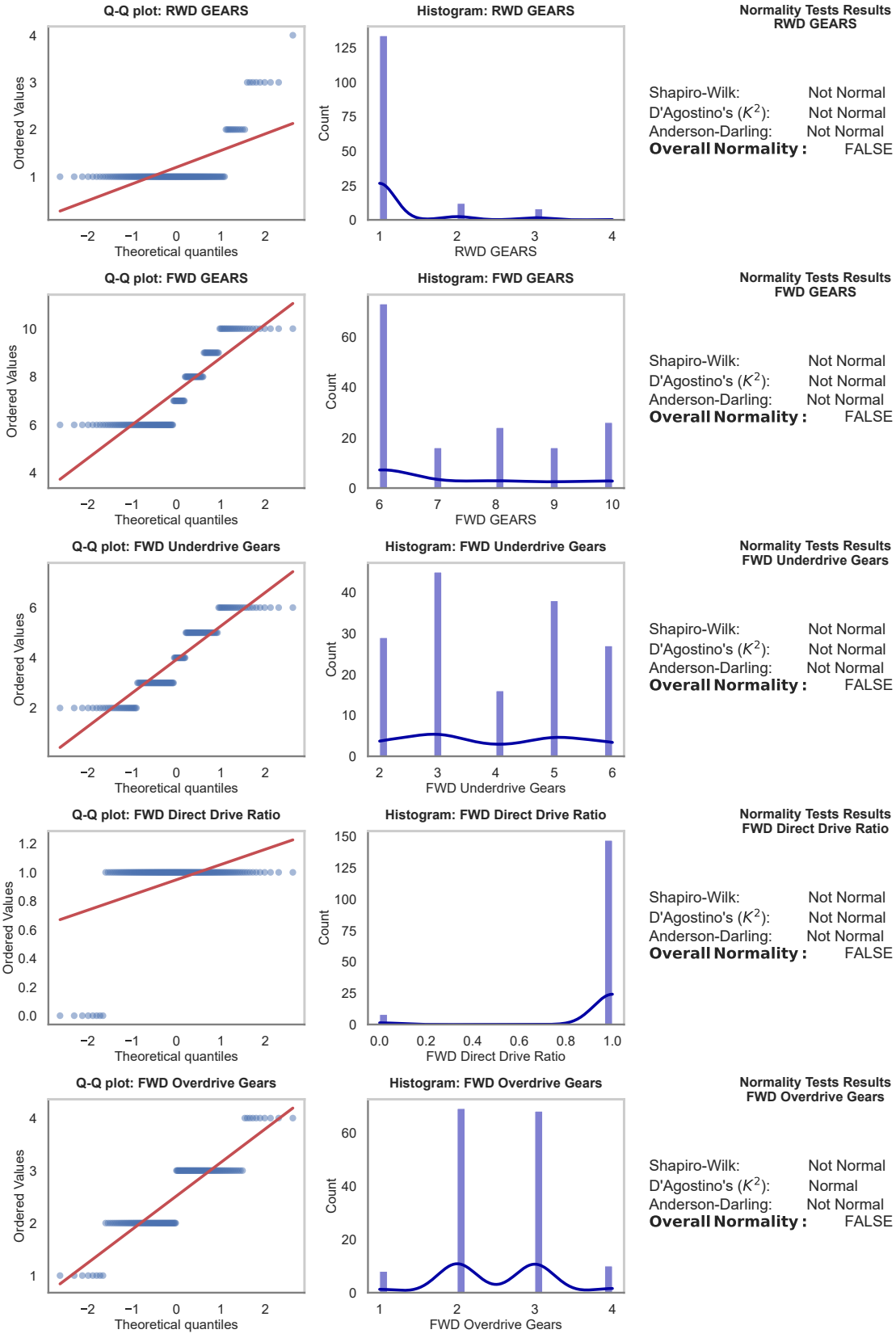

Source: Author.

Figure 288 – Normality Tests Results (2 of 24)

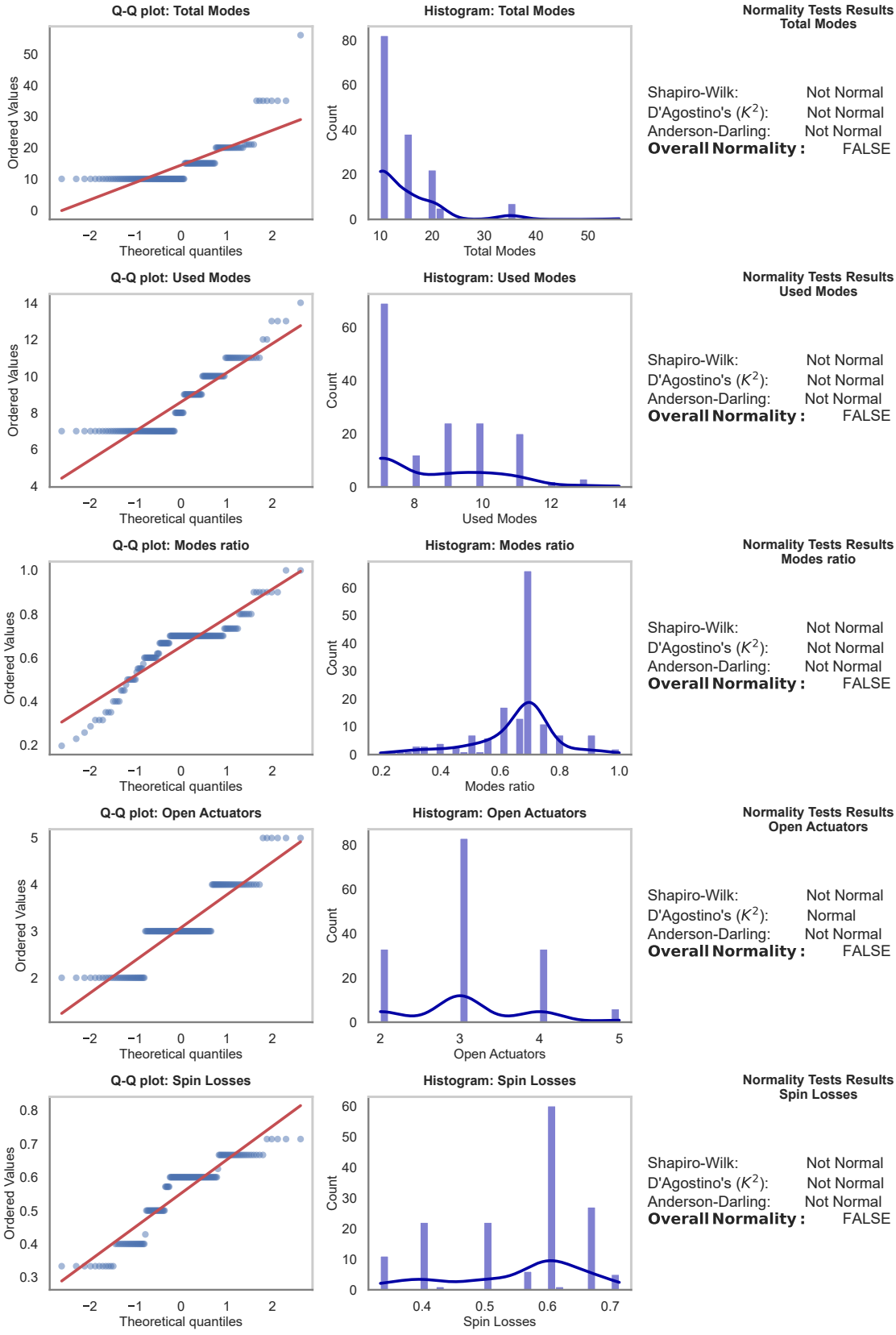

Source: Author.

Figure 289 – Normality Tests Results (3 of 24)

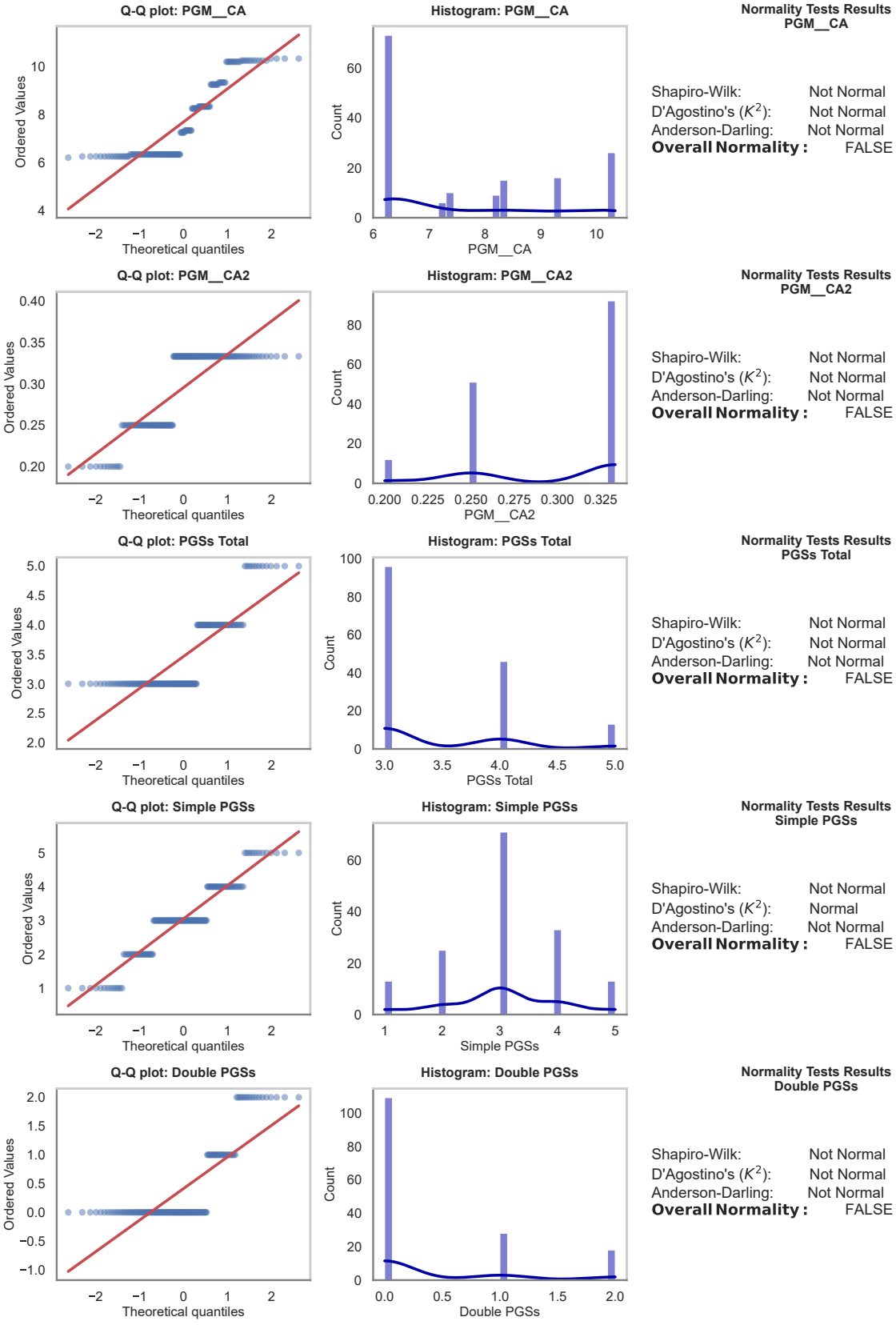

Source: Author.

Figure 290 – Normality Tests Results (4 of 24)

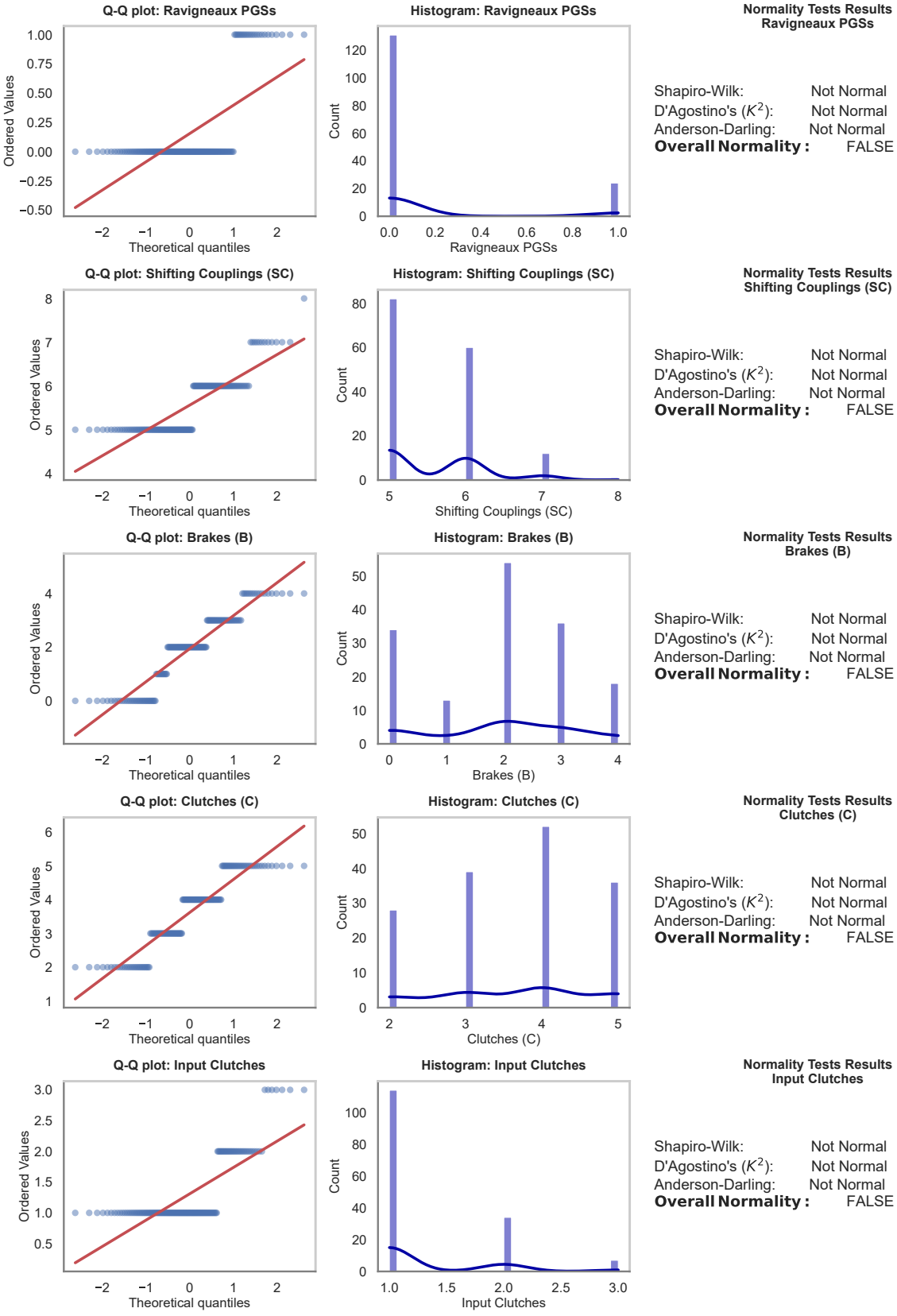

Source: Author.

Figure 291 – Normality Tests Results (5 of 24)

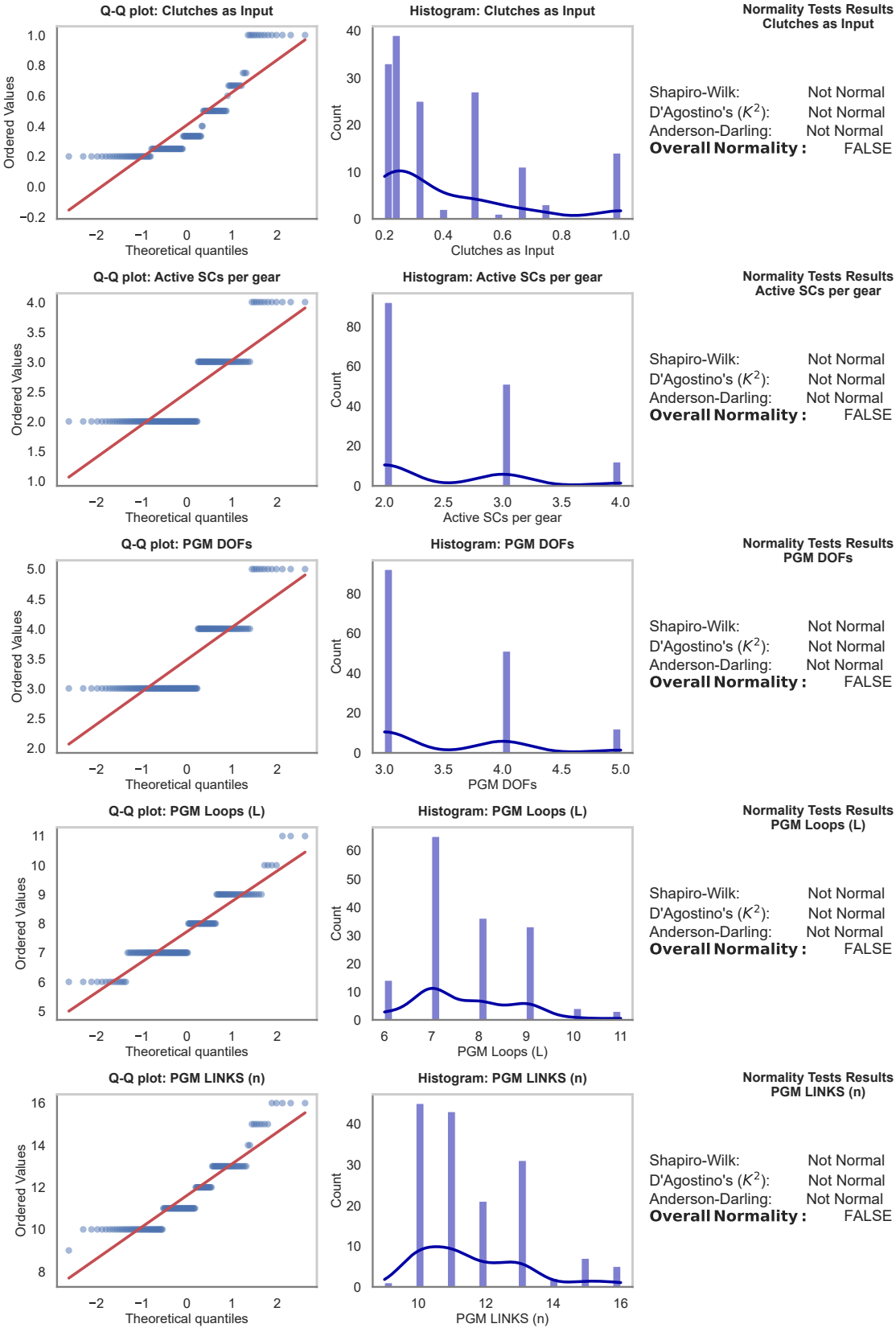

Source: Author.

Figure 292 – Normality Tests Results (6 of 24)

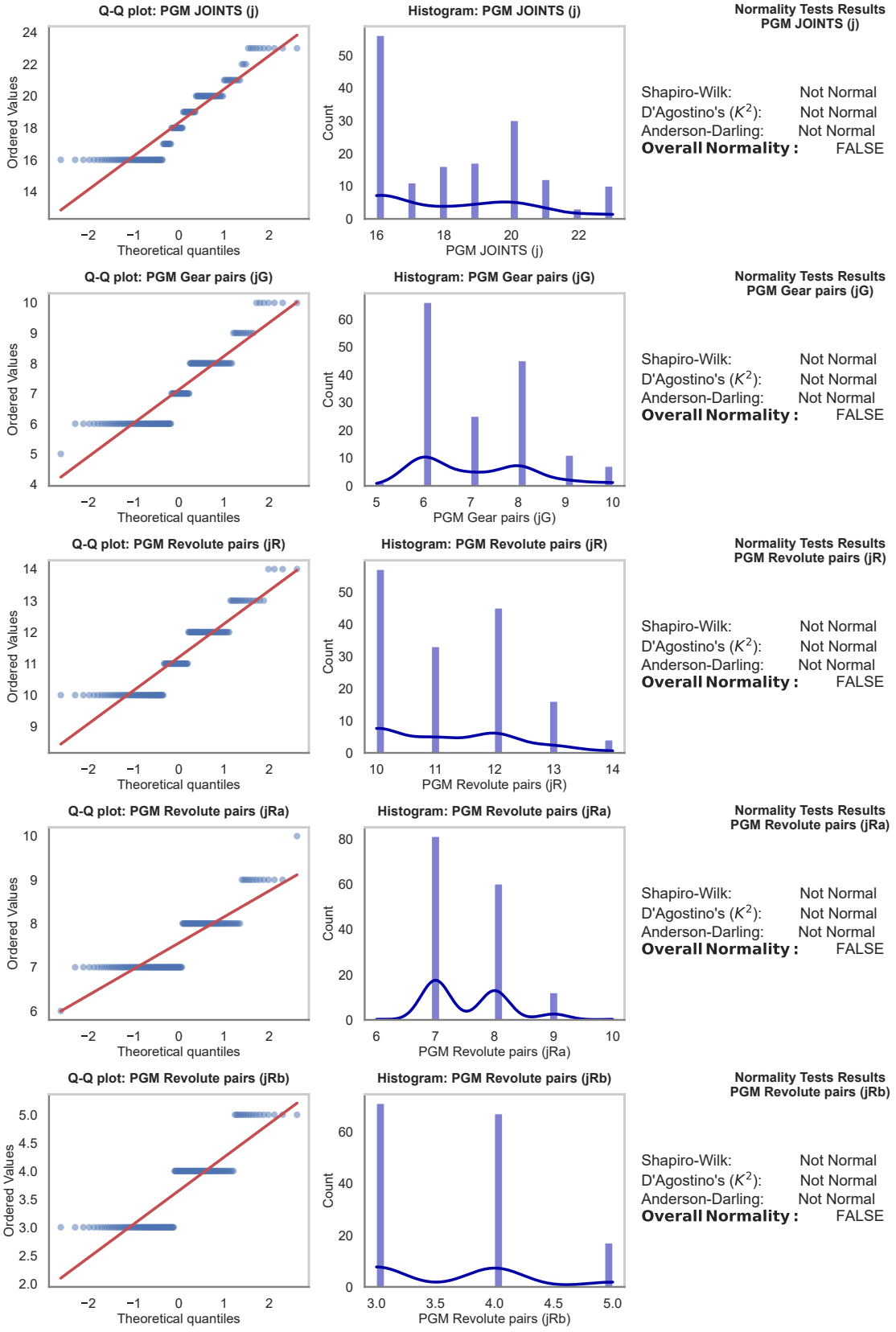

Source: Author.

Figure 293 – Normality Tests Results (7 of 24)

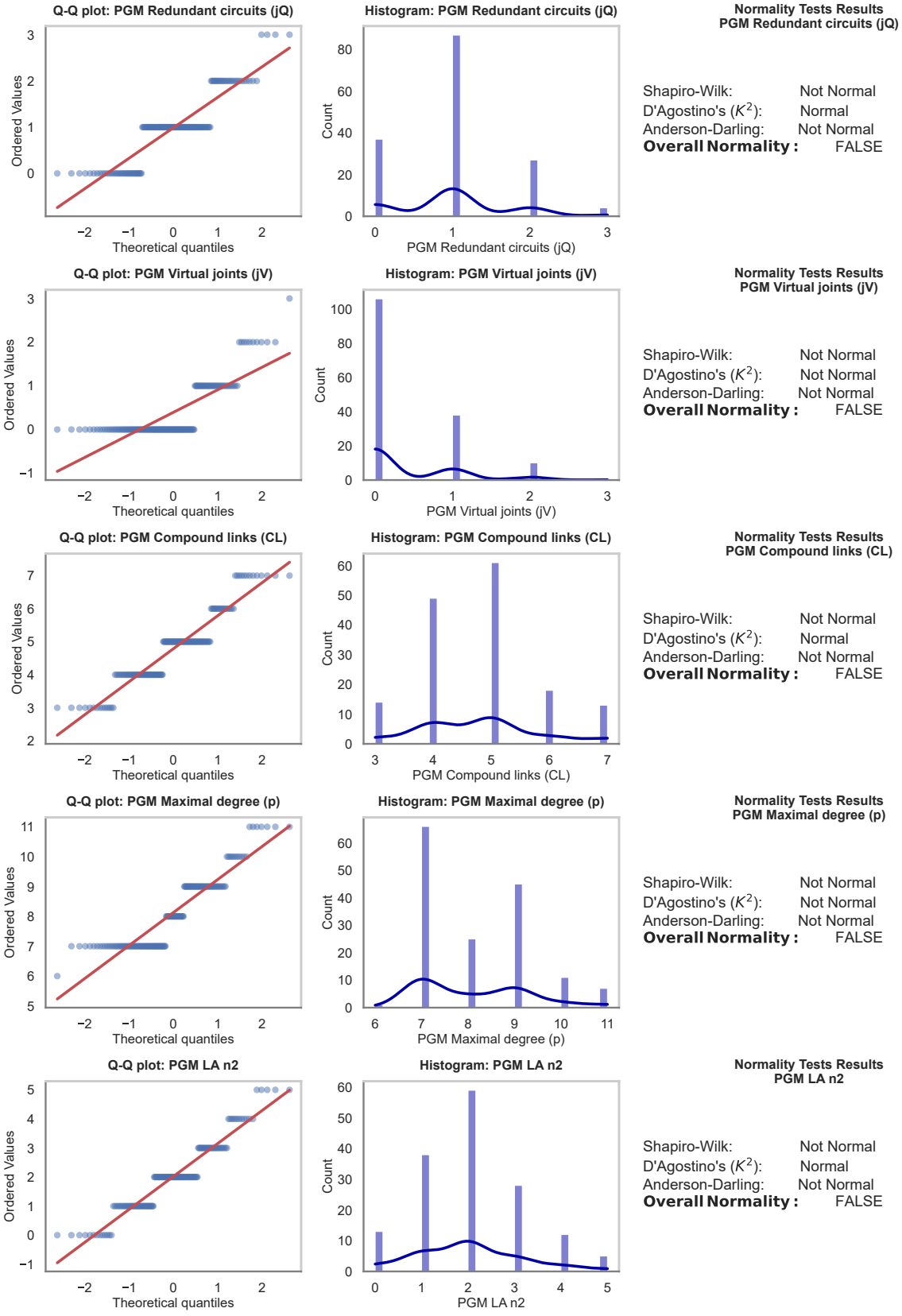

Source: Author.

Figure 294 – Normality Tests Results (8 of 24)

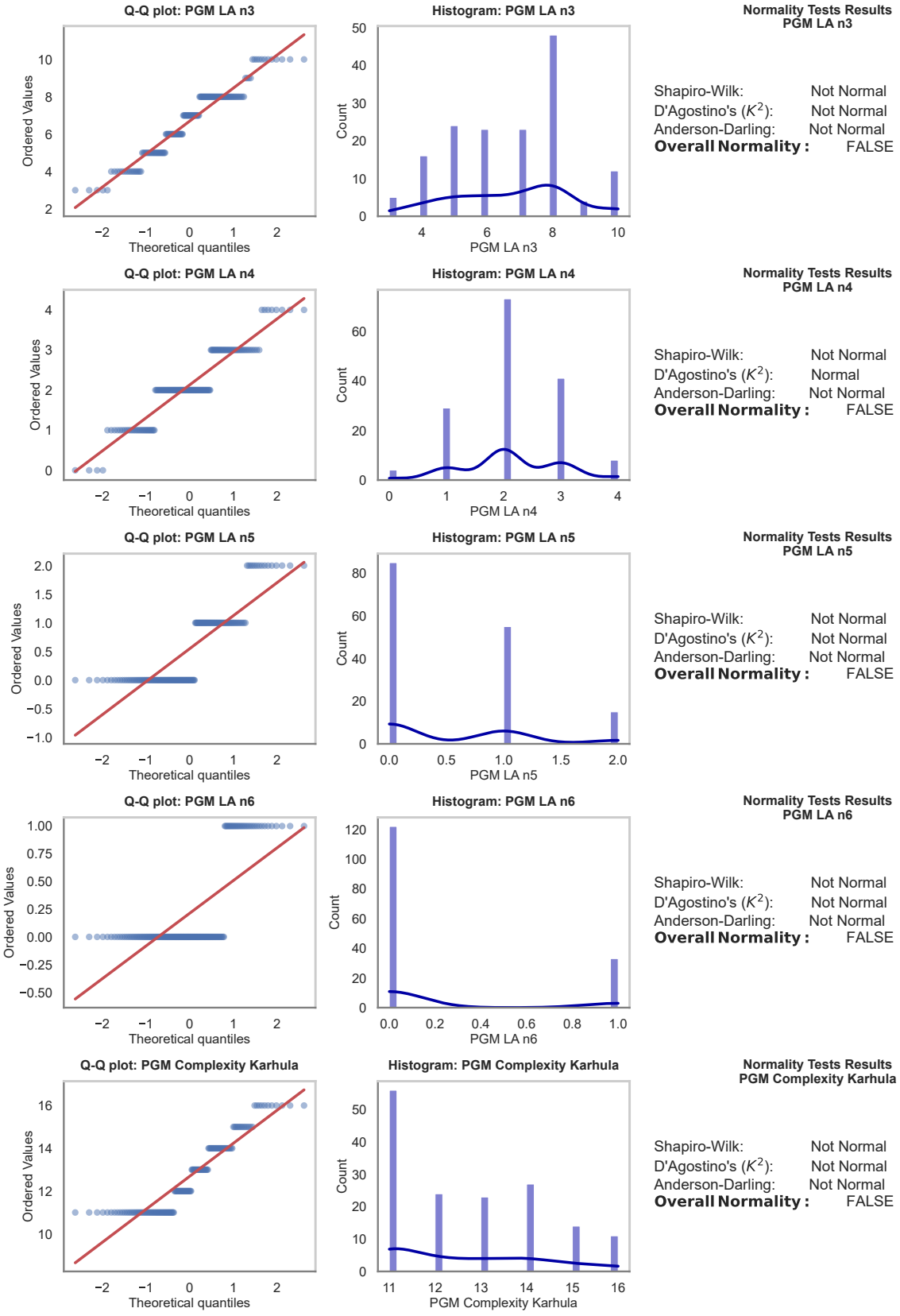

Source: Author.

Figure 295 – Normality Tests Results (9 of 24)

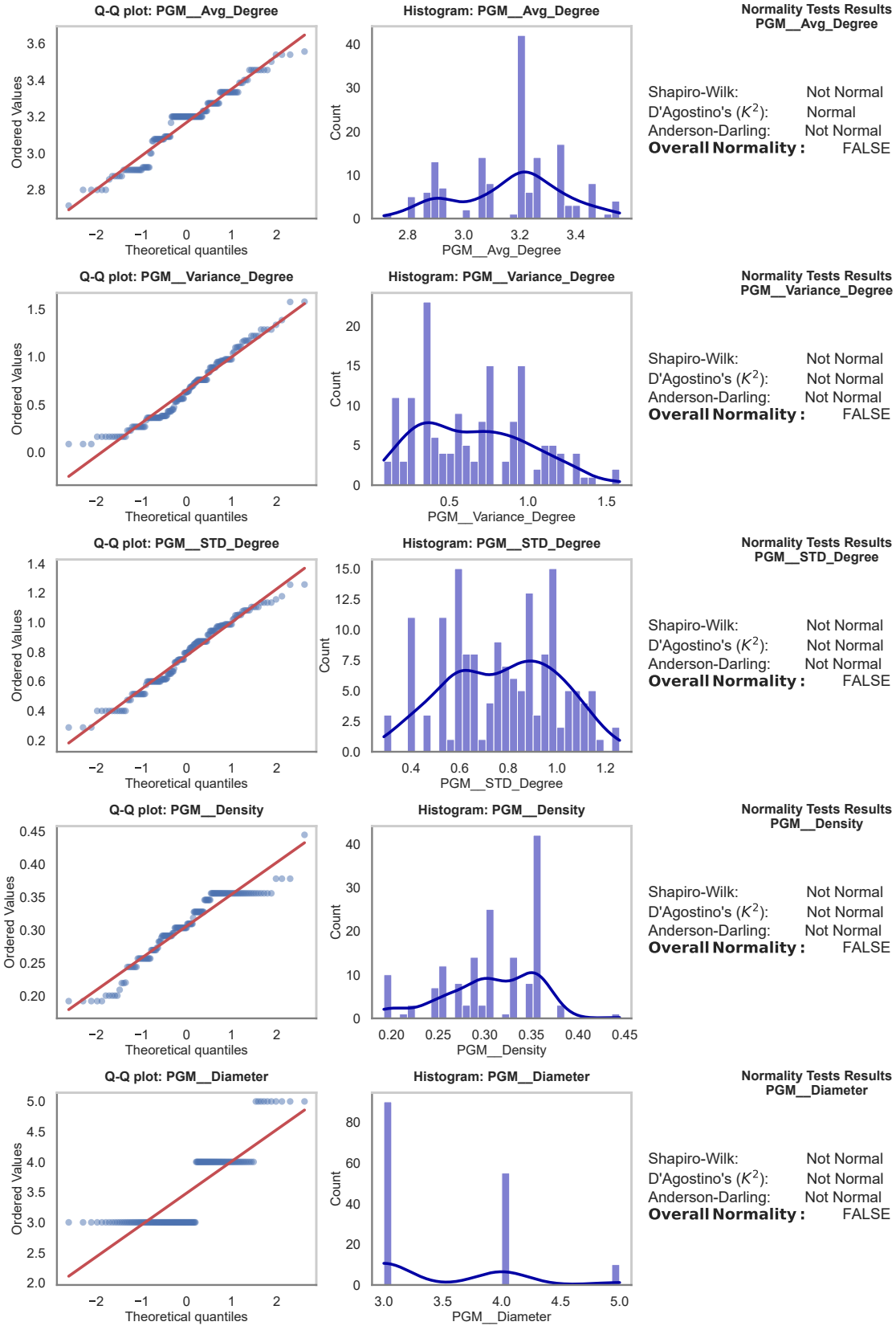

Source: Author.

Figure 296 – Normality Tests Results (10 of 24)

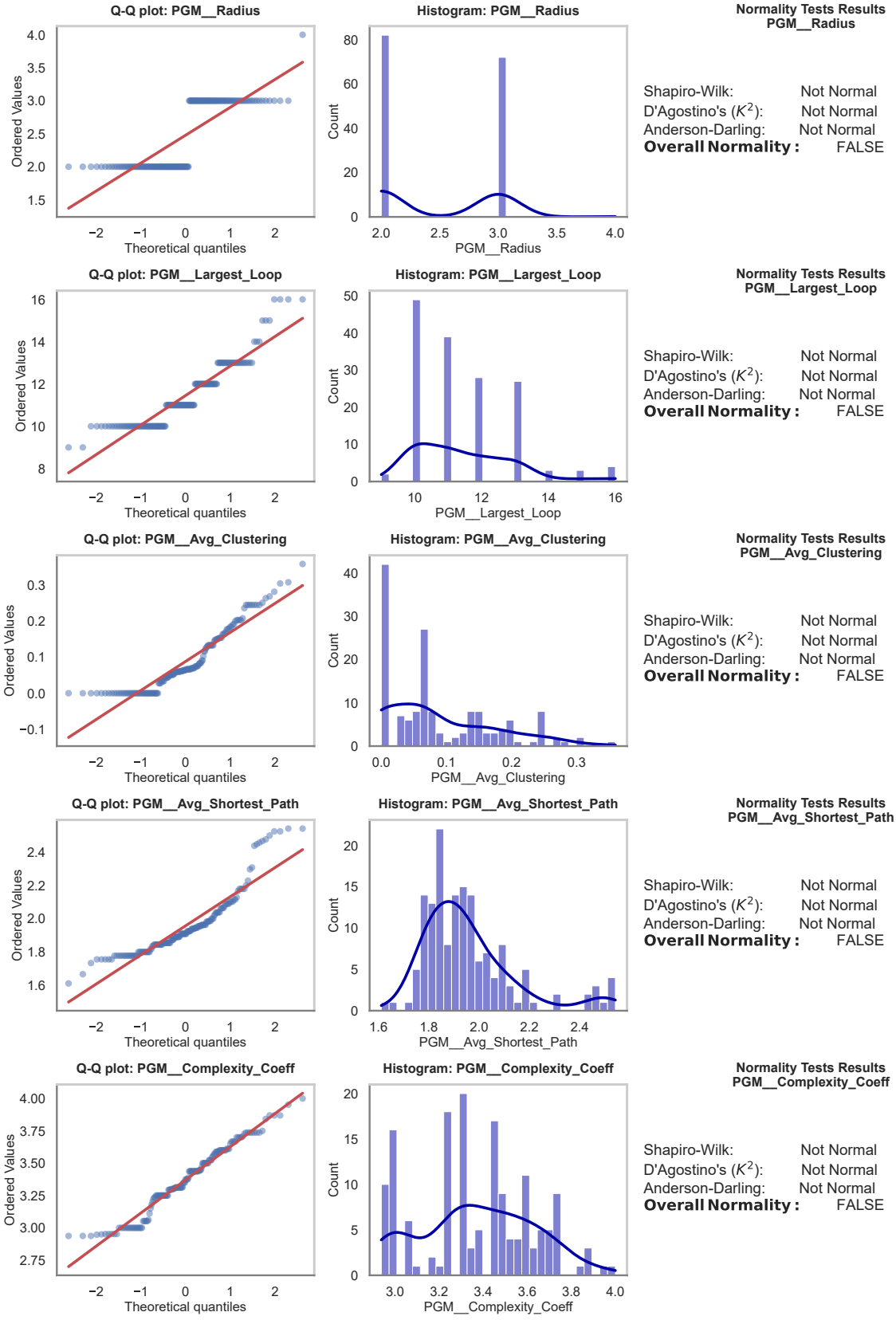

Source: Author.

Figure 297 – Normality Tests Results (11 of 24)

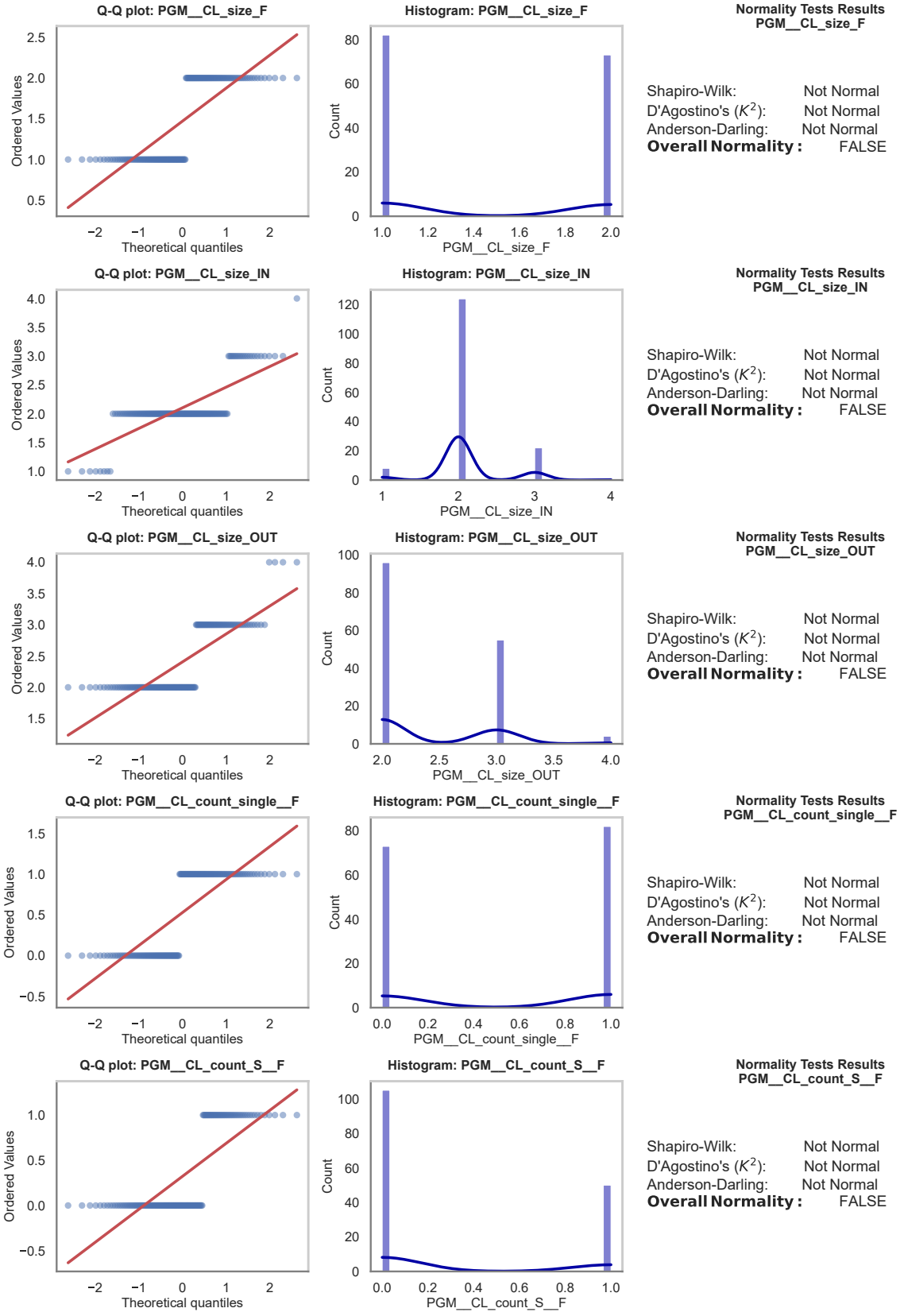

Source: Author.

Figure 298 – Normality Tests Results (12 of 24)

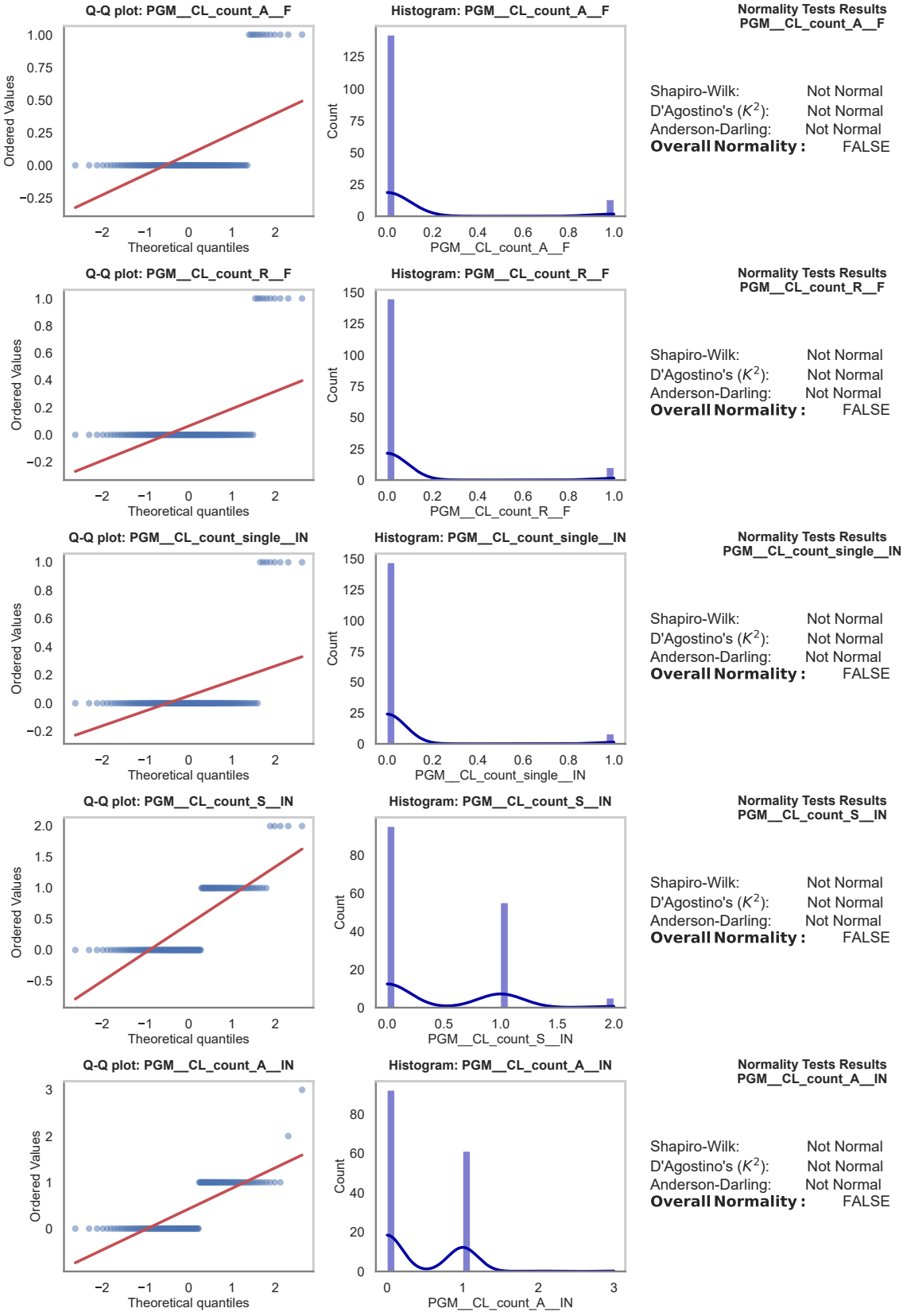

Source: Author.

Figure 299 – Normality Tests Results (13 of 24)

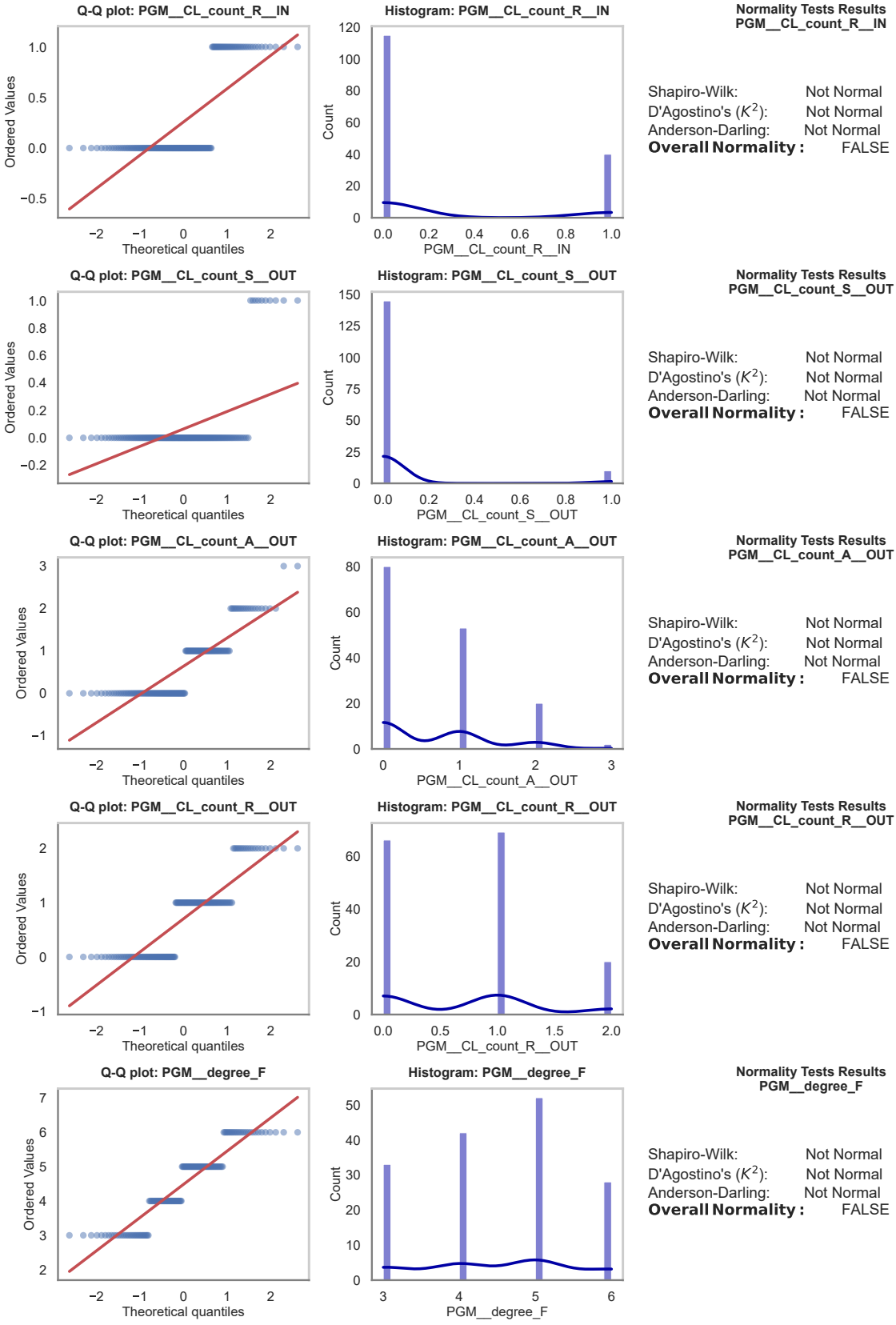

Source: Author.

Figure 300 – Normality Tests Results (14 of 24)

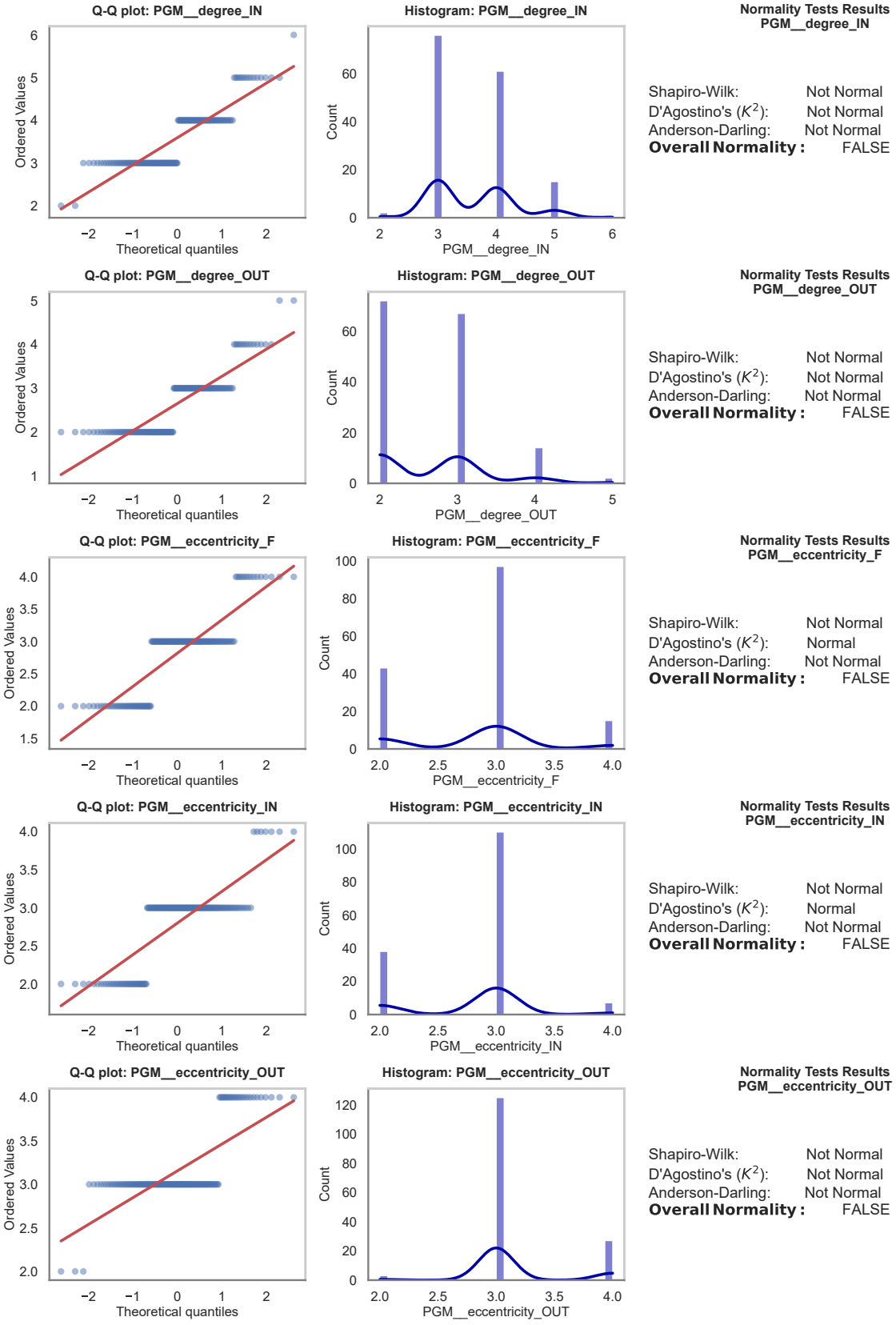

Source: Author.

Figure 301 – Normality Tests Results (15 of 24)

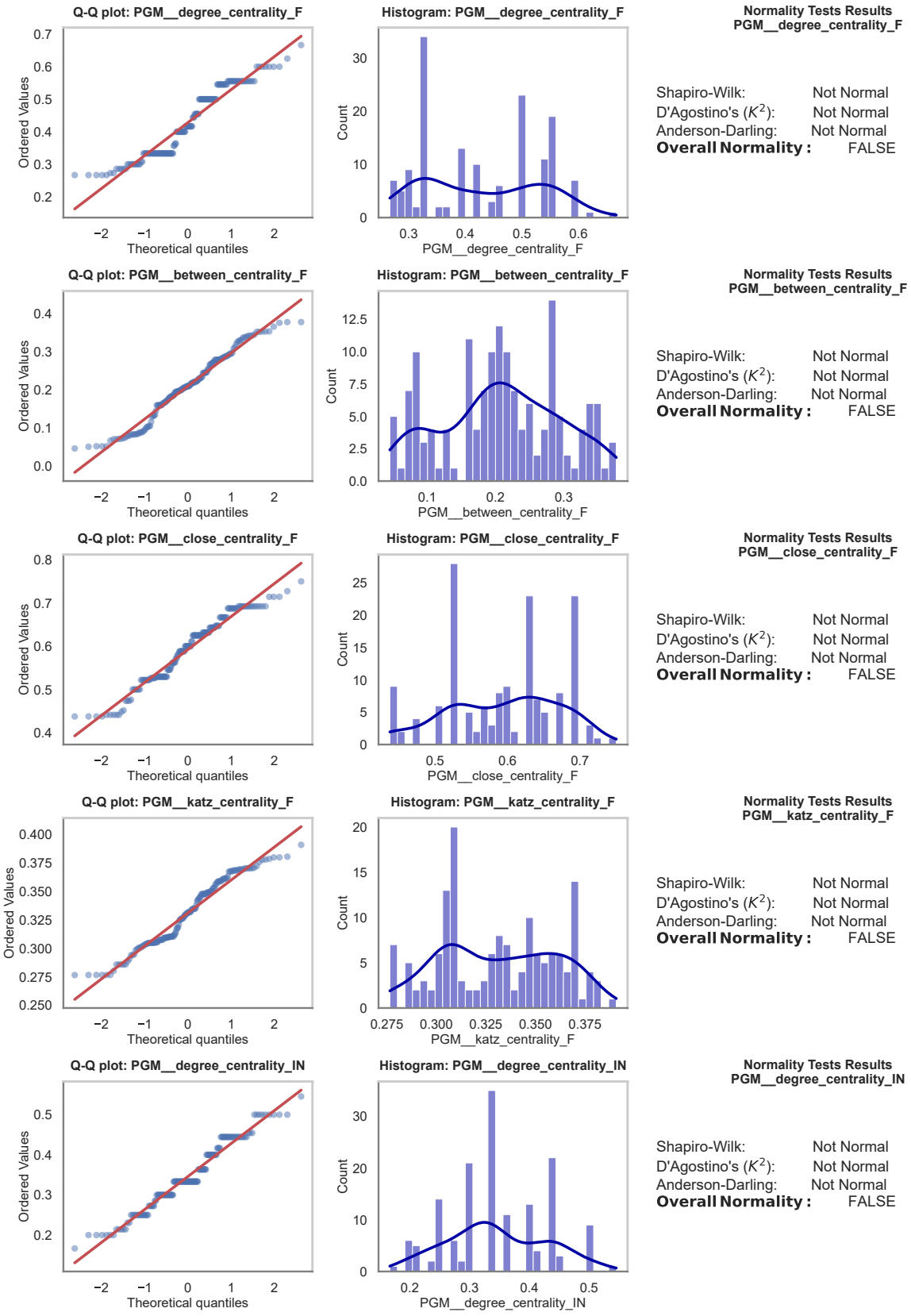

Source: Author.

Figure 302 – Normality Tests Results (16 of 24)

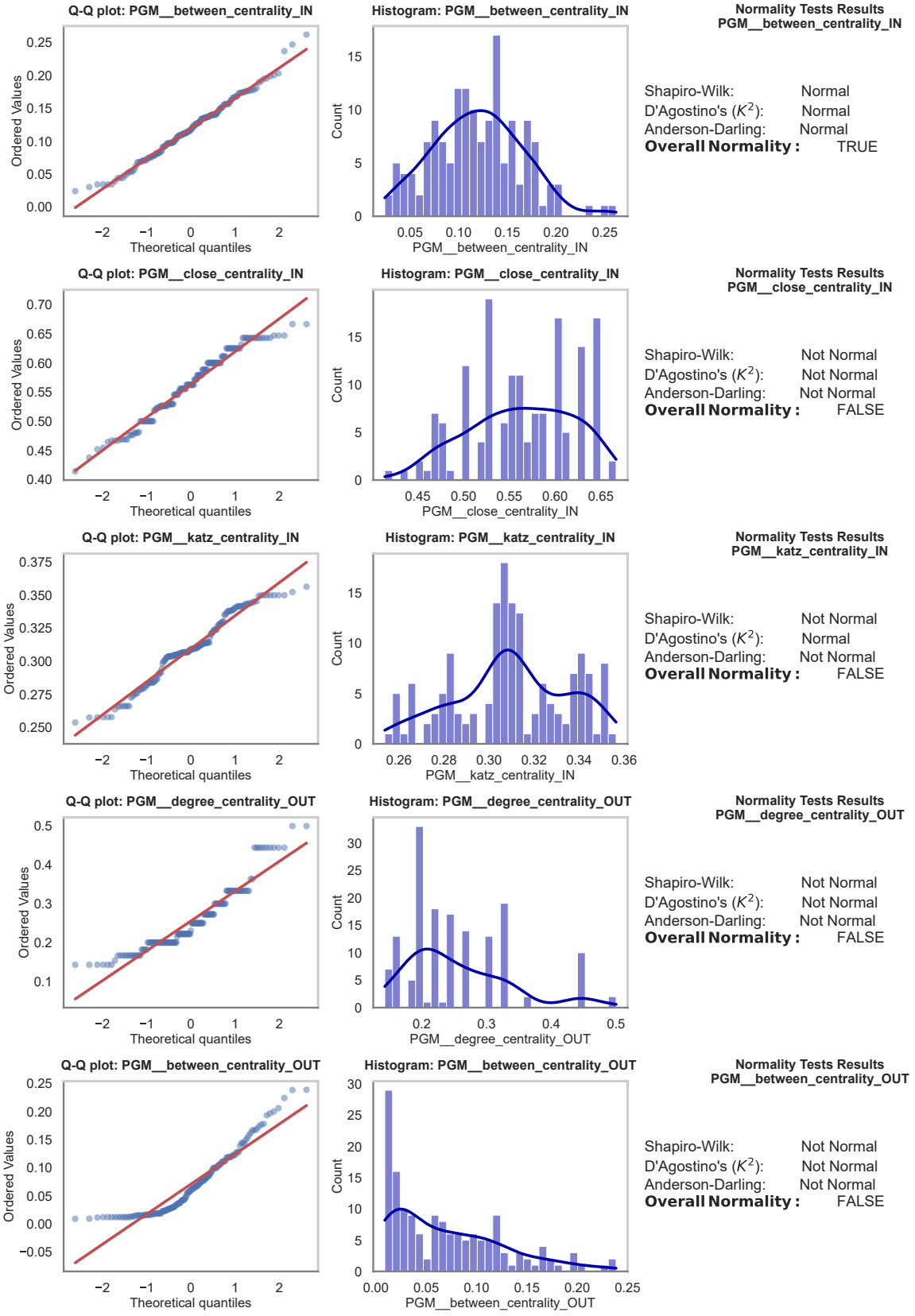

Source: Author.

Figure 303 – Normality Tests Results (17 of 24)

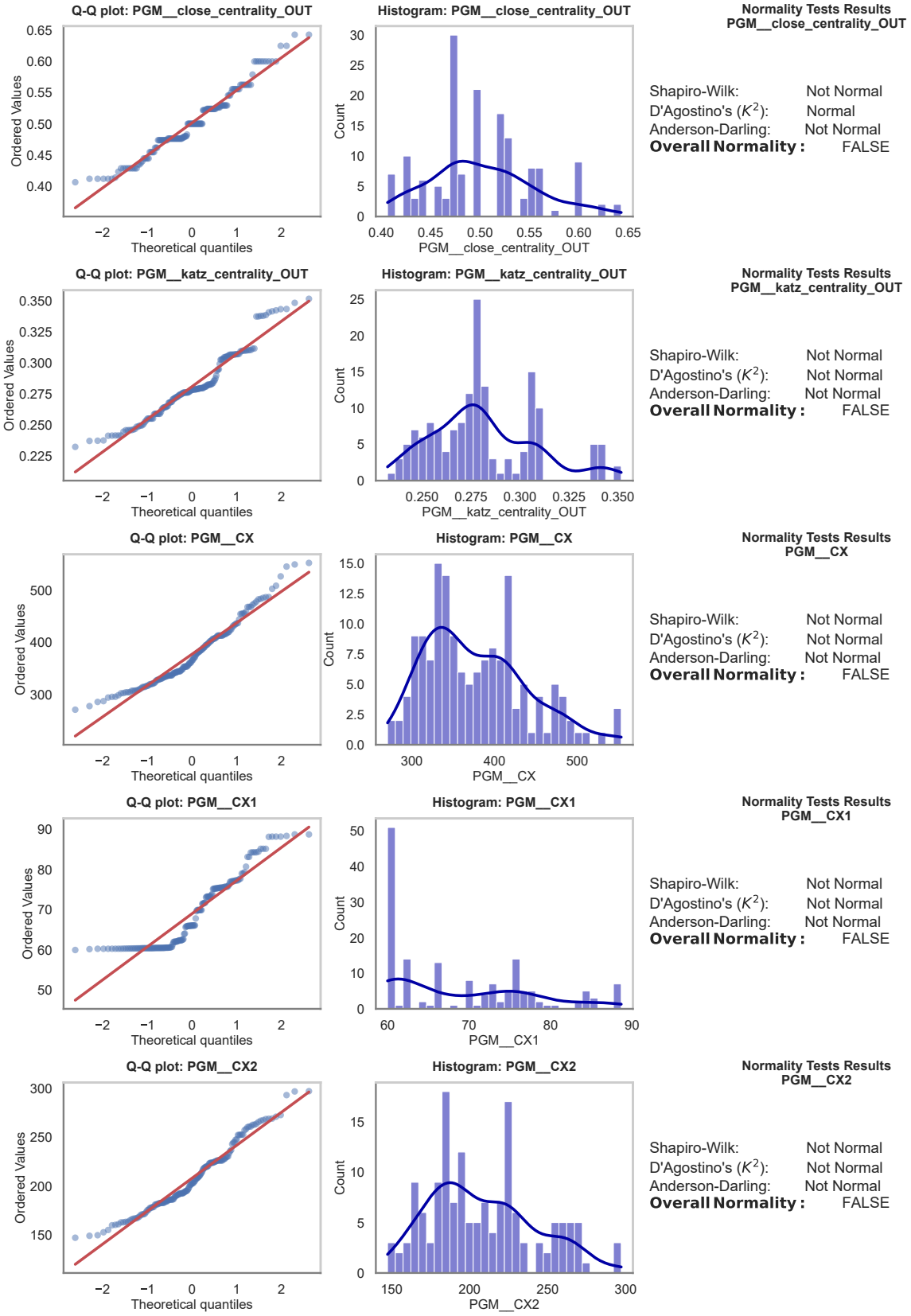

Source: Author.

Figure 304 – Normality Tests Results (18 of 24)

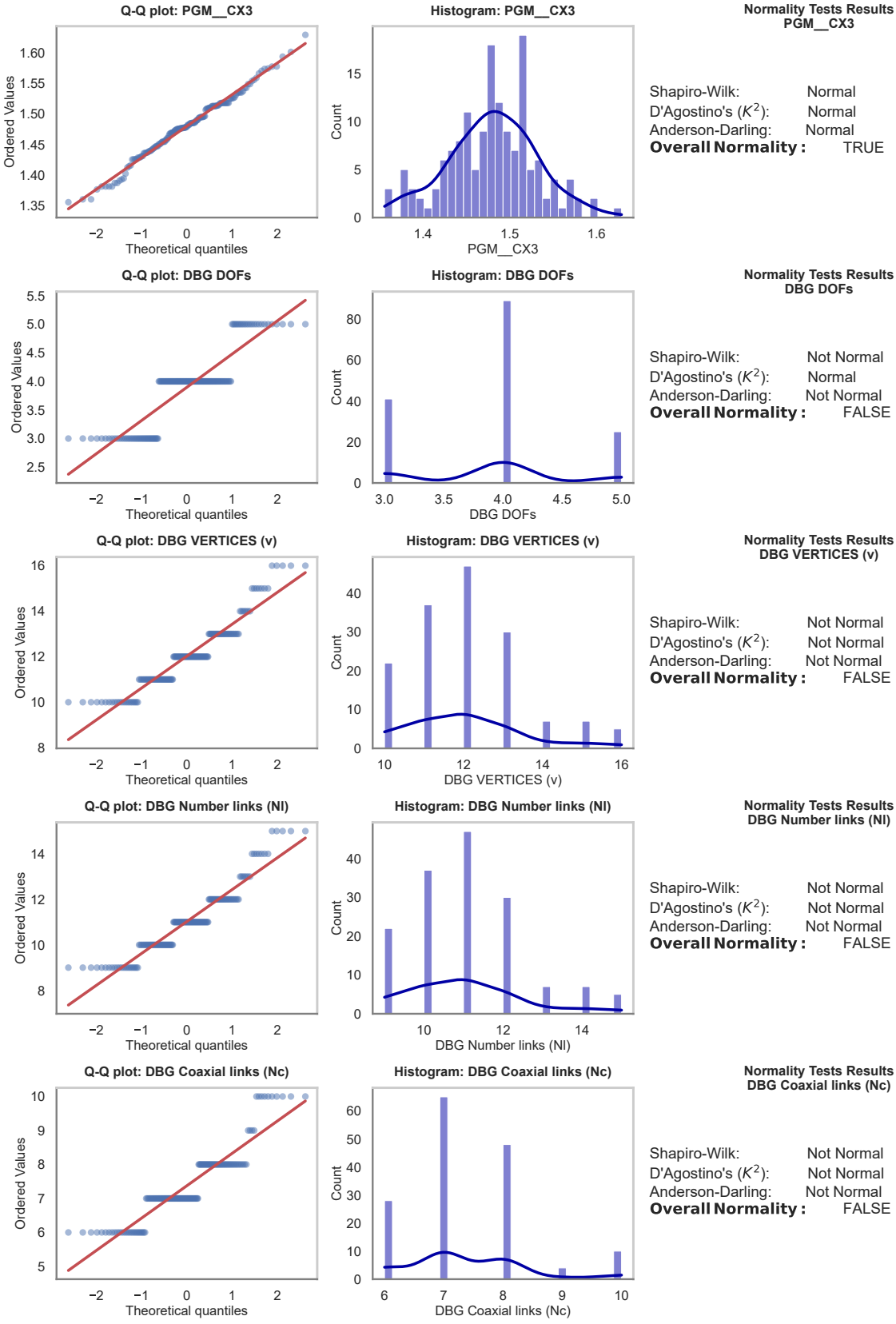

Source: Author.

Figure 305 – Normality Tests Results (19 of 24)

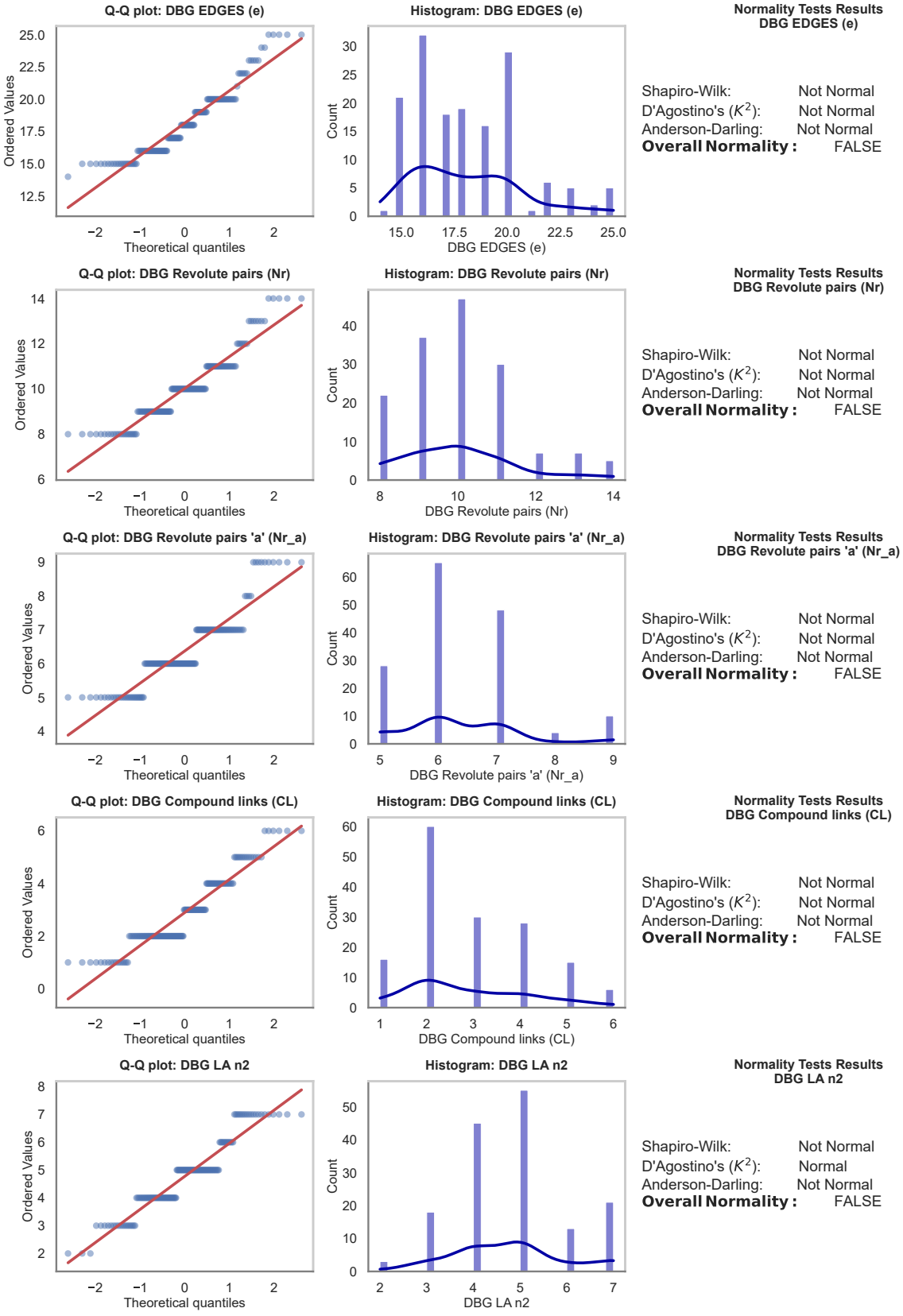

Source: Author.

Figure 306 – Normality Tests Results (20 of 24)

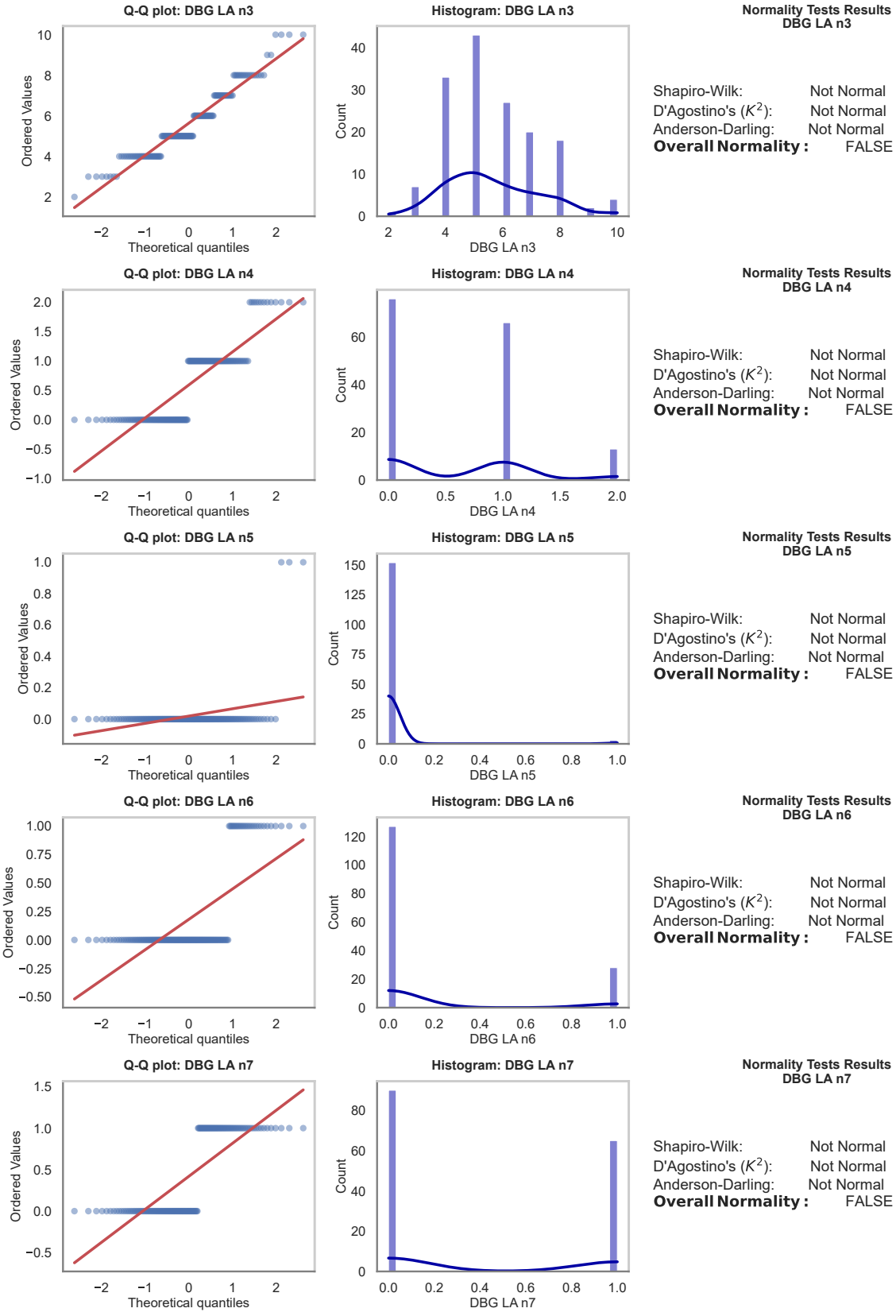

Source: Author.

Figure 307 – Normality Tests Results (21 of 24)

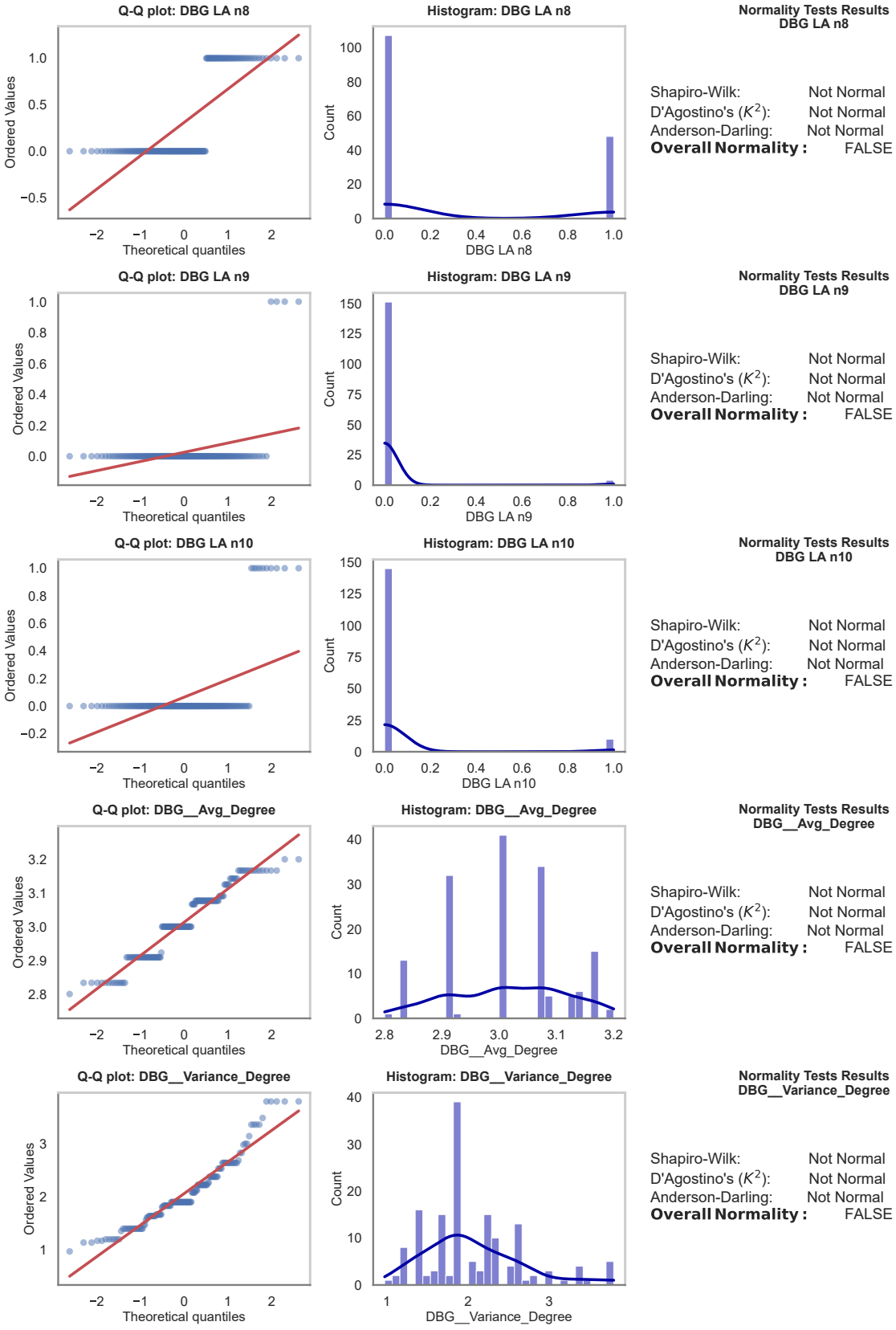

Source: Author.

Figure 308 – Normality Tests Results (22 of 24)

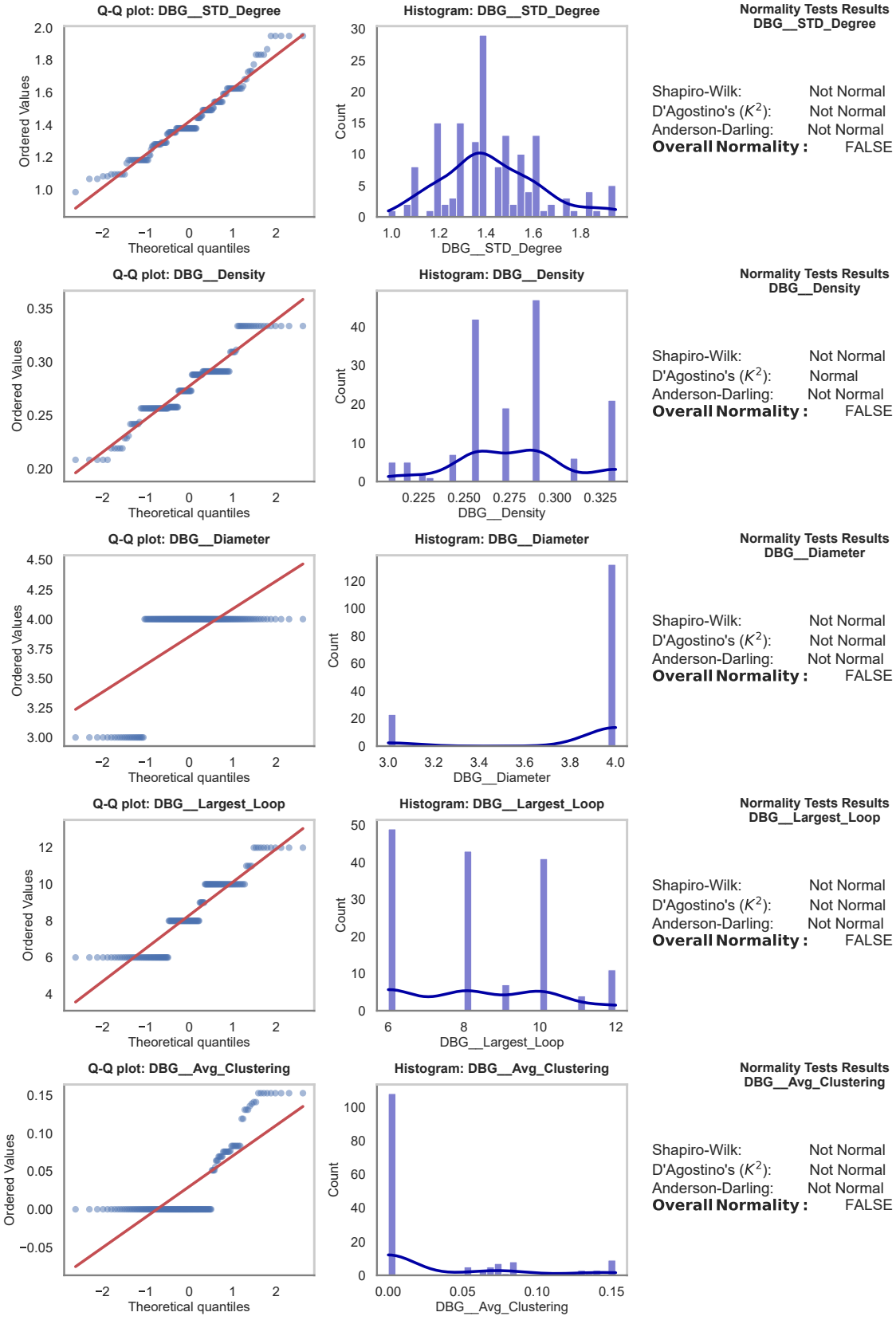

Source: Author.

Figure 309 – Normality Tests Results (23 of 24)

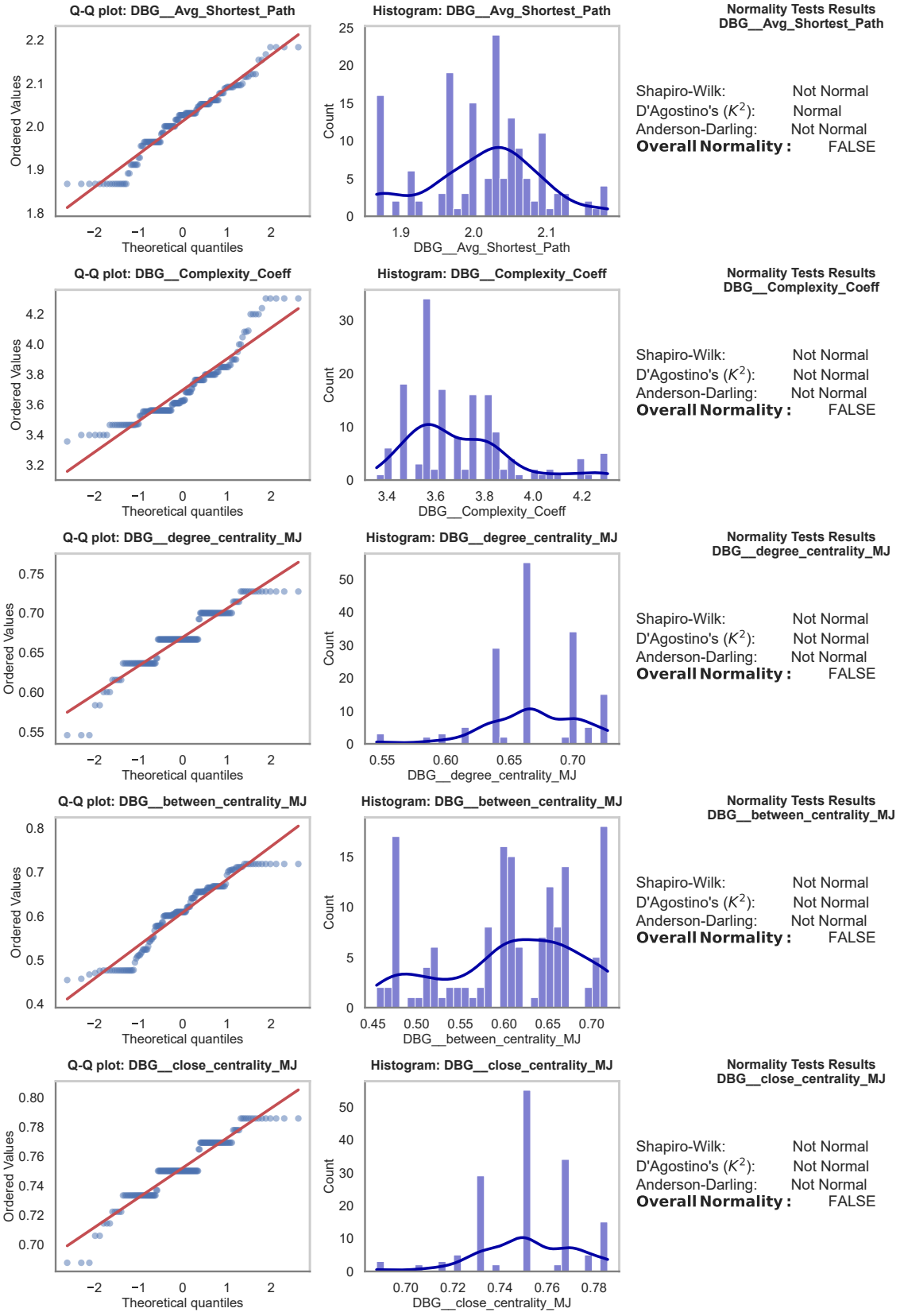

Source: Author.

Figure 310 – Normality Tests Results (24 of 24)

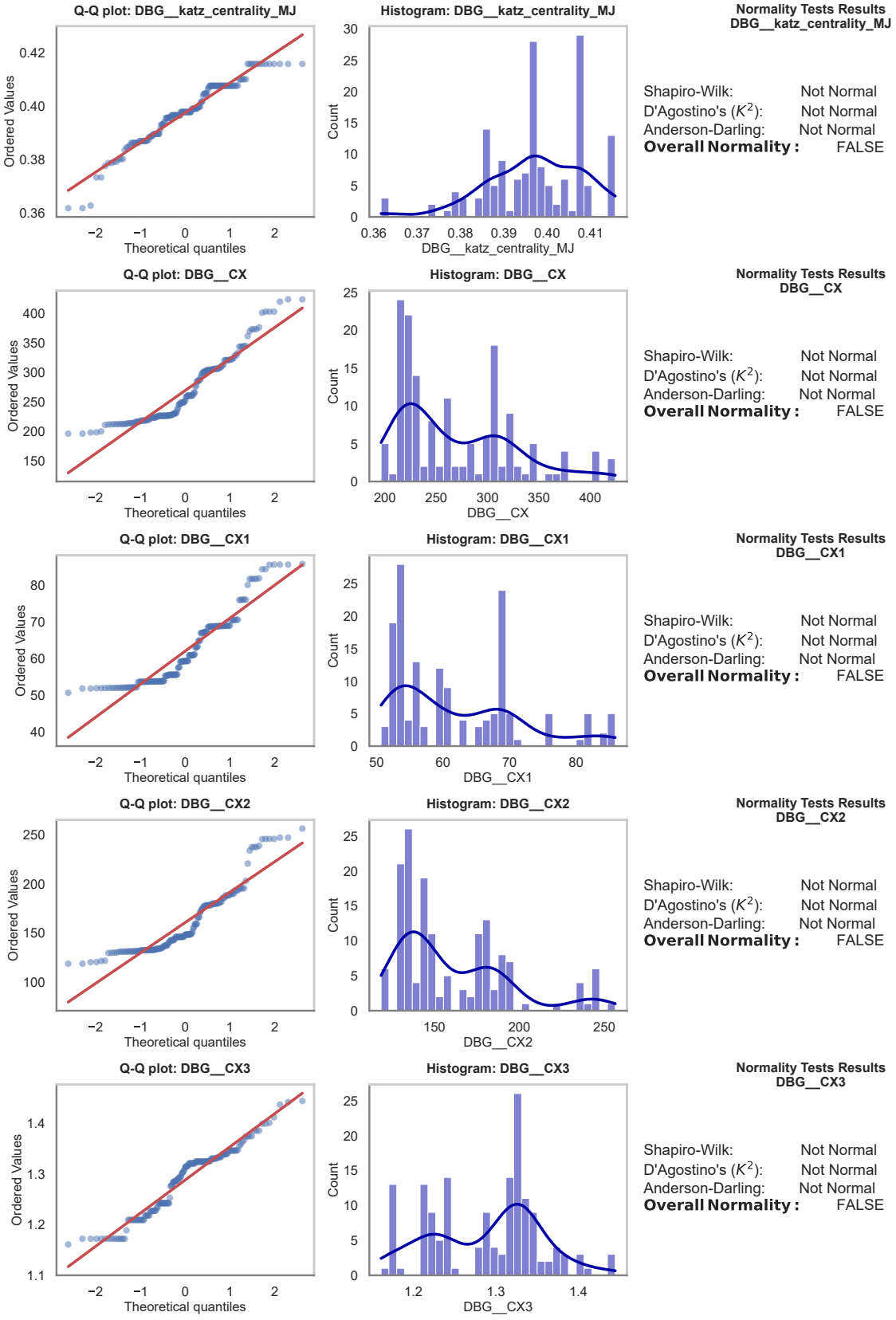

Source: Author.

B.2 RESULTS OF BIVARIATE DATA ANALYSIS

The complete features correlation heatmap is very large. To enhance its readability, it was divided into 15 sections, as illustrated in Figure 311.

Figure 311 – Correlation Heatmap Slice Map

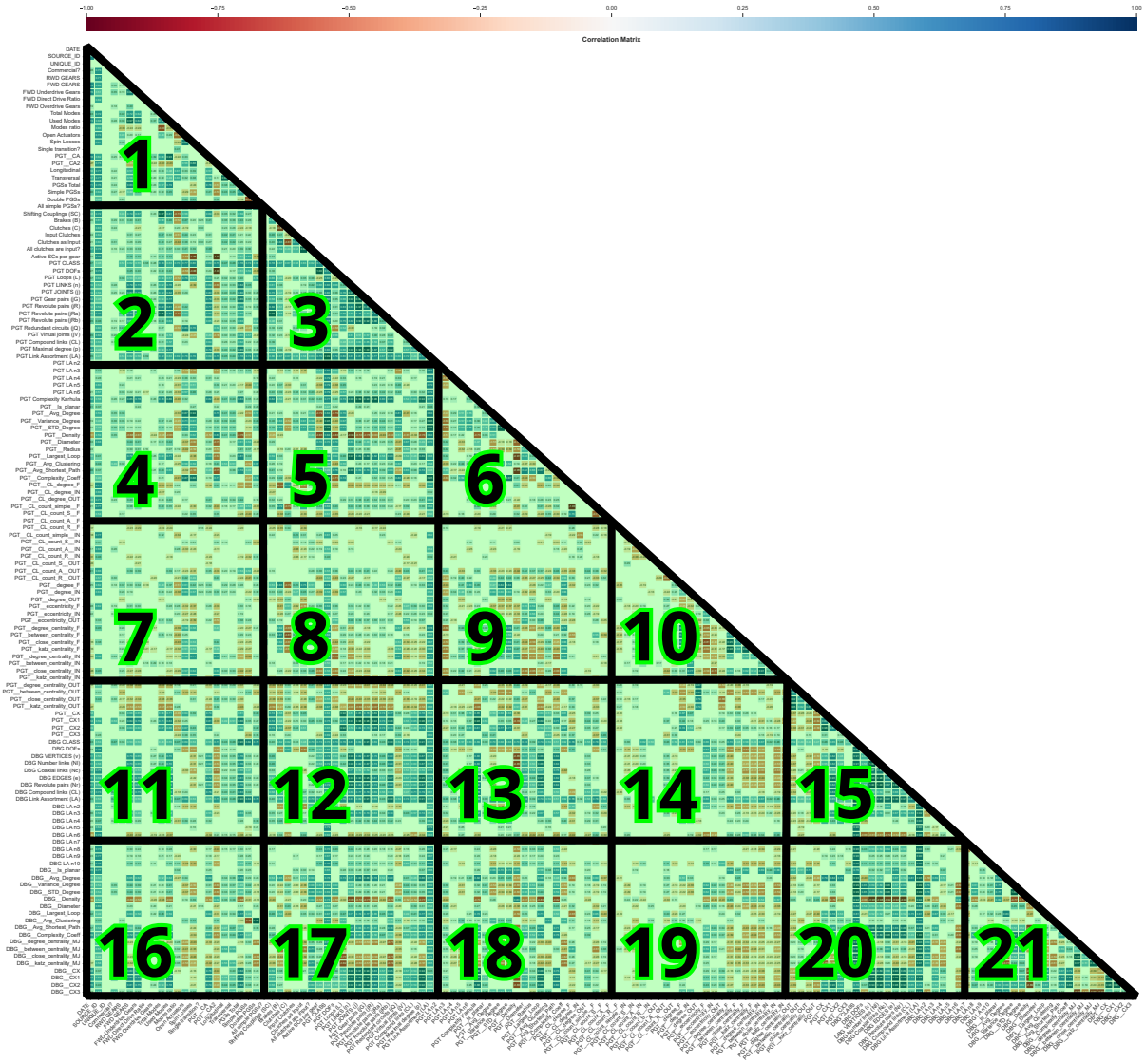

Source: Author.

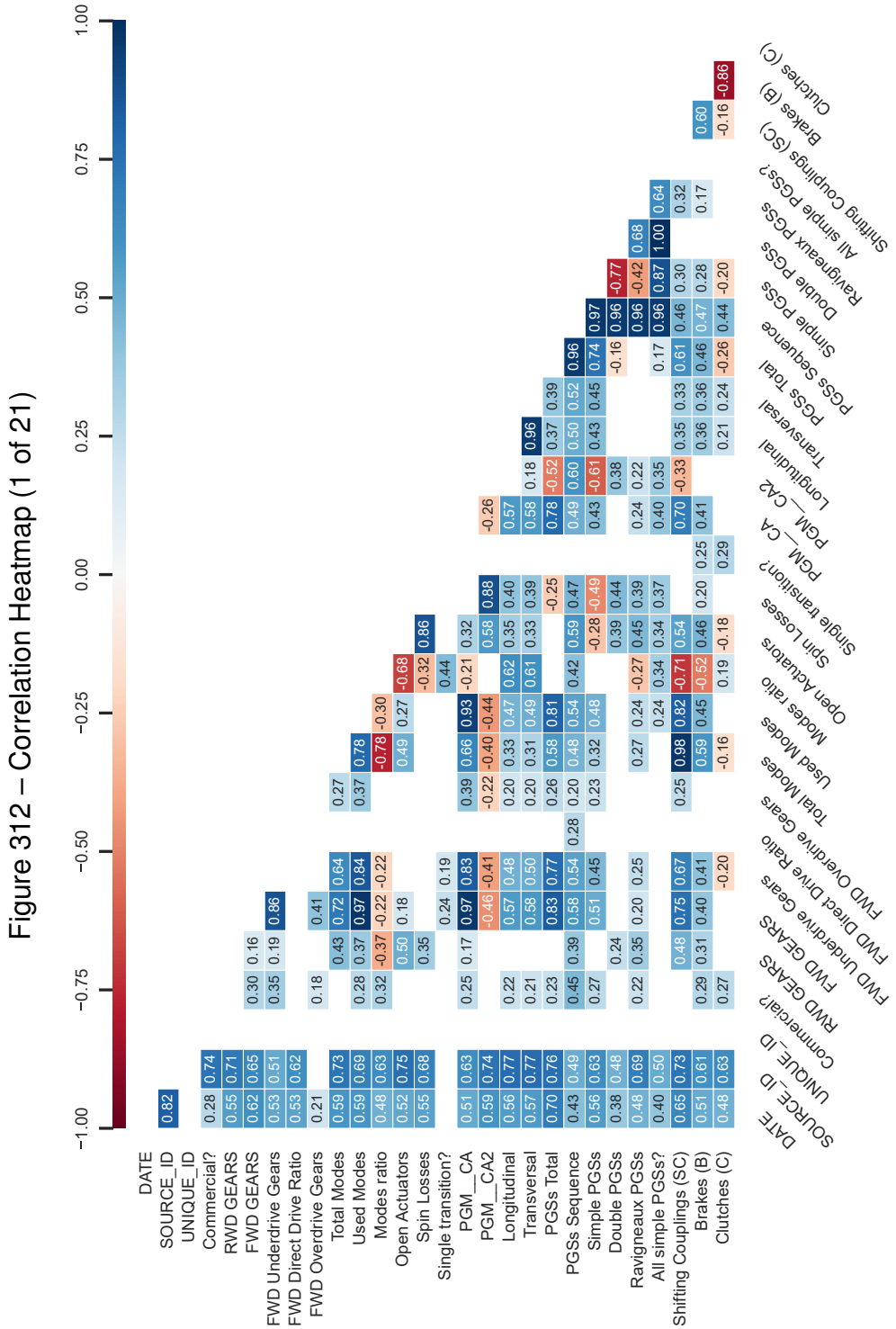

Source: Author.

Figure 313 – Correlation Heatmap (2 of 21)

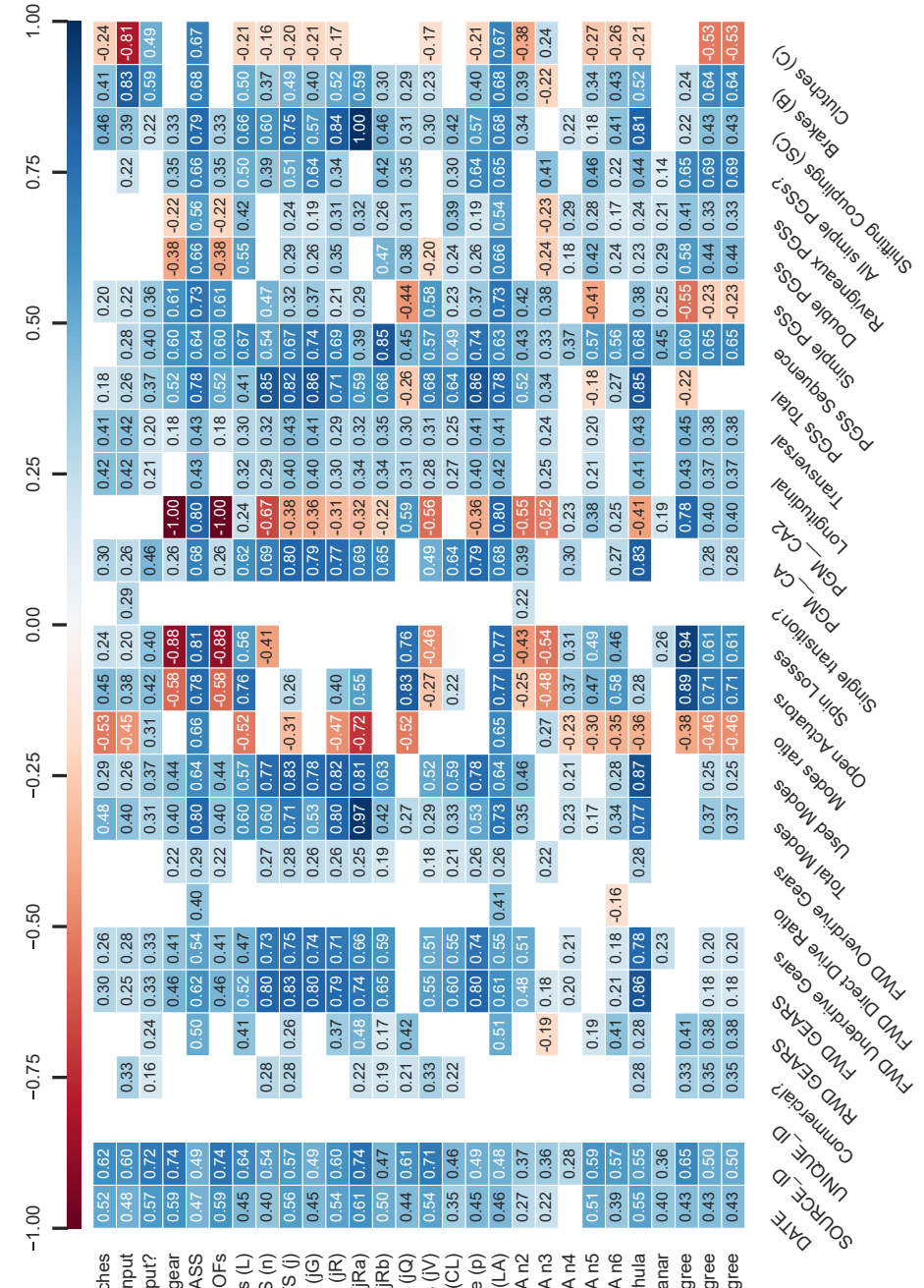

Source: Author.

Figure 314 – Correlation Heatmap (3 of 21)

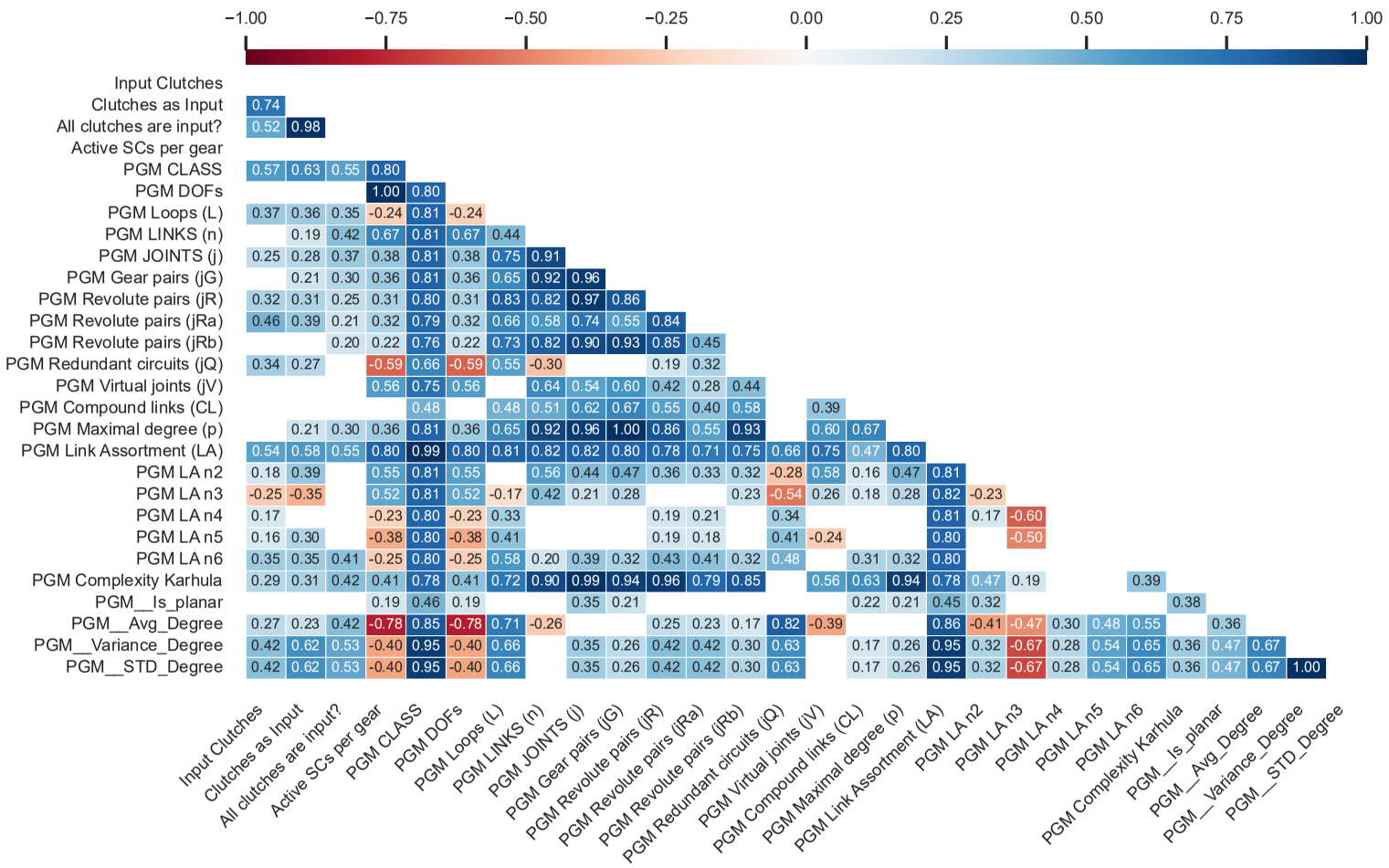

Source: Author.

Figure 315 – Correlation Heatmap (4 of 21)

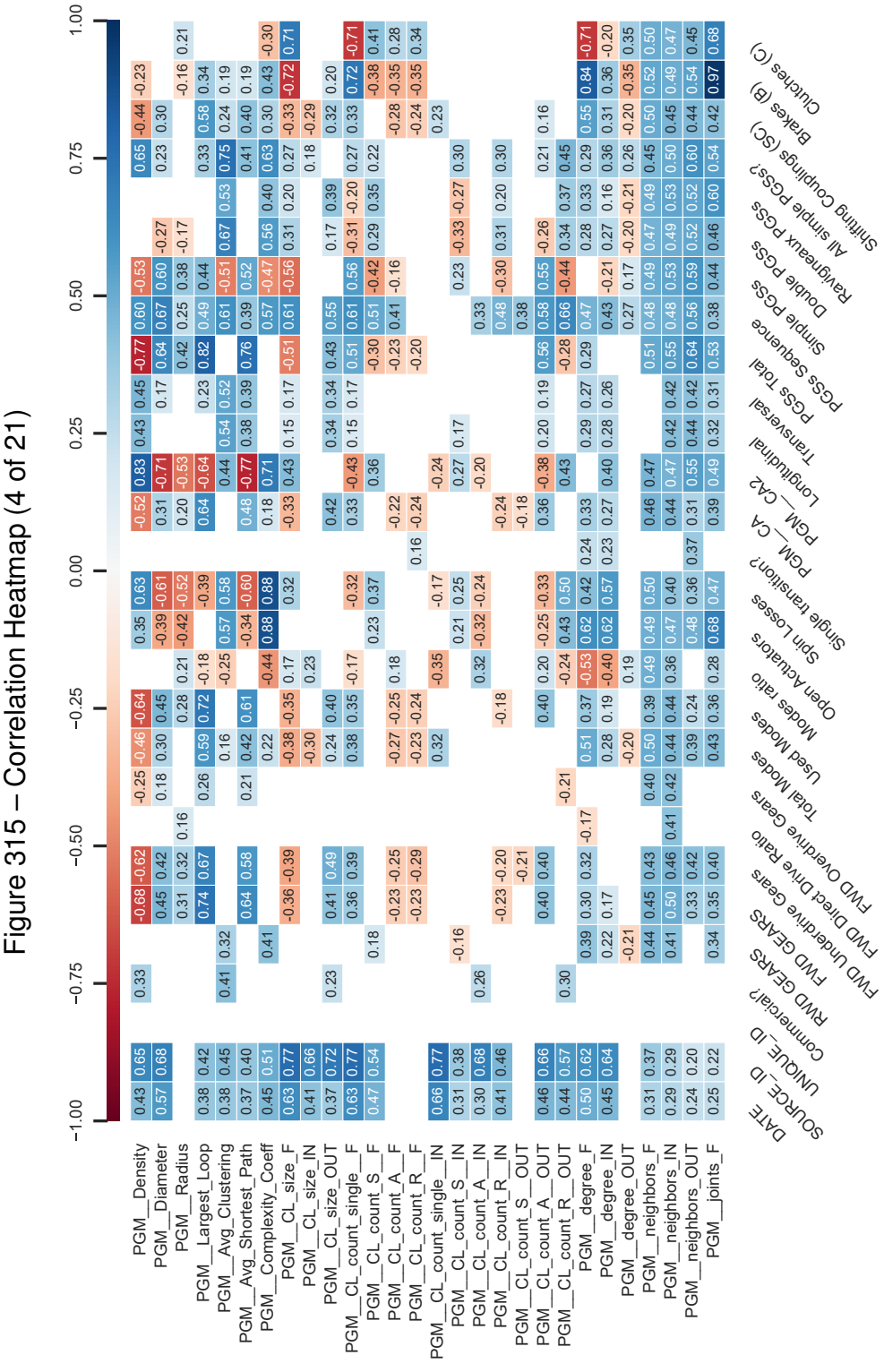

Source: Author.

Figure 316 – Correlation Heatmap (5 of 21)

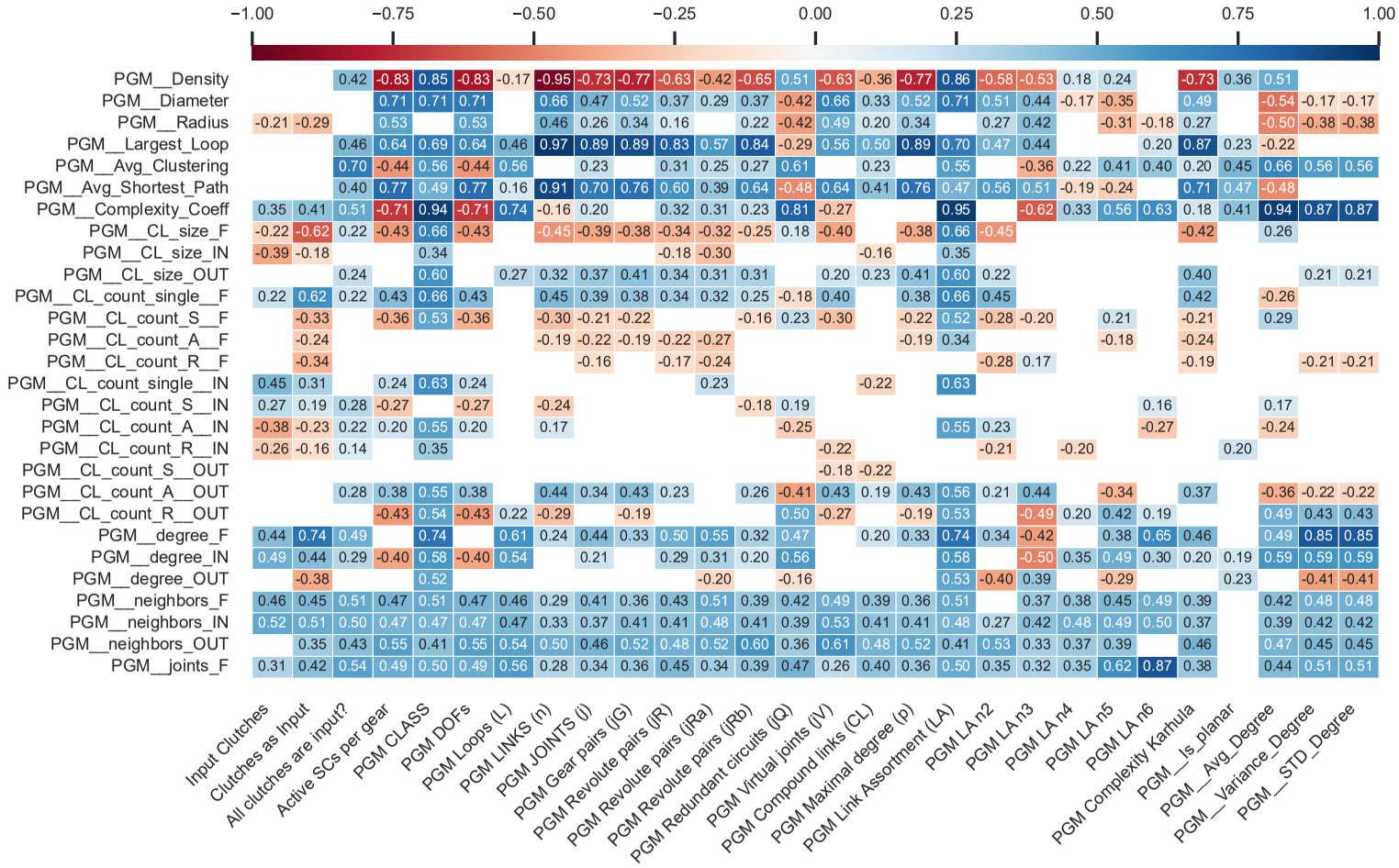

Source: Author.

Figure 317 – Correlation Heatmap (6 of 21)

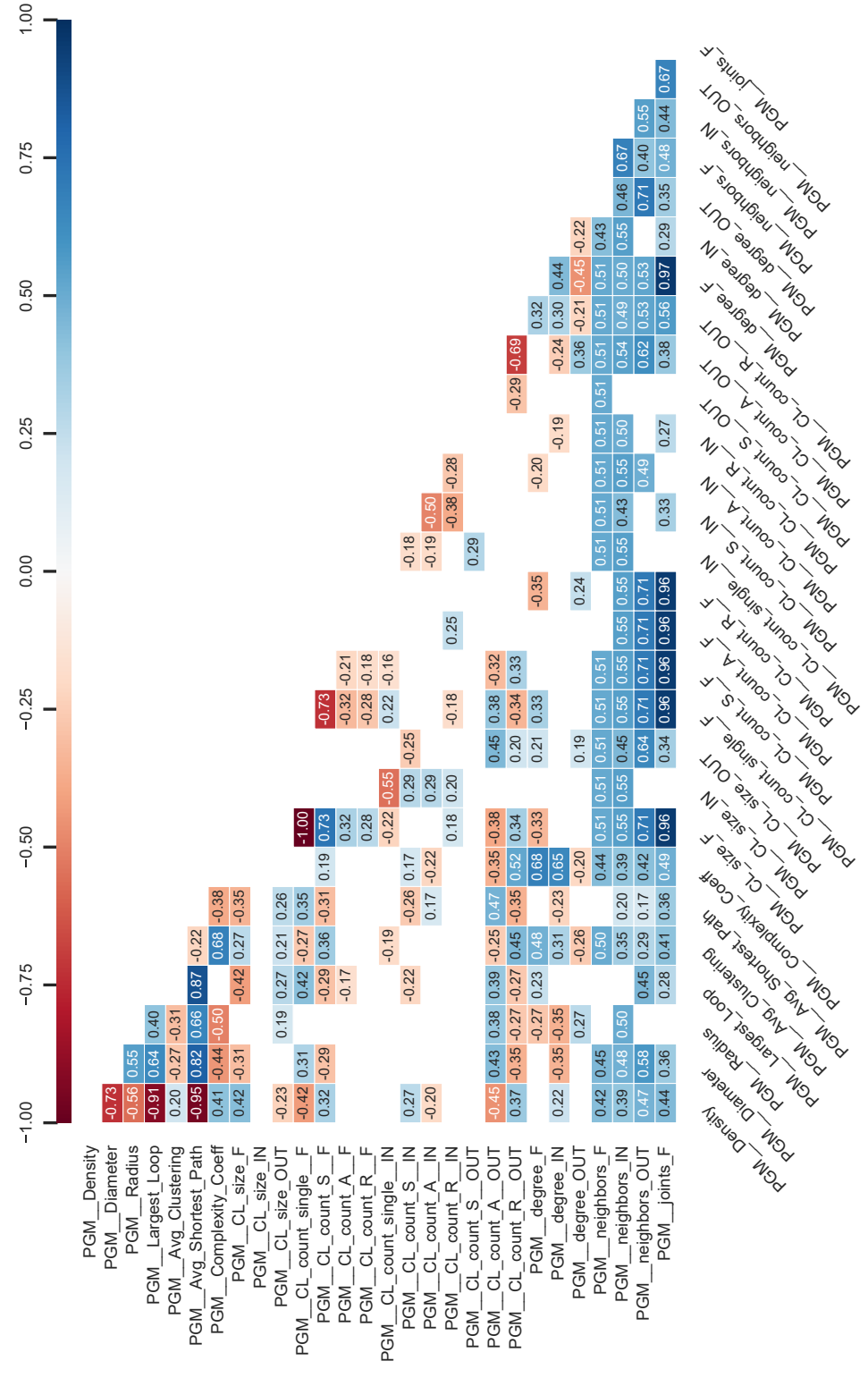

Source: Author.

Figure 318 – Correlation Heatmap (7 of 21)

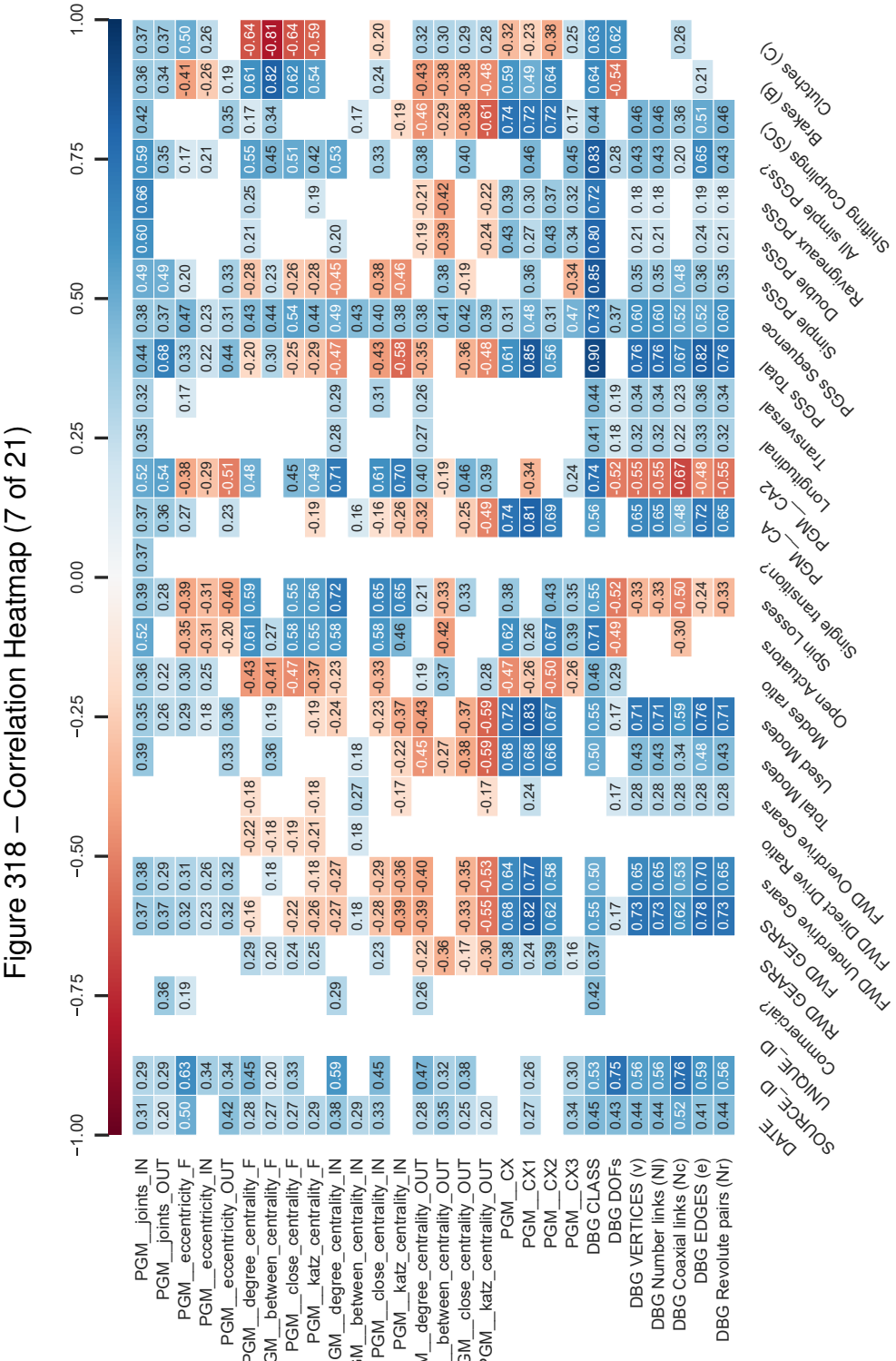

Source: Author.

Figure 319 – Correlation Heatmap (8 of 21)

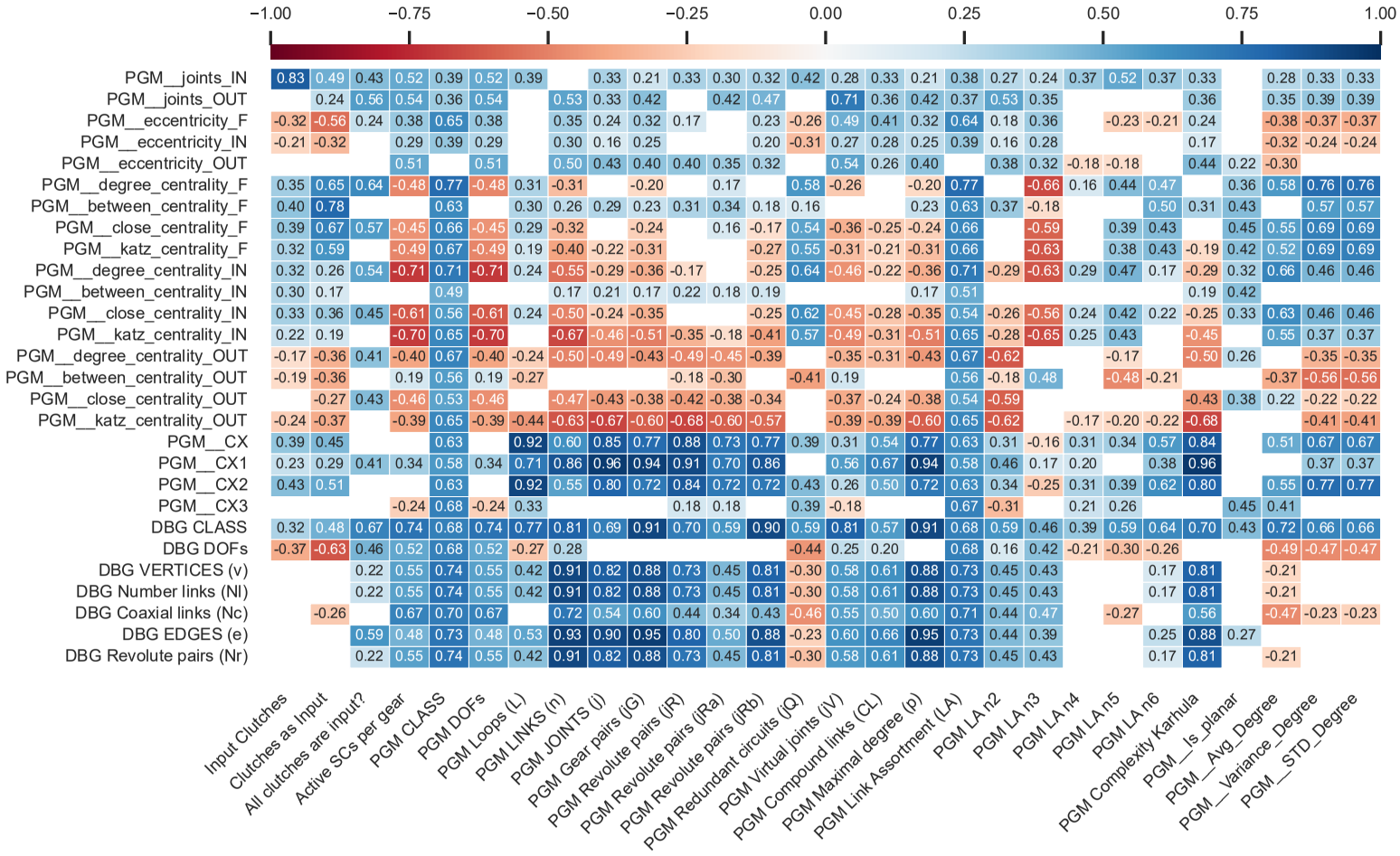

Source: Author.

Figure 320 – Correlation Heatmap (9 of 21)

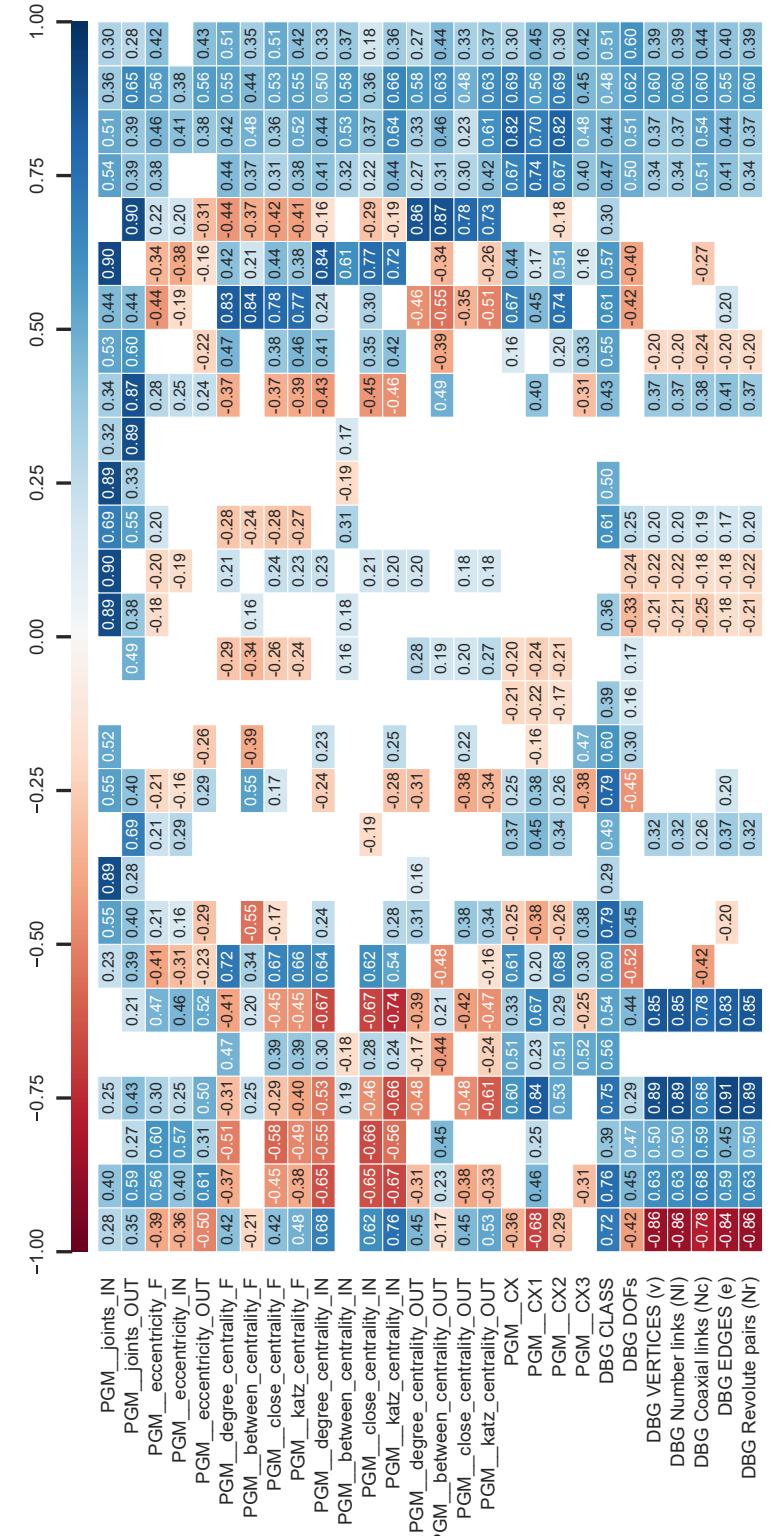

Source: Author.

Figure 321 – Correlation Heatmap (10 of 21)

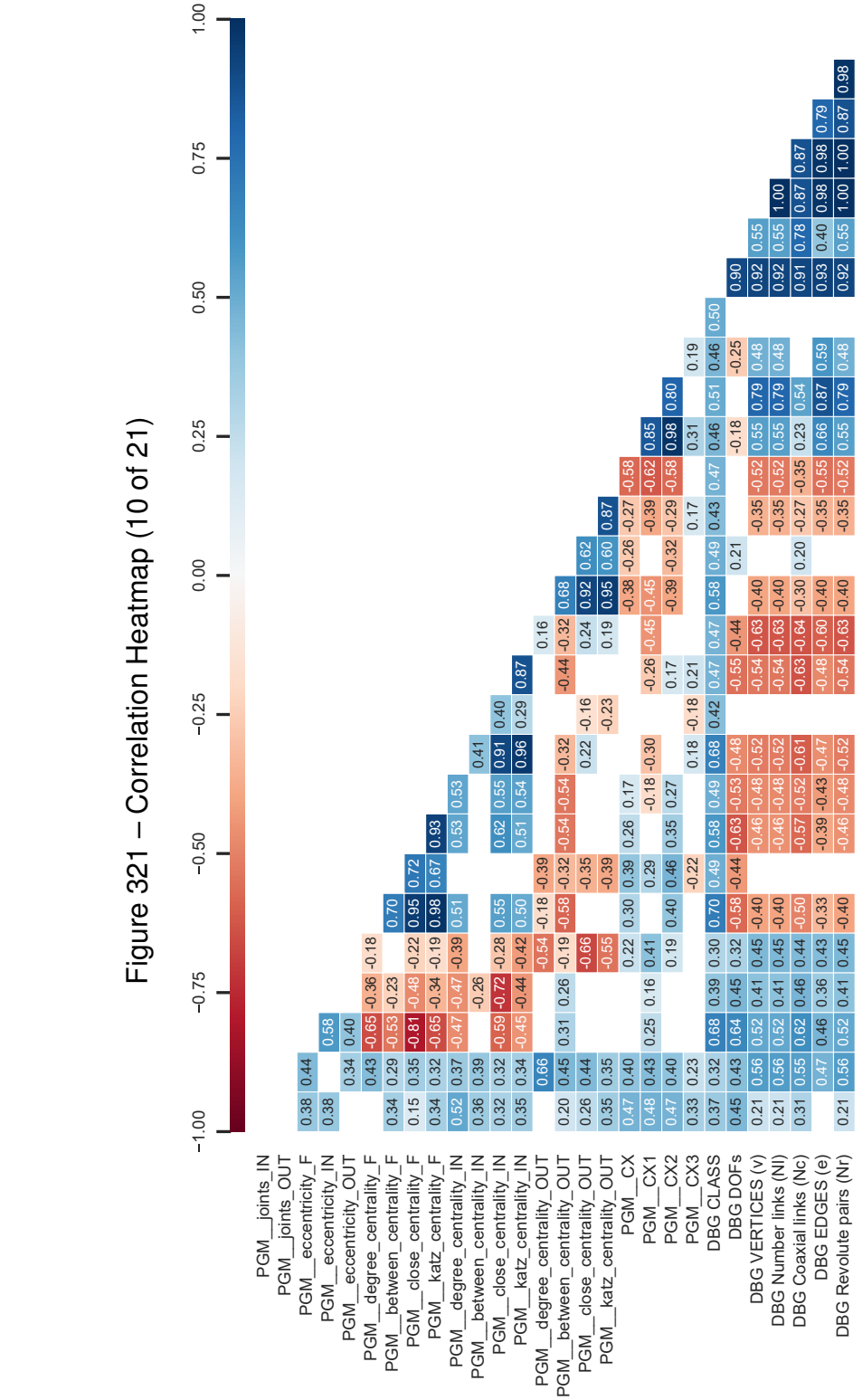

Source: Author.

Figure 322 – Correlation Heatmap (11 of 21)

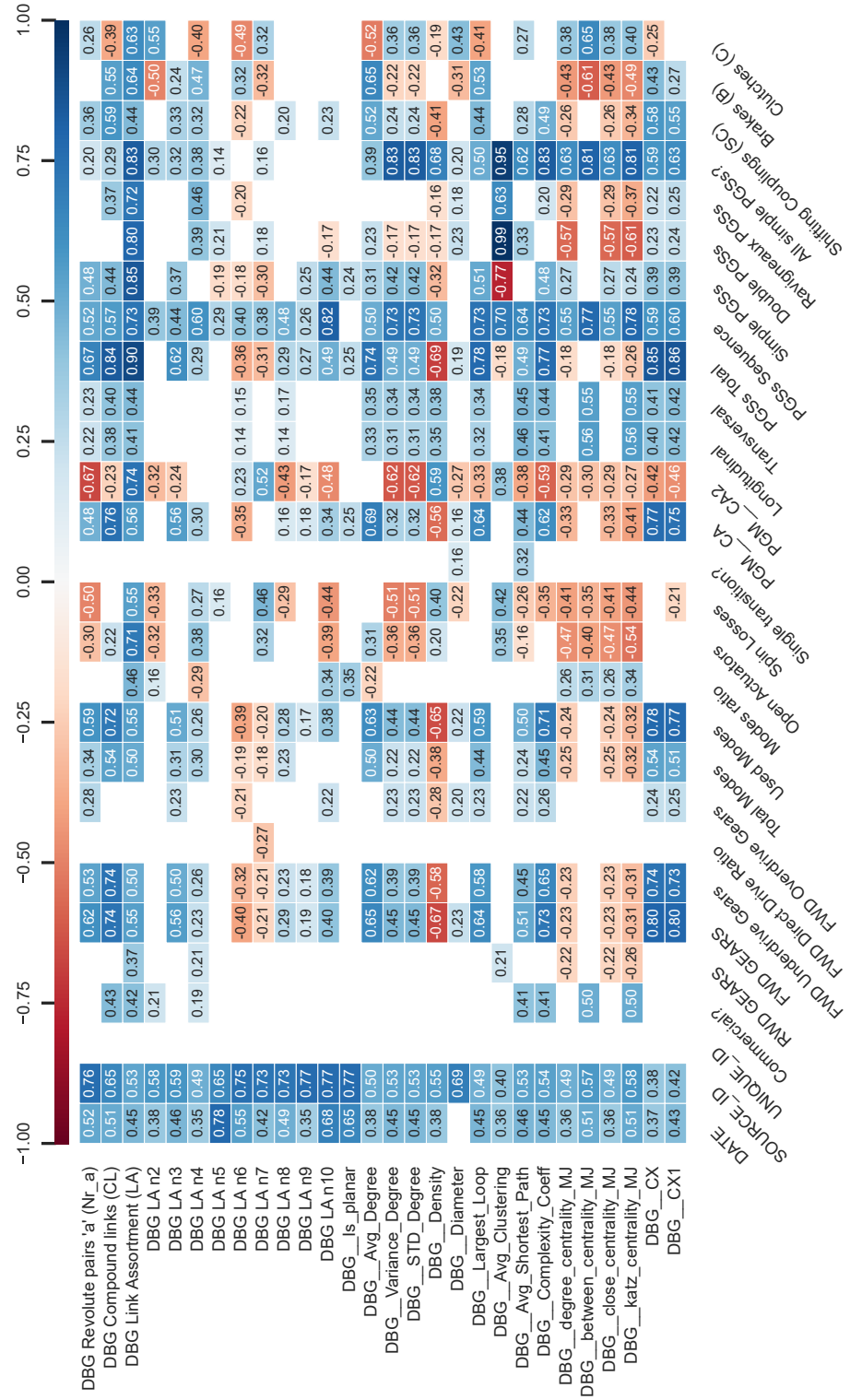

Source: Author.

Figure 323 – Correlation Heatmap (12 of 21)

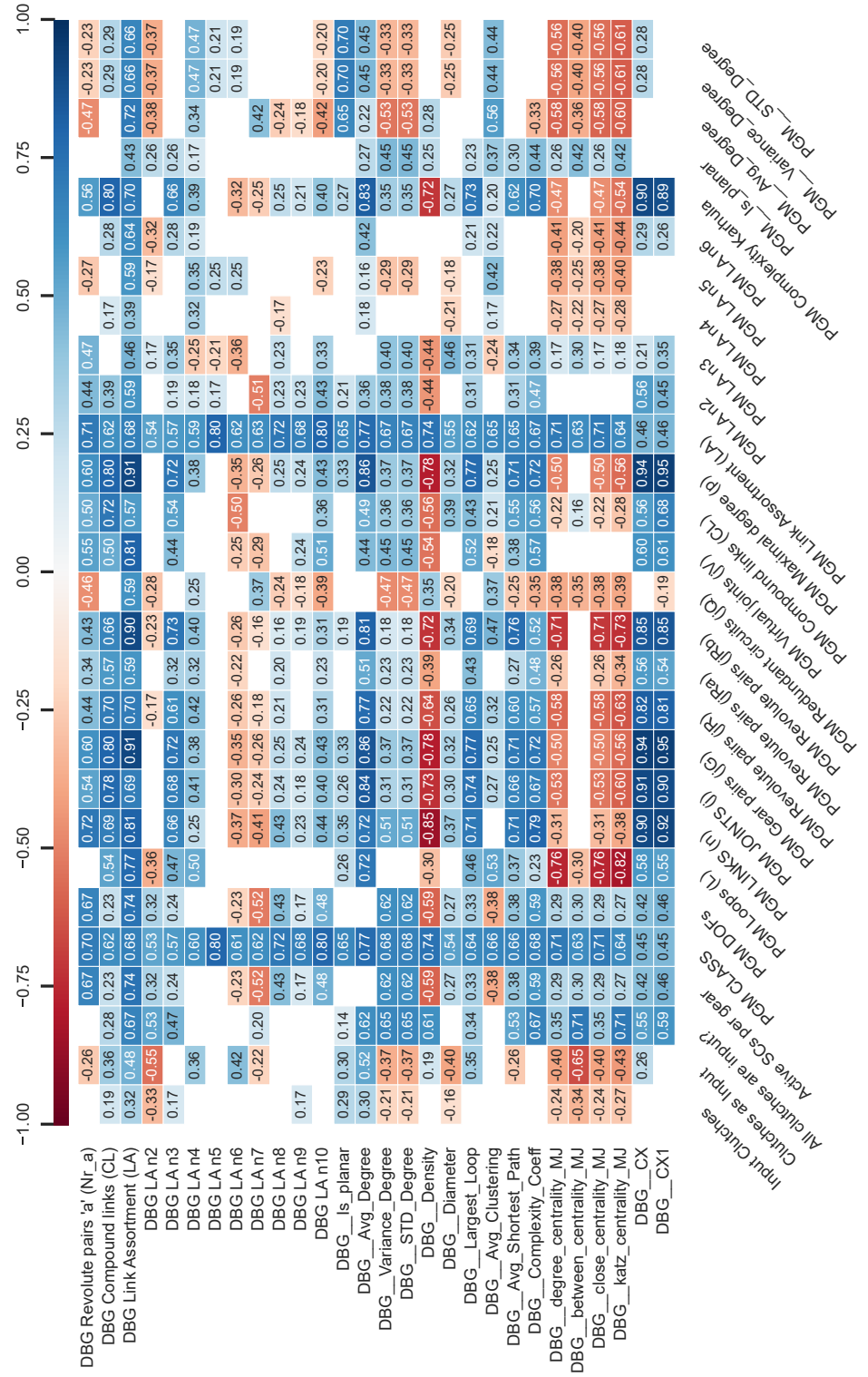

Source: Author.

Figure 324 – Correlation Heatmap (13 of 21)

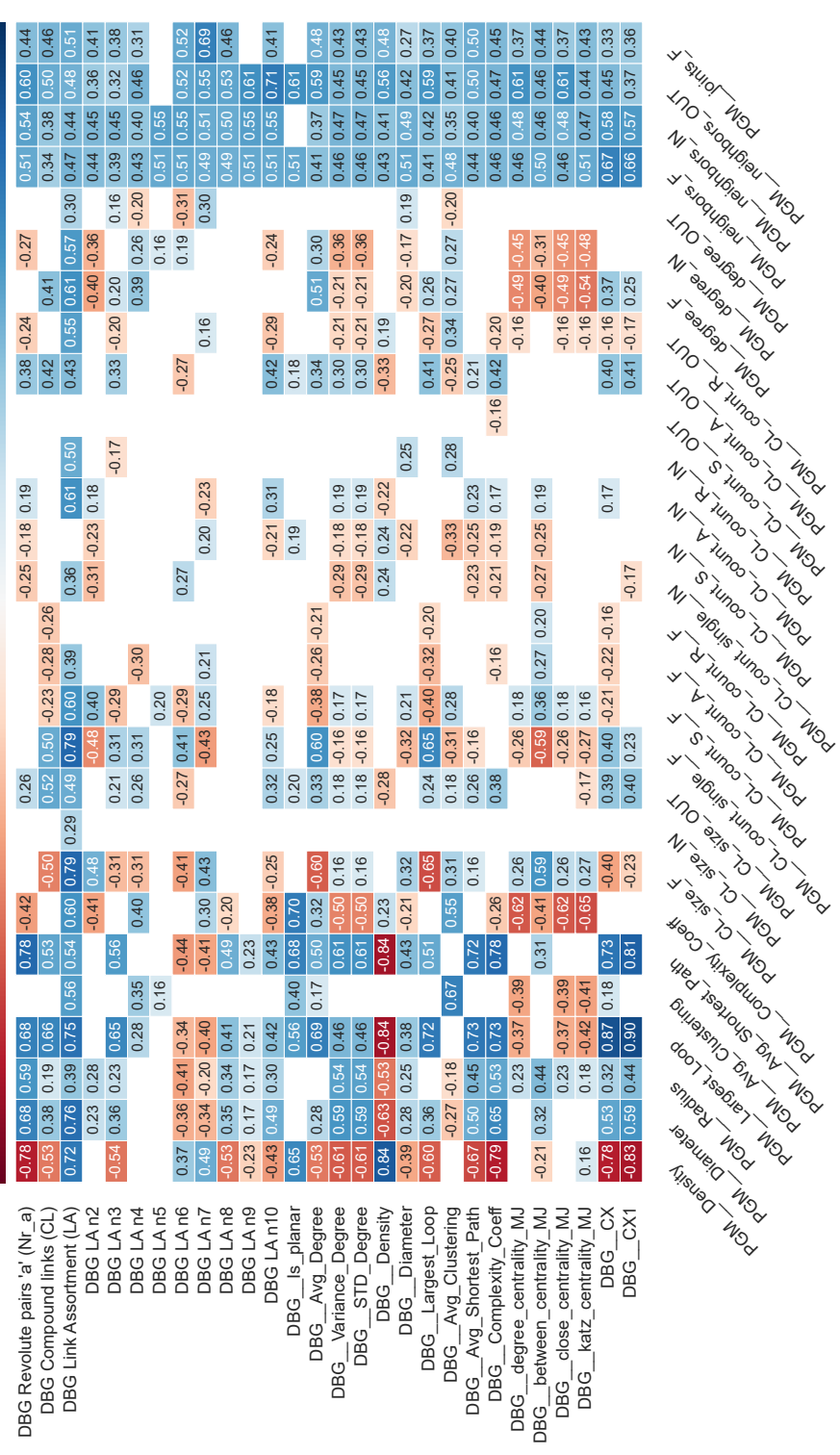

Source: Author.

Figure 325 – Correlation Heatmap (14 of 21)

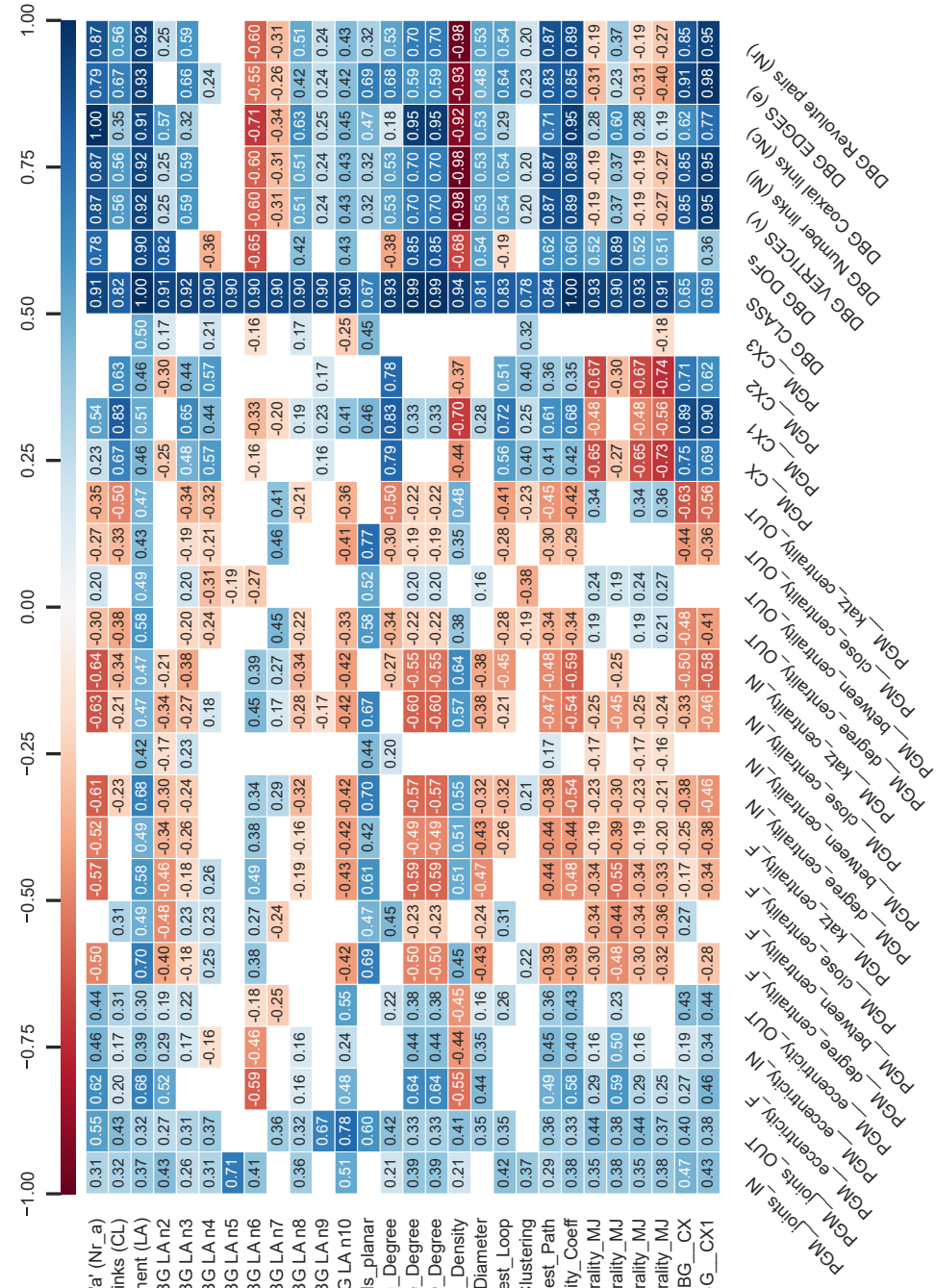

Source: Author.

Figure 326 – Correlation Heatmap (15 of 21)

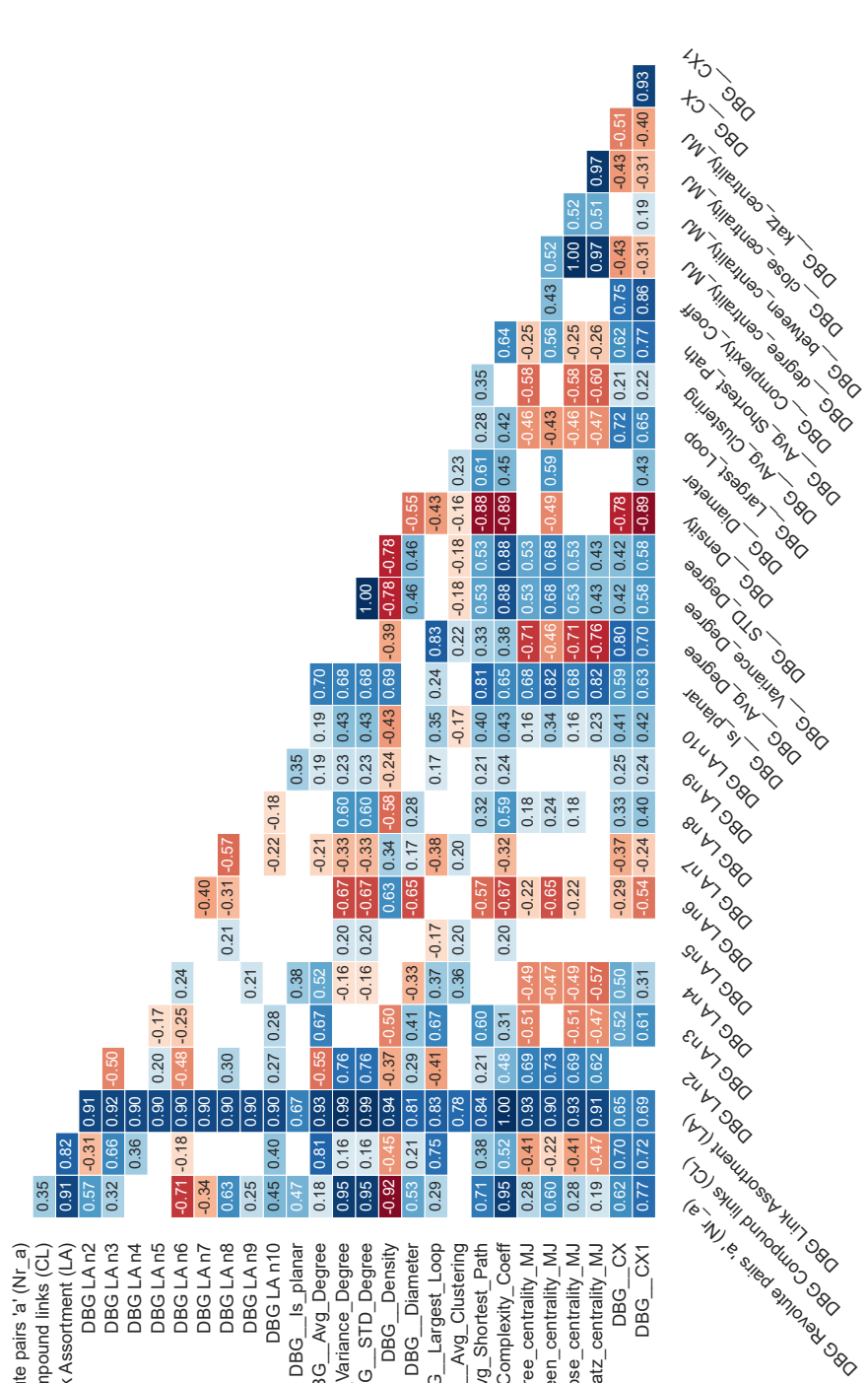

Source: Author.

Figure 327 – Correlation Heatmap (16 of 21)

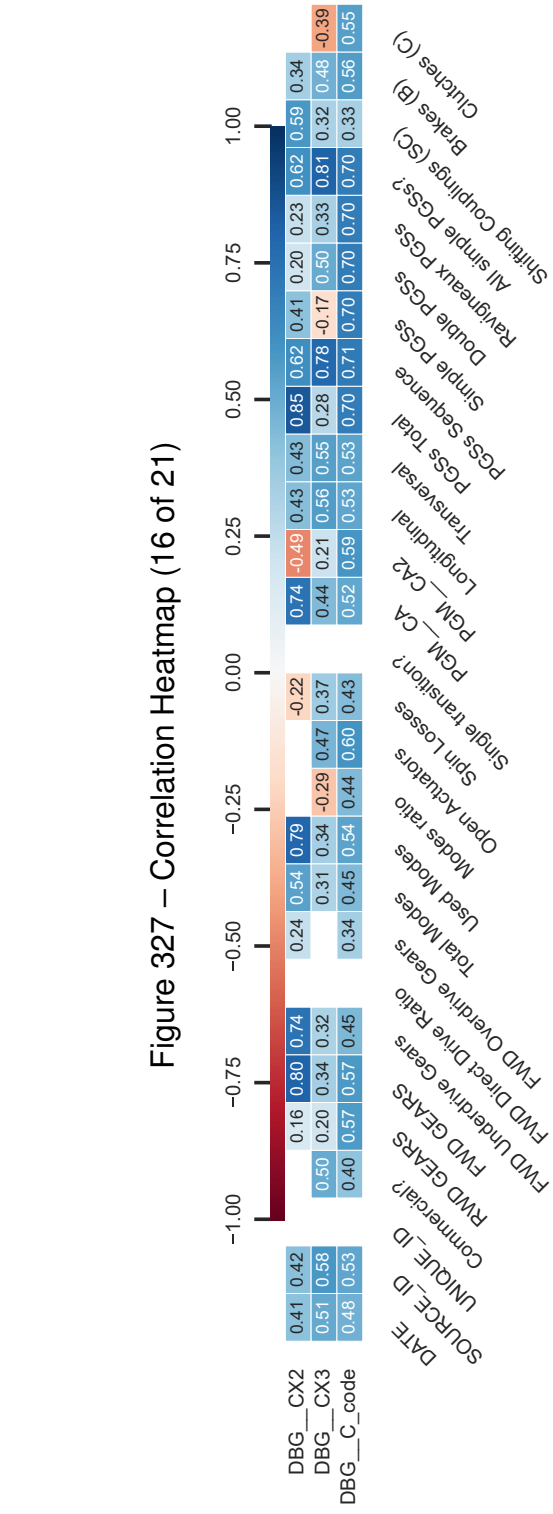

Source: Author.

Figure 328 – Correlation Heatmap (17 of 21)

Source: Author.

Figure 329 – Correlation Heatmap (18 of 21)

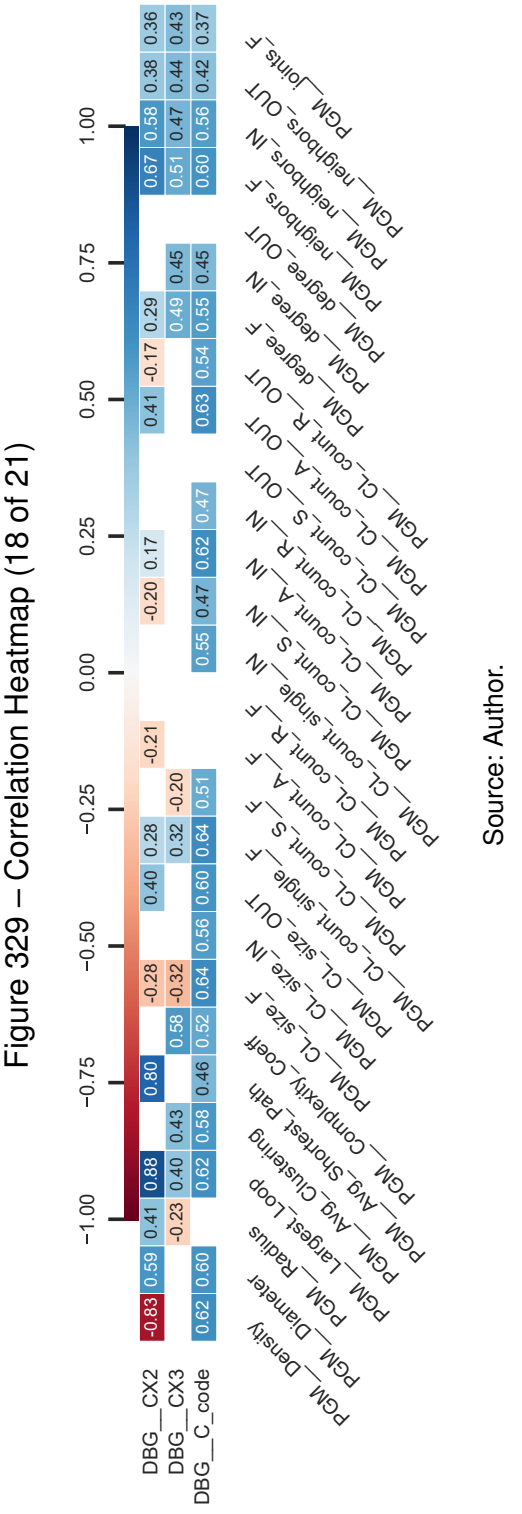

Source: Author.

Figure 330 – Correlation Heatmap (19 of 21)

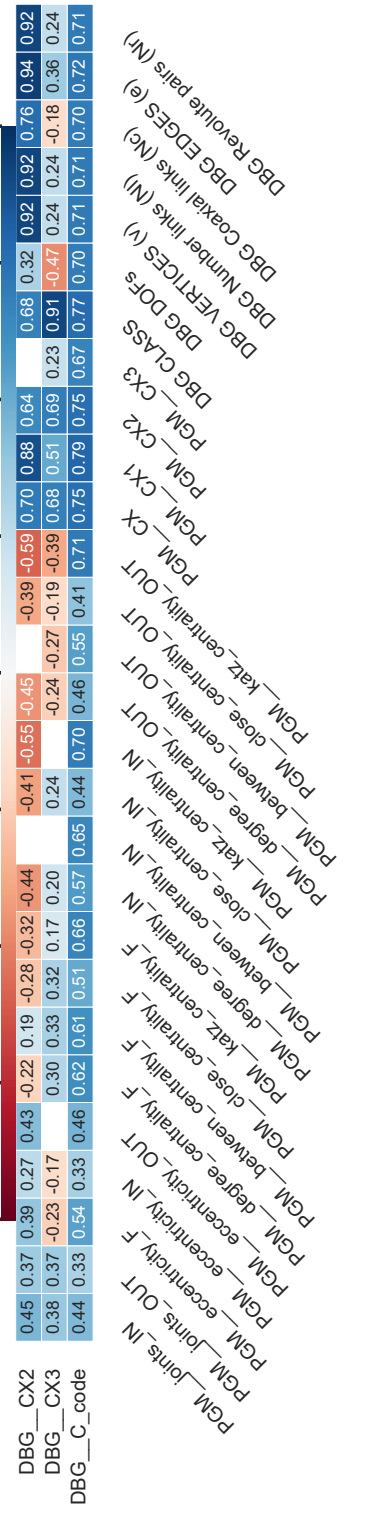

Source: Author.

Figure 331 – Correlation Heatmap (20 of 21)

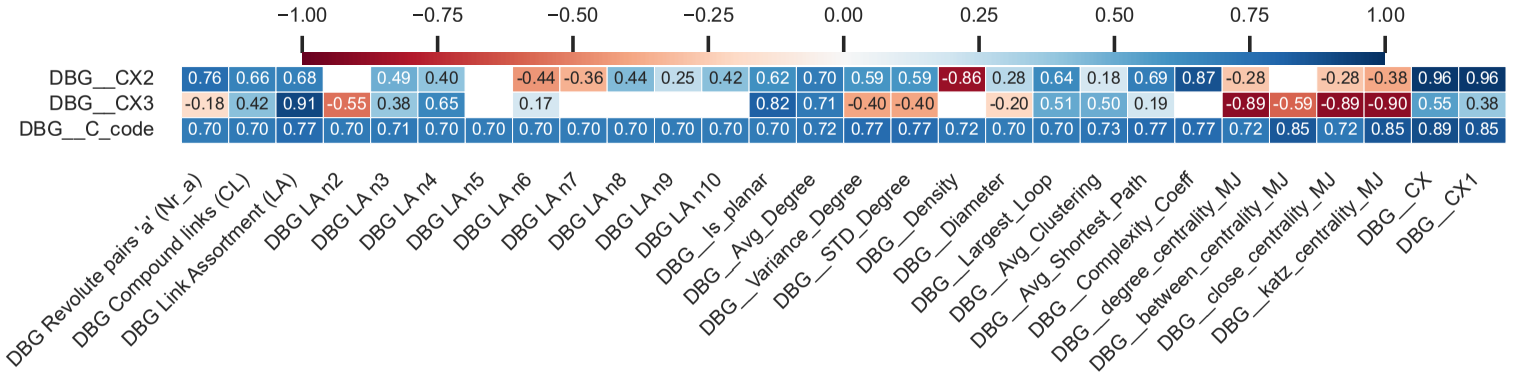

Source: Author.

Figure 332 – Correlation Heatmap (21 of 21)

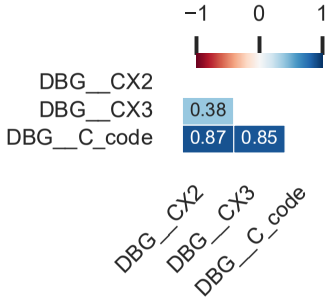

Source: Author.

B.2.1 Perfectly Correlated Features

In this section, excerpts from the complete heatmap (Appendix B.2), showcasing positive and negative perfectly correlated features, are presented.

Figure 333 – Perfectly Correlated Features (1 of 1)

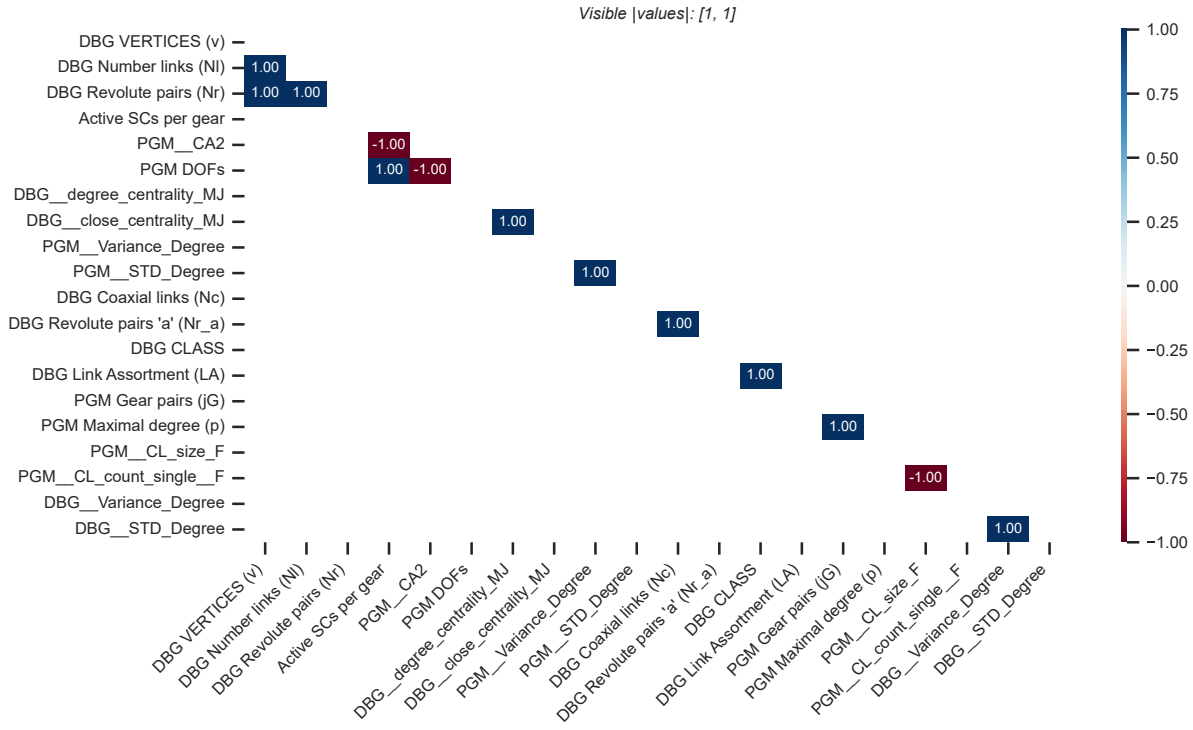

Source: Author.

B.2.2 Highly Correlated Features

In this section, excerpts from the complete heatmap (Appendix B.2), which display features absolutely correlated between 0.8 and 0.99, are presented. These features are considered to be highlyly correlated.

Figure 334 – Highly Correlated Features (1 of 19)

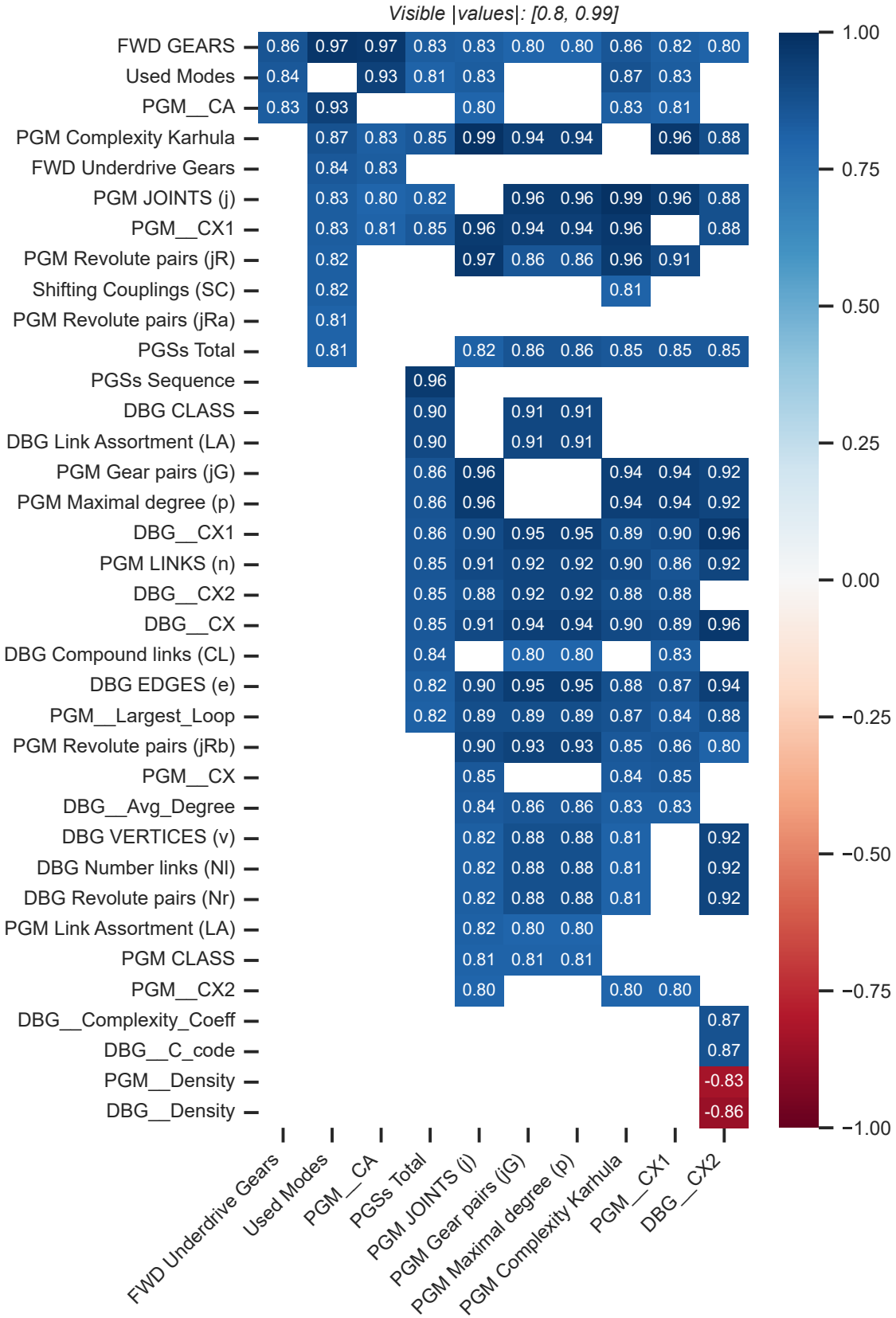

Source: Author.

Figure 335 – Highly Correlated Features (2 of 19)

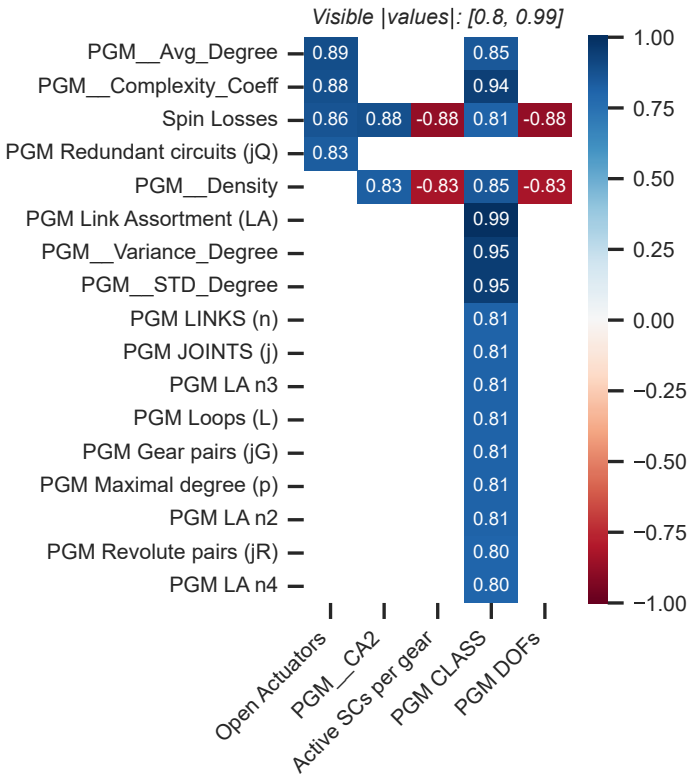

Source: Author.

Figure 336 – Highly Correlated Features (3 of 19)

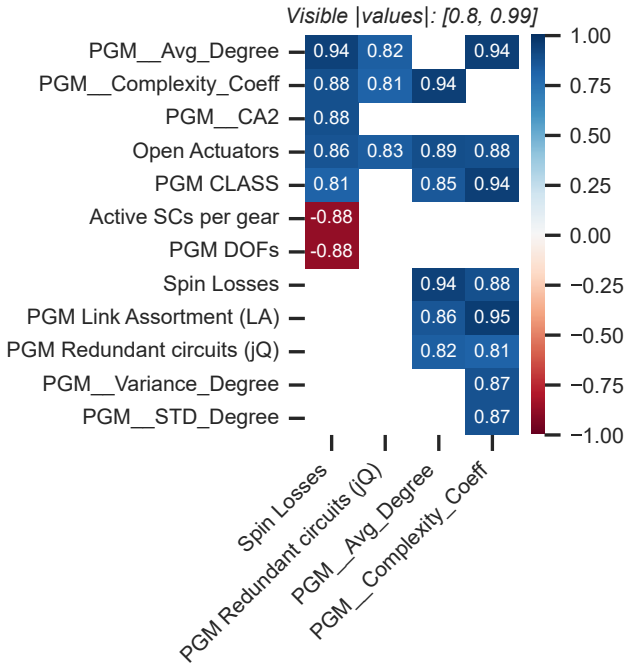

Source: Author.

Figure 337 – Highly Correlated Features (4 of 19)

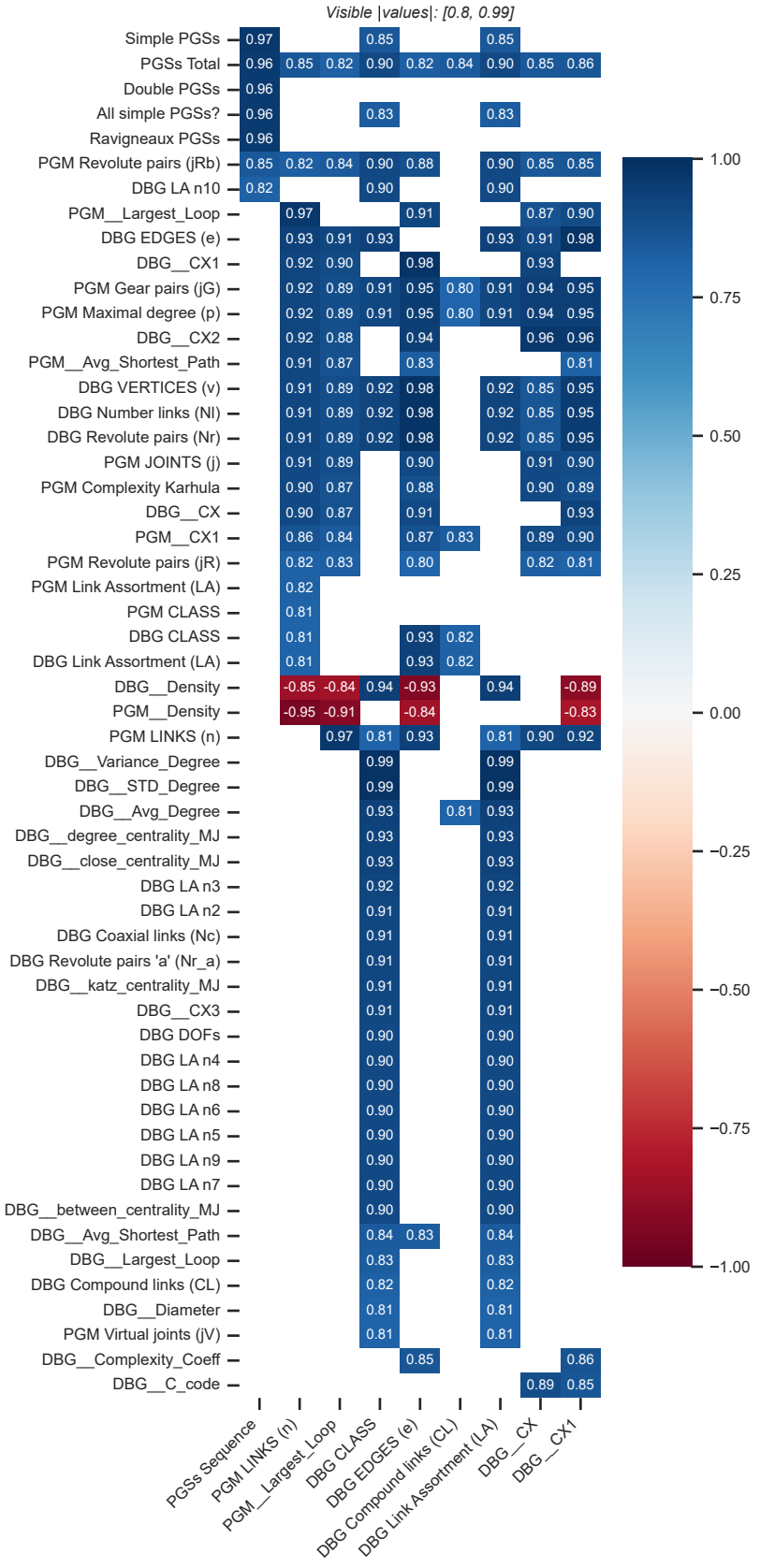

Source: Author.

Figure 338 – Highly Correlated Features (5 of 19)

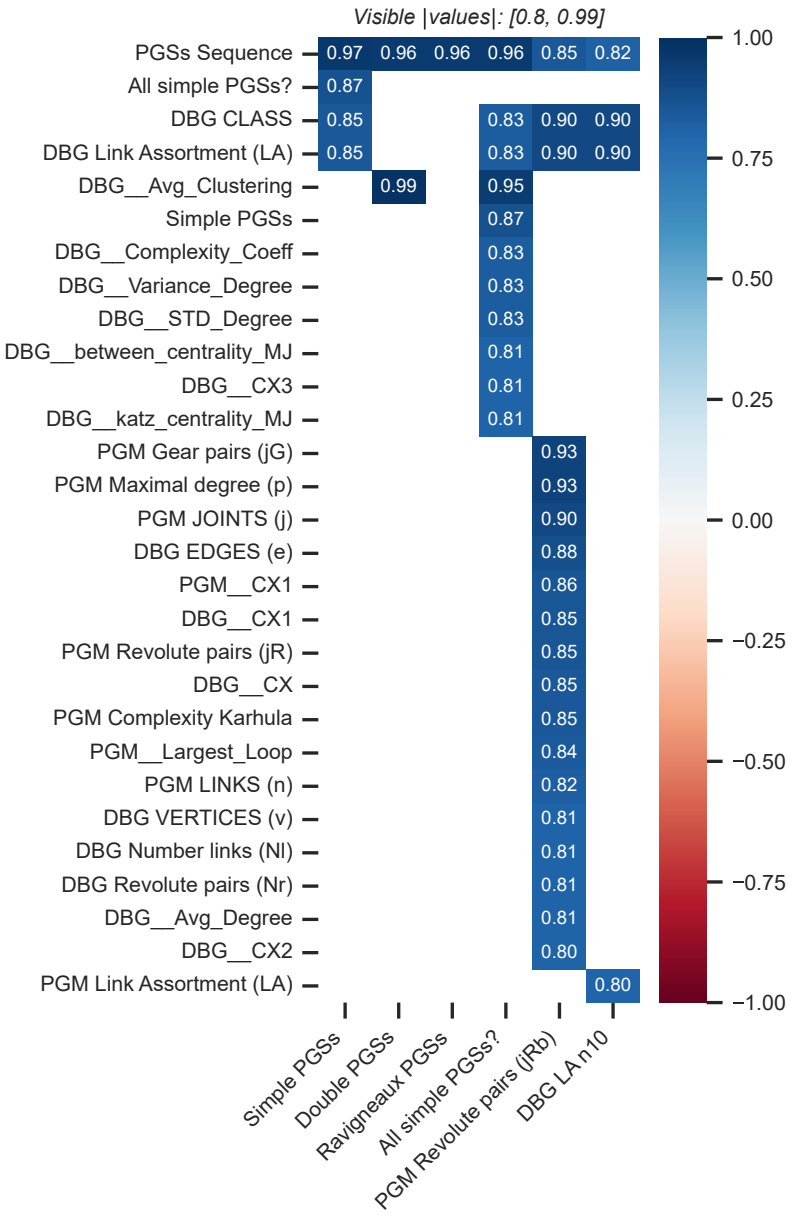

Source: Author.

Figure 339 – Highly Correlated Features (6 of 19)

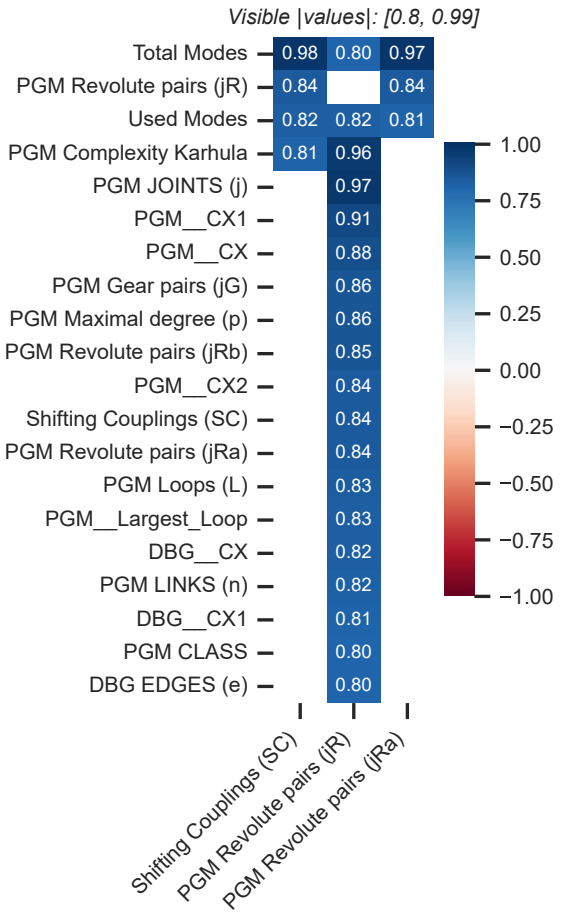

Source: Author.

Figure 340 – Highly Correlated Features (7 of 19)

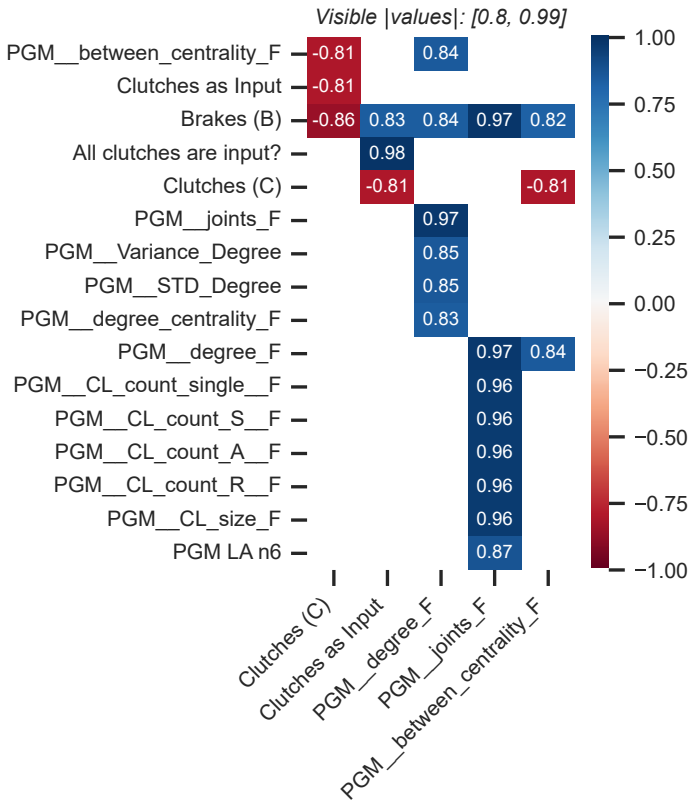

Source: Author.

Figure 341 – Highly Correlated Features (8 of 19)

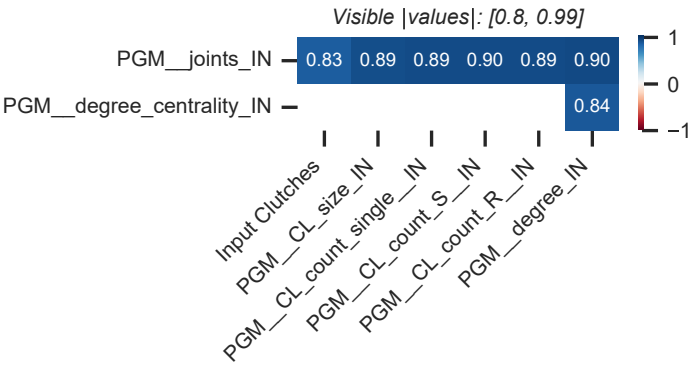

Source: Author.

Figure 342 – Highly Correlated Features (9 of 19)

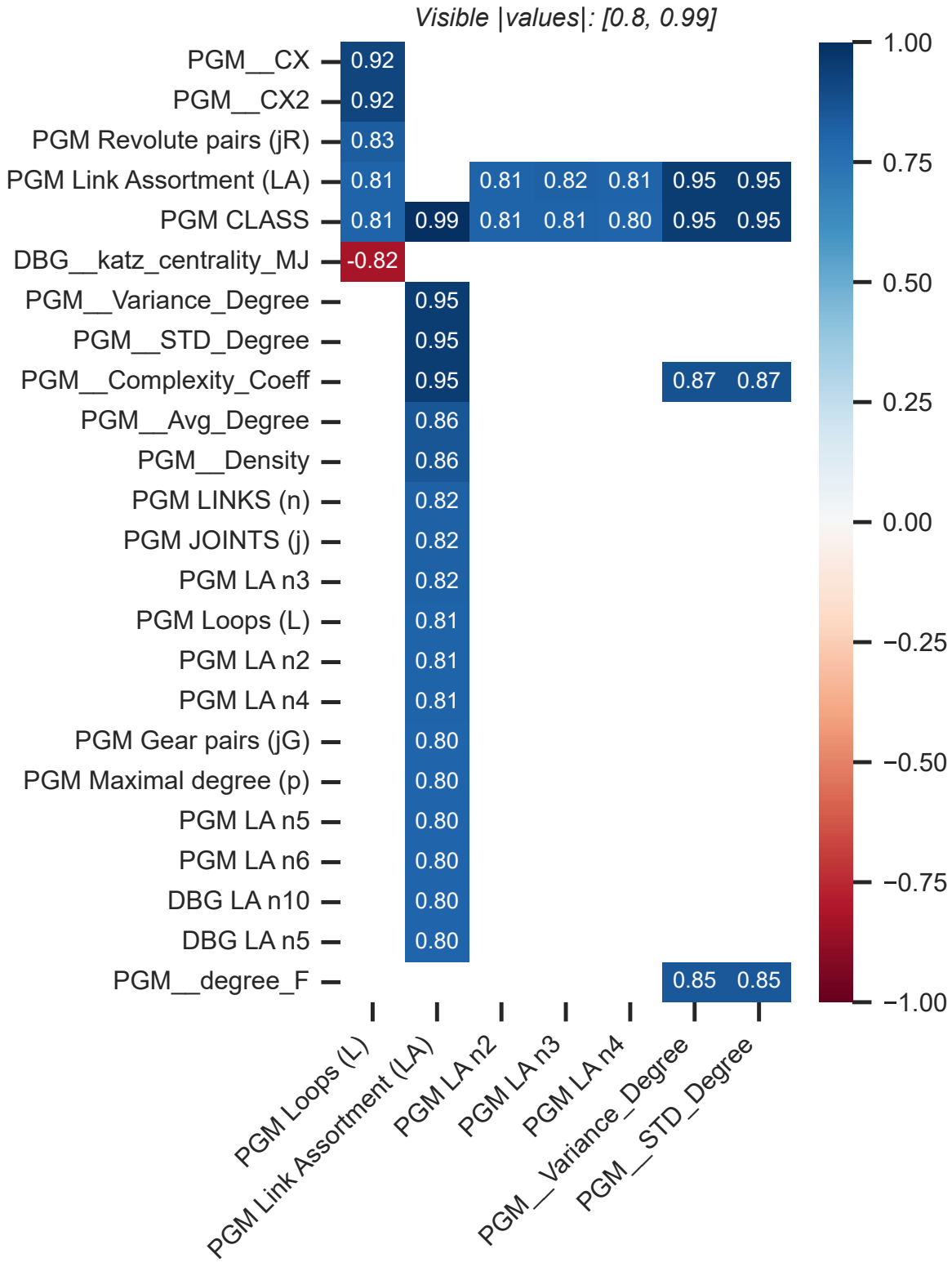

Source: Author.

Figure 343 – Highly Correlated Features (10 of 19)

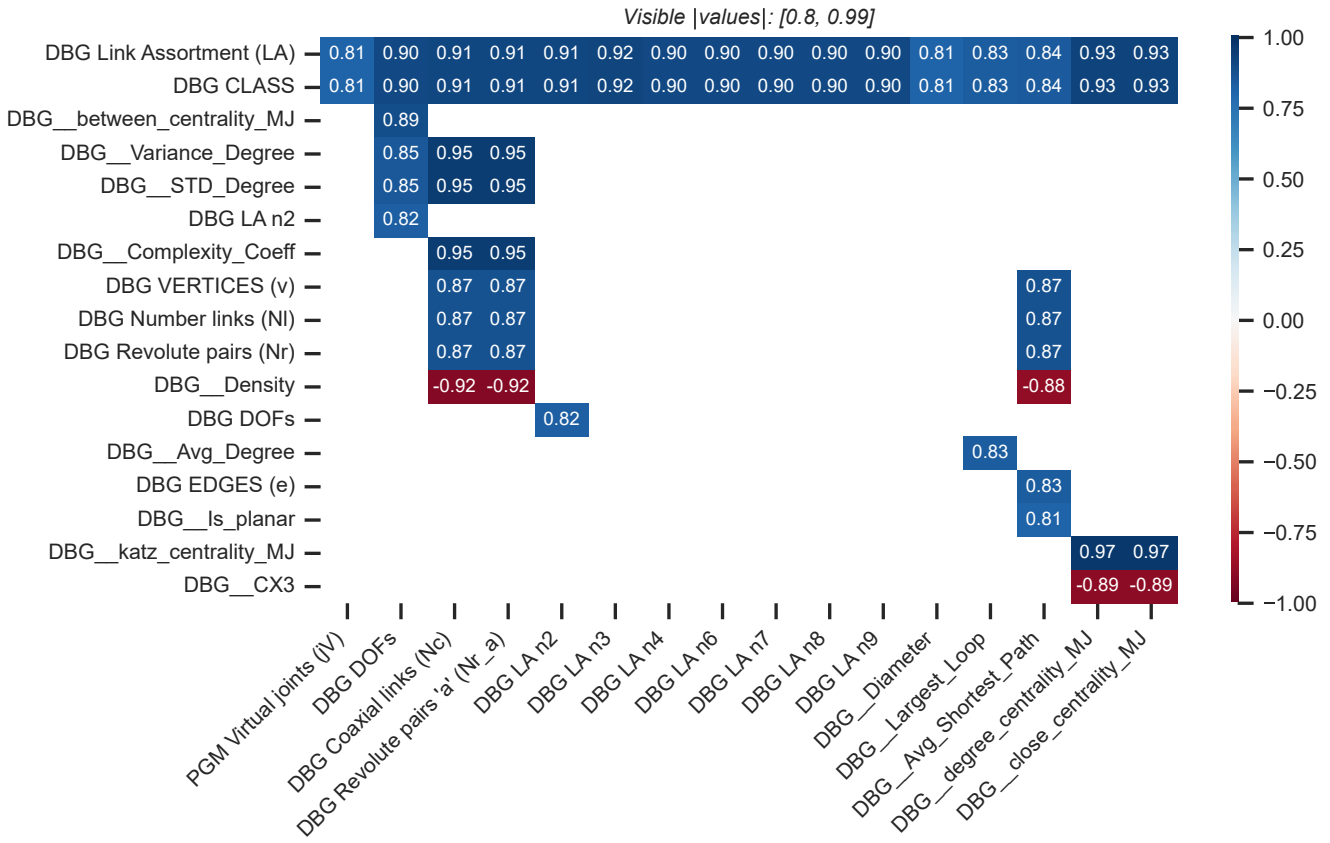

Source: Author.

Figure 344 – Highly Correlated Features (11 of 19)

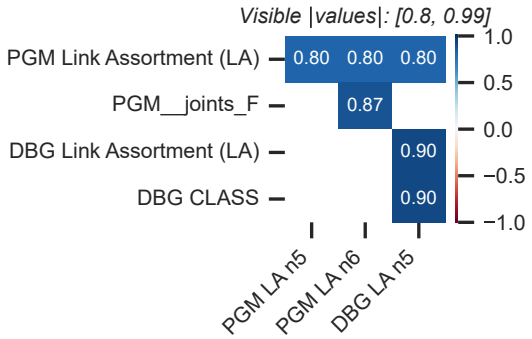

Source: Author.

Figure 345 – Highly Correlated Features (12 of 19)

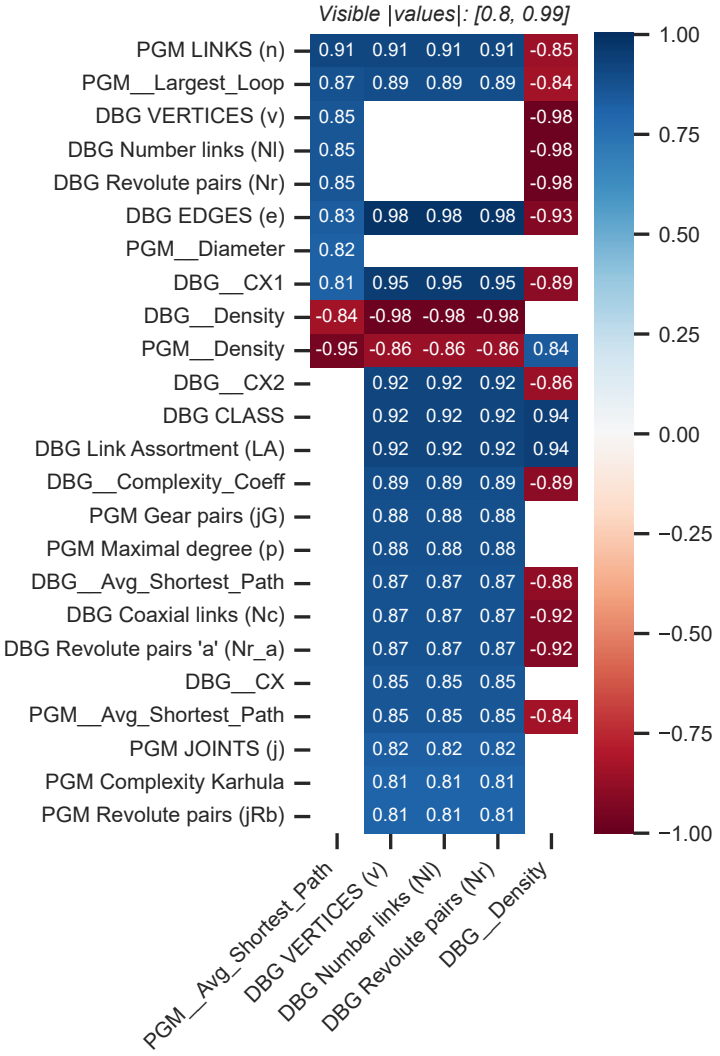

Source: Author.

Figure 346 – Highly Correlated Features (13 of 19)

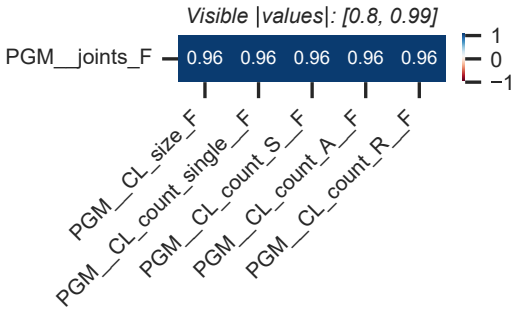

Source: Author.

Figure 347 – Highly Correlated Features (14 of 19)

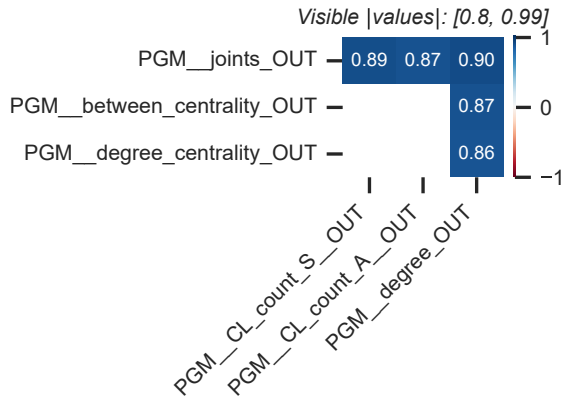

Source: Author.

Figure 348 – Highly Correlated Features (15 of 19)

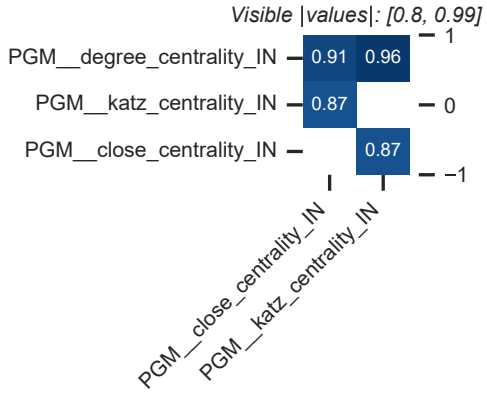

Source: Author.

Figure 349 – Highly Correlated Features (16 of 19)

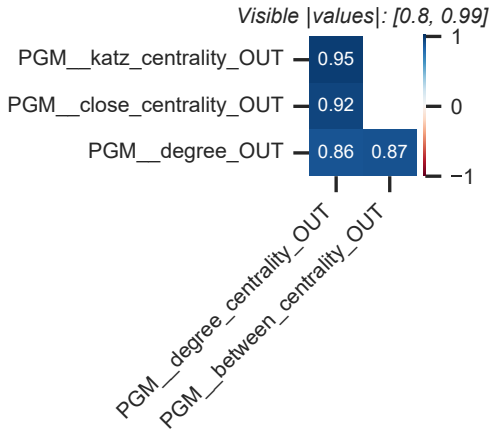

Source: Author.

Figure 350 – Highly Correlated Features (17 of 19)

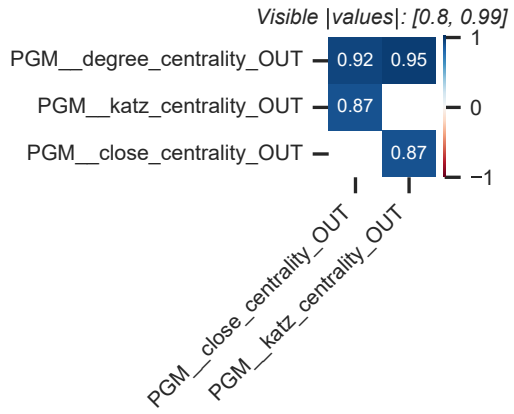

Source: Author.

Figure 351 – Highly Correlated Features (18 of 19)

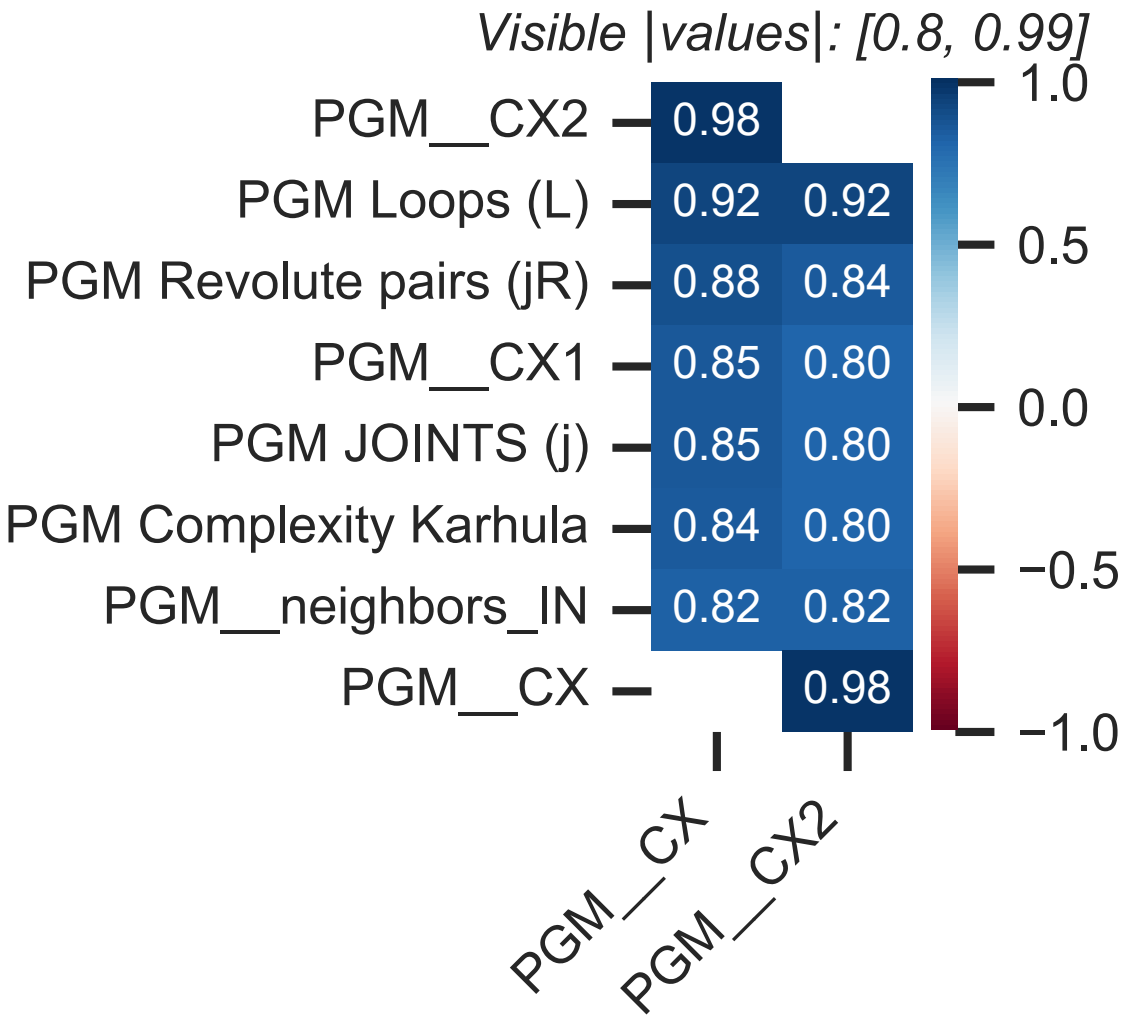

Source: Author.

Figure 352 – Highly Correlated Features (19 of 19)

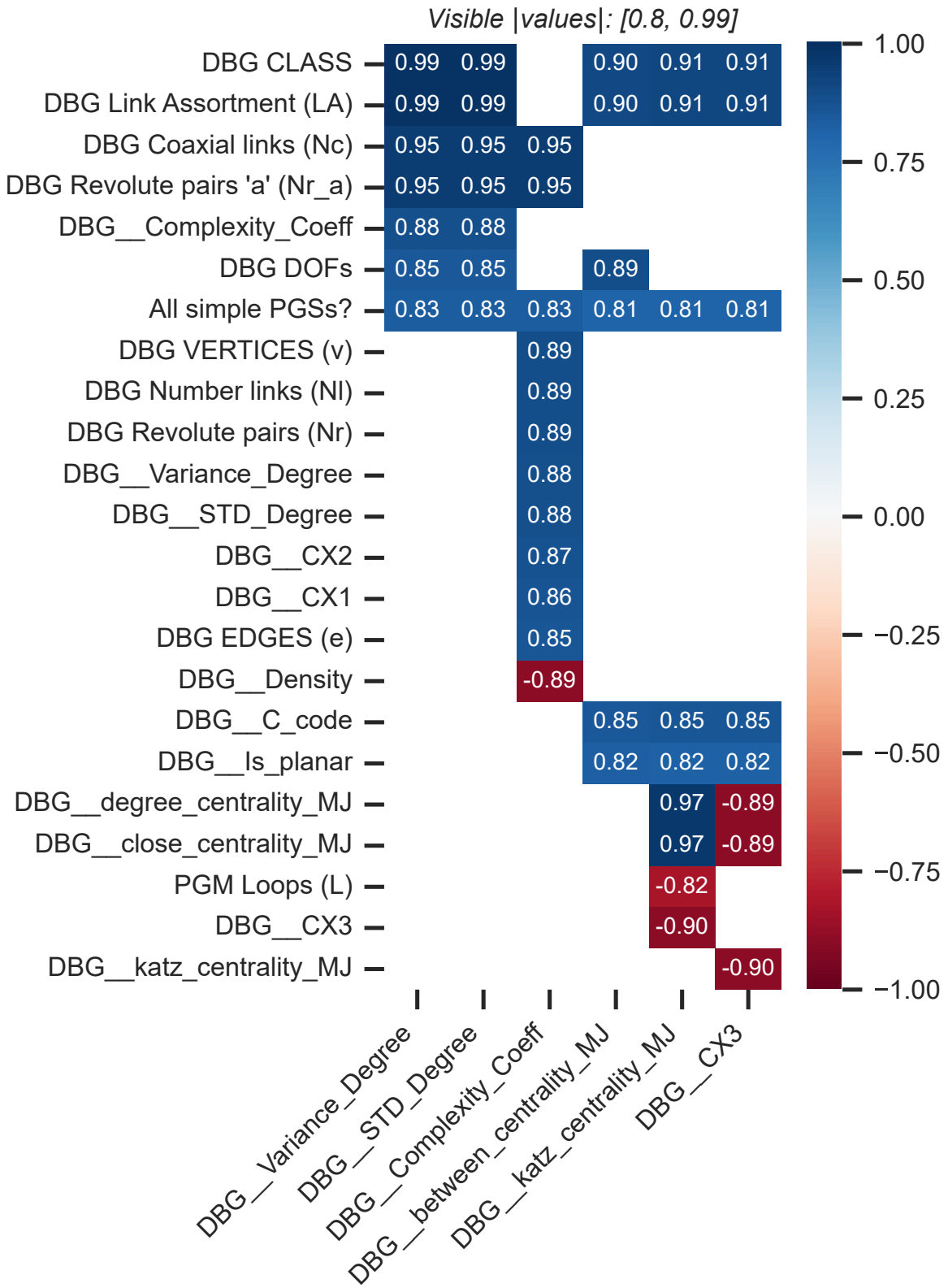

Source: Author.

B.3 RESULTS OF LINK ANALYSIS

The Frame (F), Input (IN), and Output (OUT) links were analyzed to determine their compound compositions, adjacency connections, and centrality measures. The results were segmented by three primary characteristics: the number of forward gears, the total count of PGSs, and the commercial status. Graphical representations of these results for each link are provided in the following sections.

B.3.1 Frame (F) Link Results

Figure 353 – Frame (F) compound links analysis

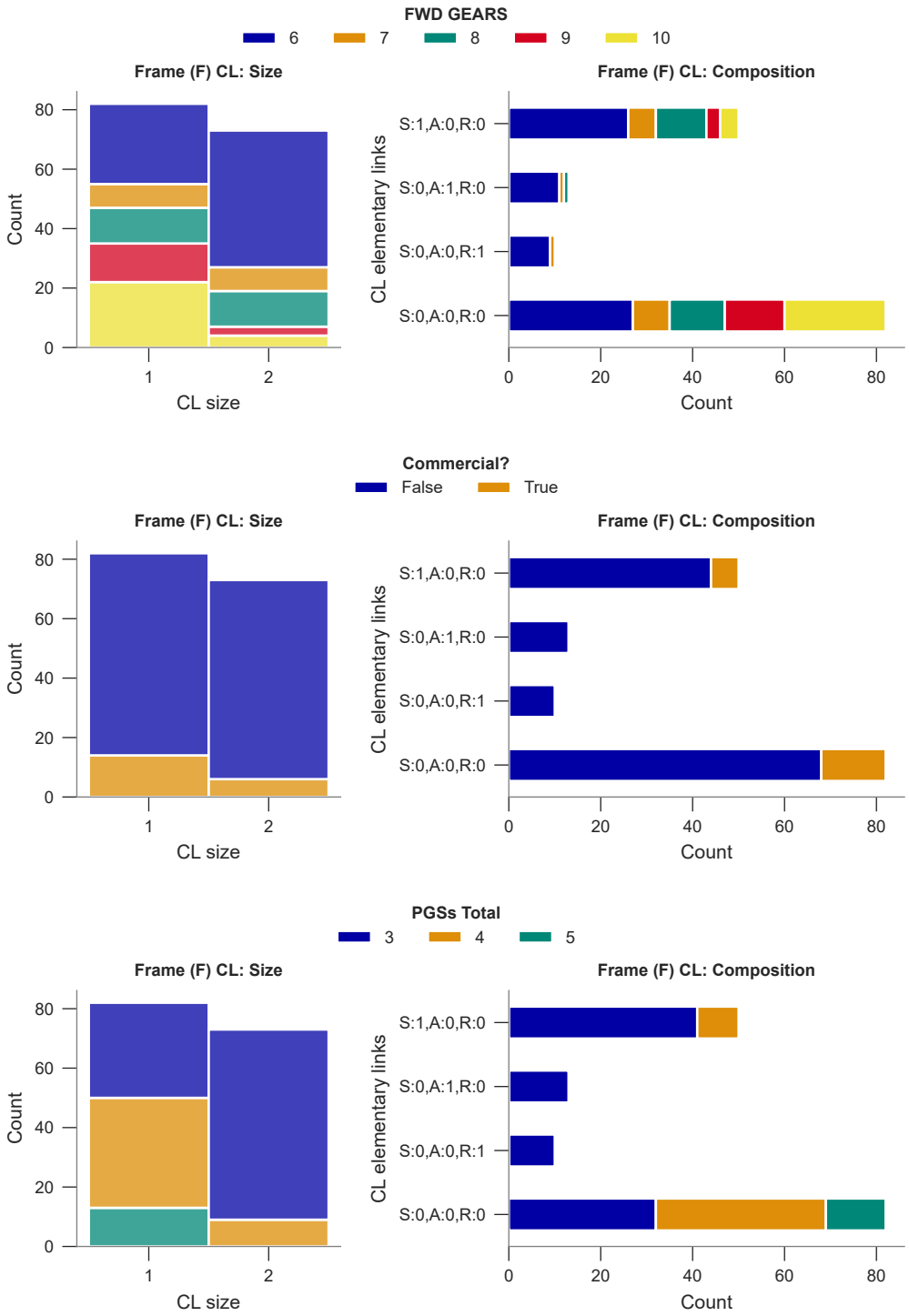

Source: Author.

Figure 354 – Frame (F) adjacency analysis by *FWD GEARS*

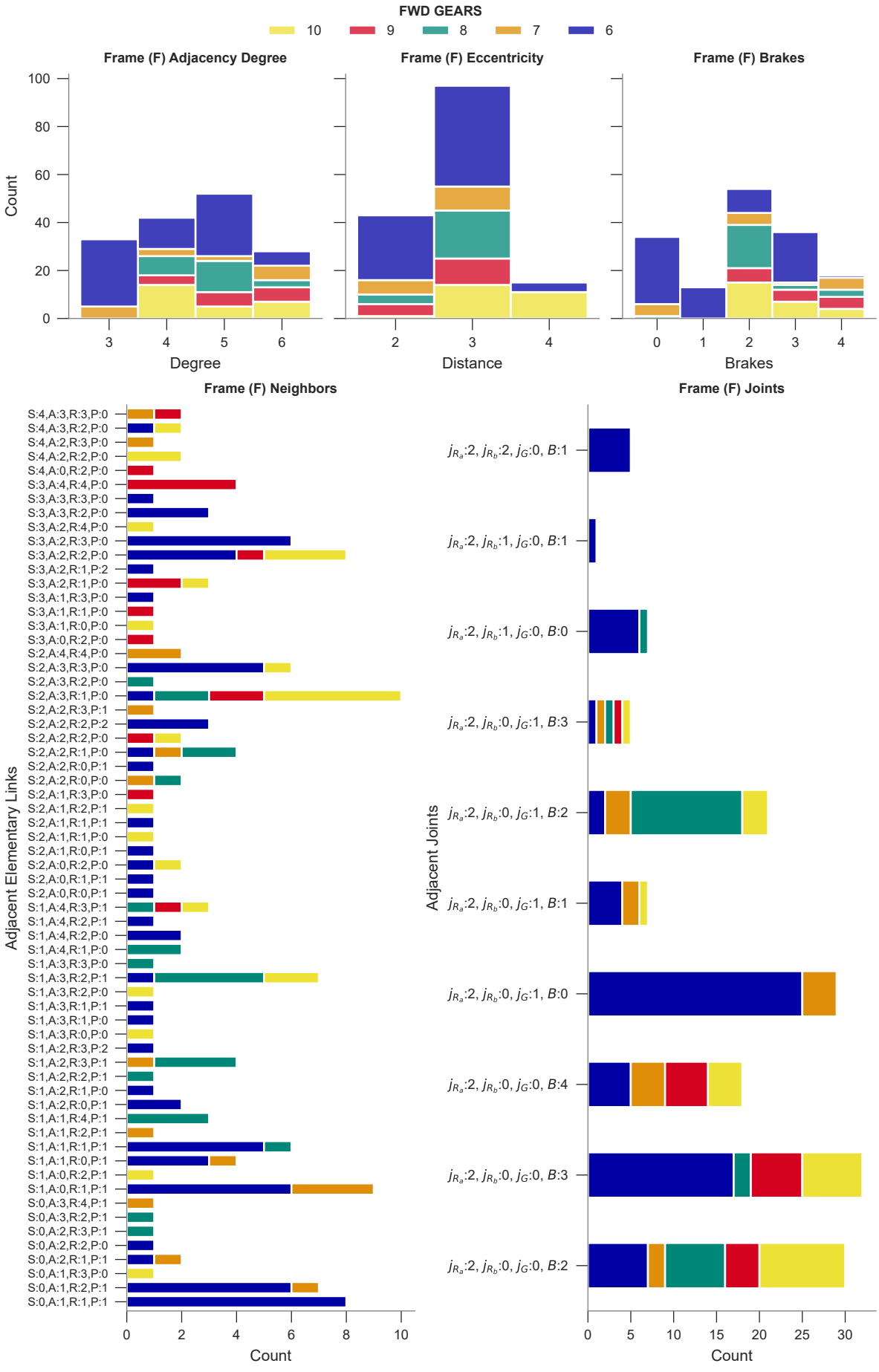

Source: Author.

Figure 355 – Frame (F) adjacency analysis by *Commercial*

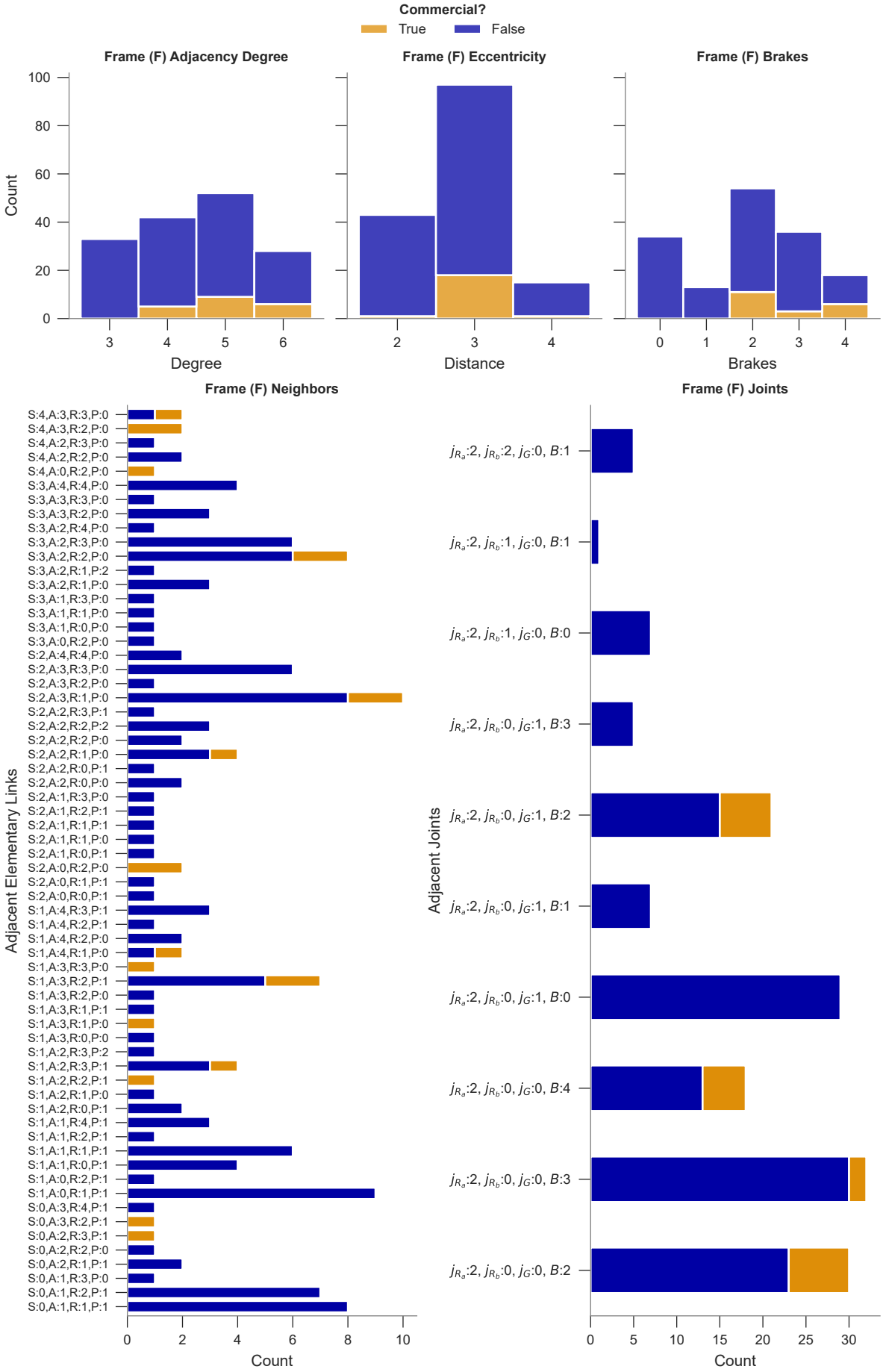

Source: Author.

Figure 356 – Frame (F) adjacency analysis by *PGSs Total*

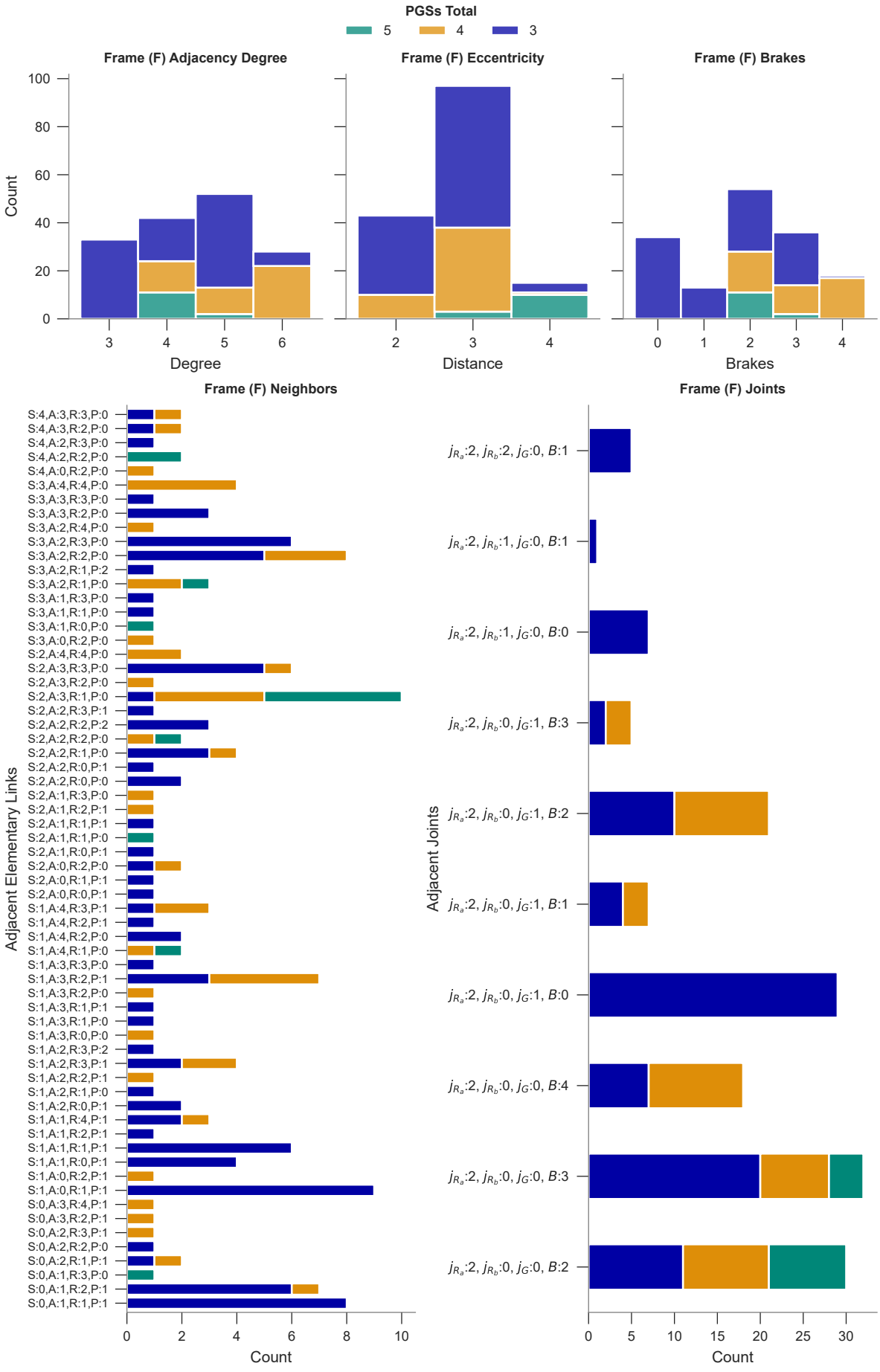

Source: Author.

Figure 357 – Frame (F) centrality analysis

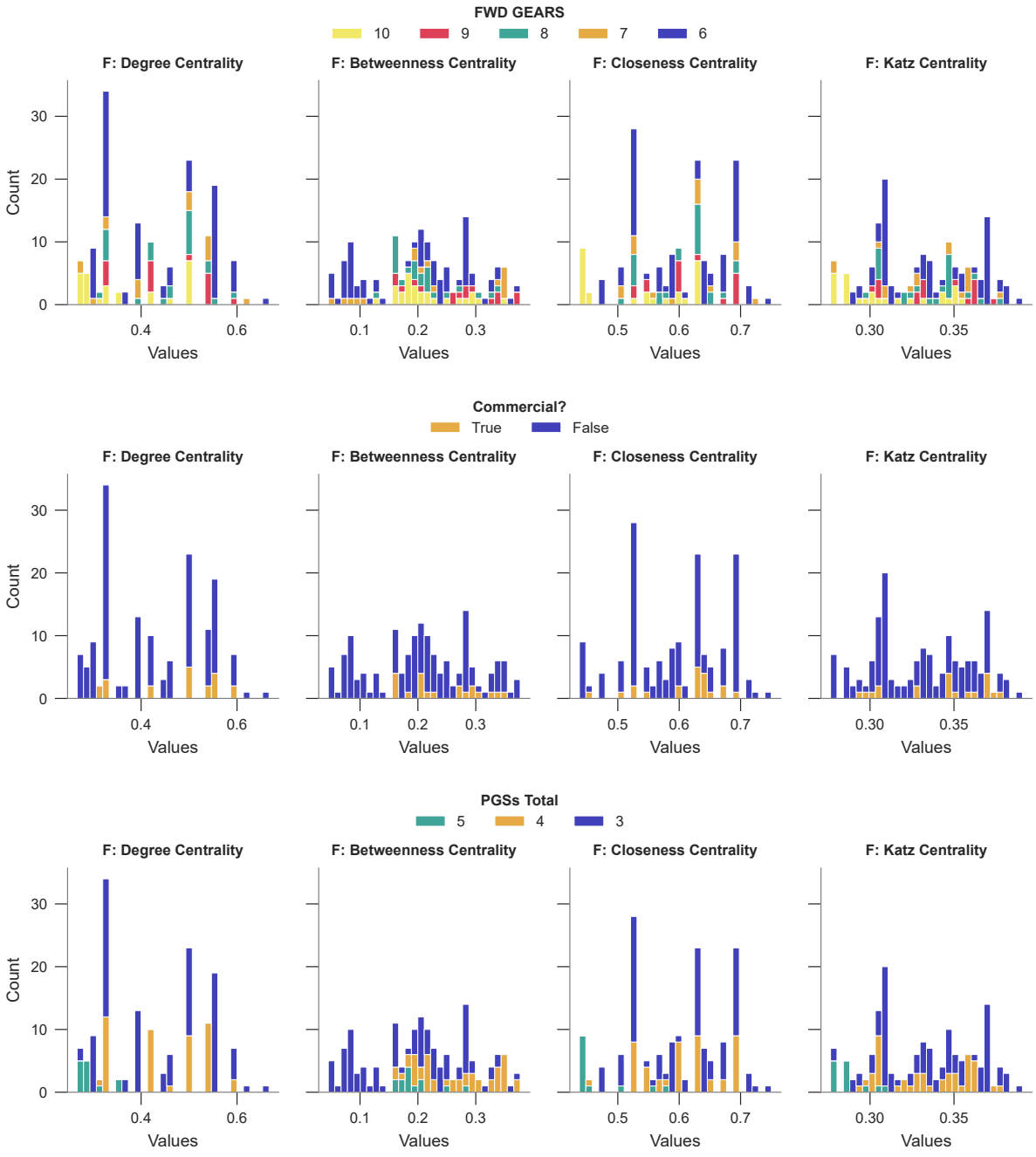

Source: Author.

B.3.2 Input (IN) Link Results

Figure 358 – Input (IN) compound links analysis

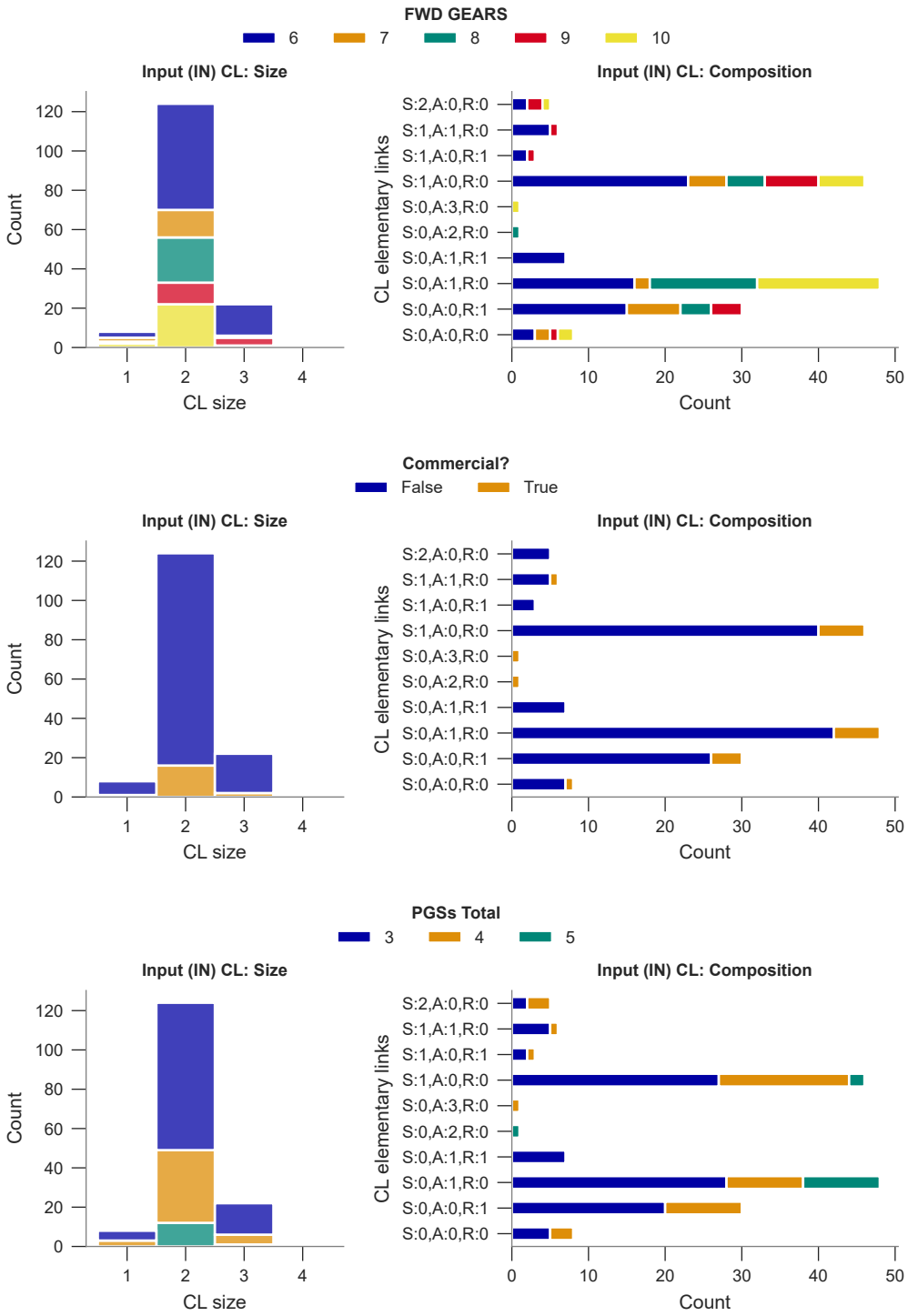

Source: Author.

Figure 359 – Input (IN) adjacency analysis by *FWD GEARS*

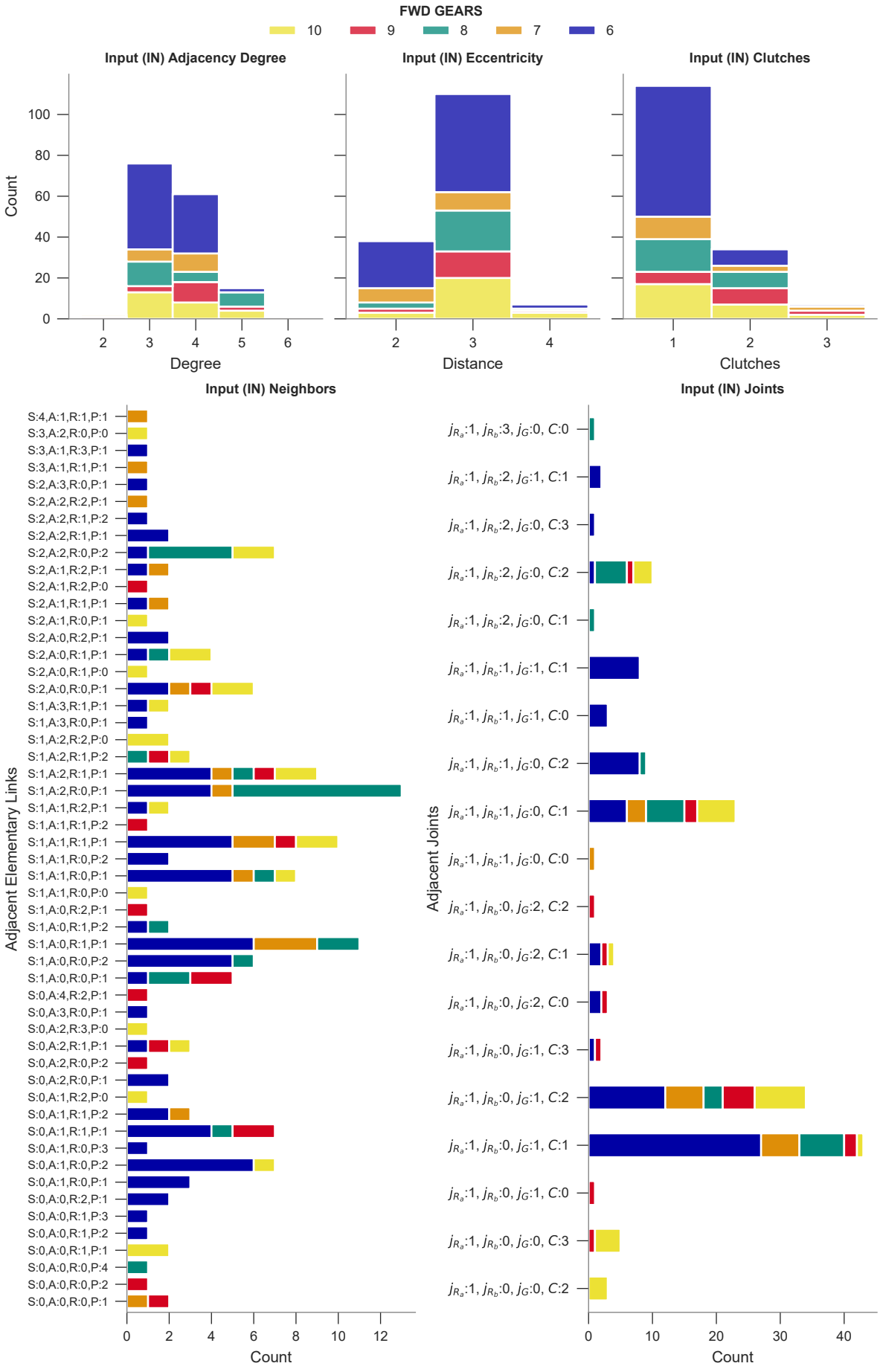

Source: Author.

Figure 360 – Input (IN) adjacency analysis by *Commercial*

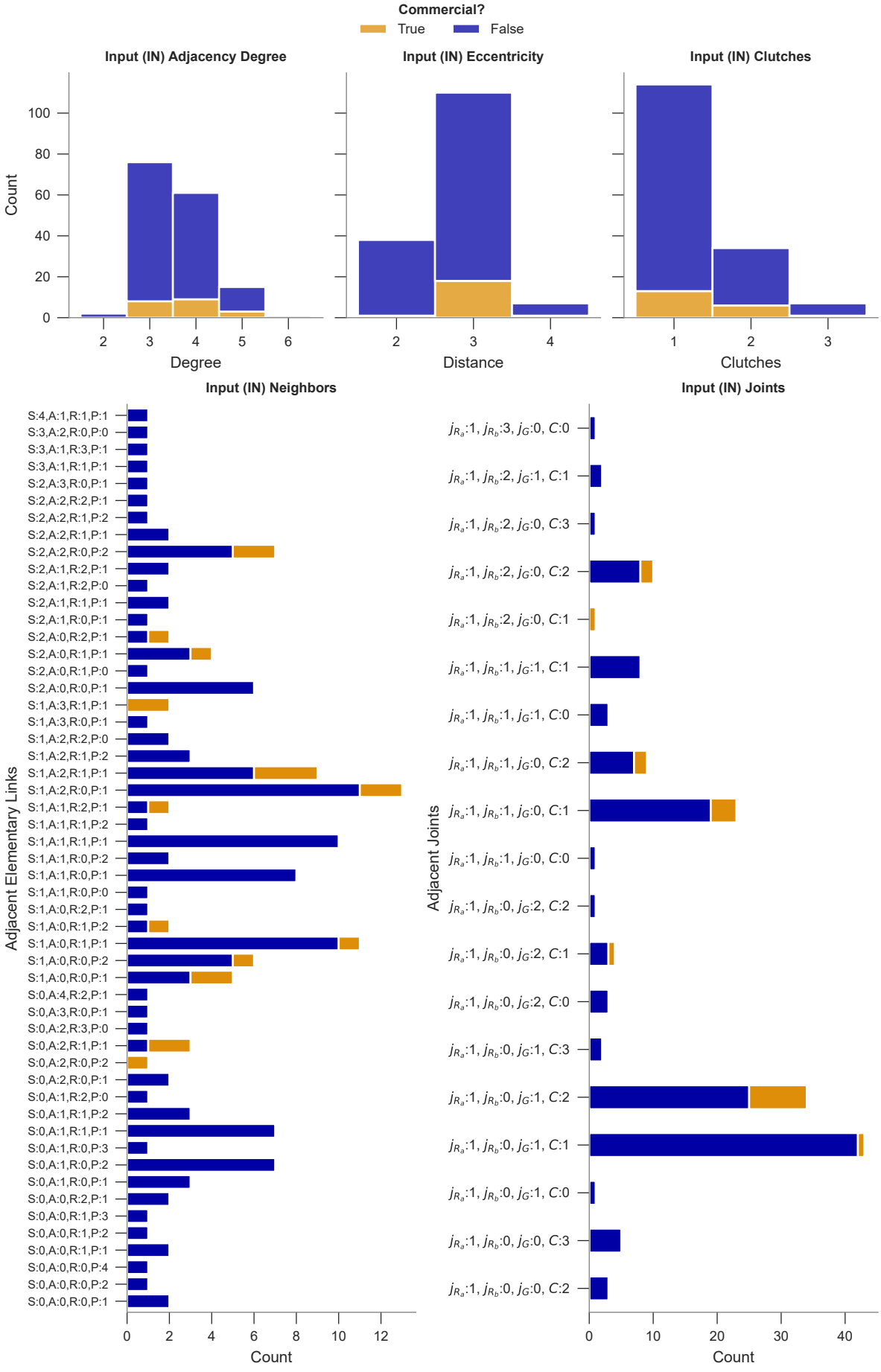

Source: Author.

Figure 361 – Input (IN) adjacency analysis by *PGSs Total*

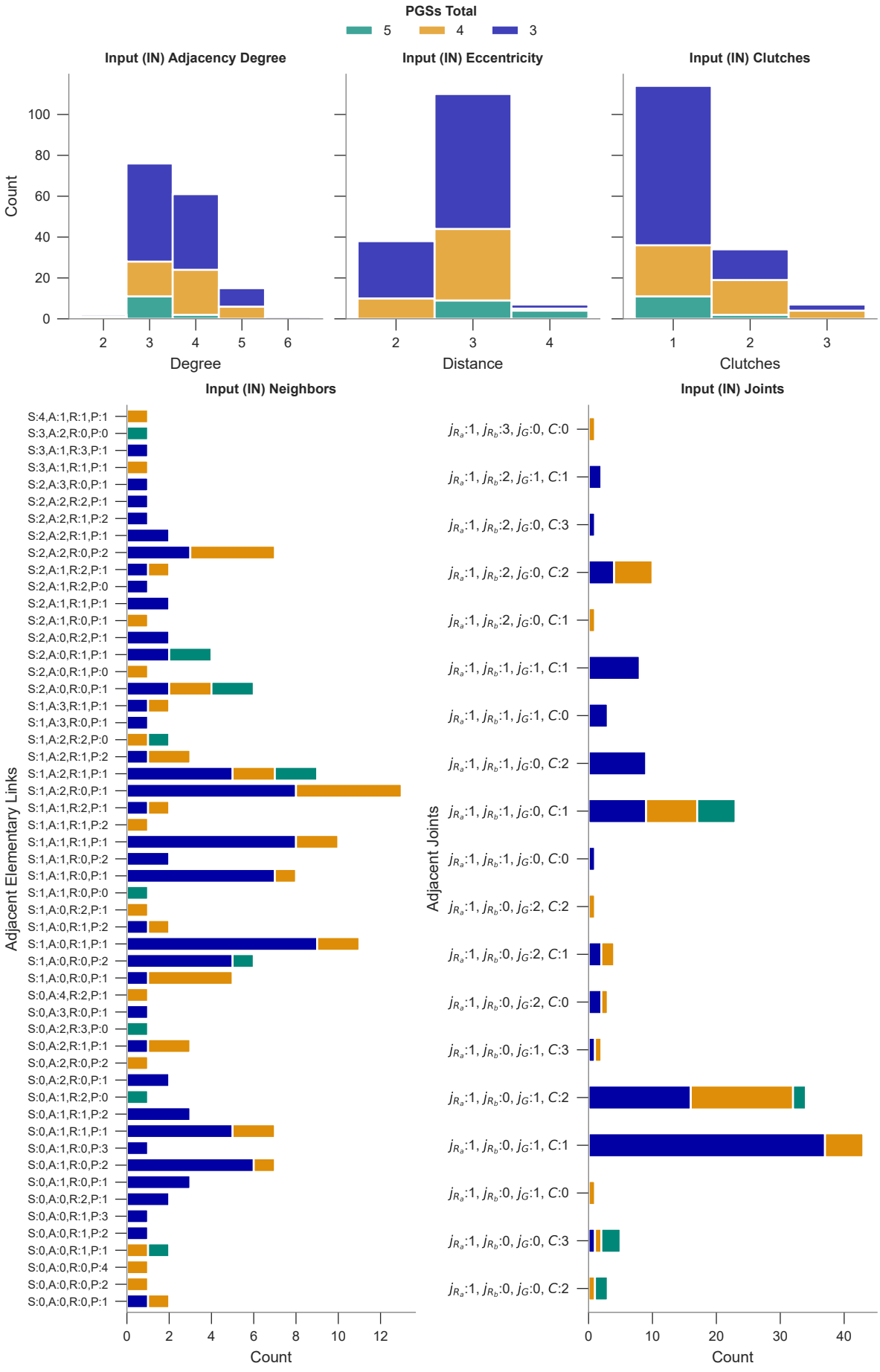

Source: Author.

Figure 362 – Input (IN) centrality analysis

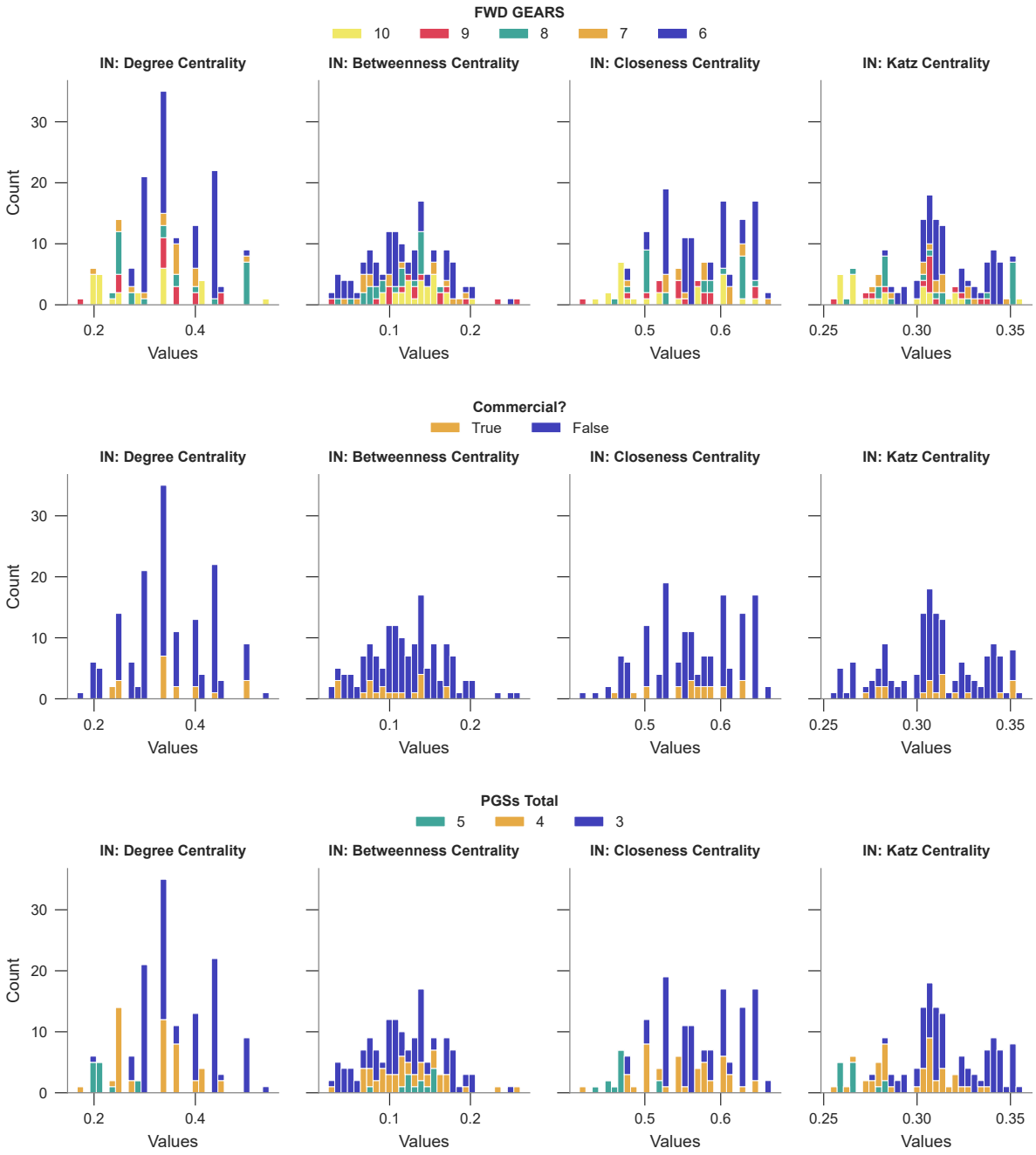

Source: Author.

B.3.3 Output (OUT) Link Results

Figure 363 – Output (OUT) compound links analysis

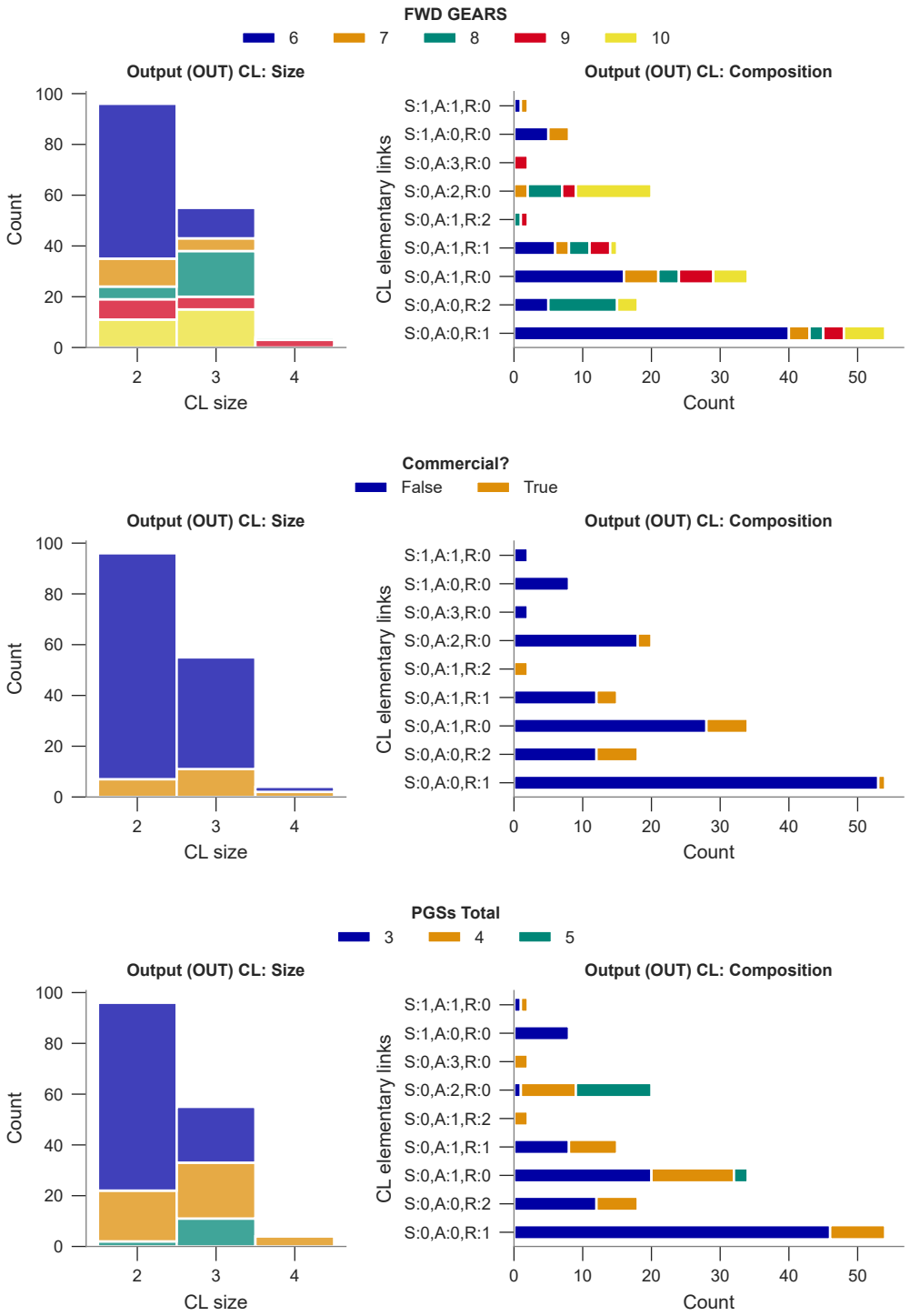

Source: Author.

Figure 364 – Output (OUT) adjacency analysis by *FWD GEARS*

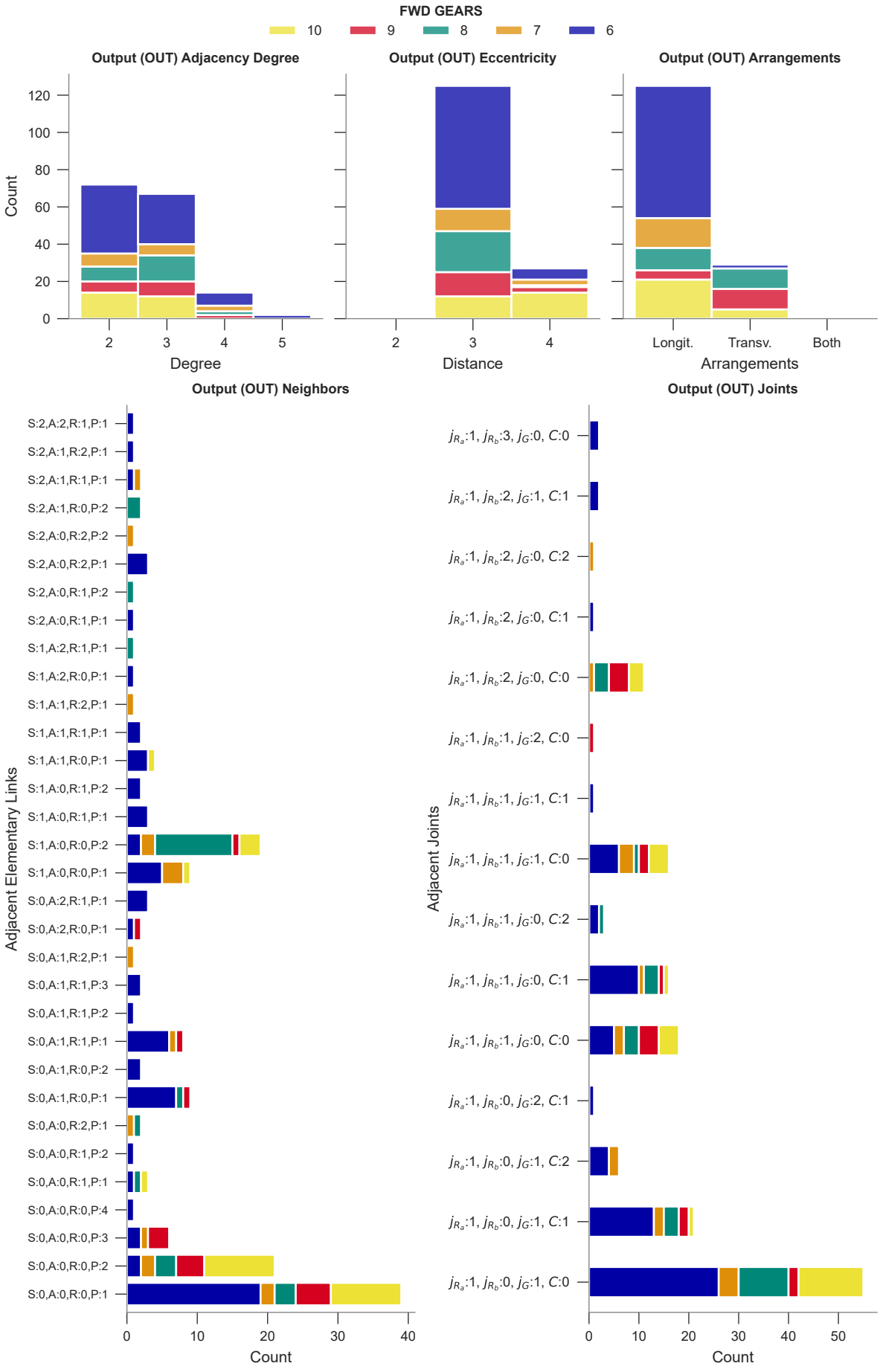

Source: Author.

Figure 365 – Output (OUT) adjacency analysis by *Commercial*

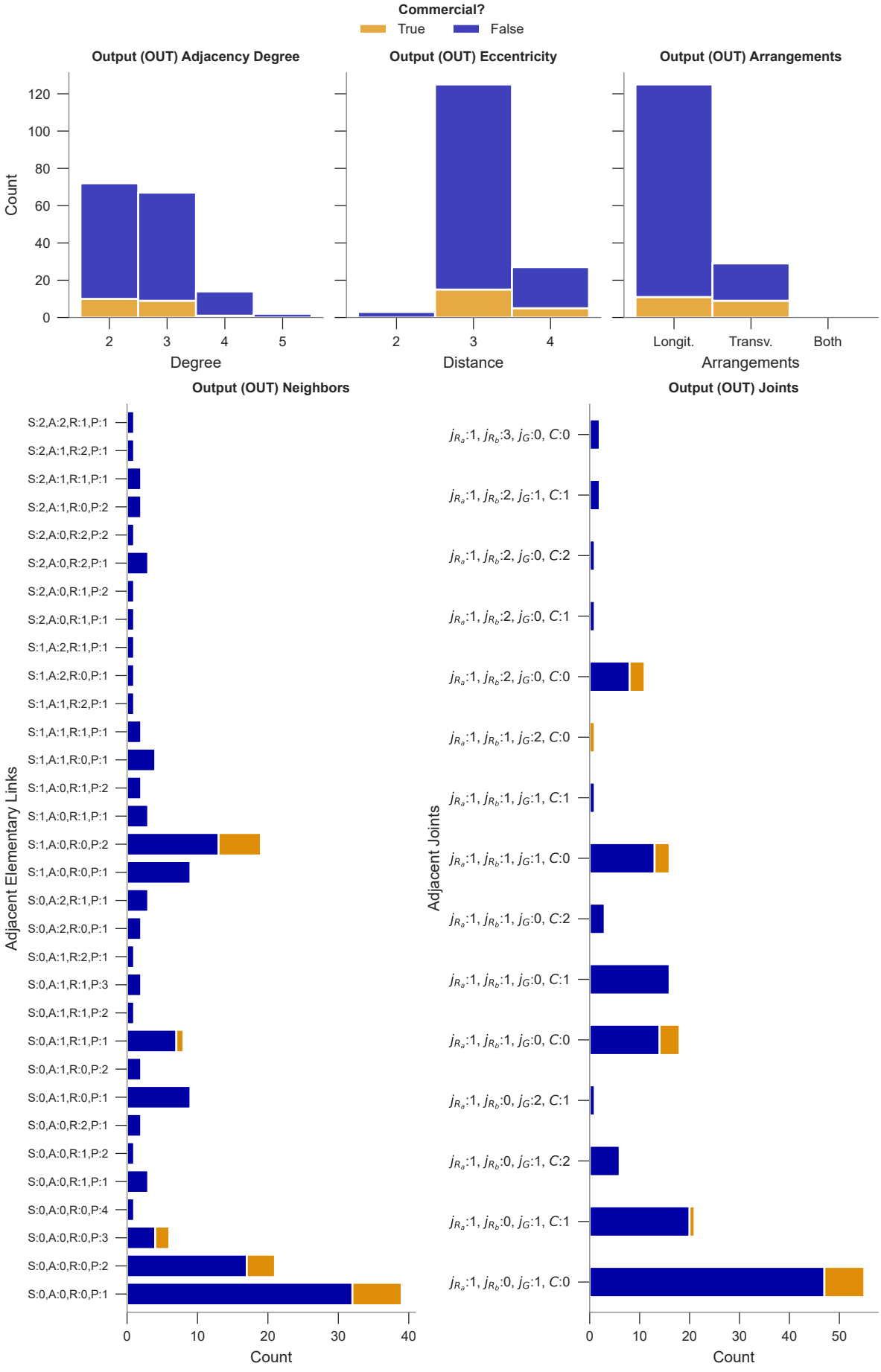

Source: Author.

Figure 366 – Output (OUT) adjacency analysis by *PGSs Total*

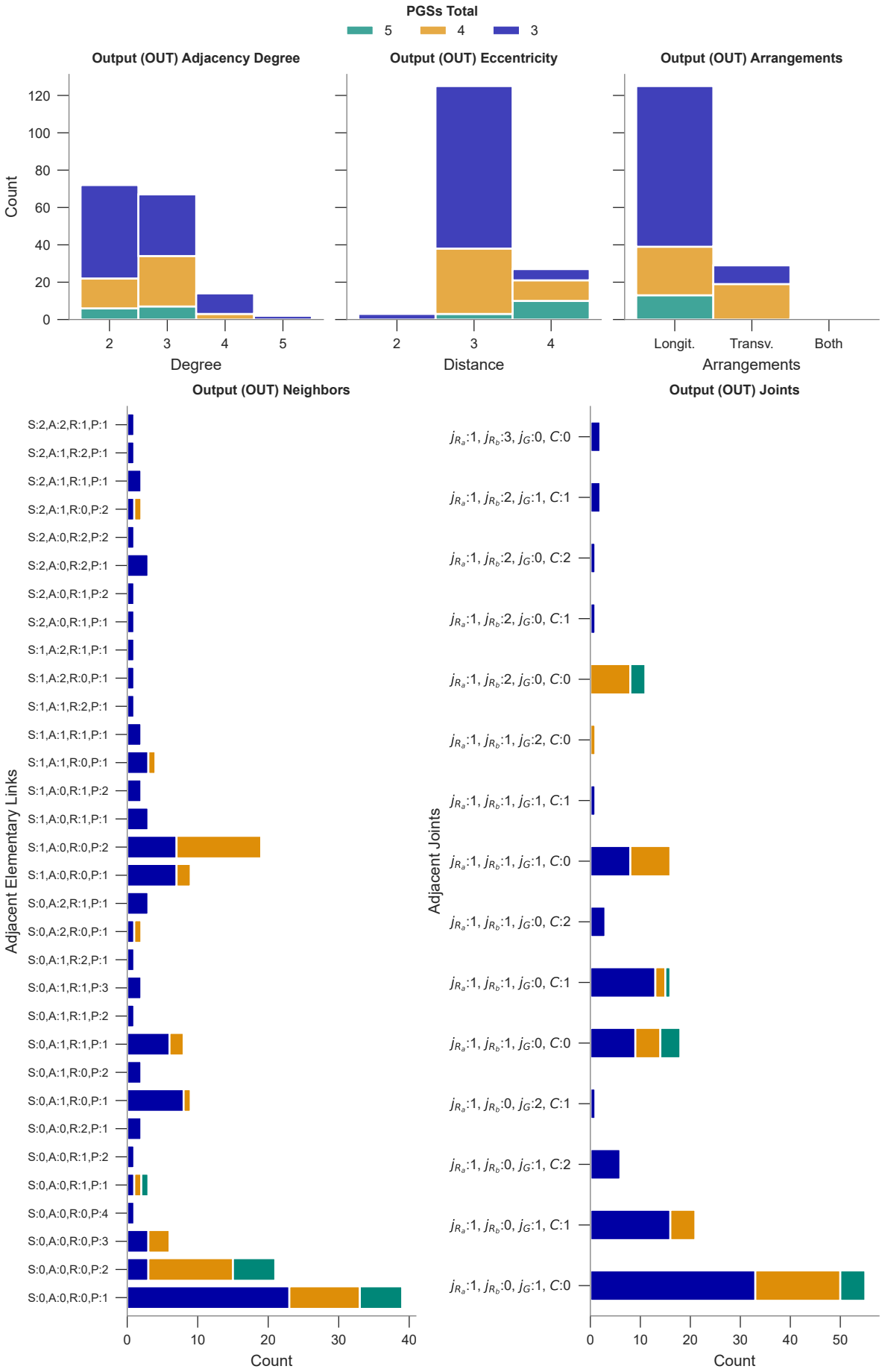

Source: Author.

Figure 367 – Output (OUT) centrality analysis

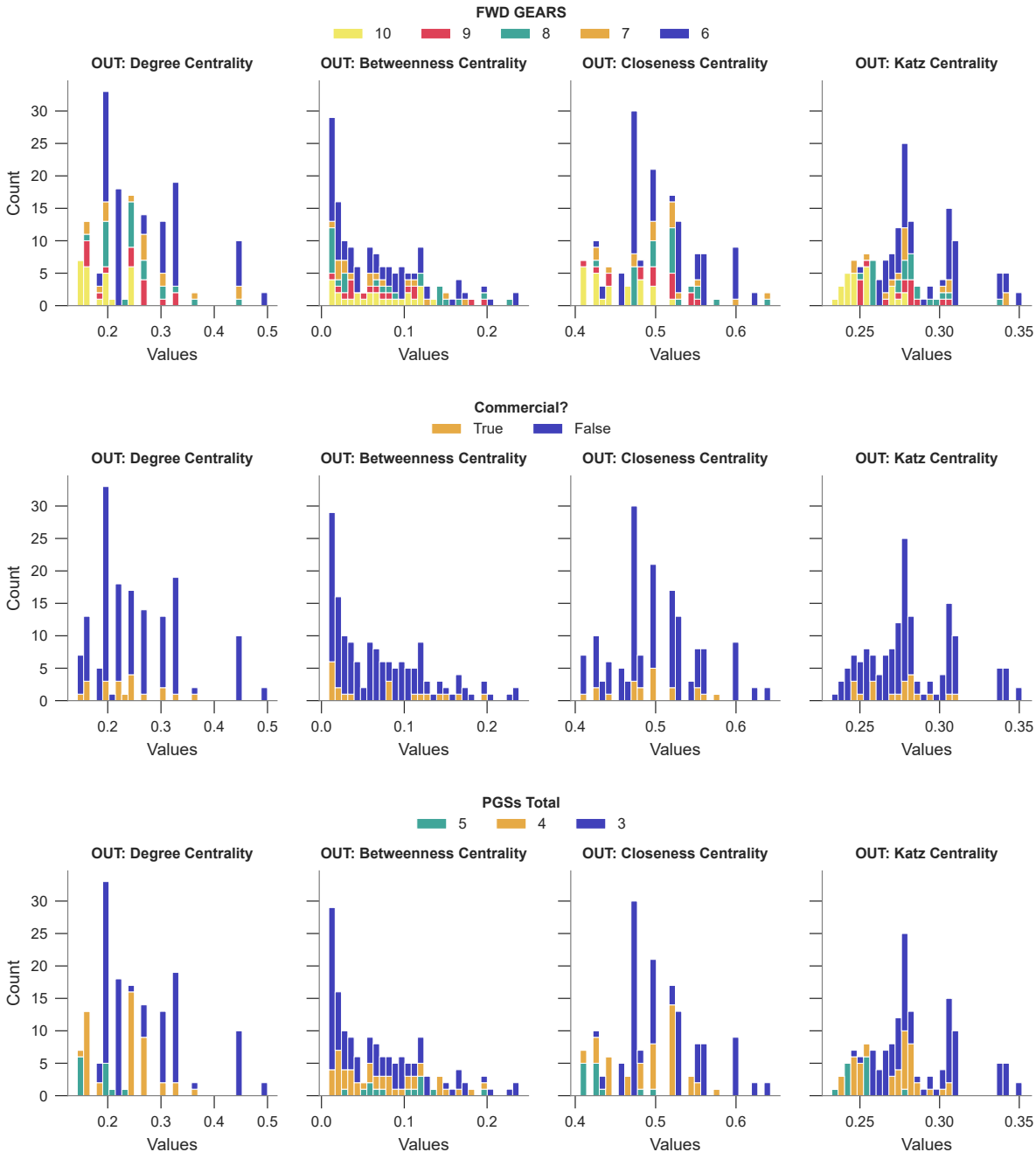

Source: Author.

B.4 RESULTS OF FEATURE SELECTION

The 15 most relevant features selected through four methods and two aggregators for each target feature discussed in Section 5.4.4 are detailed in this section.

Function Overview

It was developed a Python function to execute a series of steps, each contributing to the overall objective of identifying and ranking the most significant features for a given target feature in the PGM database. Four methods are employed to assess feature importance:

- *Random Forest Classifier*: Utilized for its inherent ability to provide feature importance, this method offers a view based on ensemble learning.
- *Recursive Feature Elimination (RFE)*: This technique uses Logistic Regression to iteratively remove features, focusing on those that contribute most to the prediction accuracy. As RFE importance results in a ranking, features with lower ranking implies greater importance.
- *Univariate Statistics*: F-scores for numerical features and Chi-squared scores for categorical features provide a statistical basis for feature selection.
- *L1 Regularization (Lasso Regression)*: This approach highlights features that remain significant even after applying regularization, which helps in reducing overfitting.

The function synthesizes information from the various methods into two aggregated rankings:

- *Weighted Ranking*: This combines the different rankings, emphasizing the methods considered more reliable, with predefined weights: Weighted Rank = 0.35 $\times$ RF + 0.35 $\times$ RFE + 0.1 $\times$ Lasso + 0.2 $\times$ F-Scores + 0.2 $\times$ Chi-Squared
- *Mean Ranking*: Averages the rankings from each method, providing a balanced view across all techniques.

Visual representation provides clear, comparative bar charts for each method's feature importance and the aggregated rankings.

Results by target feature

The outcome of this function is a comprehensive ranking of the 15 most relevant features based on multi-faceted approach to reduce the risk of bias inherent in any single method and to provide a robust basis for selecting features for further PGM design requirements. The visualization of the results for each target feature is presented below.

Figure 368 – 15 most relevant features for commercial status 'TRUE'.

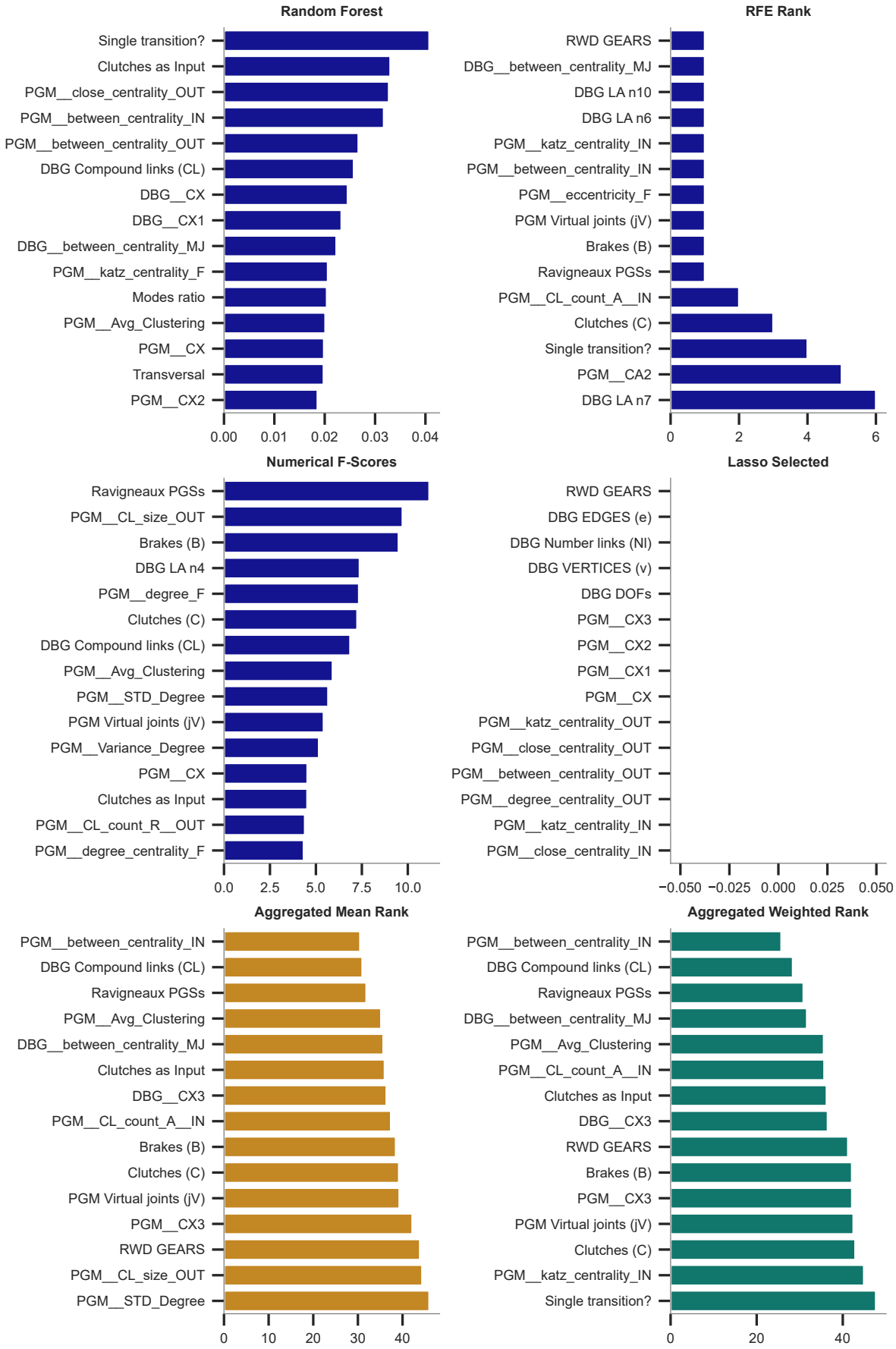

Source: Author.

Figure 369 – 15 most relevant features for total count of 3 elementary PGSs.

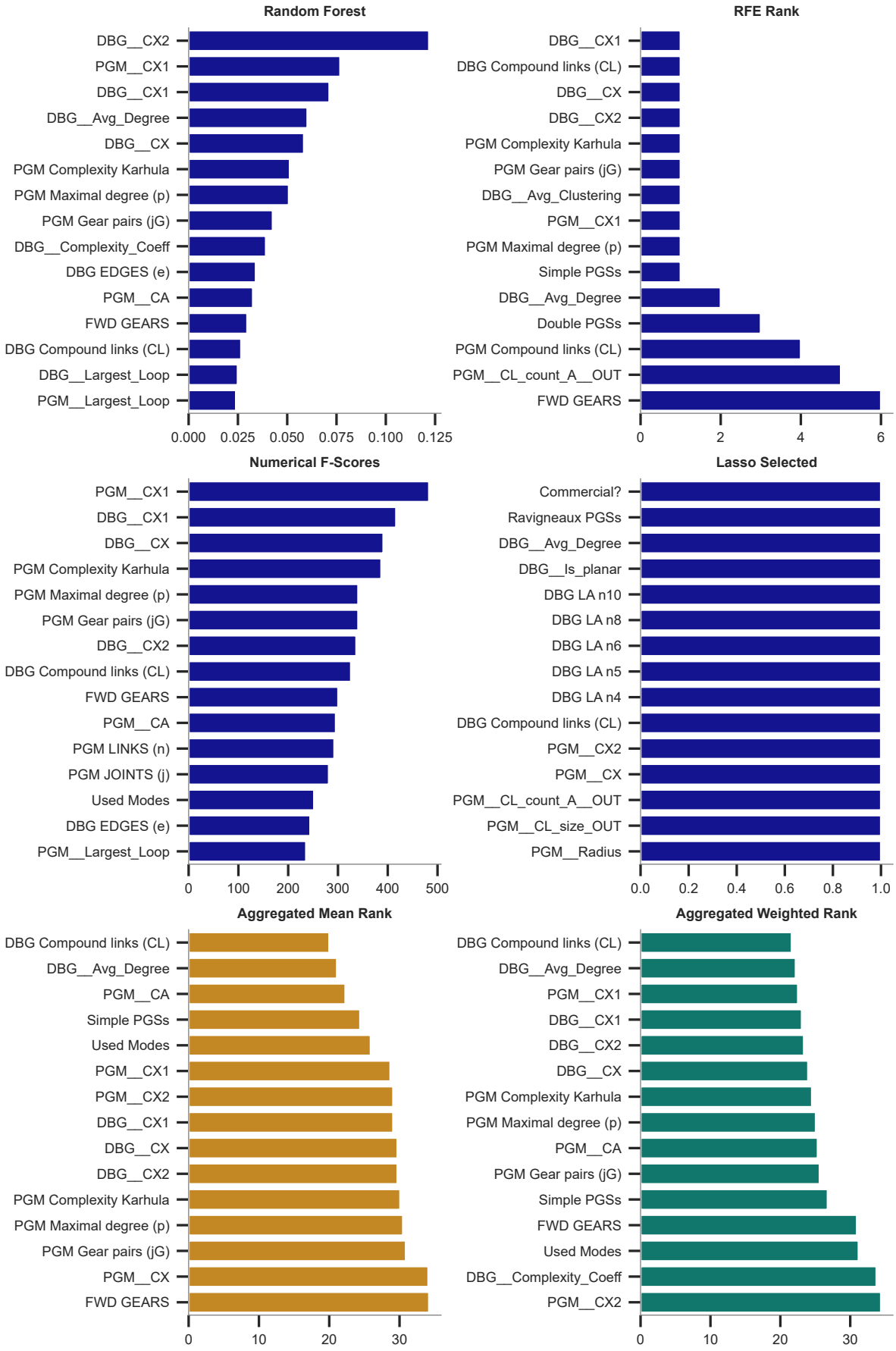

Source: Author.

Figure 370 – 15 most relevant features for total count of 4 elementary PGSs.

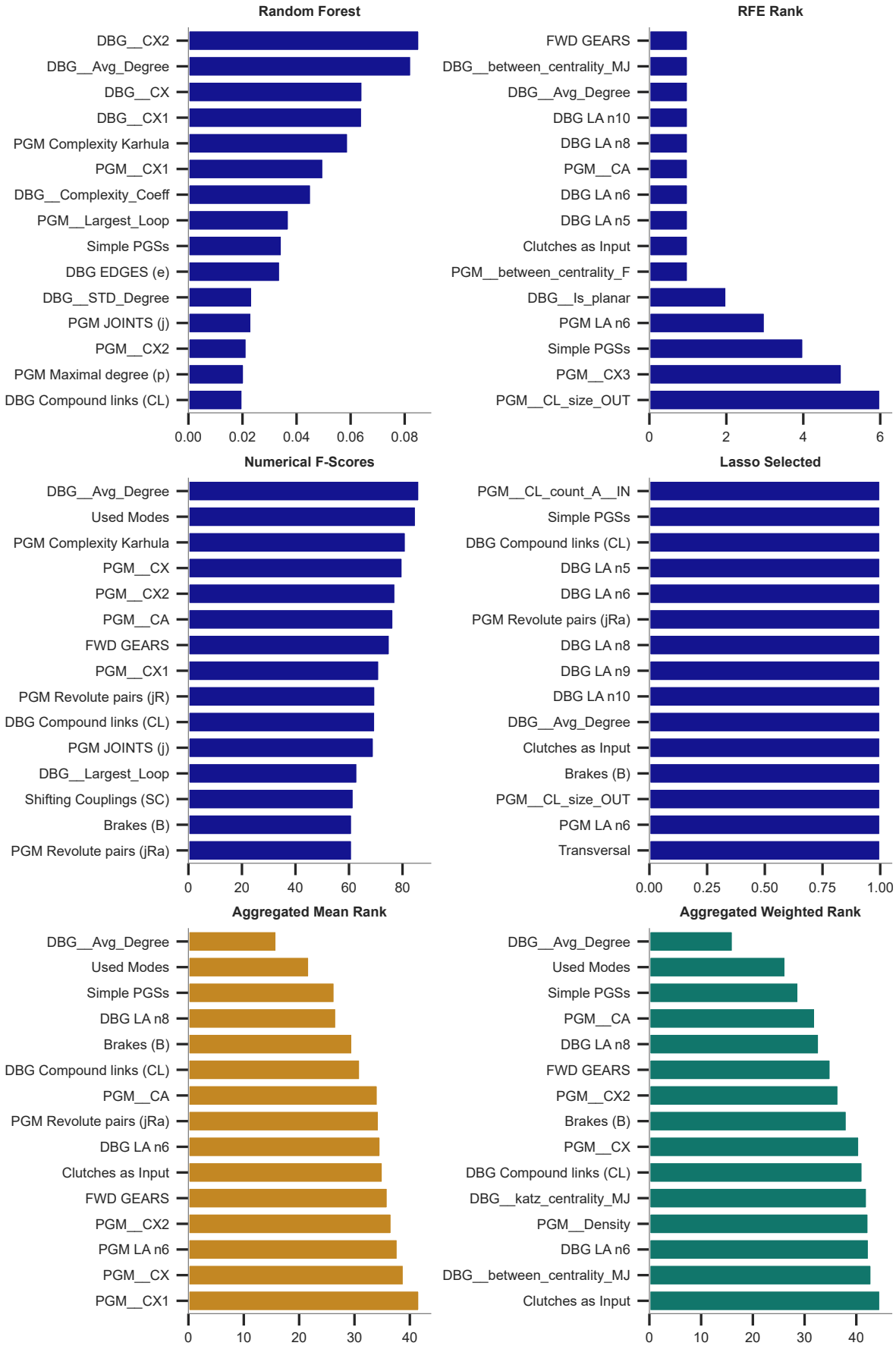

Source: Author.

Figure 371 – 15 most relevant features for total count of 5 elementary PGSs.

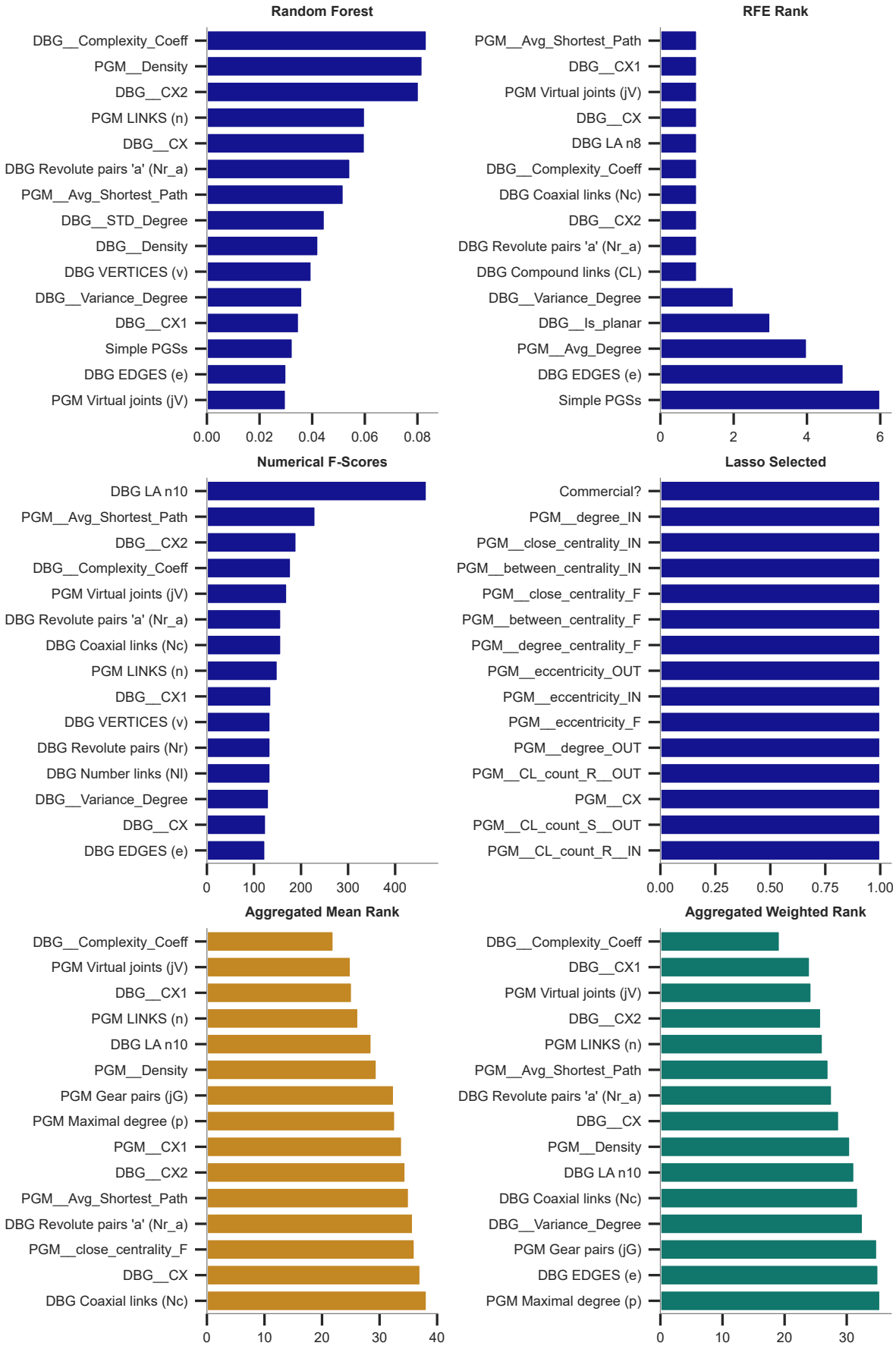

Source: Author.

Figure 372 – 15 most relevant features for 6 forward speeds.

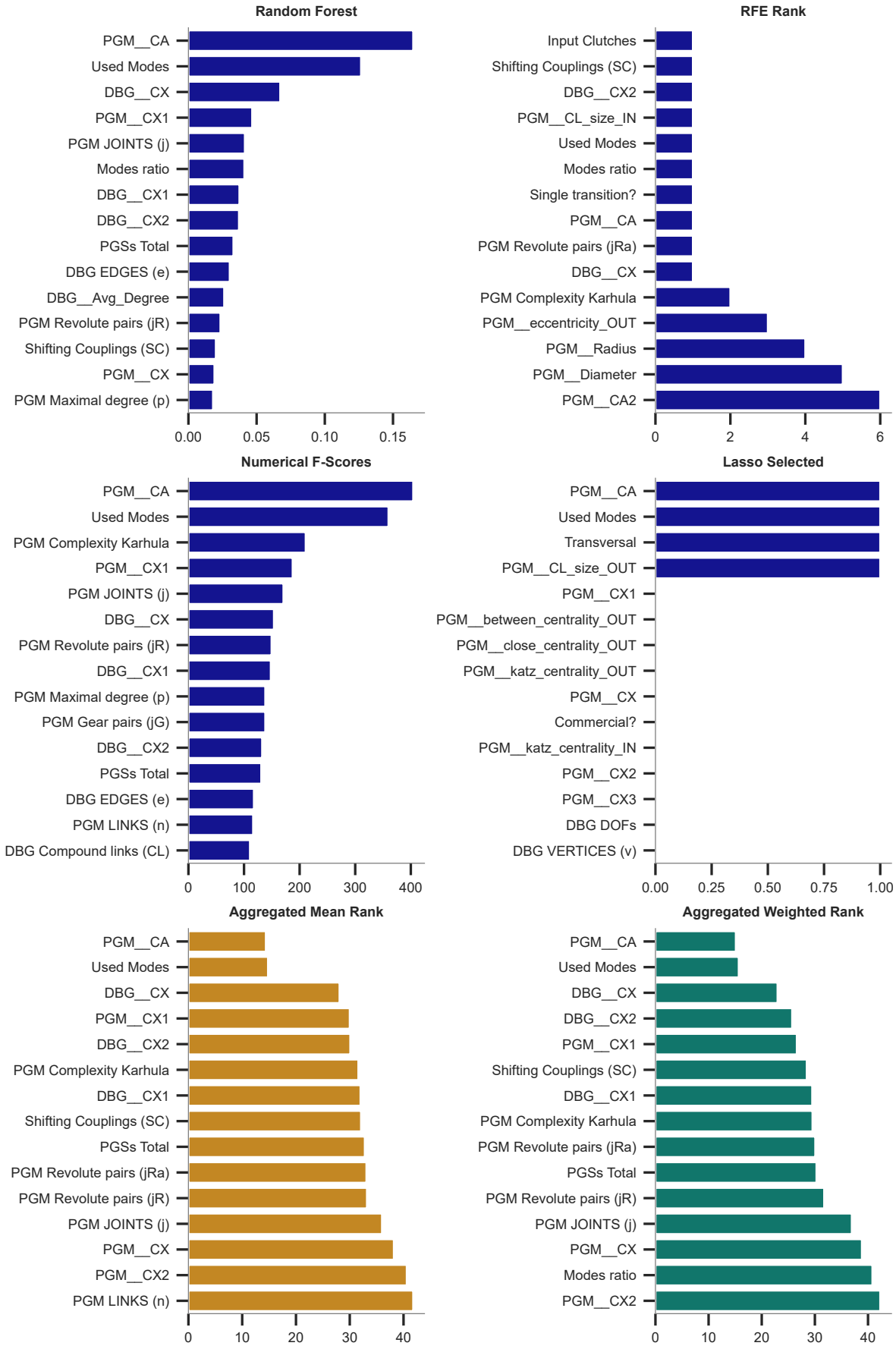

Source: Author.

Figure 373 – 15 most relevant features for 7 forward speeds.

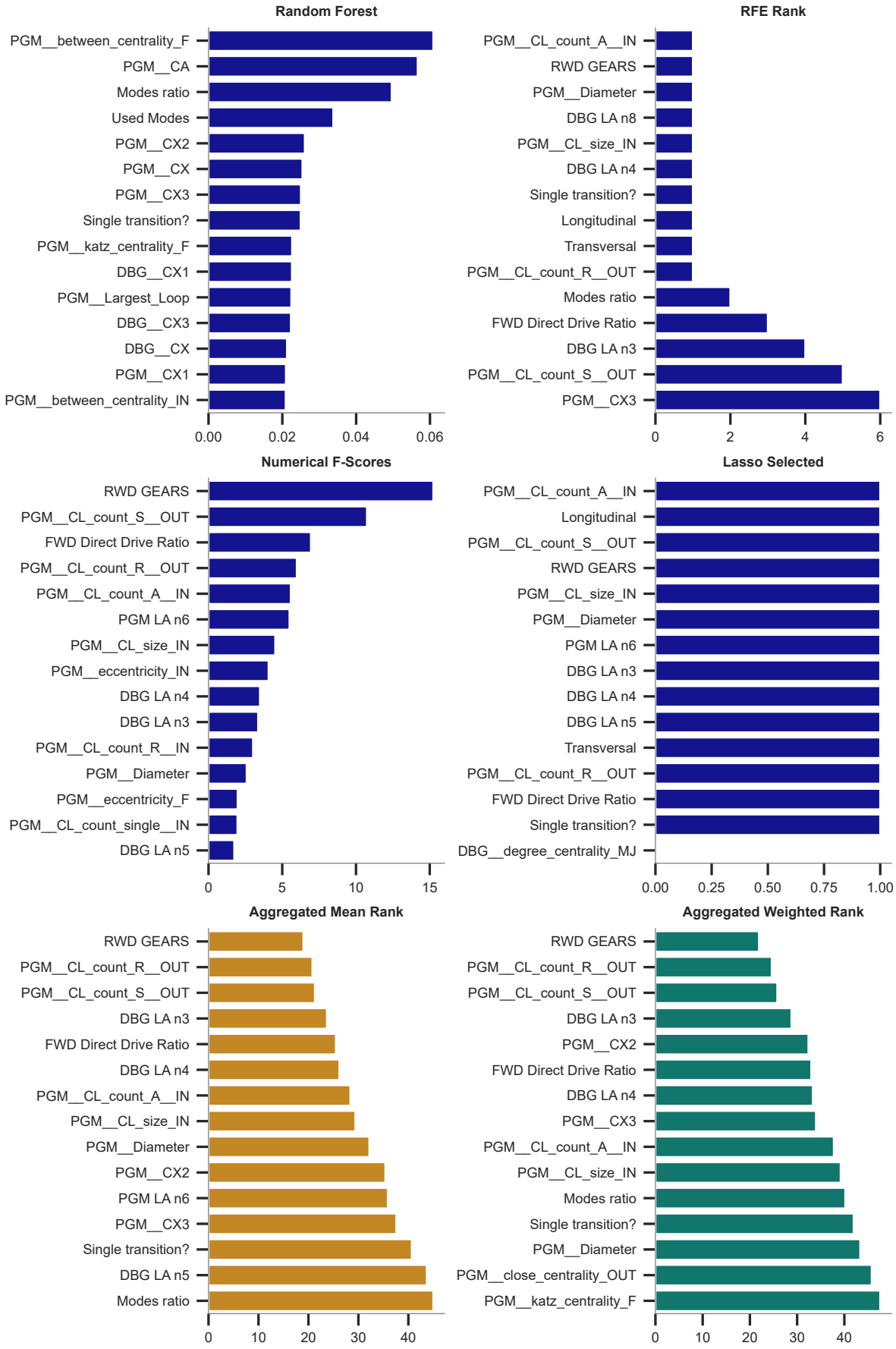

Source: Author.

Figure 374 – 15 most relevant features for 8 forward speeds.

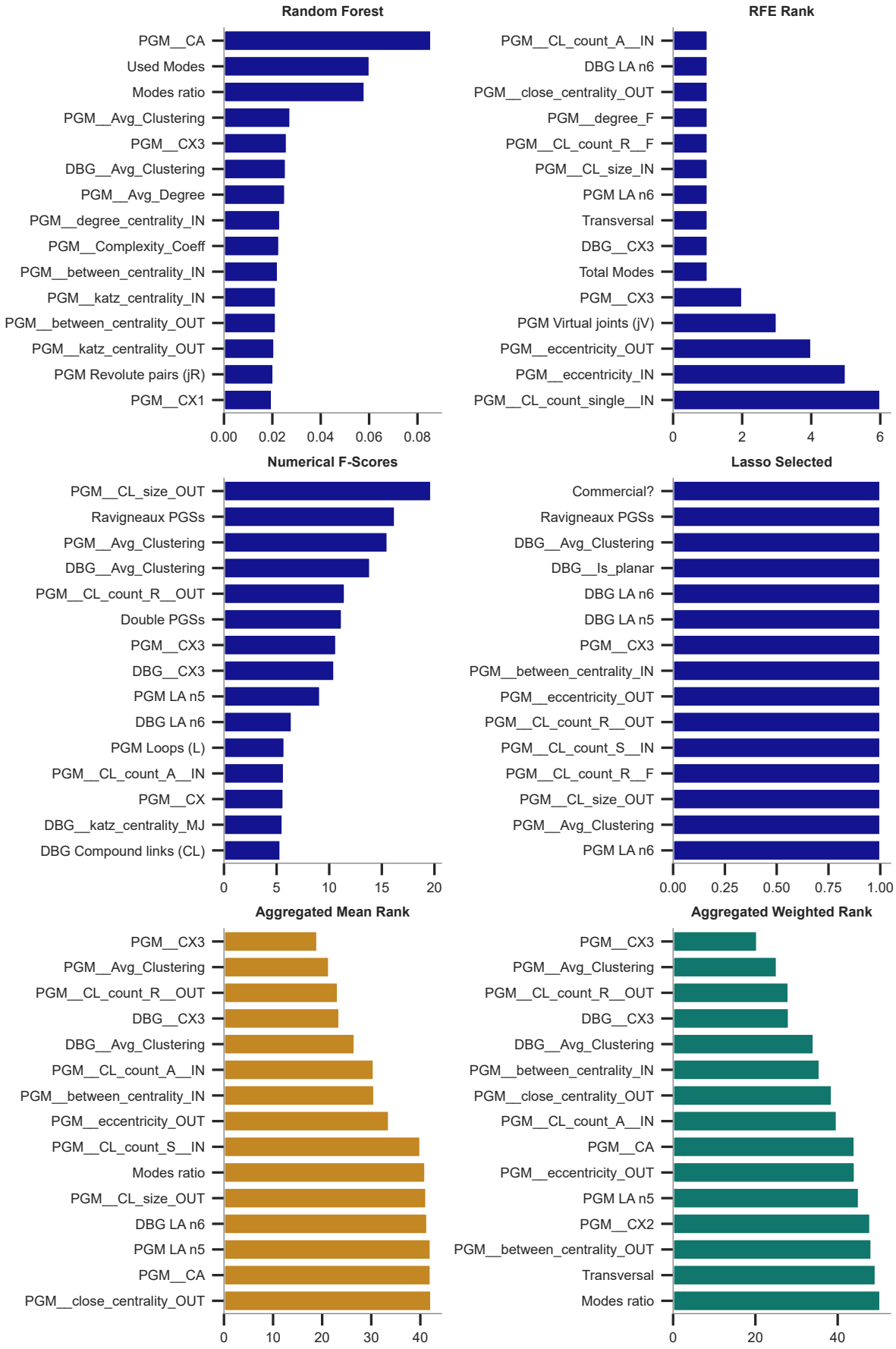

Source: Author.

Figure 375 – 15 most relevant features for 9 forward speeds.

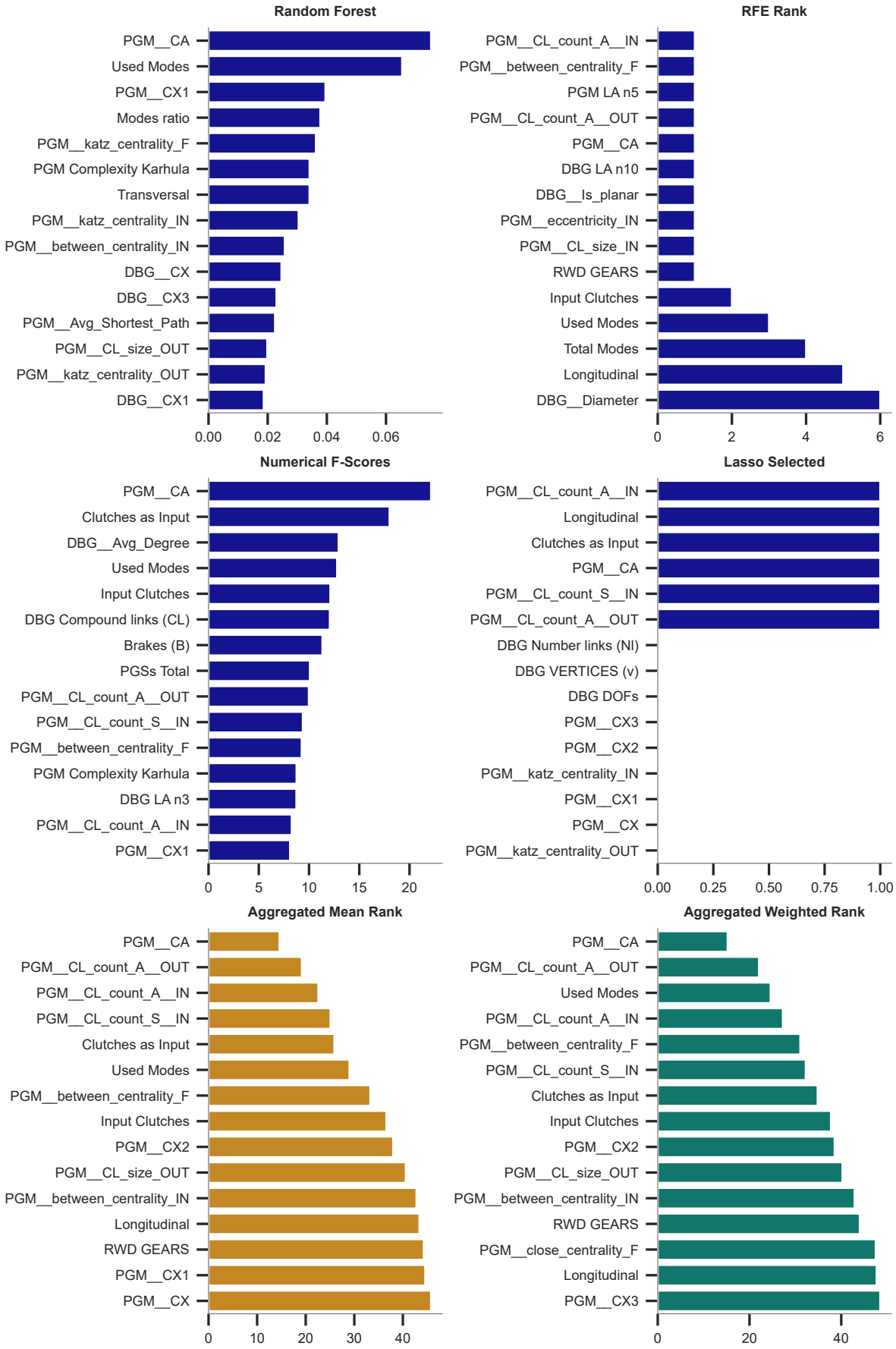

Source: Author.

Figure 376 – 15 most relevant features for 10 forward speeds.

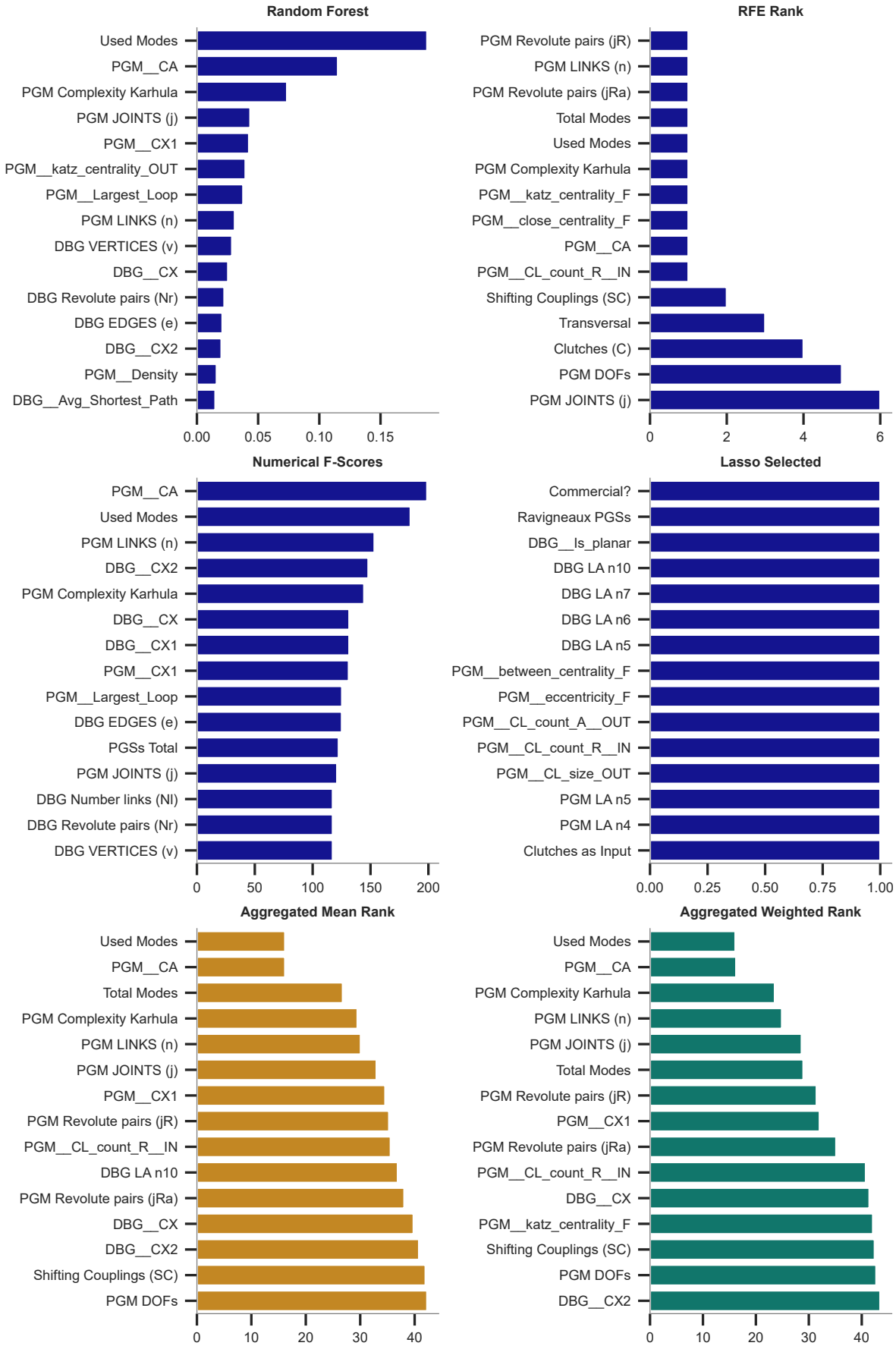

Source: Author.